

*Inria*

RESEARCH CENTER  
Sophia Antipolis - Méditerranée

FIELD

Activity Report 2019

## Section New Results

Edition: 2020-03-21





1. ABS Project-Team	4
2. ACUMES Project-Team	7
3. AROMATH Project-Team	14
4. ATHENA Project-Team	22
5. BIOCORE Project-Team	33
6. BIOVISION Project-Team	42
7. CAMIN Project-Team	52
8. CASTOR Project-Team	66
9. CHORALE Team	71
10. COATI Project-Team	80
11. COFFEE Project-Team (section vide)	94
12. DATASHAPE Project-Team	95
13. DIANA Project-Team	104
14. ECUADOR Project-Team	112
15. EPIONE Project-Team	115
16. FACTAS Project-Team	133
17. FOCUS Project-Team	145
18. GRAPHDECO Project-Team	151
19. GRAPHIK Project-Team	161
20. HEPHAISTOS Project-Team	166
21. INDES Project-Team	172
22. Kairos Project-Team	183
23. LEMON Project-Team	190
24. MATHNEURO Project-Team	192
25. MCTAO Project-Team	203
26. MORPHEME Project-Team	208
27. NACHOS Project-Team	222
28. NEO Project-Team	231
29. PRIVATICS Project-Team	241
30. STAMP Project-Team	247
31. Stars Project-Team	254
32. TITANE Project-Team	278
33. TOSCA Team	288
34. WIMMICS Project-Team	294
35. ZENITH Project-Team	302

## ABS Project-Team

# 5. New Results

## 5.1. Modeling interfaces and contacts

**Keywords:** docking, scoring, interfaces, protein complexes, Voronoi diagrams, arrangements of balls.

### 5.1.1. Characterizing molecular flexibility by combining IRMSD measures

**Participants:** F. Cazals, R. Tetley.

The root mean square deviation (RMSD) and the least RMSD are two widely used similarity measures in structural bioinformatics. Yet, they stem from global comparisons, possibly obliterating locally conserved motifs. In this work [16], we correct these limitations with the so-called *combined RMSD*, which mixes independent IRMSD measures, each computed with its own rigid motion. The combined RMSD is relevant in two main scenarios, namely to compare (quaternary) structures based on motifs defined from the sequence (domains, SSE), and to compare structures based on structural motifs yielded by local structural alignment methods.

We illustrate the benefits of combined RMSD over the usual IRMSD on three problems, namely (i) the assignment of quaternary structures for hemoglobin (scenario #1), (ii) the calculation of structural phylogenies (case study: class II fusion proteins; scenario #1), and (iii) the analysis of conformational changes based on combined RMSD of rigid structural motifs (case study: one class II fusion protein; scenario #2). Using these, we argue that the combined RMSD is a tool of choice to perform positive and negative discrimination of degree of freedom, with applications to the design of move sets and collective coordinates.

Executables to compute combined RMSD are available within the Structural Bioinformatics Library (<http://sbl.inria.fr>).

## 5.2. Modeling the flexibility of macro-molecules

**Keywords:** protein, flexibility, collective coordinate, conformational sampling dimensionality reduction.

### 5.2.1. Wang-Landau Algorithm: an adapted random walk to boost convergence

**Participants:** F. Cazals, A. Chevallier.

The Wang-Landau (WL) algorithm is a recently developed stochastic algorithm computing densities of states of a physical system, and also performing numerical integration in high dimensional spaces. Since its inception, it has been used on a variety of (bio-)physical systems, and in selected cases, its convergence has been proved. The convergence speed of the algorithm is tightly tied to the connectivity properties of the underlying random walk.

In this work [19], we propose an efficient random walk that uses geometrical information to circumvent the following inherent difficulties: avoiding overstepping strata, toning down concentration phenomena in high-dimensional spaces, and accommodating multidimensional distributions. These improvements are especially well suited to improve calculations on a per basin basis – included anharmonic ones.

Experiments on various models stress the importance of these improvements to make WL effective in challenging cases. Altogether, these improvements make it possible to compute density of states for regions of the phase space of small biomolecules.

### 5.2.2. Survey of the analysis of continuous conformational variability of biological macromolecules by electron microscopy

**Participant:** F. Cazals.

*In collaboration with a group of colleagues led by J. M. Carazo, CSIC, Biocomputing Unit, National Center for Biotechnology, Spain.*

Single-particle analysis by electron microscopy is a well established technique for analyzing the three-dimensional structures of biological macromolecules. Besides its ability to produce high-resolution structures, it also provides insights into the dynamic behavior of the structures by elucidating their conformational variability. In this work [17], the different image-processing methods currently available to study continuous conformational changes are reviewed.

### 5.3. Algorithmic foundations

**Keywords:** Computational geometry, computational topology, optimization, data analysis.

#### 5.3.1. Comparing two clusterings using matchings between clusters of clusters

**Participants:** F. Cazals, D. Mazauric, R. Tetley.

*In collaboration with R. Watrigant, University Lyon I.*

Clustering is a fundamental problem in data science, yet, the variety of clustering methods and their sensitivity to parameters make clustering hard. To analyze the stability of a given clustering algorithm while varying its parameters, and to compare clusters yielded by different algorithms, several comparison schemes based on matchings, information theory and various indices (Rand, Jaccard) have been developed. In this work [15], we go beyond these by providing a novel class of methods computing meta-clusters within each clustering— a meta-cluster is a group of clusters, together with a matching between these.

Let the intersection graph of two clusterings be the edge-weighted bipartite graph in which the nodes represent the clusters, the edges represent the non empty intersection between two clusters, and the weight of an edge is the number of common items. We introduce the so-called  $D$ -Family matching problem on intersection graphs, with  $D$  the upper-bound on the diameter of the graph induced by the clusters of any meta-cluster. First we prove  $NP$ -completeness and  $APX$ -hardness results, and unbounded approximation ratio of simple strategies. Second, we design exact polynomial time dynamic programming algorithms for some classes of graphs (in particular trees). Then, we prove spanning-tree based efficient heuristic algorithms for general graphs.

Our experiments illustrate the role of  $D$  as a scale parameter providing information on the relationship between clusters within a clustering and in-between two clusterings. They also show the advantages of our built-in mapping over classical cluster comparison measures such as the variation of information (VI).

#### 5.3.2. Low-Complexity Nonparametric Bayesian Online Prediction with Universal Guarantees

**Participant:** F. Cazals.

*In collaboration with A. Lhéritier, Amadeus SA.*

In this work [18], we propose a novel nonparametric online predictor for discrete labels conditioned on multivariate continuous features. The predictor is based on a feature space discretization induced by a full-fledged  $k$ -d tree with randomly picked directions and a recursive Bayesian distribution, which allows to automatically learn the most relevant feature scales characterizing the conditional distribution. We prove its pointwise universality, i.e., it achieves a normalized log loss performance asymptotically as good as the true conditional entropy of the labels given the features. The time complexity to process the  $n$ -th sample point is  $O(\log n)$  in probability with respect to the distribution generating the data points, whereas other exact nonparametric methods require to process all past observations. Experiments on challenging datasets show the computational and statistical efficiency of our algorithm in comparison to standard and state-of-the-art methods.

#### 5.3.3. How long does it take for all users in a social network to choose their communities?

**Participant:** D. Mazauric.

*In collaboration with J.-C. Bermond (Coati project-team), A. Chaintreau (Columbia University), and G. Ducoffe (National Institute for Research and Development in Informatics, Bucharest).*

In this work [14], we consider a community formation problem in social networks, where the users are either friends or enemies. The users are partitioned into conflict-free groups (*i.e.*, independent sets in the *conflict graph*  $G^- = (V, E)$  that represents the enmities between users). The dynamics goes on as long as there exists any set of at most  $k$  users,  $k$  being any fixed parameter, that can change their current groups in the partition *simultaneously*, in such a way that they all strictly increase their utilities (number of friends *i.e.*, the cardinality of their respective groups minus one). Previously, the best-known upper-bounds on the maximum time of convergence were  $\mathcal{O}(|V|\alpha(G^-))$  for  $k \leq 2$  and  $\mathcal{O}(|V|^3)$  for  $k = 3$ , with  $\alpha(G^-)$  being the independence number of  $G^-$ . Our first contribution in this paper consists in reinterpreting the initial problem as the study of a dominance ordering over the vectors of integer partitions. With this approach, we obtain for  $k \leq 2$  the tight upper-bound  $\mathcal{O}(|V| \min \{\alpha(G^-), \sqrt{|V|}\})$  and, when  $G^-$  is the empty graph, the exact value of order  $\frac{(2|V|)^{3/2}}{3}$ . The time of convergence, for any fixed  $k \geq 4$ , was conjectured to be polynomial. In this paper we disprove this. Specifically, we prove that for any  $k \geq 4$ , the maximum time of convergence is in  $\Omega(|V|^{\Theta(\log |V|)})$ .

## ACUMES Project-Team

## 6. New Results

### 6.1. Macroscopic traffic flow models on networks

**Participants:** Régis Duvigneau, Nikodem Dymski, Paola Goatin, Nicolas Laurent-Brouty, Elena Rossi, Shuxia Tang, Alexandre Bayen [UC Berkeley, CA, USA], Enrico Bertino [Politecnico Milano, Italy], Guillaume Costeseque [Cerema, Nantes], Alexander Keimer [UC Berkeley, CA, USA], Antonella Ferrara [U Pavia, Italy], Adriano Festa [Politecnico Torino, Italy], Mauro Garavello [U Milano-Bicocca, Italy], Thibault Liard [DeustoTech, Spain], Benedetto Piccoli [U Rutgers, NJ, USA], Giulia Piacentini [U Pavia, Italy].

**Bounded acceleration.** In [50], we study a mathematical model accounting for the boundedness of traffic acceleration at a macroscopic scale that was introduced in [137]. Our model is built on a first order macroscopic PDE model coupled with an ODE describing the trajectory of the leader of a platoon accelerating at a given constant rate. We propose a Wave Front Tracking Algorithm to construct approximate solutions. We use this algorithm to prove the existence of solutions to the associated Cauchy Problem, and provide some numerical examples illustrating the solution behaviour.

This work was part of N. Laurent-Brouty's PhD thesis.

**Moving bottlenecks on road networks.** In [48], we generalize the Lighthill-Witham-Richards model for vehicular traffic coupled with moving bottlenecks introduced in [6] to the case of road networks. Such models can be applied to study the traffic evolution in the presence of a slow-moving vehicle, like a bus. At last, a numerical experiment is shown.

This work was part of N. Dymski's PhD thesis.

**Traffic control by autonomous vehicles.** Autonomous vehicles (AVs) allow new ways of regulating the traffic flow on road networks. Most of available results in this direction are based on microscopic approaches, where ODEs describe the evolution of regular cars and AVs. In [49], we propose a multiscale approach, based on recently developed models for moving bottlenecks. Our main result is the proof of existence of solutions for open-loop controls with bounded variation.

**Vehicle platooning in highway traffic.** In [52], we consider a model describing the presence of a platoon of vehicles moving in the traffic flow. The model consists of a coupled PDE-ODE system describing the interaction between the platoon and the surrounding traffic flow. The scalar conservation law takes into account the main traffic evolution, while the ODEs describe the trajectories of the initial and final points of the platoon, whose length can vary in time. The presence of the platoon acts as a road capacity reduction, resulting in a space-time discontinuous flux function. We describe the solutions of Riemann problems and design a finite volume numerical scheme sharply capturing non-classical discontinuities. Some numerical tests are presented to show the effectiveness of the method.

This work is part of G. Piacentini's PhD thesis.

**Well-posedness of conservation laws on networks with finite buffers.** In [51], we introduce a model dealing with conservation laws on networks and coupled boundary conditions at the junctions. In particular, we introduce buffers of fixed arbitrary size and time dependent split ratios at the junctions, which represent how traffic is routed through the network, while guaranteeing spill-back phenomena at nodes. Having defined the dynamics at the level of conservation laws, we lift it up to the Hamilton-Jacobi (H-J) formulation and write boundary datum of incoming and outgoing junctions as functions of the queue sizes and vice-versa. The Hamilton-Jacobi formulation provides the necessary regularity estimates to derive a fixed-point problem in a proper Banach space setting, which is used to prove well-posedness of the model. Finally, we detail how to apply our framework to a non-trivial road network, with several intersections and finite-length links.

This work was realized in the framework of the IIP ORESTE and was part of N. Laurent-Brouty's PhD thesis.

**Traffic flow on multi-lane networks.** In [28], we prove the well-posedness of a system of balance laws describing macroscopically the traffic flow on a multi-lane road network. Motivated by real applications, we allow for the presence of space discontinuities both in the speed law and in the number of lanes. This allows to describe a number of realistic situations. Existence of solutions follows from compactness results on a sequence of Godunov's approximations, while  $L^1$ -stability is obtained by the doubling of variables technique. Some numerical simulations illustrate the behaviour of solutions in sample cases.

**Minimum time boundary controls.** The paper [35] is motivated by the practical problem of controlling traffic flow by imposing restrictive boundary conditions. For a one-dimensional congested road segment, we study the minimum time control problem of how to control the upstream vehicular flow appropriately to regulate the downstream traffic into a desired (constant) free flow state in minimum time. We consider the Initial-Boundary Value Problem (IBVP) for a scalar nonlinear conservation law, associated to the Lighthill-Whitham-Richards (LWR) Partial Differential Equation (PDE), where the left boundary condition, also treated as a valve for the traffic flow from the upstream, serves as a control. Besides, we set absorbing downstream boundary conditions. We prove first a comparison principle for the solutions of the considered IBVP, subject to comparable initial, left and right boundary data, which provides estimates on the minimal time required to control the system. Then we consider a (sub-) optimal control problem and we give numerical results based on Godunov scheme. The article serves as a starting point for studying time-optimal boundary control of the LWR model and for computing numerical results.

This work was realized in the framework of the IIP ORESTE.

**Impact of on-line navigation devices in traffic flows.** In [34], we consider a macroscopic multi-population traffic flow model on networks accounting for the presence of drivers (or autonomous vehicles) using navigation devices to minimize their instantaneous travel cost to destination. The strategic choices of each population differ in the degree of information about the system: while part of the agents knows only the structure of the network and minimizes the traveled distance, others are informed of the current traffic distribution, and can minimize their travel time avoiding the most congested areas. In particular, the different route choices are computed solving eikonal equations on the road network and they are implemented at road junctions. The impact on traffic flow efficiency is illustrated by numerical experiments. We show that, even if the use of routing devices contributes to alleviate congestion on the whole network, it also results in increased traffic on secondary roads. Moreover, the generalized use of real-time information can even deteriorate the efficiency of the network.

**Uncertainty quantification in a macroscopic traffic flow model calibrated on GPS data.** In [18], we analyze the inclusion of one or more random parameters into the deterministic Lighthill-Whitham-Richards traffic flow model and use a semi-intrusive approach to quantify uncertainty propagation. To verify the validity of the method, we test it against real data coming from vehicle embedded GPS systems, provided by AUTOROUTES TRAFIC.

## 6.2. Non-local conservation laws

**Participants:** Felisia Angela Chiarello, Paola Goatin, Elena Rossi, Jan Friedrich [U Mannheim, Germany], Simone Göttlich [U Mannheim, Germany], Jennifer Kotz [U Mannheim, Germany], Luis Miguel Villada [U Bio-Bio, Chile].

F.A. Chiarello's PhD thesis focused on non-local conservation laws. In [23], we proved the stability of entropy weak solutions, considering smooth kernels. We obtained an estimate on the dependence of the solution with respect to the kernel function, the speed and the initial datum, applying the doubling of variables technique. We also provided some numerical simulations illustrating the dependencies above for some cost functionals derived from traffic flow applications.

In the paper [22], we proved the existence for small times of weak solutions for a class of non-local systems in one space dimension, arising in traffic modeling. We approximated the problem by a Godunov type numerical scheme and we provided uniform  $L^\infty$  and BV estimates for the sequence of approximate solutions. We showed some numerical simulations illustrating the behavior of different classes of vehicles and we analyzed two cost functionals measuring the dependence of congestion on traffic composition.

We also conducted a study on Lagrangian-Antidiffusive Remap schemes (previously proposed for classical hyperbolic systems) for the above mentioned non-local multi-class traffic flow model. The error and convergence analysis show the effectiveness of the method, which is first order, in sharply capturing shock discontinuities, and better precision with respect to other methods as Lax-Friedrichs or Godunov (even 2nd order). A journal article about these results has been published [24]. Besides, high-order numerical schemes for the same model were proposed in [78].

Finally, in [21], we present a model for a class of non-local conservation laws arising in traffic flow modeling at road junctions. Instead of a single velocity function for the whole road, we consider two different road segments, which may differ for their speed law and number of lanes (hence their maximal vehicle density). We use an upwind type numerical scheme to construct a sequence of approximate solutions and we provide uniform  $L^\infty$  and total variation estimates. In particular, the solutions of the proposed model stay positive and below the maximum density of each road segment. Using a Lax-Wendroff type argument and the doubling of variables technique, we prove the well-posedness of the proposed model. Finally, some numerical simulations are provided and compared with the corresponding (discontinuous) local model.

Besides, in [31], we focus on finite volume approximation schemes to solve a non-local material flow model in two space dimensions. Based on the numerical discretisation with dimensional splitting, we prove the convergence of the approximate solutions, where the main difficulty arises in the treatment of the discontinuity occurring in the flux function. In particular, we compare a Roe-type scheme to the well-established Lax-Friedrichs method and provide a numerical study highlighting the benefits of the Roe discretisation. We also prove the  $L^1$ -Lipschitz continuous dependence on the initial datum, ensuring the uniqueness of the solution.

### 6.3. Isogeometric Discontinuous Galerkin method for compressible flows

**Participants:** Régis Duvigneau, Stefano Pezzano, Maxime Stauffert.

The co-existence of different geometrical representations in the design loop (CAD-based and mesh-based) is a real bottleneck for the application of design optimization procedures in industry, yielding a major waste of human time to convert geometrical data. Isogeometric analysis methods, which consists in using CAD bases like NURBS in a Finite-Element framework, were proposed a decade ago to facilitate interactions between geometry and simulation domains.

We investigate the extension of such methods to Discontinuous Galerkin (DG) formulations, which are better suited to hyperbolic or convection-dominated problems. Specifically, we develop a DG method for compressible Euler and Navier-Stokes equations, based on rational parametric elements, that preserves exactly the geometry of boundaries defined by NURBS, while the same rational approximation space is adopted for the solution [37]. The following research axes are considered in this context:

- **Adaptive refinement**  
Properties of NURBS functions are used to define an adaptive refinement strategy, which refines locally the discretization according to an error indicator, while describing exactly CAD geometries whatever the refinement level. The resulting approach exhibits an optimal convergence rate and capture efficiently local flow features, like shocks or vortices, avoiding refinement due to geometry approximation [36], [47].
- **Arbitrary Eulerian-Lagrangian formulation**  
To enable the simulation of flows around moving bodies, an Arbitrary Eulerian-Lagrangian (ALE) formulation is proposed in the context of the isogeometric DG method. It relies on a NURBS-based boundary velocity, integrated along time over moving NURBS elements. The gain of using exact-geometry representations is clearly quantified [39].
- **Isogeometric shape optimization**  
On the basis of the isogeometric DG method, we develop a shape optimization procedure with sensitivity analysis, entirely based on NURBS representations [40]. The mesh, the shape parameters as well as the flow solutions are represented by NURBS, which avoids any geometrical conversion and allows to exploit NURBS properties, like regularity, hierarchy, etc.



## 6.4. Sensitivity analysis for unsteady flows

**Participants:** Régis Duvigneau, Maxime Stauffert, Camilla Fiorini [UVST], Christophe Chalons [UVST].

The adjoint equation method, classically employed in design optimization to compute functional gradients, is not well suited to complex unsteady problems, because of the necessity to solve it backward in time. Therefore, we investigate the use of the sensitivity equation method, which is integrated forward in time, in the context of compressible flows. More specifically, the following research axes are considered:

- **Sensitivity analysis in presence of shocks**  
While the sensitivity equation method is a common approach for parabolic systems, its use for hyperbolic ones is still tedious, because of the generation of discontinuities in the state solution, yielding Dirac distributions in the sensitivity solution. To overcome this difficulty, we investigate a modified sensitivity equation, that includes an additional source term when the state solution exhibits discontinuities, to avoid the generation of delta-peaks in the sensitivity solution. We consider as typical example the 1D compressible Euler equations. Different approaches are tested to integrate the additional source term: a Roe solver, a Godunov method and a moving cells approach. Applications to uncertainty quantification in presence of shocks are demonstrated and compared to the classical Monte-Carlo method [26]. This study is achieved in collaboration with C. Chalons and C. Fiorini from University of Versailles.
- **High-order derivatives**  
For problems with regular solution, we investigate the recursive use of the sensitivity equation method to estimate high-order derivatives of the solution with respect to parameters of interest. Such derivatives provide useful information for optimization or uncertainty quantification. More precisely, the third-order derivatives of flow solutions governed by 2D compressible Navier-Stokes equations are estimated with a satisfactory accuracy.
- **Shape sensitivity analysis**  
When shape parameters are considered, the evaluation of flow sensitivities is more difficult, because equations include an additional term, involving flow gradient, due to the fact that the parameter affects the boundary condition location. To overcome this difficulty, we propose to solve sensitivity equations using an isogeometric Discontinuous Galerkin (DG) method, which allows to estimate accurately flow gradients at boundary and consider boundary control points as shape parameters. First results obtained for 2D compressible Euler equations exhibit a sub-optimal convergence rate, as expected, but a better accuracy with respect to a classical DG method [40].

## 6.5. Optimization of nano-phonic devices

**Participants:** Mickaël Binois, Régis Duvigneau, Mahmoud Elsaywy [NACHOS team], Alexis Gobé [NACHOS team], Stéphane Lanteri [NACHOS team].

In collaboration with NACHOS Project-Team, we consider the optimization of optical meta-surface devices, which are able to alter light properties by operating at nano-scale. In the context of Maxwell equations, modified to account for nano-scale phenomena, the geometrical properties of materials are optimized to achieve a desired electromagnetic wave response, such as change of polarization, intensity or direction. This task is especially challenging due to the computational cost related to the 3D time-accurate simulations and the difficulty to handle the different geometrical scales in optimization.

A first study, comparing an evolution strategy and a Bayesian optimization algorithm, demonstrates the potentiality of the proposed approach [25], [38].

## 6.6. Sequential learning of active subspace

**Participants:** Mickaël Binois, Nathan Wycoff [Virginia Tech], Stefan Wild [ANL].



Continuing a work started at Argonne National Laboratory, in [53] we consider the combination of Gaussian process regression modeling with the active subspace methods (ASMs), which have become a popular means of performing subspace sensitivity analysis on black-box functions. Naively applied, however, ASMs require gradient evaluations of the target function. In the event of noisy, expensive, or stochastic simulators, evaluating gradients via finite differencing may be infeasible. In such cases, often a surrogate model is employed, on which finite differencing is performed. When the surrogate model is a Gaussian process, we show that the ASM estimator is available in closed form, rendering the finite-difference approximation unnecessary. We use our closed-form solution to develop acquisition functions focused on sequential learning tailored to sensitivity analysis on top of ASMs. We also show that the traditional ASM estimator may be viewed as a method of moments estimator for a certain class of Gaussian processes. We demonstrate how uncertainty on Gaussian process hyperparameters may be propagated to uncertainty on the sensitivity analysis, allowing model-based confidence intervals on the active subspace. Our methodological developments are illustrated on several examples.

## 6.7. The Kalai-Smorodinski solution for many-objective Bayesian optimization

**Participants:** Mickaël Binois, Victor Picheny [Prowler.io], Abderrahmane Habbal.

Extending the short paper [67] on the use of the game-theoretic Kalai-Smorodinski solution in Bayesian optimization, we have refined the definition of solutions, discussed underlying assumptions, and shown empirically the improved performance of our proposed approach over naive heuristics. A realistic hyperparameter tuning problem with eight objectives as well as an expensive calibration problem with nine objectives have been considered as well.

In parallel, we have substantially improved the efficiency of the implementation, enabled specific treatment of calibration problems as well as handling noise in the GPGame package <https://cran.r-project.org/web/packages/GPGame>.

## 6.8. Heteroskedastic Gaussian process modeling and sequential design

**Participants:** Mickaël Binois, Robert Gramacy [Virginia Tech].

An increasing number of time-consuming simulators exhibit a complex noise structure that depends on the inputs. For conducting studies with limited budgets of evaluations, new surrogate methods are required in order to simultaneously model the mean and variance fields. To this end, in [43] we present the hetGP package <https://cran.r-project.org/web/packages/hetGP>, implementing many recent advances in Gaussian process modeling with input-dependent noise. First, we describe a simple, yet efficient, joint modeling framework that relies on replication for both speed and accuracy. Then we tackle the issue of data acquisition leveraging replication and exploration in a sequential manner for various goals, such as for obtaining a globally accurate model, for optimization, or for contour finding. Reproducible illustrations are provided throughout.

## 6.9. Direct and adaptive approaches to multi-objective optimization

**Participants:** Jean-Antoine Désidéri, Régis Duvigneau.

We formulate in a unified way the major theoretical results obtained by the authors in the domain of multi-objective differential optimization, discuss illustrative examples, and present a brief discussion of the related software developments made at Inria. The development is split in two connected parts. In Part A, the Multiple Gradient Descent Algorithm (MGDA), referred to as the direct approach, is a general construction of a descent method in the multi-objective optimization context. The algorithm provides a technique for determining Pareto optimal solutions in constrained problems as an extension of the classical steepest-descent method. In Part B, another problematics is posed, referred to as the adaptive approach. It is meant to be developed after a Pareto-optimal solution with respect to a set of primary cost functions subject to constraints has been elected in a first phase of optimization carried out by application of MGDA, or another effective multi-objective optimization technique, possibly an evolutionary strategy. This second phase of optimization permits to construct a continuum of neighboring solutions for which novel cost functions, designated as secondary cost

functions, are reduced at the cost of a moderate degradation of the Pareto-stationarity condition of the primary cost functions. In this way, the entire optimization process demonstrates a form of adaptivity to the result of the first phase [42].

## 6.10. Platform for prioritized multi-objective optimization

**Participant:** Jean-Antoine Désidéri.

A multi-objective differentiable optimization algorithm had been proposed to solve problems presenting a hierarchy in the cost functions,  $\{f_j(\mathbf{x})\}$  ( $j = 1, \dots, M \geq 2$ ;  $\mathbf{x} \in \Omega_a \subseteq \mathbb{R}^n$ ). The first cost functions for which  $j \in \{1, \dots, m\}$  ( $1 \leq m < M$ ) are considered to be of preponderant importance; they are referred to as the “primary cost functions” and are subject to a “prioritized” treatment, in contrast with the tail ones, for which  $j \in \{m + 1, \dots, M\}$ , referred to as the “secondary cost functions”. The problem is subject to the nonlinear constraints,  $c_k(\mathbf{x}) = 0$  ( $k = 1, \dots, K$ ). The cost functions  $\{f_j(\mathbf{x})\}$  and the constraint functions  $\{c_k(\mathbf{x})\}$  are all smooth, say  $C^2(\Omega_a)$ . The algorithm was first introduced in the case of two disciplines ( $m = 1, M = 2$ ), and successfully applied to optimum shape design optimization in compressible aerodynamics concurrently with a secondary discipline [101] [105]. An initial admissible point  $\mathbf{x}_A^\star$  that is Pareto-optimal with respect to the sole primary cost functions (subject to the constraints) is assumed to be known. Subsequently, a small parameter  $\varepsilon \in [0, 1]$  is introduced, and it is established that a continuum of Nash equilibria  $\{\bar{\mathbf{x}}_\varepsilon\}$  exists for all small enough  $\varepsilon$ . The continuum originates from  $\mathbf{x}_A^\star$  ( $\bar{\mathbf{x}}_0 = \mathbf{x}_A^\star$ ). Along the continuum: (i) the Pareto-stationarity condition exactly satisfied by the primary cost functions at  $\mathbf{x}_A^\star$  is degraded by a term  $O(\varepsilon^2)$  only, whereas (ii) the secondary cost functions initially decrease, at least linearly with  $\varepsilon$  with a negative derivative provided by the theory. Thus, the secondary cost functions are reduced while the primary cost functions are maintained to quasi Pareto-optimality. In this report, we firstly recall the definition of the different steps in the computational Nash-game algorithm assuming the functions all have known first and second derivatives (here without proofs). Then we show how, in the absence of explicitly known derivatives, the continuum of Nash equilibria can be calculated approximately via the construction of quadratic surrogate functions. Numerical examples are provided and commented [41].

## 6.11. Non-convex multiobjective optimization under uncertainty: a descent algorithm. Application to sandwich plate design and reliability

**Participants:** Quentin Mercier [Onera DADS, Châtillon], Fabrice Poirion [Onera DADS, Châtillon], Jean-Antoine Désidéri.

A novel algorithm for solving multiobjective design optimization problems with non-smooth objective functions and uncertain parameters is presented. The algorithm is based on the existence of a common descent vector for each sample of the random objective functions and on an extension of the stochastic gradient algorithm. The proposed algorithm is applied to the optimal design of sandwich material. Comparisons with the genetic algorithm NSGA-II and the DMS solver are given and show that it is numerically more efficient due to the fact that it does not necessitate the objective function expectation evaluation. It can moreover be entirely parallelizable. Another simple illustration highlights its potential for solving general reliability problems, replacing each probability constraint by a new objective written in terms of an expectation. Moreover, for this last application, the proposed algorithm does not necessitate the computation of the (small) probability of failure [141].

## 6.12. Inverse Cauchy-Stokes problems solved as Nash games

**Participants:** Abderrahmane Habbal, Marwa Ouni [PhD, LAMSIN, Univ. Tunis Al Manar], Moez Kallel [LAMSIN, Univ. Tunis Al Manar].

We extend in two directions our results published in [30] to tackle ill posed Cauchy-Stokes inverse problems as Nash games. First, we consider the problem of detecting unknown pointwise sources in a stationary viscous fluid, using partial boundary measurements. The considered fluid obeys a steady Stokes regime, the boundary measurements are a single compatible pair of Dirichlet and Neumann data, available only on a partial accessible part of the whole boundary. This inverse source identification for the Cauchy-Stokes problem is ill-posed for both the sources and missing data reconstructions, and designing stable and efficient algorithms is challenging. We reformulate the problem as a three-player Nash game. Thanks to a source identifiability result derived for the Cauchy-Stokes problem, it is enough to set up two Stokes BVP, then use them as state equations. The Nash game is then set between 3 players, the two first targeting the data completion while the third one targets the detection of the number, location and magnitude of the unknown sources. We provided the third player with the location and magnitude parameters as strategy, with a cost functional of Kohn-Vogelius type. In particular, the location is obtained through the computation of the topological sensitivity of the latter function. We propose an original algorithm, which we implemented using Freefem++. We present 2D numerical experiments for many different test-cases. The obtained results corroborate the efficiency of our 3-player Nash game approach to solve parameter or shape identification for Cauchy-Stokes problems.

The second direction is dedicated to the solution of the data completion problem for non-linear flows. We consider two kinds of non linearities leading to either a non newtonian Stokes flow or to Navier-Stokes equations. Our recent numerical results show that it is possible to perform a one-shot approach using Nash games : players exchange their respective state information and solve linear systems. At convergence to a Nash equilibrium, the states converge to the solution of the non linear systems. To the best of our knowledge, this is the first time such an approach is applied to solve Inverse problems for nonlinear systems.

### **6.13. Virtual FFR quantified with a generalized flow model using Windkessel boundary conditions ; Application to a patient-specific coronary tree**

**Participants:** Abderrahmane Habbal, Keltoum Chahour [PhD, ACUMES and EMI, Univ. Mohammed V], Rajae Aboulaich [EMI, Univ. Mohammed V], Nejib Zemzemi [Inria Bordeaux, EPI CARMEN], Mickaël Binois.

Fractional flow reserve (FFR) has proved its efficiency in improving patients diagnosis. From both economical and clinical viewpoints, a realistic simulation of vascular blood flow inside the coronary arteries could be a better alternative to the invasive FFR. In this view, we consider a 2D reconstructed left coronary tree with two artificial lesions of different degrees. We use a generalized fluid model with a Carreau law and use a coupled multidomain method to implement Windkessel boundary conditions at the outlets. We introduce our methodology to quantify the virtual FFR, and lead several numerical experiments. We compare FFR results from Navier Stokes versus generalized flow model, and for Windkessel versus traction free outlets boundary conditions or mixed outlets boundary conditions. We also investigate some sources of uncertainty that the FFR index might encounter during the invasive procedure, in particular the arbitrary position of the distal sensor. The computational FFR results show that the degree of stenosis is not enough to classify a lesion, while there is a good agreement between Navier Stokes and the non Newtonian flow model adopted in classifying coronary lesions. Furthermore, we highlight that the lack of standardization while making FFR measurement might be misleading regarding the significance of stenosis [76].

## AROMATH Project-Team

### 5. New Results

#### 5.1. Truncated Normal Forms for Solving Polynomial Systems: Generalized and Efficient Algorithms

**Participant:** Bernard Mourrain.

In [16], we consider the problem of finding the isolated common roots of a set of polynomial functions defining a zero-dimensional ideal  $I$  in a ring  $R$  of polynomials over  $\mathbb{C}$ . Normal form algorithms provide an algebraic approach to solve this problem. The framework presented in Telen et al. (2018) uses truncated normal forms (TNFs) to compute the algebra structure of  $R/I$  and the solutions of  $I$ . This framework allows for the use of much more general bases than the standard monomials for  $R/I$ . This is exploited in this paper to introduce the use of two special (non-monomial) types of basis functions with nice properties. This allows, for instance, to adapt the basis functions to the expected location of the roots of  $I$ . We also propose algorithms for efficient computation of TNFs and a generalization of the construction of TNFs in the case of non-generic zero-dimensional systems. The potential of the TNF method and usefulness of the new results are exposed by many experiments.

This is a joint work with Simon Telen and Marc Van Barel, Department of Computer Science - K.U.Leuven.

#### 5.2. Implicit representations of high-codimension varieties

**Participants:** Ioannis Emiris, Clément Laroche, Christos Konaxis.

In [8], we study implicitization, which usually focuses on plane curves and (hyper)surfaces, in other words, varieties of codimension 1. We shift the focus on space curves and, more generally, on varieties of codimension larger than 1, and discuss approaches that are not sensitive to base points. Our first contribution is a direct generalization of an implicitization method based on interpolation matrices for objects of high codimension given parametrically or as point clouds. Our result shows the completeness of this approach which, furthermore, reduces geometric operations and predicates to linear algebra computations. Our second, and main contribution is an implicitization method of parametric space curves and varieties of codimension  $> 1$ , which exploits the theory of Chow forms to obtain the equations of conical (hyper)surfaces intersecting precisely at the given object. We design a new, practical, randomized algorithm that always produces correct output but possibly with a non-minimal number of surfaces. For space curves, which is the most common case, our algorithm returns 3 surfaces whose polynomials are of near-optimal degree; moreover, computation reduces to a Sylvester resultant. We illustrate our algorithm through a series of examples and compare our Maple code with other methods implemented in Maple. Our prototype is not faster but yields fewer equations and is more robust than Maple's `implicitize`. Although not optimized, it is comparable with Gröbner bases and matrix representations derived from syzygies, for degrees up to 6.

#### 5.3. Saturation of Jacobian ideals: Some applications to nearly free curves, line arrangements and rational cuspidal plane curves

**Participant:** Alexandru Dimca.

In [6] we describe the minimal resolution of the ideal  $I_f$ , the saturation of the Jacobian ideal of a nearly free plane curve  $(C : f) = 0$ . In particular, it follows that this ideal  $I_f$  can be generated by at most 4 polynomials. Some applications to rational cuspidal plane curves are given, and a natural related question is raised.

This is a joint work with Gabriel Sticlaru (Ovidius University of Constanta).

## 5.4. Matrix formulae for Resultants and Discriminants of Bivariate Tensor-product Polynomials

**Participants:** Laurent Busé, Angelos Mantzaflaris.

The construction of optimal resultant formulae for polynomial systems is one of the main areas of research in computational algebraic geometry. However, most of the constructions are restricted to formulae for unmixed polynomial systems, that is, systems of polynomials which all have the same support. Such a condition is restrictive, since mixed systems of equations arise frequently in many problems. Nevertheless, resultant formulae for mixed polynomial systems is a very challenging problem. In [5], we introduce a square, Koszul-type, matrix, the determinant of which is the resultant of an arbitrary (mixed) bivariate tensor-product polynomial system. The formula generalizes the classical Sylvester matrix of two univariate polynomials, since it expresses a map of degree one, that is, the elements of the corresponding matrix are up to sign the coefficients of the input polynomials. Interestingly, the matrix expresses a primal-dual multiplication map, that is, the tensor product of a univariate multiplication map with a map expressing derivation in a dual space. In addition we prove an impossibility result which states that for tensor-product systems with more than two (affine) variables there are no universal degree-one formulae, unless the system is unmixed. Last but not least, we present applications of the new construction in the efficient computation of discriminants and mixed discriminants.

This is joint work with Elias Tsigaridas (Ouragan, Inria).

## 5.5. Implicitizing rational curves by the method of moving quadrics

**Participants:** Laurent Busé, Clément Laroche, Fatmanur Yildirim.

In [4], a new technique for finding implicit matrix-based representations of rational curves in arbitrary dimension is introduced. It relies on the use of moving quadrics following curve parameterizations, providing a high-order extension of the implicit matrix representations built from their linear counterparts, the moving planes. The matrices we obtain offer new, more compact, implicit representations of rational curves. Their entries are filled by linear and quadratic forms in the space variables and their ranks drop exactly on the curve. Typically, for a general rational curve of degree  $d$  we obtain a matrix whose size is half of the size of the corresponding matrix obtained with the moving planes method. We illustrate the advantages of these new matrices with some examples, including the computation of the singularities of a rational curve.

## 5.6. Separation bounds for polynomial systems

**Participants:** Ioannis Emiris, Bernard Mourrain.

In [9] we rely on aggregate separation bounds for univariate polynomials to introduce novel worst-case separation bounds for the isolated roots of zero-dimensional, positive-dimensional, and overdetermined polynomial systems. We exploit the structure of the given system, as well as bounds on the height of the sparse (or toric) resultant, by means of mixed volume, thus establishing adaptive bounds. Our bounds improve upon Canny's Gap theorem [9]. Moreover, they exploit sparseness and they apply without any assumptions on the input polynomial system. To evaluate the quality of the bounds, we present polynomial systems whose root separation is asymptotically not far from our bounds. We apply our bounds to three problems. First, we use them to estimate the bit-size of the eigenvalues and eigenvectors of an integer matrix; thus we provide a new proof that the problem has polynomial bit complexity. Second, we bound the value of a positive polynomial over the simplex: we improve by at least one order of magnitude upon all existing bounds. Finally, we asymptotically bound the number of steps of any purely subdivision-based algorithm that isolates all real roots of a polynomial system.

This is a joint work with E. Tsigaridas (Ouragan).

## 5.7. Sparse polynomial interpolation: sparse recovery, super resolution, or Prony?

**Participant:** Bernard Mourrain.

In [12], we show that the sparse polynomial interpolation problem reduces to a discrete super-resolution problem on the  $n$ -dimensional torus. Therefore the semidefinite programming approach initiated by Candès & Fernandez-Granda in the univariate case can be applied. We extend their result to the multivariate case, i.e., we show that exact recovery is guaranteed provided that a geometric spacing condition on the supports holds and the number of evaluations are sufficiently many (but not many). It also turns out that the sparse recovery LP-formulation of  $\ell_1$ -norm minimization is also guaranteed to provide exact recovery *provided that* the evaluations are made in a certain manner and even though the Restricted Isometry Property for exact recovery is not satisfied. (A naive sparse recovery LP-approach does not offer such a guarantee.) Finally we also describe the algebraic Prony method for sparse interpolation, which also recovers the exact decomposition but from less point evaluations and with no geometric spacing condition. We provide two sets of numerical experiments, one in which the super-resolution technique and Prony's method seem to cope equally well with noise, and another in which the super-resolution technique seems to cope with noise better than Prony's method, at the cost of an extra computational burden (i.e. a semidefinite optimization).

This is a joint work with Cédric Josz and Jean-Bernard Lasserre (Équipe Méthodes et Algorithmes en Commande, LAAS).

## 5.8. Computing minimal Gorenstein covers

**Participant:** Bernard Mourrain.

In [7], we analyze and present an effective solution to the minimal Gorenstein cover problem: given a local Artin  $k$ -algebra  $A = k[[x_1, \dots, x_n]]/I$ , compute an Artin Gorenstein  $k$ -algebra  $G = k[[x_1, \dots, x_n]]/I$  such that  $\ell(G) - \ell(A)$  is minimal. We approach the problem by using Macaulay's inverse systems and a modification of the integration method for inverse systems to compute Gorenstein covers. We propose new characterizations of the minimal Gorenstein cover and present a new algorithm for the effective computation of the variety of all minimal Gorenstein covers of  $A$  for low Gorenstein colength. Experimentation illustrates the practical behavior of the method.

This is a joint work with Juan Elias and Roser Homs (Dep. de Matemàtiques i Informàtica, Universitat de Barcelona).

## 5.9. Symmetry Preserving Interpolation

**Participants:** Erick David Rodriguez Bazan, Evelyne Hubert.

In [22], we address multivariate interpolation in the presence of symmetry. Interpolation is a prime tool in algebraic computation while symmetry is a qualitative feature that can be more relevant to a mathematical model than the numerical accuracy of the parameters. The article shows how to exactly preserve symmetry in multivariate interpolation while exploiting it to alleviate the computational cost. We revisit minimal degree and least interpolation with symmetry adapted bases, rather than monomial bases. This allows to construct bases of invariant interpolation spaces in blocks, capturing the inherent redundancy in the computations. We show that the so constructed symmetry adapted interpolation bases alleviate the computational cost of any interpolation problem and automatically preserve any equivariance of their interpolation problem might have.

## 5.10. Skew-Symmetric Tensor Decomposition

**Participant:** Bernard Mourrain.

In [2], we introduce the "skew apolarity lemma" and we use it to give algorithms for the skew-symmetric rank and the decomposition of tensors in  $\wedge^d V_{\mathbb{C}}$  with  $d \leq 3$  and  $\dim V_{\mathbb{C}} \leq 8$ . New algorithms to compute the rank and a minimal decomposition of a tri-tensor are also presented.



This is a joint work with Enrique Arrondo (UCM - Universidad Complutense de Madrid, Spain), Alessandra Bernardi (Department of Mathematics, University of Trento, Italy) Pedro Macias Marques (Departamento de Matemática da Universidade de Évora, Spain).

### 5.11. On the maximal number of real embeddings of minimally rigid graphs in $\mathbb{R}^2$ , $\mathbb{R}^3$ and $\mathbb{S}^2$

**Participants:** Ioannis Emiris, Evangelos Bartzos.

In [3], we study the Rigidity theory studies the properties of graphs that can have rigid embeddings in the  $d$ -dimensional Euclidean space, or on a sphere and other manifolds which in addition satisfy certain edge length constraints. One of the major open problems in this field is to determine lower and upper bounds on the number of realizations with respect to a given number of vertices. This problem is closely related to the classification of rigid graphs according to their maximal number of real embeddings. In this paper, we are interested in finding edge lengths that can maximize the number of real embeddings of minimally rigid graphs in the plane, space, and on the sphere. We use algebraic formulations to provide upper bounds. To find values of the parameters that lead to graphs with a large number of real realizations, possibly attaining the (algebraic) upper bounds, we use some standard heuristics and we also develop a new method inspired by coupler curves. We apply this new method to obtain embeddings in  $\mathbb{R}^3$ . One of its main novelties is that it allows us to sample efficiently from a larger number of parameters by selecting only a subset of them at each iteration. Our results include a full classification of the 7-vertex graphs according to their maximal numbers of real embeddings in the cases of the embeddings in  $\mathbb{R}^2$  and  $\mathbb{R}^3$ , while in the case of  $\mathbb{S}^2$  we achieve this classification for all 6-vertex graphs. Additionally, by increasing the number of embeddings of selected graphs, we improve the previously known asymptotic lower bound on the maximum number of realizations.

This is a joint work with E. Tsigaridas (Ouragan), and J. Legersky (JK University, Linz, Austria).

### 5.12. Voronoï diagram of orthogonal polyhedra in two and three dimensions

**Participants:** Ioannis Emiris, Christina Katsamaki.

In [20], we study Voronoï diagrams, which are a fundamental geometric data structure for obtaining proximity relations. We consider collections of axis-aligned orthogonal polyhedra in two and three-dimensional space under the max-norm, which is a particularly useful scenario in certain application domains. We construct the exact Voronoï diagram inside an orthogonal polyhedron with holes defined by such polyhedra. Our approach avoids creating full-dimensional elements on the Voronoï diagram and yields a skeletal representation of the input object. We introduce a complete algorithm in 2D and 3D that follows the subdivision paradigm relying on a bounding-volume hierarchy; this is an original approach to the problem. The complexity is adaptive and comparable to that of previous methods. Under a mild assumption it is  $O(n/D)$  in 2D or  $O(na^2/D^2)$  in 3D, where  $n$  is the number of sites, namely edges or facets resp.,  $D$  is the maximum cell size for the subdivision to stop, and  $a$  bounds vertex cardinality per facet. We also provide a numerically stable, open-source implementation in Julia, illustrating the practical nature of our algorithm.

The software was developed during Katsamaki's internship in 2018 at Sophia-Antipolis under the supervision of Bernard Mourrain. The problem has been proposed by our industrial collaborator ANSYS Hellas. The paper is based on Katsamaki's MSc thesis.

### 5.13. Near-Neighbor Preserving Dimension Reduction for Doubling Subsets of $L_1$

**Participants:** Ioannis Emiris, Ioannis Psarros.

In [21], we study randomized dimensionality reduction which has been recognized as one of the fundamental techniques in handling high-dimensional data. Starting with the celebrated Johnson-Lindenstrauss Lemma, such reductions have been studied in depth for the Euclidean ( $L_2$ ) metric, but much less for the Manhattan ( $L_1$ ) metric. Our primary motivation is the approximate nearest neighbor problem in  $L_1$ . We exploit its reduction to the decision-with-witness version, called approximate nearest neighbor, which incurs a roughly logarithmic overhead. In 2007, Indyk and Naor, in the context of approximate nearest neighbors, introduced the notion of nearest neighbor-preserving embeddings. These are randomized embeddings between two metric spaces with guaranteed bounded distortion only for the distances between a query point and a point set. Such embeddings are known to exist for both  $L_2$  and  $L_1$  metrics, as well as for doubling subsets of  $L_2$ . The case that remained open were doubling subsets of  $L_1$ . In this paper, we propose a dimension reduction by means of a near neighbor-preserving embedding for doubling subsets of  $L_1$ . Our approach is to represent the pointset with a carefully chosen covering set, then randomly project the latter. We study two types of covering sets:  $c$ -approximate  $r$ -nets and randomly shifted grids, and we discuss the tradeoff between them in terms of preprocessing time and target dimension. We employ Cauchy variables: certain concentration bounds derived should be of independent interest.

This is joint work with Vassilis Margonis (NKUA), and is based on his MSc thesis.

## 5.14. On the cross-sectional distribution of portfolio returns

**Participants:** Ioannis Emiris, Apostolos Chalkis.

The aim of the paper [24] is to study the distribution of portfolio returns across portfolios, and for given asset returns. We focus on the most common type of investment, considering portfolios whose weights are non-negative and sum up to 1. We provide algorithms and formulas from computational geometry and the literature on splines to compute the exact values of the probability density function, and of the cumulative distribution function, at any point. We also provide closed form solutions for the computation of its first four moments, and an algorithm to compute the higher moments. All algorithms and formulas allow also for equal asset returns.

This is a joint work with Ludovic Calès (JRC - European Commission - Joint Research Centre, Ispra).

## 5.15. Enumerating the morphologies of non-degenerate Darboux cyclides

**Participant:** Bernard Mourrain.

In [19] we provide an enumeration of all possible morphologies of non-degenerate Darboux cyclides. Based on the fact that every Darboux cyclide in  $\mathbb{R}^3$  is the stereographic projection of the intersection surface of a sphere and a quadric in  $\mathbb{R}^4$ , we transform the enumeration problem of morphologies of Darboux cyclides to the enumeration of the algebraic sequences that characterize the intersection of a sphere and a quadric in  $\mathbb{R}^4$ .

This is a joint work with Mingyang Zhao, Xiaohong Jia (KLMM - Key Laboratory of Mathematics Mechanization, Beijing, China), Changhe Tu (Shandong University, China), Wenping Wang (Computer Graphics Group, Department of Computer Science, Hong Kong, China).

## 5.16. Anisotropic convolution surfaces

**Participants:** Alvaro Fuentes Suarez, Evelyne Hubert.

Convolution surfaces with 1D skeletons have been limited to close-to-circular normal sections. The new formalism and method presented in [10] allows for ellipsoidal normal sections. Anisotropy is prescribed on  $G^1$  skeletal curves, chosen as circular splines, by a rotation angle and the three radii of an ellipsoid at each extremity. This lightweight model creates smooth shapes that previously required tweaking the skeleton or supplementing it with 2D pieces. The scale invariance of our formalism achieves excellent radii control and thus lends itself to approximate a variety of shapes. The construction of a scaffold is extended to skeletons with  $G^1$  branches. It projects onto the convolution surface as a quad mesh with skeleton bound edge-flow.



This is a joint work with Cédric Zanni (MFX Inria NGE).

### 5.17. A non-iterative method for robustly computing the intersections between a line and a curve or surface

**Participant:** Laurent Busé.

The need to compute the intersections between a line and a high-order curve or surface arises in a large number of finite element applications. Such intersection problems are easy to formulate but hard to solve robustly. In [18], we introduce a non-iterative method for computing intersections by solving a matrix singular value decomposition (SVD) and an eigenvalue problem. That is, all intersection points and their parametric coordinates are determined in one-shot using only standard linear algebra techniques available in most software libraries. As a result, the introduced technique is far more robust than the widely used Newton-Raphson iteration or its variants. The maximum size of the considered matrices depends on the polynomial degree  $q$  of the shape functions and is  $2q \times 3q$  for curves and  $6q^2 \times 8q^2$  for surfaces. The method has its origin in algebraic geometry and has here been considerably simplified with a view to widely used high-order finite elements. In addition, the method is derived from a purely linear algebra perspective without resorting to algebraic geometry terminology. A complete implementation is available from <http://bitbucket.org/nitro-project/>.

This is joint work with Xiao Xiao and Fehmi Cirak (Cambridge, UK).

### 5.18. Cooperative Visual-Inertial Sensor Fusion: the Analytic Solution

**Participant:** Bernard Mourrain.

In [15], we analyze the visual–inertial sensor fusion problem in the cooperative case of two agents, and prove that this sensor fusion problem is equivalent to a simple polynomial equations system that consists of several linear equations and three polynomial equations of second degree. The analytic solution of this polynomial equations system is easily obtained by using an algebraic method. In other words, this letter provides the analytic solution to the visual–inertial sensor fusion problem in the case of two agents. The power of the analytic solution is twofold. From one side, it allows us to determine the relative state between the agents (i.e., relative position, speed, and orientation) without the need of an initialization. From another side, it provides fundamental insights into all the theoretical aspects of the problem. This letter mainly focuses on the first issue. However, the analytic solution is also exploited to obtain basic structural properties of the problem that characterize the observability of the absolute scale and the relative orientation. Extensive simulations and real experiments show that the solution is successful in terms of precision and robustness.

This is a joint work with Agostino Martinelli and Alexander Oliva (CHROMA, Inria Grenoble).

### 5.19. Overlapping Multi-Patch Structures in Isogeometric Analysis

**Participant:** Angelos Mantzaflaris.

In isogeometric analysis (IGA) the domain of interest is usually represented by B-spline or NURBS patches, as they are present in standard CAD models. Complex domains can often be represented as a union of simple overlapping subdomains, parameterized by (tensor-product) spline patches. Numerical simulation on such overlapping multi-patch domains is a serious challenge in IGA. To obtain non-overlapping subdomains one would usually reparameterize the domain or trim some of the patches. Alternatively, one may use methods that can handle overlapping subdomains. In [13] we propose a non-iterative, robust and efficient method defined directly on overlapping multi-patch domains. Consequently, the problem is divided into several sub-problems, which are coupled in an appropriate way. The resulting system can be solved directly in a single step. We compare the proposed method with iterative Schwarz domain decomposition approaches and observe that our method reduces the computational cost significantly, especially when handling subdomains with small overlaps. Summing up, our method significantly simplifies the domain parameterization problem, since we can represent any domain of interest as a union of overlapping patches without the need to introduce trimming curves/surfaces. The performance of the proposed method is demonstrated by several numerical experiments for the Poisson problem and linear elasticity in two and three dimensions.

This is a joint work with S. Kargaran, B. Jüttler, S. Kleiss and T. Takacs. (RICAM - Johann Radon Institute for Computational and Applied Mathematics and Institute of Applied Geometry, Linz, Austria)

## 5.20. First Order Error Correction for Trimmed Quadrature in Isogeometric Analysis

**Participant:** Angelos Mantzaflaris.

In [23] we develop a specialized quadrature rule for trimmed domains, where the trimming curve is given implicitly by a real-valued function on the whole domain. We follow an error correction approach: In a first step, we obtain an adaptive subdivision of the domain in such a way that each cell falls in a pre-defined base case. We then extend the classical approach of linear approximation of the trimming curve by adding an error correction term based on a Taylor expansion of the blending between the linearized implicit trimming curve and the original one. This approach leads to an accurate method which improves the convergence of the quadrature error by one order compared to piecewise linear approximation of the trimming curve. It is at the same time efficient, since essentially the computation of one extra one-dimensional integral on each trimmed cell is required. Finally, the method is easy to implement, since it only involves one additional line integral and refrains from any point inversion or optimization operations. The convergence is analyzed theoretically and numerical experiments confirm that the accuracy is improved without compromising the computational complexity.

This is joint work with B. Jüttler and F. Scholz. (Institute of Applied Geometry, Linz, Austria).

## 5.21. Consistent discretization of higher-order interface models for thin layers and elastic material surfaces, enabled by isogeometric cut-cell methods

**Participant:** Angelos Mantzaflaris.

Many interface formulations, e.g. based on asymptotic thin interphase models or material surface theories, involve higher-order differential operators and discontinuous solution fields. In [11] we are taking first steps towards a variationally consistent discretization framework that naturally accommodates these two challenges by synergistically combining recent developments in isogeometric analysis and cut-cell finite element methods. Its basis is the mixed variational formulation of the elastic interface problem that provides access to jumps in displacements and stresses for incorporating general interface conditions. Upon discretization with smooth splines, derivatives of arbitrary order can be consistently evaluated, while cut-cell meshes enable discontinuous solutions at potentially complex interfaces. We demonstrate via numerical tests for three specific nontrivial interfaces (two regimes of the Benveniste–Miloh classification of thin layers and the Gurtin–Murdoch material surface model) that our framework is geometrically flexible and provides optimal higher-order accuracy in the bulk and at the interface.

This is joint work with Zhilin Han, Changzheng Cheng, (HFUT - Hefei University of Technology, China), Chien-Ting Wu, S. Stoter, S. Mogilevskaya, and D. Schillinger (Department of Civil, Environmental and Geo-Engineering, University of Minnesota, USA).

## 5.22. Design of Self-Supporting Surfaces with Isogeometric Analysis

**Participant:** Angelos Mantzaflaris.

Self-supporting surfaces are widely used in contemporary architecture, but their design remains a challenging problem. This paper aims to provide a heuristic strategy for the design of complex self-supporting surfaces. In our method, presented in [17] non-uniform rational B-spline (NURBS) surfaces are used to describe the smooth geometry of the self-supporting surface. The equilibrium state of the surface is derived with membrane shell theory and Airy stresses within the surfaces are used as tunable variables for the proposed heuristic design strategy. The corresponding self-supporting shapes to the given stress states are calculated by the nonlinear isogeometric analysis (IGA) method. Our validation using analytic catenary surfaces shows that the proposed

method finds the correct self-supporting shape with a convergence rate one order higher than the degree of the applied NURBS basis function. Tests on boundary conditions show that the boundary's influence propagates along the main stress directions in the surface. Various self-supporting masonry structures, including models with complex topology, are constructed using the presented method. Compared with existing methods such as thrust network analysis and dynamic relaxation, the proposed method benefits from the advantages of NURBS-based IGA, featuring smooth geometric description, good adaption to complex shapes and increased efficiency of computation.

This is joint work with Yang Xia, Ping Hu (Dalian University of Technology, China), Bert Jüttler (Institute of Applied Geometry, Linz, Austria), Hao Pan (Microsoft Research Asia, China), Wenping Wang (CSE - Department of Computer Science and Engineering, HKUST, Honk Kong, China).

### **5.23. Low-rank space-time decoupled isogeometric analysis for parabolic problems with varying coefficients**

**Participant:** Angelos Mantzaflaris.

In [14] we present a space-time isogeometric analysis scheme for the discretization of parabolic evolution equations with diffusion coefficients depending on both time and space variables. The problem is considered in a space-time cylinder in  $\mathbb{R}^{d+1}$ , with  $d = 2, 3$  and is discretized using higher-order and highly-smooth spline spaces. This makes the matrix formation task very challenging from a computational point of view. We overcome this problem by introducing a low-rank decoupling of the operator into space and time components. Numerical experiments demonstrate the efficiency of this approach.

This work was done jointly with F. Scholz and I. Touloupoulos (RICAM - Johann Radon Institute for Computational and Applied Mathematics, Linz, Austria).

## ATHENA Project-Team

## 7. New Results

### 7.1. Computational Diffusion MRI

#### 7.1.1. Coarse-Grained Spatiotemporal Acquisition Design for Diffusion MRI

**Participants:** Patryk Filipiak, Rutger Fick [TheraPanacea, Paris], Alexandra Petiet [ICM, CENIR, Paris], Mathieu Santin [ICM, CENIR, Paris], Anne-Charlotte Philippe [ICM, CENIR, Paris], Stéphane Lehericy [ICM, CENIR, Paris], Demian Wassermann [Inria Parietal], Rachid Deriche.

Acquisition protocols that allow to capture time-dependent changes in diffusion signal require long imaging time. We address this issue through an optimized subsampling scheme that maximizes accuracy of the spatiotemporal diffusion signal representation,  $q_T$ -dMRI, for given time constraints. Our proposed coarse-grained variant of the problem reduces the space of feasible acquisition parameters compared to the fine-grained approach causing no significant deterioration of a reconstruction accuracy in most of the studied cases.

This work has been published in [25].

#### 7.1.2. A Computational Framework For Generating Rotation Invariant Features And Its Application In Diffusion MRI

**Participants:** Mauro Zucchelli, Samuel Deslauriers-Gauthier, Rachid Deriche.

In this work, we present a novel computational framework for analytically generating a complete set of algebraically independent Rotation Invariant Features (RIF) given the Laplace-series expansion of a spherical function. Our computational framework provides a closed-form solution for these new invariants, which are the natural expansion of the well known spherical mean, power-spectrum and bispectrum invariants. We highlight the maximal number of algebraically independent invariants which can be obtained from a truncated Spherical Harmonic (SH) representation of a spherical function and show that most of these new invariants can be linked to statistical and geometrical measures of spherical functions, such as the mean, the variance and the volume of the spherical signal. Moreover, we demonstrate their application to dMRI signal modeling including the Apparent Diffusion Coefficient (ADC), the diffusion signal and the fiber Orientation Distribution Function (fODF). In addition, using both synthetic and real data, we test the ability of our invariants to estimate brain tissue microstructure in healthy subjects and show that our framework provides more flexibility and open up new opportunities for innovative development in the domain of microstructure recovery from diffusion MRI.

This work has been published in [20].

#### 7.1.3. A Novel Characterization of Traumatic Brain Injury in White Matter with Diffusion MRI Spherical-Harmonics Rotation Invariants

**Participants:** Mauro Zucchelli, Samuel Deslauriers-Gauthier, Drew Parker [Penn Applied Connectomics and Imaging Group, Philadelphia], Junghoon John Kim [Department of Molecular, Cellular & Biomedical Sciences, New York], Ragini Verma [Penn Applied Connectomics and Imaging Group, Philadelphia], Rachid Deriche.

The current DTI-based markers of traumatic brain injury are able to capture affected WM in the brain, but miss the areas of crossing fibers and complex WM due to the simplicity of the model. In this work, we use a novel set of spherical-harmonics rotation invariant indices, recently proposed in the literature. We demonstrate that these 12 invariants capture all the information provided by DTI. But in addition, they capture differences in complex WM, beyond DTI measures. This combined with the clinical feasibility of the method, paves the way for them to be used as better markers of brain injury.

This work has been published in [31].

#### 7.1.4. *The Dmipy Toolbox: Diffusion MRI Multi-Compartment Modeling and Microstructure Recovery Made Easy*

**Participants:** Rutger Fick [TheraPanacea, Paris], Demian Wassermann [Inria Parietal], Rachid Deriche.

Non-invasive estimation of brain microstructure features using diffusion MRI (dMRI)—known as Microstructure Imaging—has become an increasingly diverse and complicated field over the last decades. Multi-compartment (MC)-models, representing the measured diffusion signal as a linear combination of signal models of distinct tissue types, have been developed in many forms to estimate these features. However, a generalized implementation of MC-modeling as a whole, providing deeper insights in its capabilities, remains missing. To address this fact, we present Diffusion Microstructure Imaging in Python (Dmipy), an open-source toolbox implementing PGSE-based MC-modeling in its most general form. Dmipy allows on-the-fly implementation, signal modeling, and optimization of any user-defined MC-model, for any PGSE acquisition scheme. Dmipy follows a “building block”-based philosophy to Microstructure Imaging, meaning MC-models are modularly constructed to include any number and type of tissue models, allowing simultaneous representation of a tissue’s diffusivity, orientation, volume fractions, axon orientation dispersion, and axon diameter distribution. In particular, Dmipy is geared toward facilitating reproducible, reliable MC-modeling pipelines, often allowing the whole process from model construction to parameter map recovery in fewer than 10 lines of code. To demonstrate Dmipy’s ease of use and potential, we implement a wide range of well-known MC-models, including IVIM, AxCaliber, NODDI(x), Bingham-NODDI, the spherical mean-based SMT and MC-MDI, and spherical convolution-based single- and multi-tissue CSD. By allowing parameter cascading between MC-models, Dmipy also facilitates implementation of advanced approaches like CSD with voxel-varying kernels and single-shell 3-tissue CSD. By providing a well-tested, user-friendly toolbox that simplifies the interaction with the otherwise complicated field of dMRI-based Microstructure Imaging, Dmipy contributes to more reproducible, high-quality research.

This work has been published in [12].

#### 7.1.5. *Effects of tractography filtering on the topology and interpretability of connectomes.*

**Participants:** Matteo Frigo, Samuel Deslauriers-Gauthier, Drew Parker [Penn Applied Connectomics and Imaging Group, Philadelphia], Abdol Aziz Ould Ismail [Penn Applied Connectomics and Imaging Group, Philadelphia], Junghoon John Kim [Department of Molecular, Cellular & Biomedical Sciences, New York], Ragini Verma [Penn Applied Connectomics and Imaging Group, Philadelphia], Rachid Deriche.

The analysis of connectomes and their associated network metrics forms an important part of clinical studies. These connectomes are based on tractography algorithms to estimate the structural connectivity between brain regions. However, tractography algorithms, are prone to false positive connections and this affects the quality of the connectomes. Several tractography filtering techniques (TFTs) have been proposed to alleviate this issue in studies, but their effect on connectomic analyses of pathology has not been investigated. The aim of this work is to investigate how TFTs affect network metrics and their interpretation in the context of clinical studies.

This work has been published in [29]

#### 7.1.6. *Spherical convolutional neural network for fiber orientation distribution function and micro-structure parameter estimation from dMRI*

**Participants:** Sara Sedlar, Samuel Deslauriers-Gauthier, Théodore Papadopoulos, Rachid Deriche.

Convolutional neural networks (CNNs) are proven to be a powerful tool for many computer vision problems where the data is acquired on a regular grid in Euclidean space. As the dMRI signals used in our experiments are acquired on spheres, we have investigated spherical CNN model (S2-CNN). In regular CNNs, during convolution, kernels are translated over the input feature maps with equidistant steps. In S2-CNN, both kernels and feature maps are represented in the 3D rotation group -  $SO(3)$  manifold. A rotation in  $SO(3)$  is analogous to a translation in Euclidean space. However, there is no regular equidistant grid in  $SO(3)$ . As a consequence,

the convolution is performed in the rotational harmonics (Fourier) domain. In this work, we investigate how the S2-CNN can be adapted to properties of dMRI data, such as antipodal symmetry, the presence of Rician noise, multiple sampling shells, etc.

This work currently in progress.

### 7.1.7. *Adaptive phase correction of diffusion-weighted images*

**Participants:** Marco Pizzolato [Signal Processing Lab (LTS5), EPFL, Lausanne], Guillaume Gilbertb [MR Clinical Science, Philips Healthcare Canada, Markham, ON], Jean-Philippe Thiran [Signal Processing Lab (LTS5), EPFL, Lausanne], Maxime Descoteaux [Université de Sherbrooke, Sherbrooke], Rachid Deriche.

Phase correction (PC) is a preprocessing technique that exploits the phase of images acquired in Magnetic Resonance Imaging (MRI) to obtain real-valued images containing tissue contrast with additive Gaussian noise, as opposed to magnitude images which follow a non-Gaussian distribution, e.g. Rician. PC finds its natural application to diffusion-weighted images (DWIs) due to their inherent low signal-to-noise ratio and consequent non-Gaussianity that induces a signal overestimation bias that propagates to the calculated diffusion indices. PC effectiveness depends upon the quality of the phase estimation, which is often performed via a regularization procedure. We show that a suboptimal regularization can produce alterations of the true image contrast in the real-valued phase-corrected images. We propose adaptive phase correction (APC), a method where the phase is estimated by using MRI noise information to perform a complex-valued image regularization that accounts for the local variance of the noise. We show, on synthetic and acquired data, that APC leads to phase-corrected real-valued DWIs that present a reduced number of alterations and a reduced bias. The substantial absence of parameters for which human input is required favors a straightforward integration of APC in MRI processing pipelines.

This work has been published in [17].

### 7.1.8. *Towards validation of diffusion MRI tractography: bridging the resolution gap with 3D Polarized Light Imaging*

**Participants:** Abib Olushola Yessouffou Alimi, Samuel Deslauriers-Gauthier, Rachid Deriche.

Three-dimensional Polarized Light Imaging (3D-PLI) is an optical approach presented as a good candidate for validation of diffusion Magnetic Resonance Imaging (dMRI) results such as orientation estimates (fiber Orientation Distribution Functions) and tractography. We developed an analytical approach to reconstruct fiber ODFs from 3D-PLI datasets. From these fODFs, here we compute brain fiber tracts via dMRI-based probabilistic tractography algorithm. Reconstructed fODFs at different scales proves the ability to bridge the resolution gap between 3D-PLI and dMRI, demonstrating, therefore, a great promise to validate diffusion MRI tractography thanks to multi-scale fiber tracking based on 3D-PLI.

This work has been published in [21].

### 7.1.9. *Analytical Fiber ODF Reconstruction in 3D Polarized Light Imaging: Performance Assessment*

**Participants:** Abib Olushola Yessouffou Alimi, Samuel Deslauriers-Gauthier, Felix Matuschke [INM-1 - Institute of Neuroscience and Medicine, Jülich], Daniel Schmitz [INM-1 - Institute of Neuroscience and Medicine, Jülich], Markus Axer [INM-1 - Institute of Neuroscience and Medicine, Jülich], Rachid Deriche.

Three dimensional Polarized Light Imaging (3D-PLI) allows to map the spatial fiber structure of postmortem tissue at a sub-millimeter resolution, thanks to its birefringence property. Different methods have been recently proposed to reconstruct the fiber orientation distribution function (fODF) from high-resolution vector data provided by 3D-PLI. Here, we focus on the analytical fODF computation approach, which uses the spherical harmonics to represent the fODF and analytically computes the spherical harmonics coefficients via the spherical Fourier transform. This work deals with the assessment of the performance of this approach on rich synthetic data which simulates the geometry of the neuronal fibers and on human brain dataset. A computational complexity and robustness to noise analysis demonstrate the interest and great potential of the approach.



This work has been published in [22].

## 7.2. Unveiling brain activity using M/EEG

### 7.2.1. *Fast Approximation of EEG Forward Problem and Application to Tissue Conductivity Estimation*

**Participants:** Kostiantyn Maksymenko, Maureen Clerc, Théodore Papadopoulo.

Bioelectric source analysis in the human brain from scalp electroencephalography (EEG) signals is sensitive to the conductivity of the different head tissues. Conductivity values are subject dependent, so non-invasive methods for conductivity estimation are necessary to fine tune the EEG models. To do so, the EEG forward problem solution (so-called lead field matrix) must be computed for a large number of conductivity configurations. Computing one lead field requires a matrix inversion which is computationally intensive for realistic head models. Thus, the required time for computing a large number of lead fields can become impractical. In this work, we propose to approximate the lead field matrix for a set of conductivity configurations, using the exact solution only for a small set of basis points in the conductivity space. Our approach accelerates the computing time, while controlling the approximation error. Our method is tested for brain and skull conductivity estimation, with simulated and measured EEG data, corresponding to evoked somato-sensory potentials. This test demonstrates that the used approximation does not introduce any bias and runs significantly faster than if exact lead field were to be computed.

This work has been published in [15].

### 7.2.2. *Data-driven cortical clustering to provide a family of plausible solutions to the M/EEG inverse problem*

**Participants:** Maureen Clerc, Kostiantyn Maksymenko, Théodore Papadopoulo.

The Magneto/Electroencephalography (M/EEG) inverse problem consists in reconstructing cortical activity from M/EEG measurements. It is an ill-posed problem. Hence prior hypotheses are needed to constrain the solution space. In this work, we consider that the brain activity which generates the M/EEG signals is supported by single or multiple connected cortical regions. As opposed to methods based on convex optimization, which are forced to select one possible solution, we propose a cortical clustering based approach, which is able to find several candidate regions. These regions are different in term of their sizes and/or positions but fit the data with similar accuracy. We first show that even under the hypothesis of a single active region, several source configurations can similarly explain the data. We then use a multiple signal classification (MUSIC) approach to recover multiple active regions with our method. We validate our method on simulated and measured MEG data. Our results show that our method provides a family of plausible solutions which both accord with the priors and similarly fit the measurements.

This work has been published in [8].

### 7.2.3. *Convolutional autoencoder for waveform learning*

**Participants:** Sara Sedlar, Maureen Clerc, Rachid Deriche, Théodore Papadopoulo.

Electro- or Magneto-encephalographic (M/EEG) signals measured on the scalp can be modeled as a linear combination of source signals occurring in different cortical regions. Analysis of specific recurrent waveforms from measurements can help in the evaluation of several neurological disorders such as epilepsy, Alzheimer's disease, and narcolepsy. In addition, detection of the neural events evoked by certain stimuli is crucial for brain-computer interfaces. Such M/EEG signals are quite faint and inherently affected by an important noise, generated by irrelevant brain activities, by other organs, by external ambient noise or imperfections of the measuring devices. In addition, there are intra- and inter-subject variabilities, meaning that the relevant waveforms vary in terms of amplitudes, shapes, and time delays. This makes waveform learning on such signals a quite complex task. In order to address these problems, a number of dictionary (here waveforms) learning based approaches has been proposed. The common framework behind those approaches is an

alternative estimation of data-driven waveforms and their corresponding activations in terms of amplitudes and positions over time. Motivated by the success of these methods and the advances in deep learning, we propose a method based on a convolutional auto-encoder that aims at improving more traditional approaches. Auto-encoders are unsupervised neural network models that have been successfully used for data compression, feature learning, denoising and clustering. Auto-encoders are composed of an encoder which creates a code also known as bottle-neck and decoder that is supposed to reconstruct input signal given the code. By penalizing reconstruction loss function with certain constraints we can guide the auto-encoder to perform compression, denoising, clustering etc. For the moment, the properties of the model are investigated on single-channel synthetic data imitating three types of neurological activities (spikes, short oscillatory and low frequency saw-tooth waveforms) mixed using a realistic leadfield matrix (source space to sensor space transform).

This work is in current progress.

#### **7.2.4. Automatic detection of epileptic seizures by video-EEG**

**Participants:** Mamoudou Sano, Hugo Cadis [IPMC], Fabrice Duprat [IPMC], Massimo Mantegazza [IPMC], Maureen Clerc, Théodore Papadopoulo.

Epilepsy is a serious condition that affects almost 50 million people worldwide. Despite several generations of antiepileptic treatments, the rate of drug-resistant patients remains around 30% and the discovery of new pharmacological targets is therefore a crucial issue.

In order to find pharmacological targets, several animal models make it possible to study the mechanisms of establishment of epileptic disease, or epileptogenesis, and the consequences of repeated spontaneous attacks which characterize epilepsy. Recording an electroencephalogram (EEG) remains the best way to understand these mechanisms. However, the placement of electrodes on small animals such as mice is difficult or even impossible depending on the age of the animal or other used protocols. The use of video recordings over several days, weeks or months makes it possible to observe the animals with a minimum of disturbances and to assess the severity of the crises on a behavioral scale. In both cases, the visual analysis of hundreds of hours of video and/or EEG recordings is very long and error-prone.

The goal of this joint IPMC, ATHENA work was to improve acquisition techniques and develop software tools to automate both EEG and video analysis. EEG analysis was based on the "Adaptive Waveform Learning" that was developed in the group a few years ago [61]. This is work in progress.

### **7.3. Combined fMRI, M/EEG and dMRI**

#### **7.3.1. White Matter Information Flow Mapping from Diffusion MRI and EEG.**

**Participants:** Samuel Deslauriers-Gauthier, Jean-Marc Lina [ETS - Ecole de Technologie Supérieure, Montréal], Russel Butler [Université de Sherbrooke, Sherbrooke], Kevin Whittingstall [Université de Sherbrooke, Sherbrooke], Pierre-Michel Bernier [Université de Sherbrooke, Sherbrooke], Maxime Descoteaux [Université de Sherbrooke, Sherbrooke], Rachid Deriche.

The human brain can be described as a network of specialized and spatially distributed regions. The activity of individual regions can be estimated using electroencephalography and the structure of the network can be measured using diffusion magnetic resonance imaging. However, the communication between the different cortical regions occurring through the white matter, coined information flow, cannot be observed by either modalities independently. Here, we present a new method to infer information flow in the white matter of the brain from joint diffusion MRI and EEG measurements. This is made possible by the millisecond resolution of EEG which makes the transfer of information from one region to another observable. A subject specific Bayesian network is built which captures the possible interactions between brain regions at different times. This network encodes the connections between brain regions detected using diffusion MRI tractography derived white matter bundles and their associated delays. By injecting the EEG measurements as evidence into this model, we are able to estimate the directed dynamical functional connectivity whose delays are supported by the diffusion MRI derived structural connectivity. We present our results in the form of information flow



diagrams that trace transient communication between cortical regions over a functional data window. The performance of our algorithm under different noise levels is assessed using receiver operating characteristic curves on simulated data. In addition, using the well-characterized visual motor network as grounds to test our model, we present the information flow obtained during a reaching task following left or right visual stimuli. These promising results present the transfer of information from the eyes to the primary motor cortex. The information flow obtained using our technique can also be projected back to the anatomy and animated to produce videos of the information path through the white matter, opening a new window into multi-modal dynamic brain connectivity.

This work has been published in [11].

### **7.3.2. Structural connectivity to reconstruct brain activation and effective connectivity between brain regions**

**Participants:** Brahim Belaoucha, Théodore Papadopoulo.

Understanding how brain regions interact to perform a specific task is very challenging. EEG and MEG are two non-invasive imaging modalities that allow the measurement of brain activation with high temporal resolution. Several works in EEG/MEG source reconstruction show that estimating brain activation can be improved by considering spatio-temporal constraints but only few of them use structural information to do so. In this work, we present a source reconstruction algorithm that uses brain structural connectivity, estimated from diffusion MRI (dMRI), to constrain the EEG/MEG source reconstruction. Contrarily to most source reconstruction methods which reconstruct activation for each time instant, the proposed method estimates an initial reconstruction for the first time instants and a multivariate autoregressive model that explains the data in further time instants. This autoregressive model can be thought as an estimation of the effective connectivity between brain regions. We called this algorithm iterative Source and Dynamics reconstruction (iSDR). This paper presents the overall iSDR approach and how the proposed model is optimized to obtain both brain activation and brain region interactions. The accuracy of our method is demonstrated using synthetic data in which it shows a good capability to reconstruct both activation and connectivity. iSDR is also tested with real data (face recognition task). The results are in phase with other works published with the same data and others that used different imaging modalities with the same task showing that the choice of using an autoregressive model gives relevant results.

This work has been submitted to the non-invasive brain imaging special issue of Journal of Neural Engineering.

### **7.3.3. Estimation of Axon Conduction Delay, Conduction Speed, and Diameter from Information Flow using Diffusion MRI and MEG.**

**Participants:** Samuel Deslauriers-Gauthier, Rachid Deriche.

The different lengths and conduction velocities of axons connecting cortical regions of the brain yield information transmission delays which are believed to be fundamental to brain dynamics. While early work on axon conduction velocity was based on ex vivo measurements, more recent work makes use of a combination of diffusion Magnetic Resonance Imaging (MRI) tractography and electroencephalography (EEG) to estimate axon conduction velocity in vivo. An essential intermediary step in this later strategy is to estimate the inter hemispheric transfer time (IHTT) using EEG. The IHTT is estimated by measuring the latency between the peaks or by computing the lag to maximum correlation on contra lateral electrodes. These approaches do not take the subjects anatomy into account and, due to the limited number of electrodes used, only partially leverage the information provided by EEG. In our previous work, we proposed a method, named Connectivity Informed Maximum Entropy on the Mean (CIMEM), to estimate information flow in the white matter of the brain. CIMEM is built around a Bayesian network which represents the cortical regions of the brain and their connections, observed using diffusion MRI tractography. This Bayesian network is used to constrain the EEG inverse problem and estimate which white matter connections are used to transfer information between cortical regions. In our previous work, CIMEM was used to infer the information flow in the white matter by assuming a constant conduction velocity for all connections. In this context, the conduction speed, and thus the delays, were inputs used to help constrain the problem. Here, we instead assume that the connection used

to transfer information across the hemispheres is known, due the design of the acquisition paradigm, but that its conduction velocity must be estimated.

This work has been published in [23].

#### **7.3.4. Estimation of Axonal Conduction Speed and the Inter Hemispheric Transfer Time using Connectivity Informed Maximum Entropy on the Mean**

**Participants:** Samuel Deslauriers-Gauthier, Rachid Deriche.

The different lengths and conduction velocities of axons connecting cortical regions of the brain yield information transmission delays which are believed to be fundamental to brain dynamics. A critical step in the estimation of axon conduction speed in vivo is the estimation of the inter hemispheric transfer time (IHTT). The IHTT is estimated using electroencephalography (EEG) by measuring the latency between the peaks of specific electrodes or by computing the lag to maximum correlation on contra lateral electrodes. These approaches do not take the subject's anatomy into account and, due to the limited number of electrodes used, only partially leverage the information provided by EEG. Using the previous published Connectivity Informed Maximum Entropy on the Mean (CIMEM) method, we propose a new approach to estimate the IHTT. In CIMEM, a Bayesian network is built using the structural connectivity information between cortical regions. EEG signals are then used as evidence into this network to compute the posterior probability of a connection being active at a particular time. Here, we propose a new quantity which measures how much of the EEG signals are supported by connections, which is maximized when the correct conduction delays are used. Using simulations, we show that CIMEM provides a more accurate estimation of the IHTT compared to the peak latency and lag to maximum correlation methods.

This work has been published in [24].

#### **7.3.5. A Unified Model for Structure–function Mapping Based on Eigenmodes**

**Participants:** Samuel Deslauriers-Gauthier, Rachid Deriche.

Characterizing the connection between brain structure and brain function is essential for understanding how behaviour emerges from the underlying anatomy. To this end, a common representation of the brain is that of a network, where nodes represent cortical and sub-cortical gray matter volumes and edges represent the strength of structural or functional connectivity. A convenient representation of this network is that of a matrix, where entries represent the strength of the structural connectivity (SC) or functional connectivity (FC) between nodes. A number of studies have shown that the network structure of the white matter shapes functional connectivity, leading to the idea that it should be possible to predict the function given the structure. A strategy is to learn a direct mapping from the SC matrix to the FC matrix. In this work, we show that the mappings currently proposed in the literature can be generalized to a single model and that this model can be used to generate new structure-function mappings. We tested our general model on 40 subjects of the Human Connectome Project and demonstrated that for specific choices of parameters, our model reduces to previously proposed models and yields comparable results. However, by allowing to choose the eigenvalue and eigenvector mapping independently, our models can also produce novel mapping that improve the prediction of FC from SC.

This work is currently under submission to OHBM.

#### **7.3.6. Connectivity-informed spatio-temporal MEG source reconstruction: Simulation results using a MAR model**

**Participants:** Ivana Kojcic, Théodore Papadopoulo, Samuel Deslauriers-Gauthier, Rachid Deriche.

Recovering brain activity from M/EEG measurements is an ill-posed problem and prior constraints need to be introduced in order to obtain unique solution. The majority of the methods use spatial and/or temporal constraints, without taking account of long-range connectivity. In this work, we propose a new connectivity-informed spatio-temporal approach to constrain the inverse problem using supplementary information coming from diffusion MRI. We present results based on simulated brain activity using a Multivariate Autoregressive Model, with realistic subject anatomy obtained from Human Connectome Project dataset.

This work has been published in [35].

### 7.3.7. *Connectivity-informed solution for spatio-temporal M/EEG source reconstruction*

**Participants:** Ivana Kojcic, Théodore Papadopoulos, Samuel Deslauriers-Gauthier, Rachid Deriche.

Recovering brain activity from M/EEG measurements is an ill-posed problem and prior constraints need to be introduced in order to obtain unique solution. The majority of the methods use spatial and/or temporal constraints, without taking account of long-range connectivity. In this work, we propose a new connectivity-informed spatio-temporal approach to constrain the inverse problem using supplementary information coming from diffusion MRI. We present results based on simulated brain activity obtained with realistic subject anatomy from Human Connectome Project dataset.

This work has been published in [34].

### 7.3.8. *Deconvolution of fMRI Data using a Paradigm Free Iterative Approach based on Partial Differential Equations*

**Participants:** Isa Costantini, Samuel Deslauriers-Gauthier, Rachid Deriche.

Functional magnetic resonance imaging (fMRI) is a technique which indirectly measures neural activations via the blood oxygenated level dependent (BOLD) signal. So far, few approaches have been proposed to regularize the fMRI data, while recovering the underlying activations at the voxel level. In particular, for task fMRI, voxels time courses are fitted on a given experimental paradigm. To avoid the necessity of a priori information on the pattern, supposing the brain works with blocks of constant activation, Farouj et al. has developed a deconvolution approach which solves the optimizations problem by splitting it into two regularization problems, i.e. spatial and temporal. Starting from this idea, we propose a paradigm-free iterative algorithm based on partial differential equations (PDEs) which minimizes the image variations, while preserving sharp transitions (i.e. brain activations), in the space and the time dimensions at once.

This work has been published in [27].

### 7.3.9. *Novel 4-D Algorithm for Functional MRI Image Regularization using Partial Differential Equations*

**Participants:** Isa Costantini, Samuel Deslauriers-Gauthier, Rachid Deriche.

State-of-the-art techniques for denoising functional MRI (fMRI) images consider the problems of spatial and temporal regularization as decoupled tasks. In this work we propose a partial differential equations (PDEs)-based algorithm that acts directly on the 4-D fMRI image. Our approach is based on the idea that large image variations should be preserved as they occur during brain activation, but small variations should be smoothed to remove noise. Starting from this principle, by means of PDEs we were able to smooth the fMRI image with an anisotropic regularization, thus recovering the location of the brain activations in space and their timing and duration.

This work has been published in [28].

### 7.3.10. *Spatially Varying Monte Carlo Sure for the Regularization of Biomedical Images*

**Participants:** Marco Pizzolato [Signal Processing Lab (LTS5), EPFL, Lausanne], Erick Jorge Canales-Rodríguez [Radiology Department CHUV, Lausanne], Jean-Philippe Thiran [Signal Processing Lab (LTS5), EPFL, Lausanne], Rachid Deriche.

Regularization, filtering, and denoising of biomedical images requires the use of appropriate filters and the adoption of efficient regularization criteria. It has been shown that the Stein's Unbiased Risk Estimate (SURE) can be used as a proxy for the mean squared error (MSE), thus giving an effective criterion for choosing the regularization amount as to that minimizing SURE. Often, due to the complexity of the adopted filters and solvers, this proxy must be calculated with a Monte Carlo method. In practical biomedical applications, however, images are affected by spatially-varying noise distributions, which must be taken into account. We propose a modification to the Monte Carlo method, called svSURE, that accounts for the spatial variability of the noise variance, and show that it correctly estimates the MSE in such cases.

This work has been published in [30].

### **7.3.11. *The visual word form area (VWFA) is part of both language and attention circuitry***

**Participants:** Lang Chen, Demian Wasserman, Daniel Abrams, John Kochalka, Guillermo Gallardo-Diez, Vinod Menon.

While predominant models of visual word form area (VWFA) function argue for its specific role in decoding written language, other accounts propose a more general role of VWFA in complex visual processing. However, a comprehensive examination of structural and functional VWFA circuits and their relationship to behavior has been missing. Here, using high-resolution multimodal imaging data from a large Human Connectome Project cohort (N=313), we demonstrate robust patterns of VWFA connectivity with both canonical language and attentional networks. Brain-behavior relationships revealed a striking pattern of double dissociation: structural connectivity of VWFA with lateral temporal language network predicted language, but not visuo-spatial attention abilities, while VWFA connectivity with dorsal fronto-parietal attention network predicted visuo-spatial attention, but not language abilities. Our findings support a multiplex model of VWFA function characterized by distinct circuits for integrating language and attention, and point to connectivity-constrained cognition as a key principle of human brain organization.

This work has been published in [10].

## **7.4. Brain Computer Interfaces**

### **7.4.1. *Augmenting Motor Imagery Learning for Brain-Computer Interfacing Using Electrical Stimulation as Feedback***

**Participants:** Saugat Bhattacharyya [School of Bio-Science and Engineering, Calcutta], Mitsuhiro Hayashibe [Tohoku University, Sendai], Maureen Clerc.

Brain-computer Interfaces (BCI) and Functional electrical stimulation (FES) contribute significantly to induce cortical learning and to elicit peripheral neuronal activation processes and thus, are highly effective to promote motor recovery. This study aims at understanding the effect of FES as a neural feedback and its influence on the learning process for motor imagery tasks while comparing its performance with a classical visual feedback protocol. The participants were randomly separated into two groups: one group was provided with visual feedback (VIS) while the other received electrical stimulation (FES) as feedback. Both groups performed various motor imagery tasks while feedback was provided in form of a bi-directional bar for VIS group and targeted electrical stimulation on the upper and lower limbs for FES group. The results shown in this paper suggest that the FES based feedback is more intuitive to the participants, hence, the superior results as compared to the visual feedback. The results suggest that the convergence of BCI with FES modality could improve the learning of the patients both in terms of accuracy and speed and provide a practical solution to the BCI learning process in rehabilitation.

This work, obtained in the context of the BCI-LIFT IPL, has been published in [9].

### **7.4.2. *Adaptive parameter setting in a code modulated visual evoked potentials BCI***

**Participants:** Federica Turi, Maureen Clerc.

Code-modulated visual evoked potentials (c-VEPs) BCI are designed for high-speed communication. The setting of stimulus parameters is fundamental for this type of BCI, because stimulus parameters have an influence on the performance of the system. In this work we design a c-VEP BCI for word spelling, in which it is possible to find the optimal stimulus presentation rate per each subject thanks to an adaptive setting parameter phase. This phase takes place at the beginning of each session and allows to define the stimulus parameters that are used during the spelling phase. The different stimuli are modulated by a binary m-sequence circular-shifted by a different time lag and a template matching method is applied for the target detection. We acquired data from 4 subjects in two sessions. The results obtained for the offline spelling show the variability between subjects and therefore the importance of subject-dependent adaptation of c-VEP BCI.

This work has been published in [32].

#### **7.4.3. Participation to the Cybathlon BCI Series**

**Participants:** Karine Leclerc [Centre René Labreuil, Le Cannet], Magali Mambrucchi [Centre René Labreuil, Le Cannet], Amandine Audino, Pierre Giacalone, Federica Turi, Maureen Clerc, Théodore Papadopoulo.

The CYBATHLON is a unique championship in which people with physical disabilities compete against each other to complete everyday tasks using state-of-the-art technical assistance systems. Athena participated in the CYBATHLON BCI Series that took place on September 8th, 2019 as a satellite event of the Graz Brain-Computer Interface Conference. Athena was part of a bigger Inria team which encompassed also the Inria Bordeaux Sud-Ouest Potioc team (participants from Bordeaux are not listed). For both Inria sub-teams, it was a first participation to such a competition : we learned a lot about the practical issues of working with people with physical disabilities and on all the practical issues that can encounter a BCI user out of the lab. The actual competition consisted of driving a car on a track by issuing three types of commands (Left, Right, Lights) using mental imagery. Even though our pilot finished last, she was for each run leading the race till a few seconds before its end. A great satisfaction was to see that the software that we built worked reliably out of the lab (many teams have had troubles in issuing commands and had to redo a race). Yet, this required a lot of last minute work to integrate smoothly in the competition system: we learned a lot in this respect. The poster [36] summarises this effort.

#### **7.4.4. BCI Performance prediction**

**Participants:** Maureen Clerc, Nathalie Gayraud, Laurent Bougrain [NeuroSys Project-Team], Sébastien Rimbert [NeuroSys Project-Team], Stéphanie Fleck [Perseus].

Predicting a subject's ability to use a Brain Computer Interface (BCI) is one of the major issues in the BCI domain. Relevant applications of forecasting BCI performance include the ability to adapt the BCI to the needs and expectations of the user, assessing the efficiency of BCI use in stroke rehabilitation, and finally, homogenizing a research population. A limited number of recent studies have proposed the use of subjective questionnaires, such as the Motor Imagery Questionnaire Revised-Second Edition (MIQ-RS). Our results showed no significant correlation between BCI performance and the MIQ-RS scores. However, we reveal that BCI performance is correlated to habits and frequency of practicing manual activities. This work is an outcome of the BCI-LIFT IPL and was published in [18]. Another joint publication [19] investigated median nerve stimulation as a new approach to detect intraoperative awareness during General Anesthesia.

#### **7.4.5. EEG Classification of Auditory Attention**

**Participants:** Joan Belo, Johann Benerradi, Maureen Clerc, Michel Pascal [Nice Music Conservatory], Daniele Schön [Institut de Neurosciences des Systèmes].

In a Master's thesis [33] in collaboration with Nice Music Conservatory and Institut de Neurosciences des Systèmes, we focused on analyzing auditory attention of human participants who are presented two auditory streams, simultaneously on left and right. By analyzing the EEG signals measured, the problem is to detect to which stream the participant is attending. Auditory Attention is also the topic of the PhD thesis of Joan Belo, funded by a CIFRE with Oticon Medical.

#### **7.4.6. Innovative Brain-Computer Interface based on motor cortex activity to detect accidental awareness during general anesthesia**

**Participants:** Sébastien Rimbert, Philippe Guerci, Nathalie Gayraud, Claude Meistelman, Laurent Bougrain.

Accidental Awareness during General Anesthesia (AAGA) occurs in 1-2% of high-risk practice patients and is responsible for severe psychological trauma, termed post-traumatic stress disorder (PTSD). Currently, monitoring techniques have limited accuracy in predicting or detecting AAGA. Since the first reflex of a patient experiencing AAGA is to move, a passive Brain-Computer Interface (BCI) based on the detection of an intention of movement would be conceivable to alert the anesthetist and prevent this phenomenon. However, the way in which the propofol (an anesthetic drug commonly used for inducing and maintaining general anesthesia) affects the motor brain activity and is reflected by the electroencephalo-graphic (EEG) signal has been poorly investigated and is not clearly understood. The goal of this forward-looking study is to investigate the motor activity behavior with step-wise increase of propofol doses in 4 healthy subjects and provide a proof of concept for such an innovative BCI.

This work has been published in [26].



## BIOCORE Project-Team

## 7. New Results

### 7.1. Mathematical methods and methodological approach to biology

#### 7.1.1. Mathematical analysis of biological models

##### 7.1.1.1. Mathematical study of ecological models

**Participants:** Frédéric Grogard, Ludovic Mailleret, Suzanne Touzeau, Clotilde Djuikem, Israël Tankam Chedjou.

*Semi-discrete models.* Semi-discrete models have shown their relevance in the modeling of biological phenomena whose nature presents abrupt changes over the course of their evolution [41]. We used such models and analyzed their properties in several practical situations, some of them requiring such a modeling to describe external perturbations of natural systems such as harvest, and others to take seasonality into account. We developed such models in the context of the analysis of the effect of stochasticity and Allee effects on the introduction of populations [14], seasonality in the dynamics of coffee leaf rust [59] and of banana and plantain burrowing nematodes [67], as well as for the protection of plant resistance against root-knot nematodes [66].

*Models in plant epidemiology.* We developed and analysed dynamical models describing plant-parasite interactions, in order to better understand, predict and control the evolution of damages in crops. We considered several pathosystems, further described in Section 7.2.3, describing and controlling the impact on plants of fungi [59], [39], viruses [36], nematodes [67], [66], and pests [60].

##### 7.1.1.2. Estimation and control

**Participants:** Frédéric Grogard, Ludovic Mailleret, Suzanne Touzeau, Yves Fotso Fotso, Samuel Nilusmas, Israël Tankam Chedjou.

*Parameter identification in complex systems.* In complex biological systems, identifying model parameters is a challenge that raises identifiability issues. To fit a within-host immunological model to a large data set of individual viremia profiles, we developed an Approximate Bayesian Computation (ABC)-like method that yielded several parameter sets compatible with the data and reflecting the variability among individuals [25]. This work benefited from the resources and support of NEF computation cluster.

*Optimal control and optimisation.* We developed several approaches to control the evolution of crop pests. To reduce crop losses due to plant-parasitic nematodes, we optimised (i) rotation strategies between resistant and susceptible cultivars of horticultural crops [76], or (ii) fallow periods between plantain cropping seasons [67]. These optimisation problems were solved on a finite time horizon. They benefited from the resources and support of NEF computation cluster.

We also solved an optimal control problem to limit the damages due to coffee berry borers [60]. It consisted in designing the most cost-efficient application of a biopesticide over time. Using Pontryagin's maximum principle, we determined the existence and structure of the solution. The problem was solved numerically using BOCOP (<https://www.bocop.org/>).

##### 7.1.1.3. Analysis of multistability and periodic behavior with hybrid models

**Participants:** Madalena Chaves, Eleni Firippi.

*Probabilistic dynamics tool for hybrid models* In a collaboration with D. Figueiredo and M.A. Martins from the University of Aveiro, Portugal (project PHC Pessoa), a tool was developed for simulating weighted reactive models [55]. These are essentially discrete models with dynamics described by state transition graphs: each transition has a given weight and the graph has the capacity to alter its accessibility relations.

M. Chaves and M.A. Martins jointly edited a book with selected papers from the Symposium on Molecular Logic and Computational Synthetic Biology [70], gathering work on different formalisms and applications of hybrid models.

*Coupling and synchronization of piecewise linear systems* This work studies the coupling of  $N$  identical positive feedback loops described by piecewise linear differential equations. Under diffusive coupling, and for different conditions on the coupling parameters, the  $N$  systems may synchronize or, alternatively, generate a set of new steady states that form a specific pattern [49]. An unexpected result is the existence of a special relationship between the number of components  $N$  and the maximal concentration-to-activity threshold ratio ( $V_1/(\gamma_1\theta_1)$ ). This relationship implies that, for very specific parameter sets, the  $N$  compartments cannot be guaranteed to synchronize.

#### 7.1.1.4. Dynamics of complex feedback architectures

**Participants:** Madalena Chaves, Jean-Luc Gouzé.

To analyze the closed-loop dynamics of metabolic pathways under gene regulation, we propose a method to construct a state transition graph for a given regulatory architecture consisting of a pathway of arbitrary length, with any number of genetic regulators, and under any combination of positive and negative feedback loops [19]. Using this formalism, we analyze a “metabolator”-like mechanism (a pathway with two metabolites and three enzymes) and prove the existence of two co-existing oscillatory behaviors: damped oscillations towards a fixed point or sustained oscillations along a periodic orbit [20].

#### 7.1.2. Metabolic and genomic models

**Participants:** Jean-Luc Gouzé, Olivier Bernard, Valentina Baldazzi, Lucie Chambon, Carlos Martinez Von Dossow, Agustin Yabo, Alex Dos Reis de Souza, Walid Djema, Sofya Maslovskaya.

*Analysis and reduction of a model of sugar metabolism in peach fruit.* Predicting genotype-to-phenotype relationships is a big challenge for plant biology and breeding. A model of sugar metabolism in peach fruit has been recently developed and applied to 10 peach varieties [80]. A reduction pipeline combining several reduction strategies has been developed to reduce both model size and nonlinearity and allow for further application to virtual breeding (collaboration with B. Quilot-Turion and Mohamed Memmah (INRA Avignon) as part of the PhD thesis of Hussein Kanso) [64]. A paper is currently under revision for Mathematical Biosciences.

*Analysis of an integrated cell division-endoreduplication and expansion model.* The development of a new organ depends on cell-cycle progression and cell expansion, but the interaction and coordination between these processes is still unclear [27]. An integrated model of fruit development has been developed and used to test different interaction schemes, by comparing simulation results to the observed cell size distribution in tomato fruit [15].

*Modeling cell growth and resource allocation.* In the framework of the Maximic project (collaboration with IBIS team) and as a follow up of our previous work [82], we investigated the impact of energy metabolism on cell’s strategy for resource allocation. Preliminary results show that the inclusion of energy costs leads to the emergence of a trade-off between growth rate and yield, as experimentally observed in many bacterial cells .

The allocation of cellular resources can strongly influence not only the rate of cell growth but also the resulting cell size [78]. To better investigate the connection between proteome allocation and cell volume, the original model by Giordano et al. [82] has been connected to a biophysical model of cell growth, explicitly describing cell volume increase as a function of cell’s internal pressure and mechanical properties. The resulting model will be used to investigate the mechanisms (control of osmotic pressure or wall mechanics) behind cell size control under different environmental constraints [84].

*Optimal allocation of resources in a bacterium.* We study by techniques of optimal control the optimal allocation between metabolism and gene expression during growth of bacteria, in collaboration with Inria IBIS and MCTAO project-teams. We developed different versions of the problem, and consider a new problem where the aim is to optimize the production of a product [68], [40], [50], (ANR project Maximic, PhD thesis of A. Yabo). We also study variations of the model, for example in the chemostat [57]. The precise mathematical analysis of the optimal behavior (turnpike property) is under investigation.



*A synthetic community of bacteria.* In the framework of IPL Cosy, we study the coexistence of two strains of bacteria *E. Coli* in a bioreactor. The strains have been modified synthetically to achieve some goals. The aim is to obtain a better productivity in the consortium than in a single strain, by control technics. The description of models is in revision for Plos Comp. Biol.

In collaboration with team VALSE (Lille), we also studied several problems of estimation and robust stabilization related to IPL Cosy, for two bacterial species in a bioreactor [53], [54].

*Control of a model of synthesis of a virulence factor.* In collaboration with J.-A. Sepulchre (UCA), we modeled the production of a virulence factor by a bacterium in a continuous stirred tank reactor. The production of this enzyme is genetically regulated, and degrades a polymeric external substrate into monomers [37]. We also studied the problem of periodic inputs for maximization of some yield [97].

*Hybrid control of genetic networks.* We designed control strategies based on the measurement and control of a unique gene within positive or negative loops of genetic networks, in order to stabilize the system around its unstable fixed point. The quantized nature of genetic measurements and the new synthetic control approaches available in biology encourage the use of piecewise constant control laws. A specific partitioning of the state space and the study of successive repulsive regions allow to show global convergence and global stability for the resulting system [18]. Several other control strategies are studied [47], [48], [46]. This is part of the PhD thesis of L. Chambon.

### 7.1.3. Biochemical and signaling models

**Participants:** Madalena Chaves, Eleni Firippi, Sofia Almeida, Marielle Péré, Luis Gomes Pereira, Jérémie Roux.

#### 7.1.3.1. Analysis and coupling of biological oscillators

*Modeling, analysis and coupling of the mammalian cell cycle and clock* A transcriptional model of the mammalian circadian clock was developed in [13] and its parameters calibrated against experimental data from F. Delaunay's lab. A cell cycle model was also previously developed by us [77]. The interactions between the two oscillators are investigated under uni- or bi-directional coupling schemes [44]. Numerical simulations replicate the oscillators' period-lock response and recover observed clock to cell cycle period ratios such as 1:1, 3:2 and 5:4 (as observed in experiments, F. Delaunay's lab). This work is in collaboration with F. Delaunay (ANR ICycle) and part of the PhD thesis of Sofia Almeida.

*Period-control in a coupled system of two genetic oscillators* In the context of ANR project ICycle, we consider two reduced models that mimic the dynamics of the cell cycle and clock oscillators and study the effect of each oscillator on the coupled system, from a synthetic biology perspective [56]. The first observation is that oscillator A is more likely to be the controller of the coupled system period when the dynamics of oscillator B becomes stable due to the coupling strength. Another interesting observation is that the coupled system exhibits oscillatory dynamics over an increased region of the parameter space. This work is part of the PhD thesis of Eleni Firippi (ANR ICycle).

#### 7.1.3.2. Modeling the apoptotic signaling pathway

*A detailed model of the death receptor layer* In a collaboration with J. Roux and within project Imodrez, the goal is to study the origins of cell-to-cell variability in response to anticancer drugs and provide a link between complex cell signatures and cell response phenotype. In a first approach, we constructed a detailed model to represent the death receptor-ligand binding and subsequent signaling cascade [11]. This model was used to study the effect of intrinsic and extrinsic noise sources, and suggested the need to expand a set of reactions on the model, to account for the observed cell heterogeneity (this was part of the PhD thesis of Luis Pereira).

*A basic model to explore the effect of a positive feedback loop* Analysis of the detailed apoptosis receptor model uncovered a set of reactions for which the introduction of a positive feedback loop from caspase 8 was able to significantly increase the range of variability in the model in response to extrinsic noise. To better understand this mechanism and the role of positive loop in cell response variability, we are constructing a reduced model representing only the basic components: death ligand and receptor, caspase 8 and two intermediate complexes. This is part of the work of the PhD student Marielle Péré.

## 7.2. Fields of application

### 7.2.1. Bioenergy

#### 7.2.1.1. Modelling microalgae production

**Participants:** Olivier Bernard, Antoine Sciandra, Walid Djema, Ignacio Lopez, David Demory, Ouassim Bara, Jean-Philippe Steyer.

##### *Experimental developments*

*Running experiments in controlled dynamical environments.* The experimental platform made of continuous photobioreactors driven by a set of automaton controlled by the ODIN software is a powerful and unique tool which gave rise to a quantity of very original experiments. Such platform improved knowledge of several biological processes such as lipid accumulation or cell cycle under light fluctuation, etc [69].

This experimental platform was used to control the long term stress applied to a population of microalgae [72]. This Darwinian selection procedure generated several new strains more resistant to oxidative stresses after several months in the so called selectiostats [58].

Experiments were run to understand the interactions in a simplified ecosystem between microalgae and cyanobacteria. The initial idea was to use a nitrogen fixing cyanobacteria providing nitrogen to the microalgae. It turns out that negative interactions appear in this ecosystem, first because of the mutual shadowing of these organisms, and second because of the production of allelopathic substances inhibiting the competitive organisms [79].

On top of this, we carried out outdoor pilot experiments with solar light. We tested the impact of various temperatures, resulting from different shadowing configurations on microalgal growth rate.

Experimental work was also carried out in collaboration with the Inalve startup with microalgal biofilm to determine the impact of light and dark sequences on cell growth and photoacclimation [26], [63]. The architecture of the biofilms was also observed for different species with confocal microscopic techniques [23].

These works have been carried out in collaboration with A. Talec and E. Pruvost (CNRS/Sorbonne Université -Oceanographic Laboratory of Villefranche-sur-Mer LOV).

*Metabolism of carbon storage and lipid production.* A metabolic model has been set up and validated for the microalgae *Isochrysis lutea*, on the basis of the DRUM framework , in order to simulate autotrophic, heterotrophic and mixotrophic growth, and to determine how to reduce substrate inhibition. The model was extended for other substrates such as glucose or glycerol. A simplified model was developed by I. Lopez to represent the dynamics of polar lipids, especially when faced to higher oxygen concentration. In particular, this model represents the microalgae growth under different conditions of temperature, light and oxygen.

*Modeling photosynthetic biofilms.* Several models have been developed to represent the growth of microalgae within a biofilm. A first structured physiological model, extending the one proposed in [95] uses mixture theory to represent the microalgae growth, based on the consideration of intracellular reserves triggering the processes of growth, respiration and excretion. We consider separately the intracellular storage carbon (lipids and carbohydrates) and the functional part of microalgae . Another approach accounts for the dynamics of the light harvesting systems when cells are submitted to rapid successions of light and dark phases [28], [71]. A simpler model was developed and used to identify the optimal working mode of a process based on photosynthetic biofilm growing on a conveyor belt [45]. The model was used to identify the worldwide potential of microalgal biofilms under different climates [26].

##### *Modeling microalgae production processes.*

A synthesis has been written on the different aspects for developing models of microalgae in the field of wastewater treatment [38]. The paper is completed by a position paper proposing guidelines for the development of models in biotechnology [31]. A model representing the dynamics of microalgae when growing in suboptimal conditions of light, nitrogen and phosphorus was developed. It consists in an extension of the Droop model accounting for the two quota of nitrogen and phosphorus [65]. This was the topic of the

internship of Luis Plaza Alvarez. The model also represents the pigment acclimation to various light intensities. We have studied in [75] the response of a Droop model forced by periodic light or temperature signals. We transformed the model into a planar periodic system generating a monotone dynamical system. Combined with results on periodic Kolmogorov equations, the global dynamics of the system can be described.

#### *Modeling thermal adaptation in microalgae.*

Experiments have been carried out in collaboration with A.-C. Baudoux (Biological Station of Roscoff) in order to study growth of various species of the microalgae genus *Micromonas* at different temperatures. After calibration of our models, we have shown that the pattern of temperature response is strongly related to the site where cells were isolated. We derived a relationship to extrapolate the growth response from isolation location. With this approach, we proved that the oceanwide diversity of *Micromonas* species is very similar to the oceanwide diversity of the phytoplankton [22]. We have used Adaptive Dynamics theory to understand how temperature drives evolution in microalgae. We could then predict the evolution of this biodiversity in a warming ocean and show that phytoplankton must be able to adapt within 1000 generation to avoid a drastic reduction in biodiversity [22].

*Modeling viral infection in microalgae.* In collaboration with A.-C. Baudoux (Biological Station of Roscoff) a model was developed to account for the infection of a *Micromonas* population, with population of susceptible, infected and also free viruses. The model turned out to accurately reproduce the infection experiments at various temperatures, and the reduction of virus production above a certain temperature [22]. The model was then extrapolated to the whole ocean to better understand how the warming will impact the mortality due to viruses.

### 7.2.1.2. Control and Optimization of microalgae production

#### *Optimization of the bioenergy production systems*

A model predictive control algorithm was run based on simple microalgae models coupled with physical models where culture depth influences thermal inertia. Optimal operation in continuous mode for outdoor cultivation was determined when allowing variable culture depth. Assuming known weather forecasts considerably improved the control efficiency [21].

#### *Control of microalgal biofilms.*

Determining the optimal operating conditions for a rotating algal biofilm process [63] is a difficult question. A 1D model was developed, and the gradient associated to the productivity at the process scale was computed. Then the conditions maximizing productivity were derived, playing on the conveyor belt velocity and geometry [71].

*Interactions between species.* We have proposed an optimal control strategy to select in minimal time the microalgal strain with the lowest pigment content [51]. The control takes benefit from photoinhibition to compute light stresses penalizing the strains with a higher pigment content and finally selecting microalgae with lower chlorophyll content. Another optimal control problem was considered for selecting a strain of interest within two species competing for the same substrate, when dynamics is represented by a Droop model [52], [73], [74]. In both cases, the optimal control derived from the Pontryagin maximum principle also exhibit a turnpike behaviour. This is a collaboration with team MCTAO.

Strategies to improve the temperature response have also been studied. We modelled the adaptive dynamics for a population submitted to a variable temperature [58]. This was used at the LOV to design experiments with periodic temperature stresses aiming at enhancing polyunsaturated long chain fatty acids content of *Tisochrysis lutea* [72].

### 7.2.1.3. Modelling mitochondrial inheritance patterns

Most eukaryotes inherit their mitochondria from only one of their parents. When there are different sexes, it is almost always the maternal mitochondria that are transmitted. Indeed, maternal uniparental inheritance has been reported for the brown alga *Ectocarpus* but we show in this study [33] that different strains of *Ectocarpus* can exhibit different patterns of inheritance: *Ectocarpus siliculosus* strains showed maternal uniparental inheritance, as expected, but crosses using different *Ectocarpus* species 7 strains exhibited either

paternal uniparental inheritance or an unusual pattern of transmission where progeny inherited either maternal or paternal mitochondria, but not both. A possible correlation between the pattern of mitochondrial inheritance and male gamete parthenogenesis was investigated. Moreover, in contrast to observations in the green lineage, we did not detect any change in the pattern of mitochondrial inheritance in mutant strains affected in life cycle progression. Finally, an analysis of field-isolated strains provided evidence of mitochondrial genome recombination in both *Ectocarpus* species.

## 7.2.2. Biological depollution

### 7.2.2.1. Control and optimization of bioprocesses for depollution

**Participants:** Olivier Bernard, Carlos Martinez Von Dossow, Jean-Luc Gouzé.

We consider artificial ecosystems including microalgae, cyanobacteria and bacteria in interaction. The objective is to more efficiently remove inorganic nitrogen and phosphorus from wastewater, while producing a microalgal biomass which can be used for biofuel or bioplastic production. Models have been developed including predators grazing the microalgae. Experiments with nitrogen fixing cyanobacteria were carried out, and simple models of the ecosystem were developed to assess the potential of such organisms to support the nitrogen need of microalgae [79].

### 7.2.2.2. Coupling microalgae to anaerobic digestion

**Participants:** Olivier Bernard, Antoine Sciandra, Jean-Philippe Steyer, Frédéric Grogard, Carlos Martinez Von Dossow.

The coupling between a microalgal pond and an anaerobic digester is a promising alternative for sustainable energy production and wastewater treatment by transforming carbon dioxide into methane using light energy. The ANR Phycover project is aiming at evaluating the potential of this process [96].

We have proposed several models to account for the biodiversity in the microalgal pond and for the interaction between the various species. These models were validated with data from the Saur company. More specifically, we have included in the microalgae model the impact of the strong turbidity, and derived a theory to better understand the photolimitation dynamics especially when accounting for the photo-inhibition in the illuminated periphery of the reactor [91]. Control strategies playing with the dilution rate, shadowing or modifying depth were then proposed [90].

Finally, a study of the possible sensors which would enhance the monitoring of these process was proposed [30], [29]

### 7.2.2.3. Life Cycle Assessment

**Participants:** Olivier Bernard, Jean-Philippe Steyer, Marjorie Alejandra Morales Arancibia.

*Environmental impact assessment.* To follow up the pioneering life cycle assessment (LCA) work of [87], we identified the obstacles and limitations which should receive specific research efforts to make microalgae production environmentally sustainable [93].

In the Purple Sun ANR-project, we studied a new paradigm to improve the energy balance by combining biofuel production with photovoltaic electricity. The LCA of a greenhouse with, at the same time, photovoltaic panels and low emissivity glasses was carried out. Depending on the period of the year, changing the species can both improve productivity and reduce environmental footprint [34].

We have also studied the environmental impact of protein production from microalgae in an algal biofilm process and compared it to other sources (fisheries, soy,...). This study confirms the interest of microalgae for reducing the environmental impact.

This work is the result of a collaboration with Arnaud Helias of INRA-LBE (Laboratory of Environmental Biotechnology, Narbonne).

## 7.2.3. Design of ecologically friendly plant production systems

### 7.2.3.1. Controlling plant arthropod pests

**Participants:** Frédéric Grogard, Ludovic Mailleret, Suzanne Touzeau, Yves Fotso Fotso.

*Optimization of introduction processes.* The question of how many and how frequently natural enemies should be introduced into crops to most efficiently fight a pest species is an important issue of integrated pest management. The topic of optimization of natural enemies introductions has been investigated for several years [89], and extends more generally to pulse perturbations in population dynamics.

A central theoretical result concerns the unveiling of the crucial influence of within-predator density dependent processes. To evaluate this theoretical prediction in a more realistic, stochastic and spatially explicit setting, a stochastic individual based model has been built in Python MESA, on the basis of a previous work in NetLogo. Extensive simulatory experiments were performed to assess the effects of density dependent processes as well as spatial structure and stochasticity on augmentative biological control performance and variability [88]. The modelling platform is interactive and can be accessed online at <http://popintro.sophia.inra.fr/>.

In a more general setting, we studied the impact on the introduction success of a population of the interplay of Allee effects, stochasticity in introduction sizes, and occurrence of catastrophes that temporarily wipe out the population. The mean first passage time (MFPT) for a population to reach a viable size was used as a measure of establishment success for the introduction processes [14].

*Characteristics of space and the behavior and population dynamics of biological control agents.* We studied the influence of the spatial structure and characteristics of the environment on the establishment and spread of biological control agents through computer simulations and laboratory experiments on parasitoids of the genus *Trichogramma*. This was the topic of Thibaut Morel Journal [94] and Marjorie Haond's PhD theses [85]. The last article associated with Thibaut Morel Journal's Thesis appeared this year [35]. We explored the influence of different characteristics of the structural connectivity of an invaded habitat on the invading population. We demonstrated how spread was hindered by habitat clusters and accelerated by the presence of hubs. These results highlight the importance of considering the structure of the invaded area to predict the outcome of invasions.

In a different study stemming from Marjorie Haond Thesis, we showed how habitat richness [86] as represented by its local carrying capacity can positively influence the spreading speed of an expanding population. This work has been published as a preprint recommended by *Peer Community in Ecology* and is on the verge to be submitted to a regular scientific journal. This work has been performed in collaboration with Elodie Vercken (ISA) and Lionel Roques (BioSP, Avignon).

In a different context, we studied how predatory mite population development can be enhanced by the provision of artificial habitats. One paper focused on the influence of different artificial materials on the oviposition and survival of predatory mites appeared this year [16]. This topic was also at the core of the Master 2 internship of Lucas Etienne [81] during which he studied the combined influences of artificial habitats and additional food on the development of a predatory mite and on the control of a phytophagous mite. An article reporting on this study is currently under preparation.

*Modelling and control of coffee berry borers.* We developed a model describing the coffee berry borer dynamics based on the insect life-cycle and the berry availability during a single cropping season. A control was introduced, based on a biopesticide (entomopathogenic fungus such as *Beauveria bassiana*) that is sprayed and persist on the berries. An optimal control problem was solved (see Section 7.1.1.2 ). The aim was to maximise the yield at the end of the cropping season, while minimising the borer population for the next cropping season and the control costs. Depending on the initial pest infestation, the optimal solution structure varied [60], [62]. This research pertains to Yves Fotso Fotso's PhD thesis, who visited BIOCORE during 5 months in 2019 through the EPITAG associate team.

#### 7.2.3.2. Controlling plant pathogens

**Participants:** Frédéric Grogard, Ludovic Mailleret, Suzanne Touzeau, Clotilde Djuikem.

*Sustainable management of plant resistance.* We studied other plant protection methods dedicated to fight plant pathogens. One such method is the introduction of plant strains that are resistant to one pathogen. This often leads to the appearance of virulent pathogenic strains that are capable of infecting the resistant plants.



We have developed a (spatio-)temporal epidemiological model of the phoma stem canker of oilseed rape, to test and assess the durability of deployment strategies of various cultivars. Based on this model, we aim at developing a user-friendly, upgradeable and efficient simulation tool designed for researchers as well as non academic partners from technical institutes and agriculture cooperatives. We hence applied and obtained the SiDRes AMDT, which will start in 2020.

A stochastic model was developed to help determine the efficiency of pyramiding qualitative resistance and quantitative resistance narrowing population bottlenecks exerted on plant viruses, the latter aiming at slowing down virus adaptation to the qualitative resistance. It showed the efficiency of pyramiding when the fitness cost of RB virus variants in susceptible plants is intermediate [36]. This study provides a framework to select plants with appropriate virus-evolution-related traits to avoid or delay resistance breakdown. This was done in collaboration with Frédéric Fabre (INRA Bordeaux) and Benoît Moury (INRA Avignon).

*Taking advantage of plant diversity and immunity to minimize disease prevalence.* An epidemiological model of gene-for-gene interaction considering a mechanism related to the specific defense response of plants, the systemic acquired resistance (SAR) was developed. SAR provides a sort of immunity to virulent pathogens for resistant plants having undergone an infection attempt by an avirulent pathogen. This model showed that there exists an optimal host mixture that ensures the lowest plant disease prevalence, so as to optimize the crop yield. It is especially efficient for pathogens with a low or intermediate basic reproduction rate and hosts with a high SAR efficiency [61]. This was done in collaboration with Pauline Clin and Frédéric Hamelin (Agrocampus Ouest).

#### 7.2.3.3. Plant-nematode interactions

**Participants:** Valentina Baldazzi, Frédéric Grogard, Ludovic Mailleret, Suzanne Touzeau, Israël Tankam Chedjou, Samuel Nilusmas.

Plant-parasitic nematodes are small little-mobile worms that feed and reproduce on plant roots, generating considerable losses in numerous crops all over the world. Most eco-friendly plant protection strategies are based on the use of resistant crops, but agricultural practices also contribute to nematode control.

Based on an interaction model between plantain roots and *Radopholus similis*, we solved an optimisation problem (see Section 7.1.1.2). It aimed at determining the duration between cropping seasons (fallow period) that maximises the farmer's cumulated yield, which is affected by the nematode population, while minimising the costs of nematode control and nursery-bought pest-free suckers, on a fixed time horizon that lasts several cropping seasons. Fallow periods reduce the nematode population in the soil, as these pests need roots to feed on and reproduce. For a relatively long time horizon, deploying one season less than the maximum possible number of cropping seasons resulted in a better multi-seasonal profit. The optimal solution consisted in applying long fallows at the beginning, to drastically reduce the nematode population. The profit was lower for more regular fallows, but the final soil infestation was also lower [67]. This research pertains to Israël Tankam Chedjou's PhD thesis, who visited BIOCORE during 5 months in 2019 through the EPITAG associate team.

We also studied resistance-based root-knot nematode control. As virulent nematodes exhibit a reduced fitness on susceptible crops, alternating resistant and susceptible plants could help increase the efficiency and durability of such control methods. Optimal crop rotations (see Section 7.1.1.2) were characterised by low ratios of resistant plants and were robust to parameter uncertainty. Rotations provided significant gains over resistant-only strategies, especially for intermediate fitness costs and severe epidemic contexts. Switching from the current general deployment of resistant crops to custom rotation strategies could not only maintain or increase crop yield, but also preserve the few and valuable R-genes available. This research pertains to Samuel Nilusmas' PhD thesis. This work has been published as a pre-print [76] and is currently under review. It has also been presented at several national and international conferences this year [66], [42].

#### 7.2.3.4. Optimality/games in population dynamics

**Participants:** Frédéric Grogard, Ludovic Mailleret, Pierre Bernhard.



*Optimal resource allocation.* Mycelium growth and sporulation are considered for phytopathogenic fungi. For biotrophic fungi, a flow of resource is uptaken by the fungus without killing its host; in that case, life history traits (latency-sporulation strategy) have been computed based on a simple model considering a single spore initiating the mycelium, several spores in competition and applying optimal resource allocation, and several spores in competition through a dynamic game through the analytico-numerical solution of the Hamilton-Jacobi-Bellman-Isaacs equation [39]. This work is done with Fabien Halkett of INRA Nancy.

*Optimal foraging and residence times variations.* In this work, we built on our re-analysis of the Marginal Value Theorem (MVT) [4] to study the effect on the optimal foraging strategy of habitat conversion, whereby patches are converted from one existing type to another, hence changing the frequency of each type in the environment. We studied how realized fitness and the average rate of movement should respond to changes in the frequency distribution of patch-types, and how they should covary. We found that the initial pattern of patch-exploitation in a habitat can help predict the qualitative responses of fitness and movement rate following habitat conversion. We conclude that taking into account behavioral responses may help better understand the ecological consequences of habitat conversion [17].

## BIOVISION Project-Team

# 7. New Results

## 7.1. High tech vision aid-systems for low-vision patients

### 7.1.1. Multilayered Analysis of Newspaper Structure and Design

**Participants:** Hui-Yin Wu, Pierre Kornprobst.

The understanding of newspaper document structure can help in the adaptation of text and visual content for different devices and media [53], as well as, in the context of low vision, to enhance accessibility by combining magnification and text-to-speech aids. However, automated segmentation of complex document structures like newspapers remains an ongoing challenge due its dense layout with numerous visual and textual design elements [38], [44].

To address this challenge, we propose a multi-layered analysis of structure and design, presented in [27]. Taking images of newspaper front pages as input, our approach uses a combination of computer vision techniques to segment newspapers with complex layouts into meaningful blocks of varying degrees of granularity, and convolutional neural network (CNN) to classify each block. The final output presents a visualization of the various design elements present in the newspaper such as in Figure 2 . Compared to previous approaches, our method introduces a much larger set of design-related labels (23 labels against less than 10 before) resulting in a very fine description of the pages, with high accuracy (83%), as shown in Figure 3

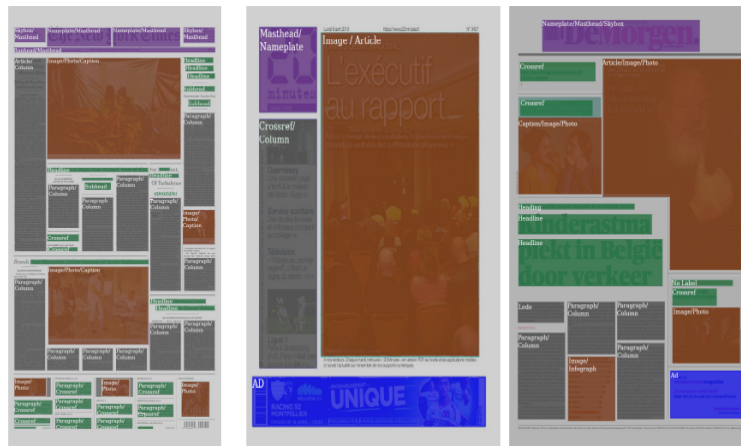


Figure 2. Visualization of the classification results on three different newspapers in our test set. Colors indicate primary categories as masthead elements (purple), text column (gray), ads (blue), images (brown) and minor text elements (green). Original images copyright of (from left to right) New York Times, 20 Minutes, and DeMorgan, courtesy of Newseum.

This work is presented in [27].

### 7.1.2. Towards accessible news reading design in virtual reality for low vision

**Participants:** Hui-Yin Wu, Aurélie Calabrèse, Pierre Kornprobst.

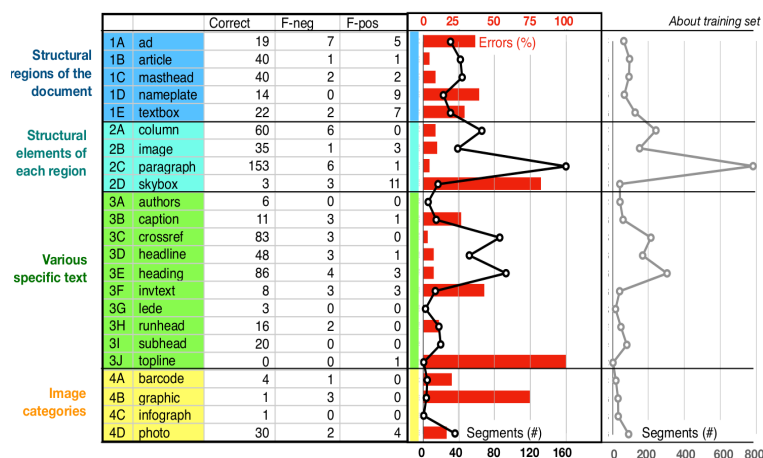


Figure 3. Classification result per categories. Results are presented in the table, showing the number of design elements that are correctly classified, false-negative (i.e. missing label), and false-positive (i.e. wrongly assigned label). Then a red chart shows the errors together with the number of segments (black line) used for the test dataset. To the right, the grey curve indicates the number of segments which were available in the training set.

Low-vision conditions resulting in partial loss of the visual field strongly affect patients' daily tasks and routines, and none more prominently than the ability to access text. Though vision aids such as magnifiers, digital screens, and text-to-speech devices can improve overall accessibility to text, news media, which is non-linear and has complex and volatile formatting, bars low-vision patients from easy access to essential news content [54].

Our aim is to position virtual reality as the next step towards accessible and enjoyable news reading for the low vision. Our ongoing work, which we present in [26], consists of an extensive review into existing research on low-vision reading technologies and accessibility for modern news media. From previous research and studies, we then conduct an analysis into the advantages of virtual reality for low-vision reading and propose comprehensive guidelines for visual accessibility design in virtual reality, with a focus on reading. This is coupled with a hands-on study of eight reading applications in virtual reality to evaluate how accessibility design is currently implemented in existing products. Finally, we present a framework that integrates the design principles resulting from our analysis and study, and implement a proof-of-concept for this framework using browser-based graphics (Figure 4 and 5) to demonstrate the feasibility of our proposal with modern virtual reality technology.

This work is presented in [26].

## 7.2. Human vision understanding through joint experimental and modeling studies, for normal and dystrophic vision

### 7.2.1. From micro- to macroscopic description of the retina

#### 7.2.1.1. Retinal Waves

**Participants:** Dora Matzakos-Karvouniari [Laboratoire Jean-Alexandre Dieudonné, (LJAD), Nice, France], Bruno Cessac, Lionel Gil [Institut de Physique de Nice (InPhyNi), France].

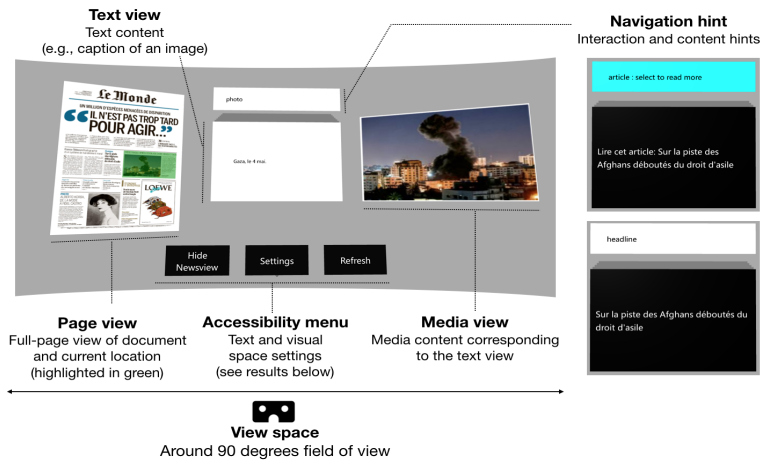


Figure 4. Application prototype: The global overview of the newspaper page is shown side-by-side with the enlarged text and images of the highlighted region. Navigation hints above the card show what type of content is displayed (e.g. photo, heading, paragraph) and whether the card can be selected (i.e. highlighted in light blue) to reveal further content. Text and images of the newspaper are purely for demonstrating a proof-of-concept. Excerpted from 7 May 2019 issue of ©Le Monde.

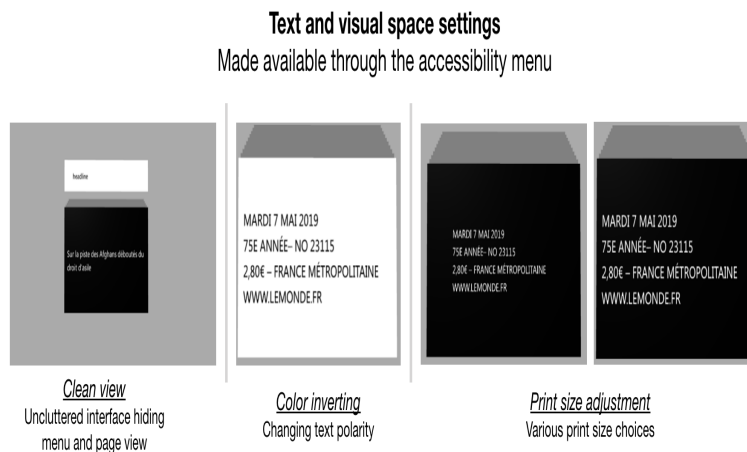


Figure 5. The accessibility menu provides a number of functions including (1) showing/hiding the page and menu view to personalize the view space, (2) invert foreground and background color only for text content, and (3) change the print size. Text on the cards excerpted from 7 May 2019 issue of ©Le Monde

Retinal waves are bursts of activity occurring spontaneously in the developing retina of vertebrate species, contributing to the shaping of the visual system organization: retina circuitry shaping, retinotopy, eye segregation [63], [47], [58], [48]. They stop a few weeks after birth. Wave activity begins in the early development, long before the retina is responsive to light. It was recently found that they can be reinitiated pharmacologically in the adult mammalian retina [46]. This could have deep consequences on therapy for several degenerative retinal diseases. The mechanism of their generation, in developing, or adult retinas, remains however incompletely understood [64].

We have proposed a model for stage II retinal waves - induced by bursting Starburst Amacrine Cells (SACs) coupled by acetylcholine - with two objectives: (i) being sufficiently close to biophysics to explain and propose experiments and (ii) affording a mathematical analysis [14], [34]. From a bifurcations analysis we have highlighted several relevant biophysical parameters controlling waves generation, mainly regulating potassium and calcium dynamics. We thus explain how SACs in different species exhibit a large variability in their bursting periods with a common mechanism.

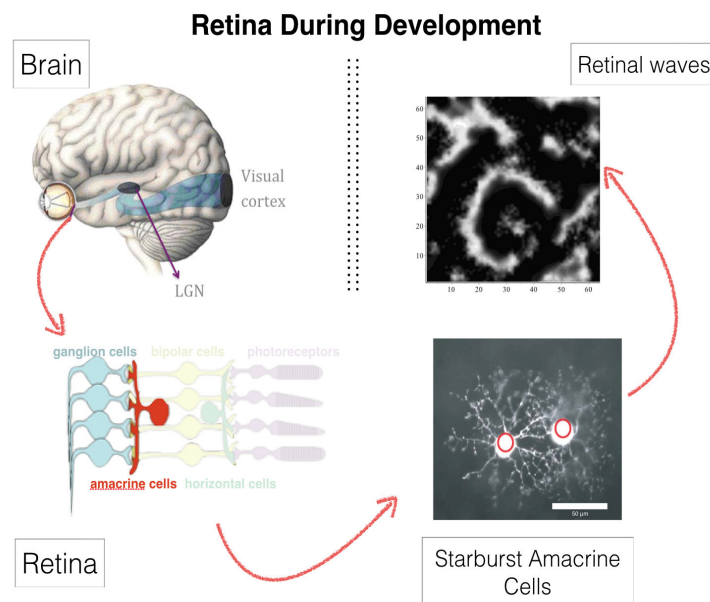


Figure 6. Top left. View of the human visual system. Bottom left. Right after birth the retina is not fully developed (shadowed parts). The retinal waves (top right) contributes to this development. They are mediated by specific cells (Starburst Amacrine Cells in stage II, bottom right).

Based on this biophysical model we have analysed here the dynamics of retinal waves and their statistics. We show that, despite the acetylcholine coupling intensity has been experimentally observed to change during development, SACs retinal waves can nevertheless stay in a regime with power law distributions, reminiscent of a critical regime. Thus, this regime occurs on a range of coupling parameters instead of a single point as in usual phase transitions. We explain this phenomenon thanks to a coherence-resonance mechanism, where noise is responsible for the broadening of the critical coupling strength range. This work has been presented in [14], [16], [25]

#### 7.2.1.2. Anticipation in the retina and the visual cortex VI

**Participants:** Bruno Cessac, Frédéric Chavane [Institut de Neurosciences de la Timone (CNRS and Aix-Marseille Université, France)], Alain Destexhe [Institute de Neurosciences Paris-Saclay (UNIC)], Sandrine

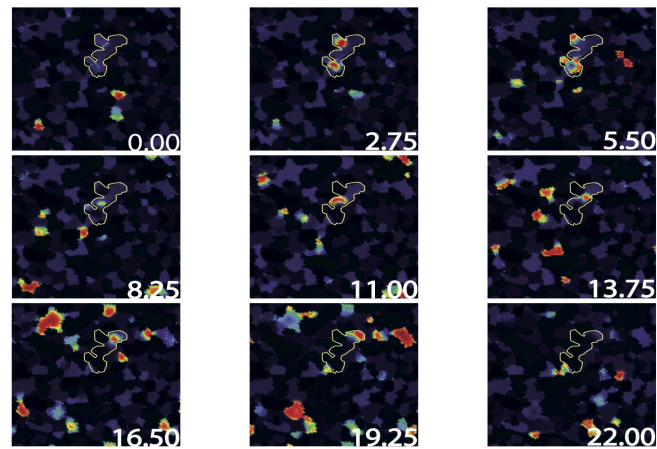


Figure 7. Example of the two dimensional time evolution of the calcium concentration  $C$ . Dark regions correspond to low calcium concentration while red corresponds to high concentration (wave). The time (in s) is displayed in the bottom right corner. The same thin white line in the center of each image, delimits a closed domain where wave propagates almost periodically. Hence, after the sequence shown above which correspond to a single period, a new one takes place a time later with a new wave following almost the same trajectory. The domain delimited by the white line is circled with high sAHP regions and therefore slowly evolves with time. A numerical movie is available on the website : <https://www.youtube.com/watch?v=shMR3NMCBDE>

Chemla [Institut de Neurosciences de la Timone (CNRS and Aix-Marseille Université, France)], Selma Souihel, Matteo Di Volo [Institute de Neuroscience Paris-Saclay (UNIC)].

This work has been done in the context of the ANR Trajectory and Selma Souihel Thesis [11].

Vision is initiated in the retina, where light is converted into electrical signals by photoreceptors, sent to bipolar cells then ganglion cells, generating spike trains. Visual information is then transmitted to the thalamus via the optic nerve which in turn transmits it to the visual cortex. The retinal processing alone takes time, up to 150 ms, not to mention the time lags introduced by synaptic transmissions between the three processing units. This shows that the existence of compensatory mechanisms to reduce processing delays is absolutely essential. These compensatory mechanisms are known as anticipation. Anticipation first occurs at the level of the retina and is further carried out by the primary visual cortex. In its first occurrence, anticipation is either characterized by a shift in the the peak response, or a short range wave of activation. In the second case, it is characterized by a wider range wave of activation.

The first contribution of this work is the development of a generalized 2D model of the retina, mimicking three types of ganglion cells : Fast OFF cells with gain control, direction selective cells with gap junction connectivity, and differential motion cells connected through an upstream amacrine circuit, able of anticipating different kinds of moving stimuli. The second contribution is to use our retina model as an input to a mean field cortical model to reproduce motion anticipation as observed in voltage sensitive dye imaging recordings. Throughout our work, we will study the effect of non linear phenomena involved in anticipation, as well as connectivity, both at the level of the retina and the primary visual cortex. The integrated retino-cortical model allowed us to study the effects of anticipation on two-dimensional stimuli, and to highlight the collaborative aspect of anticipation mechanisms in the retina and the cortex.

This work has been presented in [17], [22], [20], [34], [21], [11]



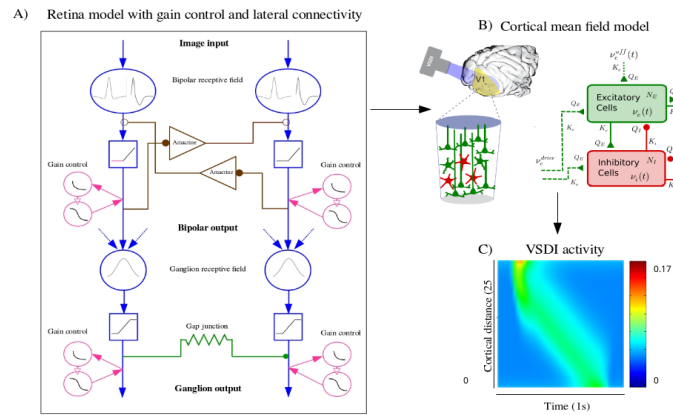


Figure 8. Schematic of our retino cortical model for anticipation. Left. Structure of the retinal model with 3 pathways: Blue: Gain control. Green: Gap junctions laterally connecting Ganglion Cells. Brown. Amacrine cells lateral connectivity. Right top. Cortical model (from Destexhe-Boustani 2009). Bottom. Simulation of VSDI activity in response to a moving bar.

### 7.2.1.3. Dynamical synapse in the retina

**Participants:** Bruno Cessac, Simone Ebert, Olivier Marre [Institut de la Vision (IdV), Paris, France], Romain Veltz [MathNeuro].

A very sophisticated example of the computations within the retina is observed when the visual system is exposed to a periodic stimulus, such as a regular series of flashes. If the retina would simply respond proportionally to the stimulus input, one might expect that ganglion cells would become entrained into aperiodic activity, responding to each flash. When the stimulus sequence ends, the activity would end as well. However, ganglion cells can exhibit various different kinds of response patterns to this form of stimulation shown in Figure 3. At the beginning of the stimulus, cells typically respond to the first flash of this new stimulus with a peak of activity, but then very rapidly decay in the amplitude of their response to the following flashes. Most remarkably, when the flash sequence ends ganglion cells do not just stop to respond, but in fact may generate a pulse of activity signalling the missing stimulus. This property of indicating a deviation from an expected pattern has been termed the Omitted Stimulus Response (OSR) (Schwartz, Harris, Shrom, Berry, 2007). The aim of this study was to implement and compare the two existing models of Omitted Stimulus Response in the retina, as well as exploring potential mechanisms that may be involved in generating it. Especially synaptic mechanisms may provide an explanation here, but the integration of such a mechanism into an OSR model has not been explored yet. A potential synaptic property that provides an interesting candidate to test here would be short-term plasticity (STP), which modulates synaptic efficacy depending on the previous activity in a short time interval (Blitz, Foster, Regehr, 2004). STP thus modulates signal transmission and a consecutive spike pattern and has been found to take place within the retina (Dunn, Rieke, 2008). Examining the models' underlying mechanisms, advantages and disadvantages as well as similarities and differences will provide a good foundation to modify existing models by adding potential mechanisms and exploring their effect on a ganglion cell response to a periodic stimulus. Ultimately, this may help shedding light on cellular properties in a neuronal circuit as of as few as 3 cells can contribute to already interpreting information from the environment.

This work has been presented in [32]. It has led to experiments done in the Institut de la Vision by S. Ebert (internship Biovision) and O. Marre (Institut de la Vision (IdV), Paris, France) in November 2019.

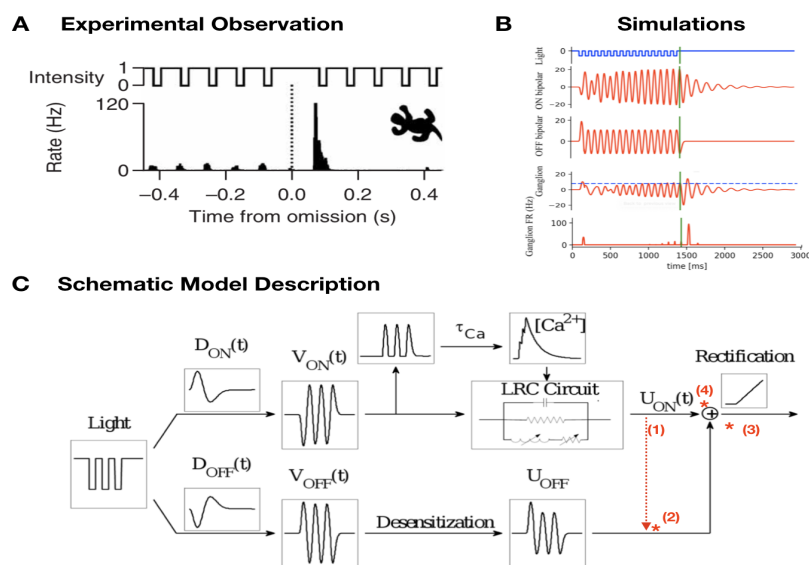


Figure 9. A. Experimentally observed Omitted Stimulus Response (OSR) to a periodic flash sequence. B. Simulations performed with an existing Model from Gao et al., 2009. C. Schematic description of the used 'Calcium-tuned Oscillator' Model from Gao et al., 2009. It is based on a feedforward circuit consisting of two different pathways with different intrinsic processing steps. Both pathways are combined to represent the synaptic input ganglion cells, who's activity with generate an Omitted Stimulus Response. Planned modifications planned are marked in red. (1) a presynaptic connection before summation of both pathways. (2),(3),(4) are synapses where short term synaptic plasticity could occur.

## 7.2.2. Numerical modelling of the retina in normal and pathological conditions

### 7.2.2.1. Probing retinal function with a multi-layered simulator

**Participants:** Bruno Cessac, Gerrit Hilgen [Institute of Neuroscience (ION), Newcastle, UK], Evgenia Kartsaki, Evelyne Sernagor [Institute of Neuroscience (ION), Newcastle, UK].

Our brain can recreate images from interpreting a stream of information emitted by one million parallel channels in the retina. This ability is partly due to the astonishing functional and anatomical diversity of the retinal ganglion cells (RGCs), each interpreting a different feature of the visual scene. How precisely this complexity is encoded in the spike trains produced by the population of RGCs is, however, largely unknown. Adding to the complexity, RGCs “speak” to each other during complex tasks (especially motion handling), via amacrine cells (ACs - lateral connectivity). To decipher their role, we study an experimental setting where neurons co-express the genes *Grik4* or *Scnn1a* and excitatory or inhibitory DREADDs (Designer Receptors Exclusively Activated by Designer Drugs), activated by the designer drug CNO. Switching on or off RGCs and/or ACs cells may not only impact the RGCs individual response but also their concerted activity to different stimuli, thus allowing us to understand how they contribute to the encoding of complex visual scenes. However, it is difficult to distinguish on pure experimental grounds the effect of CNO when both cell types express DREADDs, as these cells “antagonise” each other. Contrarily, numerical simulation can afford it. Here, we propose a novel simulation platform that can reflect normal and impaired retinal function (from single-cell to large-scale level). It is able to handle different visual processing circuits and allows us to visualise responses to visual scenes (movies). In addition, the platform allows simulation of retinal responses when DREADD-expressing cell subclasses are either silenced or excited with CNO. To demonstrate how our simulator works, we deploy a circuit that handles motion on a large-scale level and study how the retina responds to visual scenes by visualising retinal processing at each level. The simulator also provides a tunable parameter to control the CNO effect (excitation or inhibition). Consequently, it facilitates the disentanglement of the effect of CNO on ACs and RGCs. Nevertheless, simulations and experiments are widely complementary. Experiments are necessary to constrain the numerical model and check its validity (especially, its predictions), while the computational approach affords to explore aspects that cannot be easily achieved experimentally.

This work has been presented in [24], [19], [33]

### 7.2.2.2. Simulating the cortical activity evoked by artificial retinal implants

**Participants:** Teva Andréoletti, Bruno Cessac, Frédéric Chavane [Institut de Neurosciences de la Timone (CNRS and Aix-Marseille Université, France)], Sébastien Roux [Institut de Neurosciences de la Timone (CNRS and Aix-Marseille Université, France)].

Recent advances in neuroscience and microelectronics opens up the possibility of partially restoring vision to blind patients using retinal prostheses. These are devices capturing the light of a visual scene and converting it to electric impulses sent by a matrix of electrodes chirurgically fixed on the retina. The stimulation of an electrode elicits an activation in the visual cortex that evokes a percept similar to a light spot called phosphene. The joint stimulation of electrodes allows to reproduce simple shapes (letters, objects, stairs) and to restore a low resolution vision to blind people (see Fig 1). This domain of research is however at an early stage compared to cochlear implants. Especially, the way an electric stimulation activates the visual cortex is still poorly understood. The group of F. Chavane (NeOpTo team at INT Marseille) has used mesoscopic recordings of cortical activity (optical imaging) to better understand the activity evoked by stimulation of the retina with implanted multi electrodes arrays (Roux et al 2016 eLife). Their results show that local stimulation of the retina evoked a cortical activity that is up to 10 times larger than what is expected based on the activity evoked by visual stimuli. This result is in line with known poor resolutions of percepts evoked by stimulation of artificial retinas implanted in blind patients. This observed spread of evoked cortical activity is now better understood. An important effect, evidenced by Roux et al (2017) <https://elifesciences.org/articles/12687> is the asymmetrical spread of electric activity induced by the direct activation of retinal cells axons away from their somata.

This effect can be modelled at the level of a single electrode with a significant match to experimental measurement. Retinal prostheses integrate hundreds of electrodes and this model can be used to anticipate the simultaneous activation of several electrodes reproducing the shape of an object (Fig 1). This figure has been produced by a retina simulator, called Macular, developed by the Biovision team at Inria, and aiming at reproducing the retina response to stimulation in normal (stimulation by light) and pathological conditions (electric stimulation by prostheses) <https://team.inria.fr/biovision/macular-software/>. In a previous work <https://hal.inria.fr/hal-02292831> [28], [29] we have been able to numerically model the effect of the static joint stimulation of electrodes in retina prostheses on the primary visual cortex (V1) and to compare it to normal vision.

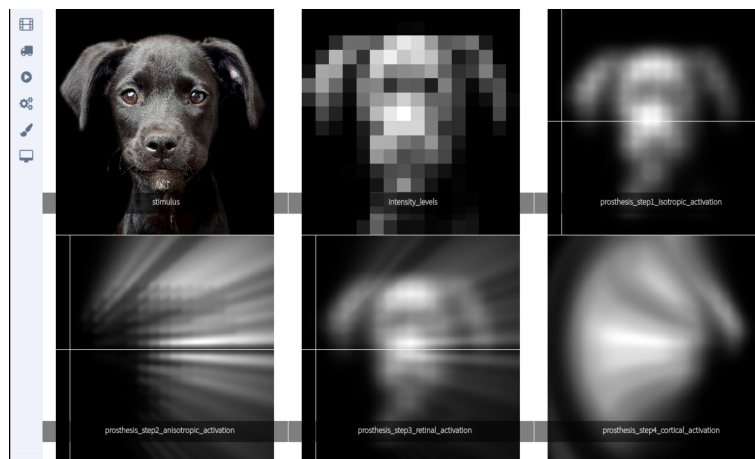


*Figure 10. Simulation of the retinal and cortical response to a prosthesis simulation. An image (up-left) is digitalized into small squares (up-left). Each square corresponds to the degree of activation of a corresponding electrode in retinal implant (up-right). The electric stimulation activates neurones en passant of retinal cells leading to non linear diffusion (left bottom) and an effective stimulation pattern (down-middle) which is blurred in comparison to the expected stimulation pattern (up-right). The induced cortical representation is shown in the bottom-right figure.*

This work has been presented in [28], [29]

## 7.3. Neuronal modelling

### 7.3.1. Linear response in neuronal networks: from neurons dynamics to collective responses

**Participant:** Bruno Cessac.

We have reviewed two examples where the linear response of a neuronal network submitted to an external stimulus can be derived explicitly, including network parameters dependence. This is done in a statistical physics-like approach where one associates to the spontaneous dynamics of the model a natural notion of Gibbs distribution inherited from ergodic theory or stochastic processes. These two examples are the Amari-Wilson-Cowan mode and a conductance based Integrate and Fire model

This work has been published in [13], [31], [18].

### 7.3.2. *On the role of Nav1.7 sodium channels in chronic pain: an experimental and computational study*

**Participants:** Lyle Armstrong [Institute of Neuroscience (ION), Newcastle, UK], Alberto Capurro [Institute of Neuroscience (ION), Newcastle, UK], Bruno Cessac, Jack Thornton [Institute of Neuroscience (ION), Newcastle, UK], Evelyne Sernagor [Institute of Neuroscience (ION), Newcastle, UK].

Chronic pain is a global healthcare problem with a huge societal impact. Its management remains generally unsatisfactory, with no single treatment clinically approved in most cases. In this study we use an in vitro model of erythromelalgia consisting of dorsal root ganglion neurons derived from human induced pluripotent stem cells obtained from a patient (carrying the mutation F1449V) and a control subject. We combine neurophysiology and computational modelling to focus on the Nav1.7 voltage gated sodium channel, which acts as an amplifier of the receptor potential in nociceptive neurons and plays a critical role in erythromelalgia due to gain of function mutations causing the channel to open with smaller depolarisations. Using extracellular recordings, we found that the scorpion toxin OD1 (a Nav1.7 channel opener) increases dorsal root ganglion cell excitability in cultures obtained from the control donor, evidenced by an increase in spontaneous discharges, firing rate and spike amplitude. In addition, we confirmed previous reports of voltage clamp experiments concerning an increase in spontaneous discharge in the patient cell cultures and the analgesic effects of the Nav1.7 blocker PF-05089771. Our findings are explained with a conductance-based model of the dorsal root ganglion neuron, exploring its behaviour for different values of half activation voltage and inactivation removal rate of the Nav1.7 current. Erythromelalgia was simulated through a decrease of the Nav1.7 half activation voltage, turning previously subthreshold stimuli to pain-inducing, and successfully counteracted with the channel blocker. The painful effects of OD1 were simulated through a quicker removal of Nav1.7 inactivation that reproduced the effects of the toxin not only on the spike frequency but also on its amplitude. This work has been submitted to J. Neuroscience. [30].

### 7.3.3. *Ghost attractors in spontaneous brain activity: wandering in a repertoire of functionally relevant BOLD phaselocking solutions*

**Participants:** Joana Cabral [Department of Psychiatry, Medical Sciences Division, University of Oxford, UK], Bruno Cessac, Gustavo Deco [Catalan Institute for Research and Advance Studies (ICREA), Spain], Morten L. Kringelbach [University of Oxford, UK], Jakube Vohryzek [Center for Music in the Brain, Department of Clinical Medicine, Aarhus University, Denmark].

Functionally relevant network patterns form transiently in brain activity during rest, where a given subset of brain areas exhibits temporally synchronized BOLD signals. To adequately assess the biophysical mechanisms governing intrinsic brain activity, a detailed characterization of the dynamical features of functional networks is needed from the experimental side to inform theoretical models. In this work, we use an open-source fMRI dataset from 100 unrelated participants from the Human Connectome Project and analyse whole-brain activity using Leading Eigenvector Dynamics Analysis, which focuses on the detection of recurrent phase-locking patterns in the BOLD signal. Borrowing tools from dynamical systems theory, we characterise spontaneous brain activity in the form of trajectories within a low-dimensional phase space. Decomposing the phase space into Voronoi-like cells using k-means clustering algorithm, we demonstrate that the cluster centroids (representing recurrent BOLD phase-locking patterns) closely overlap with previously identified resting-state networks. We further demonstrate that the metric associated with the phase-locking patterns shows moderate reliability across recordings indicating potential existence of subject specific dynamical landscapes. Our results point to the hypothesis that functional brain networks behave as ghost attractor states in a low-dimensional phase space, providing insights into the evolutionary rules governing brain activity in the spontaneous state and reinforcing the importance of addressing brain function within the framework of dynamical systems theory. This work has been submitted to Frontiers in Systems Neuroscience.

## CAMIN Project-Team

## 6. New Results

### 6.1. Selectivity of implanted neural electrical stimulation

**Participants:** Lucie William, David Guiraud, Charles Fattal, Christine Azevedo, Arthur Haiarrassary.

In the context of using a multi-contact cuff electrode positioned around a trunk nerve to activate selectively the fascicles leading to selective movements, a pre-clinical study was performed on the sciatic nerve of four rabbits (Lab. Chirurgie Experimentale, Institut de Biologie, University of Montpellier). The purpose was to compare and classify six different currents configuration (current ratios) (Fig.8 ) with a 12- contact cuff electrode using selectivity, robustness (i.e. ability to maintain selectivity within a range of current amplitudes) and efficiency (i.e. electrical consumption of the considered multipolar configuration *versus* the electrical consumption of the reference whole-ring configuration) indexes.

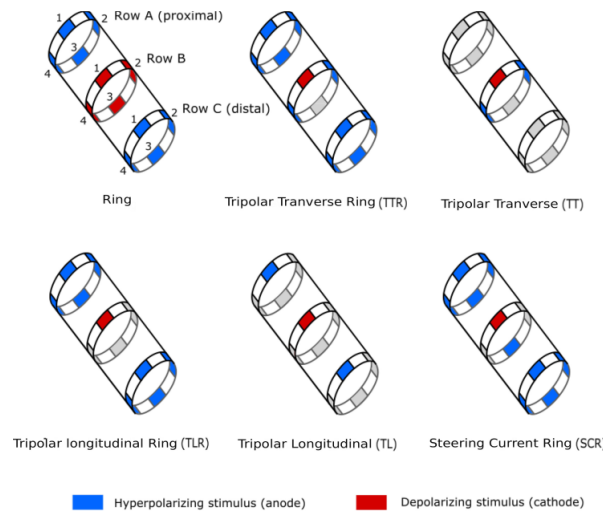


Figure 8. Six different configurations of the 12-contact electrode were tested: Ring, Tripolar Transverse Ring (TTR), Tripolar Transverse (TT), Tripolar Longitudinal Ring (TLR), Tripolar Longitudinal (TL), Steering Current Ring (SCR)

Results indicated that the optimal configuration depends on the weights applied to selectivity robustness and efficiency criteria. Tripolar transverse is the most robust configuration and the less efficient, whereas tripolar longitudinal ring is efficient but not robust. New configurations issued from a previous theoretical study we carried out such as steering current ring appears as good compromise between the 3 criteria [18].

The PhD of Lucie William (started in October 2019) will be the continuation of this work in the context of neural electrical stimulation of complete quadriplegic human participants (AGILIS project).

### 6.2. Selective Neural Electrical Stimulation to restores Hand and Forearm Movements in Individuals with Complete Tetraplegia

**Participants:** David Guiraud, Charles Fattal, Christine Azevedo, Mélissa Dali, Jacques Teissier [Beau Soleil clinic, Montpellier], Anthony Géllys [Propara Rehab. Center, Montpellier].



Selective neural electrical stimulation of radial and median nerves enables the activation of functional movements in the paralyzed hand of individuals with tetraplegia. In eight participants (Clinique Beau Soleil and Propara Rehabilitation Center, Montpellier) with complete tetraplegia, during a programmed surgery and under complete anesthesia, we demonstrated that selective stimulation based on multicontact cuff electrodes and optimized current spreading over the active contacts provided isolated, compound, functional and strong movements. Several configurations were needed to target different areas within the nerve to obtain all the envisioned movements. We further confirmed that the upper limb nerves have muscle specific fascicles, which makes possible to activate isolated movements. The future goal is to provide patients with functional restoration of object grasping and releasing with a minimally invasive solution: only two cuff electrodes above the elbow. This will be the objective of AGILIS project supported by EIT Health.

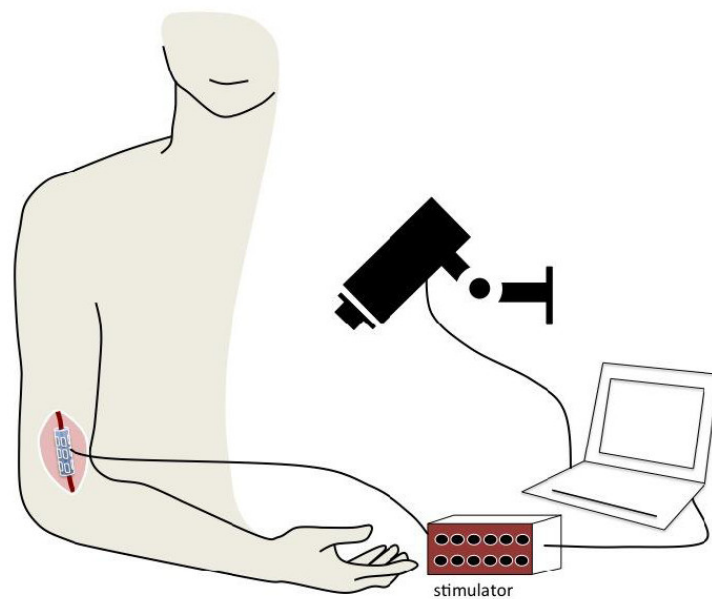


Figure 9. Neural electrical stimulation of radial or median nerve using a multi-contact cuff electrode allows to elicit different individual or grouped muscle contractions inducing different fingers and wrist movements.

### 6.3. Assisted Grasping in Individuals with Tetraplegia: Improving Control through Residual Muscle Contraction and Movement

**Participants:** Lucas Fonseca [UnB, Brazil], David Guiraud, Charles Fattal, Christine Azevedo, Arthur Hiarrassary, Camilo Silva, Anthony Gélys [Propara Rehab. Center, Montpellier].

Individuals who sustained a spinal cord injury often lose important motor skills, and cannot perform basic daily living activities. Several assistive technologies, including robotic assistance and functional electrical stimulation, have been developed to restore lost functions. However, designing reliable interfaces to control assistive devices for individuals with C4–C8 complete tetraplegia remains challenging. Although with limited grasping ability, they can often control upper arm movements via residual muscle contraction. We have explored the feasibility of drawing upon these residual functions to pilot two devices, a robotic hand and an electrical stimulator. We studied two modalities, supra-lesional electromyography (EMG), and upper arm inertial sensors (IMU). We interpreted the muscle activity or arm movements of subjects with tetraplegia

attempting to control the opening/closing of a robotic hand, and the extension/flexion of their own contralateral hand muscles activated by electrical stimulation. Two groups of participants with quadriplegia were recruited (Clinique Propara, Montpellier): eight subjects issued EMG-based commands; nine other subjects issued IMU-based commands. For each participant, we selected at least two muscles or gestures detectable by our algorithms. Despite little training, all participants could control the robot's gestures or electrical stimulation of their own arm via muscle contraction or limb motion [20].

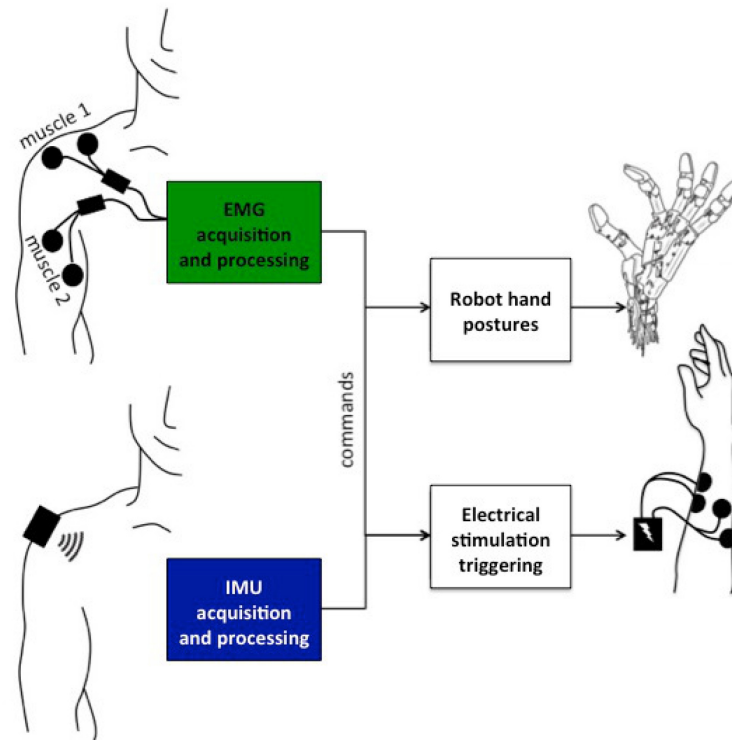


Figure 10. Protocol principle. EMG or IMU signals are converted into commands for the robotic hand or the electrical stimulator. The robotic hand has three possible gestures: at-rest, open and close. The electrical stimulator can receive three commands: no stimulation, stimulate channel 1 (wrist flexion) or stimulate channel 2 (wrist extension). Users are able to observe the outcome of their input and use it as biofeedback.

In the AGILIS project supported by EIT Health, we intend to extend this approach to participants with 2 implanted electrodes on median and radial nerves participating in a 30-days clinical study (APHP, Paris and Clinique La Châtaigneraie, Menucourt).

We are currently working on the software that is responsible for acquiring sensor data and controlling the stimulator (§5.2.4). The previous algorithms are being implemented in a single platform focusing on the 30-days clinical study. The residual motion based system was improved based on the results published in [20]. It is also faster and more efficient. The inertial sensors now have higher frequency, which leads to higher accuracy of movement classification, particularly with faster movements.

## 6.4. Modeling and simulation of a human hand

**Participants:** Daniel Simon, Ahmed Farek.

The AGILIS stimulation system is intended to generate grasping action on some objects such as balls and cans. A high-fidelity hand model and associated simulation software was developed to anticipate real experiments and help for the system identification and tuning [30]. The hand model uses 23 degrees of freedom for the wrist and fingers. 28 muscles are considered, including the 12 muscles which are expected to be activated using electrical stimulation of the median and radial nerves. Others are also considered in the model as, even if not stimulated, they contribute to the hand and fingers movements through passive forces when extended. Several actuation models are investigated to allow for the identification of muscles-to-movements relations.

The active forces provided by the stimulated muscles are computed thanks to the original model developed over the past years by the team, where the inputs are currents injected to muscles or nerves. The fingers are assumed to interact with the grasped object through elastic contacts and limited friction.

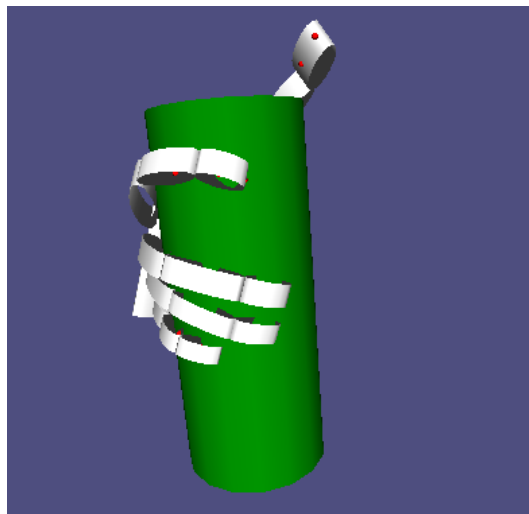


Figure 11. Simulation of a stimulated hand grasping a can

## 6.5. Functional impact of a self-triggered grasping neuroprosthesis in post-stroke subjects

**Participants:** David Gasq, Christine Azevedo, Ronan Le Guillou, Jérôme Froger [CHU Nîmes, France].

The improvement of the grasp abilities remains a challenge in the 50% of post-stroke subjects who have not recovered functional grasping due to paralysis of the finger's extensor muscles. The ePrehension-Stroke is a prospective, bicentric (promoted by the CHU de Nîmes), multi-crossover, blinded evaluation study which assesses the functional impact of a self-triggered grasping neuroprosthesis. We have developed a specific software, NeuroPrehens, which controls external electrical stimulations applied over finger's extensor muscles and was triggered by voluntary head movements or electromyography activity of leg muscles. The main objective is to assess the impact of the self-triggered grasping neuroprosthesis on the ability to perform a standardized task of grasping, moving and releasing either a glass (palmar grasp) or a spoon (key pinch), compared to the absence of neuroprosthesis use. Secondary objectives are to assess (1) the preferential modes of neuroprosthesis control, (2) the impact of the neuroprosthesis on a standardized unimanual grip scale (Action Arm Research Test), (3) the psycho-social impacts (Psychosocial Impact of Assistive Devices Scale questionnaire) and the subject's satisfaction and tolerance (Quebec User Assessment of Satisfaction with Assistive Technology questionnaire) related to neuroprosthesis use. Over 20 subjects planned to include until

June 2020, we have included 8 subjects since July 2019. The prospects of this pilot study are to develop a fully wearable and self-piloted neuroprosthesis that can be used in daily life by the largest number of post-stroke subjects who have not recovered active grasping abilities.

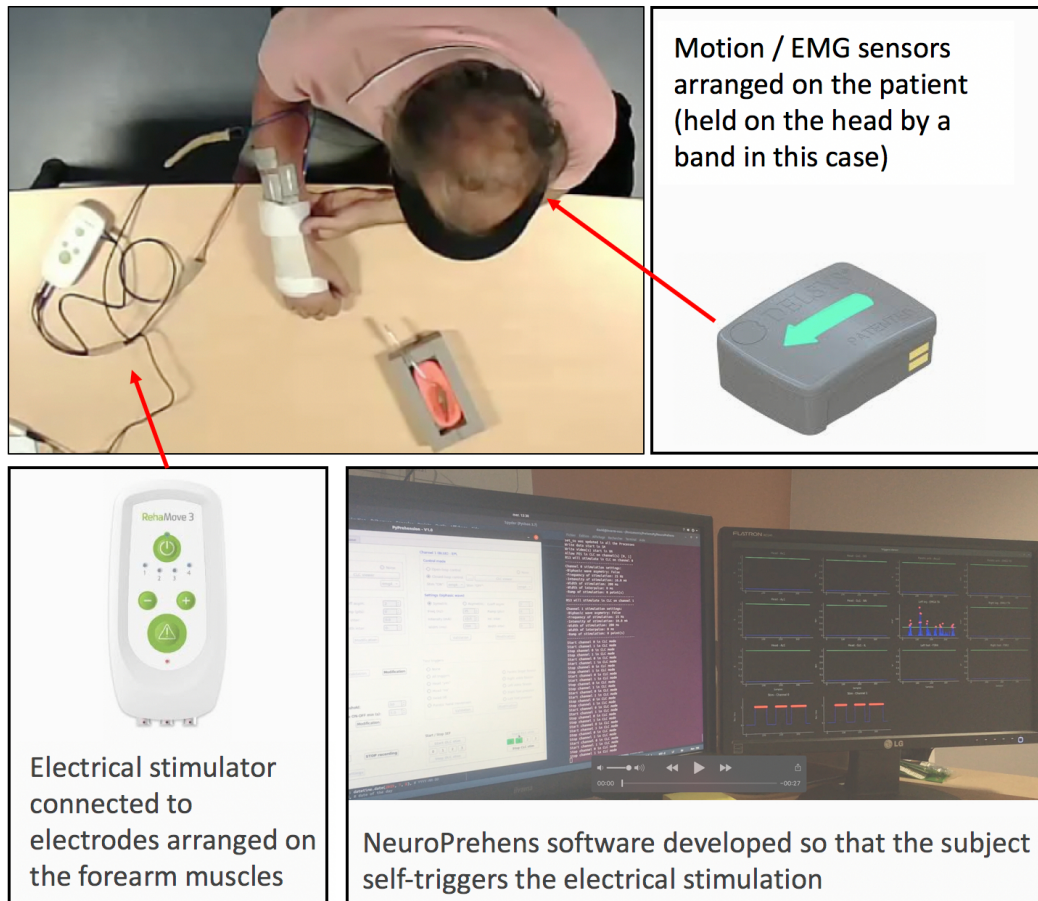


Figure 12. Experimental device constituting the self-triggered grasping neuroprosthesis.

## 6.6. Near-infrared spectroscopy time course under hypercapnia

**Participants:** Victor Vagné, David Guiraud, Vincent Costalat [CHU Montpellier], Emmanuelle Le-Bars, Stephane Perrey.

Partial arterial pressure of carbon dioxide (CO<sub>2</sub>) modulates cerebral blood flow through vasoreactivity mechanism. Near infrared spectroscopy (NIRS) can be used to record these changes in cerebral hemodynamics. However, no laterality comparison of the NIRS signal has been performed despite being a prerequisite for the use of such method in a vasoreactivity monitoring context. We propose to investigate laterality of NIRS signal in response to a CO<sub>2</sub>-inhalation-based hypercapnia paradigm in healthy volunteers.

**Methods:** Eleven healthy volunteers (6 women, 5 men, mean age:  $31 \pm 11$ ) underwent a 3-block-design inhalation paradigm: normoxia (5min, “baseline”) – hypercapnia (2min, “stimulation”) – normoxia (5min, “post-stimulation”). NIRS signal was measured using a two-channel oximeter (INVOS 5100C, Medtronic,

USA) with sensors placed symmetrically on both the left and right sides on each subject's forehead. Additional heart rate (HR) monitoring was performed simultaneously. Based on the NIRS mean signal pattern, an a priori model of parametric identification was applied for each channel to quantify parameters of interest (amplitude, time delay, excitation and relaxation time) for each inhalation block.

Results: HR increased significantly during the stimulation block. The quality of the model was satisfactory: mean absolute error between modeled and experimental signals were lower than the resolution of the device. No significant lateralization were found between left and right values of most of the parameters.

Conclusion: Due to the lack of lateralization, this parametric identification of NIRS responses to hypercapnia could bring light to a potential asymmetry and be used as a biomarker in patients with cerebrovascular diseases.

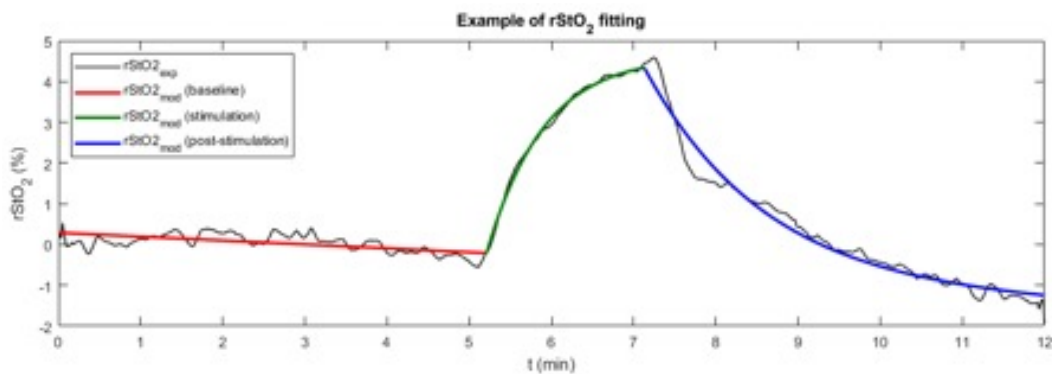


Figure 13. Example of curve fitting on NIRS signal with a compartmental first order model in response to a 2-min hypercapnic stimulus.

## 6.7. EPIONE

**Participants:** David Andreu, David Guiraud, Arthur Hiairassary.

The project was completed in 2017 but major publications were issued in 2018 and 2019 reporting the most important results of both stimulation of the upper and lower limbs in amputees to restore sensations using 4 TIME electrodes. We developed original algorithms that convert signals acquired from sensors of the artificial lower limb, namely the prosthetic limb, into stimulus to the afferent branches of the sciatic nerve. This pioneering work shows that not only the gait performances were greatly enhanced but also the phantom pain relief was effective with a long lasting after stopping the therapy [22] [21]. These results follows the previous ones obtained on the upper limb with similar results [23].

## 6.8. FES-assisted cycling

**Participants:** Benoît Sijobert, Ronan Le Guillou, Charles Fattal, Christine Azevedo, Martin Schmoll, Emerson Fachin-Martins [UNB, Brazil], Henrique Resende [UFMG, Brazil], David Lobato [UNB, Brazil].

Our team is working for several years on FES-assisted cycling for individuals with spinal cord injury. We intend to improve cycling accessibility to a larger population in order to propose exercising and leisure activity to improve quality of life and self esteem. On this context we have been working on three aspects this year: 1) improving training to be able to propose patients in rehabilitation centers a simplified and acceptable protocol to prepare muscles to cycling, 2) improving usability in a rehabilitation context to ease and simplify the access to FES-cycling, 3) better understanding fatigue phenomena to improve cycling performances.



A funding (EDF Foundation) has been obtained by our clinical partner "CRF La Châtaigneraie" to perform a clinical protocol to follow up the physical preparation of individuals with spinal cord injury to manage overground active pedaling after 4 months of 3 sessions per week training at home. The protocol has been approved by an ethical committee (§3.3 ). One of the participants will be involved in Cyathlon 2020 event. The inclusions began in September 2019. A longitudinal follow-up will allow to precisely assess the performances progress along the training period. After the 4-months at home training the participants will be using the overground cycling platform that has been developed by our team (§5.2.2 ).



*Figure 14. Muscular preparation for overground cycling training. Left: Participant executing strengthening program with conventional multichannel stimulator (CEFAR); Right: Participant performing endurance training on FES-ergocycle.*

It has been shown that FES-cycling of subjects with Spinal Cord Injuries (SCI) results in physiological and psychological positive effects such as cardiovascular training, decrease in pressure sores occurrence and self-esteem improvements. However, the use of this technology has often remained restricted to indoor and stationary ergometers in clinical contexts, partly due to the small amount (10–25 W) of power produced and the requirement of experimented users to finely tuned the stimulation patterns needed to stimulate lower limb muscles with an adequate modality. Our latest study on this subject introduces a novel approach of a Functional Electrical Stimulation (FES) controller intended for FES-induced cycling based on inertial measurement units (IMUs). This study aimed at simplifying the design of electrical stimulation timing patterns while providing a method adapted to different users and devices. In most of the different studies and commercial devices, the crank angle is used as an input to trigger stimulation onset. We propose to use instead thigh inclination as the reference information to build stimulation timing patterns. The tilting angles of both thighs are estimated from one inertial sensor located above each of the knees. An IF-THEN rules algorithm detects online and automatically the thigh peak angles in order to start and stop the stimulation of quadriceps muscles depending on these events. One participant with complete paraplegia was included and was able to propel a recumbent trike using the proposed approach after a very short setting time. This new modality opens the way to a



simpler and user-friendly method to automatically design FES-induced cycling stimulation patterns, adapted to a clinical use, to multiple bike geometries and user morphologies. Using the online peak knee flexion algorithm developed in the study presented in last years section 6.2 to continuously detect this event, we validated a novel approach in order to trigger the quadriceps stimulation at the beginning of the pushing phase. These results can be seen in Figure 15 . Enabling this method to take into account a possible sliding in seat position without requiring an accurate placement of the IMUs or a geometrical model of the individual [24].

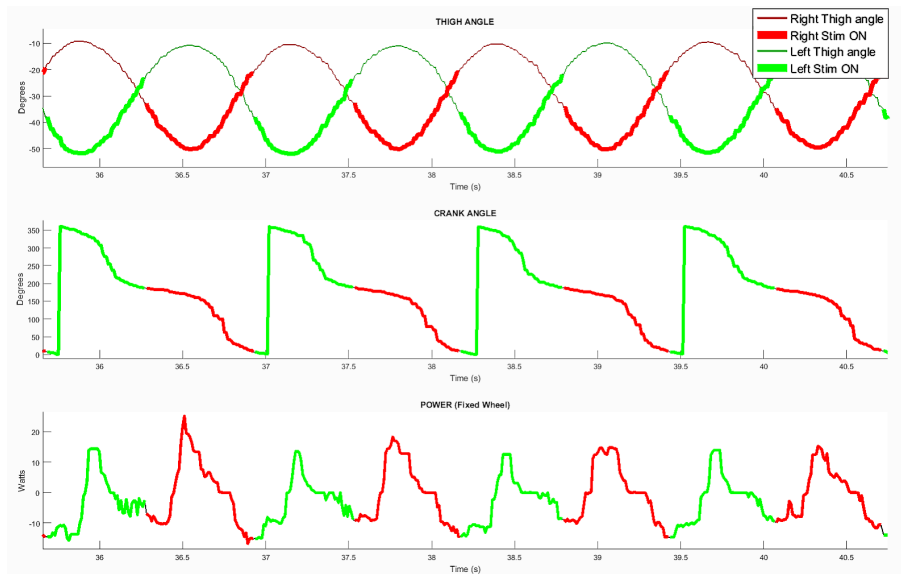


Figure 15. Data sample illustrating the results over four pedalling cycles in home trainer condition. TOP: Left (green) and right (red) thigh tilting angles - MIDDLE: crank angle - BOTTOM: developed power. The two stimulation channels activation are highlighted.

Another important aspect concerning FES-cycling is the pilots ability to resist fatigue for a prolonged time. Muscular activation as a result of electrical nerve stimulation is known to introduce a rather quick onset of fatigue. Therefore different approaches have been tested in literature to reduce the effective stimulation frequency received by individual motor-units. Several studies were able to show improvements using distributed multichannel stimulation against conventional single channel stimulation. A direct comparison between the different techniques is difficult as all studies use different methods of quantifying muscular fatigue. Further most studies fail to mention measured absolute values during a contraction at maximum strength. Therefore our team was designing a new testing protocol in collaboration with the University of Brasilia (CACAO Associate team) with the aim to assess muscular fatigue of currently published and new electrode positions against conventional single channel stimulation (baseline) in a more practical setting. The fatigue testing protocol was tailored to mimic 10 min FES-cycling at 50 RPM using an isokinetic dynamometer (Biodex System 4). Assuming a torque-production of 40 percent of the maximal torque-production-capacity of a well-trained quadriceps muscle to be sufficient for FES-cycling. The active torque produced at this starting level was measured in a series of contractions, tracking the decline of torque. The study was conducted in Brasilia on 3 individuals expressing a complete spinal cord injury. All participants were enrolled in a FES-training program for about 14months. All participants were highly motivated and fulfilled the demanded inclusion criteria ensuring a safe execution of the protocol. For every subject both legs were measured individually leading to an overall sample size of  $n=6$ . Currently the data-analysis is still in progress. The results of this study should lead to optimized stimulation techniques to prolong the onset of fatigue during FES-cycling.



Figure 16. Overground cycling. The participant was able to propel the recumbent trike over a 40 meter corridor.

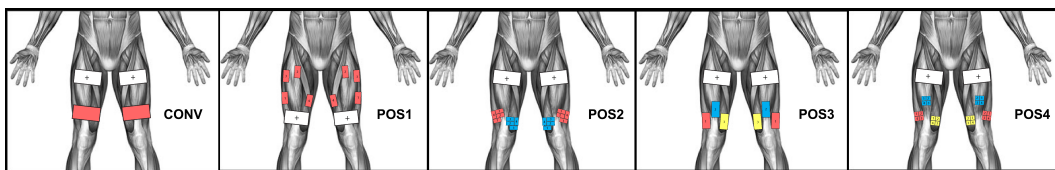


Figure 17. Electrode configurations examined. Electrodes marked with “+” were the Anodes (reference electrodes). CONV: Standard electrode configuration 40 Hz delivered to one pair of electrodes; POS1: One channel with 40 Hz distributed over 4 electrodes – common anode; POS2: Two channels with each 40 Hz distributed via 4 electrodes – common anode; POS3: Three channels of 40 Hz each delivered to one electrode – common anode; POS4: Three channels with each 40 Hz distributed via 4 electrodes – common anode

## 6.9. Breathing detection via tracheal sounds

**Participants:** Xinyue Lu, David Guiraud, Christine Azevedo, Serge Renaux [Neuroresp], Thomas Similowski [Hosp. LA Salpêtrière, Paris].

Individuals with a respiratory paralysis are essentially supplied by mechanical ventilation. However, severe drawbacks of mechanical ventilation were reported: low autonomy, high health costs, infection risk, etc. If patients’ phrenic nerves and diaphragms are still functional, implanted diaphragm pacing can provide them a more natural respiration. Compared to classic mechanical ventilation, implanted diaphragm pacing can cancel some of the disadvantages mentioned above, and can also help to significantly improve speech and recover some olfactory sensation.

But existing implanted diaphragm pacing systems can not monitor patient’s induced respiration and they stimulate at constant intensity and frequency - they work in open-loop. It means that stimulation intensity,

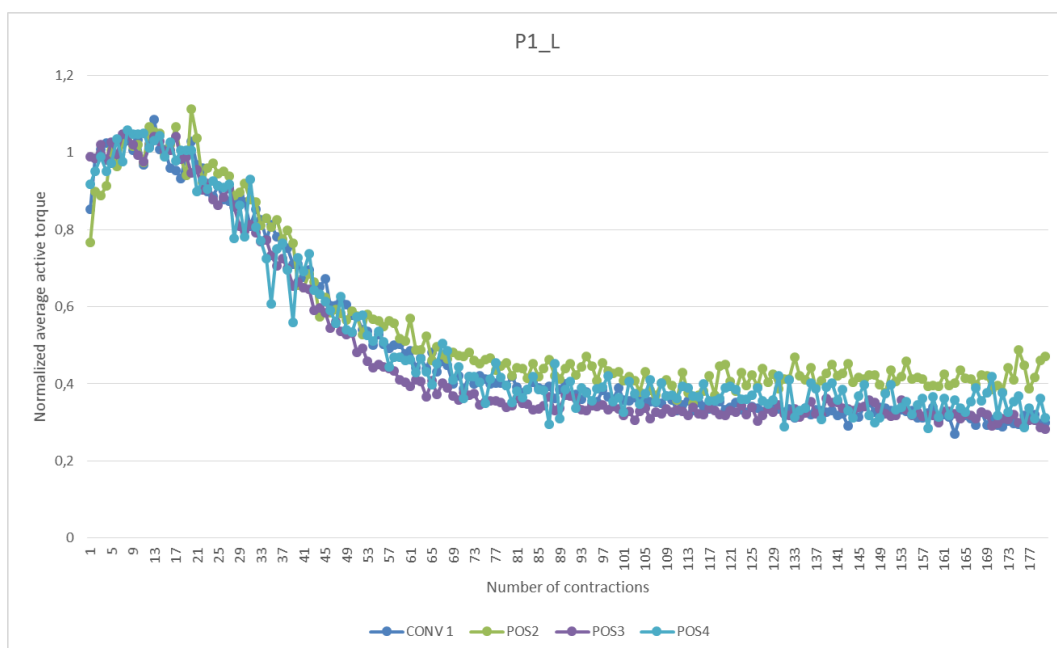


Figure 18. Preliminary data retrieved of the left leg of patient 1. The average active torque of the first 20 contractions was used to normalize fatigue curves. POS1 was excluded from the figure due to exaggerated fluctuations in torque.

pulse width and frequency are fixed at the installation of the implant, updated at each control visit, but do not adapt to patient's continuous situation evolution because of the absence of respiratory monitoring. To close the loop, an ambulatory respiratory monitoring solution needs to be developed. Adding adaptive abilities to existing systems would improve the efficiency of the delivered stimulation.

The gold standard for apnea/hypoventilation evaluation is the polygraph, which includes an pulse oximeter and at least one respiratory flow sensor. In a clinical use, flow sensors could be nasal cannula, pneumotachograph, thermistor or plethysmograph. But these sensors need to be placed over the face or are sensitive to patient's movements. They are therefore not compatible with an implanted diaphragm pacing system which is portable and for a daily living use. With this in mind, this study investigated an acoustic method. The proposed tracheal sounds recording requires only one tiny microphone fixed on the neck with a support, which is the only physical contact with the patient.



Figure 19. The position of microphone to record tracheal sounds.

Many previous studies have shown some positive results on respiration analysis from tracheal sounds in sleep apnea, especially for obstructive sleep apnea. But only few methods are developed for real-time applications (processing delay within seconds) with robustness requirements, indeed, all these studies have been carried out in quiet and controlled acoustic environments with stable sources of noises, and with limited movements of the subjects (during sleep).

In collaboration with NEURORESP company and La Salpêtrière Hospital (Paris) we are investigating the possibility to perform a real-time and continuous breathing detection (day and night), even during wakefulness in noisy environments. We proposed the method with tracheal sounds recorded on the neck at suprasternal notch (Fig. 19). This method is noninvasive and easy to apply. And the recorded tracheal sounds contain not only respiratory sounds, but also heart beats sounds (as phonocardiogram: PCG) so that some basic cardiac information, as cardiac rhythm, could be calculated. Furthermore, inspired by ECG-derived respiration, the similar method could also be applied on obtained PCG to get respiratory information.

The proposed method has been tested on 30 recordings from 15 healthy subjects with different respiratory condition, one example is shown in Fig. 20. We proposed a new algorithm to detect respiration phases, by combining the signal processing both in the temporal (envelope and PCG-derived respiration) and the frequency domains. We assessed the performances of the algorithm in emulated noisy environments. The accuracy, sensibility and specificity of system are all superior to 90%. The result is good enough to show a proof of such a conception. Furthermore, a tracheal sounds recording from a patient under implanted phrenic nerve stimulation has shown that the recording system has the possibility to capture an image of stimulation impulse from the wireless transmission. Getting the synchronization with respiratory sounds and stimulation signals can help to verify and even to adjust patient's stimulation parameters.

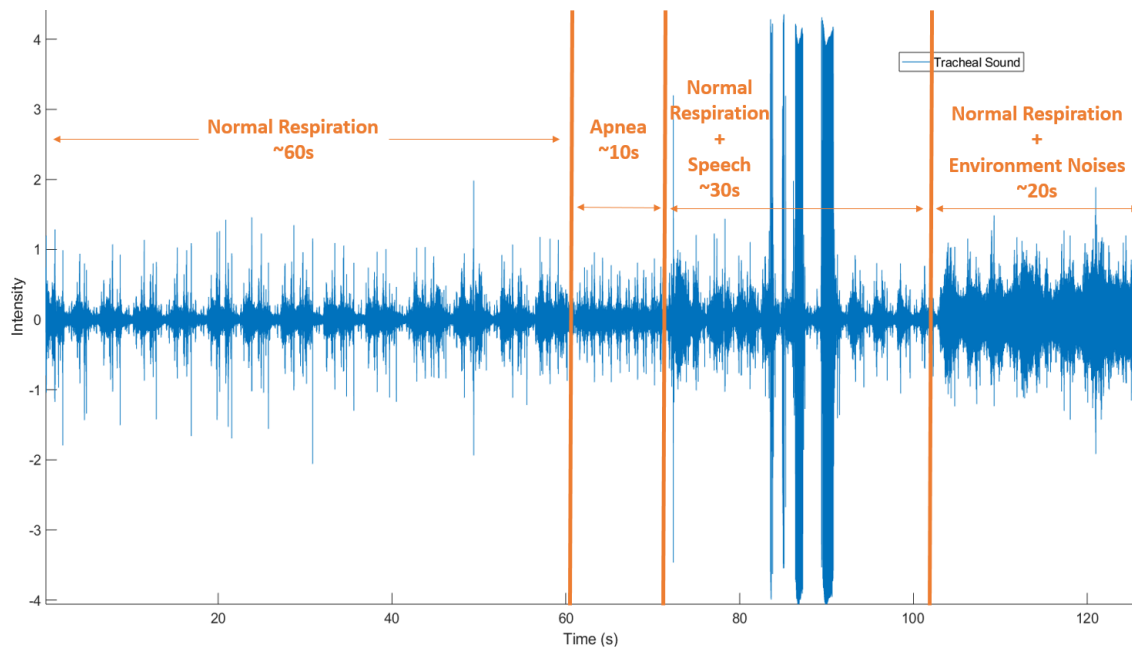


Figure 20. One example of a 2-min recording of tracheal sounds.

## 6.10. Attenuation and Delay of Remote Potentials Evoked by Direct Electrical Stimulation During Brain Surgery

**Participants:** Anthony Boyer, Hugues Duffau [CHU Montpellier], Emmanuel Mandonnet [CHU Lari-boisière], Marion Vincent, Sofiane Ramdani [LIRMM], David Guiraud, François Bonnetblanc.

Direct electrical stimulation (DES) is used to perform functional brain mapping during awake surgery but its electrophysiological effects remain by far unknown. DES may be coupled with the measurement of evoked potentials (EPs) to study the conductive and integrative properties of activated neural ensembles and probe the spatiotemporal dynamics of short- and long-range networks. We recorded ECoG signals on two patients undergoing awake brain surgery and measured EPs on functional sites after cortical stimulations, using combinations of stimulation parameters. EPs were similar in shape but delayed in time and attenuated in amplitude when elicited from a different gyrus or remotely from the recording site. We were able to trigger remote EPs using low stimulation intensities. We propose different activation and electrophysiological propagation mechanisms following DES based on activated neural elements [15].

Electrodes of both ECoG strips are numbered from 1 to 4 and from 5 to 8. The Sylvian fissure and central sulcus are highlighted by a white dashed lines and annotated "SyF" and "Cs" respectively. For P1, experimental DES was applied on: (1) the Wernicke's area (S1), associated with complete anomia; (2) the ventral premotor cortex (S2), which led to movement and counting interruptions. Strip 1 spans over both temporal and parietal lobe with: electrode 1 over the most posterior part of the superior temporal gyrus; electrode 2 over the Sylvian fissure; electrodes 3 and 4 over the adjacent supramarginal gyrus. Strip 2 spans over the precentral gyrus with: electrodes 5 to 7 over the ventral premotor cortex; electrode 8 is bordering with the most posterior part of the partially resected dorsolateral prefrontal cortex. For P2, experimental DES was applied on: (1) the middle part of the superior temporal gyrus (S1) which led to complete anomia; (2) the precentral gyrus (S2), which induced articulatory disorders. Strip 1 spans over the superior temporal gyrus with: electrodes 1 and 2 over its middle third; electrodes 3 and 4 over its most posterior part. Strip 2 spans over the precentral

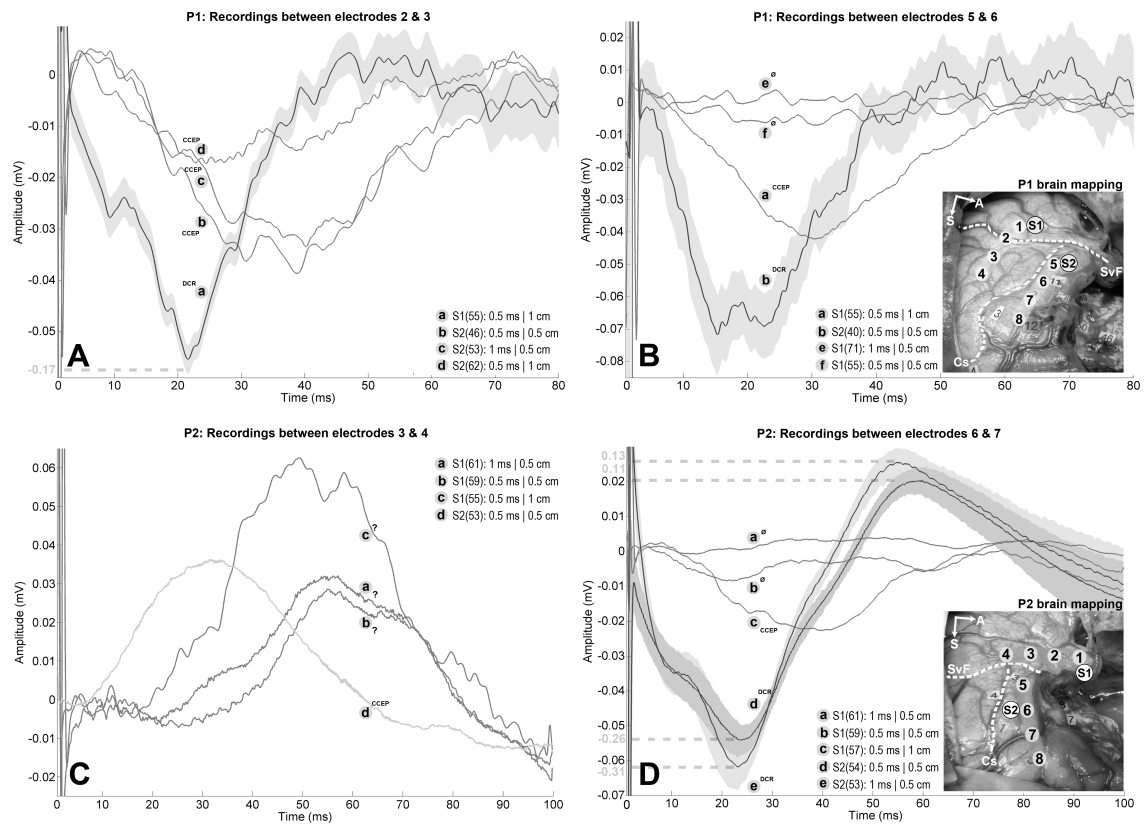


Figure 21. P1 and P2 brain mappings: Pictures illustrating the stimulation sites (S1, S2) and ECoG positioning with respect to the initial 60 Hz cortical brain mapping (numbered paper tags).



and dorsolateral prefrontal gyri with: electrodes 5 and 6 over the ventral premotor cortex; electrodes 7 and 8 are respectively bordering and within the adjacent dorsolateral prefrontal cortex. Tumor was about 164 cm<sup>3</sup> for P1 and 150 cm<sup>3</sup> for P2. The number of averaged stimuli is reported within parentheses for each trace. 99% confidence interval estimated for DCRs are represented by grey surfaces to demonstrate that CCEPs do not belong to them. Additional traces corresponding to variations of stimulation parameters were added if available, regardless of the presence of EPs. A: Differential recordings between electrodes 2 and 3 for P1 while stimulating S1 (-170  $\mu$ V, 21 ms delay) and S2 (amplitudes ranging from -40  $\mu$ V to -17  $\mu$ V, delays ranging from 25 ms to 38 ms). EPs following S2 stimulation are CCEPs because of the presence of the central fissure between the stimulation and recording sites. The EP measured after stimulating S1 is ambiguous because electrode 2 lies on the Sylvian fissure, but the short latency and enhanced amplitude with regard to the CCEPs suggest a DCR. Note the dashed line indicating a different amplitude scale for the DCR, which was reduced by a factor 3 for visualization purposes. B: Differential recordings between electrodes 5 and 6 for P1 while stimulating S2 (-75  $\mu$ V, 20 ms delay) and S1 (-44  $\mu$ V, 30 ms delay). EP following S1 stimulation is a CCEP because of the presence of the Sylvian fissure between the stimulation and recording sites. EP following S2 stimulation should be viewed as DCR as it was recorded on the same gyrus and it showed shorter latency and enhanced amplitude in comparison with the CCEP. C: Differential recordings between electrodes 3 and 4 for P2 while stimulating S1 (amplitudes ranging from +29  $\mu$ V to +62  $\mu$ V, delays ranging from 52 ms to 62 ms) and S2 (+36  $\mu$ V, 32 ms delay). EP following S2 stimulation is a CCEP because of the presence of the Sylvian fissure between the stimulation and recording sites. EPs following S1 stimulations should be viewed as DCRs as they are recorded on the same gyrus but the latencies and amplitudes appeared unusual. EPs are positive because of differential measure. D: Differential recordings between electrodes 6 and 7 for P2 while stimulating S2 (amplitudes ranging from -260  $\mu$ V to -310  $\mu$ V, 20 ms delay) and S1 (-24  $\mu$ V, 38 ms delay). EP following S1 stimulation is a CCEP because of the presence of the Sylvian fissure and the operative cavity between the stimulation and recording sites. EPs following S2 are likely DCRs as they are recorded on the same gyrus, which is corroborated by their short latencies and maximized amplitudes with regard to the CCEP. Note the dashed lines indicating different amplitude scales for the DCRs, which were reduced by a factor 5 for visualization purposes.

## CASTOR Project-Team

### 4. New Results

#### 4.1. On the identification of the electron temperature profile from polarimetry Stokes vector measurements in Tokamak free-boundary equilibrium reconstruction

**Participants:** Blaise Faugeras, Francesco Orsitto.

This paper reports numerical investigations on the identification of the electron temperature profile  $T_e$  from interferometry and polarimetry Stokes vector measurements with the equilibrium code NICE (Newton direct and Inverse Computation for Equilibrium). This latter enables the consistent resolution of the inverse equilibrium reconstruction problem in the framework of nonlinear free-boundary equilibrium coupled to the Stokes model equation for polarimetry. We find that for ITER plasma with high  $I_p$ ,  $N_e$  and  $T_e$  the identification from noisy measurements is possible (Project EUROfusion / WP01Jet Campaigns (WPJET1)).

#### 4.2. Equilibrium reconstruction for the JT-60SA tokamak

**Participant:** Blaise Faugeras.

Twin experiments were performed with this tokamak geometry in the framework of the EUROfusion / WP10 JT-60SA (WPSA) project.

#### 4.3. Plasma boundary reconstruction for the ISTTOK tokamak

**Participants:** Blaise Faugeras, Rui Coelho, R. Santos.

Plasma boundary reconstruction is one of the main tools to provide a reliable control and tokamak performance. We explore the feasibility for the ISTTOK tokamak (Portugal) of a reconstruction method based on calculated vacuum magnetic flux map and plasma intersection with the wall. We show that via square wave input response curves and pre-processing of the poloidal field coil currents, it is possible to build for ISTTOK a simple scaling model for the effective equilibrium magnetic fields, and perform plasma boundary reconstruction using the algorithm VacTH. This algorithm, included in the NICE numerical code suite, relies on the decomposition of the poloidal flux in toroidal harmonics. The reconstructed plasma boundary is shown for a given discharge and its shape and position are shown to evolve consistently with the typical timescale evolution of ISTTOK discharges. This provides an opportunity of using this plasma boundary reconstruction method as a diagnostic tool for ISTTOK.

#### 4.4. Implementation of a method enabling error bar computations for all reconstructed equilibrium quantities

**Participant:** Blaise Faugeras.

Error bars on control variables are directly given by the inverse of the Hessian of the minimized cost function. This is not the case for other quantities such as the safety factor profile for example, and the computation of error bars for these important output quantities necessitate the non-trivial computation of their (discrete) derivatives with respect to the control variables as well as the state variables.

#### 4.5. New developments on the code NICE

**Participant:** Blaise Faugeras.

Developments have been done on the code NICE:

- Implementation of a mode 'without plasma' for magnetostatic computations.
- Implementation of pressure constraints in NICE for IMAS tested on JET data.
- Regular updates of the relaxed NICE actor in IMAS (EUROfusion / WP13 Code Development for Integrated Modeling)
- A Matlab interface has been developed to run the free boundary direct, evolutive, and inverse static modes of NICE.

#### 4.6. Automatic identification of the plasma equilibrium operating space in tokamaks

**Participants:** Blaise Faugeras, Xia Song, Eric Nardon, Holger Heumann.

In order to identify the plasma equilibrium operating space for future tokamaks, a new objective function is introduced in the inverse static free-boundary equilibrium code FEEQS.M. This function comprises terms which penalize the violation of the central solenoid and poloidal field coils limitations (currents and forces). The penalization terms do not require any weight tuning. Hence, this new approach automates to a large extent the identification of the operating space. As an illustration, the new method is applied on the ITER 15 and 17MA inductive scenarios, and similar operating spaces compared to previous works are found. These operating spaces are obtained within a few ( $\sim 3$ ) hours of computing time on a single standard CPU.

#### 4.7. Automating the design of Tokamak experiment scenarios

**Participants:** Jacques Blum, Holger Heumann.

The real-time control of plasma position, shape and current in a tokamak has to be ensured by a number of electrical circuits consisting of voltage suppliers and axisymmetric coils. Finding good target voltages/currents for the control systems is a very laborious, non-trivial task due to non-linear effects of plasma evolution. We introduce here an optimal control formulation to tackle this task and present in detail the main ingredients for finding numerical solutions: the finite element discretization, accurate linearizations and Sequential Quadratic Programming. Case studies for the tokamaks WEST and HL-2M highlight the flexibility and broad scope of the proposed optimal control formulation.

#### 4.8. Coupling NICE-METIS

**Participants:** Jean François Artaud, Jacques Blum, Cédric Boulbe, Blaise Faugeras.

The free boundary equilibrium code NICE has been coupled to the fast transport solver METIS in a Matlab workflow. A first test case has been proposed on ITER. This work has been done for the project Eurofusion WPCD.

#### 4.9. Advances in high order mixed finite elements for Maxwell's equations

**Participant:** Francesca Rapetti.

The implementation of high order curl- or div-conforming finite element spaces is quite delicate, especially in the three-dimensional case. I have worked on an implementation strategy, which has been applied in the open source finite element software FreeFem++. In particular, I have used the inverse of a generalized Vandermonde matrix to build a basis of generators in duality with the degrees of freedom, which then provides in FreeFem++ an easy-to-use but powerful interpolation operator. With Marcella Bonazzoli, now at the Inria Team DEFI in Saclay, I have carefully addressed the problem of applying the same Vandermonde matrix to possibly differently oriented tetrahedra of the mesh over the computational domain. [17]

High order mixed finite element spaces generally lack natural choices of bases but they do have spanning families. I have worked on these FEs for simplicial meshes and proven theoretically their effectiveness. I have also commented on some aspects of a new set of degrees of freedom, the so-called weights on the small simplices, to represent discrete functions in these spaces [11].

#### 4.10. Construction of divergence-free bases

**Participants:** Francesca Rapetti, Ana Alonso Rodriguez.

I have worked to propose and analyze an efficient algorithm for the computation of a basis of the space of divergence-free Raviart-Thomas finite elements. The algorithm is based on graph techniques. The key point is to realize that, with very natural degrees of freedom for fields in the space of Raviart-Thomas finite elements of degree  $r + 1$  and for elements of the space of discontinuous piecewise polynomial functions of degree  $r \geq 0$ , the matrix associated with the divergence operator is the incidence matrix of a particular graph. By choosing a spanning tree of this graph, it is possible to identify an invertible square submatrix of the divergence matrix and to compute easily the moments of a field in the space of Raviart-Thomas finite elements with assigned divergence. The analyzed approach is then used to construct a basis of the space of divergence-free Raviart-Thomas finite elements. The numerical tests show that the performance of the algorithm depends neither on the topology of the domain nor on the polynomial degree  $r$  [16].

#### 4.11. First steps to polytopal/polyhedral meshes

**Participant:** Francesca Rapetti.

Merging ideas from compatible discretisations and polyhedral methods, I have worked with D. Di Pietro and J. Droniou to construct novel fully discrete polynomial de Rham sequences of arbitrary degree on polygons and polyhedra. The spaces and operators that appear in these sequences are directly amenable to computer implementation. Besides proving exactness, we have shown that the usual sequence of Finite Element spaces forms, through appropriate interpolation operators, a commutative diagram with other proposed sequence, which ensures suitable approximation properties. A discussion on reconstructions of potentials and discrete L2-products completes the work [14].

#### 4.12. $C^1$ finite elements on triangular meshes

**Participants:** Hervé Guillard, Ali Elarif, Boniface Nkonga.

In order to avoid some mesh singularities that arise when using quadrangular elements for complex geometries and flux aligned meshes, the use of triangular elements is a possible option that we have studied in the past years. However due to the appearance of fourth order terms in the PDE systems that we are interested in, pure Galerkin methods require the use of finite element methods with  $C^1$  continuity. The PhD thesis of Ali Elarif that has begun in october 2017 is devoted to the study of these methods for complex PDE models encountered in plasma physics. Relying on the work previously done on steady elliptic PDE, this year we applied these finite element methods to some evolution problems like the incompressible Navier-Stokes and MHD equations in stream-function formulation. Error estimates in  $H^2$  norms have been obtained using standard finite element techniques. The simulation of some instabilities encountered in plasma physics have been done with very satisfactory results.

#### 4.13. Modelling of acoustic streaming

**Participants:** Hervé Guillard, Argyris Delis [TUC, Crete].

Acoustic streaming is a particularly interesting example of the interaction of phenomena occurring on two different time scales. From a practical point of view, it is mainly used to generate a slow motion in microfluidic devices by means of high frequency acoustic sources. Modelling of these interaction is a challenge : taking into account the high frequency phenomena is prohibitively expensive but on the other hand, there is no universal agreement on existing averaged models. In order to have reference simulations, we have constructed a numerical code solving the compressible Navier-Stokes equations with high-order accuracy using compact schemes. Comparison with asymptotic analytical results has been done and shows that the code is able to simulate acoustic waves propagation in a stable way on long time scale, a property that is essential for the study of this phenomenon.

#### 4.14. Mortar finite element methods

**Participants:** Hervé Guillard, Francesca Rapetti.

Hermite-Bezier finite element modeling is the standard method used to discretize the MHD equations in codes such as JOEK. This finite element family allows for an accurate description of the magnetic topology using flux aligned grids where the iso-parametric curved elements match the magnetic flux level sets. However, the description of complex material geometries is difficult with this family of finite element. We have begun to study the use of discretization methods using overlapping meshes where one mesh is composed of quadrangular Hermite-Bezier finite element while the second one is made of triangular elements.

#### 4.15. Collisions in gyrokinetic equation

**Participants:** Afeintou Sangam, Vladimir T. Tikhonchuk.

Charged particles in plasma in strong magnetic fields undergo a complicated motion, which is a combination of a fast cyclotron gyration around the magnetic field lines and a relatively slow dynamics along and across the magnetic field lines. Gyrokinetic equations, devised to describe plasma under such conditions, eliminate the fast cyclotron gyration from the equation of motion, thus reducing the space-velocity phase space dimension from six to five.

Originally, the gyrokinetic formulation was devised for a collisionless plasmas. The quest for retaining collisions in gyrokinetic equations is ongoing. Collisions are important if one wants to describe the transport properties of a magnetized plasma on a macroscopic level. A description of the transport of energy and momentum was proposed in Refs. [18], [20], [19], [22], [21]. However, mathematical description of collisions in these works is too complicated for numerical implementation. We develop a simplified description of collision operators in the gyrokinetic formulation that preserve the pertinent conservation features and suitable for numerical modeling. A comparison of these operators with several test cases is under investigation.

#### 4.16. Singular solutions of dispersive systems

**Participants:** S. Gavriluk, B. Nkonga, K-M Shyue, L. Truskinovsky.

We study a dispersive regularization of p-system. The governing equations are the Euler- Lagrange equations for a Lagrangian depending not only on the velocity and density, but also on the first material derivative of density. Such regularization arises, in particular, in the modeling of waves in solids, in bubbly fluids as well as in the theory of water waves. We show that such terms are not always regularizing. The solution can develop shocks even in the presence of dispersive terms. In particular, we construct such a shock solution that connects a constant state to a periodic wave train. The corresponding shock speed coincides with the velocity of the wave train. The generalized Rankine-Hugoniot relations (jump relations) are also obtained. The numerical evidence of the existence of such shocks is demonstrated in the case of the Serre-Green-Naghdi equations describing long surface water waves. In particular, it has been shown that such waves can dynamically be formed

#### **4.17. A path conservative finite volume method for a shear shallow water model**

**Participants:** P. Chandrashekar, B. Nkonga, A. K. Meena, A. Bhole.

The shear shallow water model provides a higher order approximation for shallow water flows by including the effect of vertical shear in the model. This model can be derived from the depth averaging process by including the second order velocity fluctuations, which are neglected in the classical shallow water approximation. The resulting model has a non-conservative structure, which resembles the 10-moment equations from gas dynamics. This structure facilitates the development of path conservative schemes and we construct HLL, 3-wave and 5-wave HLLC-type solvers. An explicit and semi-implicit MUSCL-Hancock type second order scheme is proposed for the time integration. Several test cases including roll waves show the performance of the proposed modeling and numerical strategy.

#### **4.18. Full MHD Modeling of Shattered Pellet Injection**

**Participants:** B. Nkonga, P. Chandrashekar, A. Bhole.

To avoid disruptions, the first thing to do is to operate as far as possible from disruptions operational limits. It means that plasma scenarios must be designed taking these limits into account. The challenge is to deal with peeling-ballooning instabilities called Edge Localized Modes (ELMs) which are characterized by the quasi-periodic relaxation of the pressure pedestal profile which results in the expelling of particles and energy from the bulk plasma to the edge. Injecting of impurities is one of the solutions to change the pedestal profile and mitigate MHD instabilities. The current design of the ITER DMS (Disruption Mitigation System) is a hybrid system using Massive Gas Injection (MGI) and Shattered Pellet Injection (SPI), methods which have demonstrated their efficiency on current tokamaks (JET, DIII-D, ...). Considering that the plasma is composed of impurities, main ion core and set of electrons, premixed "Full MHD" formulation has been proposed. This model assumes that, for any control volume, the plasma is locally neutral and at the thermal and coronal equilibrium. Properties of this model are under analysis, according to the tabulated equation of state. A numerical approximation in the Jorek Code is also under progress. This work has been done in the context of the JET program 2019.



## CHORALE Team

# 6. New Results

## 6.1. Task based world modeling and understanding

### 6.1.1. Hidden robot

**Participants:** John Thomas (Master student), Philippe Martinet, Paolo Salaris, Sébastien Briot (LS2N-ARMEN)

When robots want to execute a task, they require to have an adequate representation of the environment where they will evolve. In model based approach, it is classical to describe environment using Metric Map where the function of perception (localization) and control (Path or trajectory tracking) refer to Cartesian state. In sensor based control, the methodology "teaching by showing" has been developed during the last 30 years. The concept of sensory memory has been then introduced in order to represent the task to be executed in sensor space. This concept is used in order to represent the task directly in the sensor space for a particular set of sensors. In summary, building the representation of the task (or the environment) is building the sensory memory, defining a particular motion (or trajectory) is defining a particular occurrence of sensor features, and executing the task is done when a control is designed to perceive the same as stored in the sensory memory. This approach has shown great ability in terms of robustness. However, it is still difficult to analyze the singularities and to demonstrate the stability property for those approaches (mainly when it is necessary to control 6 degree of freedom). In 2013, Sébastien Briot and Philippe Martinet have studied the visual servoing scheme of a Gough-Stewart Platform [18] and shown that it exists an hidden robot in the controller that can be used to study the behaviour and properties of it. The Hidden robot allows to transform the analysis of the controller by viewing it as a parallel robot. Recently, this concept has been applied to study the singularities of the visual servoing scheme of points and of lines [19]. This work continues in the framework of the ANR project SESAME.

The idea of the new initial work done in 2019, is to find a methodology to design a task by using the Hidden robot concept. Navigation of a mobile robot has been considered in a first time. The followed methodology considers a topological navigation framework where a successive interaction situation are modelled by using an hidden robot: in some words, navigation is done by using a set of successive hidden parallel robots holding the robot when moving. At least two main question have been identified: What is the structure of the virtual robot which fits to task to be done? and Where to fix (or How to select) the anchors of this virtual robots?

For the first question, the idea is, considering different kind of features, to define a virtual parallel robot based on virtual legs. These virtual legs are directly linked to the considered feature. We have studied two cases, distance and angle, considering that existing sensors allow us to obtain the corresponding extracted features. After the modeling of sensors features, different control laws have been investigated allowing to produce motion of the mobile platform. The corresponding hidden robots and the properties have been studied.

For the second question, two methods have been investigated using selection matrix of features or weighted features. The main used criteria is the transmissibility index which relates the faculty of motion transmission of the virtual parallel mechanism.

This work [52] is preliminary and on going. We already have obtained preliminary results in simulation allowing a mobile platform to evolve in a dedicated environment. It was the work done by John Thomas under the supervision of Philippe Martinet and Paolo Salaris.

### 6.1.2. End to end navigation

**Participants:** Renato Martins (Post-doc), Patrick Rives

This research deals with the problem of end-to-end learning for navigation in dynamic and crowded scenes solely from visual information. We investigate the problem of navigating an unknown space to reach a target of interest, for instance “doors”, exploring the possibilities given by data-driven based models in the context of ANR MOBI-Deep project around the guidance of visually impaired people. A successful agent navigation policy requires learning general relationships between the agent actions, safety rules and its surrounding environment. We started studying a simple guidance model (turn left, right or stop), whose guidance task is to remain inside a specific region of the scene (to avoid collision). This is equivalent to take the action to stay in the center of a corridor (indoor scene) or road (outdoor scenario). We first evaluate a relatively small supervised net composed of sixteen ResNet convolutional layers. This model was trained with real images from the Udacity autonomous driving challenge, but presented limited generalization when tested in either non-structured scenes or in scenes with humans. In order to overcome these limitations, we plan to train an A3C agent (Asynchronous Actor-Critic Agent) to learn the action policies in a reinforcement learning scheme, using data acquired of virtual environments with crowds. We also plan to evaluate the use of inputs from different levels as: scene semantic segmentation; depth inference from monocular images; and human and object detection information in the learning scheme.

### 6.1.3. *Semantization of scene*

**Participants:** Mohammed Boussaha (PhD, IGN), E. Fernandez-Moral, R. Martins, Patrick Rives

The work carried out in the ANR PlaTINUM project concerns the semantic labeling of images [17] acquired by agents (autonomous vehicles or pedestrians) moving in an urban-like environment and their accurate localization and guidance. A semantic labeling based on a machine learning approach (CNN) was developed. A same methodology is used to semantize virtual images built from a textured 3D mesh representation of the environment and images from the camera handled by the agents. Several strategies have been studied to exploit complementary information, such as color and depth for improving the accuracy of semantization. Our results show that exploiting this complementarity requires to perfectly align the different sources of informations. We proposed a new approach to the problem of calibration of heterogeneous multi sensors systems [41], [44]. We also looked for evaluating a new metric to quantify the accuracy of semantization provided by the CNN by taking into account the boundaries of semantized objects during the learning step. As a consequence, we show that weighting the boundary pixels in the images allows to segment more clearly the navigable areas used by different agents such as pedestrians (sidewalks) and cars (road). The results of this research were published in [29], [30]. The CNN used for labeling images acquired by different image sensors (perspective and spherical) was pre-trained from public datasets with perspective images of urban-like environments (simulated or real). In the context of the Platinum ANR project, a fine-tuning was done with some spherical images acquired in Rouen by the IGN Stereopolis vehicle and then hand-labelled. A Docker version of the software has been made available on the project server in order to be used by the other partners.

A localization method has also been implemented to exploit information of color, depth and semantics (when this information is available). An estimation of the agent position (6DOF, rotation and translation) is computed thanks to a dense method that minimizes the geometric, photometric and semantic differences between a spherical view provided by a SIG (Système d’Information Géographique) data base hosted in a cloud server and the current view of the agent.

During the last year of the project, the methods developed in PlaTINUM were consolidated and validated on the data acquired in Rouen. As originally planned in the project, Inria enlisted the help of iXblue-division Robopec to integrate the various functions developed during the project. This software, called Perception360, will be from now the software platform for all perception developments in the Inria CHORALE team.

### 6.1.4. *Optical Flow Estimation Using Deep Learning In Spherical Images*

**Participants:** Haozhou Zhang (Master), Cédric Demonceaux (Vibot), Guillaume Allibert

In a complex environment such as in a forest, the autonomous navigation is a challenging problem due to many constraints such as the loss of GPS signals because dense and unstructured environments (branches, foliage, ...) reduce the visibility. Without GPS signals, a vision system with the ability to capture everything going on around you seems more valuable than ever and crucial to navigate in this environment. Spherical images offer great benefits over classical cameras wherever a wide field of view is essential.

The equirectangular projection is a popular representation of images taken by spherical cameras. In this projection, the latitude and longitude of the spherical images are projected to horizontal and vertical coordinates on a 2D plane. However, this equirectangular projection suffers from distortions, especially in polar regions. In this case, the density of features is no longer regular at different latitudes of the images. As a result, traditional image processing methods that have been used for perspective images do not have good performance when they are applied to equirectangular images.

Optical flow estimation is a basic problem of computer vision [50]. It is generally used as input of algorithm for autonomous navigation. Given two successive images, it estimates the motion vector in 2D (in x and y direction) for each pixel from between the two input images. Optical flow is usually considered as a good approximation of the true physical motion mapped on the image plane. It provides a concise description of the direction and velocity of the motion. In [24] and [36], CNNs which are capable of solving the optical flow estimation problem as a supervised learning task are proposed and became the standard for optical flow estimation. However, the dataset used to train [24], [36] is only based on perspective images. Even if they can be used directly with spherical images as input, the high distortions coming from equirectangular projection drastically reduce the global performance of these networks. One possible way to solve this issue is to train the networks proposed in [24], [36] with spherical images. Unfortunately, these databases do not exist and generating them would be a long and costly process.

In the Master's Hoazhou [55], we have proposed a solution to overcome this issue in proposing an adaptation of FlowNet networks to deal with the distortions in the equirectangular projection of spherical images. The proposed approach lies a distortion aware convolution used as convolution layers in the network to deal with distortions in equirectangular images. The proposed networks allows the models to be trained by perspective images and be applied to spherical images using an adapted convolution which is coherent with the spherical image. This solution avoids training a large number of spherical images which is not available and costly to generate.

## 6.2. Multi-sensory perception and control

### 6.2.1. Autonomous Parking Maneuvers

**Participants:** David Perez Morales (PhD, LS2N-ARMEN), Olivier Kermorgant (LS2N-ARMEN), Salvador Dominguez Quijada (LS2N-ARMEN), Philippe Martinet

Automated parking is used as new functionality to sell different model of cars right now. Mainly, the different versions of parking abilities are not autonomous and are based on motion planning only. There is no ability to evolve in dynamic environment: it remains automated in static environment, or even an assistant to park under the control of the driver. The purpose of the PhD work of David Perez Morales was to investigate how the problem of autonomous parking by using different sensor based techniques is able to handle any kind of parking situations (parallel, perpendicular, diagonal) for parking an unparking (backward and forward).

Two different frameworks has been developed. The first framework, using a Multi-Sensor-Based Control (MSBC) approach [47], [48], [46], [45] allows to formalize different parking and unparking operations in a single maneuver with either backward or forward motions. Building upon the first one and by using an MPC strategy [49], a Multi-Sensor-Based Predictive Control (MSBPC) framework has been developed, allowing the vehicle to park autonomously (with multiple maneuvers, if required) into perpendicular and diagonal parking spots with both forward and backward motions and into parallel ones with backward motions in addition to unpark from parallel spots with forward motions. These frameworks have been tested extensively using a robotized Renault ZOE with positive outcomes and now they are part of the autonomous driving architecture being developed at LS2N.

In 2019, the main focus was on MSBPC, and on taking into account the dynamic aspect in the environment (mainly pedestrians). Detection and tracking for pedestrian has been included in the perception aspect, in parallel to the detection of empty spots for parking. An additional terms has been added as a constraint in the cost function to be minimized in order to take into account the dynamic aspect, and a mechanism has been put in place in order to switch automatically the maneuver. In presence of pedestrian, an additional maneuver is engaged, which is what human are generally doing if place is enough for performing safely the maneuver. Comparison with state of the art motion planning approach have been done in simulation. The proposed method have demonstrated the efficiency while the others fails in a very long set of maneuvers. Real experiments have been done also in presence of pedestrians.

### 6.2.2. Platoon control and observer

**Participants:** Ahmed Khalifa (Post-Doc, LS2N-ARMEN), Olivier Kermorgant (LS2N-ARMEN), Salvador Dominguez Quijada (LS2N-ARMEN), Philippe Martinet

In the framework of the ANR Valet project, we are interested in platooning control of cars for a service of VALET Parking where it is necessary to join a platoon (after unparking), to evolve among the platoon, and leave the platoon (for parking). We are considering the case when the leader is autonomous (following an already defined path) or manually driven by a human (the path must be build on line). The lateral controller to follow a path has been designed earlier [23] and the localization technique largely evaluated experimentally [33]. The main exteroceptive sensor is the Velodyne VLP16.

The first work [38] [15] concerned the design of a distributed longitudinal controller for car-like vehicles platooning that travel in an urban environment. The presented control strategy combines the platoon maintaining, gap closure, and collision avoidance functionality into a unified control law. A consensus-based controller designed in the path coordinates is the basis of the proposed control strategy and its role is to achieve position and velocity consensus among the platoon members taking into consideration the nature of the motion in an urban environment. For platoon creation, gap closure scenario is highly recommended for achieving a fast convergence of the platoon. For that, an algorithm is proposed to adjust the controller parameters online. A longitudinal collision between followers can occur due to several circumstances. Therefore, the proposed control strategy considers the assurance of collision avoidance by the guarantee of a minimum safe inter-vehicle distance. Convergence of the proposed algorithm is proved in the different modes of operations. Finally, studies are conducted to demonstrate and validate the efficiency of the proposed control strategy under different driving conditions. To better emulate a realistic setup, the controller is tested by an implementation of the car-like vehicles platoon in a vehicular mobility simulator called ICARS, which considers the real vehicle dynamics and other platooning staff in urban environments.

The second work [14] addresses the problem of controlling the longitudinal motion of car-like vehicles platoon navigating in an urban environment that can improve the traffic flow with a minimum number of required communication links. To achieve a higher traffic flow, a constant-spacing policy between successive vehicles is commonly used but this is at a cost of increased communication links as the leader information must broadcast to all the followers. Therefore, we propose a distributed observer-based control law that depends on a hybrid source of neighbours information in which a sensor-based link is used to get the predecessor position while the leader information is acquired through a communication-based link. Then, an observer is designed and integrated into the control law such that the velocity information of the predecessor can be estimated. We start by presenting the platoon model defined in the Curvilinear coordinates with the required transformation between that coordinate and the Cartesian Coordinates so that one can design the control law directly in the Curvilinear coordinates. After that, internal and string stability analysis are conducted. Finally, we provide simulation results, through dynamic vehicular mobility simulator called ICARS, to illustrate the feasibility of the proposed approach and corroborate our theoretical findings.

Both work have been tested in real with a platoon of 3 up to 4 cars.

### 6.2.3. High speed visual servoing

**Participants:** Franco Fusco (PhD, LS2N-ARMEN), Olivier Kermorgant (LS2N-ARMEN), Philippe Martinet

Controlling high speed robot with visual feedback may require to develop more complex models including the dynamics of the robots and the environment. Some previous work done in the field of dynamic visual feedback of parallel robots [42] have demonstrated the efficiency regarding the classical Joint computed torque control. Also, it has been shown that it is also possible to develop more complex interaction models [20].

In recent years, many efforts have been dedicated to extend Sampling-based planning algorithms to solve problems involving constraints, such as geometric loop-closure, which lead the valid Configuration Space to collapse to a lower-dimensional manifold. One proposed solution considers an approximation of the constrained Configuration Space that is obtained by relaxing constraints up to a desired tolerance. The resulting set has then non-zero measure, allowing therefore to exploit classical planning algorithms to search for a path that connects two given states. When the constraints involve kinematic loops in the system, relaxation generally bears to undesired contact forces, which needs to be compensated during execution by a proper control action. We propose a new tool that exploits relaxation to plan in presence of constraints [32]. Local motions inside the approximated manifold are found as the result of an iterative scheme that uses Quadratic Optimization to proceed towards a new sample without falling outside the relaxed region. By properly guiding the exploration, paths are found with smaller relaxation factors and the need of a dedicated controller to compensate errors is reduced. We complete the analysis by showing the feasibility of the approach with experiments on a real manipulator platform.

The commonly exploited approach in visual servoing is to use a model that expresses the rate of change of a set of features as a function of sensor twist. These schemes are commonly used to obtain a velocity command, which needs to be tracked by a low-level controller. Another approach that can be exploited consists in going one step further and to consider an acceleration model for the features. This strategy allows also to obtain a natural and direct link with the dynamic model of the controlled system. The work done in [13] aims at comparing the use of velocity and acceleration-based models in feed-back linearization for Visual Servoing. We consider the case of a redundant manipulator and discuss what this implies for both control techniques. By means of simulations, we show that controllers based on features acceleration give better results than those based on velocity in presence of noisy feedback signals.

We are working to propose new prediction models for Visual Predictive Control that can lead to both better motions in the feature space and shorter sensor trajectories in 3D. Contrarily to existing local models based only on the Interaction Matrix, it is proposed to integrate acceleration information provided by second-order models. This helps to better estimate the evolution of the image features, and consequently to evaluate control inputs that can properly steer the system to a desired configuration. By means of simulations, the performances of these new predictors are shown and compared to those of a classical model. Real experiments confirm the validity of the approach and show that the increased complexity.

#### 6.2.4. Proactive and social navigation

**Participants:** Maria Kabtoul (PhD), Wanting Jin (Master), Anne Spalanzani (CHROMA), Philippe Martinet, Paolo Salaris

In the last decade, many works have been done concerning navigation of robots among humans [34], [27] or human robots interaction [22], [31]. In very few cases, a robot can realize an intention to move.

In this work, we would like that robots can express their needs for sharing spaces with humans in order to perform their task (i.e. navigation in crowded environments). This requires to be proactive and adapt to the behavior by exploiting the potential collaborative characteristics of the nearby environment of the robots.

In the framework of the ANR project HIANIC, Maria Kabtoul is doing her PhD on the topic Proactive Social navigation for autonomous vehicles among crowds. We consider shared spaces where humans and cars are able to evolve simultaneously. The first step done in this way is to introduce a pedestrian to vehicle interaction behavioral model. The model estimates the pedestrian's cooperation with the vehicle in an interaction scenario by a quantitative time-varying function. Then, the trajectory of the pedestrian is predicted based on its cooperative behavior. Both parts of the model are tested and validated using real-life recorded scenarios of pedestrian-vehicle interaction. The model is capable of describing and predicting agents' behaviors when interacting with a vehicle in both lateral and frontal crossing scenarios.



In the framework of the ANR project MOBI-DEEP, we have addressed the problem of navigating a robot in a constrained human-like environment. We provide a method to generate a control strategy that enables the robot to proactively move in order to induce desired and socially acceptable cooperative behaviors in neighboring pedestrians. Contrary to other control strategies that simply aim to passively avoid neighboring pedestrians, this approach greatly simplifies the navigation task for both robots and humans, especially in crowded and constrained environments. In order to reach this objective, the co-navigation process between humans and robots is formalized as a multi-objective optimization problem and a control strategy for the robot is obtained by using the Model Predictive Control (MPC) approach. The Social Force Model (SFM) is used to predict the human motion in cooperative situations. Different social behaviors of humans when moving in a group are also taken into account to generate the proper robot motion. Moreover, a switching strategy between purely reactive (if cooperation is not possible) and proactive-cooperative planning depending on the evaluation of the human intentions is also provided. Simulations under different navigation scenarios show how the proactive-cooperative planner enables the robot to generate more socially and understandable behaviors.

This work has been done by Wanting Jin during her Master thesis [37].

### 6.2.5. Safe navigation

**Participants:** Luiz Guardini (PhD), Anne Spalanzani (CHROMA), Christian Laugier (CHROMA), Philippe Martinet, Anh-Lam Do (Renault), Thierry Hermitte (Renault)

Today, car manufacturer are selling systems to brake in presence of obstacle. Those systems are based on the fact that the risk of collision is always detected and well evaluated. Their action are limited on brake only, which is in some case not sufficient to limit the risk. A global and safe system must be more efficient in environment perception awareness and also in action to be decided (break, steer, acceleration). In such a case, it is very complicated to find the best solution as long as we have to evaluate the different solutions in a near horizon in terms of risk of colisions and severity injuries. Car manufacturer are interested to find solution (i.e evaluation of trajectories (planification and action) in terms of risks and injuries.

Evaluating a scene to perform a collision avoidance maneuver is a hard task for both humans and (semi-) autonomous vehicles. There are some cases though that collision avoidance is inevitable. Interpreting the scene for a possible collision avoidance is difficult already a difficult task. Choosing how to mitigate the damage seems even harder, specially when humans have only a split of second to decide how to proceed.

Intending to decrease the reaction time and to increase safety on dangerous driving situations, one can rely on intelligent systems. Nevertheless, autonomous vehicles simulation and testing usually focus on risk assessment and path planing on regular driving conditions [40]. For instance, Waymo from Google, still do not have the full capability of avoiding collision initiated by other vehicles [28].

Developing Advanced Driver Assistance Systems (ADAS) technologies is one alternative for these emergency scenarios. It includes systems such as Active Braking System (ABS), Forward Collision Warning (FCW) and Collision Avoidance (CA). The latter is one of the most complex systems developed in order to assure safety. It perceives technologies such as Advanced Emergency Braking (AEB) and Autonomous Emergency Steering (AES) System. Those systems attempt to avoid the crash or at least reduce its severity. Developing a CA system starts by assessing the available information in the scene. This is made by establishing safe zones that the vehicle can access. The notion of safety of severity is usually addressed by the concept of risk. Risk can be intuitively understood as the likelihood and severity of the damage that an object of interest may suffer or cause in the future. Threat Assessment (also referred as Risk Assessment or Hazard Assessment) makes use of such concept.

The excellence of the data evidenced in the scene plays a major role in risk assessment and mitigation. Up to date, objects in the scene are not contextualized. For instance, pedestrians are treated as forbidden zones whereas cars are allowed to be collided when mitigation is necessary. This might be a correct assessment in some cases, but not always. The injury risk changes independently to each object according to aspects on the scene, such as the impact velocity and angle of collision.



This work focus on the development of a probabilistic cost map that expresses the Probability of Collision with Injury Risk (PCIR). On top of the information gathered by sensors, it includes the severity of injury in the event of a collision between ego and the objects in the scene. This cost map provides enhanced information to perform vehicle motion planning in emergency trajectories where collision is impending.

We represent the environment though probabilistic occupancy grids. It endures agile and robust sensor interpretation mechanisms and incremental discovery procedures. It also handles uncertainty thanks to probabilistic reasoning [25].

We use the Conditional Monte Carlo Dense Occupancy Tracker (CMCDOT developed in CHROMA). It is a generic spatial occupancy tracker that infers dynamics of the scene through a hybrid representation of the environment. The latter consists of static and dynamic occupancy, empty spaces and unknown areas. This differentiation enables the use of state-specific models as well as relevant confidence estimation and management of dataless areas [51].

Although CMCDOT occupancy grid leads to a very reliable global occupancy of the environment, it works on a sub-object level, meaning that the grid by itself does not carry the information on object classification. To overcome this, Erkent et al [26] proposes a method, which estimates an occupancy grid containing detailed semantic information. The semantic characteristics include classes like road, car, pedestrian, sidewalk, building, vegetation, etc.

The proposed Probabilistic risk map has been built and validation has been done in simulation using Gazebo using different scenarios (identified by the car manufacturer).

### 6.2.6. 3D Autonomous navigation using Model Predictive Path Integral approach

**Participants:** Ihab Mohamed (PhD), Guillaume Allibert, Philippe Martinet

Having a safe and reliable system for autonomous navigation of autonomous systems such as Unmanned Aerial Vehicles (UAVs) is a highly challenging and partially solved problem for robotics communities, especially for cluttered and GPS-denied environments such as dense forests, crowded offices, corridors, and warehouses. Such a problem is very important for solving many complex applications, such as surveillance, search-and-rescue, and environmental mapping. To do so, UAVs should be able to navigate with complete autonomy while avoiding all kinds of obstacles in real-time. To this end, they must be able to (i) perceive their environment, (ii) understand the situation they are in, and (iii) react appropriately.

To solve this problem, the applications of the path-integral control theory have recently become more prevalent. One of the most noteworthy works is Williams's iterative path integral method, namely, Model Predictive Path Integral (MPPI) control framework Williams et al. [53]. In this method, the control sequence is iteratively updated to obtain the optimal solution based on importance sampling of trajectories. In Williams et al [54], authors derived a different iterative method in which the control- and noise-affine dynamics constraints, on the original MPPI framework, are eliminated. This framework is mainly based on the information-theoretic interpretation of optimal control using KL-divergence and free energy, while it was previously based on the linearization of Hamilton-Jacob Bellman (HJB) equation and application of Feynman-Kac lemma.

The attractive features of MPPI controller, over alternative methods, can be summarized as: (i) a derivative-free optimization method, i.e., no need for derivative information to find the optimal solution; (ii) no need for approximating the system dynamics and cost functions with linear and quadratic forms, i.e., non-linear and non-convex functions can be naturally employed, even that dynamics and cost models can be easily represented using neural networks; (iii) planning and execution steps are combined into a single step, providing an elegant control framework for autonomous vehicles.

In the context of autonomous navigation, it is observed that the MPPI controller has been mainly applied to the tasks of aggressive driving and UAVs navigation in cluttered environments. For instance, to navigate in cluttered environments, the obstacle map is assumed to be known (either available a priori or built off-line), and only static 2D floor-maps are used. Conversely, in practice, the real environments are often partially observable, with dynamic obstacles. Moreover, only 2D navigation tasks are performed, which limits the applicability of the control framework.

For this reason, our work focuses on MPPI for 2D and 3D navigation tasks in cluttered environments, which are inherently uncertain and partially observable. To the best of our knowledge, this point has not been reported in the literature, presenting a generic MPPI framework that opens up new directions for research.

We propose a generic Model Predictive Path Integral (MPPI) control framework that can be used for 2D or 3D autonomous navigation tasks in either fully or partially observable environments, which are the most prevalent in robotics applications. This framework exploits directly the 3D-voxel grid, e.g., OctoMap [35], acquired from an on-board sensing system for performing collision-free navigation. We test the framework, in realistic RotorS-based simulation, on goal-oriented quadrotor navigation tasks in a 2D/3D cluttered environment, for both fully and partially observable scenarios. Preliminary results demonstrate that the proposed framework works perfectly, under partial observability, in 2D and 3D cluttered environments.

We demonstrate our proposed framework on a set of simulated quadrotor navigation tasks in a 2D and 3D cluttered environment, assuming that: (i) there is a priori knowledge about the environment (namely, fully observable case); (ii) there is not any a priori information (namely, partially observable case); here, the robot is building and updating the map, which represents the environment, online as it goes along.

### 6.2.7. Perception-aware trajectory generation for robotic systems

Participant: Paolo Salaris, Marco Cagnetti (PostDoc, RAINBOW), Valerio Paduano (Master, RAINBOW), Paolo Robuffo Giordano (RAINBOW)

We now focus on our planned research activities on task-oriented perception and control of a robotic system engaged in executing a task. The main objective is to improve the execution of a given task by fruitfully *coupling action and perception*. We aim at finding the correct balance between efficient task execution and quality of the information content since the amount of the latter has an impact on the possibility of correctly executing the task. Indeed, a robot needs to solve an estimation problem in order to safely move in unstructured environments and accomplishing a task. For instance, it has to self-calibrate and self-localize w.r.t. the environment while, at the same time, a map of the surroundings may be built. These possibilities are highly influenced by the quality and amount of sensor information (i.e., available measurements), especially in case of limited sensing capabilities and/or low cost (noisy) sensors.

For nonlinear systems (i.e., the most of the robotics systems of our interest) the amount and quality of the collected information depends on the robot trajectories. It is hence important to find, among all possible trajectories able to accomplish a task, the most informative ones. One crucial point in this context, also known as *active sensing control*, is the choice of an appropriate *measure of information* to be optimized. The Observability Gramian (OG) measures the level of observability of the *initial state* and hence, its maximization (e.g. by maximizing its smallest eigenvalue) actually increase the amount of information about the initial state and hence improves the performances in estimating (observing) the initial state of the robot. However, when the objective is to estimate the current/future state of the robot (which is implicitly the goal of most of the previous literature in this subject, and of our research too), the OG is *not* the right metric even if is often used in the literature for this goal. Recently, in [12], we showed that, the right metric is instead the *Constructibility Gramian* (CG) that indeed quantifies the amount of information about the current/future state, which is obviously the state of interest for the sake of motion control/task execution. We then propose an *online* optimal sensing control problem whose objective is to determine at *runtime*, i.e. anytime a new estimate is provided by the employed observer (an EKF in our case), the future trajectory that maximizes the smallest eigenvalue of the CG. We applied our machinery to two robotics platforms: a unicycle vehicle and a quadrotor UAV moving on a vertical plane, both measuring two distances w.r.t. two markers located in the environment. Results show the effectiveness of our solution not only for pure robot's state estimation, but also with instances of active self-calibration and map building.

The proposed solution is not able to cope with the process/actuation noise as CG is not able to measure its degrading effects on the current amount of the collected information and by consequence its negative effects in the estimation process. For all the cases where an EKF is used as an observer, we overcame this issue in [21] where we minimized the largest eigenvalue of the covariance matrix of the EKF that is the solution of the Riccati differential equation.

We also extended the methodology to the problem of shared control by proposing a shared control active perception method aimed at fusing the high-level skills of a human operator in accomplishing complex tasks with the capabilities of a mobile robot in maximizing the acquired information from the onboard sensors for improving its state estimation (localization). In particular, a persistent autonomous behaviour, expressed in terms of a cyclic motion represented by a closed B-Spline, is executed by the robot. The human operator is in charge of modifying online some geometric properties of this path for executing a given task (e.g., exploration). The path is then autonomously processed by the robot, resulting in an actual path that tries to follow the human's commands while, at the same time, maximizing online the acquired information from the sensors. This work has been done by Valerio Paduano during his Master thesis [43] and submitted to ICRA 2020.

Recently we are also working on extending the methodology to Multiple Robot Systems (in particular a group of quadrotor UAVs). In this context, the goal is to propose an optimal and *online* trajectory planning framework for addressing the localization problem of a group of multiple robots without requiring the rigidity condition. In particular, by leveraging our recent work on optimal online active estimation, we will propose the use of CG for quantifying the localization accuracy, and develop an *online* decentralized optimal trajectory planning able to optimize the CG during the robot motion. We particularly focus on the *online* component, since the planned trajectory are *continuously refined* during the robot motion by exploiting the (continuously converging) decentralized estimation of the robot relative poses. In order to illustrate the approach, we will consider the localization problem for a group of quadrotor UAVs measuring relative distances with maximum range sensing constraints and a decentralized Extended Kalman Filter [39] that estimates the relative configuration of each robot in the group w.r.t. a special one (randomly chosen in the group).

## COATI Project-Team

# 7. New Results

## 7.1. Network Design and Management

**Participants:** Julien Bensmail, Jean-Claude Bermond, Christelle Caillouet, David Coudert, Frédéric Giroire, Frédéric Havet, Nicolas Nisse, Stéphane Pérennes, Joanna Moulrierac, Foivos Fioravantes, Adrien Gausseran, Andrea Tomassilli.

Network design is a very wide subject which concerns all kinds of networks. In telecommunications, networks can be either physical (backbone, access, wireless, ...) or virtual (logical). The objective is to design a network able to route a (given, estimated, dynamic, ...) traffic under some constraints (e.g. capacity) and with some quality-of-service (QoS) requirements. Usually the traffic is expressed as a family of requests with parameters attached to them. In order to satisfy these requests, we need to find one (or many) paths between their end nodes. The set of paths is chosen according to the technology, the protocol or the QoS constraints.

We mainly focus on the following topics: Firstly, we study Software Defined Networking (SDN) and Network Function Virtualization (NFV) and how to exploit their potential benefits. We propose algorithms for the Provisioning Service Function Chains (SFC) and algorithms to reconfigure the SFC in order to improve the network operational costs without any interruption (with a *make-before-break approach*) and Virtual Network Functions (VNF) placement algorithms to address the mono- and multi-tenant issues in edge and core networks. We also propose algorithms for distributed Mininet<sup>0</sup> in order to improve the performance, and also bandwidth-optimal failure recovery scheme for robust programmable networks. Secondly, we study optimization problems within optical networks: wavelength reconfiguration for seamless migration and spectrum assignment in elastic optical tree-networks. Thirdly, we study the scheduling of network tasks within a data center while taking into account the communication between the network resources. We also study distributed link scheduling in wireless networks. Finally, we investigate on the placement of drones for maximizing the coverage of a landscape by drones in order to localize targets or collect data from sensors.

### 7.1.1. Software Defined Networks and Network Function Virtualization

Recent advances in networks such as Software Defined Networking (SDN) and Network Function Virtualization (NFV) are changing the way network operators deploy and manage Internet services. On the one hand, SDN introduces a logically centralized controller with a global view of the network state. On the other hand, NFV enables the complete decoupling of network functions from proprietary appliances and runs them as software applications on general purpose servers. In such a way, network operators can dynamically deploy Virtual Network Functions (VNFs). SDN and NFV, both separately, bring to network operators new opportunities for reducing costs, enhancing network flexibility and scalability, and shortening the time-to-market of new applications and services. Moreover, the centralized routing model of SDN jointly with the possibility of instantiating VNFs on demand may open the way for an even more efficient operation and resource management of networks. For instance, an SDN/NFV-enabled network may simplify the Service Function Chain (SFC) deployment and provisioning by making the process easier and cheaper. We addressed several questions in this context.

In [15], we aim at investigating how to leverage both SDN and NFV in order to exploit their potential benefits. We took steps to address the new opportunities offered in terms of network design, network resilience, and energy savings, and the new problems that arise in this new context, such as the optimal network function placement in the network. We show that a symbiosis between SDN and NFV can improve network performance and significantly reduce the network's Capital Expenditure (CapEx) and Operational Expenditure (OpEx).

<sup>0</sup>Mininet provides a virtual test bed and development environment for software-defined networks (SDN). See <http://mininet.org>.

In [50], [57], [58], we consider the problem of reconfiguring SFC with the goal of bringing the network from a sub-optimal to an optimal operational state. We propose optimization models based on the *make-before-break* mechanism, in which a new path is set up before the old one is torn down. Our method takes into consideration the chaining requirements of the flows and scales well with the number of nodes in the network. We show that, with our approach, the network operational cost defined in terms of both bandwidth and installed network function costs can be reduced and a higher acceptance rate can be achieved, while not interrupting the flows.

In [59], we consider the placement of functions in 5G networks in which functions must not only be deployed in large central data centers, but also in the edge. We propose an algorithm that solves the Virtual Network Function Chain Placement Problem allowing a fine management of these rare resources in order to respond to the greatest number of requests possible. Because networks can be divided into several entities belonging to different tenants who are reluctant to reveal their internal topologies, we propose a heuristic that allows the NFV orchestrator to place the function chains based only on an abstract view of the infrastructure network. We leverage this approach to address the complexity of the problem in large mono- or multi-tenant networks. We analyze the efficiency of our algorithm and heuristic with respect to a wide range of parameters and topologies.

In [53], [80], [69], we rethink the network dimensioning problem with protection against Shared Risk Link Group (SLRG) failures in the SDN context. We propose a path-based protection scheme with a global rerouting strategy, in which, for each failure situation, there may be a new routing of all the demands. Our optimization task is to minimize the needed amount of bandwidth. After discussing the hardness of the problem, we develop a scalable mathematical model that we handle using the Column Generation technique. Through extensive simulations on real-world IP network topologies and on random generated instances, we show the effectiveness of our method. Finally, our implementation in OpenDaylight demonstrates the feasibility of the approach and its evaluation with Mininet shows that technical implementation choices may have a dramatic impact on the time needed to reestablish the flows after a failure takes place.

Finally, in [49], [78], [79], we consider the problem of performing large scale SDN networks simulations in a distributed environment. Indeed, networks have become complex systems that combine various concepts, techniques, and technologies. Hence, modelling or simulating them is now extremely complicated and researchers massively resort to prototyping techniques. Among other tools, Mininet is the most popular when it comes to evaluate SDN propositions. It allows to emulate SDN networks on a single computer. However, under certain circumstances experiments (e.g., resource intensive ones) may overload the host running Mininet. To tackle this issue, we propose Distrinet [49], [78], [79], a way to distribute Mininet over multiple hosts. Distrinet uses the same API than Mininet, meaning that it is compatible with Mininet programs. Distrinet is generic and can deploy experiments in Linux clusters or in the Amazon EC2 cloud. Thanks to optimization techniques, Distrinet minimizes the number of hosts required to perform an experiment given the capabilities of the hosting infrastructure, meaning that the experiment is run in a single host (as Mininet) if possible. Otherwise, it is automatically deployed on a platform using a minimum amount of resources in a Linux cluster or with a minimum cost in Amazon EC2.

## 7.1.2. Optimization of optical networks operation

### 7.1.2.1. Wavelength Defragmentation for Seamless Migration

Dynamic traffic in optical networks leads to spectrum fragmentation, which significantly reduces network performance, i.e., increases blocking rate and reduces spectrum usage. Telecom operators face the operational challenge of operating non-disruptive defragmentation, i.e., within the *make-before-break* paradigm when dealing with lightpath rerouting in wavelength division multiplexed (WDM) fixed-grid optical networks. In [39], we propose a *make-before-break* (MBB) Routing and Wavelength Assignment (RWA) defragmentation process, which provides the best possible lightpath network provisioning, i.e., with minimum bandwidth requirement. We tested extensively the models and algorithms we propose on four network topologies with different GoS (Grade of Service) defragmentation triggering events. We observe that, for a given throughput, the spectrum usage of the best *make-before-break* lightpath rerouting is always less than 2.5% away from that of an optimal lightpath provisioning.

### 7.1.2.2. *On spectrum assignment in elastic optical tree-networks*

To face the explosion of the Internet traffic, a new generation of optical networks is being developed; the Elastic Optical Networks (EONs). EONs use the optical spectrum efficiently and flexibly, but that gives rise to more difficulty in the resource allocation problems. In [31], we study the problem of Spectrum Assignment (SA) in Elastic Optical Tree-Networks. Given a set of traffic requests with their routing paths (unique in the case of trees) and their spectrum demand, a spectrum assignment consists in allocating to each request an interval of consecutive slots (spectrum units) such that a slot on a given link can be used by at most one request. The objective of the SA problem is to find an assignment minimizing the total number of spectrum slots to be used. We prove that SA is NP-hard in undirected stars of 3 links and in directed stars of 4 links, and show that it can be approximated within a factor of 4 in general stars. Afterwards, we use the equivalence of SA with a graph coloring problem (interval coloring) to find constant-factor approximation algorithms for SA on binary trees with special demand profiles.

## 7.1.3. *Scheduling*

### 7.1.3.1. *When Network Matters: Data Center Scheduling with Network Tasks*

We consider in [51] the placement of jobs inside a data center. Traditionally, this is done by a task orchestrator without taking into account network constraints. According to recent studies, network transfers represent up to 50% of the completion time of classical jobs. Thus, network resources must be considered when placing jobs in a data center. In this paper, we propose a new scheduling framework, introducing network tasks that need to be executed on network machines alongside traditional (CPU) tasks. The model takes into account the competition between communications for the network resources, which is not considered in the formerly proposed scheduling models with communication. Network transfers inside a data center can be easily modeled in our framework. As we show, classical algorithms do not efficiently handle a limited amount of network bandwidth. We thus propose new provably efficient algorithms with the goal of minimizing the makespan in this framework. We show their efficiency and the importance of taking into consideration network capacity through extensive simulations on workflows built from Google data center traces.

### 7.1.3.2. *Distributed Link Scheduling in Wireless Networks*

In [55], we investigate distributed transmission scheduling in wireless networks. Due to interference constraints, “neighboring links” cannot be simultaneously activated, otherwise transmissions will fail. Here, we consider any binary model of interference. We use the model described by Bui, Sanghavi, and Srikant in [85], [93]. We assume that time is slotted and during each slot there are two phases: one control phase which determines what links will be activated and a data phase in which data are sent. We assume random arrivals on each link during each slot, so that a queue is associated to each link. Since nodes do not have a global knowledge of the network, our aim (like in [85], [93]) is to design for the control phase a distributed algorithm which determines a set of non-interfering links. To be efficient the control phase should be as short as possible; this is done by exchanging control messages during a constant number of mini-slots (constant overhead). In this paper, we design the first fully distributed local algorithm with the following properties: it works for any arbitrary binary interference model; it has a constant overhead (independent of the size of the network and the values of the queues), and it does not require any knowledge of the queue-lengths. We prove that this algorithm gives a maximal set of active links, where in each interference set there is at least one active link. We also establish sufficient conditions for stability under general Markovian assumptions. Finally, the performance of our algorithm (throughput, stability) is investigated and compared via simulations to that of previously proposed schemes.

### 7.1.3.3. *Backbone colouring and algorithms for TDMA scheduling*

We investigate graph colouring models for the purpose of optimizing TDMA link scheduling in Wireless Networks. Inspired by the BPRN-colouring model recently introduced by Rocha and Sasaki, we introduce a new colouring model, namely the BMRN-colouring model, which can be used to model link scheduling problems where particular types of collisions must be avoided during the node transmissions.



In [25], we initiate the study of the BMRN-colouring model by providing several bounds on the minimum number of colours needed to BMRN-colour digraphs, as well as several complexity results establishing the hardness of finding optimal colourings. We also give a special focus on these considerations for planar digraph topologies, for which we provide refined results. Some of these results extend to the BPRN-colouring model as well. We notably prove that every planar digraph can be 8-BMRN\*-coloured, while there exist planar digraphs for which 8 colours are needed in a BMRN\*-colouring [72]. We also proved that the problem of deciding whether a planar digraph can be  $k$ -BMRN\*-coloured is NP-hard for every  $k \in \{3, \dots, 6\}$ .

### 7.1.4. Optimizing drone coverage

#### 7.1.4.1. Self-organized UAV-based Supervision and Connectivity

The use of drones has become more widespread in recent years. Many use cases have been developed involving these autonomous vehicles, ranging from simple delivery of packages to complex emergency situations following catastrophic events. The miniaturization and very low cost of these machines make it possible today to create large meshes to ensure network coverage in disaster areas, for instance. However, the problems of scaling up and self-organization are necessary to solve problems in these use cases.

In the position paper [45], we first present different new requirements for the deployment of unmanned aerial vehicles (UAV) networks, involving the use of many drones. Then, we introduce solutions from distributed algorithms and real-time data processing to ensure quasi-optimal solutions to the raised problems.

In [44], [65], we propose VESPA, a distributed algorithm using only one-hop information of the drones, to discover targets with unknown location and auto-organize themselves to ensure connectivity between them and the sink in a multi-hop aerial wireless network. We prove that connectivity, termination and coverage are preserved during all stages of our algorithm, and we evaluate the algorithm performances through simulations. Comparison with a prior work shows the efficiency of VESPA both in terms of discovered targets and number of used drones.

#### 7.1.4.2. Optimal placement of drones for fast sensor energy replenishment using wireless power transfer

Lifetime is the main issue of wireless sensors networks. Since the nodes are often placed in inaccessible places, the replacement of their battery is not an easy task. Moreover, the node maintenance is a costly and time consuming operation when the nodes are high in numbers. Energy harvesting technologies have recently been developed to replenish part or all of the required energy that allows a node to function. In [47], [48], we use dedicated chargers carried by drones that can fly over the network and transmit energy to the nodes using radio-frequency (RF) signals. We formulate and optimally solve the Optimal Drone Placement and Planning Problem (OD3P) by using a given number of flying drones, in order to efficiently recharge wireless sensor nodes. Unlike other works in the literature, we assume that the drones can trade altitude with coverage and recharge power, while each drone can move across different positions in the network to extend coverage. We present a linear program as well as a fast heuristic algorithm to meet the minimum energy demands of the nodes in the shortest possible amount of time. Our simulation results show the effectiveness of our approaches for network scenarios with up to 50 sensors and a  $50 \times 50$ m terrain size.

#### 7.1.4.3. Efficient Data Collection and Tracking with Flying Drones

Data collection is an important mechanism for wireless sensor networks to be viable. In [34], we address the Aerial Data Collection Problem (ADCP) from a set of mobile wireless sensors located on the ground, using a fleet of flying devices. The objective is i) to deploy a set of UAVs in a 3D space to cover and collect data from all the mobile wireless sensors at each time step through a ground-to-air communication, ii) to send these data to a central base station using multi-hop wireless air-to-air communications through the network of UAVs, iii) while minimizing the total deployment cost (communication and deployment) over time. The Aerial Data Collection Problem (ADCP) is a complex time and space coverage, and connectivity problem. We first present a mixed-integer linear program solving ADCP optimally for small instances. Then, we develop a second model solved by column generation for larger instances, with optimal or heuristic pricing programs. Results show that our approach provides very accurate solutions minimizing the data collection cost. Moreover, only a very small number of columns are generated throughout the resolution process, showing the efficiency of our approach.

### 7.1.5. Other results

#### 7.1.5.1. The Structured Way of Dealing with Heterogeneous Live Streaming Systems

In peer-to-peer networks for video live streaming, peers can share the forwarding load in two types of systems: unstructured and structured. In unstructured overlays, the graph structure is not well-defined, and a peer can obtain the stream from many sources. In structured overlays, the graph is organized as a tree rooted at the server and parent-child relationships are established between peers. Unstructured overlays ensure robustness and a higher degree of resilience compared to the structured ones. Indeed, they better manage the dynamics of peer participation or churn. Nodes can join and leave the system at any moment. However, they are less bandwidth efficient than structured overlays. In [54], we propose new simple distributed repair protocols for video live streaming structured systems. We show, through simulations and with real traces from Twitch, that structured systems can be very efficient and robust to failures, even for high churn and when peers have very heterogeneous upload bandwidth capabilities.

#### 7.1.5.2. Optimal SF Allocation in LoRaWAN Considering Physical Capture and Imperfect Orthogonality

In [46], we propose a theoretical framework for maximizing the long range wide-area networks (LoRaWAN) capacity in terms of the number of end nodes, when they all have the same traffic generation process. The model optimally allocates the spreading factor to the nodes so that attenuation and collisions are optimized. We use an accurate propagation model considering Rayleigh channel, and we take into account physical capture and imperfect spreading factors (SF) orthogonality while guaranteeing a given transmission success probability to each served node in the network. Numerical results show the effectiveness of our SF allocation policy. Our framework also quantifies the maximum capacity of single cell networks and the gain induced by multiplying the gateways on the covered area. We finally evaluate the impact of physical capture and imperfect SF orthogonality on the SF allocation and network performances.

## 7.2. Graph Algorithms

**Participants:** Julien Bensmail, Jean-Claude Bermond, David Coudert, Frédéric Giroire, Frédéric Havet, Emanuele Natale, Nicolas Nisse, Stéphane Pérennes, Francois Dross, Fionn Mc Inerney, Thibaud Trollet.

COATI is interested in the algorithmic aspects of Graph Theory. In general we try to find the most efficient algorithms to solve various problems of Graph Theory and telecommunication networks. We use Graph Theory to model various network problems. We study their complexity and then we investigate the structural properties of graphs that make these problems hard or easy.

### 7.2.1. Complexity of graph problems

#### 7.2.1.1. Fully Polynomial FPT Algorithms for Some Classes of Bounded Clique-width Graphs.

Recently, hardness results for problems in P were achieved using reasonable complexity theoretic assumptions such as the Strong Exponential Time Hypothesis. According to these assumptions, many graph theoretic problems do not admit truly subquadratic algorithms. A central technique used to tackle the difficulty of the above mentioned problems is fixed-parameter algorithms with polynomial dependency in the fixed parameter (P-FPT). Applying this technique to clique-width, an important graph parameter, remained to be done. In [35], we study several graph theoretic problems for which hardness results exist such as cycle problems, distance problems and maximum matching. We give hardness results and P-FPT algorithms, using clique-width and some of its upper bounds as parameters. We believe that our most important result is an algorithm in  $O(k^4 \cdot n + m)$ -time for computing a maximum matching where  $k$  is either the modular-width of the graph or the  $P_4$ -sparseness. The latter generalizes many algorithms that have been introduced so far for specific subclasses such as cographs. Our algorithms are based on preprocessing methods using modular decomposition and split decomposition. Thus they can also be generalized to some graph classes with unbounded clique-width.

### 7.2.1.2. Explicit Linear Kernels for Packing Problems

During the last years, several algorithmic meta-theorems have appeared (Bodlaender et al. [83], Fomin et al. [88], Kim et al. [90]) guaranteeing the existence of linear kernels on sparse graphs for problems satisfying some generic conditions. The drawback of such general results is that it is usually not clear how to derive from them constructive kernels with reasonably low explicit constants. To fill this gap, we recently presented [89] a framework to obtain explicit linear kernels for some families of problems whose solutions can be certified by a subset of vertices. In [37], we enhance our framework to deal with packing problems, that is, problems whose solutions can be certified by collections of *subgraphs* of the input graph satisfying certain properties.  $\mathcal{F}$ -Packing is a typical example: for a family  $\mathcal{F}$  of connected graphs that we assume to contain at least one planar graph, the task is to decide whether a graph  $G$  contains  $k$  vertex-disjoint sub-graphs such that each of them contains a graph in  $\mathcal{F}$  as a minor. We provide explicit linear kernels on sparse graphs for the following two orthogonal generalizations of  $\mathcal{F}$ -Packing: for an integer  $\ell \geq 1$ , one aims at finding either minor-models that are pairwise at distance at least  $\ell$  in  $G$  ( $\ell$ - $\mathcal{F}$ -Packing), or such that each vertex in  $G$  belongs to at most  $\ell$  minors-models ( $\mathcal{F}$ -Packing with-Membership). Finally, we also provide linear kernels for the versions of these problems where one wants to pack *subgraphs* instead of minors.

### 7.2.1.3. Low Time Complexity Algorithms for Path Computation in Cayley Graphs.

We study the problem of path computation in Cayley Graphs (CG) from an approach of word processing in groups. This approach consists in encoding the topological structure of CG in an automaton called Diff, then techniques of word processing are applied for computing the shortest paths. In [17], we present algorithms for computing the  $K$ -shortest paths, the shortest disjoint paths and the shortest path avoiding a set of nodes and edges. For any CG with diameter  $D$ , the time complexity of the proposed algorithms is  $O(KD|\text{Diff}|)$ , where  $|\text{Diff}|$  denotes the size of Diff. We show that our proposal outperforms the state of art of topology-agnostic algorithms for disjoint shortest paths and stays competitive with respect to proposals for specific families of CG. Therefore, the proposed algorithms set a base in the design of adaptive and low-complexity routing schemes for networks whose interconnections are defined by CG.

### 7.2.1.4. Convex hull in graphs.

In [40], we prove that, given a closure function the smallest preimage of a closed set can be calculated in polynomial time in the number of closed sets. This implies that there is a polynomial time algorithm to compute the convex hull number of a graph, when all its convex subgraphs are given as input. We then show that deciding if the smallest preimage of a closed set is logarithmic in the size of the ground set is LOGSNP-hard if only the ground set is given. A special instance of this problem is to compute the dimension of a poset given its linear extension graph, that is conjectured to be in P.

The intent to show that the latter problem is LOGSNP-complete leads to several interesting questions and to the definition of the isometric hull, i.e., a smallest isometric subgraph containing a given set of vertices  $S$ . While for  $|S| = 2$  an isometric hull is just a shortest path, we show that computing the isometric hull of a set of vertices is NP-complete even if  $|S| = 3$ . Finally, we consider the problem of computing the isometric hull number of a graph and show that computing it is  $\Sigma_2^P$  complete.

## 7.2.2. Combinatorial games in graphs

### 7.2.2.1. Graph searching and combinatorial games in graphs.

The Network Decontamination problem consists of coordinating a team of mobile agents in order to clean a contaminated network. The problem is actually equivalent to tracking and capturing an invisible and arbitrarily fast fugitive. This problem has natural applications in network security in computer science or in robotics for search or pursuit-evasion missions. Many different objectives have been studied: the main one being the minimization of the number of mobile agents necessary to clean a contaminated network.

Many environments (continuous or discrete) have also been considered. In the book chapter [61], we focus on networks modeled by graphs. In this context, the optimization problem that consists of minimizing the number of agents has a deep graph-theoretical interpretation. Network decontamination and, more precisely, *graph searching* models, provide nice algorithmic interpretations of fundamental concepts in the Graph Minors theory by Robertson and Seymour.

For all these reasons, graph searching variants have been widely studied since their introduction by Breish (1967) and mathematical formalizations by Parsons (1978) and Petrov (1982). The book chapter [61] consists of an overview of the algorithmic results on graph decontamination and graph searching. Moreover, [19] is the preface to the special issue of TCS on the 8th Workshop on GRAPh Searching, Theory and Applications, Anogia, Crete, Greece, April 10 - April 13, 2017.

In [52], we focus on another game with mobile agents in a graph. Precisely, in the eternal domination game played on graphs, an attacker attacks a vertex at each turn and a team of guards must move a guard to the attacked vertex to defend it. The guards may only move to adjacent vertices on their turn. The goal is to determine the eternal domination number  $\gamma_{all}^\infty$  of a graph which is the minimum number of guards required to defend against an infinite sequence of attacks. [52] continues the study of the eternal domination game on strong grids  $P_n \boxtimes P_m$ . Cartesian grids  $P_n \square P_m$  have been vastly studied with tight bounds existing for small grids such as  $k \times n$  grids for  $k \in \{2, 3, 4, 5\}$ . It was recently proven that  $\gamma_{all}^\infty(P_n \square P_m) = \gamma(P_n \square P_m) + O(n + m)$  where  $\gamma(P_n \square P_m)$  is the domination number of  $P_n \square P_m$  which lower bounds the eternal domination number [91]. We prove that, for all  $n, m \in \mathbb{N}^*$  such that  $m \geq n$ ,  $\lfloor \frac{nm}{9} \rfloor + \Omega(n + m) = \gamma_{all}^\infty(P_n \boxtimes P_m) = \lceil \frac{nm}{9} \rceil + O(m\sqrt{n})$  (note that  $\lceil \frac{nm}{9} \rceil$  is the domination number of  $P_n \boxtimes P_m$ ). Our technique may be applied to other “grid-like” graphs.

In [66], we adapt the techniques of [91] to prove that the eternal domination number of strong grids is upper bounded by  $\frac{mn}{7} + O(m + n)$ . While this does not improve upon a recently announced bound of  $\lceil \frac{m}{3} \rceil \lceil \frac{n}{3} \rceil + O(m\sqrt{n})$  [52] in the general case, we show that our bound is an improvement in the case where the smaller of the two dimensions is at most 6179.

#### 7.2.2.2. The Orthogonal Colouring Game

In [18], we introduce the Orthogonal Colouring Game, in which two players alternately colour vertices (from a choice of  $m \in N$  colours) of a pair of isomorphic graphs while respecting the properness and the orthogonality of the colouring. Each player aims to maximize her score, which is the number of coloured vertices in the copy of the graph she owns. Our main result is that the second player has a strategy to force a draw in this game for any  $m \in N$  for graphs that admit a strictly matched involution. An involution  $\sigma$  of a graph  $G$  is strictly matched if its fixed point set induces a clique and any non-fixed point  $v \in V(G)$  is connected with its image  $\sigma(v)$  by an edge. We give a structural characterization of graphs admitting a strictly matched involution and bounds for the number of such graphs. Examples of such graphs are the graphs associated with Latin squares and sudoku squares.

In [62], we prove that recognising graphs that admit a strictly matched involution is NP-complete.

#### 7.2.2.3. Complexity of Games Compendium

Since games and puzzles have been studied under a computational lens, researchers unearthed a rich landscape of complexity results showing deep connections between games and fundamental problems and models in computer science. Complexity of Games (CoG, <https://steven3k.gitlab.io/isnphard-test/>) is a compendium of complexity results on games and puzzles. It aims to serve as a reference guide for enthusiasts and researchers on the topic and is a collaborative and open source project that welcomes contributions from the community.

### 7.2.3. Algorithms for social networks

#### 7.2.3.1. KADABRA, an Adaptive Algorithm for Betweenness via Random Approximation

In [32], we present KADABRA, a new algorithm to approximate betweenness centrality in directed and undirected graphs, which significantly outperforms all previous approaches on real-world complex networks. The efficiency of the new algorithm relies on two new theoretical contributions, of independent interest. The first contribution focuses on sampling shortest paths, a subroutine used by most algorithms that approximate betweenness centrality. We show that, on realistic random graph models, we can perform this task in time  $|E|^{\frac{1}{2}+o(1)}$  with high probability, obtaining a significant speedup with respect to the  $\Theta(|E|)$  worst-case performance. We experimentally show that this new technique achieves similar speedups on real-world complex networks, as well. The second contribution is a new rigorous application of the adaptive sampling technique. This approach decreases the total number of shortest paths that need to be sampled to compute

all betweenness centralities with a given absolute error, and it also handles more general problems, such as computing the  $k$  most central nodes. Furthermore, our analysis is general, and it might be extended to other settings.

### 7.2.3.2. Distributed Community Detection via Metastability of the 2-Choices Dynamics

In [56], we investigate the behavior of a simple majority dynamics on networks of agents whose interaction topology exhibits a community structure. By leveraging recent advancements in the analysis of dynamics, we prove that, when the states of the nodes are randomly initialized, the system rapidly and stably converges to a configuration in which the communities maintain internal consensus on different states. This is the first analytical result on the behavior of dynamics for non-consensus problems on non-complete topologies, based on the first symmetry-breaking analysis in such setting. Our result has several implications in different contexts in which dynamics are adopted for computational and biological modeling purposes. In the context of Label Propagation Algorithms, a class of widely used heuristics for community detection, it represents the first theoretical result on the behavior of a distributed label propagation algorithm with quasi-linear message complexity. In the context of evolutionary biology, dynamics such as the Moran process have been used to model the spread of mutations in genetic populations [Lieberman, Hauert, and Nowak 2005]; our result shows that, when the probability of adoption of a given mutation by a node of the evolutionary graph depends super-linearly on the frequency of the mutation in the neighborhood of the node and the underlying evolutionary graph exhibits a community structure, there is a non-negligible probability for species differentiation to occur.

### 7.2.3.3. On the Necessary Memory to Compute the Plurality in Multi-Agent Systems

Consensus and Broadcast are two fundamental problems in distributed computing, whose solutions have several applications. Intuitively, Consensus should be no harder than Broadcast, and this can be rigorously established in several models. Can Consensus be easier than Broadcast?

In models that allow noiseless communication, we prove in [60] a reduction of (a suitable variant of) Broadcast to binary Consensus, that preserves the communication model and all complexity parameters such as randomness, number of rounds, communication per round, etc., while there is a loss in the success probability of the protocol. Using this reduction, we get, among other applications, the first logarithmic lower bound on the number of rounds needed to achieve Consensus in the uniform GOSSIP model on the complete graph. The lower bound is tight and, in this model, Consensus and Broadcast are equivalent.

We then turn to distributed models with noisy communication channels that have been studied in the context of some bio-inspired systems. In such models, only one noisy bit is exchanged when a communication channel is established between two nodes, and so one cannot easily simulate a noiseless protocol by using error-correcting codes. An  $\Omega(\epsilon^{-2}n)$  lower bound on the number of rounds needed for Broadcast is proved by Boczkowski et al. [82] in one such model (noisy uniform PULL, where  $\epsilon$  is a parameter that measures the amount of noise). In such model, we prove a new  $\Theta(\epsilon^{-2}n \log n)$  bound for Broadcast and a  $\Theta(\epsilon^{-2} \log n)$  bound for binary Consensus, thus establishing an exponential gap between the number of rounds necessary for Consensus versus Broadcast.

### 7.2.3.4. How long does it take for all users in a social network to choose their communities?

In [30], we consider a community formation problem in social networks, where the users are either friends or enemies. The users are partitioned into conflict-free groups (i.e., independent sets in the conflict graph  $G^- = (V, E)$  that represents the enmities between users). The dynamics goes on as long as there exists any set of at most  $k$  users,  $k$  being any fixed parameter, that can change their current groups in the partition simultaneously, in such a way that they all strictly increase their utilities (number of friends i.e., the cardinality of their respective groups minus one). Previously, the best-known upper-bounds on the maximum time of convergence were  $O(|V|\alpha(G^-))$  for  $k \leq 2$  and  $O(|V|^3)$  for  $k = 3$ , with  $\alpha(G^-)$  being the independence number of  $G^-$ . Our first contribution consists in reinterpreting the initial problem as the study of a dominance ordering over the vectors of integer partitions. With this approach, we obtain for  $k \leq 2$  the tight upper-bound  $O(|V| \min \{ \alpha(G^-), \sqrt{|V|} \})$  and, when  $G^-$  is the empty graph, the exact value of order  $\frac{(2|V|)^{3/2}}{3}$ . The time of convergence, for any fixed  $k \geq 4$ , was conjectured to be polynomial. In this paper we disprove this. Specifically, we prove that for any  $k \geq 4$ , the maximum time of convergence is in  $\Omega(|V|\Theta(\log |V|))$ .



### 7.2.3.5. A Comparative Study of Neural Network Compression

There has recently been an increasing desire to evaluate neural networks locally on computationally-limited devices in order to exploit their recent effectiveness for several applications; such effectiveness has nevertheless come together with a considerable increase in the size of modern neural networks, which constitute a major downside in several of the aforementioned computationally-limited settings. There has thus been a demand of compression techniques for neural networks. Several proposals in this direction have been made, which famously include hashing-based methods and pruning-based ones. However, the evaluation of the efficacy of these techniques has so far been heterogeneous, with no clear evidence in favor of any of them over the others. In [70], we address this latter issue by providing a comparative study. While most previous studies test the capability of a technique in reducing the number of parameters of state-of-the-art networks, we follow [86] in evaluating their performance on basic architectures on the MNIST dataset and variants of it, which allows for a clearer analysis of some aspects of their behavior. To the best of our knowledge, we are the first to directly compare famous approaches such as HashedNet, Optimal Brain Damage (OBD), and magnitude-based pruning with L1 and L2 regularization among them and against equivalent-size feed-forward neural networks with simple (fully-connected) and structural (convolutional) neural networks. Rather surprisingly, our experiments show that (iterative) pruning-based methods are substantially better than the HashedNet architecture, whose compression doesn't appear advantageous to a carefully chosen convolutional network. We also show that, when the compression level is high, the famous OBD pruning heuristics deteriorates to the point of being less efficient than simple magnitude-based techniques.

## 7.3. Graph and digraph theory

**Participants:** Julien Bensmail, Frédéric Havet, Nicolas Nisse, Stéphane Pérennes, Francois Dross, Fionn Mc Inerney, Thi Viet Ha Nguyen, Nathann Cohen.

COATI studies theoretical problems in graph theory. If some of them are directly motivated by applications, others are more fundamental.

We are putting an effort on understanding better directed graphs (also called *digraphs*) and partitioning problems, and in particular colouring problems. We also try to better understand the many relations between orientations and colourings. We study various substructures and partitions in (di)graphs. For each of them, we aim at giving sufficient conditions that guarantee its existence and at determining the complexity of finding it.

To ease the reading, we split our results in this section into several subsections dedicated to particular topics.

### 7.3.1. Graph and digraph colourings

#### 7.3.1.1. Distinguishing labellings and the 1-2-3 Conjecture

We are interested in several distinguishing labelling (or edge-weighting) problems, where the general aim, given a graph, is to label the edges in such a way that certain properties are fulfilled. The main problem we have been considering is the **1-2-3 Conjecture**, which claims that every connected graph different from  $K_2$  admits a labelling with 1, 2, 3 such that no two adjacent vertices are incident to the same sum of weights. Some of our latest results provide evidence towards the 1-2-3 Conjecture. We also investigated questions inspired from the conjecture, such that the role of the weights 1, 2, 3 in the statement of the conjecture, the deep connection with proper vertex-colourings and other standard notions of graph theory.

#### 7.3.1.2. A 1-2-3-4 result for the 1-2-3 Conjecture in 5-regular graphs

To date, the best-known result towards the 1-2-3 Conjecture is due to Kalkowski, Karoński and Pfender, who proved that it holds when relaxed to 5-edge-weightings. Their proof builds upon a weighting algorithm designed by Kalkowski for a total version of the problem. In [23], we present new mechanisms for using Kalkowski's algorithm in the context of the 1-2-3 Conjecture. As a main result we prove that every 5-regular graph admits a 4-edge-weighting that permits to distinguish its adjacent vertices via their incident sums.



### 7.3.1.3. On $\{a, b\}$ -edge-weightings of bipartite graphs with odd $a, b$

For any  $S \subset \mathbb{Z}$  we say that a graph  $G$  has the  $S$ -property if there exists an  $S$ -edge-weighting  $w : E(G) \rightarrow S$  such that for any pair of adjacent vertices  $u, v$  we have  $\sum_{e \in E(v)} w(e) \neq \sum_{e \in E(u)} w(e)$ , where  $E(v)$  and  $E(u)$  are the sets of edges incident to  $v$  and  $u$ , respectively. In general, deciding if a graph  $G$  has the  $\{a, b\}$ -property is NP-complete for every  $a, b$ . This question is open for bipartite graphs however. The only known results of this sort are that bipartite graphs without the  $\{1, 2\}$ -property can be recognized easily, and similarly for 2-connected bipartite graphs without the  $\{0, 1\}$ -property. In [28], we focus on  $\{a, a + 2\}$ -edge-weightings where  $a \in \mathbb{Z}$  is odd. We show that a 2-connected bipartite graph has the  $\{a, a + 2\}$ -property if and only if it is not a so-called odd multi-cactus. In the case of trees, we show that only one case is pathological. That is, we show that all trees have the  $\{a, a + 2\}$ -property for odd  $a \neq -1$ , while there is an easy characterization of trees without the  $\{-1, 1\}$ -property.

### 7.3.1.4. 1-2-3 Conjecture in Digraphs: More Results and Directions

When arc-weighting a digraph, there are, at each vertex, two sums of incident weights: the in-coming sum  $\sigma^-$  and the out-going sum  $\sigma^+$ . Thus, there are many ways for generalizing the 1-2-3 Conjecture to digraphs. In the recent years, four main variants have been considered, where, for every arc  $\vec{uv}$ , it is required that one of  $\sigma^-(u), \sigma^+(u)$  is different from one of  $\sigma^-(v), \sigma^+(v)$ . All of these four variants are well understood, except for the one where, for every arc  $\vec{uv}$ , it is required that  $\sigma^-(u) \neq \sigma^+(v)$ . Regarding this version, Horňák, Przybyło and Woźniak recently proved that almost every digraph can be 4-arc-weighted so that, for every arc  $\vec{uv}$ , the sum of weights incoming to  $u$  is different from the sum of weights outgoing from  $v$ . They conjectured a stronger result, namely that the same statement with 3 instead of 4 should also be true. We verify this conjecture in [73]. This work takes place in a recent “quest” towards a directed version of the 1-2-3 Conjecture, the variant above being one of the last introduced ones. We take the occasion of this work to establish a summary of all results known in this field, covering known upper bounds, complexity aspects, and choosability. On the way we prove additional results which were missing in the whole picture. We also mention the aspects that remain open.

### 7.3.1.5. Edge Weights and Vertex Colours: Minimizing Sum Count

Put differently, the 1-2-3 Conjecture asks whether, via weights with very low magnitude, we can “encode” a proper vertex-colouring of any graph. Note, however, that we do not care about whether such a result colouring is optimal, i.e., whether its number of colours is close to the chromatic number. In [22], we investigate the minimum number of distinct sums/colours we can produce via a neighbour-sum-distinguishing edge-weighting of a given graph  $G$ , and the role of the assigned weights in that context. Clearly, this minimum number is bounded below by the chromatic number  $\chi(G)$  of  $G$ . When using weights of  $\mathbb{Z}$ , we show that, in general, we can produce neighbour-sum-distinguishing edge-weightings generating  $\chi(G)$  distinct sums, except in the peculiar case where  $G$  is a balanced bipartite graph, in which case  $\chi(G) + 1$  distinct sums can be generated. These results are best possible. When using  $k$  consecutive weights  $1, \dots, k$ , we provide both lower and upper bounds, as a function of the maximum degree  $\Delta$ , on the maximum least number of sums that can be generated for a graph with maximum degree  $\Delta$ . For trees, which, in general, admit neighbour-sum-distinguishing 2-edge-weightings, we prove that this maximum, when using weights 1 and 2, is of order  $2 \log_2 \Delta$ . Finally, we also establish the NP-hardness of several decision problems related to these questions.

### 7.3.1.6. On Minimizing the Maximum Color for the 1-2-3 Conjecture

In the line of the previous investigation, one way to get some sort of progress is to design proper labellings where the maximum color of a vertex is as small as possible. In [64], we investigate the consequences of labeling graphs as in the 1-2-3 Conjecture when it is further required to make the maximum resulting color as small as possible. We first investigate the hardness of determining the minimum maximum color by a labeling for a given graph, which we show is NP-complete in the class of bipartite graphs but polynomial-time solvable in the class of graphs with bounded treewidth. We then provide bounds on the minimum maximum color that can be generated both in the general context, and for particular classes of graphs. Finally, we study how using larger labels permits to reduce the maximum color.

### 7.3.1.7. Decomposing degenerate graphs into locally irregular subgraphs

A (undirected) graph is locally irregular if no two of its adjacent vertices have the same degree. A decomposition of a graph  $G$  into  $k$  locally irregular subgraphs is a partition  $E_1, \dots, E_k$  of  $E(G)$  into  $k$  parts each of which induces a locally irregular subgraph. Not all graphs decompose into locally irregular subgraphs; however, it was conjectured that, whenever a graph does, it should admit such a decomposition into at most three locally irregular subgraphs. This conjecture was verified for a few graph classes in recent years. It was introduced because it was noticed that, in some contexts, there are connections between locally irregular decompositions and the 1-2-3 Conjecture. In [63], we consider the decomposability of degenerate graphs with low degeneracy. Our main result is that decomposable  $k$ -degenerate graphs decompose into at most  $3k + 1$  locally irregular subgraphs, which improves on previous results whenever  $k \leq 9$ . We improve this result further for some specific classes of degenerate graphs, such as bipartite cacti,  $k$ -trees, and planar graphs. Although our results provide only little progress towards the leading conjecture above, the main contribution of this work is rather the decomposition schemes and methods we introduce to prove these results.

### 7.3.1.8. A general decomposition theory for the 1-2-3 Conjecture and locally irregular decompositions

In [21], we propose an approach encapsulating locally irregular decompositions and proper labelings. As a consequence, we get another interpretation of several existing results related to the 1-2-3 Conjecture. We also come up with new related conjectures, to which we give some support.

### 7.3.1.9. Decomposability of graphs into subgraphs fulfilling the 1-2-3 Conjecture

In particular, one of the side problems we run into is decomposing graphs into subgraphs verifying the 1-2-3 Conjecture. In [29], we prove that every  $d$ -regular graph,  $d \geq 2$ , can be decomposed into at most 2 subgraphs (without isolated edges) fulfilling the 1-2-3 Conjecture if  $d \notin \{10, 11, 12, 13, 15, 17\}$ , and into at most 3 such subgraphs in the remaining cases. Additionally, we prove that in general every graph without isolated edges can be decomposed into at most 24 subgraphs fulfilling the 1-2-3 Conjecture, improving the previously best upper bound of 40. Both results are partly based on applications of the Lovász Local Lemma.

### 7.3.1.10. On the 2-edge-coloured chromatic number of grids

The oriented (2-edge-coloured, respectively) chromatic number  $\chi_o(G)$  ( $\chi_2(G)$ , respectively) of an undirected graph  $G$  is defined as the maximum oriented (2-edge-coloured, respectively) chromatic number of an orientation (signature, respectively) of  $G$ . Although the difference between  $\chi_o(G)$  and  $\chi_2(G)$  can be arbitrarily large, there are, however, contexts in which these two parameters are quite comparable. In [24], we compare the behaviour of these two parameters in the context of (square) grids. While a series of works has been dedicated to the oriented chromatic number of grids, we are not aware of any work dedicated to their 2-edge-coloured chromatic number. We investigate this throughout this paper. We show that the maximum 2-edge-coloured chromatic number of a grid lies between 8 and 11. We also focus on 2-row grids and 3-row grids, and exhibit bounds on their 2-edge-coloured chromatic number, some of which are tight. Although our results indicate that the oriented chromatic number and the 2-edge-coloured chromatic number of grids are close in general, they also show that these parameters may differ, even for easy instances.

### 7.3.1.11. From light edges to strong edge-colouring of 1-planar graphs

A strong edge-colouring of an undirected graph  $G$  is an edge-colouring where every two edges at distance at most 2 receive distinct colours. The strong chromatic index of  $G$  is the least number of colours in a strong edge-colouring of  $G$ . A conjecture of Erdős and Nešetřil, stated back in the 80's, asserts that every graph with maximum degree  $\Delta$  should have strong chromatic index at most roughly  $1.25\Delta^2$ . Several works in the last decades have confirmed this conjecture for various graph classes. In particular, lots of attention have been dedicated to planar graphs, for which the strong chromatic index decreases to roughly  $4\Delta$ , and even to smaller values under additional structural requirements. In [26], we initiate the study of the strong chromatic index of 1-planar graphs, which are those graphs that can be drawn on the plane in such a way that every edge is crossed at most once. We provide constructions of 1-planar graphs with maximum degree  $\Delta$  and strong chromatic index roughly  $6\Delta$ . As an upper bound, we prove that the strong chromatic index of a 1-planar graph with maximum degree  $\Delta$  is at most roughly  $24\Delta$  (thus linear in  $\Delta$ ). In the course of proving the latter result, we prove, towards a conjecture of Hudák and Šugerek, that 1-planar graphs with minimum degree 3 have edges both of whose ends have degree at most 29.

### 7.3.1.12. Pushable chromatic number of graphs with degree constraints

Pushable homomorphisms and the pushable chromatic number  $\chi_p$  of oriented graphs were introduced by Klostermeyer and MacGillivray in 2004. They notably observed that, for any oriented graph  $\vec{G}$ , we have  $\chi_p(\vec{G}) \leq \chi_o(\vec{G}) \leq 2\chi_p(\vec{G})$ , where  $\chi_o(\vec{G})$  denotes the oriented chromatic number of  $\vec{G}$ . This stands as first general bounds on  $\chi_p$ . This parameter was further studied in later works.

In [71], we consider the pushable chromatic number of oriented graphs fulfilling particular degree conditions. For all  $\Delta \geq 29$ , we first prove that the maximum value of the pushable chromatic number of an oriented graph with maximum degree  $\Delta$  lies between  $2^{\frac{\Delta}{2}-1}$  and  $(\Delta - 3) \cdot (\Delta - 1) \cdot 2^{\Delta-1} + 2$  which implies an improved bound on the oriented chromatic number of the same family of graphs. For subcubic oriented graphs, that is, when  $\Delta \leq 3$ , we then prove that the maximum value of the pushable chromatic number is 6 or 7. We also prove that the maximum value of the pushable chromatic number of oriented graphs with maximum average degree less than 3 lies between 5 and 6. The former upper bound of 7 also holds as an upper bound on the pushable chromatic number of planar oriented graphs with girth at least 6.

## 7.3.2. Graph and digraph decompositions

### 7.3.2.1. Edge-partitioning a graph into paths: beyond the Barát-Thomassen conjecture

In 2006, Barát and Thomassen conjectured that there is a function  $f$  such that, for every fixed tree  $T$  with  $t$  edges, every  $f(t)$ -edge-connected graph with its number of edges divisible by  $t$  has a partition of its edges into copies of  $T$ . This conjecture was recently verified in [81] by, in particular, some members of COATI. In [27], we further focus on the path case of the Barát-Thomassen conjecture. Before the aforementioned general proof was announced, several successive steps towards the path case of the conjecture were made, notably by Thomassen [94], [95], [96], until this particular case was totally solved by Botler, Mota, Oshiro and Wakabayashi [84]. Our goal in this work was to propose an alternative proof of the path case with a weaker hypothesis: Namely, we prove that there is a function  $f$  such that every  $f(t)$ -edge-connected graph with minimum degree  $f(t)$  has an edge-partition into paths of length  $t$  whenever  $t$  divides the number of edges. We also show that 24 can be dropped to 4 when the graph is eulerian.

### 7.3.2.2. Constrained ear decompositions in graphs and digraphs.

Ear decompositions of graphs are a standard concept related to several major problems in graph theory like the Traveling Salesman Problem. For example, the Hamiltonian Cycle Problem, which is notoriously NP-complete, is equivalent to deciding whether a given graph admits an ear decomposition in which all ears except one are trivial (i.e. of length 1). On the other hand, a famous result of Lovász states that deciding whether a graph admits an ear decomposition with all ears of odd length can be done in polynomial time. In [38], we study the complexity of deciding whether a graph admits an ear decomposition with prescribed ear lengths. We prove that deciding whether a graph admits an ear decomposition with all ears of length at most  $\ell$  is polynomial-time solvable for all fixed positive integer  $\ell$ . On the other hand, deciding whether a graph admits an ear decomposition without ears of length in  $\mathcal{F}$  is NP-complete for any finite set  $\mathcal{F}$  of positive integers. We also prove that, for any  $k \geq 2$ , deciding whether a graph admits an ear decomposition with all ears of length  $0 \pmod k$  is NP-complete.

We also consider the directed analogue to ear decomposition, which we call handle decomposition, and prove analogous results : deciding whether a digraph admits a handle decomposition with all handles of length at most  $\ell$  is polynomial-time solvable for all positive integer  $\ell$ ; deciding whether a digraph admits a handle decomposition without handles of length in  $\mathcal{F}$  is NP-complete for any finite set  $\mathcal{F}$  of positive integers (and minimizing the number of handles of length in  $\mathcal{F}$  is not approximable up to  $n(1 - \epsilon)$ ); for any  $k \geq 2$ , deciding whether a digraph admits a handle decomposition with all handles of length  $0 \pmod k$  is NP-complete. Also, in contrast with the result of Lovász, we prove that deciding whether a digraph admits a handle decomposition with all handles of odd length is NP-complete. Finally, we conjecture that, for every set  $\mathcal{A}$  of integers, deciding whether a digraph has a handle decomposition with all handles of length in  $\mathcal{A}$  is NP-complete, unless there exists  $h \in \mathbb{N}$  such that  $\mathcal{A} = \{1, \dots, h\}$ .

### 7.3.3. Substructures in graphs and digraphs

#### 7.3.3.1. Subdivisions in Digraphs of Large Out-Degree or Large Dichromatic Number

In 1985, Mader conjectured the existence of a function  $f$  such that every digraph with minimum out-degree at least  $f(k)$  contains a subdivision of the transitive tournament of order  $k$ . This conjecture is still completely open, as the existence of  $f(5)$  remains unknown. In this paper, we show that if  $D$  is an oriented path, or an in-arborescence (i.e., a tree with all edges oriented towards the root) or the union of two directed paths from  $x$  to  $y$  and a directed path from  $y$  to  $x$ , then every digraph with minimum out-degree large enough contains a subdivision of  $D$ . Additionally, we study Mader's conjecture considering another graph parameter. The dichromatic number of a digraph  $D$  is the smallest integer  $k$  such that  $D$  can be partitioned into  $k$  acyclic subdigraphs. We show in [16] that any digraph with dichromatic number greater than  $4m(n-1)$  contains every digraph with  $n$  vertices and  $m$  arcs as a subdivision.

#### 7.3.3.2. Bipartite spanning sub(di)graphs induced by 2-partitions

For a given 2-partition  $(V_1, V_2)$  of the vertices of a (di)graph  $G$ , we study properties of the spanning bipartite subdigraph  $BG(V_1, V_2)$  of  $G$  induced by those arcs/edges that have one end in each  $V_i, i \in \{1, 2\}$ . In [20], we determine, for all pairs of non-negative integers  $k_1, k_2$ , the complexity of deciding whether  $G$  has a 2-partition  $(V_1, V_2)$  such that each vertex in  $V_i$  (for  $i \in \{1, 2\}$ ) has at least  $k_i$  (out-)neighbours in  $V_{3-i}$ . We prove that it is NP-complete to decide whether a digraph  $D$  has a 2-partition  $(V_1, V_2)$  such that each vertex in  $V_1$  has an out-neighbour in  $V_2$  and each vertex in  $V_2$  has an in-neighbour in  $V_1$ . The problem becomes polynomially solvable if we require  $D$  to be strongly connected. We give a characterization of the structure of NP-complete instances in terms of their strong component digraph. When we want higher in-degree or out-degree to/from the other set the problem becomes NP-complete even for strong digraphs. A further result is that it is NP-complete to decide whether a given digraph  $D$  has a 2-partition  $(V_1, V_2)$  such that  $BD(V_1, V_2)$  is strongly connected. This holds even if we require the input to be a highly connected eulerian digraph.

#### 7.3.3.3. Metric Dimension: from Graphs to Oriented Graphs

The metric dimension  $MD(G)$  of an undirected graph  $G$  is the cardinality of a smallest set of vertices that allows, through their distances to all vertices, to distinguish any two vertices of  $G$ . Many aspects of this notion have been investigated since its introduction in the 70's, including its generalization to digraphs.

In [42], [43], we study, for particular graph families, the maximum metric dimension over all strongly-connected orientations, by exhibiting lower and upper bounds on this value. We first exhibit general bounds for graphs with bounded maximum degree. In particular, we prove that, in the case of subcubic  $n$ -node graphs, all strongly-connected orientations asymptotically have metric dimension at most  $\frac{n}{2}$ , and that there are such orientations having metric dimension  $\frac{2n}{5}$ . We then consider strongly-connected orientations of grids. For a torus with  $n$  rows and  $m$  columns, we show that the maximum value of the metric dimension of a strongly-connected Eulerian orientation is asymptotically  $\frac{nm}{2}$  (the equality holding when  $n, m$  are even, which is best possible). For a grid with  $n$  rows and  $m$  columns, we prove that all strongly-connected orientations asymptotically have metric dimension at most  $\frac{2nm}{3}$ , and that there are such orientations having metric dimension  $\frac{nm}{2}$ .

### 7.3.4. Bio-informatics motivated problems

#### 7.3.4.1. Overlaying a hypergraph with a graph with bounded maximum degree

A major problem in structural biology is the characterization of low resolution structures of macro-molecular assemblies. One subproblem of this very difficult question is to determine the plausible contacts between the subunits (e.g. proteins) of an assembly, given the lists of subunits involved in all the complexes. This problem can be conveniently modelled by graphs and hypergraphs. Let  $G$  and  $H$  be respectively a graph and a hypergraph defined on a same set of vertices, and let  $F$  be a fixed graph. We say that  $GF$ -overlays a hyperedge  $S$  of  $H$  if  $F$  is a spanning subgraph of the subgraph of  $G$  induced by  $S$ , and that it  $F$ -overlays  $H$  if it  $F$ -overlays every hyperedge of  $H$ . Motivated by structural biology, we study in [68] the computational complexity of two problems. The first problem,  $(\Delta \leq k)F$ -Overlay, consists in deciding whether there is a graph with maximum degree at most  $k$  that  $F$ -overlays a given hypergraph  $H$ . It is a particular case of the

second problem  $\text{Max } (\Delta \leq k)F\text{-Overlay}$ , which takes a hypergraph  $H$  and an integer  $s$  as input, and consists in deciding whether there is a graph with maximum degree at most  $k$  that  $F$ -overlays at least  $s$  hyperedges of  $H$ . We give a complete polynomial/NP-complete dichotomy for the  $\text{Max } (\Delta \leq k)F\text{-Overlay}$  problems depending on the pairs  $(F, k)$ , and establish the complexity of  $(\Delta \leq k)F\text{-Overlay}$  for many pairs  $(F, k)$ .

**COFFEE Project-Team (section vide)**



## DATASHAPE Project-Team

### 5. New Results

#### 5.1. Algorithmic aspects of topological and geometric data analysis

##### 5.1.1. Sampling and Meshing Submanifolds

**Participants:** Jean-Daniel Boissonnat, Siargey Kachanovich.

*In collaboration with Mathijs Wintraecken (IST Austria).*

This work [41], [11] presents a rather simple tracing algorithm to sample and mesh an  $m$ -dimensional submanifold of  $\mathbb{R}^d$  for arbitrary  $m$  and  $d$ . We extend the work of Dobkin et al. to submanifolds of arbitrary dimension and codimension. The algorithm is practical and has been thoroughly investigated from both theoretical and experimental perspectives. The paper provides a full description and analysis of the data structure and of the tracing algorithm. The main contributions are : 1. We unify and complement the knowledge about Coxeter and Freudenthal-Kuhn triangulations. 2. We introduce an elegant and compact data structure to store Coxeter or Freudenthal-Kuhn triangulations and describe output sensitive algorithms to compute faces and cofaces or any simplex in the triangulation. 3. We present a manifold tracing algorithm based on the above data structure. We provide a detailed complexity analysis along with experimental results that show that the algorithm can handle cases that are far ahead of the state-of-the-art.

##### 5.1.2. Topological correctness of PL-approximations of isomanifolds

**Participant:** Jean-Daniel Boissonnat.

*In collaboration with Mathijs Wintraecken (IST Austria).*

Isomanifolds are the generalization of isosurfaces to arbitrary dimension and codimension, i.e. manifolds defined as the zero set of some multivariate multivalued function  $f : \mathbb{R}^d \rightarrow \mathbb{R}^{d-n}$ . A natural (and efficient) way to approximate an isomanifold is to consider its Piecewise-Linear (PL) approximation based on a triangulation  $\mathcal{T}$  of the ambient space  $\mathbb{R}^d$ . In this paper [43], we give conditions under which the PL-approximation of an isomanifold is topologically equivalent to the isomanifold. The conditions are easy to satisfy in the sense that they can always be met by taking a sufficiently fine triangulation  $\mathcal{T}$ . This contrasts with previous results on the triangulation of manifolds where, in arbitrary dimensions, delicate perturbations are needed to guarantee topological correctness, which leads to strong limitations in practice. We further give a bound on the Fréchet distance between the original isomanifold and its PL-approximation. Finally we show analogous results for the PL-approximation of an isomanifold with boundary.

##### 5.1.3. Dimensionality Reduction for $k$ -Distance Applied to Persistent Homology

**Participants:** Jean-Daniel Boissonnat, Kunal Dutta.

*In collaboration with Shreya Arya (Duke University)*

Given a set  $P$  of  $n$  points and a constant  $k$ , we are interested in computing the persistent homology of the Čech filtration of  $P$  for the  $k$ -distance, and investigate the effectiveness of dimensionality reduction for this problem, answering an open question of Sheehy [*Proc. SoCG, 2014*] [38]. We first show using the Johnson-Lindenstrauss lemma, that the persistent homology can be preserved up to a  $(1 \pm \epsilon)$  factor while reducing dimensionality to  $O(k \log n / \epsilon^2)$ . Our main result shows that the target dimension can be improved to  $O(\log n / \epsilon^2)$  under a reasonable and naturally occurring condition. The proof involves a multi-dimensional variant of the Hanson-Wright inequality for subgaussian quadratic forms and works when the random matrices are used for the Johnson-Lindenstrauss mapping are subgaussian. This includes the Gaussian matrices of Indyk-Motwani, the sparse random matrices of Achlioptas and the Ailon-Chazelle fast Johnson-Lindenstrauss transform. To provide evidence that our condition encompasses quite general situations, we show that it is satisfied when the points are independently distributed (i) in  $\mathbb{R}^D$  under a subgaussian distribution, or (ii) on a spherical shell in  $\mathbb{R}^D$  with a minimum angular separation, using Gershgorin's theorem. Our results also show that the JL-mapping preserves up to a  $(1 \pm \epsilon)$  factor, the Rips and Delaunay filtrations for the  $k$ -distance, as well as the Čech filtration for the approximate  $k$ -distance of Buchet et al.

#### 5.1.4. Edge Collapse and Persistence of Flag Complexes

**Participants:** Jean-Daniel Boissonnat, Siddharth Pritam.

In this article [42], we extend the notions of dominated vertex and strong collapse of a simplicial complex as introduced by J. Barmak and E. Miniam and build on the initial success of [30]. We say that a simplex (of any dimension) is dominated if its link is a simplicial cone. Domination of edges appear to be very powerful and we study it in the case of flag complexes in more detail. We show that edge collapse (removal of dominated edges) in a flag complex can be performed using only the 1-skeleton of the complex. Furthermore, the residual complex is a flag complex as well. Next we show that, similar to the case of strong collapses, we can use edge collapses to reduce a flag filtration  $\mathcal{F}$  to a smaller flag filtration  $\mathcal{F}^c$  with the same persistence. Here again, we only use the 1-skeletons of the complexes. The resulting method to compute  $\mathcal{F}^c$  is simple and extremely efficient and, when used as a preprocessing for Persistence Computation, leads to gains of several orders of magnitude wrt the state-of-the-art methods (including our previous approach using strong collapse). The method is exact, irrespective of dimension, and improves performance of Persistence Computation even in low dimensions. This is demonstrated by numerous experiments on publicly available data.

#### 5.1.5. DTM-based Filtrations

**Participants:** Frédéric Chazal, Marc Glisse, Raphael Tinarrage.

*In collaboration with Anai, Hirokazu and Ike, Yuichi and Inakoshi, Hiroya and Umeda, Yuhei (Fujitsu Labs).*

Despite strong stability properties, the persistent homology of filtrations classically used in Topological Data Analysis, such as, e.g. the Čech or Vietoris-Rips filtrations, are very sensitive to the presence of outliers in the data from which they are computed. In [15], we introduce and study a new family of filtrations, the DTM-filtrations, built on top of point clouds in the Euclidean space which are more robust to noise and outliers. The approach adopted in this work relies on the notion of distance-to-measure functions, and extends some previous work on the approximation of such functions.

#### 5.1.6. Recovering the homology of immersed manifolds

**Participant:** Raphael Tinarrage.

Given a sample of an abstract manifold immersed in some Euclidean space, in [57], we describe a way to recover the singular homology of the original manifold. It consists in estimating its tangent bundle -seen as subset of another Euclidean space- in a measure theoretic point of view, and in applying measure-based filtrations for persistent homology. The construction we propose is consistent and stable, and does not involve the knowledge of the dimension of the manifold.

#### 5.1.7. Regular triangulations as lexicographic optimal chains

**Participant:** David Cohen-Steiner.

*In collaboration with André Lieutier and Julien Vuillamy (Dassault Systèmes).*

We introduce [46] a total order on  $n$ -simplices in the  $n$ -Euclidean space for which the support of the lexicographic-minimal chain with the convex hull boundary as boundary constraint is precisely the  $n$ -dimensional Delaunay triangulation, or in a more general setting, the regular triangulation of a set of weighted points. This new characterization of regular and Delaunay triangulations is motivated by its possible generalization to submanifold triangulations as well as the recent development of polynomial-time triangulation algorithms taking advantage of this order.

#### 5.1.8. Discrete Morse Theory for Computing Zigzag Persistence

**Participant:** Clément Maria.

*In collaboration with Hannah Schreiber (Graz University of Technology, Austria)*

We introduce a framework to simplify zigzag filtrations of general complexes using discrete Morse theory, in order to accelerate the computation of zigzag persistence. Zigzag persistence is a powerful algebraic generalization of persistent homology. However, its computation is much slower in practice, and the usual optimization techniques cannot be used to compute it. Our approach is different in that it preprocesses the filtration before computation. Using discrete Morse theory, we get a much smaller zigzag filtration with same persistence. The new filtration contains general complexes. We introduce new update procedures to modify on the fly the algebraic data (the zigzag persistence matrix) under the new combinatorial changes induced by the Morse reduction. Our approach is significantly faster in practice [35].

### 5.1.9. Computing Persistent Homology with Various Coefficient Fields in a Single Pass

**Participants:** Jean-Daniel Boissonnat, Clément Maria.

This article [18] introduces an algorithm to compute the persistent homology of a filtered complex with various coefficient fields in a single matrix reduction. The algorithm is output-sensitive in the total number of distinct persistent homological features in the diagrams for the different coefficient fields. This computation allows us to infer the prime divisors of the torsion coefficients of the integral homology groups of the topological space at any scale, hence furnishing a more informative description of topology than persistence in a single coefficient field. We provide theoretical complexity analysis as well as detailed experimental results. The code is part of the Gudhi software library.

### 5.1.10. Exact computation of the matching distance on 2-parameter persistence modules

**Participant:** Steve Oudot.

*In collaboration with Michael Kerber (T.U. Graz) and Michael Lesnick (SUNY).*

The matching distance is a pseudometric on multi-parameter persistence modules, defined in terms of the weighted bottleneck distance on the restriction of the modules to affine lines. It is known that this distance is stable in a reasonable sense, and can be efficiently approximated, which makes it a promising tool for practical applications. In [31] we show that in the 2-parameter setting, the matching distance can be computed exactly in polynomial time. Our approach subdivides the space of affine lines into regions, via a line arrangement. In each region, the matching distance restricts to a simple analytic function, whose maximum is easily computed. As a byproduct, our analysis establishes that the matching distance is a rational number, if the bigrades of the input modules are rational.

### 5.1.11. Decomposition of exact pfd persistence bimodules

**Participant:** Steve Oudot.

*In collaboration with Jérémy Cochoy (Symphonia).*

In [24] we identify a certain class of persistence modules indexed over  $\mathbb{R}^2$  that are decomposable into direct sums of indecomposable summands called blocks. The conditions on the modules are that they are both pointwise finite-dimensional (pfd) and exact. Our proof follows the same scheme as the one for pfd persistence modules indexed over  $\mathbb{R}$ , yet it departs from it at key stages due to the product order not being a total order on  $\mathbb{R}^2$ , which leaves some important gaps open. These gaps are filled in using more direct arguments. Our work is motivated primarily by the study of interlevel-sets persistence, although the proposed results reach beyond that setting.

### 5.1.12. Level-sets persistence and sheaf theory

**Participants:** Nicolas Berkouk, Steve Oudot.

*In collaboration with Grégory Ginot (Paris 13).*

In [39] we provide an explicit connection between level-sets persistence and derived sheaf theory over the real line. In particular we construct a functor from 2-parameter persistence modules to sheaves over  $\mathbb{R}$ , as well as a functor in the other direction. We also observe that the 2-parameter persistence modules arising from the level sets of Morse functions carry extra structure that we call a Mayer-Vietoris system. We prove classification, barcode decomposition, and stability theorems for these Mayer-Vietoris systems, and we show that the aforementioned functors establish a pseudo-isometric equivalence of categories between derived constructible sheaves with the convolution or (derived) bottleneck distance and the interleaving distance of strictly pointwise finite-dimensional Mayer-Vietoris systems. Ultimately, our results provide a functorial equivalence between level-sets persistence and derived pushforward for continuous real-valued functions.

### 5.1.13. Intrinsic Interleaving Distance for Merge Trees

**Participant:** Steve Oudot.

*In collaboration with Ellen Gasparovic (Union College), Elizabeth Munch (Michigan State), Katharine Turner (Australian National University), Bei Wang (Utah), and Yusu Wang (Ohio-State).*

Merge trees are a type of graph-based topological summary that tracks the evolution of connected components in the sublevel sets of scalar functions. They enjoy widespread applications in data analysis and scientific visualization. In [49] we consider the problem of comparing two merge trees via the notion of interleaving distance in the metric space setting. We investigate various theoretical properties of such a metric. In particular, we show that the interleaving distance is intrinsic on the space of labeled merge trees and provide an algorithm to construct metric 1-centers for collections of labeled merge trees. We further prove that the intrinsic property of the interleaving distance also holds for the space of unlabeled merge trees. Our results are a first step toward performing statistics on graph-based topological summaries.

## 5.2. Statistical aspects of topological and geometric data analysis

### 5.2.1. Estimating the Reach of a Manifold

**Participants:** Frédéric Chazal, Jisu Kim, Bertrand Michel.

*In collaboration with E. Aamari (Univ. Paris-Diderot), A. Rinaldo, L. Wasserman (Carnegie Mellon University).*

In [13], various problems in manifold estimation make use of a quantity called the reach, denoted by  $\tau_M$ , which is a measure of the regularity of the manifold. This paper is the first investigation into the problem of how to estimate the reach. First, we study the geometry of the reach through an approximation perspective. We derive new geometric results on the reach for submanifolds without boundary. An estimator  $\hat{\tau}$  of  $\tau_M$  is proposed in an oracle framework where tangent spaces are known, and bounds assessing its efficiency are derived. In the case of i.i.d. random point cloud  $X_n$ ,  $\hat{\tau}(X_n)$  is showed to achieve uniform expected loss bounds over a  $C^3$ -like model. Finally, we obtain upper and lower bounds on the minimax rate for estimating the reach.

### 5.2.2. A statistical test of isomorphism between metric-measure spaces using the distance-to-a-measure signature

**Participant:** Claire Brecheteau.

In [20], we introduce the notion of DTM-signature, a measure on  $\mathbb{R}$  that can be associated to any metric-measure space. This signature is based on the function distance to a measure (DTM) introduced in 2009 by Chazal, Cohen-Steiner and Mériçot. It leads to a pseudo-metric between metric-measure spaces, that is bounded above by the Gromov-Wasserstein distance. This pseudo-metric is used to build a statistical test of isomorphism between two metric-measure spaces, from the observation of two  $N$ -samples.

The test is based on subsampling methods and comes with theoretical guarantees. It is proven to be of the correct level asymptotically. Also, when the measures are supported on compact subsets of  $\mathbb{R}^d$ , rates of convergence are derived for the  $L_1$ -Wasserstein distance between the distribution of the test statistic and its subsampling approximation. These rates depend on some parameter  $\rho > 1$ . In addition, we prove that the power is bounded above by  $\exp(-CN1/\rho)$ , with  $C$  proportional to the square of the aforementioned pseudo-metric between the metric-measure spaces. Under some geometrical assumptions, we also derive lower bounds for this pseudo-metric.

An algorithm is proposed for the implementation of this statistical test, and its performance is compared to the performance of other methods through numerical experiments.

### 5.2.3. *On the choice of weight functions for linear representations of persistence diagrams*

**Participant:** Vincent Divol.

*In collaboration with Wolfgang Polonik (UC Davis).*

Persistence diagrams are efficient descriptors of the topology of a point cloud. As they do not naturally belong to a Hilbert space, standard statistical methods cannot be directly applied to them. Instead, feature maps (or representations) are commonly used for the analysis. A large class of feature maps, which we call linear, depends on some weight functions, the choice of which is a critical issue. An important criterion to choose a weight function is to ensure stability of the feature maps with respect to Wasserstein distances on diagrams. In [21], we improve known results on the stability of such maps, and extend it to general weight functions. We also address the choice of the weight function by considering an asymptotic setting; assume that  $\mathbb{X}_n$  is an i.i.d. sample from a density on  $[0, 1]^d$ . For the Čech and Rips filtrations, we characterize the weight functions for which the corresponding feature maps converge as  $n$  approaches infinity, and by doing so, we prove laws of large numbers for the total persistences of such diagrams. Those two approaches (stability and convergence) lead to the same simple heuristic for tuning weight functions: if the data lies near a  $d$ -dimensional manifold, then a sensible choice of weight function is the persistence to the power  $\alpha$  with  $\alpha \geq d$ .

### 5.2.4. *Understanding the Topology and the Geometry of the Persistence Diagram Space via Optimal Partial Transport*

**Participants:** Vincent Divol, Théo Lacombe.

Despite the obvious similarities between the metrics used in topological data analysis and those of optimal transport, an optimal-transport based formalism to study persistence diagrams and similar topological descriptors has yet to come. In [48], by considering the space of persistence diagrams as a measure space, and by observing that its metrics can be expressed as solutions of optimal partial transport problems, we introduce a generalization of persistence diagrams, namely Radon measures supported on the upper half plane. Such measures naturally appear in topological data analysis when considering continuous representations of persistence diagrams (e.g. persistence surfaces) but also as limits for laws of large numbers on persistence diagrams or as expectations of probability distributions on the persistence diagrams space. We study the topological properties of this new space, which will also hold for the closed subspace of persistence diagrams. New results include a characterization of convergence with respect to transport metrics, the existence of Fréchet means for any distribution of diagrams, and an exhaustive description of continuous linear representations of persistence diagrams. We also showcase the usefulness of this framework to study random persistence diagrams by providing several statistical results made meaningful thanks to this new formalism.

## 5.3. Topological approach for multimodal data processing

### 5.3.1. *A General Neural Network Architecture for Persistence Diagrams and Graph Classification*

**Participants:** Frédéric Chazal, Théo Lacombe, Martin Royer.

*In collaboration with Mathieu Carrière (Columbia Univ.) and Umeda Yuhei and Ike Yuichi (Fujitsu Labs).*

Persistence diagrams, the most common descriptors of Topological Data Analysis, encode topological properties of data and have already proved pivotal in many different applications of data science. However, since the (metric) space of persistence diagrams is not Hilbert, they end up being difficult inputs for most Machine Learning techniques. To address this concern, several vectorization methods have been put forward that embed persistence diagrams into either finite-dimensional Euclidean space or (implicit) infinite dimensional Hilbert space with kernels. In [44], we focus on persistence diagrams built on top of graphs. Relying on extended persistence theory and the so-called heat kernel signature, we show how graphs can be encoded by (extended) persistence diagrams in a provably stable way. We then propose a general and versatile framework for learning vectorizations of persistence diagrams, which encompasses most of the vectorization techniques used in the literature. We finally showcase the experimental strength of our setup by achieving competitive scores on classification tasks on real-life graph datasets.

### 5.3.2. *Topological Data Analysis for Arrhythmia Detection through Modular Neural Networks*

**Participant:** Frédéric Chazal.

*In collaboration with Umeda Yuhei and Meryll Dindin (Fujitsu Labs).*

In [47], we present an innovative and generic deep learning approach to monitor heart conditions from ECG signals. We focus our attention on both the detection and classification of abnormal heartbeats, known as arrhythmia. We strongly insist on generalization throughout the construction of a deep-learning model that turns out to be effective for new unseen patient. The novelty of our approach relies on the use of topological data analysis as basis of our multichannel architecture, to diminish the bias due to individual differences. We show that our structure reaches the performances of the state-of-the-art methods regarding arrhythmia detection and classification.

### 5.3.3. *ATOL: Automatic Topologically-Oriented Learning*

**Participants:** Frédéric Chazal, Martin Royer.

*In collaboration with Umeda Yuhei and Ike Yiuchi (Fujitsu Labs).*

There are abundant cases for using Topological Data Analysis (TDA) in a learning context, but robust topological information commonly comes in the form of a set of persistence diagrams, objects that by nature are uneasy to affix to a generic machine learning framework. In [56], we introduce a vectorisation method for diagrams that allows to collect information from topological descriptors into a format fit for machine learning tools. Based on a few observations, the method is learned and tailored to discriminate the various important plane regions a diagram is set into. With this tool one can automatically augment any sort of machine learning problem with access to a TDA method, enhance performances, construct features reflecting underlying changes in topological behaviour. The proposed methodology comes with only high level tuning parameters such as the encoding budget for topological features. We provide an open-access, ready-to-use implementation and notebook. We showcase the strengths and versatility of our approach on a number of applications. From emulous and modern graph collections to a highly topological synthetic dynamical orbits data, we prove that the method matches or beats the state-of-the-art in encoding persistence diagrams to solve hard problems. We then apply our method in the context of an industrial, difficult time-series regression problem and show the approach to be relevant.

### 5.3.4. *Inverse Problems in Topological Persistence: a Survey*

**Participant:** Steve Oudot.

*In collaboration with Elchanan Solomon (Duke).*

In [27] we review the literature on inverse problems in topological persistence theory. The first half of the survey is concerned with the question of surjectivity, i.e. the existence of rightinverses, and the second half focuses on injectivity, i.e. left inverses. Throughout, we highlight the tools and theorems that underlie these advances, and direct the reader's attention to open problems, both theoretical and applied.



### 5.3.5. Intrinsic Topological Transforms via the Distance Kernel Embedding

**Participants:** Clément Maria, Steve Oudot.

*In collaboration with Elchanan Solomon (Duke).*

Topological transforms are parametrized families of topological invariants, which, by analogy with transforms in signal processing, are much more discriminative than single measurements. The first two topological transforms to be defined were the Persistent Homology Transform and Euler Characteristic Transform, both of which apply to shapes embedded in Euclidean space. The contribution of this work [54] is to define topological transforms that depend only on the intrinsic geometry of a shape, and hence are invariant to the choice of embedding. To that end, given an abstract metric measure space, we define an integral operator whose eigenfunctions are used to compute sublevel set persistent homology. We demonstrate that this operator, which we call the distance kernel operator, enjoys desirable stability properties, and that its spectrum and eigenfunctions concisely encode the large-scale geometry of our metric measure space. We then define a number of topological transforms using the eigenfunctions of this operator, and observe that these transforms inherit many of the stability and injectivity properties of the distance kernel operator.

### 5.3.6. A Framework for Differential Calculus on Persistence Barcodes

**Participant:** Steve Oudot.

*In collaboration with Jacob Leygonie and Ulrike Tillmann (Oxford).*

In [52], we define notions of differentiability for maps from and to the space of persistence barcodes. Inspired by the theory of diffeological spaces, the proposed framework uses lifts to the space of ordered barcodes, from which derivatives can be computed. The two derived notions of differentiability (respectively from and to the space of barcodes) combine together naturally to produce a chain rule that enables the use of gradient descent for objective functions factoring through the space of barcodes. We illustrate the versatility of this framework by showing how it can be used to analyze the smoothness of various parametrized families of filtrations arising in topological data analysis.

## 5.4. Experimental research and software development

### 5.4.1. Robust Stride Detector from Ankle-Mounted Inertial Sensors for Pedestrian Navigation and Activity Recognition with Machine Learning Approaches

**Participants:** Bertrand Beauflis, Frédéric Chazal, Bertrand Michel.

*In collaboration with Marc Grelet (Sysnav).*

In [16], a stride detector algorithm combined with a technique inspired by zero velocity update (ZUPT) is proposed to reconstruct the trajectory of a pedestrian from an ankle-mounted inertial device. This innovative approach is based on sensor alignment and machine learning. It is able to detect 100% of both normal walking strides and more than 97% of atypical strides such as small steps, side steps, and backward walking that existing methods can hardly detect. This approach is also more robust in critical situations, when for example the wearer is sitting and moving the ankle or when the wearer is bicycling (less than two false detected strides per hour on average). As a consequence, the algorithm proposed for trajectory reconstruction achieves much better performances than existing methods for daily life contexts, in particular in narrow areas such as in a house. The computed stride trajectory contains essential information for recognizing the activity (atypical stride, walking, running, and stairs). For this task, we adopt a machine learning approach based on descriptors of these trajectories, which is shown to be robust to a large of variety of gaits. We tested our algorithm on recordings of healthy adults and children, achieving more than 99% success. The algorithm also achieved more than 97% by children suffering from movement disorders. Compared to most algorithms in the literature, this original method does not use a fixed-size sliding window but infers this last in an adaptive way

### 5.4.2. Robust pedestrian trajectory reconstruction from inertial sensor

**Participants:** Bertrand Beauflis, Frédéric Chazal, Bertrand Michel.

*In collaboration with Marc Grelet (Sysnav).*

In [28], a strides detection algorithm combined with a technique inspired by Zero Velocity Update (ZUPT) is proposed using inertial sensors worn on the ankle. This innovative approach based on a sensors alignment and machine learning can detect both normal walking strides and atypical strides such as small steps, side steps and backward walking that existing methods struggle to detect. As a consequence, the trajectory reconstruction achieves better performances in daily life contexts for example, where a lot of these kinds of strides are performed in narrow areas such as in a house. It is also robust in critical situations, when for example the wearer is sitting and moving the ankle or bicycling, while most algorithms in the literature would wrongly detect strides and produce error in the trajectory reconstruction by generating movements. Our algorithm is evaluated on more than 7800 strides from seven different subjects performing several activities. We validated the trajectory reconstruction during motion capture sessions by analyzing the stride length. Finally, we tested the algorithm in a challenging situation by plotting the computed trajectory on the building map of an 5 hours and 30 minutes office worker recording.

## 5.5. Algorithmic and Combinatorial Aspects of Low Dimensional Topology

### 5.5.1. Treewidth, crushing and hyperbolic volume

**Participant:** Clément Maria.

*In collaboration with Jessica S. Purcell (Monash University, Australia)*

The treewidth of a 3-manifold triangulation plays an important role in algorithmic 3-manifold theory, and so it is useful to find bounds on the tree-width in terms of other properties of the manifold. In [26], we prove that there exists a universal constant  $c$  such that any closed hyperbolic 3-manifold admits a triangulation of tree-width at most the product of  $c$  and the volume. The converse is not true: we show there exists a sequence of hyperbolic 3-manifolds of bounded tree-width but volume approaching infinity. Along the way, we prove that crushing a normal surface in a triangulation does not increase the carving-width, and hence crushing any number of normal surfaces in a triangulation affects tree-width by at most a constant multiple.

### 5.5.2. Parameterized complexity of quantum knot invariants

**Participant:** Clément Maria.

In [53], we give a general fixed parameter tractable algorithm to compute quantum invariants of links presented by diagrams, whose complexity is singly exponential in the carving-width (or the tree-width) of the diagram. In particular, we get a  $O(N^{3/2cw} \text{poly}(n))$  time algorithm to compute any Reshetikhin-Turaev invariant-derived from a simple Lie algebra  $\mathfrak{g}$  of a link presented by a planar diagram with  $n$  crossings and carving-width  $cw$ , and whose components are coloured with  $\mathfrak{g}$ -modules of dimension at most  $N$ . For example, this includes the  $N$ th-coloured Jones polynomial and the  $N$ th-coloured HOMFLYPT polynomial.

## 5.6. Miscellaneous

### 5.6.1. Material Coherence from Trajectories via Burau Eigenanalysis of Braids

**Participant:** David Cohen-Steiner.

*In collaboration with Melissa Yeung and Mathieu Desbrun (Caltech).*

In this paper [58], we provide a numerical tool to study material coherence from a set of 2D Lagrangian trajectories sampling a dynamical system, i.e., from the motion of passive tracers. We show that eigenvectors of the Burau representation of a topological braid derived from the trajectories have levelsets corresponding to components of the Nielsen-Thurston decomposition of the dynamical system. One can thus detect and identify clusters of space-time trajectories corresponding to coherent regions of the dynamical system by solving an eigenvalue problem. Unlike previous methods, the scalable computational complexity of our braid-based approach allows the analysis of large amounts of trajectories. Studying two-dimensional flows and their induced transport and mixing properties is key to geophysical studies of atmospheric and oceanic processes.

However, one often has only sparse tracer trajectories (e.g., positions of buoys in time) to infer the overall flow geometry. Fortunately, topological methods based on the theory of braid groups have recently been proposed to extract structures from such a sparse set of trajectories by measuring their entanglement. This braid viewpoint offers sound foundations for the definition of coherent structures. Yet, there has been only limited efforts in developing practical tools that can leverage topological properties for the efficient analysis of flow structures: handling a larger number of trajectories remains computationally challenging. We contribute a new and simple computational tool to extract Lagrangian structures from sparse trajectories by noting that the eigenstructure of the Burau matrix representation of a braid of particle trajectories can be used to reveal coherent regions of the flows. Detection of clusters of space-time trajectories corresponding to coherent regions of the dynamical system can thus be achieved by solving a simple eigenvalue problem. This paper establishes the theoretical foundations behind this braid eigenanalysis approach, along with numerical validations on various flows.

### **5.6.2. Quantitative stability of optimal transport maps and linearization of the 2-Wasserstein space**

**Participants:** Alex Delalande, Frédéric Chazal.

*In collaboration with Quentin Mérigot (Institut de Mathématiques d'Orsay).*

In [55], we study an explicit embedding of the set of probability measures into a Hilbert space, defined using optimal transport maps from a reference probability density. This embedding linearizes to some extent the 2-Wasserstein space, and enables the direct use of generic supervised and unsupervised learning algorithms on measure data. Our main result is that the embedding is (bi-)Holder continuous, when the reference density is uniform over a convex set, and can be equivalently phrased as a dimension-independent Hölder-stability results for optimal transport maps.

## DIANA Project-Team

# 6. New Results

## 6.1. Service Transparency

### 6.1.1. *From Network Traffic Measurements to QoE for Internet Video*

**Participants:** Muhammad Jawad Khokhar, Thibaut Ehlinger, Chadi Barakat.

Video streaming is a dominant contributor to the global Internet traffic. Consequently, monitoring video streaming Quality of Experience (QoE) is of paramount importance to network providers. Monitoring QoE of video is a challenge as most of the video traffic of today is encrypted. In this work, we consider this challenge and present an approach based on controlled experimentation and machine learning to estimate QoE from encrypted video traces using network level measurements only. We consider a case of YouTube and play out a wide range of videos under realistic network conditions to build ML models (classification and regression) that predict the subjective MOS (Mean Opinion Score) based on the ITU P.1203 model along with the QoE metrics of startup delay, quality (spatial resolution) of playout and quality variations, and this is using only the underlying network Quality of Service (QoS) features. We comprehensively evaluate our approach with different sets of input network features and output QoE metrics. Overall, our classification models predict the QoE metrics and the ITU MOS with an accuracy of 63-90% while the regression models show low error; the ITU MOS (1-5) and the startup delay (in seconds) are predicted with a root mean square error of 0.33 and 2.66 respectively. The results of this work were published in [26] and can be found with further details in the PhD manuscript of Muhammad Jawad Khokhar graduated in October 2019.

### 6.1.2. *When Deep Learning meets Web Measurements to infer Network Performance*

**Participants:** Imane Taibi, Chadi Barakat.

Web browsing remains one of the dominant applications of the internet, so inferring network performance becomes crucial for both users and providers (access and content) so as to be able to identify the root cause of any service degradation. Recent works have proposed several network troubleshooting tools, e.g, NDT, MobiPerf, SpeedTest, Fathom. Yet, these tools are either computationally expensive, less generic or greedy in terms of data consumption. The main purpose of this work funded by the IPL BetterNet is to leverage passive measurements freely available in the browser and machine learning techniques (ML) to infer network performance (e.g., delay, bandwidth and loss rate) without the addition of new measurement overhead. To enable this inference, we propose a framework based on extensive controlled experiments where network configurations are artificially varied and the Web is browsed, then ML is applied to build models that estimate the underlying network performance. In particular, we contrast classical ML techniques (such as random forest) to deep learning models trained using fully connected neural networks and convolutional neural networks (CNN). Results of our experiments show that neural networks have a higher accuracy compared to classical ML approaches. Furthermore, the model accuracy improves considerably using CNN. These results were published in [28].

### 6.1.3. *On Accounting for Screen Resolution in Adaptive Video Streaming: A QoE-Driven Bandwidth Sharing Framework*

**Participants:** Othmane Belmoukadam, Muhammad Jawad Khokhar, Chadi Barakat.

Screen resolution along with network conditions are main objective factors impacting the user experience, in particular for video streaming applications. Terminals on their side feature more and more advanced characteristics resulting in different network requirements for good visual experience. Previous studies tried to link MOS (Mean Opinion Score) to video bit rate for different screen types (e.g., CIF, QCIF, and HD). We leverage such studies and formulate a QoE-driven resource allocation problem to pinpoint the optimal bandwidth allocation that maximizes the QoE (Quality of Experience) over all users of a provider located behind the same bottleneck link, while accounting for the characteristics of the screens they use for video payout. For our optimization problem, QoE functions are built using curve fitting on data sets capturing the relationship between MOS, screen characteristics, and bandwidth requirements. We propose a simple heuristic based on Lagrangian relaxation and KKT (Karush Kuhn Tucker) conditions for a subset of constraints. Numerical simulations show that the proposed heuristic is able to increase overall QoE up to 20% compared to an allocation with TCP look-alike strategies implementing max-min fairness. Later, we use a MPEG/DASH implementation in the context of ns-3 and show that coupling our approach with a rate adaptation algorithm can help increasing QoE while reducing both resolution switches and number of interruptions. Our framework and the first validation results were published in [20].

#### **6.1.4. Tuning optimal traffic measurement parameters in virtual networks with machine learning**

**Participants:** Karyna Gogunska, Chadi Barakat.

With the increasing popularity of cloud networking and the widespread usage of virtualization as a way to offer flexible and virtual network and computing resources, it becomes more and more complex to monitor this new virtual environment. Yet, monitoring remains crucial for network troubleshooting and analysis. Controlling the measurement footprint in the virtual network is one of the main priorities in the process of monitoring as resources are shared between the compute nodes of tenants and the measurement process itself. In this paper, first, we assess the capability of machine learning to predict measurement impact on the ongoing traffic between virtual machines; second, we propose a data-driven solution that is able to provide optimal monitoring parameters for virtual network measurement with minimum traffic interference. These results were published in [25] and are part of the PhD manuscript of Karyna Gogunska graduated in December 2019.

#### **6.1.5. Collaborative Traffic Measurement in Virtualized Data Center Networks**

**Participants:** Houssam Elbouanani, Chadi Barakat.

Data center network monitoring can be carried out at hardware networking equipment (e.g. physical routers) and/or software networking equipment (e.g. virtual switches). While software switches offer high flexibility to deploy various monitoring tools, they have to utilize server resources, esp. CPU and memory, that can no longer be reserved fully to service users' traffic. In this work we closely examine the costs of (i) sampling packets ; (ii) sending them to a user-space program for measurement; and (iii) forwarding them to a remote server where they will be processed in case of lack of resources locally. Starting from empirical observations, we derive an analytical model to accurately predict ( $R^2 = 99.5\%$ ) the three aforementioned costs, as a function of the sampling rate. We next introduce a collaborative approach for traffic monitoring and sampling that maximizes the amount of collected traffic without impacting the data center's operation. We analyze, through numerical simulations, the performance of our collaborative solution. The results show that it is able to take advantage of the uneven loads on the servers to maximize the amount of traffic that can be sampled at the scale of a data center. The resulting gain can reach 200% compared to a non collaborative approach. These results were published in [23].

#### **6.1.6. Distributed Privacy Preserving Platform for Ridesharing Services**

**Participants:** Damien Saucez, Yevhenii Semenko.

The sharing economy fundamentally changed business and social interactions. Interestingly, while in essence this form of collaborative economy allows people to directly interact with each other, it is also at the source of the advent of eminently centralized platforms and marketplaces, such as Uber and Airbnb. One may be concerned with the risk of giving the control of a market to a handful of actors that may unilaterally fix their own rules and threaten privacy. Within the Data Privacy project of the UCAJedi Idex Academy 5 and House of Human and Social Sciences, Technologies and Uses Theme, we have proposed a holistic solution to address privacy issues in the sharing economy. We considered the case of ridesharing and proposed a decentralized architecture which gives the opportunity to shift from centralized platforms to decentralized ones. Digital communications in our proposition are specifically designed to preserve data privacy and avoid any form of centralization. A blockchain is used in our proposition to guarantee the essential roles of a marketplace, but in a decentralized way. Our evaluation shows that privacy protection without trusted entities comes at the cost of harder scalability than an approach with a trusted third party. However, our numerical evaluation on real data and our Android prototype shows the practical feasibility of our approach. The results obtained in this activity are published in 12th International Conference on Security, Privacy, and Anonymity in Computation, Communication, and Storage (SpaCCS) 2019, Atlanta [31] and documented in a research report [35].

### ***6.1.7. Missed by Filter Lists: Detecting Unknown Third-Party Trackers with Invisible Pixels***

**Participants:** Imane Fouad, Arnaud Legout, Natasa Sarafijanovic-Djukic.

Web tracking has been extensively studied over the last decade. To detect tracking, previous studies and user tools rely on filter lists. However, it has been shown that filter lists miss trackers. In this paper, we propose an alternative method to detect trackers inspired by analyzing behavior of invisible pixels. By crawling 84,658 webpages from 8,744 domains, we detect that third-party invisible pixels are widely deployed: they are present on more than 94.51% of domains and constitute 35.66% of all third-party images. We propose a fine-grained behavioral classification of tracking based on the analysis of invisible pixels. We use this classification to detect new categories of tracking and uncover new collaborations between domains on the full dataset of 4,216,454 third-party requests. We demonstrate that two popular methods to detect tracking, based on EasyList & EasyPrivacy and on Disconnect lists respectively miss 25.22% and 30.34% of the trackers that we detect. Moreover, we find that if we combine all three lists, 379,245 requests originated from 8,744 domains still track users on 68.70% of websites. This work will appear in PETS 2020 [24].

### ***6.1.8. Privacy implications of switching ON a light bulb in the IoT world***

**Participants:** Mathieu Thiery, Arnaud Legout.

The number of connected devices is increasing every day, creating smart homes and shaping the era of the Internet of Things (IoT), and most of the time, end-users are unaware of their impacts on privacy. In this work, we analyze the ecosystem around a Philips Hue smart white bulb in order to assess the privacy risks associated to the use of different devices (smart speaker or button) and smartphone applications to control it. We show that using different techniques to switch ON or OFF this bulb has significant consequences regarding the actors involved (who mechanically gather information on the user's home) and the volume of data sent to the Internet (we measured differences up to a factor 100, depending on the control technique we used). Even when the user is at home, these data flows often leave the user's country, creating a situation that is neither privacy friendly (and the user is most of the time ignorant of the situation), nor sovereign (the user depends on foreign actors), nor sustainable (the extra energetic consumption is far from negligible). We therefore advocate a complete change of approach, that favors local communications whenever sufficient. The preprint documenting this work has been published as research report [40].

### ***6.1.9. ElectroSmart***

**Participants:** Arnaud Legout, Mondri Ravi, David Migliacci, Abdelhakim Akodadi, Yanis Boussad.

We are currently evaluating the relevance to create a startup for the ElectroSmart project. We are quite advanced in the process and the planned creation is June 2020. There is a "contrat de transfert" ready between Inria and ElectroSmart to transfer the PI from Inria to the ElectroSmart company (when it will be created). Arnaud Legout the future CEO of the company obtained the "autorisation de création d'entreprise" from Inria. ElectroSmart has been incubated in PACA Est in December 2018.



The three future co-founder of ElectroSmart (Arnaud Legout, Mondri Ravi, David Migliacci) followed the Digital Startup training from Inria/EM Lyon.

The goal of ElectroSmart is to help people reduce their exposure to EMF and offer a solution to reduce symptoms associated with exposure to EMF. Electrosensitivity, is known to be a complex and multifactorial syndrome that impacts hundreds of millions of persons worldwide. We aim to commercialize the first treatment of electrosensitivity based on non-deceptive placebo (called open-label placebo). It is known today that placebo are an effective treatment to subjective symptoms (which is the case for several symptoms associated with electrosensitivity). The problem with placebo was that it was assumed that it must be deceptive to be efficient. Kaptchuk et al. showed recently that non-deceptive placebo are as effective as deceptive placebo, so the ethical usage of placebo is now possible. ElectroSmart want to be the first company to commercialize non-deceptive placebo for electrosensitive persons. For details, see <https://electrosmart.app/>.

## 6.2. Open Network Architecture

### 6.2.1. Constrained Software Defined Networks

**Participant:** Damien Saucez.

The objective of the ANR JCJC DET4ALL project was to offer the ability to multiplex constrained networks with real time and safety requirements on Ethernet network not initially thought for strict constraints. The reason for this move to Ethernet is to reduce the cost of networking solutions in automotive and industrial applications. We advocate that this move requires to rely on Software Defined Networking (SDN) that enables a programmatic approach to networking, hence offering modularity and flexibility. The challenge with SDN is to be able to certify the behaviour of the system while keeping the solution generic. Within DET4ALL we put the first element in place to show that the previous works that proposed programming languages and abstractions for best-effort network could be leveraged to offering safety properties and determinism in real-time industrial and automotive networks. More precisely, we have demonstrated that Linear Temporal Logic (LTL) can be used in real-time networks to demonstrate that real-time constraints are always respected. We built a strawman to show that the Temporal NetKat language was adapted to express real-time constraints of networks even though it was not initially design for that purpose. Given that Temporal NetKat relies on LTL and an algebra, it is a good candidate to prove the correct behaviour of a SDN network which logic would be implemented with such a language. In the continuation of this work, we have determined what would be necessary to be able to provide provable live network updates in real time network without service degradation. This work is published in [30] and will be detailed in the next subsection. Due the leave of Damien Saucez to Safran for one year starting October 1st 2019, the activity on this project had to be stopped as it was in the context of an ANR JCJC project.

### 6.2.2. NUTS: Network Updates in Real Time Systems

**Participants:** Damien Saucez, Walid Dabbous.

Recent manufacturing trends have highlighted the need to adapt to volatile, fast-moving, and customer-driven markets. To keep pace with ever quicker product lifecycles, shorter order lead times and growing product variants, factories will become distributed modular cyber-physical systems interconnected by complex communication networks. We advocate that the Software Define Networking (SDN) concept with its programmatic approach to networking is a key enabler for the so-called Industry 4.0 because it provides flexibility and the possibility to formally reason on networks. We have identified that a critical point to address is how to support safe network updates of deterministic real-time communication SDN. To achieve this goal 4 elements are required. First a declarative language with LTL support is needed to express the constraints. Second, a programmable data-plane with the ability to provide real-time constraints indications must be provided in order to assess the behaviour of the forwarding elements. Such language does not exist yet however among the data-plane languages currently on the market some provide the ability to add annotations that could be used to reach our objective. Third, we have identified that deterministic algorithms had to be used to provide a verifiable sequence of network updates in order to make live updates without service degradations. Finally, mathematical techniques must be used to provide bounds on the network updates. Network Calculus can be used for that objective. This study was published as a poster in SOSR'19 [30].

### 6.2.3. *A Joint range extension and localization for LPWAN*

**Participants:** Mohamed Naoufal Mahfoudi, Gayatri Sivados, Othmane Bensouda Korachi, Thierry Turletti, Walid Dabbous.

We have proposed Snipe, a novel system offering joint localization and range extensions for LPWANs. Although LPWAN systems such as Long Range (LoRa) are designed to achieve high communication range with low energy consumption, they suffer from fading in obstructed environments with dense multipath components, and their localization system is sub-par in terms of accuracy. In this work, MIMO techniques are leveraged to achieve a higher signal-to-noise ratio at both the end device and the gateway while providing an opportunistic accurate radar-based system for localization with limited additional cost. This work has been published at Internet Technology Letters [15].

### 6.2.4. *Online Robust Placement of Service Chains for Large Data Center Topologies*

**Participants:** Ghada Moualla, Thierry Turletti, Damien Saucez.

The trend today is to deploy applications and more generally Service Function Chains (SFCs) in public clouds. However, before being deployed in the cloud, chains were deployed on dedicated infrastructures where software, hardware, and network components were managed by the same entity, making it straightforward to provide robustness guarantees. By moving their services to the cloud, the users lose their control on the infrastructure and hence on the robustness. We propose an online algorithm for robust placement of service chains in data centers. Our placement algorithm determines the required number of replicas for each function of the chain and their placement in the data center. Our simulations on large data-center topologies with up to 30,528 nodes show that our algorithm is fast enough such that one can consider robust chain placements in real time even in a very large data center and without the need of prior knowledge on the demand distribution. This work has been published at IEEE Access [16].

### 6.2.5. *Bandwidth-optimal Failure Recovery Scheme for Robust Programmable Networks*

**Participants:** Giuseppe Di Lena, Damien Saucez, Thierry Turletti.

With the emergence of Network Function Virtualization (NFV) and Software Defined Networking (SDN), efficient network algorithms considered too hard to be put in practice in the past now have a second chance to be considered again. In this context, we rethink the network dimensioning problem with protection against Shared Risk Link Group (SLRG) failures. In this work, we consider a path-based protection scheme with a global rerouting strategy, in which, for each failure situation, there may be a new routing of all the demands. Our optimization task is to minimize the needed amount of bandwidth. After discussing the hardness of the problem, we develop a scalable mathematical model that we handle using the Column Generation technique. Through extensive simulations on real-world IP network topologies and on random generated instances, we show the effectiveness of our method. Finally, our implementation in OpenDaylight demonstrates the feasibility of the approach and its evaluation with Mininet shows that technical implementation choices may have a dramatic impact on the time needed to reestablish the flows after a failure takes place. This work has been presented at the IEEE International Conference on Cloud Networking (CloudNet), November 2019, at Coimbra in Portugal [29] and documented in a research report [36]. A poster version is published in IFIP-Networking in Warsaw [41].

### 6.2.6. *Efficient Pull-based Mobile Video Streaming leveraging In-Network Functions*

**Participants:** Indukala Naladala, Thierry Turletti.

There has been a considerable increase in the demand for high quality mobile video streaming services, while at the same time, the video traffic volume is expected to grow exponentially. Consequently, maintaining high quality of experience (QoE) and saving network resources are becoming crucial challenges to solve. In this work, we propose a name-based mobile streaming scheme that allows efficient video content delivery by exploiting a smart pulling mechanism designed for information-centric networks (ICNs). The proposed mechanism enables fast packet loss recovery by leveraging in-network caching and coding. Through an experimental evaluation of our mechanism over an open wireless testbed and the Internet, we demonstrate that the proposed scheme leads to higher QoE levels than classical ICN and TCP-based streaming mechanisms.

This work will be presented at the IEEE Consumer Communications & Networking Conference (CCNC), in January 2020 at Las Vegas, USA [27]. The following link <https://github.com/fit-r2lab/demo-cefore> includes the artefacts that allows to reproduce performance results shown in the paper.

### **6.2.7. Low Cost Video Streaming through Mobile Edge Caching: Modelling and Optimization**

**Participants:** Luigi Vigneri, Chadi Barakat.

Caching content at the edge of mobile networks is considered as a promising way to deal with the data tsunami. In addition to caching at fixed base stations or user devices, it has been recently proposed that an architecture with public or private transportation acting as mobile relays and caches might be a promising middle ground. While such mobile caches have mostly been considered in the context of delay tolerant networks, in this work done in collaboration with Eurecom with the support of the UCN@Sophia Labex, we argue that they could be used for low cost video streaming without the need to impose any delay on the user. Users can prefetch video chunks into their playout buffer from encountered vehicle caches (at low cost) or stream from the cellular infrastructure (at higher cost) when their playout buffer empties while watching the content. Our main contributions are: (i) to model the playout buffer in the user device and analyze its idle periods which correspond to bytes downloaded from the infrastructure; (ii) to optimize the content allocation to mobile caches, to minimize the expected number of non-offloaded bytes. We perform trace-based simulations to support our findings showing that up to 60 percent of the original traffic could be offloaded from the main infrastructure. These contributions were published in the IEEE Transactions on Mobile Computing journal [18].

### **6.2.8. Quality of Experience-Aware Mobile Edge Caching through a Vehicular Cloud**

**Participants:** Luigi Vigneri, Chadi Barakat.

Densification through small cells and caching in base stations have been proposed to deal with the increasing demand for Internet content and the related overload on the cellular infrastructure. However, these solutions are expensive to install and maintain. Instead, using vehicles acting as mobile caches might represent an interesting alternative. In this work, we assume that users can query nearby vehicles for some time, and be redirected to the cellular infrastructure when the deadline expires. Beyond reducing costs, in such an architecture, through vehicle mobility, a user sees a much larger variety of locally accessible content within only few minutes. Unlike most of the related works on delay tolerant access, we consider the impact on the user experience by assigning different retrieval deadlines per content. We provide the following contributions: (i) we model analytically such a scenario; (ii) we formulate an optimization problem to maximize the traffic offloaded while ensuring user experience guarantees; (iii) we propose two variable deadline policies; (iv) we perform realistic trace-based simulations, and we show that, even with low technology penetration rate, more than 60% of the total traffic can be offloaded which is around 20% larger compared to existing allocation policies. These results were published in the IEEE Transactions on Mobile Computing journal [19].

### **6.2.9. Machine Learning for Next-Generation Intelligent Transportation Systems**

**Participants:** Tingting Yuan, Thierry Turletti, Chadi Barakat.

Intelligent Transportation Systems, or ITS for short, includes a variety of services and applications such as road traffic management, traveler information systems, public transit system management, and autonomous vehicles, to name a few. It is expected that ITS will be an integral part of urban planning and future cities as it will contribute to improved road and traffic safety, transportation and transit efficiency, as well as to increased energy efficiency and reduced environmental pollution. On the other hand, ITS poses a variety of challenges due to its scalability and diverse quality-of-service needs, as well as the massive amounts of data it will generate. In this survey, we explore the use of Machine Learning (ML), which has recently gained significant traction, to enable ITS. In the context of the Drive associated team, we did a comprehensive survey of the current state-of-the-art of how ML technology has been applied to a broad range of ITS applications and services, such as cooperative driving and road hazard warning, and identify future directions for how ITS can use and benefit from ML technology. The survey is documented in [42].

## 6.3. Experimental Evaluation

### 6.3.1. Exploiting the cloud for Mininet performance

**Participants:** Giuseppe Di Lena, Damien Saucez, Thierry Turletti.

Networks have become complex systems that combine various concepts, techniques, and technologies. As a consequence, modelling or simulating them is now extremely complicated and researchers massively resort to prototyping techniques. Among other tools, Mininet is the most popular when it comes to evaluate SDN propositions. It allows to emulate SDN networks on a single computer. However, under certain circumstances experiments (e.g., resource intensive ones) may overload the host running Mininet. To tackle this issue, we propose Distrinet, a way to distribute Mininet over multiple hosts. Distrinet uses the same API than Mininet, meaning that it is compatible with Mininet programs. Distrinet is generic and can deploy experiments in Linux clusters or in the Amazon EC2 cloud. Thanks to optimization techniques, Distrinet minimizes the number of hosts required to perform an experiment given the capabilities of the hosting infrastructure, meaning that the experiment is run in a single host (as Mininet) if possible. Otherwise, it is automatically deployed on a platform using a minimum amount of resources in a Linux cluster or with a minimum cost in Amazon EC2. This work has been presented at the IEEE International Conference on Cloud Networking (CloudNet) [22]. Distrinet has been demonstrated both at the IEEE CloudNet conference and at the ACM CoNEXT conference in Orlando USA in December 2019 [39].

### 6.3.2. Distributed Network Experiment Emulation

**Participants:** Giuseppe Di Lena, Damien Saucez, Thierry Turletti, Walid Dabbous.

With the ever growing complexity of networks, researchers have to rely on test-beds to be able to fully assess the quality of their propositions. In the meanwhile, Mininet offers a simple yet powerful API, the goldilocks of network emulators. We advocate that the Mininet API is the right level of abstraction for network experiments. Unfortunately it is designed to be run on a single machine. To address this issue we developed a distributed version of Mininet-Distrinet-that can be used to perform network experiments in any Linux-based testbeds, either public or private. To properly use testbed resources and avoid over-commitment that would lead to inaccurate results, Distrinet uses optimization techniques that determine how to orchestrate the experiments within the testbed. Its programmatic approach, its ability to work on various testbeds, and its optimal management of resources make Distrinet a key element to reproducible research. This work has been presented at the Global Experimentation for Future Internet - Workshop (GeFi) workshop November 2019, at Coimbra in Portugal [38].

### 6.3.3. Evaluating smartphone performance for cellular power measurement. Under submission

**Participants:** Yanis Boussad, Arnaud Legout.

From crowdsourced data collection to automation and robotics, mobile smartphones are well suited for various use cases given the rich hardware components they feature. Researchers can now have access to various sensors such as barometers, magnetometers, orientation sensors, in addition to multiple wireless technologies all on a single and relatively cheap mobile smartphone. In this work, we study the performance of smartphones to measure cellular wireless power. We performed our experiments inside an anechoic chamber in order to compare the measurements of smartphone to the ones obtained with professional spectrum analyzer. We first evaluate the effect of orientation on the received power, then we propose a way to improve the accuracy of smartphone power measurements by using the orientation sensors. We improve the accuracy of the measurements from 25 dBm RMSE to no more than 6 dBm RMSE. We also show how we can exploit the characteristics of the reception pattern of the smartphone to determine the angle of arrival of the signal. The results of this work are described in a research report under submission [32].

### 6.3.4. Towards Reproducible Wireless Experiments Using R2lab

**Participants:** Mohamed Naoufal Mahfoudi, Thierry Parmentelat, Thierry Turletti, Walid Dabbous.

Reproducibility is key in designing wireless systems and evaluating their performance. Trying to reproduce wireless experiments allowed us to identify some pitfalls and possible ways to simplify the complex task of avoiding them. In this research report, we expose a few considerations that we learned are instrumental for ensuring the reproducibility of wireless experiments. Then we describe the steps we have taken to make our experiments easy to reproduce. We specifically address issues related to wireless hardware, as well as varying propagation channel conditions. We show that extensive knowledge of the used hardware and of its design is required to guarantee that the inner state of the system has no negative impact on performance evaluation and experimental results. As for variability of channel conditions, we make the case that a special setup or testbed is necessary so that one can control the ambient wireless propagation environment, using for instance, an anechoic chamber like R2lab. This work is published as research report [33].

### ***6.3.5. A step towards runnable papers using R2lab***

**Participants:** Thierry Parmentelat, Mohamed Naoufal Mahfoudi, Thierry Turetletti, Walid Dabbous.

In this research report, we present R2lab, an open, electromagnetically insulated research testbed dedicated to wireless networking. We describe the hardware capabilities currently available in terms of Software Defined Radio, and the software suite made available to deploy experiments. Using a generic experiment example, we show how it all fits into a notebook-based approach to getting closer to runnable papers. This work is published as research report [34].

## ECUADOR Project-Team

### 6. New Results

#### 6.1. Towards Algorithmic Differentiation of C++

**Participants:** Laurent Hascoët, Valérie Pascual, Frederic Cazals [ABS team, Inria Sophia-Antipolis].

Our goal is to extend Tapenade for C++. We further developed our external parser for C++, built on top of Clang-LLVM <https://clang.llvm.org/>. This parser is now connected to the input formalism “IL” of Tapenade. Tapenade now manages enough constructs of Object languages to be able to build its own Internal Representation (IR) and to regenerate back from the IR a non-transformed C++ source.

In the present development stage, this back-and-forth chain works on several small C++ codes. Still, many issues remain on the large example provided by the ABS team. We are working to solve those progressively. The lack of serious development documentation on the Clang internals obviously doesn't help.

The next development stage will be to adapt the analysis and differentiation components of Tapenade to the new Object constructs of the IR. This development has not started yet. Upstream this development, we need to devise an extended AD model correspondingly. This research part is in progress.

#### 6.2. AD of mixed-language codes

**Participants:** Valérie Pascual, Laurent Hascoët.

We extend Tapenade to differentiate codes that mix different languages, for both tangent and adjoint modes of AD. Our motivating application is Calculix, a 3-D Structural Finite Element code that mixes Fortran and C. This year we improved the memory representation of Tapenade's IR to handle the C-Fortran memory correspondence (commons, structs...) defined by the Fortran standard.

C files (aka “translation units”) and Fortran modules are two instances of the more general notion of “package” for which we have developed a unified representation in Tapenade, that also handles C++ namespaces.

#### 6.3. Application to large industrial codes

**Participants:** Valérie Pascual, Laurent Hascoët, Bruno Maugars [ONERA], Sébastien Bourasseau [ONERA], Cédric Content [ONERA], Jose I. Cardesa [IMFT], Christophe Airiau [IMFT].

We support industrial users with their first experiments of Algorithmic Differentiation of large in-house codes. This concerned two industrial codes this year.

One application is with ONERA on their ElsA CFD platform (Fortran 90). This is the continuation of a collaboration started in 2018. Both tangent and adjoint models of the kernel of ElsA were built successfully with Tapenade. This year's work was mostly about improving efficiency. It is worth noticing that this application was performed inside ONERA by ONERA engineers (Bruno Maugars, Sébastien Bourasseau, Cédric Content) with no need for installation of ElsA inside Inria. We take this as a sign of maturity of Tapenade. Our contribution is driven by development meetings, in which we point out some strategies and tool options to improve efficiency of the adjoint code. As a result from these discussions, we developed improved strategies and AD model, that will be useful to other tools. These improvements deal mostly with the adjoint of vectorized code. We prepared together an article that describes the architecture of a modular and AD-friendly ElsA, together with the corresponding extensions of the AD model of Tapenade. This article has been submitted to “Computers and Fluids”.



The other application ultimately targets AD of the “Jaguar” code, developed jointly by ONERA, CERFACS, and IMFT in Toulouse. This is a collaboration with Jose I. Cardesa and Christophe Airiau, both at IMFT. After a relatively easy tangent differentiation, most of the effort was devoted to obtaining a running and efficient adjoint code. Not too surprisingly, the main source of trouble was the Message-Passing parallel aspect on the application code. This underlined a lack of debugging support for adjoint-differentiated code. Given the runtime of the simulation that we consider (from hours to a few days on a 4110 processors platform), efficiency is crucial. We used the optimal binomial checkpointing scheme at the time-stepping level. However, performance of the adjoint code can probably be improved further with a better checkpointing scheme on the call tree. This calls in particular for AD-specific performance profiling tools, that we are planning to develop. We prepared together an article that describes this successful experiment, which is now submitted to “Journal of Computational Science”.

Two collaborations are in preparation for next year, one with Jan Hueckelheim at Argonne National Lab. about SIMD parallel codes, and one with Stefano Carli at KU Leuven about adjoint AD of the plasma code SOLPS-ITER.

## 6.4. Control of approximation errors

**Participants:** Alain Dervieux, Loic Frazza [Gamma3 team, Inria-Saclay], Adrien Loseille [Gamma3 team, Inria-Saclay], Frédéric Alauzet [Gamma3 team, Inria-Saclay], Anca Belme [university of Paris 6], Alexandre Carabias [Lemma].

Reducing approximation errors as much as possible is a particular kind of optimal control problem. We formulate it exactly this way when we look for the optimal metric of the mesh, which minimizes a user-specified functional (goal-oriented mesh adaptation). In that case, the usual methods of optimal control apply, using adjoint states that can be produced by Algorithmic Differentiation.

This year, we published the final revised versions of two conference papers [23], [21], we published in a journal the final version of the adjoint-based mesh adaptation for Navier-Stokes flows [16]), and we published in “Numerical Methods in Fluids” a work on nonlinear correctors extending [22]. Let us also mention the final publication of the book “Uncertainty Management for Robust Industrial Design in Aeronautics”, edited by C. Hirsch et al. in the Springer series Notes on Numerical Fluid Mechanics and Multidisciplinary Design (2019) in which we have contributed chapters 20, 21, 45, and 48.

The monography on mesh adaptation currently being written by Alauzet, Loseille, Koobus and Dervieux now involves all its chapters (14 chapters) and is being finalized.

## 6.5. Turbulence models

**Participants:** Alain Dervieux, Bruno Koobus, Stephen Wornom.

Modeling turbulence is an essential aspect of CFD. The purpose of our work in hybrid RANS/LES (Reynolds Averaged Navier-Stokes / Large Eddy Simulation) is to develop new approaches for industrial applications of LES-based analyses. In the applications targetted (aeronautics, hydraulics), the Reynolds number can be as high as several tens of millions, far too high for pure LES models. However, certain regions in the flow can be predicted better with LES than with usual statistical RANS models. These are mainly vortical separated regions as assumed in one of the most popular hybrid models, the hybrid Detached Eddy Simulation (DES) model. Here, “hybrid” means that a blending is applied between LES and RANS. An important difference between a real life flow and a wind tunnel or basin is that the turbulence of the flow upstream of each body is not well known.

The development of hybrid models, in particular DES in the litterature, has raised the question of the domain of validity of these models. According to theory, these models should not be applied to flow involving laminar boundary layers (BL). But industrial flows are complex flows and often present regions of laminar BL, regions of fully developed turbulent BL and regions of non-equilibrium vortical BL. It is then mandatory for industrial use that the new hybrid models give a reasonable prediction for all these types of flow. We concentrated on evaluating the behavior of hybrid models for laminar BL and for vortical wakes. While less predictive than pure LES on laminar BL, some hybrid models still give reasonable predictions for rather low Reynolds numbers.

We have developed a new model relying on the hybridation of a DES model based on a  $k-\epsilon$  closure with our dynamic VMS model [13] [11]. Our purpose is to propose a model rather predictive in condition where the engineer has not much information concerning the turbulence in the flow under study. This year, we continued to improve this model and to test it for a large set of configurations with Reynolds numbers ranging from low (laminar flows) to very large.

## 6.6. High order approximations

**Participants:** Alain Dervieux, Bruno Koobus, Stephen Wornom, Tanya Kozubskaya [Keldysh Institute of Russian Academy].

High order approximations for compressible flows on unstructured meshes are facing many constraints that increase their complexity i.e. their computational cost. This is clear for the largest class of approximation, the class of  $k$ -exact schemes, which rely on a local polynomial representation of degree  $k$ . We are investigating schemes which would solve as efficiently as possible the dilemma of choosing between an approximation with a representation inside macro-elements which finally constrains the mesh, and a representation around each individual cell, as in vertex formulations. This is a cooperation with the Keldysh Institute of Russian Academy which whom we have already developed several families of superconvergent schemes.

## 6.7. Aeroacoustics

**Participants:** Alain Dervieux, Bruno Koobus, Stephen Wornom, Tanya Kozubskaya [Keldysh Institute of Russian Academy].

The progress in highly accurate schemes for compressible flows on unstructured meshes (together with advances in massive parallelization of these schemes) allows us to solve problems previously out of reach. The three teams of Montpellier university (coordinator), Inria-Sophia and Keldysh Institute of Moscow have written a proposal for cooperation on the subject of the extension of these methods to simulate the noise emission of rotating machines (helicopters, future aerial vehicles, unmanned aerial vehicles, wind turbines...). The proposal has been selected by ANR and RSF (Russian Science Foundation) for support for a program duration of 4 years.

## EPIONE Project-Team

## 6. New Results

### 6.1. Medical Image Analysis

#### 6.1.1. Learning a Probabilistic Model for Diffeomorphic Registration and Motion Modeling

**Participants:** Julian Krebs [Correspondant], Hervé Delingette, Tommaso Mansi [Siemens Healthineers, Princeton, NJ, USA], Nicholas Ayache.

*This work is funded by Siemens Healthineers, Princeton, NJ, USA*

deformable registration, probabilistic motion modeling, artificial intelligence, latent variable model, deformation transport

We developed a probabilistic approach for multi-scale deformable image registration in 3-D using conditional variational autoencoder [16], [58] and extended it to a motion model by using cardiac MRI image sequences [40]. This includes:

- A probabilistic formulation of the registration problem through unsupervised learning of an encoded deformation model.
- A generative motion model using explicit time-dependent temporal convolutional networks (Fig. 4).
- Demonstration on cardiac cine-MRI for cardiac motion tracking, simulation, transport and temporal super-resolution.

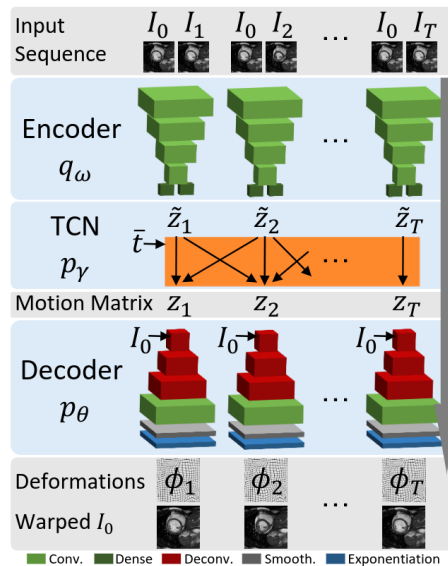


Figure 4. Probabilistic motion model: the encoder  $q_\omega$  projects the image pair  $(I_0, I_t)$  to a probabilistic low-dimensional deformation encoding  $\tilde{z}_t$  from which the temporal convolutional network  $p_\gamma$  constructs the motion matrix  $z \in \mathbb{R}^{d \times T}$ . The decoder  $p_\theta$  maps the motion matrix to the deformations  $\phi_t$ .

### 6.1.2. Predicting PET-derived demyelination from multimodal MRI using sketcher-refiner adversarial training for multiple sclerosis

**Participants:** Wen Wei [Correspondent], Nicholas Ayache, Olivier Colliot [ARAMIS].

*This work is done in collaboration with the Aramis-Project team of Inria in Paris and the researchers at the Brain and Spinal Cord Institute (ICM) located in Paris.*

Multiple Sclerosis, MRI, PET, GANs

By using multiparametric MRI, we proposed to use a 3D FCNN to predict FLAIR MRI which is used clinically for the detection of WM lesions [26]. In addition, we proposed Sketcher-Refiner GANs to predict PET-derived demyelination from multiparametric MRI [25] with the following contributions:

- Learning the complex relationship between myelin content and multimodal MRI data;
- Comparing quantitatively our approach to other state-of-the-art techniques;
- Proposing visual attention saliency maps to better interpret the neural networks;
- Comparing different combinations of MRI modalities and features to assess which is the optimal input;

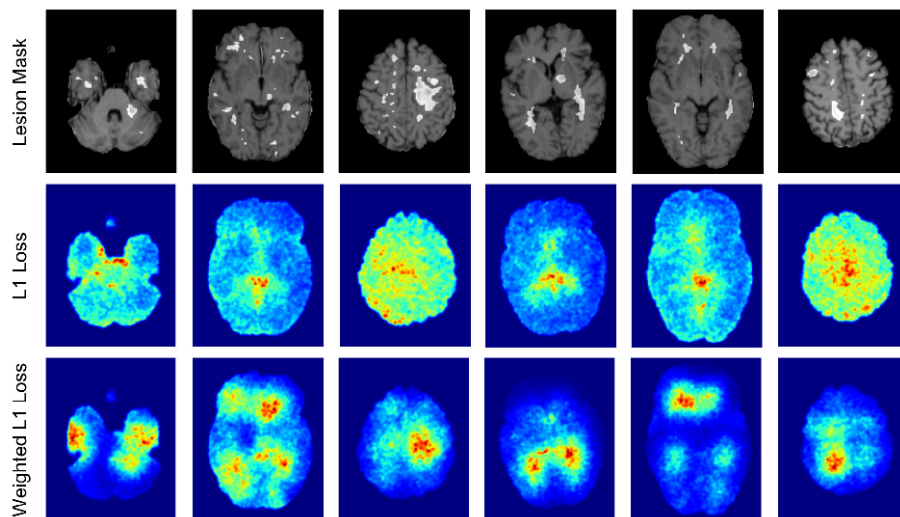


*Figure 5. The proposed visual attention saliency map. The white regions shown in first row are MS lesion masks. The second row shows some examples of the attention of neural networks when L1 loss is used as the traditional constraint in the loss function, without the specific weighting scheme that we proposed. The third row shows the corresponding attention of neural networks when our proposed weighted L1 loss is applied. It is clear that our designed loss function is able to effectively shift the attention of neural networks towards MS lesions.*

### 6.1.3. Patch Based Bayesian Mesh Registration

**Participants:** Paul Blanc-Durand [Correspondant], Hervé Delingette.

*A 1 year grant from APHP*

Bayesian Modeling, Mesh deformation, Mechanical model

The objective of this work is to co-register two lung CT scans of the same patient acquired at different breathing cycle based on an elastic and Bayesian model of lung deformation. Its originality stems from the joint estimation of a displacement fields and its derivatives (gradient matrix) defined from a tetrahedral mesh. Inference is performed in two alternating steps including the optimization of local affine transforms and the global optimization of the displacement.

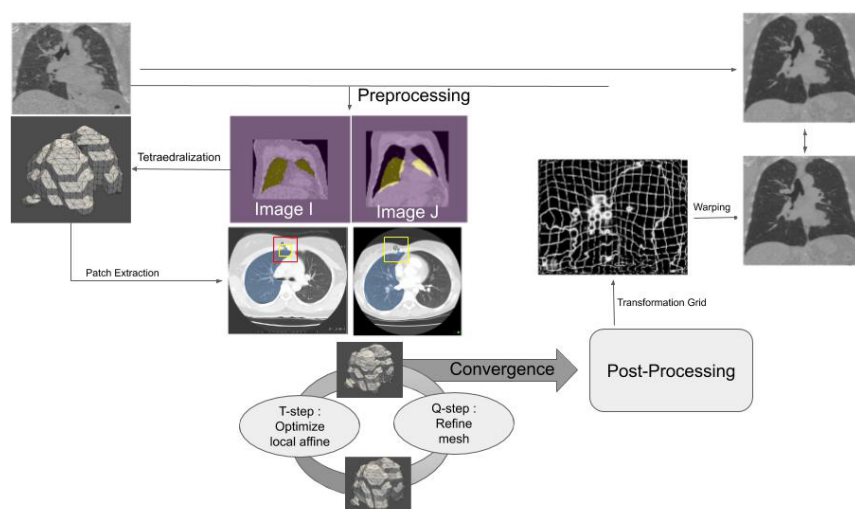


Figure 6. Patches are extracted around vertices of mesh. During *T*-step, we aim to optimize an affine transform centered on a vertice of image *I* (the moving image) to image *J* (the fixed image). The affine transform is regularized under a probabilistic model taking into account the deformation of the mesh. During *Q*-step, we developed an elastical model of lung which homogenize predictions. After few epochs, convergence is achieved.

## 6.2. Imaging & Phenomics, Biostatistics

### 6.2.1. Statistical learning on large databases of heterogeneous imaging, cognitive and behavioral data

**Participants:** Luigi Antelmi [Correspondent], Nicholas Ayache, Philippe Robert, Marco Lorenzi.

Supported by the French government, through the UCA<sup>JEDI</sup> Investments in the Future project managed by the National Research Agency (ANR) ref. num. ANR-15-IDEX-01, our research is within the MNC3 initiative (Médecine Numérique: Cerveau, Cognition, Comportement), in collaboration with the Institut Claude Pompidou (CHU of Nice). Computational facilities are funded by the grant AAP Santé 06 2017-260 DGA-DSH, and by the Inria Sophia Antipolis - Méditerranée, "NEF" computation cluster.

statistical learning, joint analysis, neuroimaging

The aim of our work is to build scalable learning models for the joint analysis of heterogeneous biomedical data, to be applied to the investigation of neurological and neuropsychiatric disorders from collections of brain imaging, body sensors, biological and clinical data available in current large-scale databases such as ADNI<sup>0</sup> and local clinical cohorts.

<sup>0</sup><http://adni.loni.usc.edu/>

We developed a probabilistic latent variable model able to account for heterogeneous data modalities jointly [6]. In the latent space, this is achieved by constraining the variational distribution of each modality to a common target prior. Moreover, we added *ad hoc* prior distribution and parameterization for the latent space to induce sparsity (Fig. 7 a). This approach is capable to highlight meaningful relationships among biomarkers in the context of Alzheimer’s disease (Fig. 7 b) that can be used to develop optimal strategies for disease quantification and prediction.

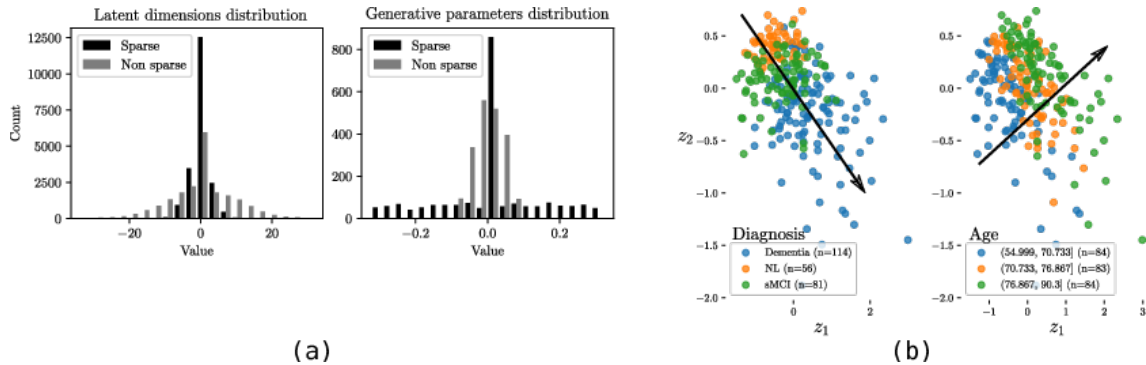


Figure 7. (a) Effect of variational dropout on a synthetic experiment modeled with the Multi-Channel VAE. As expected, the minimum amount of non-zero components of the latent variables (left) and generative parameters (right) is obtained with the sparse model. (b) Stratification of the ADNI subjects (test data) in the sparse latent space. In the same space it is possible to stratify subjects in the test-set by disease status (left) and by age (right) in almost orthogonal directions.

### 6.2.2. Joint Biological & Imaging markers for the Diagnosis of severe lung diseases

**Participants:** Benoit Audelan [Correspondant], Hervé Delingette, Nicholas Ayache.

Lung cancer, Early detection, Biomarkers, Segmentation quality control

Lung cancer is among the most common cancer and is considered to be one of the most important public health problem. In recent years, immunotherapy has revolutionized cancer treatments but its efficiency is varying among patients. To prevent possible negative side effects there is a critical need in reliable biomarkers capable of predicting the response to immunotherapy treatments. We analyzed the performance of different biomarkers and studied their combination through logistic regression and decision tree models, as part of a joint project with the IRCAN laboratory (Pr P. Hofman, Dr S. Heeke) at Nice hospital [13].

Furthermore, we investigated the issue of automated quality control assessment of image segmentations, which are a key point of medical image processing pipelines. We propose a novel unsupervised quality control approach based on simple intensity and smoothness assumptions [30]. We introduce a novel spatial prior which allows an automatic estimation of all parameters through Bayesian learning. The approach was tested on various medical imaging datasets (Fig. 8).

### 6.2.3. Modelling and inference of protein dynamics in neurodegenerative diseases across brain networks

**Participants:** Sara Garbarino [Correspondant], Marco Lorenzi.

Sara Garbarino acknowledges financial support from the French government managed by L’Agence Nationale de la Recherche under Investissements d’Avenir UCA JEDI (ANR-15-IDEX-01) through the project “AtroProDem: A data-driven model of mechanistic brain Atrophy Propagation in Dementia”.



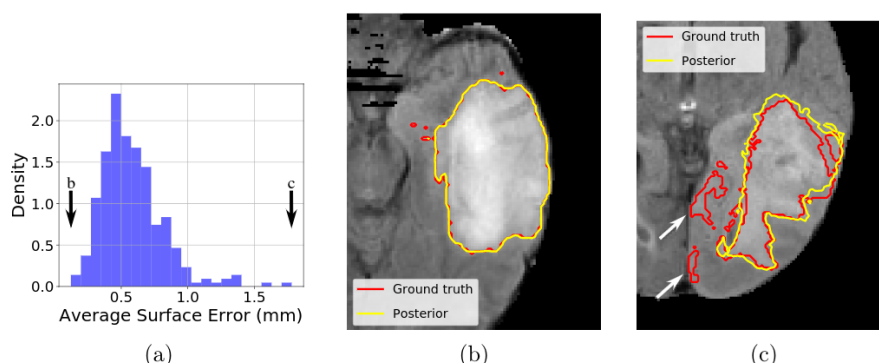


Figure 8. Unsupervised quality control of the BRATS 2017 challenge training set. Distribution of the Average Surface Error (a). Example of a segmentation explained by the model (b). Example of a segmentation not explained by the model (c).

Gaussian Processes, Bayesian non-parametric modelling, neuroimaging data, protein dynamics, brain network

In this project we propose the first unified framework for the joint estimation of long term neurodegenerative disease progression and kinetic parameters describing pathological protein dynamics across brain networks [48]. The model is expressed within a constrained Gaussian Process regression setting. We use stochastic variational inference for scalable inference and uncertainty quantification. Experiments on simulated data and on AV45-PET brain imaging data measuring topographic amyloid deposition in Alzheimer’s disease show that our model accurately recovers prescribed rates along graph dynamics and precisely reconstructs the underlying progression.

## 6.3. Computational Anatomy & Geometric Statistics

### 6.3.1. Riemannian Geometric Statistics in Medical Image Analysis

**Participants:** Xavier Pennec [Correspondant], Stefan Sommer [CPH Univ, DK], Tom Fletcher [University of Virginia at Charlottesville, USA].

*This work is partially funded by the ERC-Adv G-Statistics*

Geometric statistics, Riemannian geometry, medical image analysis, computational anatomy

There has been a growing need in the medical image computing community for principled methods to process nonlinear geometric data. Riemannian geometry has emerged as one of the most powerful mathematical and computational frameworks for analyzing such data. In the book *Riemannian Geometric Statistics in Medical Image Analysis* [53], we provided an introduction to the core methodology for performing statistics on Riemannian manifolds and more general nonlinear spaces followed by a presentation of state-of-the-art methods in medical image analysis.

We provided more specifically an introduction chapter on differential and Riemannian geometry [56] (with S. Sommer and T. Fletcher), a comprehensive chapter on symmetric positive definite matrices (SPD) and manifold value image processing [55], and reference chapter on the affine connection setting for transformation groups including the stationary velocity fields parametrisation of diffeomorphisms and its use in medical image registration for longitudinal modeling of Alzheimer’s disease [54] (with M. Lorenzi) and a chapter on the statistical bias on the estimation in quotient space [52] (with N. Miolane and L Devillier).

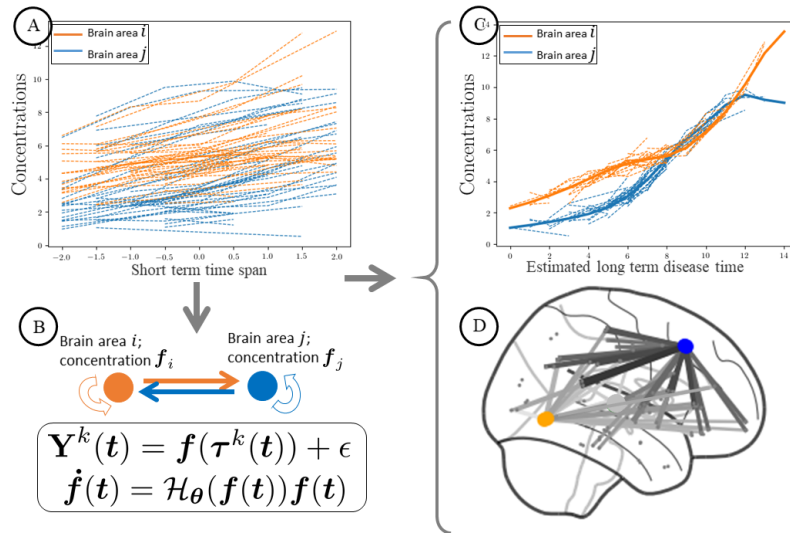


Figure 9. Schematic representation of the proposed framework. Regional protein concentrations are collected for a number of subjects over a short term time span (A). The dynamics of such concentrations are described in terms of a dynamical system for the vector of concentrations (B). The proposed framework estimates such parameters encoding the strength of propagation (D) and the long term protein concentrations with respect to the estimated long term time axis (C).

### 6.3.2. Effect of curvature on the Empirical Fréchet mean estimation in manifolds

**Participant:** Xavier Pennec [Correspondant].

*This work is funded by the ERC-Adv G-Statistics*

Geometric statistics, empirical Fréchet mean

Statistical inference in manifolds most often rely on the Fréchet mean in the Riemannian case, or on exponential barycenters in affine connection spaces. The uncertainty of the empirical mean estimation with a fixed number of samples is a key question. In sufficient concentration conditions, a central limit theorem was established in Riemannian manifolds by Bhattacharya and Patrangenaru in 2005. We propose in [62] an asymptotic development valid in Riemannian and affine cases which better explain the role of the curvature in the modulation of the speed of convergence of the empirical mean. We also establish a non-asymptotic development in high concentration which shows a statistical bias on the empirical mean in the direction of the average gradient of the curvature. These curvature effects become important with large curvature and can drastically modify the estimation of the mean. They could partly explain the phenomenon of sticky means recently put into evidence in stratified spaces, notably in the case of negative curvature.

### 6.3.3. Shape Analysis with diffeomorphisms

**Participants:** Nicolas Guigui [Correspondant], Shuman Jia, Maxime Sermesant, Xavier Pennec.

*This work is partially funded by the ERC-Adv G-Statistics*

Shape Analysis, parallel transport, LDDMM, symmetry

The statistical analysis of temporal deformations and inter-subject variability relies on shape registration and parallel transport of deformations (Figure 10). However, the numerical integration and optimization required lead to important numerical errors. This work aims at improving the numerical consistency and reproducibility

of the Pole Ladder scheme to perform parallel transport. We propose a modification of this scheme using registration errors [39] and define different types of errors to evaluate the accuracy: the involutivity and transvectivity. We test our method on 138 cardiac shapes and demonstrate improved numerical consistency for both types of errors.

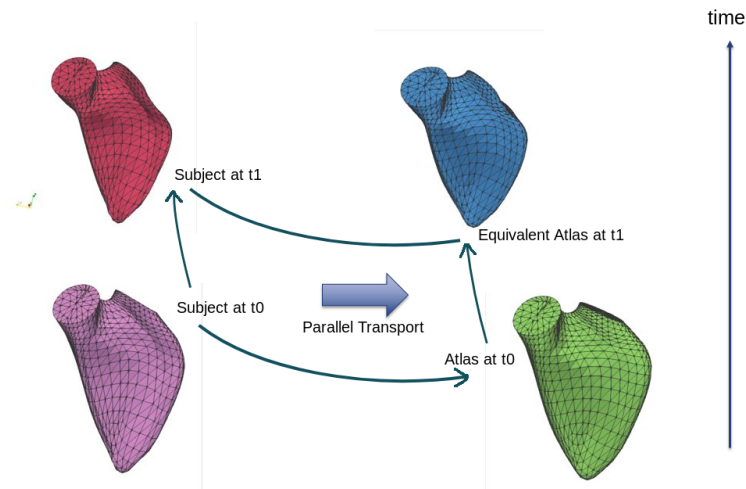


Figure 10. Illustration of our framework using parallel transport to normalize individual temporal deformations to an atlas.

#### 6.3.4. Classification of Riemannian metrics on the manifold of symmetric positive definite matrices

**Participants:** Yann Thanwerdas [Correspondant], Xavier Pennec.

*This work is partially funded by the ERC-Adv G-Statistics and by the IDEX UCA-JEDI ANR-15-IDEX-01 through an excellence OPhD fellowship.*

Symmetric Positive Definite matrices, Riemannian metrics, dually flat manifolds

Symmetric Positive Definite matrices have been used in many fields of medical data analysis. Many Riemannian metrics have been defined on this manifold but the choice of the Riemannian structure lacks a set of principles that could lead one to choose properly the metric. We introduced several families of Riemannian metrics supported by a deformation principle and a principle of balanced metrics:

1. Power-Affine and Deformed-Affine metrics [43], that highlight relations between the affine-invariant, the polar-affine and the log-Euclidean metrics ;
2. Mixed-Power-Euclidean and Mixed-Power-Affine metrics [42], that highlight relations between many Riemannian metrics, as shown on Figure 11 .

#### 6.3.5. Statistical shape analysis of faces for computer aided dermatology and plastic surgery

**Participants:** Florent Jousse [Correspondant], Xavier Pennec, Hervé Delingette, Matilde Gonzalez.

*Supported by the company Quantificare through a CIFRE funding.*

Gaussian Processes, non rigid registration

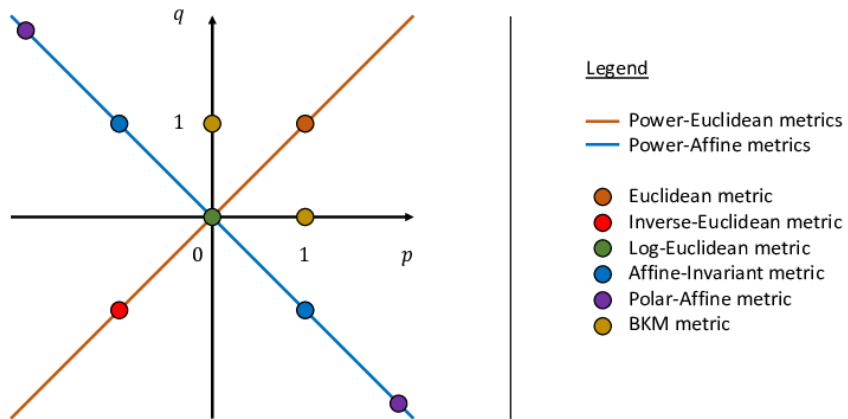


Figure 11. The family of Mixed-Power-Euclidean metrics

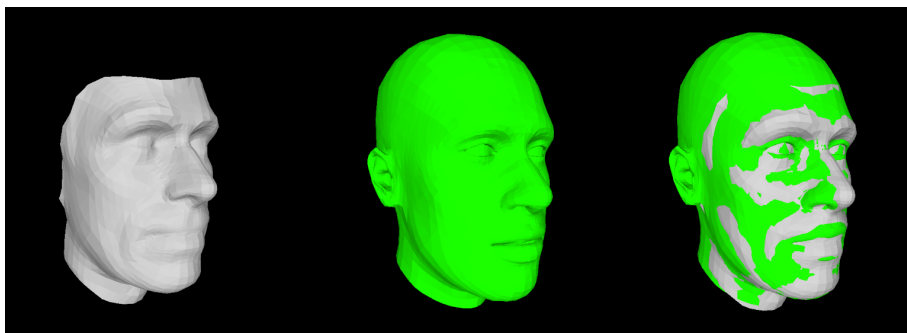


Figure 12. Example of facial template fitting. The white mesh (target) has been acquired by stereoscopy while the green one is a template mesh that has been deformed to fit the target.

The objective of this work is to model complex face deformations related to natural aging, facial expressions, surgical interventions or posture motions to improve the 3D reconstruction of faces and to normalize their analysis. It includes the development of non-rigid registration methods of textured meshes and their statistical modeling through Gaussian processes.

### 6.3.6. Brain Morphometry in the MAPT clinical trial

**Participants:** Raphaël Sivera [Correspondant], Hervé Delingette, Marco Lorenzi, Xavier Pennec, Nicholas Ayache.

*This work is partially funded by the ERC-Adv G-Statistics*

Longitudinal deformation modeling, multivariate statistics, brain morphology, Alzheimer's disease, clinical trial.

- We proposed a complete framework for statistical hypothesis testing on mass-multivariate data. This framework builds on the recent works on multivariate statistics in neuroimaging to propose a generic approach adapted to the study of longitudinal deformations [3].
- This framework is used in the context of the MAPT study to highlight a significant effect of the multidomain intervention on the brain morphological changes (see Figure 13 ) [22].

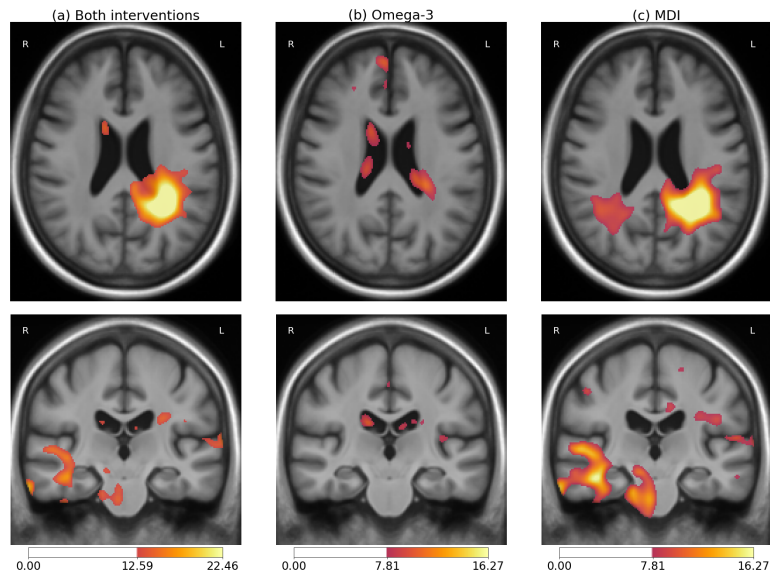


Figure 13. Localization of the MAPT treatments effect on the longitudinal morphological changes for: (a) both categorical variables associated with the omega-3 supplementation and the multidomain intervention, (b) omega-3 only, (c) multidomain intervention only. Color bars indicate the magnitude of the z-values for the likelihood-ratio test. High values indicate a difference in the morphological changes that is associated with the treatment status.

### 6.3.7. Statistical Learning of Heterogeneous Data in Large-Scale Clinical Databases

**Participants:** Clement Abi Nader [Correspondant], Nicholas Ayache, Philippe Robert, Marco Lorenzi.

Gaussian Process, Alzheimer's Disease, Disease Progression Modelling

The aim of this thesis is to develop a spatio-temporal model of Alzheimer's Disease (AD) progression based on multi-modal brain data. We assume that the brain progression is characterized by independent spatio-temporal sources that we want to separate. We estimate brain structures involved in the disease progression at different resolutions thus dealing with the non-stationarity of medical images, while assigning to each of them a monotonic temporal progression using Gaussian processes (Figure 14). We also compute an individual time-shift parameter to assess the disease stage of each subject. This work has been accepted for publication in the journal *NeuroImage* [5]

## 6.4. Computational Physiology

### 6.4.1. Deep Learning based Metal Artifacts Reduction in post-operative Cochlear Implant CT Imaging

**Participants:** Zihao Wang [Correspondant], Clair Vandersteen, Thomas Demarcy, Dan Gnansia, Charles Raffaelli, Nicolas Guevara, Hervé Delingette.

*This work is funded by the Provence-Alpes-Côte-d'Azur region, the Université Côte d'Azur and Oticon Medical through CIMPLE <https://team.inria.fr/epione/en/research/cimple/> research project.*

Generative Adversarial Network, Metal Artifacts Reduction, Cochlea Implantation

We propose a 3D metal artifact reduction method using convolutional neural networks for post-operative cochlear implant imaging.[44]

- Learn metal artifacts reduction by using pre-operative images and metal artifacts simulation to create image pairs for training GANs.
- Metal artifacts simulation starts from a cochlea implantation fusion image and ends with the simulated post-operative image.(Fig. 15)
- A 3D generative adversarial network (MARGANs) to create an image with a reduction of metal artifacts.
- Evaluations on ten patients show the effectiveness of artefact reduction compared to two classical methods.

### 6.4.2. Kinematic Spiral Shape Recognition in the Human Cochlea

**Participants:** Wilhelm Wimmer [Correspondant], Clair Vandersteen, Nicolas Guevara, Marco Caversaccio, Hervé Delingette.

*Supported by the Swiss National Science Foundation (no. P400P2\_180822) and the French government (UCA JEDI - ANR-15-IDEX-01).*

Approximate maximum likelihood, kinematic surface recognition, natural growth

To improve therapies for hearing loss and deafness, e.g., with auditory neuroprostheses, we developed a reliable detection algorithm for the cochlear modiolar axis in CT images (Fig. 16). The algorithm was tested in an experimental study with 4 experts in 23 human cochlea CT data sets [45] [27]. Our experiments showed that the algorithm reduces the alignment error providing more reliable modiolar axis detection for clinical and research applications.

## 6.5. Computational Cardiology & Image-Based Cardiac Interventions

### 6.5.1. Cardial Electrophysiological Model Learning and Personalisation

**Participants:** Nicolas Cedilnik [Correspondant], Ibrahim Ayed [Sorbonne, LIP6, Paris], Hubert Cochet [IHU Liryc, Bordeaux], Patrick Gallinari [Sorbonne, LIP6, Paris], Maxime Sermesant.

*This work is funded by the IHU Liryc, Bordeaux.*

modelling, electrophysiology, ventricular tachycardia, ischemic cardiomyopathy



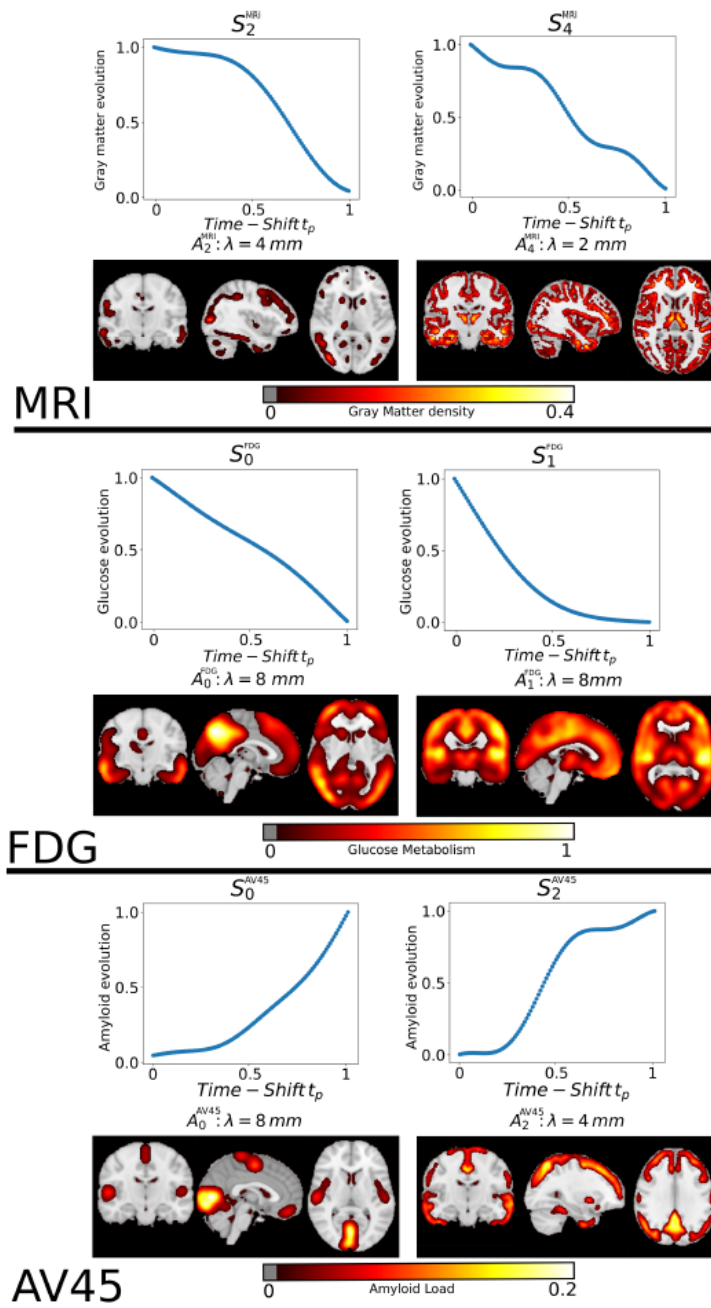


Figure 14. Estimated spatio-temporal processes affecting the brain during Alzheimer's Disease for three different imaging markers.

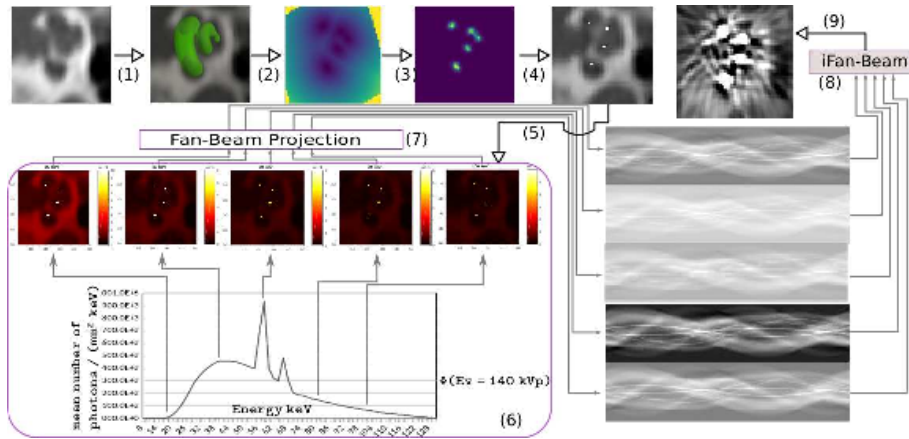


Figure 15. CI metal artifacts simulation workflow starting from a pre-operative image and ending with the simulated post-operative image after 9 processing steps.

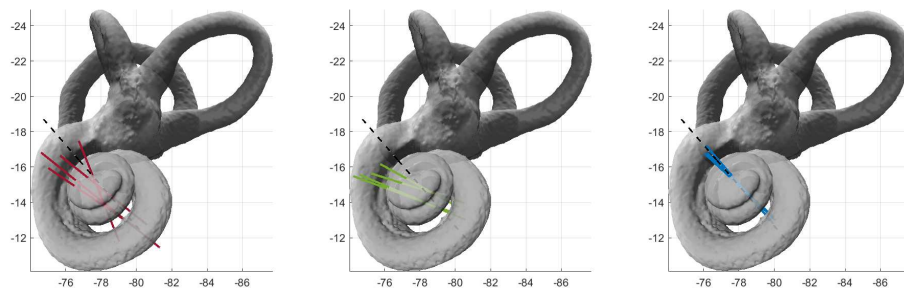


Figure 16. Visualization of the bony labyrinth with reference modiolar axis (dashed line). Modiolar axes after manual landmark-based (left), PCA-based (middle), and robust kinematic detection (right) in CT data are shown for comparison.

This project aims at making electrophysiological model personalisation enter clinical practice in interventional cardiology. During this year:

- we evaluated a fully automated computed tomography-based model personalisation framework in the context of post-ischemic ventricular tachycardia [35],
- we developed a model personalisation methodology based on invasive data in our participation in the STACOM2019 modelling challenge [37],
- we proposed a deep learning based approach to replace numerical integration of partial differential equations used in cardiac modelling [32], see Figure 17 .

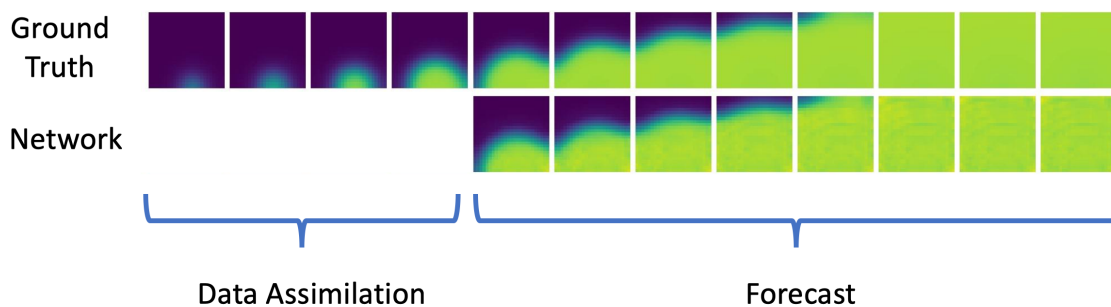


Figure 17. Transmembrane potential obtained with a reaction diffusion model (top) and forecasted by EP-Net (bottom) for one slice of a tissue slab

### 6.5.2. Deep Learning Formulation of ECGI for Data-driven Integration of Spatiotemporal Correlations and Imaging Information

**Participants:** Tania Marina Bacoyannis [Correspondant], Hubert Cochet [IHU Liryc, Bordeaux], Maxime Sermesant.

*This work is funded within the ERC Project ECSTATIC with the IHU Liryc, in Bordeaux.*

Deep Learning, Electrocardiographic Imaging, Inverse problem of ECG, Electrical simulation, Generative Model.

Electrocardiographic imaging (ECGI) aims at reconstructing the electrical activity of the heart using body surface potentials. To achieve this one has to solve the ill-posed inverse problem of the torso propagation. We propose in [33] a novel Deep Learning method based on Conditional Variational Autoencoder able to solve ECGI inverse problem in 2D. This generative probabilistic model learns geometrical and spatio-temporal information and enables to generate the corresponding activation map of the specific heart.

120 activation maps and the corresponding Body Surface Potentials (BSP) were generated using the dipole formulation. 80% of the simulated data was used for training and 20% for testing. We generate 10 probable solutions for each given input using our model. The Mean Squarre Error (MSE) metric over all the tests was 0.095. As results we were able to observe that the reconstruction performs well. Next, we will extend the model in 3D and test it on real data provided by the IHU Liryc.

### 6.5.3. Discovering the link between cardiovascular pathologies and neurodegeneration through biophysical and statistical models of cardiac and brain images

**Participants:** Jaume Banus Cobo [Correspondant], Marco Lorenzi, Maxime Sermesant.

*Université Côte d'Azur (UCA)*

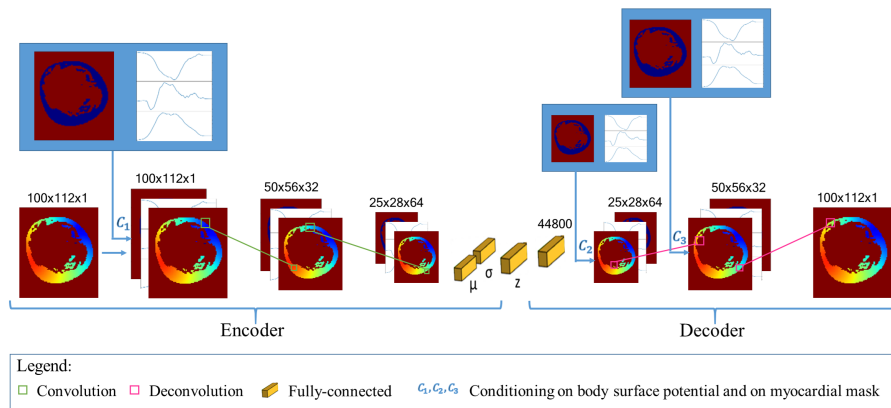


Figure 18. Architecture of our conditioned generative model (encoder) and our conditioned variational approximation (decoder)

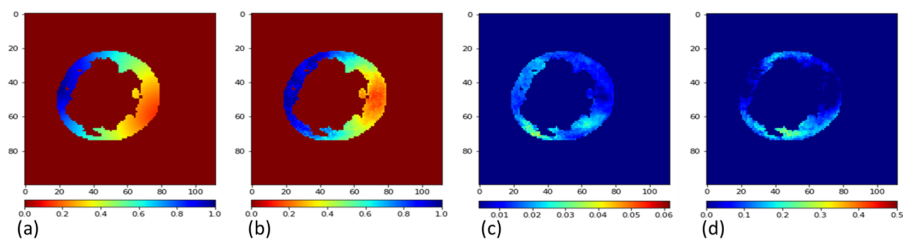


Figure 19. (a) Simulated and (b) predicted mean activation maps for proposed deep learning based ECGI, (c) Standard deviation map calculated over 10 predictions, (d) error map, difference between predicted and simulated activation maps.

## Lumped models - Biophysical simulation - Statistical learning

The project aims at developing a computational model of the relationship between cardiac function and brain damage from large-scale clinical databases of multi-modal and multi-organ medical images. The model is based on advanced statistical learning tools for discovering relevant imaging features related to cardiac dysfunction and brain damage; these features are combined within a unified mechanistic framework to providing a novel understanding of the relationship between cardiac function, vascular pathology and brain damage. [34]

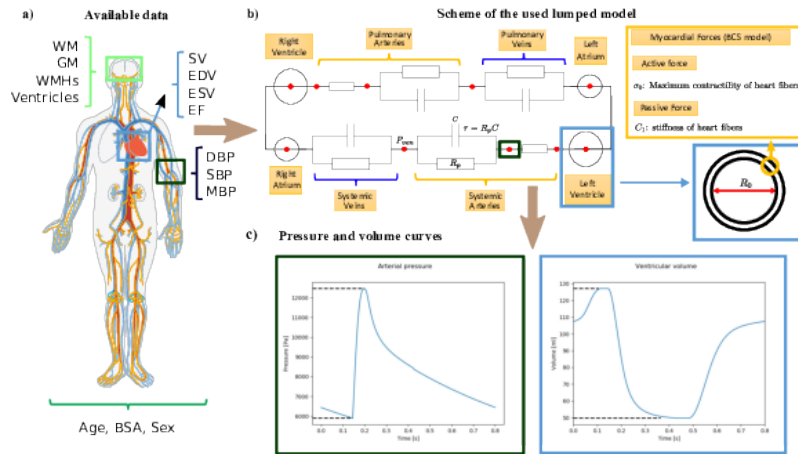


Figure 20. a) Summary of the available data for each subject, including cardiac data, socio-demographic information, blood pressure measurements and brain volumetric indicators. b) Simplified representation of the lumped model showing the parameters used in the personalisation.  $\tau$  characterizes the contractility of the main systemic arteries,  $R_p$  the peripheral resistance,  $P_{ven}$  the venous pressure right after the capillaries,  $R_0$  the radius of the left ventricle,  $\sigma_0$  the contractility of the cardiac fibers and  $C_1$  their stiffness. A more detailed representation of the myocardial forces is omitted for the sake of clarification. c) Example of the pressure and volume curves that can be obtained from the model, from these curves we extract scalar indicators to match the available clinical data.

#### 6.5.4. Parallel transport of surface deformations from pole ladder to symmetrical extension

**Participants:** Shuman Jia [Correspondant], Nicolas Guigui, Nicolas Duchateau, Pamela Mocerì, Maxime Sermesant, Xavier Pennec.

The authors acknowledge the partial funding by the Agence Nationale de la Recherche (ANR)/ERA CoSysMedSysAFib and ANR MIGAT projects.

We proposed a general scheme to perform statistical modeling of the temporal deformation of the heart, directly based on meshes. We encoded the motion and the intersubject shape variations, with diffeomorphisms parameterized either by stationary SVFs or by time-varying velocity fields in the LDDMM framework.

Experiments on a 4D right-ventricular endocardial meshes database demonstrated the stability of our transport algorithm, of importance for the assessment of pathological changes. The method is adaptable to other anatomies with temporal or longitudinal data.

#### 6.5.5. Machine Learning and Pulmonary hypertension

**Participants:** Yingyu Yang [Correspondant], Stephane Gillon, Jaume Banus Cobo, Pamela Mocerì, Maxime Sermesant.

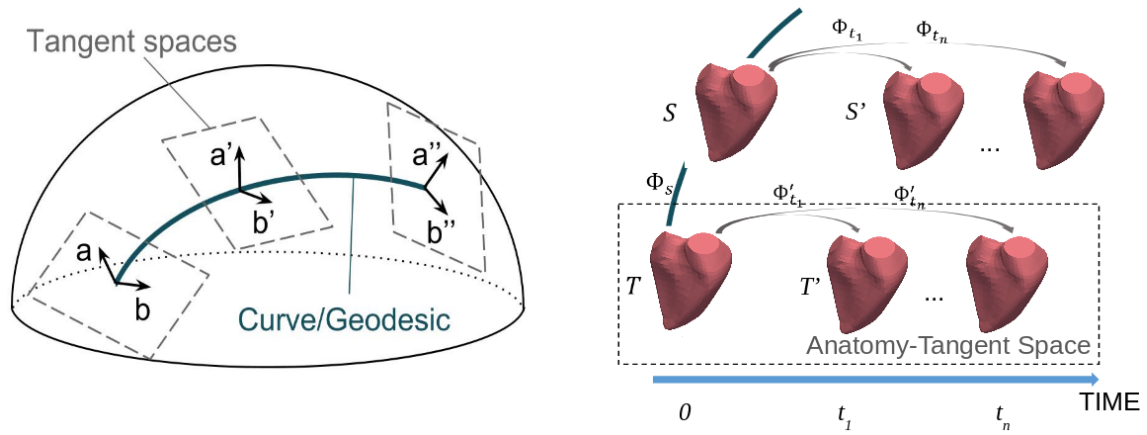


Figure 21. Illustration of parallel transport of vectors  $a$  and  $b$  along a curve (left) and its application to cardiac imaging (right) with a focus on surfaces.

cardiac modelling, machine learning

Right heart catheterisation is considered as the gold standard for the assessment of patients with suspected pulmonary hyper-tension. It provides clinicians with meaningful data, such as pulmonary capillary wedge pressure and pulmonary vascular resistance, however its usage is limited due to its invasive nature. Non-invasive alternatives, like Doppler echocardiography could present insightful measurements of right heart but lack detailed information related to pulmonary vasculature. In order to explore non-invasive means, we studied a dataset of 95 pulmonary hypertension patients, which includes measurements from echocardiography and from right-heart catheterisation. We used data extracted from echocardiography to conduct cardiac circulation model personalisation and tested its prediction power of catheter data. Standard machine learning methods were also investigated for pulmonary artery pressure prediction. Our preliminary results demonstrated the potential prediction power of both data-driven and model-based approaches. It was published as "Non-Invasive Pressure Estimation in Patients with Pulmonary Arterial Hypertension: Data-driven or Model-based?" accepted at 10th Workshop on Statistical Atlases and Computational Modelling of the Heart, Oct 2019, Shenzhen, China [46]

#### 6.5.6. Style Data Augmentation for Robust Segmentation of Multi-Modality Cardiac MRI

**Participants:** Buntheng Ly [Correspondent], Hubert Cochet [IHU Liryc, Bordeaux], Maxime Sermesant.

Image Segmentation. Multi-modality, Cardiac Magnetic Resonance Imaging, Late Gadolinium Enhanced, Deep Learning

We propose a data augmentation method to improve the segmentation accuracy of the convolutional neural network on multi-modality cardiac magnetic resonance dataset [41].

The strategy aims to reduce over-fitting of the network toward any specific intensity or contrast of the training images by introducing diversity in these two aspects, as shown in figure 23 .

#### 6.5.7. Towards Hyper-Reduction of Cardiac Models using Poly-Affine Deformation

**Participants:** Gaëtan Desrues [Correspondant], Hervé Delingette, Maxime Sermesant.

Model Order Reduction, Finite Elements Method, Affine Transformation, Meshless



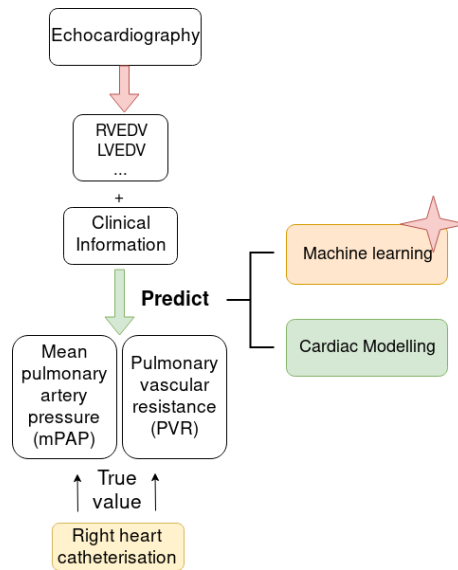


Figure 22. The main idea and logic of this work

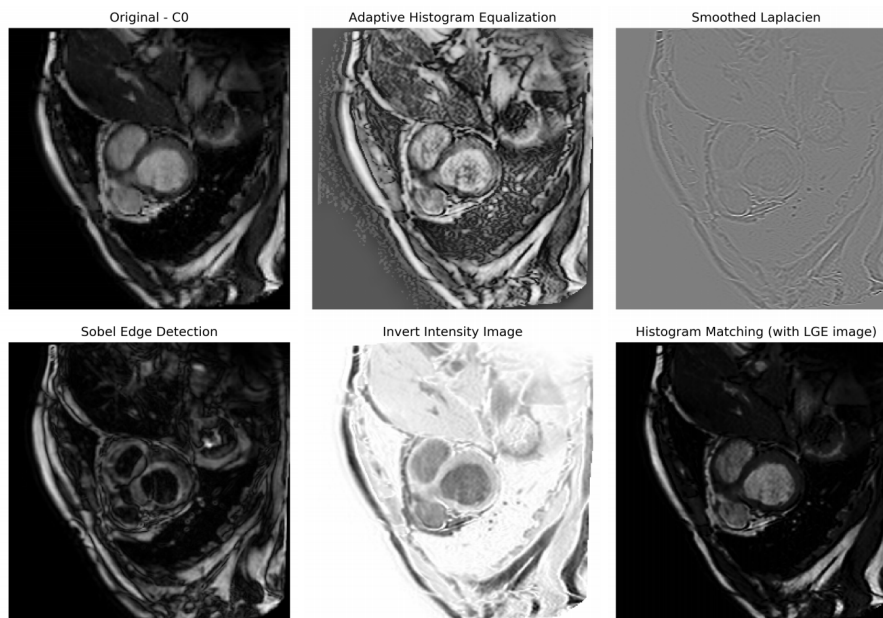


Figure 23. Different variation of input images and the image processing methods used. C0 denotes the steady-state free precessing CMR modality image.

Patient-specific 3D models can help in improving therapy selection, treatment optimization and interventional training. However, these simulations generally have an important computational cost. The aim of this project is to optimize a 3D electromechanical model of the heart for faster simulations [38]. The cardiac deformation is approached by a reduced number of degrees of freedom represented by affine transformations (frames in Figure 24 b) located at the center of the AHA regions (Figure 24 a). The displacement of the material points are computed using region-based shape functions (Figure 24 c).

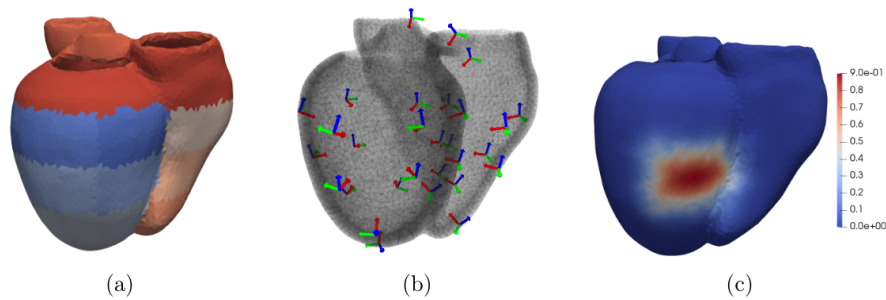


Figure 24. Framework on a cardiac topology. AHA regions (a). Affine degrees of freedom (b). Shape function in one region (c).

## FACTAS Project-Team

## 6. New Results

### 6.1. Inverse problems for Poisson-Laplace equations

**Participants:** Paul Asensio, Laurent Baratchart, Sylvain Chevillard, Juliette Leblond, Jean-Paul Marmorat, Konstantinos Mavreas, Masimba Nemaire.

#### 6.1.1. Inverse magnetization issues from planar data

The overall goal is here to determine magnetic properties of rock samples (*e.g.* meteorites or stalactites), from weak field measurements close to the sample that can nowadays be obtained using SQUIDs (superconducting quantum interference devices). Depending on the geometry of the rock sample, the magnetization distribution can either be considered to lie in a plane (thin sample) or in a parallelepiped of thickness  $r$ . Some of our results apply to both frameworks (the former appears as a limiting case when  $r$  goes to 0), while others concern the 2-D case and have no 3-D counterpart as yet.

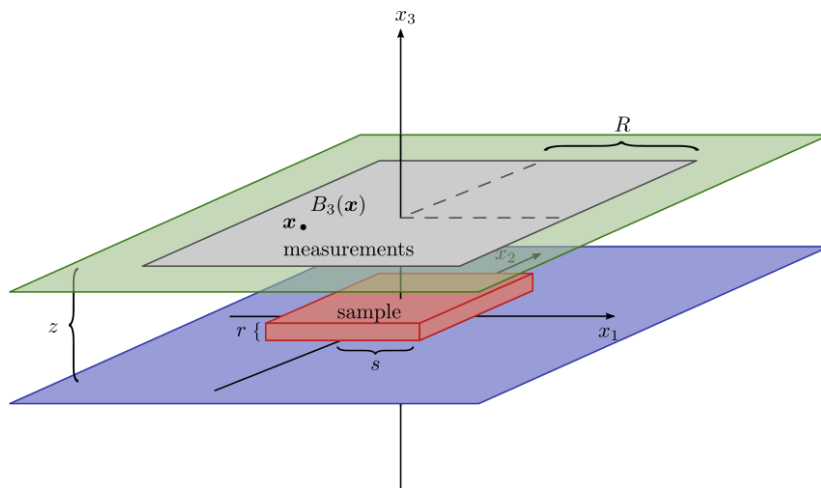


Figure 3. Schematic view of the experimental setup

Figure 3 presents a schematic view of the experimental setup: the sample lies on a horizontal plane at height 0 and its support is included in a parallelepiped. The vertical component  $B_3$  of the field produced by the sample is measured in points of a horizontal square at height  $z$ .

We pursued our investigation of the recovery of magnetizations modeled by signed measures on thin samples, and we singled out an interesting class that we call slender samples. These are sets of zero measure in  $\mathbb{R}^3$ , the complement of which has all its connected components of infinite measure. For such samples, we showed that consistent recovery is possible, in the Morozov discrepancy limit, by penalizing the total variation when either the support of the magnetization is purely 1-unrectifiable (which holds in particular for dipolar models) or the magnetization is unidirectional (an assumption of physical interest because igneous rocks acquire magnetization by cooling down in some ambient field). These notions play a role similar to sparsity in this infinite-dimensional context. An article has been published to report on these results [16]. Moreover, in the case of planar samples (which are certainly slender), a loop decomposition of divergence free measures was

obtained, which sharpens in the 2-D setting the structure theorem of [77], and allowed us to prove, using in addition the real analyticity of the operators relating the magnetization to the field, that the argument of the minimum of the regularized criterion  $\|f - B_3\mu\|_2^2 + \lambda\|\mu\|_{TV}$  is unique; here,  $\mu$  is the measure representing the magnetization with respect to which the criterion gets optimized,  $f$  is the data and  $\lambda > 0$  a regularization parameter, while  $\|\mu\|_{TV}$  is the total variation of  $\mu$ . An implementation using a variant of the FISTA algorithm has been set up which yields promising results when measurements are carried out on a relatively large surface patch. Yet, a deeper understanding on how to adjust the parameters of the method is required. This topic is studied in collaboration with D. Hardin and C. Villalobos from Vanderbilt University.

We also continued investigating the recovery of the moment of a magnetization, an important physical quantity which is in principle easier to reconstruct than the full magnetization because it is simply a vector in  $\mathbb{R}^3$  that only depends on the field (*i.e.* magnetizations that produce the zero field also have zero moment). For the case of thin samples, we published an article reporting the construction of linear estimators for the moment from the field, based on the solution of certain bounded extremal problems in the range of the adjoint of the forward operator [15]. On a related side, we also setup other linear estimators based on asymptotic results, in the previous years. These estimators are not limited to thin samples and can in principle estimate the net moment of 3D samples, provided that the dimensions of the sample are small with respect to the measurement area. Numerical experiments confirm that linear estimators (both kinds) make essential use of field values taken at the boundary of the measurement area, and are easily blurred by noise. We experimentally confirmed this sensitivity on a rather simple case: a small spherule has been magnetized in a controlled way by our partners at MIT, and its net moment has been measured by a classical magnetometer. The spherule has then been measured with the SQUID microscope, with several choices for important parameters (height of the sensor with respect to the spherule, sensitivity of the instrument, size of the 2D rectangle on which measurements are performed, size of the sample step). We applied our (asymptotics based) linear estimator on these experimental maps and they turn out to be clearly affected, especially when the data at the edges of the map are involved. The nature of the noise due to the microscope itself (electronic and quantization noise) might play an important role, as it is known to be non-white, and therefore can affect our methods which sum it up. Subsequently, we now envisage the possibility of modeling the structure of the noise to pre-process the data.

Finally, we considered a simplified 2-D setup for magnetizations and magnetic potentials (of which the magnetic field is the gradient). When both the sample and the measurement set are parallel intervals, we set up some best approximation issues related to inverse recovery and relevant BEP problems in Hardy classes of holomorphic functions, see Section 3.3.1 and [25], which is joint work with E. Pozzi (Department of Mathematics and Statistics, St Louis Univ., St Louis, Missouri, USA). Note that, in the present case, the criterion no longer acts on the boundary of the holomorphy domain (namely, the upper half-plane), but on a strict subset thereof, while the constraint acts on the support of the approximating function. Both involve functions in the Hilbert Hardy space of the upper half-plane.

### 6.1.2. Inverse magnetization issues from sparse cylindrical data

The team Factas was a partner of the ANR project MagLune on Lunar magnetism, headed by the Geophysics and Planetology Department of Cerege, CNRS, Aix-en-Provence, which ended this year (see Section 8.2.1). Recent studies let geoscientists think that the Moon used to have a magnetic dynamo for a while. However, the exact process that triggered and fed this dynamo is still not understood, much less why it stopped. The overall goal of the project was to devise models to explain how this dynamo phenomenon was possible on the Moon.

The geophysicists from Cerege went a couple of times to NASA to perform measurements on a few hundreds of samples brought back from the Moon by Apollo missions. The samples are kept inside bags with a protective atmosphere, and geophysicists are not allowed to open the bags, nor to take out samples from NASA facilities. Moreover, the process must be carried out efficiently as a fee is due to NASA by the time when handling these moon samples. Therefore, measurements were performed with some specific magnetometer designed by our colleagues from Cerege. This device measures the components of the magnetic field produced by the sample, at some discrete set of points located on circles belonging to three cylinders (see Figure 4). The objective of Factas is to enhance the numerical efficiency of post-processing data obtained with this magnetometer.

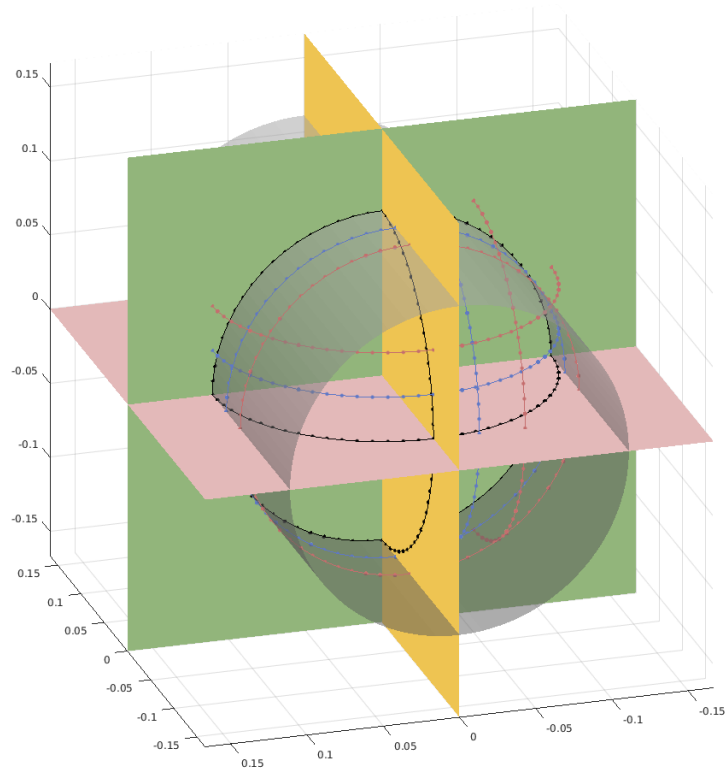


Figure 4. Typical measurements obtained with the instrument of Cerege. Measurements of the field are performed on nine circles, given as sections of three cylinders. On each circle, only one component of the field is measured: the component  $B_h$  along the axis of the corresponding cylinder (blue points), the component  $B_n$  radial with respect to the circle (black points), or the component  $B_\tau$  tangential to the circle (red points).

Under the hypothesis that the field can be well explained by a single magnetic pointwise dipole, and using ideas similar to those underlying the FindSources3D tool (see Sections 3.4.3 and 6.1.3), we try to recover the position and the moment of the dipole using the available measurements. This work, which is still ongoing, constitutes the topic of the PhD thesis of K. Mavreas, whose defense is scheduled on January 31, 2020. In a given cylinder, using the associated cylindrical system of coordinates, recovering the position of the dipole boils down to determine its height  $z$ , its radial distance  $\rho$  and its azimuth  $\phi$ . We use the fact that, whatever component of the field is measured, the (square of the) measurements performed on the circle at height  $h$  correspond to a rational function of the form  $p(z)/(z - u_h)^5$  where  $p$  is a polynomial of degree at most 4 and  $u_h$  is the complex number  $u_h = \frac{1+\rho^2+(h-z)^2}{\rho} e^{i\phi}$ . The numerator  $p$  depends on the moment of the dipole, on the height  $h$  and on the kind of component which is measured. In contrast,  $u_h$  can be estimated by rational approximation techniques, which allows one to obtain  $\phi$  directly and gives the relation  $\rho|u_h| = 1 + \rho^2 + (h - z)^2$ . Combining the relations obtained at several heights, we proposed several methods to estimate  $\rho$  and  $z$ .

This year has been mostly devoted to running numerical experiments on synthetic examples. The first important observation is that the minimization criterion that we use to recover  $u_h$  can have local minima achieving very small values, and that can sometimes erroneously be considered as the global minimum. We started studying theoretically this phenomenon, see Section 6.7.1. This means that the relative error  $\varepsilon = |u_h - \widetilde{u}_h|/|u_h|$  between the theoretical minimum  $u_h$  and the value  $\widetilde{u}_h$  estimated by our algorithm can vary from almost 0 to more than 50%, even when the data used as measurements exactly correspond to the field produced by a magnetic dipole. The second important observation is that the statistical distribution of  $\varepsilon$  (when the position of the dipole is uniformly chosen within a cylinder with a moment uniformly chosen on the unit sphere) depends on the measured component of the field. Figure 5 shows the distribution experimentally observed. The vertical component of the field noticeably leads to better estimates for  $u_h$  than both other components. The third important observation that we made is that the presence of noise on the measurements, even moderate, significantly alters the quality of the estimation of  $u_h$ . Figure 6 shows the distribution experimentally observed in the same conditions as before, but using data contaminated with a random normal noise with standard deviation 5% of the maximal absolute value of the measured component.

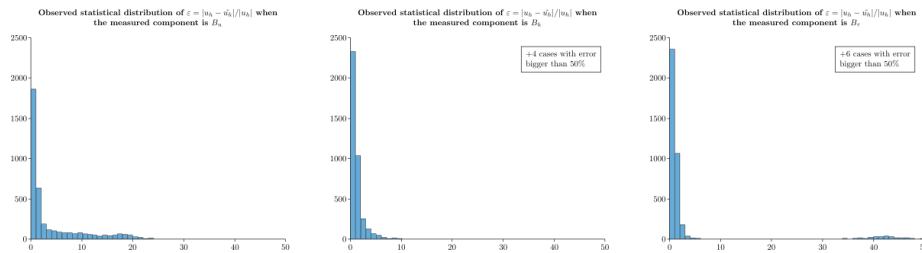


Figure 5. Different statistical behavior of the error of the recovered pole position, depending on the measured component of the field. Each bar indicates the number of cases observed with an error within the range of abscissas of the bar. The experiment has been performed with 4000 dipoles whose position and moment were randomly chosen (uniformly inside a cylinder, and on the unit sphere, respectively).

These observations are somehow bad news, as the method we propose is based on recovering the position of the dipole by using the values  $u_h$  collected at several heights  $h$ . However, our experiments also revealed an unexpected good news: while the estimation of  $u_h$  itself is often bad, as soon as the data are not perfect, its argument (from which  $\phi$  is immediately deduced) turns out to be fairly well recovered. This is illustrated in Figure 7 which shows, on the set of experiments of Figure 6, the position of the 4000 dipoles, with a color indicating whether  $\varepsilon$  is big (left part of the figure) and whether the error on the argument of  $u_h$  is big (right part of the figure). As can be seen, the angular error is most of the time smaller than  $10^\circ$ , even for dipoles



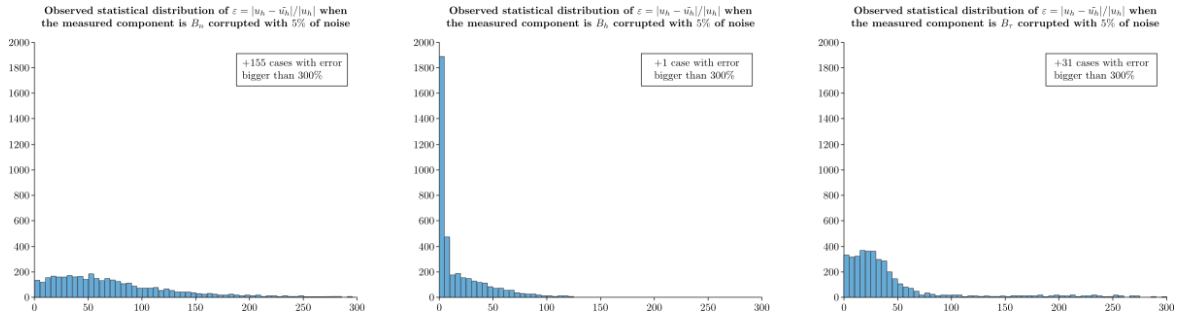


Figure 6. Statistical behavior of the error of the recovered pole position, when the measurement are corrupted with a centered Gaussian noise with standard deviation 5% of the maximal absolute value of the measured component. The setup is otherwise the same as in Figure 5.

for which  $\varepsilon$  is fairly big. This phenomenon is probably due to the fact that local minima of the criterion tends to have a complex argument close to the complex argument of the global minimum, a phenomenon that we started to study theoretically (see Section 6.7.1).

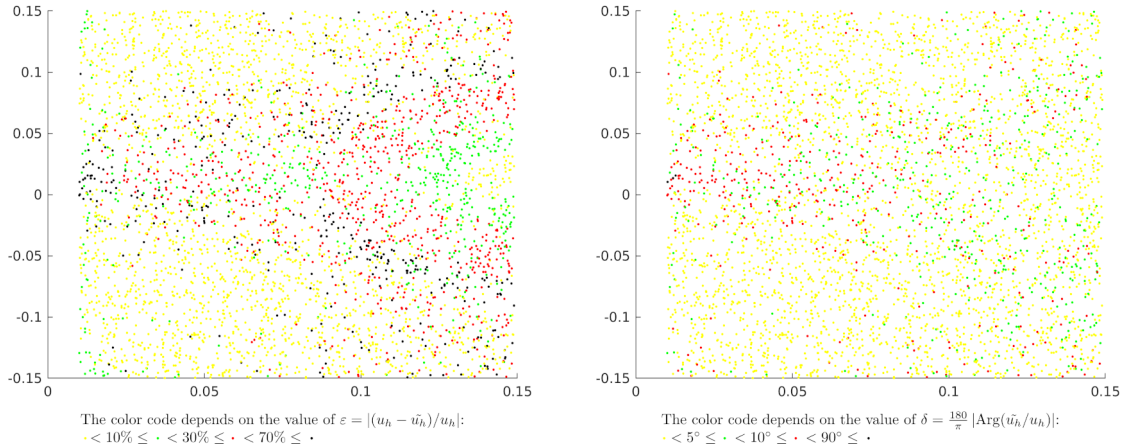


Figure 7. Each dot corresponds to the position of a dipole of the set of experiments described in Figure 6. What is shown is indeed  $(\rho, z)$  where  $\rho$  and  $z$  correspond to, respectively, the radial distance and height of the dipole position, expressed in cylindrical coordinates. The position is displayed with a dot whose color indicates the order of magnitude of the modulus of the relative error (figure on the left) and of the angle error (figure on the right) committed in the recovery of the value  $u_h$ .

### 6.1.3. Inverse problems in medical imaging

In 3-D, functional or clinically active regions in the cortex are often modeled by pointwise sources that have to be localized from measurements, taken by electrodes on the scalp, of an electrical potential satisfying a

Laplace equation (EEG, electroencephalography). In the works [8], [42] on the behavior of poles in best rational approximants of fixed degree to functions with branch points, it was shown how to proceed via best rational approximation on a sequence of 2-D disks cut along the inner sphere, for the case where there are finitely many sources (see Section 4.3).

In this connection, a dedicated software FindSources3D (FS3D, see Section 3.4.3) is being developed, in collaboration with the Inria team Athena and the CMA - Mines ParisTech. Its Matlab version now incorporates the treatment of MEG data, the aim being to handle simultaneous EEG–MEG recordings available from our partners at INS, hospital la Timone, Marseille. Indeed, it is now possible to use simultaneously EEG and MEG measurement devices, in order to measure both the electrical potential and a component of the magnetic field (its normal component on the MEG helmet, that can be assumed to be spherical). This enhances the accuracy of our source recovery algorithms. Note that FS3D takes as inputs actual EEG measurements, like time signals, and performs a suitable singular value decomposition in order to separate independent sources.

It appears that, in the rational approximation step, *multiple* poles possess a nice behavior with respect to branched singularities. This is due to the very physical assumptions on the model from dipolar current sources: for EEG data that correspond to measurements of the electrical potential, one should consider *triple* poles; this will also be the case for MEG – magneto-encephalography – data. However, for (magnetic) field data produced by magnetic dipolar sources, like in Section 6.1.2, one should consider poles of order five. Though numerically observed in [9], there is no mathematical justification so far why multiple poles generate such strong accumulation of the poles of the approximants (see Section 6.7.1). This intriguing property, however, is definitely helping source recovery and will be the topic of further study. It is used in order to automatically estimate the “most plausible” number of sources (numerically: up to 3, at the moment).

This year, we started considering a different class of models, not necessarily dipolar, and related estimation algorithms. Such models may be supported on the surface of the cortex or in the volume of the encephalon. We represent sources by vector-valued measures, and in order to favor sparsity in this infinite-dimensional setting we use a TV (i.e. total variation) regularization term as in Section 6.1.1. The approach follows that of [16] and is implemented through two different algorithms, whose convergence properties are currently being studied. Tests on synthetic data from a few dipolar sources provide results of different qualities that need to be better understood. In particular, a weight is being added in the TV term in order to better identify deep sources. This is the topic of the starting PhD research of P. Asensio and M. Nemaire. Ultimately, the results will be compared to those of FS3D and other available software tools.

## 6.2. Matching problems and their applications

**Participants:** Laurent Baratchart, Martine Olivi, Gibin Bose, David Martinez Martinez, Fabien Seyfert.

### 6.2.1. Multiplexer synthesis via interpolation and common junction design

In the context of David Martinez Martinez’s PhD funded partly by CNES the synthesis of multiplexer responses was considered using multipoint matching techniques. Indeed, synthesizing the response of multiplexer composed of a set of channel filters connected via common manifold junction to a common port can be seen as a matrix version application of our multipoint matching result for filters [7]. For short a simultaneous matching solutions is sought for, where each channel filter matches the load it is connected at specified matching frequencies. The difficulty here is that the load seen by each filter, depends explicitly of the response of the other filters by means of the common junction’s response: the multiplexer synthesis problem is therefore, in general, strictly harder than the filter multipoint matching problem, and can’t be solved by a sequential solving of independent «scalar» problems. A notable exception to this statement is obtained when a totally decoupling common junction is considered. This somehow artificial situation was taken as a start of a continuation algorithm, during which the decoupling junction response is moved step by step via a linear trajectory towards the target junction while the simultaneous matching problem is solved all along via a differential predictor corrector method. Whereas all «accidents» of branch point type that can occur during this procedure are not classified yet, one major obstruction to the continuation process is the occurrence of manifold peaks. The latter are due to resonances occurring in the manifold junction and yield total reflection at some frequencies

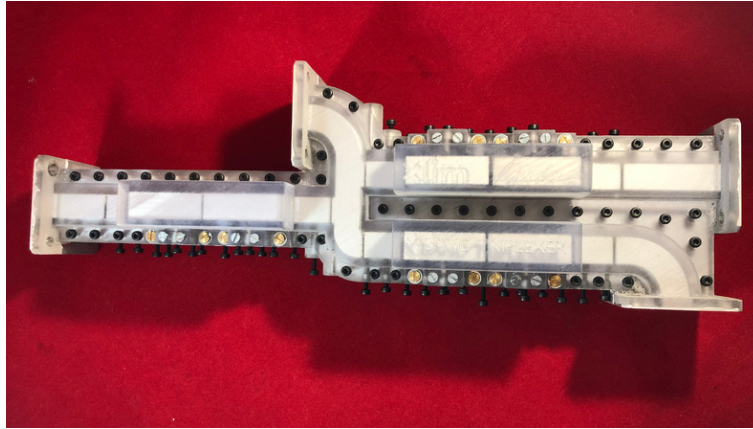


Figure 8. Compact triplexer synthesized via matrix multi-point interpolation techniques and realized via 3D printing.

of the channel ports. When latter coincide with the matching frequencies of a particular channel filter, the simultaneous matching problem has no solution, and the continuation algorithm fails irredeemably.

We therefore gave a full characterization of this manifold peaks and designed a heuristic approach to avoid their appearance during the continuation process. We showed that they only depend on the out of band response of the channel filters, and can in first approximation be considered as constant along the continuation process and estimated by a full wave simulation of each channel filter. This is then used within a triangular adjustment procedure that looks for possible manifold length adjustments (within the channel filters, and between that channel filters and the manifold junction) that guaranties the absence of manifold peaks within the band of each channel filter. Details of this procedure that give important information to the designer about the feasibility of an effective multiplexer response by means of given manifold T-junction, and this before any channel filter optimization procedure, are detailed in [23], [18] and were presented at Eumc 2019. In connection with the previously described continuation procedure, it was used to design a compact triplexer, based on frequency specifications considered as «hard to fulfill» and furnished by CNES. The triplexer was then realized using 3D printing techniques at Xlim (S. Bila and O. Tantot) our long standing academical partners on these topics (see Figure 8 ). This work is part of the PhD thesis [14] defended by David Martinez Martinez at the end of June.

### 6.2.2. Uniform matching and global optimality considerations: application to a reference tracking problem

This problem was proposed by Pauline Kergus, PhD student at Onera (Toulouse). In her PhD, she studied the following data driven problem: given frequency measurements of a plant, find a controller which allows to follow a given reference model. The approach she proposed was to directly identify the controller from frequency measurements induced on the controller by the closed loop. Of course the quality of the controller, and in particular its stability, highly depend on the chosen reference model. The question is thus: how to choose a good reference model  $M$  with a minimum of information on the plant? The reference model is linked to the sensitivity function  $S$  by the relation  $M + S = 1$ . The sensitivity function is an important design tool in control. To ensure closed loop stability, it should be stable and satisfy some interpolation conditions at the unstable poles and zeros of the plant [28]. Its shape reflect the performances of the closed loop:  $S$  should be small at low frequencies to ensure a good tracking accuracy, as well as disturbance rejection; while to ensure noise rejection,  $S$  should go to 1 at infinity (the reference model  $1 - S$  should be small at high frequencies). The shaping problem for the sensitivity function can be stated in a manner almost similar to the matching

problem described below: find a Schur function with minimum infinite norm in a frequency band  $[0, w_c]$ , where  $w_c$  is the chosen cutoff frequency, while satisfying some interpolatory constraints. The main difference that prevents for using the convex relaxation method proposed below is the condition at infinity. An alternative optimization method is under study. To get a non-optimal solution to the problem, Pauline Kergus proposed a simple way to enforce the interpolation conditions from a given well-shaped reference model. To compute the unstable poles and zeros of the plant, which is the minimal required information, she uses our software PISA <https://project.inria.fr/pisa/working/project/>. Examples illustrating the advantages and limitations of the method were studied. The results were reported in the journal paper [17] and presented at the CDC 2019 in Nice.

### 6.3. Stability assessment of microwave amplifiers and design of oscillators

**Participants:** Laurent Baratchart, Sylvain Chevillard, Martine Olivi, Fabien Seyfert, Sébastien Fueyo, Adam Cooman.

The goal is here to help design amplifiers and oscillators, in particular to detect instability at an early stage of the design. This topic is studied in the doctoral work of S. Fueyo, co-advised with J.-B. Pomet (from the McTao Inria project-team). Application to oscillator design methodologies is studied in collaboration with Smain Amari from the Royal Military College of Canada (Kingston, Canada).

As opposed to Filters and Antennas, Amplifiers and Oscillators are active components that intrinsically entail a non-linear functioning. The latter is due to the use of transistors governed by electric laws exhibiting saturation effects, and therefore inducing input/output characteristics that are no longer proportional to the magnitude of the input signal. Hence, they typically produce non-linear distortions. A central question arising in the design of amplifiers is to assess stability. The latter may be understood around a functioning point when no input but noise is considered, or else around a periodic trajectory when an input signal at a specified frequency is applied. For oscillators, a precise estimation of their oscillating frequency is crucial during the design process. For devices operating at relatively low frequencies, time domain simulations perform satisfactorily to check stability. For complex microwave amplifiers and oscillators, the situation is however drastically different: the time step necessary to integrate the transmission line's dynamical equations (which behave like a simple electrical wire at low frequency) becomes so small that simulations are intractable in reasonable time. Moreover, most linear components of such circuits are known through their frequency response, and a preliminary, numerically unstable step is then needed to obtain their impulse response, prior to any time domain simulation.

For these reasons, the analysis of such systems is carried out in the frequency domain. In the case of stability issues around a functioning point, where only small input signals are considered, the stability of the linearized system obtained by a first order approximation of each non-linear component can be studied *via* the transfer impedance functions computed at some ports of the circuit. In recent years, we showed that under realistic dissipativity assumptions at high frequency for the building blocks of the circuit, these transfer functions are meromorphic in the complex frequency variable  $s$ , with at most finitely many unstable poles in the right half-plane [4]. Dwelling on the unstable/stable decomposition in Hardy Spaces, we developed a procedure to assess the stability or instability of the transfer functions at hand, from their evaluation on a finite frequency grid [11], that was further improved in [10] to address the design of oscillators, in collaboration with Smain Amari. This has resulted in the development of a software library called Pisa (see Section 3.4.1, aiming at making these techniques available to practitioners. Research in this direction now focuses on the links between the width of the measurement band, the density of the measurement points, and the precision with which an unstable pole, located within a certain depth into the complex plane, can be identified.

Extensions of the procedure to the strong signal case, where linearisation is considered around a periodic trajectory, have received attention over the last two years. When stability is studied around a periodic trajectory, determined in practice by Harmonic Balance algorithms, linearization yields a linear time varying dynamical system with periodic coefficients and a periodic trajectory thereof. While in finite dimension the stability of such systems is well understood via the Floquet theory, this is no longer the case in the present setting which is infinite dimensional, due to the presence of delays. Dwelling on the theory of retarded systems, S. Fueyo's

PhD work has shown last year that, for general circuits, the monodromy operator of the linearized system along its periodic trajectory is a compact perturbation of a high frequency, non dynamical operator, which is stable under a realistic passivity assumption at high frequency. Therefore, only finitely many unstable points can arise in the spectrum of the monodromy operator, and this year we established a connection between these and the singularities of the harmonic transfer function, viewed as a holomorphic function with values in periodic  $L^2$  functions. One difficulty, however, is that these singularities need not affect all Fourier coefficients, whereas harmonic balance techniques can only estimate finitely many of them. This issue, that was apparently not singled out by practitioners, is currently under examination.

We also wrote an article reporting about the stability of the high frequency system, and recast this result in terms of exponential stability of certain delay systems [24].

## 6.4. The Hardy-Hodge decomposition

**Participants:** Laurent Baratchart, Masimba Nemaire.

In a joint work with T. Qian and P. Dang from the university of Macao, we proved in previous years that on a compact hypersurface  $\Sigma$  embedded in  $\mathbb{R}^n$ , a  $\mathbb{R}^n$ -valued vector field of  $L^p$  class decomposes as the sum of a harmonic gradient from inside  $\Sigma$ , a harmonic gradient from outside  $\Sigma$ , and a tangent divergence-free field, provided that  $2 - \varepsilon < p < 2 + \varepsilon'$ , where  $\varepsilon$  and  $\varepsilon'$  depend on the Lipschitz constant of the surface. We also proved that the decomposition is valid for  $1 < p < \infty$  when  $\Sigma$  is *VMO-smooth* (*i.e.*  $\Sigma$  is locally the graph of Lipschitz function with derivatives in *VMO*). By projection onto the tangent space, this gives a Helmholtz-Hodge decomposition for vector fields on a Lipschitz hypersurface, which is apparently new since existing results deal with smooth surfaces. In fact, the Helmholtz-Hodge decomposition holds on Lipschitz surfaces (not just hypersurfaces), The Hardy-Hodge decomposition generalizes the classical Plemelj formulas from complex analysis. We pursued this year the writing of an article on this topic, and we also found that this decomposition yields a description of silent magnetizations distributions of  $L^p$ -class on a surface. A natural endeavor is now to use this description, *via* balayage, to describe volumetric silent magnetizations.

## 6.5. Identification of resonating frequencies of compact metallic objects in electromagnetic inverse scattering

**Participants:** Laurent Baratchart, Martine Olivi, Fabien Seyfert.

We started an academic collaboration with LEAT (Univ. Nice, France, pers. involved: Jean-Yves Dauvignac, Nicolas Fortino, Yasmina Zaki) on the topic of inverse scattering using frequency dependent measurements. As opposed to classical electromagnetic imaging where several spatially located sensors are used to identify the shape of an object by means of scattering data at a single frequency, a discrimination process between different metallic objects is here being sought for by means of a single, or a reduced number of sensors that operate on a whole frequency band. For short the spatial multiplicity and complexity of antenna sensors is here traded against a simpler architecture performing a frequency sweep.

The setting is shown on Figure 9 . The total field  $E_t(r, \theta, \phi)$  is the sum of the incident field  $E_i$  (here a plane wave) and scattered field  $E_s$ , that is at every point in space we have  $E_t = E_i + E_s$ . A harmonic time dependency ( $e^{j\omega t}$ , where  $j$  is the imaginary unit:  $j^2 = -1$  ) is supposed for the incident wave, so that by linearity of Maxwell equations and after a transient state, following holds,

$$E_s(r_o, \theta_o, \phi_o) = H(s = j\omega, \theta_o, \phi_o)E_i(r_e, \theta_e, \phi_e).$$

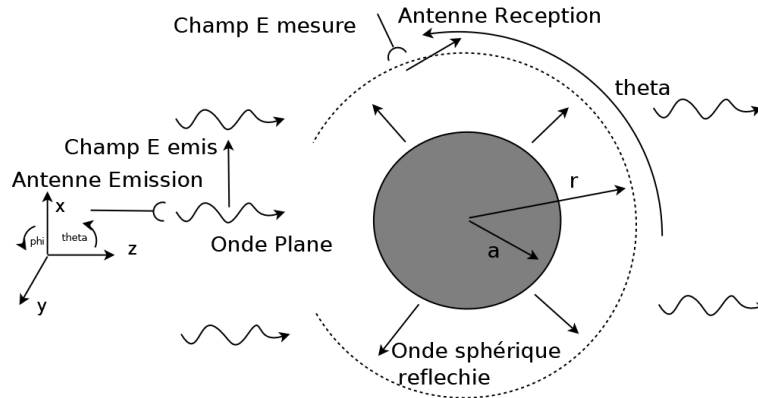


Figure 9. Sphere illuminated by an electromagnetic plane wave - measurement of the scattered wave

The subscripts  $o$  and  $e$  stand here for «observation point» and «emission point»: the scattered field at the observation point is therefore related to the emitted planar wave field at the emission point via the transfer function  $H(s = j\omega, \theta_o, \phi_o)$ . The emission point is here supposed fixed, so the dependency in  $e$  is omitted in  $H$ . Under regularity conditions on the scatterer's boundary the function  $H$  can be shown to admit an analytic continuation into the complex left half plane for the  $s$  variable, away from a discrete set (with a possible accumulation point a infinity) where it admits poles. Thus,  $H$  is a meromorphic function in the variable  $s$ . Its poles are called the resonating frequencies of the scattering object. Recovering these resonating frequencies from frequency scattering measurement, that is measurements of  $H$  at particular  $s = j\omega'_i s$  is the primary objective of this project.

In order to gain some insight we started a full study of the particular case when the scatterer is a spherical PEC (Perfectly Electric Conductor). In this case Maxwell equations can be solved «explicitly» by means of expansions in series of vectorial spherical harmonics. We showed in particular that in this case  $H$  admits following simple structure:

$$H(\omega, \theta_o, \phi_o) = R(s, \theta_o, \phi_o)e^{-\tau_1(\theta_o, \phi_o)s} + C(\theta_o, \phi_o)e^{-\tau_2(\theta_o, \phi_o)s},$$

where  $R$  is a meromorphic functions with poles at zeros of the spherical Hankel functions and their derivatives and  $C$  is independent of the frequency. Identification procedures, surprisingly close to the ones we developed in connection with amplifier stability analysis, are currently being studied to gain information about the resonating frequencies by means of a rational approximation of the function  $R$  once it has been de-embedded. Generalization of this analysis and procedure will be considered for arbitrarily compact PEC objects.

## 6.6. Imaging and modeling ancient materials

**Participants:** Vanna Lisa Coli, Juliette Leblond, Pat Vatiwutipong.

This is a recent activity of the team, linked to image classification in archaeology in the framework of the project ToMaT (see Regional Initiatives below) and to the post-doctoral stay of V. L. Coli; it is pursued in collaboration with L. Blanc-Féraud (project-team Morpheme, I3S-CNRS/Inria Sophia/iBV), D. Binder (CEPAM-CNRS, Nice), in particular.



The pottery style is classically used as the main cultural marker within Neolithic studies. Archaeological analyses focus on pottery technology, and particularly on the first stages of pottery manufacturing processes. These stages are the most demonstrative for identifying the technical traditions, as they are considered as crucial in apprenticeship processes. Until now, the identification of pottery manufacturing methods was based on macro-traces analysis, i.e. surface topography, breaks and discontinuities indicating the type of elements (coils, slabs, ...) and the way they were put together for building the pots. Overcoming the limitations inherent to the macroscopic pottery examination requires a complete access to the internal structure of the pots. Micro-computed tomography ( $\mu$ CT) has recently been used for exploring ancient materials microstructure. This non-invasive method provides quantitative data for a big set of proxies and is perfectly adapted to the analysis of Cultural heritage materials.

The main challenge of our current analyses aims to overcome the lack of existing protocols to apply in order to quantify observations. In order to characterize the manufacturing sequences, the mapping of the paste variability (distribution and composition of temper) and the discontinuities linked to different classes of pores, fabrics and/or organic inclusions appears promising. The totality of the acquired images composes a set of 2-D and 3-D surface and volume data at different resolutions and with specific physical characteristics related to each acquisition modality (multimodal and multi-scale data). Specific shape recognition methods need to be developed by application of robust imaging techniques and 3-D-shapes recognition algorithms.

In a first step, we devised a method to isolate pores from the 3-D data volumes in binary 3-D images, to which we apply a process named Hough transform (derived from Radon transform). This method, of which the generalization from 2-D to 3-D is quite recent, allows us to evaluate the presence of parallel lines going through the pores. The quantity of such lines is a good indicator of the “coiling” manufacturing, that it allows to distinguish from the other “spiral patchwork” patchwork technique, in particular. These progresses are described in [20], [22], [21], and the object of an article in preparation.

The Hough and Radon transforms can also be applied to 2-D slices of the available 3-D images displaying pores locations. In this framework, the use of Radon transform to evaluate the density of points in the image that do belong to (or almost) parallel lines appears to be quite efficient, as was seen during P. Vatiwutipong’s internship.

Other possibilities of investigation will be analyzed as well, such as machine learning techniques.

## 6.7. Behavior of poles in rational and meromorphic approximation

**Participants:** Laurent Baratchart, Sylvain Chevillard, Juliette Leblond, Martine Olivi, Fabien Seyfert.

### 6.7.1. Rational approximation

The numerous experiments that we performed on synthetic data in the context of the MagLune project (see Sections 6.1.2 and 8.2.1) revealed an intriguing behavior of the local minima of the optimization problem underlying our method. In the context of that application, we are provided with sampled values on the unit circle  $\mathbb{T}$  of a function  $f$  which is known to be of the form  $f(z) = p(z)/(z - \beta)^5$  where  $p(z) \in \mathbb{C}_4[z]$  is a polynomial of degree at most 4 with complex coefficients and  $\beta \in \mathbb{D}$  belongs to the unit disk. A key problem consists in recovering  $\beta$  from the values of  $f$  on the unit circle. The same problem occurs in the core of FindSources3D (see 3.4.3 and 6.1.3) with  $p$  being of degree at most 2 and a pole of order 3 rather than 5.

In order to estimate  $\beta$ , we seek for the global minimum on  $\mathbb{C}_4[z] \times \mathbb{D}$  of the function  $\phi$  defined by

$$\phi : (q, \alpha) \mapsto \left\| \frac{q(z)}{(z - \alpha)^5} - f(z) \right\|_{L^2(\mathbb{T})}.$$

When  $f$  is actually a rational function of the considered form,  $\phi$  obviously has a unique global minimum where it reaches the value 0. We experimentally observed that  $\phi$  usually has several local minima, some of them achieving very small values, and these minima often have a complex argument close to the argument of  $\beta$ . This behavior is unusual and contrasts with the fact the function

$$\psi : (q, \alpha_1, \dots, \alpha_5) \mapsto \left\| \frac{q(z)}{\prod_{i=1}^5 (z - \alpha_i)} - f(z) \right\|_{L^2(\mathbb{T})}$$

is known to have a unique local minimum on  $\mathbb{C}_4[z] \times \mathbb{D}^5$  (which is global) when  $f$  is a rational function of the same form.

In order to understand the reasons underlying our observations, we started studying the theoretical properties of the critical points of  $\phi$ , in the general case of a pole of order  $n \in \mathbb{N}^*$  and with a polynomial of degree less or equal to  $n - 1$  at the numerator. Our results so far are the following.

We introduce the family  $(g_j^{(\alpha)})_{j \in \mathbb{N}^*}$  where  $g_j^{(\alpha)}(z) = (1 - \bar{\alpha}z)^{j-1} / (z - \alpha)^j$  which is an orthogonal basis (for the usual  $L^2(\mathbb{T})$  Hilbert product) of the space of rational functions with a single pole (of arbitrary order) in  $\alpha$ . Thanks to this family, we prove that  $(q, \alpha)$  is a critical point of  $\phi$  if and only if  $f$  is orthogonal either to  $g_n^{(\alpha)}$  or  $g_{n+1}^{(\alpha)}$  and, for such a given  $\alpha$ ,  $q/(z - \alpha)^n$  is the orthogonal projection of  $f$  onto the rational functions of that form. The case when  $f$  is orthogonal to  $g_n^{(\alpha)}$  combined with the fact that  $q/(z - \alpha)^n$  is the orthogonal projection of  $f$  implies a pole-zero simplification of  $q/(z - \alpha)^n$  at  $z = \alpha$  and we conjecture that it exactly corresponds to local *maxima* of  $\phi$  with respect to variable  $\alpha$ . We also conjecture that the other case exactly corresponds to local *minima* of  $\phi$ . We are currently working on proving these conjectures, which should not be too hard.

We also obtained an explicit algebraic equation characterizing  $\alpha$ , and we know how to solve it when  $f$  is of the form  $1/(z - \beta)^k$  ( $1 \leq k \leq n$ ). For small values of  $n$ , we proved (and conjecture that it holds for any  $n$ ) that there are  $2k - 1$  solutions in the unit disk, all lying on the diameter passing through  $\beta$ . This is a remarkable result that somehow theoretically confirms the kind of experimental observations we got. The theoretical case of a function  $f$  with a non trivial numerator seems currently out of reach, though.

### 6.7.2. Meromorphic approximation

We showed that best meromorphic approximation on a contour, in the uniform norm, to functions with countably many branched singularities with polar closure inside the contour produces poles whose counting measure accumulate weak-\* to the Green equilibrium distribution on the cut of minimal capacity outside of which the function is single-valued. This is joint work with M. Yattselev (University of Indianapolis, Purdue University at Indianapolis). An article is currently being written on this topic.

## FOCUS Project-Team

# 7. New Results

## 7.1. Service-Oriented and Cloud Computing

**Participants:** Mario Bravetti, Maurizio Gabbrielli, Saverio Giallorenzo, Claudio Guidi, Ivan Lanese, Cosimo Laneve, Fabrizio Montesi, Gianluigi Zavattaro, Stefano Pio Zingaro.

### 7.1.1. Service-Oriented Computing and Internet of Things

Session types, i.e. types for structuring service communication, are recently being integrated into mainstream programming languages. In practice, a very important notion for dealing with such types is that of subtyping, since it allows for typing larger classes of system, where a program has not precisely the expected behavior but a similar one. We recently showed that, when asynchronous communication is considered, unfortunately, such a subtyping relation is undecidable. In [27] we present an algorithm (the first one that does not restrict type syntax or limit communication) and a tool for checking asynchronous subtyping which is sound, but not complete: in some cases it terminates without returning a final verdict. In [29] we discuss the relationship between session types and service behavioural contracts and we show the existence of a fully abstract interpretation of session types into a fragment of contracts, mapping subtyping into binary compliance-preserving contract refinement. This also yields an original undecidability result for asynchronous contract refinement.

In [43] we elaborate on our previous work on choreographies, which specify in a single artefact the expected behaviour of all the participants in a service oriented system. In particular, we extend dynamic choreographies, which model system updates at runtime, with the feature of dynamic inclusion of new unforeseen participants. In [30] we propose, in the context of platooning (a freight organization system where a group of vehicles follows a predefined trajectory maintaining a desired spatial pattern), a two layered, composable technical solution for federated platooning: a decentralized overlay network that regulates the interactions among the stakeholders, useful to mitigate issues linked to data safety and trustworthiness; and a dynamic federation platform, needed to monitor and interrupt deviant behaviors of federated members.

Finally, in [44] we focused on the use of our service-oriented language Jolie in an Internet of Things (IoT) setting. Technically, a key feature of Jolie is that it supports uniform linguistic abstractions to exploit heterogeneous communication stacks, i.e. for service oriented computing, protocols such as TCP/IP, Bluetooth, and RMI at transport level, and HTTP and SOAP at application level. We extend Jolie in order to support, uniformly as well, also the two most adopted protocols for IoT communication, i.e. CoAP and MQTT, and we report our experience on a case study on home automation.

### 7.1.2. Cloud Computing

In [18] we investigate the problem of modeling the optimal and automatic deployment of cloud applications and we experiment such an approach by applying it to the Abstract Behavioural Specification language ABS. In [28] we show that automated deployment, proven undecidable in the general case, is, instead, algorithmically treatable for the specific case of microservices: we implement an automatic optimal deployment tool and compute deployment plans for a realistic microservice architecture. In [35] we propose a core formal programming model (combining features from  $\lambda$ -calculus and  $\pi$ -calculus) for serverless computing, also known as Functions-as-a-Service: a recent paradigm aimed at simplifying the programming of cloud applications. The idea is that developers design applications in terms of functions and the infrastructure deals automatically with cloud deployment in terms of distribution and scaling.

## 7.2. Models for Reliability

**Participants:** Ivan Lanese, Dorian Medic.

### 7.2.1. Reversibility

We have continued the study of reversibility started in the past years. First, we continued to study reversibility in the context of the Erlang programming language. In particular, we devised a technique to record a program execution and replay it [37] inside the causal-consistent reversible debugger for Erlang we developed in the last years. More precisely, we may not replay the exact same execution, but any execution which is causal-consistent to it. We proved that this is enough to replay misbehaviours, hence to look for the bugs causing them. Second, we compared [48] various approaches to causal-consistent reversibility in CCS and  $\pi$ -calculus. In CCS, we showed that the two main approaches for causal-consistent reversibility, namely the ones of RCCS [51] and of CCSk [55] give rise to isomorphic LTSs (up to some structural rules). In  $\pi$ -calculus, we showed that one can define a causal semantics for  $\pi$ -calculus parametric on the data structure used to track extruded names, and that different instances capture causal semantics from the literature. All such semantics can be used to define (different) causal-consistent reversible semantics. As a final contribution, we studied reversibility in the context of Petri nets [41]. There, we do not consider causal-consistent reversibility, but a notion of local reversibility typical of Petri nets. In particular, we say that a transition is reversible if one can add a set of effect-reverses (an effect-reverse, if it can trigger, undoes the effect of the transition) to undo it in each marking reachable by it, without changing the set of reachable markings. We showed that, contrarily to what happens in bounded nets, transition reversibility is not decidable in general unbounded nets. It is however decidable in some significant subclasses of Petri nets, in particular all transitions of cyclic nets (nets where the initial marking is reachable from any state) are reversible. Finally, we show how to restructure nets by adding new places so to make their transitions reversible without altering their behaviour.

## 7.3. Probabilistic Systems and Resource Control

**Participants:** Martin Avanzini, Mario Bravetti, Raphaëlle Crubillé, Ugo Dal Lago, Francesco Gavazzo, Gabriele Vanoni, Akira Yoshimizu.

### 7.3.1. Probabilistic Programming and Static Analysis

In FoCUS, we are interested in studying probabilistic higher-order programming languages and, more generally, the fundamental properties of probabilistic computation when placed in an interactive scenario, for instance concurrency. One of the most basic but nevertheless desirable properties of programs is of course termination. Termination can be seen as a minimal guarantee about the time complexity of the underlying program. When probabilistic choice comes into play, termination can be defined by stipulating that a program is terminating if its probability of convergence is 1, this way giving rise to the notion of *almost sure termination*. Alternatively, a probabilistic program is said to be *positively almost surely terminating* if its average runtime is finite. The latter condition easily implies the former. Termination, already undecidable for deterministic (universal) programming languages, remains so in the presence of probabilistic choice, even becoming provably harder.

The FoCUS team has been the first in advocating the use of types to guarantee probabilistic termination, in the form of a monadic sized-type system [17]. Developed in collaboration with Grellois by Dal Lago, this system substantially generalises usual sized-types, and allows this way to capture probabilistic, higher-order programs which terminate almost surely. Complementary, in collaboration with Ghyselen, Avanzini and Dal Lago have recently defined a formal system for reasoning about the *expected runtime* of higher-order probabilistic programs, through a *refinement type system* capable of *modeling probabilistic effects* with exceptional accuracy [26]. To the best of our knowledge, this provides the first formal methodology for *average case complexity analysis* of higher-order programs. Remarkably, the system is also *extensionally complete*.

In 2018, we have started to investigate the foundations for *probabilistic abstract reduction systems* (*probabilistic ARSs*), which constitute a general framework to study fundamental properties of probabilistic computations, such as termination or confluence. In 2019, we have significantly revised this initial development [11]. Particularly, we have refined Lyapunov ranking functions by conceiving them as *probabilistic embeddings*. The ramifications of this work are two-fold. First, we obtain a sound and complete method for reasoning about strong positive almost sure termination. Second, this method has been instantiated in the setting of (first-order)

*probabilistic rewrite systems*, giving rise to the notion of *barycentric algebras*, generalising the well-known interpretation method. Barycentric algebras have been integrated in the termination prover *NaTT*<sup>0</sup>, confirming the feasibility of the approach.

We have also worked on higher-order model checking as a way to prove termination of probabilistic variations on higher-order recursion schemes [36], obtaining encouraging results. More specifically, an algorithm for approximating the probability of convergence of any such scheme has been designed and proved sound, although the problem of precisely computing the probability of convergence is shown to be undecidable at order 2 or higher. Finally, we have published a new version of a contribution we wrote in 2017 about how implicit computational complexity could help in proving that certain cryptographic constructions have the desired complexity-theoretic properties [12].

### 7.3.2. Higher-Order and Effectful Programs: Relational Reasoning

In FoCUS, we are also interested in relational reasoning about programs written in higher-order programming languages. In the recent years, this research has been directed to effectful programs, namely programs whose behaviour is not purely functional. Moreover, there has recently been a shift in our interests, driven by the projects REPAS and DIAPASoN, towards quantitative kinds of relational reasoning, in which programs are not necessarily dubbed equivalent (or not), but rather put at a certain distance.

The first contribution we had in this direction is due to Dal Lago and Gavazzo [31], who generalized the so-called open normal-form bisimilarity technique to higher-order programs exhibiting any kind of monadic effect. The key ingredient here is that of a relator, and allows to lift relations on a set to relations on monadic extensions to the same set. This allows to define open normal-form bisimilarity, and to prove it correct. This, together, with other contributions, have also appeared in Gavazzo's PhD Thesis, which has been successfully defended in April 2019 [10], and which has been awarded the Prize for the Best PhD Thesis in Theoretical Computer Science by the Italian Chapter of the EATCS.

We have also given the notion of differential logical relations [33], a generalization of Plotkin's logical relations in which programs are dubbed being at a certain *distance* rather than being just *equivalent*. Noticeably, this distance is not necessarily numeric, but is itself functional if the compared programs have a non-ground type. This allows to evaluate the distance between programs taking into account the possible actions the environment can make on the compared programs.

### 7.3.3. Alternative Probabilistic Models

We are also interested in exploring probabilistic models going beyond the usual ones, in which deterministic programming languages are endowed with discrete probabilistic choice.

We have first of all studied bayesian  $\lambda$ -calculi, namely  $\lambda$ -calculi in which not only an operator for probabilistic choice is available, but also one for *scoring*, which serves as the basis to model conditioning in probabilistic programming. We give a geometry of interaction model for such a typed  $\lambda$ -calculus [34], namely a paradigmatic calculus for higher-order Bayesian programming in the style of PCF. The model is based on the category of measurable spaces and partial measurable functions, and is proved adequate with respect to both a distribution-based and a sampling-based operational semantics.

We have also introduced a probabilistic extension of a framework to specify and analyze software product lines [15]. We define a syntax of the language including probabilistic operators and define operational and denotational semantics for it. We prove that the expected equivalence between these two semantic frameworks holds. Our probabilistic framework is supported by a set of scripts to show the model behavior.

## 7.4. Verification Techniques

**Participants:** Ugo Dal Lago, Adrien Durier, Daniel Hirschhoff, Ivan Lanese, Cosimo Laneve, Davide Sangiorgi, Akira Yoshimizu, Gianluigi Zavattaro.

<sup>0</sup>See <https://www.trs.css.i.nagoya-u.ac.jp/NaTT/>.

Extensional properties are those properties that constrain the behavioural descriptions of a system (i.e., how a system looks like from the outside). Examples of such properties include classical functional correctness, deadlock freedom and resource usage.

In the last year of the Focus project, we have worked on three main topics: (i) *name mobility and coinductive techniques*, (ii) *deadlock analysis*, and (iii) *cost analysis of properties* of languages for actors and for smart contracts.

#### 7.4.1. Name Mobility and Coinductive Techniques

In [19], we propose proof techniques for bisimilarity based on unique solution of equations. The results essentially state that an equation (or a system of equations) whose infinite unfolding never produces a divergence has the unique-solution property. We distinguish between different forms of divergence; derive an abstract formulation of the theorems, on generic LTSs; adapt the theorems to other equivalences such as trace equivalence, and to preorders such as trace inclusion; we compare the resulting techniques to enhancements of the bisimulation proof method (the ‘up-to techniques’). In [20], we study how to adapt such techniques to higher-order languages. In such languages proving behavioural equivalences is known to be hard, because interactions involve complex values, namely terms of the language. The soundness of proof techniques is usually delicate and difficult to establish. The language considered is the Higher-Order  $\pi$ -calculus.

The contribution [42] studies the representation of the call-by-need  $\lambda$ -calculus in the pure message-passing concurrency of the  $\pi$ -calculus, precisely the Local Asynchronous  $\pi$ -calculus, that has sharper semantic properties than the ordinary  $\pi$ -calculus. We exploit such properties to study the validity of  $\beta$ -reduction (meaning that the source and target terms of a beta-reduction are mapped onto behaviourally equivalent processes). Nearly all results presented fail in the ordinary  $\pi$ -calculus.

In [45], we investigate basic properties of the Erlang concurrency model. This model is based on asynchronous communication through mailboxes accessed via pattern matching. In particular, we consider Core Erlang (which is an intermediate step in Erlang compilation) and we define, on top of its operational semantics, an observational semantics following the approach used to define asynchronous bisimulation for the  $\pi$ -calculus. Our work allows us to shed some light on the management of process identifiers in Erlang, different from the various forms of name mobility already studied in the literature. In fact, we need to modify standard definitions to cope with such specific features of Erlang.

The paper [25] reviews the origins and the history of enhancements of the bisimulation and coinduction proof methods.

#### 7.4.2. Deadlock Analysis

The contributions [22] and [50] address deadlock analysis of Java-like programs. The two papers respectively cover two relevant features of these languages: (i) multi-threading and reentrant locks and (ii) co-ordination primitives (`wait`, `notify` and `notifyAll`). In both cases, we define a behavioral type system that associates abstract models to programs (lams and Petri Nets with inhibitor arcs) and define an algorithm for detecting deadlocks. The two systems are consistent and our technique is intended to be an effective tool for the deadlock analysis of programming languages.

The paper [16] addresses the  $\pi$ -calculus. It defines a type system for guaranteeing that typable processes never produce a run-time error and, even if they may diverge, there is always a chance for them to finish their work, i.e., to reduce to an idle process (a stronger property than deadlock freedom). The type system uses so-called *non-idempotent intersections* and, therefore, applies to a large class of processes. Indeed, despite the fact that the underlying property is  $\prod_2^0$ -complete, there is a way to show that the system is complete, i.e., that any well-behaved process is typable, although for obvious reasons infinitely many derivations need to be considered.

#### 7.4.3. Static Analysis of Properties of Concurrent Programs

We have analyzed the computational time of actor programs, following a technique similar to [52], and we have begun a new research direction that deals with the analysis of Solidity smart contracts.



In [23], we propose a technique for estimating the computational time of programs in an actor model. To this aim, we define a compositional translation function returning cost equations, which are fed to an automatic off-the-shelf solver for obtaining the time bounds. Our approach is based on so-called *synchronization sets* that capture possible difficult synchronization patterns between actors and helps make the analysis efficient and precise. The approach is proven to correctly over-approximate the worst computational time of an actor model of concurrent programs. The technique is complemented by a prototype analyzer that returns upper bound of costs for the actor model.

In [38], we analyze the behaviour of smart contracts, namely programs stored on some blockchain that control the transfer of assets between parties under certain conditions. In particular, we focus on the interactions of smart contracts and external actors (usually, humans) in order to maximize objective functions. To this aim, we define a core language of programs, which is reminiscent of Solidity, with a minimal set of smart contract primitives and we describe the whole system as a parallel composition of smart contracts and users. We therefore express the system behaviour as a first order logic formula in Presburger arithmetics and study the maximum profit for each actor by solving arithmetic constraints.

## 7.5. Computer Science Education

**Participants:** Michael Lodi, Simone Martini.

We study why and how to teach computer science principles (nowadays often referred to as “computational thinking”, CT), in the context of K-12 education. We are interested in philosophical, sociological, and historical motivations to teach computer science. Furthermore, we study what concepts and skills related to computer science are not only technical abilities, but have a general value for all students. Finally, we try to find/produce/evaluate suitable materials (tools, languages, lesson plans...) to teach these concepts, taking into account: difficulties in learning CS concepts (particularly programming); stereotypes about computer science (teachers’ and students’ mindset); teacher training (both non-specialist and disciplinary teachers); innovative teaching methodologies (primarily based on constructivist and constructionist learning theories).

### 7.5.1. Computational Thinking, Unplugged Activities, and Constructionism

We reviewed some relevant literature related to learning CS and, more specifically, programming in a constructivist and constructionist light. We investigated some cognitive aspects, for example, the notional machine and its role in understanding, misunderstanding, and difficulties of learning to program. We reviewed programming languages for learning to program, with particular focus on educational characteristics of block-based languages [24].

We analyzed the widespread but debated pedagogical approach of “unplugged activities”: activities without a computer, like physical games, used to teach CS concepts. We explicitly connect computational thinking to the “CS Unplugged” pedagogical approach, by analyzing a representative sample of CS Unplugged activities in light of CT. We found the activities map well onto commonly accepted CT concepts, although caution must be taken not to regard CS Unplugged as being a complete approach to CT education [14].

Moreover, we found similarities (e.g., kinesthetic activities) and differences (e.g., structured vs. creative activities) between Unplugged and constructivism or constructionism. We argue there is a tension between the constructivist need to link the CS concepts to actual implementations and the challenge of teaching CS principles without computers, to undermine the misconceptions of CS as “the science of computers” [13].

### 7.5.2. CS in Primary School

We designed, produced and implemented in a primary school some “unplugged + plugged” teaching materials and lesson plans [47]. The unplugged activities are structured as an incremental discovery, scaffolded by the instructors, of the fundamental concepts of structured programming (e.g., sequence, conditionals, loops, variables) but also complexity in terms of computational steps and generalization of algorithms. The plugged activities follow the creative learning approach, using Scratch as the primary tool, both for free creative expression and for learning other disciplines (e.g., drawing regular polygons).

### **7.5.3. Growth Mindset and Transfer**

Every person holds an idea (mindset) about intelligence: someone thinks it is a fixed trait, like eye colour (fixed mindset), while others believe it can grow like muscles (growth mindset). The latter is beneficial for students to have better results, particularly in STEM disciplines, and to not being influenced by stereotypes. Computer science is a subject that can be affected by fixed ideas (“geek gene”), and some (small) studies showed it can induce fixed ideas. By contrast, some claims stating that studying CS can foster a GM have emerged. However, educational research shows that the transfer of competences is hard. We measured [40] some indicators (e.g., mindset, computer science mindset) at the beginning and the end of a high school year in different classes, both CS and non-CS oriented. At the end of the year, none of the classes showed a statistically significant change in their mindset. Interestingly, non-CS oriented classes showed a significant decrease in their computer science growth mindset, which is not desirable.

## **7.6. Constraint Programming**

**Participants:** Maurizio Gabbrielli, Liu Tong.

In Focus, we sometimes make use of constraint solvers (e.g., cloud computing, service-oriented computing). Since a few years we have thus began to develop tools based on constraints and constraint solvers.

In [39] we have used constraints in the setting of Service Function Chaining (SFC) deployment. SFCs represent sequences of Virtual Network Functions that compose a service. They are found within Network Function Virtualization (NFV) and Software Defined Networking (SDN) technologies, that recently acquired a great momentum thanks to their promise of being a flexible and cost-effective solution for replacing hardware-based, vendor-dependent network middleboxes with software appliances running on general purpose hardware in the cloud.

We employ constraint programming to solve the SFC design problem. Indeed we argue that constraint programming can be effectively used to address this kind of problems because it provides expressive and flexible modeling languages which come with powerful solvers, thus providing efficient and scalable performance.

## GRAPHDECO Project-Team

### 6. New Results

#### 6.1. Computer-Assisted Design with Heterogeneous Representations

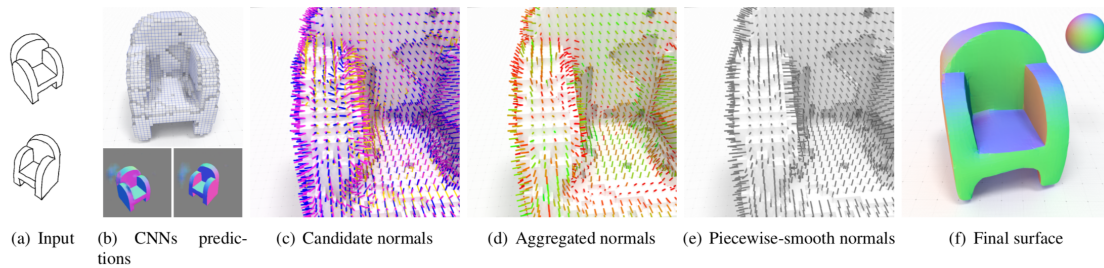


Figure 4. Our method takes as input multiple sketches of an object (a). We first apply existing deep neural networks to predict a volumetric reconstruction of the shape as well as one normal map per sketch (b). We re-project the normal maps on the voxel grid in complement to the surface normal computed from the volumetric prediction (c). We aggregate these different normals into a distribution represented by a mean vector and a standard deviation (d). We optimize this normal field to make it piecewise smooth (e) and use it to regularize the surface (f). The final surface preserves the overall shape of the predicted voxel grid as well as the sharp features of the predicted normal maps.

##### 6.1.1. Combining Voxel and Normal Predictions for Multi-View 3D Sketching

**Participants:** Johanna Delanoy, Adrien Bousseau.

Recent works on data-driven sketch-based modeling use either voxel grids or normal/depth maps as geometric representations compatible with convolutional neural networks. While voxel grids can represent complete objects – including parts not visible in the sketches – their memory consumption restricts them to low-resolution predictions. In contrast, a single normal or depth map can capture fine details, but multiple maps from different viewpoints need to be predicted and fused to produce a closed surface. We propose to combine these two representations to address their respective shortcomings in the context of a multi-view sketch-based modeling system. Our method predicts a voxel grid common to all the input sketches, along with one normal map per sketch. We then use the voxel grid as a support for normal map fusion by optimizing its extracted surface such that it is consistent with the re-projected normals, while being as piecewise-smooth as possible overall (Fig. 4). We compare our method with a recent voxel prediction system, demonstrating improved recovery of sharp features over a variety of man-made objects.

This work is a collaboration with David Coeurjolly from Université de Lyon and Jacques-Olivier Lachaud from Université Savoie Mont Blanc. The work was published in the journal *Computer & Graphics* and presented at the SMI conference [14].

##### 6.1.2. Video Motion Stylization by 2D Rigidification

**Participants:** Johanna Delanoy, Adrien Bousseau.

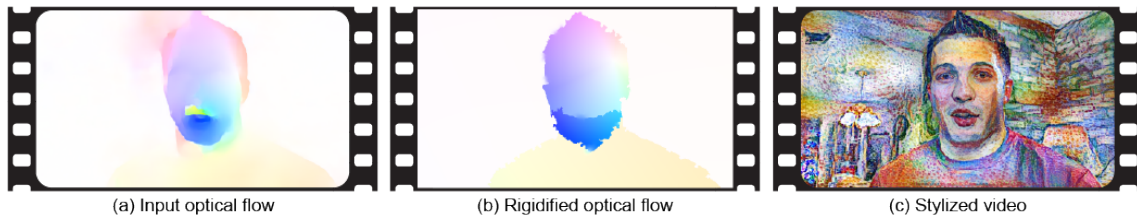


Figure 5. Our method takes as input a video and its optical flow (a). We segment the video and optimize its pixel trajectories to produce a new video that exhibits piecewise-rigid motion (b). The resulting rigidified video can be stylized with existing algorithms (c) to produce animations where the style elements (brush strokes, paper texture) produce a strong sense of 2D motion.

We introduce a video stylization method that increases the apparent rigidity of motion. Existing stylization methods often retain the 3D motion of the original video, making the result look like a 3D scene covered in paint rather than a 2D painting of a scene. In contrast, traditional hand-drawn animations often exhibit simplified in-plane motion, such as in the case of cut-out animations where the animator moves pieces of paper from frame to frame. Inspired by this technique, we propose to modify a video such that its content undergoes 2D rigid transforms (Fig. 5). To achieve this goal, our approach applies motion segmentation and optimization to best approximate the input optical flow with piecewise-rigid transforms, and re-renders the video such that its content follows the simplified motion. The output of our method is a new video and its optical flow, which can be fed to any existing video stylization algorithm.

This work is a collaboration with Aaron Hertzmann from Adobe Research. It was presented at the ACM/EG Expressive Symposium [21].

### 6.1.3. Multi-Pose Interactive Linkage Design

**Participant:** Adrien Bousseau.

We introduce an interactive tool for novice users to design mechanical objects made of 2.5D linkages. Users simply draw the shape of the object and a few key poses of its multiple moving parts. Our approach automatically generates a one-degree-of-freedom linkage that connects the fixed and moving parts, such that the moving parts traverse all input poses in order without any collision with the fixed and other moving parts. In addition, our approach avoids common linkage defects and favors compact linkages and smooth motion trajectories. Finally, our system automatically generates the 3D geometry of the object and its links, allowing the rapid creation of a physical mockup of the designed object (Fig. 6).

This work was conducted in collaboration with Gen Nishida and Daniel G. Aliaga from Purdue University, was published in Computer Graphics Forum and presented at the Eurographics conference [18].

### 6.1.4. Extracting Geometric Structures in Images with Delaunay Point Processes

**Participant:** Adrien Bousseau.

We introduce Delaunay Point Processes, a framework for the extraction of geometric structures from images. Our approach simultaneously locates and groups geometric primitives (line segments, triangles) to form extended structures (line networks, polygons) for a variety of image analysis tasks. Similarly to traditional point processes, our approach uses Markov Chain Monte Carlo to minimize an energy that balances fidelity to the input image data with geometric priors on the output structures. However, while existing point processes struggle to model structures composed of inter-connected components, we propose to embed the point process into a Delaunay triangulation, which provides high-quality connectivity by construction. We further leverage key properties of the Delaunay triangulation to devise a fast Markov Chain Monte Carlo sampler. We

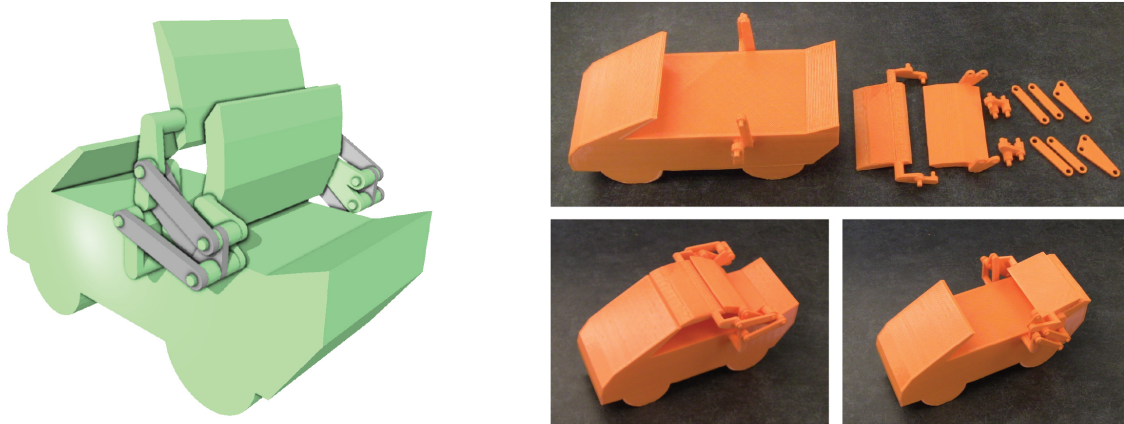


Figure 6. Our interactive system facilitates the creation (left) and fabrication (right) of mechanical objects.

demonstrate the flexibility of our approach on a variety of applications, including line network extraction, object contouring, and mesh-based image compression (see Fig. 7).

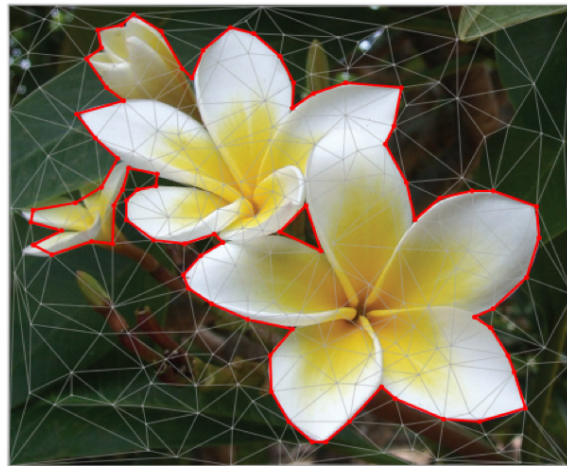


Figure 7. Our method extracts geometric structures like the countour of these flowers by optimizing a dynamic Delaunay triangulation.

This work was conducted in collaboration with Jean-Dominique Favreau and Florent Lafarge (TITANE group), and published in IEEE PAMI [16].

#### 6.1.5. Integer-Grid Sketch Vectorization

**Participants:** Tibor Stanko, Adrien Bousseau.

A major challenge in line drawing vectorization is segmenting the input bitmap into separate curves. This segmentation is especially problematic for rough sketches, where curves are depicted using multiple overdrawn



strokes. Inspired by feature-aligned mesh quadrangulation methods in geometry processing, we propose to extract vector curve networks by parametrizing the image with local drawing-aligned integer grids. The regular structure of the grid facilitates the extraction of clean line junctions; due to the grid's discrete nature, nearby strokes are implicitly grouped together. Our method successfully vectorizes both clean and rough line drawings, whereas previous methods focused on only one of those drawing types.

This work is an ongoing collaboration with David Bommes from University of Bern and Mikhail Bessmeltsev from University of Montreal. It is currently under review.

### 6.1.6. Surfacing Sparse Unorganized 3D Curves using Global Parametrization

**Participants:** Tibor Stanko, Adrien Bousseau.

Designers use sketching to quickly externalize ideas, often using a handful of curves to express complex shapes. Recent years have brought a plethora of new tools for creating designs directly in 3D. The output of these tools is often a set of sparse, unorganized curves. We propose a novel method for automatic conversion of such unorganized curves into clean curve networks ready for surfacing. The core of our method is a global curve-aligned parametrization, which allows us to automatically aggregate information from neighboring curves and produce an output with valid topology.

This work is an ongoing collaboration with David Bommes from University of Bern, Mikhail Bessmeltsev from University of Montreal, and Justin Solomon from MIT.

### 6.1.7. OpenSketch: A Richly-Annotated Dataset of Product Design Sketches

**Participants:** Yulia Gryaditskaya, Adrien Bousseau, Fredo Durand.

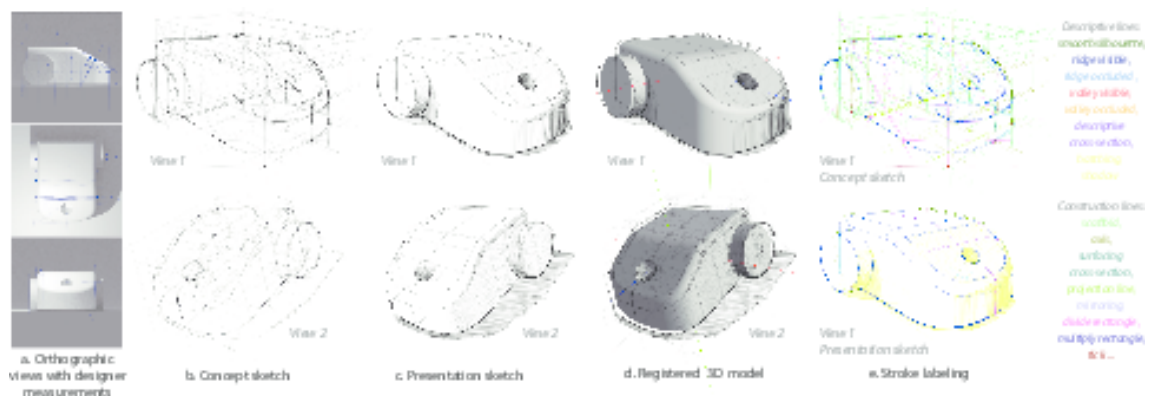


Figure 8. We showed designers three orthographic views (a) of the object and asked them to draw it from two different perspective views (b). We also asked to replicate each of their sketches as a clean presentation drawing (c). We semi-automatically registered 3D models to each sketch (d), and we manually labeled different types of lines in all concept sketches and presentation drawings from the first viewpoint (e).

Product designers extensively use sketches to create and communicate 3D shapes and thus form an ideal audience for sketch-based modeling, non-photorealistic rendering and sketch filtering. However, sketching requires significant expertise and time, making design sketches a scarce resource for the research community. We introduce *OpenSketch*, a dataset of product design sketches aimed at offering a rich source of information for a variety of computer-aided design tasks. *OpenSketch* contains more than 400 sketches representing 12 man-made objects drawn by 7 to 15 product designers of varying expertise. We provided participants with front, side and top views of these objects (Fig. 8 a), and instructed them to draw from two novel perspective



viewpoints (Fig. 8 b). This drawing task forces designers to *construct the shape* from their mental vision rather than directly copy what they see. They achieve this task by employing a variety of sketching techniques and methods not observed in prior datasets. Together with industrial design teachers, we distilled a taxonomy of line types and used it to label each stroke of the 214 sketches drawn from one of the two viewpoints (Fig. 8 e). While some of these lines have long been known in computer graphics, others remain to be reproduced algorithmically or exploited for shape inference. In addition, we also asked participants to produce clean presentation drawings from each of their sketches, resulting in aligned pairs of drawings of different styles (Fig. 8 c). Finally, we registered each sketch to its reference 3D model by annotating sparse correspondences (Fig. 8 d). We provide an analysis of our annotated sketches, which reveals systematic drawing strategies over time and shapes, as well as a positive correlation between presence of construction lines and accuracy. Our sketches, in combination with provided annotations, form challenging benchmarks for existing algorithms as well as a great source of inspiration for future developments. We illustrate the versatility of our data by using it to test a 3D reconstruction deep network trained on synthetic drawings, as well as to train a filtering network to convert concept sketches into presentation drawings. We distribute our dataset under the Creative Commons CC0 license: <https://ns.inria.fr/d3/OpenSketch>.

This work is a collaboration with Mark Sypesteyn, Jan Willem Hoftijzer and Sylvia Pont from TU Delft, Netherlands. This work was published at ACM Transactions on Graphics, and presented at SIGGRAPH Asia 2019 [17].

### 6.1.8. *Intersection vs. Occlusion: a Discrete Formulation of Line Drawing 3D Reconstruction*

**Participants:** Yulia Gryaditskaya, Adrien Bousseau, Felix Hähnlein.

The popularity of sketches in design stems from their ability to communicate complex 3D shapes with a handful of lines. Yet, this economy of means also makes sketch interpretation a challenging task, as global 3D understanding needs to emerge from scattered pen strokes. To tackle this challenge, many prior methods cast 3D reconstruction of line drawings as a global optimization that seeks to satisfy a number of geometric criteria, including orthogonality, planarity, symmetry. However, all of these methods require users to distinguish line intersections that exist in 3D from the ones that are only due to occlusions. These user annotations are critical to the success of existing algorithms, since mistakenly treating an occlusion as a true intersection would connect distant parts of the shape, with dramatic consequences on the overall optimization procedure. We propose a line drawing 3D reconstruction method that automatically discriminates 3D intersections from occlusions. This automation not only reduces user burden, it also allows our method to scale to real-world sketches composed of hundreds of pen strokes, for which the number of intersections is too high to make existing user-assisted methods practical. Our key idea is to associate each 2D intersection with a binary variable that indicates if the intersection should be preserved in 3D. Our algorithm then searches for the assignment of binary values that yields the best 3D shape, as measured with similar criteria as the ones used by prior work for 3D reconstruction. However, the combinatorial nature of this binary assignment problem prevents trying all possible configurations. Our main technical contribution is an efficient search algorithm that leverages principles of how product designers draw to reconstruct complex 3D drawings within minutes.

This work is a collaboration with Alla Sheffer (Professor at University of British Columbia) and Chenxi Liu (PhD student at University of British Columbia).

### 6.1.9. *Data-driven sketch segmentation*

**Participants:** Yulia Gryaditskaya, Felix Hähnlein, Adrien Bousseau.

Deep learning achieves impressive performance on image segmentation, which has motivated the recent development of deep neural networks for the related task of sketch segmentation, where the goal is to assign labels to the different strokes that compose a line drawing. However, while natural images are well represented as bitmaps, line drawings can also be represented as vector graphics, such as point sequences and point clouds. In addition to offering different trade-offs on resolution and storage, vector representations often come with additional information, such as stroke ordering and speed.

In this project, we evaluate three crucial design choices for sketch segmentation using deep-learning: which sketch representation to use, which information to encode in this representation, and which loss function to optimize. Our findings suggest that point clouds represent a competitive alternative to bitmaps for sketch segmentation, and that providing extra-geometric information improves performance.

#### **6.1.10. Stroke-based concept sketch generation**

**Participants:** Felix Hähnlein, Yulia Gryaditskaya, Adrien Bousseau.

State-of-the-art non-photorealistic rendering algorithms can generate lines representing salient visual features on objects. However, very few methods exist for generating lines outside of an object, as is the case for most construction lines, used in technical drawings and design sketches. Furthermore, most methods do not generate human-like strokes and do not consider the drawing order of a sketch.

In this project, we address these issues by proposing a reinforcement learning framework, where a virtual agent tries to generate a construction sketch of a given 3D model. One key element of our approach is the study and the mathematical formalization of drawing strategies used by industrial designers.

#### **6.1.11. Designing Programmable, Self-Actuated Structures**

**Participants:** David Jourdan, Adrien Bousseau.

Self-actuated structures are material assemblies that can deform from an initially simpler state to a more complex, curved one, by automatically deforming to shape. Most relevant to applications in manufacturing are self-actuated shapes that are fabricated flat, considerably reducing the cost and complexity of manufacturing curved 3D surfaces. While there are many ways to design self-actuated materials (e.g. using heat or water as actuation mechanisms), we use 3D printing to embed rigid patterns into prestressed fabric, which is then released and assumes a shape matching a given target when reaching static equilibrium.

While using a 3D printer to embed plastic curves into prestressed fabric is a technique that has been experimented on before, it has been mostly restricted to piecewise minimal surfaces, making it impossible to reproduce most shapes. By using a dense packing of 3-pointed stars, we are able to create convex shapes and positive gaussian curvature, moreover we found a direct link between the stars dimensions and the induced curvature, allowing us to build an inverse design tool that can faithfully reproduce some target shapes.

This is a collaboration with Méline Skouras of Inria Rhône Alpes and Etienne Vouga of the University of Texas at Austin.

## **6.2. Graphics with Uncertainty and Heterogeneous Content**

### **6.2.1. Multi-view relighting using a geometry-aware network**

**Participants:** Julien Philip, George Drettakis.

We propose the first learning-based algorithm that can relight images in a plausible and controllable manner given multiple views of an outdoor scene. In particular, we introduce a geometry-aware neural network that utilizes multiple geometry cues (normal maps, specular direction, etc.) and source and target shadow masks computed from a noisy proxy geometry obtained by multi-view stereo. Our model is a three-stage pipeline: two subnetworks refine the source and target shadow masks, and a third performs the final relighting. Furthermore, we introduce a novel representation for the shadow masks, which we call RGB shadow images. They reproject the colors from all views into the shadowed pixels and enable our network to cope with inaccuracies in the proxy and the non-locality of the shadow casting interactions. Acquiring large-scale multi-view relighting datasets for real scenes is challenging, so we train our network on photorealistic synthetic data. At train time, we also compute a noisy stereo-based geometric proxy, this time from the synthetic renderings. This allows us to bridge the gap between the real and synthetic domains. Our model generalizes well to real scenes. It can alter the illumination of drone footage, image-based renderings, textured mesh reconstructions, and even internet photo collections (see Fig. 9).

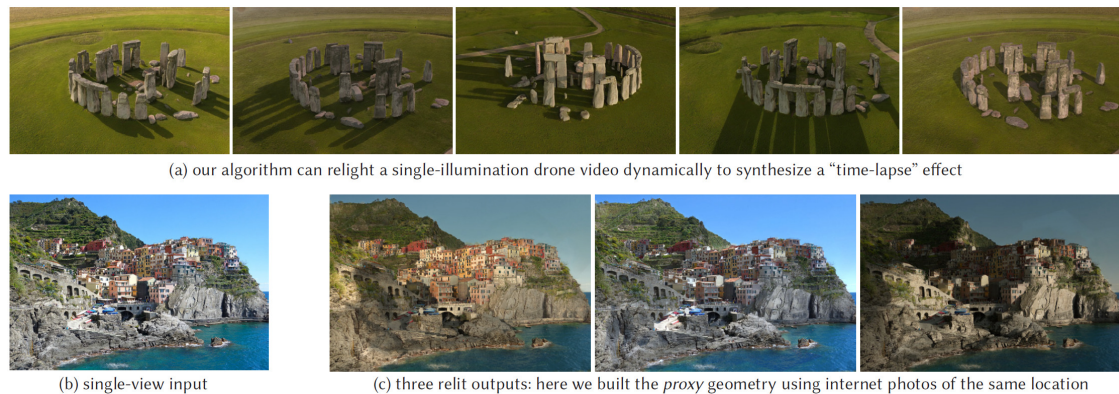


Figure 9. Results of our method: multi-view relighting using a geometry-aware network.

This work was in collaboration with M. Gharbi of Adobe Research and A. Efros and T. Zhang of UC Berkeley, and was published in ACM Transactions on Graphics and presented at SIGGRAPH 2019 [19].

### 6.2.2. Flexible SVBRDF Capture with a Multi-Image Deep Network

**Participants:** Valentin Deschaintre, Frédo Durand, George Drettakis, Adrien Bousseau.

Empowered by deep learning, recent methods for material capture can estimate a spatially-varying reflectance from a single photograph. Such lightweight capture is in stark contrast with the tens or hundreds of pictures required by traditional optimization-based approaches. However, a single image is often simply not enough to observe the rich appearance of real-world materials. We present a deep-learning method capable of estimating material appearance from a variable number of uncalibrated and unordered pictures captured with a handheld camera and flash. Thanks to an order-independent fusing layer, this architecture extracts the most useful information from each picture, while benefiting from strong priors learned from data. The method can handle both view and light direction variation without calibration. We show how our method improves its prediction with the number of input pictures, and reaches high quality reconstructions with as little as 1 to 10 images – a sweet spot between existing single-image and complex multi-image approaches – see Fig. 10 .

This work is a collaboration with Miika Aittala from MIT CSAIL. This work was published in Computer Graphics Forum, and presented at EGSR 2019 [15].

A short paper and poster summarizing this work together with our 2018 "Single-Image SVBRDF Capture with a Rendering-Aware Deep Network" was published in the Siggraph Asia doctoral consortium 2019 [22].

### 6.2.3. Guided Acquisition of SVBRDFs

**Participants:** Valentin Deschaintre, George Drettakis, Adrien Bousseau.

Another project is under development to capture a large-scale SVBRDF from a few pictures of a planar surface. Many existing lightweight methods for SVBRDF capture take as input flash pictures, which need to be acquired close to the surface of interest restricting the scale of capture. We complement such small-scale inputs with a picture of the entire surface, taken under ambient lighting. Our method then fuses these two sources of information to propagate the SVBRDFs estimated from each close-up flash picture to all pixels of the large image. Thanks to our two-scale approach, we can capture surfaces several meters wide, such as walls, doors and furniture. In addition, our method can also be used to create large SVBRDFs from internet pictures, where we use artist-designed SVBRDFs as exemplars of the small-scale behavior of the surface.

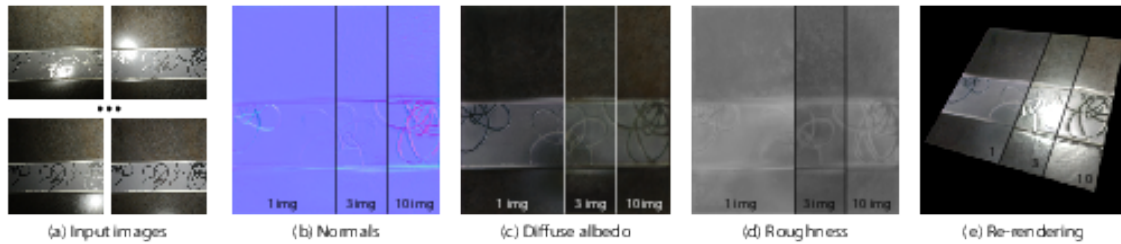


Figure 10. Our deep learning method for SVBRDF capture supports a variable number of input photographs taken with uncalibrated light-view directions (a, rectified). While a single image is enough to obtain a first plausible estimate of the SVBRDF maps, more images provide new cues to our method, improving its prediction. In this example, adding images reveals fine normal variations (b), removes highlight residuals in the diffuse albedo (c), and reveals the difference of roughness between the stone, the stripe, and the thin pattern (d).

#### 6.2.4. Mixed rendering and relighting for indoor scenes

**Participants:** Julien Philip, Michaël Gharbi, George Drettakis.

We are investigating a mixed image rendering and relighting method that allows a user to move freely in a multi-view interior scene while altering its lighting. Our method uses a deep convolutional network trained on synthetic photo-realistic images. We adapt classical path tracing techniques to approximate complex lighting effects such as color bleeding and reflections.

#### 6.2.5. DiCE: Dichoptic Contrast Enhancement for VR and Stereo Displays

**Participant:** George Drettakis.

In stereoscopic displays, such as those used in VR/AR headsets, our eyes are presented with two different views. The disparity between the views is typically used to convey depth cues, but it could be also used to enhance image appearance. We devise a novel technique that takes advantage of binocular fusion to boost perceived local contrast and visual quality of images. Since the technique is based on fixed tone curves, it has negligible computational cost and it is well suited for real-time applications, such as VR rendering. To control the trade-off between contrast gain and binocular rivalry, we conducted a series of experiments to explain the factors that dominate rivalry perception in a dichoptic presentation where two images of different contrasts are displayed (see Fig. 11). With this new finding, we can effectively enhance contrast and control rivalry in mono- and stereoscopic images, and in VR rendering, as confirmed in validation experiments.

This work was in collaboration with Durham University (G. Koulteris, past postdoc of the group), Cambridge (F. Zhong, R. Mantiuk), UC Berkeley (M. Banks) and ENS Renne (M. Chambe), and was published in ACM Transactions on Graphics and presented at SIGGRAPH Asia 2019 [20].

#### 6.2.6. Compositing Real Scenes using a relighting Network

**Participants:** Baptiste Nicolet, Julien Philip, George Drettakis.

Image-Based Rendering (IBR) allows for fast rendering of photorealistic novel viewpoints of real-world scenes captured by photographs. While it facilitates the very tedious traditional content creation process, it lacks user control over the appearance of the scene. We propose a novel approach to create novel scenes from a composition of multiple IBR scenes. This method relies on the use of a relighting network, which we first use to match the lighting conditions of each scene, and then to synthesize shadows between scenes in the final composition. This work has been submitted for publication.

#### 6.2.7. Image-based Rendering of Urban Scenes based on Semantic Information

**Participants:** Simon Rodriguez, Siddhant Prakash, George Drettakis.





Figure 11. Comparison of standard stereo images and the images with enhanced perceived contrast using our DiCE method. They can be cross-fused with the assistance of the dots above the images. Notice the enhanced contrast in the shadows and highlights of the scene. The stereo images are from *Big Buck Bunny* by Blender Foundation.

Cityscapes exhibit many hard cases for image-based rendering techniques, such as reflective and transparent surfaces. Pre-existing information about the scene can be leveraged to tackle these difficult cases. By relying on semantic information, it is possible to address those regions with tailored algorithms to improve reconstruction and rendering. This project is a collaboration with Peter Hedman from University College of London. This work has been submitted for publication.

### 6.2.8. Synthetic Data for Image-based Rendering

**Participants:** Simon Rodriguez, Thomas Leimkühler, George Drettakis.

This project explores the potential of Image-based rendering techniques in the context of real-time rendering for synthetic scenes. Accurate information can be precomputed from the input synthetic scene and used at run-time to improve the quality of approximate global illumination effects while preserving performance. This project is a collaboration with Chris Wyman and Peter Shirley from NVIDIA Research.

### 6.2.9. Densified Surface Light Fields for Human Capture Video

**Participants:** Rada Deeb, George Drettakis.

In this project, we focus on video-based rendering for mid-scale platforms. Having a mid-scale platform introduces one important problem for image-based rendering techniques due to low angular resolution. This leads to unrealistic view-dependent effects. We propose to use the temporal domain in a multidimensional surface light field approach in order to enhance the angular resolution. In addition, our approach provides a compact representation essential to dealing with the large amount of data introduced by videos compared to image-based techniques. In addition, we evaluate the use of deep encoder-decoder networks to learn a more compact representation of our multidimensional surface light field. This work is in collaboration with Edmond Boyer, MORPHEO team, Inria Grenoble.

### 6.2.10. Deep Bayesian Image-based Rendering

**Participants:** Thomas Leimkühler, George Drettakis.

Deep learning has permeated the field of computer graphics and continues to be instrumental in producing state-of-the-art research results. In the context of image-based rendering, deep architectures are now routinely used for tasks such as blending weight prediction, view extrapolation, or re-lighting. Current algorithms, however, do not take into account the different sources of uncertainty arising from the several stages of the image-based rendering pipeline. In this project, we investigate the use of Bayesian deep learning models to estimate and exploit these uncertainties. We are interested in devising principled methods which combine the expressive power of modern deep learning with the well-groundedness of classical Bayesian models.

### ***6.2.11. Path Guiding for Metropolis Light Transport***

**Participants:** Stavros Diolatzis, George Drettakis.

Path guiding has been proven to be an effective way to achieve faster convergence in Monte Carlo renderings by learning the incident radiance field. However, current path guiding techniques could be beaten by unguided path tracing due to their overhead or inability to incorporate the BSDF distribution factor. In our work, we improve path guiding and Metropolis light transport algorithms with low overhead product sampling between the incoming radiance and BSDF values. We demonstrate that our method has better convergence compared to the previous state-of-the-art techniques. Moreover, combining path guiding with MLT solves the global exploration issues ensuring convergence to the stationary distribution.

This work is an ongoing collaboration with Wenzel Jakob from Ecole Polytechnique Fédérale de Lausanne and Adrien Gruson from McGill University.

### ***6.2.12. Improved Image-Based Rendering with Uncontrolled Capture***

**Participants:** Siddhant Prakash, George Drettakis.

Current state-of-the-art Image Based Rendering (IBR) algorithms, such as Deep Blending, use per-view geometry to render candidate views and machine learning to improve rendering of novel views. The casual capture process employed introduces visible color artifacts during rendering due to automated camera settings, and incur significant computational overhead when using per-view meshes. We aim to find a global solution to harmonize color inconsistency across the entire set of images in a given dataset, and also improve the performance of IBR algorithms by limiting the use of more advanced techniques only to regions where they are required.

### ***6.2.13. Practical video-based rendering of dynamic stationary environments***

**Participants:** Théo Thonat, George Drettakis.

The goal of this work is to extend traditional Image Based Rendering to capture subtle motions in real scenes. We want to allow free-viewpoint navigation with casual capture, such as a user taking photos and videos with a single smartphone and a tripod. We focus on stochastic time-dependent textures such as waves, flames or waterfalls. We have developed a video representation able to tackle the challenge of blending unsynchronized videos.

This work is a collaboration with Sylvain Paris from Adobe Research, Miika Aittala from MIT CSAIL, and Yagiz Aksoy from ETH Zurich, and has been submitted for publication.



## GRAPHIK Project-Team

# 7. New Results

## 7.1. Ontology-Mediated Query Answering

**Participants:** Jean-François Baget, Meghyn Bienvenu, Efstathios Delivourias, Michel Leclère, Marie-Laure Mugnier, Olivier Rodriguez, Federico Ulliana.

Ontology-mediated query answering (OMQA) is the issue of querying data while taking into account inferences enabled by ontological knowledge. From an abstract viewpoint, this gives rise to *knowledge bases*, composed of an ontology and a factbase (in database terms: a database instance under incomplete data assumption). Answers to queries are logically entailed from the knowledge base.

This year, we obtained two kinds of results: *theoretical results* on fundamental issues raised by OMQA, and *practical algorithms* for OMQA on key-value stores and RDF integration systems.

### 7.1.1. Fundamental issues on OMQA with existential rules

Existential rules (a.k.a. datalog+, as this framework generalizes the deductive database language datalog) have emerged as a new ontological language in the OMQA context. Techniques for query answering under existential rules mostly rely on the two classical ways of processing rules, namely forward chaining and backward chaining. In forward chaining, known as the *chase* in database theory, the rules are applied to enrich the factbase and query answering can then be solved by evaluating the query against the *saturated* factbase (as in a classical database system, i.e., with forgetting the ontological knowledge). The backward chaining process is divided into two steps: first, the query is *rewritten* using the rules into a first-order query (typically a union of conjunctive queries, but it can be a more compact form) or into a datalog query; then the rewritten query is evaluated against the factbase (again, as in a classical database system). Depending on the considered class of existential rules, the chase and/or query rewriting may terminate or not.

#### 7.1.1.1. Decidability of chase termination for linear existential rules.

Several chase variants have long been studied in database theory. These chase variants yield logically equivalent results, but differ in their ability to detect redundancies possibly caused by the introduction of unknown individuals (nulls, blank nodes). Given a chase variant, the chase termination problem takes as input a set of existential rules and asks if this set of rules ensures the termination of the chase for any factbase. It is well-known that this problem is undecidable for all known chase variants. Hence, a crucial issue is whether chase termination becomes decidable for some known subclasses of existential rules. We considered linear existential rules, a simple yet important subclass of existential rules that generalizes database inclusion dependencies. We showed the decidability of the chase termination problem on linear rules for three main chase variants, namely skolem (a.k.a. semi-oblivious), restricted (a.k.a. standard) and core chase. The restricted chase is the most used in practice, however its study is notoriously tricky because the order in which rule applications are performed matters. Indeed, for the same factbase, some restricted chase sequences may terminate, while others may not. To obtain our results, we introduced a novel approach based on so-called derivation trees and a single notion of forbidden pattern. The simplicity of these structures make them subject to implementation. Besides the theoretical interest of a unified approach and new proofs, we provided the first positive decidability results (and complexity upper bounds) concerning the termination of the restricted chase, proving that chase termination on linear existential rules is decidable for both versions of the problem: Does every chase sequence terminate? Does some chase sequence terminate?

- ICDT 2019 [29]. In collaboration with Michael Thomazo (Inria VALDA).

### 7.1.1.2. Boundedness: Enforcing both chase termination and first-order rewritability.

We carried out the first studies on the boundedness problem for existential rules. This problem asks whether a given set of existential rules is bounded, i.e., whether there is a predefined bound on the “depth” of the chase independently from any factbase (for breadth-first chase versions, the depth corresponds to the number of breadth-first steps). It has been deeply studied in the context of datalog, where it is key to query optimization, although boundedness is undecidable in general. For datalog rules, boundedness is equivalent to a desirable property, namely first-order rewritability: a set of rules is called first-order rewritable if any conjunctive query can be rewritten into a union of conjunctive queries, whose evaluation on any factbase yields the expected answers (i.e., the relevant part of the ontology can be compiled into the rewritten query, which allows to reduce query answering to a simple query evaluation task). This equivalence does not hold for existential rules. Moreover, the notion of boundedness has to be parametrized by the chase variant, as they all behave differently with respect to termination. Beside potential practical use, the notion of boundedness is closely related to an interesting theoretical question on existential rules: what are the relationships between chase termination and first-order query rewritability? With respect to this question, we obtained the following salient result: for the oblivious and skolem (semi-oblivious) chase variants, a set of existential rules is bounded if and only if it ensures both chase termination for any factbase and first-order rewritability for any conjunctive query.

- *IJCAI 2019 [22]. In collaboration with Pierre Bourhis (Inria SPIRALS) and Sophie Tison (Inria LINKS).*

## 7.1.2. Practical Algorithms for OMQA on key-value stores and RDF integration systems

### 7.1.2.1. Ontology-mediated query answering on top of key-value stores.

Ontology-mediated query answering was mainly investigated so far based on the assumption that data conforms to relational structures (we include here RDF) and that the paradigm can be deployed on top of relational databases with conjunctive queries at the core (e.g., in SQL or SPARQL). However, this is not the prominent way on which data is today stored and exchanged, especially in the Web. Whether OMQA can be developed for non-relational structures, like those shared by increasingly popular NOSQL languages sustaining Big-Data analytics, has just begun to be investigated. Since 2016, we have been studying OMQA for key-values stores, which are systems providing fast and scalable access to JSON records. We proposed a rule language to express domain knowledge, with rules being directly applicable to key-value stores, without any translation of JSON into another data model (results published at AAI 2016 and IJCAI 2017). In 2018-2019, we implemented a prototype for MongoDB, with a restricted part of this rule language (featuring key inclusions and mandatory keys) and tree-pattern queries, and devised optimization techniques based on parallelizing query rewriting and query answering. This work is pursued within a starting PhD thesis (Olivier Rodriguez).

- *Rule-ML 2019 [31]. In collaboration with Reza Akbarinia (Inria ZENITH).*

### 7.1.2.2. Ontology-mediated query answering in RDF integration systems

Within the iCODA project devoted to data journalism and the co-supervision of Maxime Buron’s PhD thesis, we are considering the so-called Ontology-Based Data Access framework, which is composed of three components: the data level, the ontological level and mappings that relate data to facts described in the vocabulary of the ontology. Our framework more precisely considers heterogeneous data sources integrated through mappings into a (possibly virtual) RDF graph, provided with an RDFS ontology and RDFS entailment rules. The innovative aspects with respect to the state of the art are (i) SPARQL queries that extend classical conjunctive queries by the ability of querying data and ontological triples together, and (ii) Global-Local-As-View (GLAV) mappings, which can be seen as source-to-target existential rules. GLAV mappings enable the creation of unknown entities (blank nodes), which increases the amount of information accessible through the integration system. In particular, they allow one to palliate missing data values, by stating the existence of data whose values are not known in the sources. We devised, implemented and experimentally compared several query answering techniques in this setting.

- *ESWC 2019 [23], technical report [36] basis of a paper accepted to EDBT 2020. In collaboration with Maxime Buron and Ioana Manolescu (Inria CEDAR), and François Goasdoué (IRISA).*

## 7.2. Reasoning with conflicts and decision support

**Participants:** Pierre Bisquert, Patrice Buche, Michel Chein, Madalina Croitoru, Jérôme Fortin, Alain Gutierrez, Abdelraouf Hecham, Martin Jedwabny, Michel Leclère, Rallou Thomopoulos, Bruno Yun.

The work carried out during this year can be structured into two main research directions: *structured logic-based argumentation* and *collective decision making*.

### 7.2.1. Structured argumentation

To solve real-world problems we sometimes need to consider features that cannot be expressed purely (or naturally) in classical logic. Indeed, real world information is often “imperfect”: it can be partially contradictory, vague or uncertain, etc. During the evaluation period, we mostly considered reasoning in presence of conflicts. To handle this issue, as a reasoning method robust to contradiction, we have used structured argumentation, where arguments have an internal logical structure representing an inference step (i.e. some premises inducing a conclusion). In this context, arguments and their interaction are typically generated from an inconsistent knowledge base. Such arguments are in contrast to those employed in abstract argumentation where they are considered a black box (usually provided as input to a problem and not computed).

More precisely, this year, we mainly worked on two issues: the first one concerns the question of scrutinizing a structured argument, i.e. checking both the validity (“is the conclusion induced by the premisses?”) and its soundness (“is the argument valid and are its premisses true?”). This is interesting in the context of collective decision making, where participants utter arguments that can be assessed. The second one relates to the computational complexity of generating arguments from a knowledge base. Indeed, it can potentially produce a huge number of arguments, which impedes the usability of argumentation for big knowledge bases.

#### 7.2.1.1. Formalizing argument schemes and fallacies

More precisely, we have presented a logical framework allowing us to express assessment of facts and arguments together with a proof system to answer these questions. Our motivation was to clarify the notion of validity in the context of logic-based arguments along different aspects (such as the formulas used and the inference scheme). Originality lies in the possibility for the user to design their own argument schemes, i.e. specific inference patterns (e.g. expert argument, analogy argument). We showed that classical inference obtains when arguments are based on classical schemes (e.g. Hilbert axioms). We went beyond classical logic by distinguishing “proven” formulas from “uncontroversial” ones (whose negation is not proven) and provided a definition of a fallacious argument in this context.

- LPNMR 2019 [20]. In collaboration with Florence Dupin de Saint-Cyr and Philippe Besnard (IRIT).

#### 7.2.1.2. Optimising argumentation frameworks

Another problem addressed was the large number of logical arguments that can be potentially constructed from a knowledge base. To address this problem we have proposed a compact representation of the structured argumentation system under the form of hypergraphs and implemented it in the NAKED prototype. The tool allows to import a knowledge base (expressed in the existential rule framework), generate, visualise and export the corresponding argumentation hypergraph. These functions, paired with the aim of improving the extension computation efficiency, make this software an interesting tool for non-computer science experts, such as people working in the agronomy domain.

- AAMAS 2019 [33]. In collaboration with Srdjan Vesic (CRIL).

### 7.2.2. Collective decision making

In this setting we have focused towards the deliberation and voting techniques. We have investigated how deliberation can help generate or impact the structure of preferences underlying the voting process. We have implemented the PAPOW prototype [27] that allows for filtering of voters depending on their individual characteristics.

### 7.2.2.1. Argumentation as a tool to generate new preferences

We have investigated how argumentation can solve the Condorcet paradox by using the notion of extension (maxi-consistent sets of arguments) in order to compute new preferences. Our research hypothesis is that a decision made by a group of participants understanding the qualitative rationale (expressed by arguments) behind each other's preferences has better chances to be accepted and used in practice. Accordingly, we proposed a novel qualitative procedure which combines argumentation with computational social choice for modeling the collective decision-making problem. We showed that this qualitative approach produces structured preferences that can overcome major deficiencies that were exhibited in the social choice literature and affect most of the major voting rules. More precisely, we have dealt with the Condorcet Paradox and the properties of monotonicity and homogeneity, which are unsatisfiable by many voting rules.

- *PRAI 2019 [14]. In collaboration with Christos Kaklamanis and Nikos Karanikolas (CTI, Greece).*

### 7.2.2.2. Argumentation as a tool to modify individual preferences

The previous approach implies that voters are replaced by the extensions which, while it allows to circumvent the Condorcet Paradox, might prove difficult to implement as it disregards the notion of (voters') majority. Hence, we proposed a decision-making procedure based on argumentation and preference aggregation which permits us to explore the effect of reasoning and deliberation along with voting for the decision process. We represented the deliberation phase by defining a new voting argumentation framework, that uses vote and generic arguments, and its acceptability semantics based on the notion of pairwise comparisons between alternatives. We proved for these semantics some theoretical results regarding well-known properties from argumentation and social choice theory.

Moreover, we also studied the notion of unshared features (i.e., alternatives' criteria that constitute justifications of preferences for some agents but not for others) and showed under which conditions it is possible to reach a Condorcet consensus. We provided a deliberation protocol that ensures that, after its completion, the number of unshared features of the decision problem can only be reduced, which would tend to show that deliberation allows to lower the risk of Condorcet Paradox.

- *ICAART 2019 [28]. In collaboration with Christos Kaklamanis and Nikos Karanikolas (CTI, Greece). PRIMA 2019 [21].*

### 7.2.3. Discovering and qualifying authority links

We finalized this year the description of the engine SudoQual, devoted to the evaluation of link quality in document bases, developed in collaboration with ABES, the French National Agency for Academic Libraries (<http://www.abes.fr>), in the context of ANR Qualinca research project (2012-2016) (<https://www.lirmm.fr/qualinca/>). We presented the methodology and general algorithms used to discover and qualify so-called authority links (which are coreference links between entities mentioned in descriptions of documents and entities described in referential bases). Moreover, ABES has put in production this year a professional tool for documentalists, called Paprika (<https://paprika.idref.fr/>), whose kernel is the SudoQual engine.

- *KCAP 2019 [25].*

## 7.3. Miscellaneous: Automated design of biological devices

**Participants:** Michel Leclère, Guillaume Perution Kihli, Federico Ulliana.

We mention here results obtained in a collaboration with a team of biologists from the Center for Structural Biochemistry (CBS, Montpellier) on the logical computing capabilities of living organisms. More precisely, this joint work focuses on the development of a framework dedicated to the design of so-called Recombinase-based devices, whose behavior is specified as Boolean functions. We looked at the case of single-cell devices, whose expressivity limits, that is, the Boolean functions they can implement without distributing the Boolean function in several parts, are still unknown. While it is easy to determine which Boolean function is implemented by a device, the converse problem of automatically designing a device implementing a given Boolean function is a difficult task for which no automatic method exists. To tackle this problem, we experimented in the past years a combinatorial approach consisting in exhaustively generating all devices up to

a given size, then determining the Boolean function they implement. A generating program and a database for these devices were developed. This year, we achieved the first formal study of this problem, which we believe can serve as foundations for the development of new biological design solutions. A set of minimality properties naturally emerged from our study, which led us to define the notion of canonical and representative devices, by which infinitely large classes of design solutions can be finitely expressed. These results strengthen the reliability of the approach and show that our program generates all representative canonical devices. Finally, our results also indicate some interesting expressivity limits for single-cell devices. Indeed, the generation process showed that 8% among all 4-input Boolean functions cannot be implemented. We also formally proved that single-cell devices cannot implement some  $n$ -input Boolean functions, for every  $n \geq 7$ .

- *TPNC 2019 [30]. In collaboration with Jérôme Bonnet and Sarah Guiziou (CBS).*

## HEPHAISTOS Project-Team

# 6. New Results

## 6.1. Robotics

### 6.1.1. Analysis of Cable-driven parallel robots

**Participants:** Jean-Pierre Merlet [correspondant], Yves Papegay.

We have continued the analysis of suspended CDPRs for control and design purposes. This analysis is heavily dependent on the behavior of the cable. Three main models can be used: *ideal* (no deformation of the cable due to the tension, the cable shape is a straight line between the attachments points), *elastic* (cable length changes according to the tension to which it is submitted, straight line cable shape) and *sagging* (cable shape is not a line as the cable is submitted to its own mass). The different models leads to very different analysis with a complexity increasing from ideal to sagging. All cables exhibit sagging but the sagging effect is often neglected if the CDPR is relatively small while it definitively cannot be neglected for large CDPRs. The most used sagging model is the Irvine model [24]. This is a non algebraic planar model with the upper attachment point of the cable is supposed to be grounded: it provides the coordinates of the lowest attachment point  $B$  of the cable if the cable length  $L_0$  at rest and the force applied at this point are known. It takes into account both the elasticity and deformation of the cable due to its own mass. A drawback of this model is that we will be more interested in a closed-form of the  $L_0$  for a given pose of  $B$  (for the inverse kinematics of CDPR) and in alternate form of the model that will provide constraint on the force components (for the direct kinematics). We have proposed new original formulations of the Irvine model in [13] and have shown that their use drastically improve the solving time for both the inverse and direct kinematics (i.e finding all possible solutions for both problems) that are required for CDPRs control. Still the solving time of the direct kinematics is too large for the real-time direct kinematics and in that case only the current pose of the platform is of interest.

The direct kinematics relies on an accurate estimation of the cable lengths that is usually based on the measurement of the winch drum rotation. We have evaluated the influence of uncertainties in the cable length measurement on the result of the FK [19] and have shown that for a poor robot geometry (which was for example the case for the prototype described in section 6.1.2 for which the geometry was imposed) this influence may be quite large. An usual strategy to decrease this uncertainty for small to medium-sized CDPR is to use a drum with a cable spiral guide for the coiling which impose a coiling path for the cable. However this strategy is unfeasible for large and very large CDPR (that we called *Ultrabot*) for which the large length of the cables impose to have several layers on the drum and therefore leads to a more erratic coiling process that leads to possibly large errors of the cable lengths estimation. To get a better estimation of the cable lengths we have proposed an original method, based on the Vernier principle [21]. The idea is to have several small colored marks on the cable at known distances from the end-point of the cable and to have several color sensors in the mast of the CDPR. We have first shown that if 3 colors (e.g. RGB) were used, then an appropriate disposition of the marks on the cable allows to have up to 29 marks on the cable so that the sequence of 3 successive colors is always unique. Hence by coiling the cable and detecting the 3 successive color detected by a sensor allows to determine exactly the distance between the sensor and the cable end-point, i.e. to *calibrate* the cable length. Calibration is always an issue for CDPR which uses usually incremental encoders for measuring the drum rotation (which explain why we have also proposed another approach [18]). Then we have considered the sequence of color detection when coiling the cable, starting from its largest length. We have looked at the distribution of cable length changes  $\Delta\rho$  between two successive detection and have proposed a strategy that provide the distance between the marks so that this distribution is quasi-uniform with a mean value that is minimal. For example we have shown that for a 60 meters length cable having 29 marks we were able to have an almost constant  $\Delta\rho$  of 40 cm, meaning that when the cable length changes by this value, then we get an exact evaluation of the cable length at each detection. In between such detection we rely on the drum rotation measurement to estimate the cable length. Furthermore we have shown that the difference between the



expected detection time and the real one allows one to update the estimate of the drum radius, thus enabling to manage an erratic coiling process. We have initially installed this system on the prototype presented in section 6.1.2. The few initial tests were really promising but on-site we have had problems for ensuring a constant positioning of the marks on the synthetic cables. Being given the very short deployment time we have not been able to fix this problem. Consequently we have decided to use another approach based on direct measurement of the load pose with lidars, this approach being described in section 6.1.2.

We have also continued to investigate the calculation of planar cross-sections of the workspace for CDPR with sagging cables. We have shown in a previous paper that the border of this workspace was either determined by cable length limits but also by the singularity of the kinematics equations. Hence these singularities play an important role for the design of a CDPR. We have started a preliminary investigation on this topic [20]. We have shown that these singularities may be classified in two categories:

- *classical singularity* which corresponds to the singularity of parallel robots with rigid legs which basically implies that the mechanical equilibrium of the system cannot be obtained, leading to a motion of the platform even if the actuators are locked
- *full singularity* which are singularity of the kinematics equations but are not classical singularity. In this case mechanical equilibrium is obtained but the CDPR is unable to move in a given direction

We have also developed an algorithm that check if a full singularity exists in the neighborhood of a given pose and to locate it with an arbitrary accuracy.

### 6.1.2. Cable-Driven Parallel Robots for large scale additive manufacturing

**Participants:** Jean-Pierre Merlet, Yves Papegay [correspondant].

Easy to deploy and to reconfigure, dynamically efficient in large workspaces even with payloads, cable-driven parallel robots are very attractive for solving displacement and positioning problems in architectural building at large scale seems to be a good alternative to crane and industrial manipulators in the area of additive manufacturing. We have co-founded in 2015 years ago the XtreeE ([www.xtreee.eu](http://www.xtreee.eu)) start-up company that is currently one of the leading international actors in large-scale 3D concrete printing.

We have been contacted in 2018 by the artist Anne-Valérie Gasc that is interested in mimicking the 3D additive manufacturing process on large scale for a live art performance. She was interested in a mean for widespreading glass micro-beads on a given trajectory over a  $21 \times 9$ m large platform located at the contemporary art center *Les Tanneries* (figure 1), located close to Montargis. She was especially interested in using a CDPR for that purpose because of the low visual intrusivity of the cables and its ability to move large load. After a few month of discussions we agree to recycle our old MARIONET-CRANE prototype (2009) for this exhibition although the place was not the most appropriate for the CDPR as the height of the location was only 3 meters. We design as load a 80 liters drum of weight 55 kg with 40 kg of powder that was sufficient for printing one trajectory (figure 1). An on-board computer connected through wifi to a master computer was managing the lidar measurement and the opening/closing of the servo-valve controlling the powder flow. The drum was supported by 4 Dyneema cables of diameter 3mm whose output points were located at the corners of the platform and whose lengths were varying between 3 and 26 meters. The master computer was controlling the CDPR and the parameters of the system were recorded every second in log files. The development was very fast and we were not able to test a full scale installation in our laboratory for lack of the appropriate space. The on-site deployment was difficult because it has to be done in a record time, far away from our home base. The lack of height has especially a strong influence on the positioning errors of the drum that drastically increase if the cables are close to the horizontal. We solve on-site this problem by adding 3 low-cost lidars that were providing partial measurement on the drum pose. The system was fully operational a few days after the official opening of the exhibition and was at the heart of the artistic exhibition "Les Larmes du Prince - Vitrifications" (<http://www.lestanneries.fr/exposition/larmes-prince-vitrifications>), that was run during July and August under the control of a local student. The exhibition was scheduled to run 5 days per week until the end of August. During this period the CDPR has worked 174 hours (4h15mn/day), has traveled 4757 meters and has dispersed about 1.5 tons of powder. We get two failures: one of the cables has broken but without any consequence because of the redundancy of the robot and a failure of the reduction gear of one of the winch on

the exhibition closing day, which has been immediately repaired. From a scientific viewpoint we have been able to test, in this quasi-industrial context, the efficiency of a control law using external measurements of the pose and the logs, still being processed has allowed us to identify possible improvements and scientific issues regarding the modeling of the system. An unexpected benefit of using the lidars was to allow to record a profile of the powder wall at each trajectory, showing its life over time as it was always evolving because of the powder particle motion after a printing.



Figure 1. The exhibition place and the drum. Photos copyrighted Anne-Valérie Gasc, "Vitrifications", Photograph: Aurélien Mole

### 6.1.3. Killing robots

**Participant:** Jean-Pierre Merlet [correspondant].

The director, Linda Blanchet, of a theater company has contacted us for helping organizing a theater event, *Killing Robots*, centered on the story of *Hitchbot*, a passive 70cm high mannequin designed by Canadian colleagues, that was put on the side-way of roads in Canada so that people may transport it, the purpose being to study the human interaction with people during a travel from the east to the west coast of Canada. The mannequin was located through a GPS and has taken a picture of its surrounding every 20 minutes while it was active. This mannequin indeed performs this travel in 15 days and a similar experiment was then scheduled in the US, the purpose being to go from Boston to San Francisco. Unfortunately after 5 days of travel the mannequin was discovered completely dismantled in Philadelphia. The idea of Linda Blanchet's performance was to propose a thriller based on the robot data for discovering who has dismantled the robot and in parallel to have the robot interacts with the actors to describe its feeling. For that purpose it was necessary that the robot becomes actuated while keeping its appearance identical to the original model. We have therefore retrieved a clone of the original *Hitchbot* and we have actuated the arms and head, so that the robot was able to move them, adding a lidar on top of the head so that it was able to locate the actors on stage (figure 2).

The Canadian colleague have also provided a conversational agent so that the robot was able to speak with a learning process. The opening of the performance was done on November 6 at the National theater of Nice and it is now performing in various places in France. We have been present at several of them to interact with the public at the end of the performance. From a scientific viewpoint our interest in this exhibition was to better understand why adding motion to a mannequin modify drastically the perception of the robot by the public. These understanding will help to work on the factors that increase the acceptance of a technological object by the public, which is clearly a major factor for the efficiency of our assistance devices.



Figure 2. The transformed Hitchbot robot

## 6.2. Smart Environment for Human Behaviour Recognition

**Participants:** Jean-Pierre Merlet, Yves Papegay, Odile Pourtallier [correspondant], Eric Wajnberg.

The general aim of this research activity focuses on long term indoor monitoring of frail persons. In particular we are interested in early detection of daily routine and activity modifications. These modifications may indicate health condition alteration of the person and may require further medical or family care. Note that our work does not aim at detecting brutal modifications such as faintness or fall.

In our research we envisage both individual and collective housing such as rehabilitation center or retirement home.

Our work relies on the following leading ideas :

- We do not base our monitoring system on wearable devices since it appears that they may not be well accepted and worn regularly,
- Privacy advocates adequacy between the monitoring level needed by a person and the detail level of the data collected. We therefore strive to design a system fitted to the need of monitoring of the person.
- In addition to privacy concern, intrusive feature of video led us not to use it.

The main aspect that grounds this work is the ability to locate a person or a group in their indoor environment. We focus our attention to the case where several persons are present in the environment. As a matter of fact the single person case is less difficult.

### 6.2.1. Tools and data analysis for experimental systems

Two experimental systems are installed in two areas (a consultation center (Institut Claude Pompidou, ICP, Nice), and a retirement home (EHPAD Valrose, Nice)) where several types of persons (residents, visitors, staff) evolve. They are made up of virtual barriers (constituted of distance and motion sensors) displayed in the environment and connected to a PC that collects and stores the measurements of the barriers. Each crossing

of a barriers hence corresponds to a specific signal of a set of sensors. We develop a set of codes that aim to analyze the data collected to construct information on the moves of the persons in the experiment areas [23].

This year we have improved the code that yields the barrier events (time and direction of crossing of barriers) from the raw data. This allowed us to use this first step to reconstruct the individual trajectories of the users.

Although the filtering technics do not use external information (such as specific use of a zone bounded by barriers, habit of users according to time....) we can determine most of the individual trajectories of the users, even when several users evolve simultaneously in the area. Although some uncertainties remain (and could probably be improved using external knowledge), we can use the results obtained to perform a statistical analysis.

The aim on the main scientific efforts this year was to develop a detailed statistical treatment chain to extract and to visualize the events information coming from the set of movement activity detectors installed at ICP. All the (statistical and graphical) development were performed in the R software environment. Globally, two sets of information were collected, for the recorded data. The first provides a kinematic view of the presence of individuals on the mass plan of ICP during a chosen time interval. The following graph gives a static example of the kinematic graph obtained. Such a dynamic information points, for example, to specific movement activities in the medical center, at given time intervals. Figure 3 shows the presence of individuals in the corridors and consultation rooms at ICP at different times.

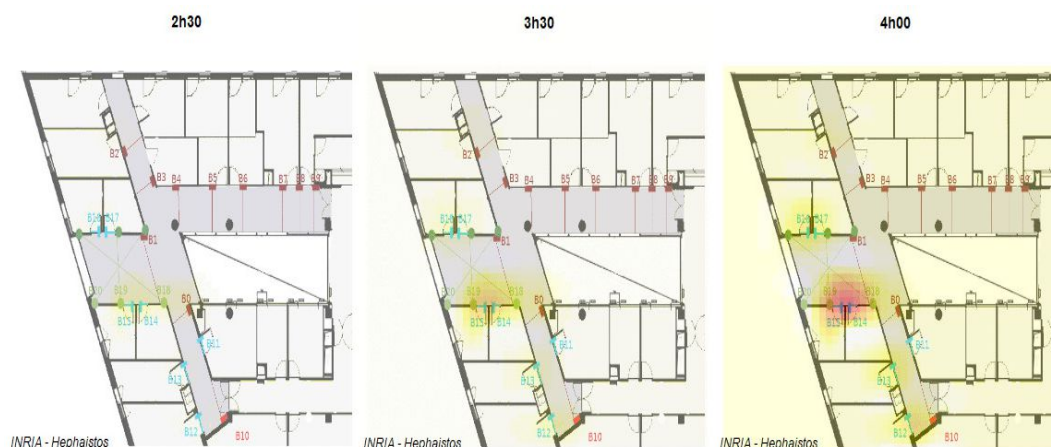


Figure 3. Three photograms on a kinematic view of the presence of individuals on the mass plan of ICP

Such a graph is only descriptive. Hence, it does not provide a functional analysis of the displacements of individuals in the medical center. In order to understand this better, the chronological movement patterns were functionally described by building, for every time interval, the transition matrix between all zones present in the analyzed medical center. After proper algebraic manipulation, the obtained transition matrices were analyzed using a factorial correspondence analysis, a multivariate method that - in this case and among other features - built graphs describing the functional movement patterns between zones. The graph presented in figure 4 gives an example of the obtained results.

The next step will be to statistically compare such results, e.g., between morning or afternoon activity, between days with or without medical consultation, etc. Results obtained might lead to a better organization of the medical activities at ICP.

### 6.3. Other medical activities

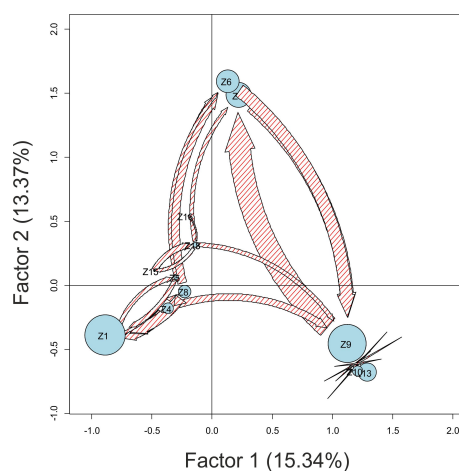


Figure 4. Example of the best factorial plan (explaining almost 30% of all the information contained in the data) obtained from a factorial correspondence analysis used to describe the functional movement patterns of individual between zones in the followed medical center during a full day of activity. Each blue circle represents a zone, with a radius proportional of its frequentation frequency. Arrows between zones (in red) are proportional to the observed flux of individual movements between zones. Only the most important arrows are presented.

**Participants:** Jean-Pierre Merlet [correspondant], Sylvain Guénon.

Eric Sejour, a surgeon at Nice hospital, has contacted us about developing a robotized system for realizing sutures in an autonomous way. Suturing is a lengthy process while in many cases this is not a complex operation. Eric Sejour mentions that developing an autonomous system allowing to manage standard wounds may be extremely interesting, especially for emergency service that are under-staffed. Instead of developing a new robot dedicated to this purpose we have proposed to Eric Sejour to build a system based on the existing manual tools that require to put the instrument in place and then simply squeezing a trigger. The placement will be realized by one of our small parallel robot, with the help of vision system to locate the edge of the wound, while the trigger squeezing will be performed by an actuator. We have obtained an Idex funding (one year for an engineer) to develop a proof-of-concept prototype that will perform the operation on silicone mockups that are used for the surgeon training.

We have had also a contact with the ergotherapist Nicolas Ciai from Nice hospital for the evaluation of patient motricity before an operation. For this evaluation the ergotherapist performs muscular testing before the operation, right after the operation and 6 months later. The exercise consists in opposing the ergotherapist palm against the musculo group that has to be tested until a force equilibrium is reached. Then the ergotherapist ranks the tonicity of the muscles on a discrete scale between 0 and 6 according to his muscular feeling. As numerous muscles have to be tested, the process is quite lengthy. Clearly this process is quite subjective and we have proposed an objectification of the process by developing a glove prototype that includes pression sensors for measuring accurately the pressure exerted by the patient. These sensors are used by a micro-computer the size of a large watch located on the wrist of the ergotherapist. This computer determines when the pressure becomes stable, in which case this pressure is displayed and recorded. A companion software will then exploit the recorded data to provide an evaluation report. Beside the objectification of the ranking, the purpose is also to speed-up the tests. Although this project is quite advanced, we are lacking of manpower to complete it so that we have presented a project to Nice hospital for funding an engineer that may complete the second version of the glove.



## INDES Project-Team

# 6. New Results

## 6.1. JavaScript Implementation and Browser Security

We have pursued the development of *Hop* and our study on efficient and secure JavaScript implementations.

### 6.1.1. JavaScript Property Caches

JavaScript objects are dynamic. At any moment of their lifetime, properties can be added or deleted. In principle a property access requires a lookup in the object itself, and, possibly, in all the objects forming its prototype chain. All fast JavaScript implementations deploy strategies to implement this lookup operation in nearly constant time. They generally rely on two ingredients: *hidden classes* and *property caches*. Hidden classes describe object memory layouts. Property caches use these descriptions to access objects directly, avoiding the normal name lookup operations. Hidden classes and property caches make property accesses comparable in speed to field accesses of traditional languages like C and Java.

Hidden classes and property caches are not new. They were invented for Self, the first dynamically typed prototype-based languages, following Smalltalk's idea that already used caches at that time for optimizing method calls. For the past ten years they have enjoyed a revival of interest after it was shown how effective they are at improving Object-Oriented languages performance in general and specially JavaScript. Today most JavaScript implementations such as V8, JavaScriptCode, and SpiderMonkey use them. Hidden classes and property caches apply in specific situations, which unfortunately means that some accesses are unoptimized or not treated very efficiently.

1. **Property addition problem:** hidden classes support the accesses of existing properties but they do not handle efficiently property addition commonly found in object constructors.
2. **Prototype properties problem:** hidden classes and property caches optimize accesses of properties directly stored in the object. They do not optimize accesses of properties stored in one of the objects composing the prototype chain.
3. **Polymorphic properties problem,** as property caches require strict hidden class equivalence for optimizing accesses, polymorphic data structures and polymorphic method invocations need special treatment to not be left unoptimized. This has been addressed by the *Polymorphic Inline Cache* technique proposed by Holzle *et al.* in previous studies, which resorts to a dynamic search in the cache history. As a linear or binary search is involved, it is not as efficient as plain property caches.

Problem 1 is critical for all existing JavaScript programs as it impacts the performance of object construction. Problems 2 and 3 will become prominent with the advent of ECMAScript 6 class-like programming style that is backed up by object prototypes. We propose solutions to these problems. At the cost of one extra test inserted at each property access, we optimize prototype property accesses. Resorting to a static analysis, we propose a technique that we call *speculative caches* for optimizing object construction.

Trading memory space for speed, we propose *cache property tables* that enable accessing polymorphic objects in constant time. For the analogy with C++ virtual tables we call these cache tables *vtables*.

We have implemented these techniques in *Hopc*, the *Hop* static JavaScript compiler and we have presented them in a conference publication [17]. We have shown how the complement and enhance property caches used for accessing object properties of JavaScript like languages. We have shown that they take over classical caches when the searched property is either stored in an object of the prototype chain or defined using accessors. They also support efficiently polymorphic and megamorphic property accesses. Finally, they also support efficient object extensions. These techniques do not apply as frequently as simple property caches that cover a vast majority of accesses. However, since they impose no overhead when not used, they can be integrated in any existing system at no run time cost. We have validated the approach with an experimental report based that shown that the presented techniques improve performance in situations where simple cache miss.



### 6.1.2. Secure JavaScript

Whereas the dynamic nature of JavaScript plays an essential role in the advantages it offers for easy and fast development, a malicious JavaScript program can easily break the integrity and confidentiality of a web or IoT application. JavaScript dynamic semantics and sharing are deeply intricately and attacker code can trivially exploit these.

We have developed a compiler, called SecureJS to offer security guarantees for JavaScript on clients, servers, and IoT devices. Our compiler is applicable to ECMAScript 5th legacy code, which in particular means that we allow for built-in JavaScript functions. Moreover, we go beyond the JavaScript language and handle a common web API, XMLHttpRequest module. The challenge is to cover most of the JavaScript language efficiently while providing strong security guarantees. For the latter, we formally define and prove the compiler's security guarantees by means of a new security property, coined as *dynamic delimited release*, for JavaScript integrity and confidentiality.

Compiled programs can be effortlessly deployed in client, server, and IoT JavaScript environments and do not require an external isolation mechanism to preserve integrity and confidentiality.

We have validated SecureJS experimentally using ECMAScript Test262 test suits. First, we have shown that SecureJS preserves the correct SecureJS semantics. Second, we have shown that it successfully implements the memory isolation needed to enforce the security property.

The current SecureJS implementation as been architected to support low-power platforms that only supports ECMAScript 5. In the future we plan to accommodate more recent version of JavaScript for the platforms that supports it. This will extend the possibility of communications between trusted and untrusted codes and this will enable more efficient implementation techniques. A paper describing this work is currently under submission.

### 6.1.3. Empowering Web Applications with Browser Extensions

Browser extensions are third party programs, tightly integrated to browsers, where they execute with elevated privileges in order to provide users with additional functionalities. Unlike web applications, extensions are not subject to the Same Origin Policy (SOP) and therefore can read and write user data on any web application. They also have access to sensitive user information including browsing history, bookmarks, credentials (cookies) and list of installed extensions. They have access to a permanent storage in which they can store data as long as they are installed in the user's browser. They can trigger the download of arbitrary files and save them on the user's device. For security reasons, browser extensions and web applications are executed in separate contexts. Nonetheless, in all major browsers, extensions and web applications can interact by exchanging messages. Through these communication channels, a web application can exploit extension privileged capabilities and thereby access and exfiltrate sensitive user information.

We have analyzed the communication interfaces exposed to web applications by Chrome, Firefox and Opera browser extensions [18]. As a result, we identified many extensions that web applications can exploit to access privileged capabilities. Through extensions' APIS, web applications can bypass SOP and access user data on any other web application, access user credentials (cookies), browsing history, bookmarks, list of installed extensions, extensions storage, and download and save arbitrary files in the user's device. Our results demonstrate that the communications between browser extensions and web applications pose serious security and privacy threats to browsers, web applications and more importantly to users. We discuss countermeasures and proposals, and believe that our study and in particular the tool we used to detect and exploit these threats, can be used as part of extensions review process by browser vendors to help them identify and fix the aforementioned problems in extensions.

## 6.2. Timing-side channels attacks

We have pursued our studies on foundations of language-based security following two axes on timing-side channels research:

### 6.2.1. Speculative constant time

The most robust way to deal with timing side-channels in software is via *constant-time* programming—the paradigm used to implement almost all modern cryptography. Constant-time programs can neither branch on secrets nor access memory based on secret data. These restrictions ensure that programs do not leak secret information via timing side channels, at least on hardware *without* microarchitectural features. However, microarchitectural features are a major source of timing side channels as the growing list of attacks (Spectre, Meltdown, etc) is showing. Moreover code deemed to be constant-time in the usual sense may in fact leak information on processors with microarchitectural features. Thus the decade-old constant-time recipes are no longer enough. We lay the foundations for constant-time in the presence of micro-architectural features that have been exploited in recent attacks: out-of-order and speculative execution. We focus on constant-time for two key reasons. First, *impact*: constant-time programming is largely used in narrow, high-assurance code—mostly cryptographic implementations—where developers already go to great lengths to eliminate leaks via side-channels. Second, *foundations*: constant-time programming is already rooted in foundations, with well-defined semantics. These semantics consider very powerful attackers have control over the cache and the scheduler. A nice effect of considering powerful attackers is that the semantics can already overlook many hardware details—e.g., since the cache is adversarially controlled there is no point in modeling it precisely—making constant-time amenable to automated verification and enforcement.

We have first defined a semantics for an abstract, three-stage (fetch, execute, and retire) machine. This machine supports out-of-order and speculative execution by modeling *reorder buffers* and *transient instructions*, respectively. Our semantics assumes that attackers have complete control over microarchitectural features (e.g., the branch target predictor), and uses adversarial execution *directives* to model adversary’s control over predictors. We have then defined *speculative constant-time*, the counterpart of *constant-time* for machines with out-of-order and speculative execution. This definition has allowed us to discover microarchitectural side channels in a principled way—all four classes of Spectre attacks as classified by Canella et al., for example, manifest as violation of our constant-time property. Our semantics even revealed a new Spectre variant, that exploits the aliasing predictor. The variant can be disabled by unsetting a flag, by illustrates the usefulness of our semantics. This study is described in a paper currently submitted.

### 6.2.2. Remote timing attacks

A common approach to deal with timing attacks is based on preventing secrets from affecting the execution time, thus achieving security with respect to a strong, *local* attacker who can measure the timing of program runs. Another approach is to allow branching on secrets but prohibit any subsequent attacker-visible side effects of the program. It is sometimes used to handle *internal timing* leaks, i.e., when the timing behavior of threads affects the interleaving of attacker-visible events via the scheduler.

While these approaches are compatible with strong attackers, they are highly restrictive for program runs as soon as they branch on a secret. It is commonly accepted that “adhering to constant-time programming is hard” and “doing so requires the use of low-level programming languages or compiler knowledge, and forces developers to deviate from conventional programming practices”.

This restrictiveness stems from the fact that there are many ways to set up timing leaks in a program. For example, after branching on a secret the program might take different time in the branches because of: (i) more time-consuming operations in one of the branches, (ii) cache effects, when in one of the branches data or instructions are cached but not in the other branch, (iii) garbage collection (GC) when in one of the branches GC is triggered but not in the other branch, and (iv) just-in-time (JIT) compilation, when in one of the branches a JIT-compiled function is called but not in the other branch. Researchers have been painstakingly addressing these types of leaks, often by creating mechanisms that are specific to some of these types. Because of the intricacies of each type, addressing their combination poses a major challenge, which these approaches have largely yet to address.

This motivates a general mechanism to tackle timing leaks independently of their type. However, rather than combining enforcement for the different types of timing leaks for strong local attackers, is there a setting

where the capabilities of attackers are perhaps not as strong, enabling us to design a general and less restrictive mechanism for a variety of timing attacks with respect to a weaker attacker?

We focus on timing leaks under *remote* execution. A key difference is that the remote attacker does not generally have a reference point of when a program run has started or finished, which significantly restricts attacker capabilities.

We illustrate remote timing attacks by two settings: a server-side setting of IoT apps where apps that manipulate private information run on a server and a client-side setting where e-voting code runs in a browser.

IFTTT (If This Then That), Zapier, and Microsoft Flow are popular IoT platforms driven by enduser programming. App makers publish their apps on these platforms. Upon installation apps manipulate sensitive information, connecting cyberphysical “things” (e.g., smart homes, cars, and fitness armbands) to online services (e.g., Google and Dropbox) and social networks (e.g., Facebook and Twitter). An important security goal is to prevent a malicious app from leaking private information of a user to the attacker.

Recent research identifies ways to leak private information by IoT apps and suggests tracking information flows in IoT apps to control these leaks. The suggested mechanisms perform data-flow (*explicit*) and control-flow (*implicit*) tracking. Unfortunately, they do not address timing leaks, implying that a malicious app maker can still exfiltrate private information, even if the app is subject to the security restrictions imposed by the proposed mechanisms.

In addition, Verificatum, an advanced client-side cryptographic library for e-voting motivates the question of remote timing leaks with respect to attackers who can observe the presence of encrypted messages on the network.

This leads us to the following general research questions:

1. What is the right model for remote timing attacks?
2. How do we rule out remote timing leaks without rejecting useful secure programs?
3. How do we generalize enforcement to multiple security levels?
4. How do we harden existing information flow tools to track remote timing leaks?
5. Are there case studies to give evidence for the feasibility of the approach?

To help answering these questions, we propose an extensional knowledge-based security characterization that captures the essence of remote timing attacks. In contrast to the local attacker that counts execution steps/time since the beginning of the execution, our model of the remote attacker is only allowed to observe inputs and outputs on attacker-visible channels, along with their timestamps. At the same time, the attacker is in charge of the potentially malicious code with capabilities to access the clock, in line with assumptions about remote execution on IoT app platforms and e-voting clients.

A timing leak is typically enabled by branching on a secret and taking different time or exhibiting different cache behavior in the branches. However, as discussed earlier, it is desirable to avoid restrictive options like forcing the execution to take constant time, prohibiting attacker-visible output any time after the branching, or prohibiting branching on a secret in the first place.

Our key observation is that for a remote attacker to successfully set up and exploit a timing leak, program behavior must follow the following pattern: (i) branching on a secret takes place in a program run, and either (ii-a) the branching is followed by more than one attacker-visible I/O event, or (ii-b) the branching is followed by one attacker-visible I/O event, and prior to the branching there is either an attacker-visible I/O event or a reading to the clock.

Based on this pattern, we design Clockwork, a monitor that rules out timing leaks. Our mechanism pushes for permissiveness. For example, runs (free of explicit and implicit flows) that do not access the clock and only have one attacker-visible I/O event are accepted.

Runs that do not perform attacker-visible I/O after branching on a secret are accepted as well. As we will see, these kinds of runs are frequently encountered in secure IoT and e-voting apps.

We implement our monitor for JavaScript, leveraging JSFlow, a state-of-the-art information flow tracker for JavaScript. We demonstrate the feasibility of the approach on a case study with IFTTT, showing how to prevent malicious app makers from exfiltrating users' private information via timing, and a case study with Verificatum, showing how to track remote timing attacks with respect to network attackers. Our case studies demonstrate both the security and permissiveness. While apps with timing leaks are rejected, benign apps that use clock and I/O operations in a non-trivial fashion are accepted.

### 6.3. Security analysis of ElGamal implementations

Throughout the last century, especially with the beginning of public key cryptography due to Diffie-Hellman, many cryptographic schemes have been proposed. Their security depends on mathematically complex problems such as integer factorization and discrete logarithm. In fact, it is thought that a cryptographic scheme is secure if it resists cryptographic attacks over a long period of time. On one hand, since certain schemes may take several years before being widely studied in depth, they become vulnerable as time passes. On the other hand, a cryptographic scheme is a provable one, if it resists cryptographic attacks relying on mathematical hypothesis.

Being easily adaptable to many kinds of cryptographic groups, the ElGamal encryption scheme enjoys homomorphic properties while remaining semantically secure, provided that the Decisional Diffie-Hellman (DDH) assumption holds on the chosen group. While the homomorphic property forbids resistance against chosen ciphertext attacks, it is very convenient for voting systems. The ElGamal encryption scheme is the most extensively used alternative to RSA, and it is the homomorphic encryption scheme almost exclusively used for voting systems. Moreover, ElGamal is the only homomorphic encryption scheme implemented by default in many hardware security modules.

In order to be provable secure, ElGamal encryption needs to be implemented on top of a group verifying the Decisional Diffie-Hellman (DDH) assumption. Since this assumption does not hold for all groups, one may have to wrap an encoding and a decoding phase to ElGamal to be able to have a generic encryption scheme.

We have submitted a paper that studies ElGamal encryption scheme libraries in order to identify which implementations respect the DDH assumption. The paper presents an analysis of 25 libraries that implement ElGamal encryption scheme in the wild. We focus our analysis on understanding whether the DDH assumption is respected in these implementations, ensuring a secure scheme in which no information about the original message could be leaked. The DDH assumption is crucial for the security of ElGamal because it ensures indistinguishability under chosen-plaintext attacks (IND-CPA). Without the DDH assumption, encryption mechanisms may leak one bit of information about the plaintext and endanger the security of the electoral system as one bit has the ability to completely invalidate privacy in an election. One way to comply with the DDH assumption is by using groups of prime order. In particular, when adopting safe primes, one can ensure the existence of a *large* prime order subgroup and restrict messages to belong to this subgroup. Mapping plaintexts into subgroups is called message encoding. Such encoding necessitates to be efficient and precisely invertible to allow decoding after the decryption.

Our results show that out of 25 analyzed libraries, 20 are wrongly implemented because they do not respect the conditions to achieve IND-CPA security under the DDH assumption. This means that encryptions using ElGamal from any of these 20 libraries leak one bit of information.

From the 5 libraries which respect the DDH assumption, we also study and compare various encoding and decoding techniques. We identify four different message encoding and decoding techniques and discuss the different designs and conclude which implementation is more efficient for voting systems.

### 6.4. Measurement and Detection of Web Tracking

#### 6.4.1. Missed by Filter Lists: Detecting Unknown Third-Party Trackers with Invisible Pixels

The Web has become an essential part of our lives: billions are using Web applications on a daily basis and while doing so, are placing *digital traces* on millions of websites. Such traces allow advertising companies, as well as data brokers to continuously profit from collecting a vast amount of data associated to the users.

*Web tracking* has been extensively studied over the last decade. To detect tracking, most of the research studies and user tools rely on *consumer protection lists*. EasyList<sup>0</sup> and EasyPrivacy<sup>0</sup> (EL&EP) are the most popular publicly maintained blacklist of known advertising and tracking domains, used by the popular browser extensions Adblock Plus<sup>0</sup> and uBlockOrigin<sup>0</sup>. Disconnect<sup>0</sup> is another very popular list for detecting domains known for tracking, used in Disconnect browser extension<sup>0</sup> and in integrated tracking protection of Firefox browser. Relying on EL&EP or Disconnect became the *de facto* approach to detect third-party tracking requests in privacy and measurement community. However it is well-known that these lists detect only known tracking and ad-related requests, and a tracker can easily avoid this detection by registering a new domain or changing the parameters of the request.

**Our contributions:** To evaluate the effectiveness of filter lists, we propose a new, fine-grained behavior-based tracking detection. Our results are based on a stateful dataset of 8K domains with a total of 800K pages generating 4M third-party requests. We make the following contributions:

- *We analyse all the requests and responses that lead to invisible pixels (by “invisible pixels” we mean  $1 \times 1$  pixel images or images without content).* Pixels are routinely used by trackers to send information or third-party cookies back to their servers: the simplest way to do it is to create a URL containing useful information, and to dynamically add an image tag into a webpage. This makes invisible pixels *the perfect suspects for tracking* and propose a new classification of tracking behaviors. Our results show that pixels are still widely deployed: they are present on more than 94% of domains and constitute 35.66% of all third-party images. We found out that pixels are responsible only for 23.34% of tracking requests, and the most popular tracking content are scripts: a mere loading of scripts is responsible for 34.36% of tracking requests.
- *We uncover hidden collaborations between third parties.* We applied our classification on more than 4M third-party requests collected in our crawl. We have detected new categories of tracking and collaborations between domains. We show that domains sync first party cookies through a *first to third party cookie syncing*. This tracking appears on 67.96% of websites.
- *We show that filter lists miss a significant number of cookie-based tracking.* Our evaluation of the effectiveness of EasyList&EasyPrivacy and Disconnect lists shows that they respectively miss 25.22% and 30.34% of the trackers that we detect. Moreover, we find that if we combine all three lists, 379,245 requests originating from 8,744 domains still track users on 68.70% of websites.
- *We show that privacy browser extensions miss a significant number of cookie-based tracking.* By evaluating the popular privacy protection extensions: Adblock, Ghostery, Disconnect, and Privacy Badger, we show that Ghostery is the most efficient among them and that all extensions fail to block at least 24% of tracking requests.

This paper [15] has been accepted for publication at the Privacy Enhancing Technologies Symposium (PETs) 2020.

#### 6.4.2. A survey on Browser Fingerprinting

This year, we have conducted a survey on the research performed in the domain of browser fingerprinting, while providing an accessible entry point to newcomers in the field. We explain how this technique works and where it stems from. We analyze the related work in detail to understand the composition of modern fingerprints and see how this technique is currently used online. We systematize existing defense solutions into different categories and detail the current challenges yet to overcome.

---

<sup>0</sup><https://easylist.to/>

<sup>0</sup><https://easylist.to/easylist/easyprivacy.txt>

<sup>0</sup><https://adblockplus.org/>

<sup>0</sup><https://github.com/gorhill/uBlock>

<sup>0</sup><https://disconnect.me/trackerprotection/blocked>

<sup>0</sup><https://disconnect.me/>

A *browser fingerprint* is a set of information related to a user's device from the hardware to the operating system to the browser and its configuration. *Browser fingerprinting* refers to the process of collecting information through a web browser to build a fingerprint of a device. Via a script running inside a browser, a server can collect a wide variety of information from public interfaces called Application Programming Interface (API) and HTTP headers. An API is an interface that provides an entry point to specific objects and functions. While some APIs require a permission to be accessed like the microphone or the camera, most of them are freely accessible from any JavaScript script rendering the information collection trivial. Contrarily to other identification techniques like cookies that rely on a unique identifier (ID) directly stored inside the browser, browser fingerprinting is qualified as completely *stateless*. It does not leave any trace as it does not require the storage of information inside the browser.

The goal of this work is twofold: first, to provide an accessible entry point for newcomers by systematizing existing work, and second, to form the foundations for future research in the domain by eliciting the current challenges yet to overcome. We accomplish these goals with the following contributions:

- A thorough survey of the research conducted in the domain of browser fingerprinting with a summary of the framework used to evaluate the uniqueness of browser fingerprints and their adoption on the web.
- An overview of how this technique is currently used in both research and industry.
- A taxonomy that classifies existing defense mechanisms into different categories, providing a high-level view of the benefits and drawbacks of each of these techniques.
- A discussion about the current state of browser fingerprinting and the challenges it is currently facing on the science, technological, business, and legislative aspects.

This work has been submitted for publication at an international journal.

## 6.5. Security Analysis of GDPR Subject Access Request Procedures

With the GDPR in place since May 2018, the rights of the European users have been strengthened. The GDPR defines users' rights and aims at protecting their personal data. Every European Data Protection Authority (DPA) provides advices, explanations and recommendations on the use of these rights. However, the GDPR does not provide any prescriptive requirements on how to authenticate a data subject request. This lack of concrete description undermines the practical effect of the GDPR: it hampers the way to exercise the subject access right, to check the lawfulness of the processing and to enforce the derived legal rights therefrom (erasure, rectification, restriction, etc).

Every data subject would like to benefit from the rights specified in GDPR, but still wonders: *How do I exercise my access right? How do I prove my identity to the controller?* These questions are critical to build trust between the data subject and the controller. The data subject is concerned with threats like *impersonation* and *abusive identity check*. Impersonation is the case of a malicious party who attempts to abuse the subject access request (SAR) by impersonating a subject to a controller. Abusive identity check occurs when a data controller is too curious and verifies the identity of a subject by asking irrelevant and unnecessary information like an electricity bill or government issued documents.

Symmetrically, every data controller needs to know how to proceed when they receive an access request: *Is the request legitimate? What is necessary to identify the subject's data?* These concerns aggravate when controllers deal with indirectly-linked identifiers, such as IP addresses, or when they have no prior contact with data subjects, as in *Google Spain*<sup>0</sup>. Most of all, data controllers want to avoid data breaches, as it can result in legal proceedings and heavy fines. Such consequence occurs in two cases: (i) the data controller releases data to an illegitimate subject, or (ii) he releases data of a subject A to a legitimate subject B.

<sup>0</sup>Google Spain SL and Google Inc. v Agencia Española de Protección de Datos (AEPD) and Mario Costeja González, Case C-131/12, <https://eur-lex.europa.eu/legal-content/EN/TXT/PDF/?uri=CELEX:62012CJ0131&from=EN>



All these questions concern the authentication procedure between the data subject and the controller. They both share a common interest in holding a strong authentication procedure to prevent impersonation and data breaches. The subject must be careful during the authentication procedure, as for providing too much personal information could compromise her right of privacy. Additionally, the controller needs to ask the appropriate information to identify the subject's data without ambiguity. There is clearly a tension during this authentication act between the controller, who tries to get as much information as possible, and the data subject who wants to provide as little as possible. Plausibly, subject access rights can probably increase the incidence of personal records being accidentally or deliberately opened to unauthorised third parties [22].

This work studies *the tension during the authentication between the data subject and the data controller*. We first evaluate the threats to the SAR authentication procedure and then we analyze the recommendations of 28 DPAs of European Union countries. We observe that four of them can potentially lead to abusive identity check. On the positive side, six of them are recommending to enforce the data minimization principle during authentication. This principle, on one hand, protects the right to privacy of data subjects, and on the other hand prevents data controllers to massively collect personal data that is not needed for authentication, thus preventing abusive identity check.

We have then evaluated the authentication procedure when exercising the access right of the 50 most popular websites and 30 third-party tracking services. Several popular websites require to systematically provide a national identity card or government-issued documents to authenticate the data subject. Among third-party tracking services, 9 of them additionally to cookies demand other personal data from the data subjects, like the identity card or the full name. We explain that such demands are not justified because additional information can not prove the ownership of the cookie.

We then provide guidelines to Data Protection Authorities, website owners and third party services on how to authenticate data subjects safely while protecting their identities, and without requesting additional unnecessary information (complying with the data minimization principle). More precisely, we explain how data controllers and data subjects must interact and how digital identifiers can be redesigned to be compliant with the GDPR.

This work has been published at the Annual Privacy Forum (APF) 2019 [13].

## 6.6. Measuring Legal Compliance of Cookie Banners

### 6.6.1. Deciphering EU legal requirements on consent and technical means to verify compliance of cookie banners

In this work, we analyze the legal requirements on how cookie banners are supposed to be implemented to be fully compliant with the ePrivacy Directive and the GDPR.

Our contribution resides in the definition of 17 operational and fine-grained requirements on cookie banner design that are legally compliant, and moreover, we define whether and when the verification of compliance of each requirement is technically feasible.

The definition of requirements emerges from a joint interdisciplinary analysis composed of lawyers and computer scientists in the domain of web tracking technologies. As such, while some requirements are provided by explicitly codified legal sources, others result from the domain-expertise of computer scientists. In our work, we match each requirement against existing cookie banners design of websites. For each requirement, we exemplify with compliant and non-compliant cookie banners.

As an outcome of a technical assessment, we verify per requirement if technical (with computer science tools) or manual (with any human operator) verification is needed to assess compliance of consent and we also show which requirements are impossible to verify with certainty in the current architecture of the Web. For example, we explain how the GDPR's requirement for revocable consent could be implemented in practice: when consent is revoked, the publisher should delete the consent cookie and communicate the withdrawal to all third parties who have previously received consent.

With this approach we aim to support practically-minded parties (compliance officers, regulators, privacy NGOs, researchers, and computer scientists) to assess compliance and detect violations in cookie banners' design and implementation, specially under the current revision of the EU ePrivacy framework.

This working paper is submitted for publication.

### 6.6.2. *Measuring Legal Compliance of Banners from IAB Europe's Transparency and Consent Framework*

As a result of the GDPR and the ePrivacy Directive, (known as "cookie law"), European users encounter cookie banners on almost every website. Many of such banners are implemented by Consent Management Providers (CMPs), who respect the IAB Europe's Transparency and Consent Framework (TCF). Via cookie banners, CMPs collect and disseminate user consent to third parties. In this work, we systematically study IAB Europe's TCF and analyze consent stored behind the user interface of TCF cookie banners. We analyze the GDPR and the ePrivacy Directive to identify legal violations in implementations of cookie banners based on the storage of consent and detect such violations by crawling 22 949 European websites.

With two automatic and semi-automatic crawl campaigns, we detect violations, and we find that: 175 websites register positive consent even if the user has not made their choice; 236 websites nudge the users towards accepting consent by pre-selecting options; and 39 websites store a positive consent even if the user has explicitly opted out. Performing extensive tests on 560 websites, we find at least one violation in 54% of them.

Finally, we provide a browser extension called "Cookie Glasses" to facilitate manual detection of violations for regular users and Data Protection Authorities.

This working paper is submitted for publication at an international conference.

## 6.7. Session Types

Session types describe communication protocols between two or more parties by specifying the sequence of exchanged messages and their functionality (sender, receiver and type of carried data). They may be viewed as the analogue, for concurrency and distribution, of data types for sequential computation. Originally conceived as a static analysis technique for an enhanced version of the  $\pi$ -calculus, session types have been subsequently embedded into a range of functional, concurrent, and object-oriented programming languages.

While binary sessions can be described by a single session type, multiparty sessions require two kinds of types: a *global type* that describes the whole session protocol, and *local types* that describe the contributions of the various participants to the protocol. The key requirement to achieve safety properties such as the absence of communication errors and deadlock-freedom, is that the local types of the processes implementing the participants be obtained as projections from the same global type (the one describing the session protocol).

We have pursued our work on multiparty session types along four main directions, in collaboration with colleagues from the Universities of Groningen, Luxemburg, Nice Sophia Antipolis, Turin and Eastern Piedmont. One of these directions is described in Section 6.8.3, the others are described below.

### 6.7.1. *Reversible Sessions with Flexible Choices*

*Reversibility* has been an active trend of research for the last fifteen years. A reversible computation is a computation that may roll back to a past state. Allowing computations to reverse is a means to improve system flexibility and reliability. In the setting of concurrent process calculi, reversible computations have been first studied for Milner's calculus CCS, then for the  $\pi$ -calculus, and only recently for typed session calculi.

Following up on our previous work on concurrent reversible sessions, we studied a simpler but somewhat more realistic calculus for concurrent reversible multiparty sessions, equipped with a flexible choice operator allowing for different sets of participants in each branch of a choice. This operator was inspired by the notion of *connecting communication* introduced by other authors to describe protocols with optional participants. Our calculus supports a compact representation of the *history* of processes and types, which facilitates the definition of rollback. Moreover, it implements a fine-tuned strategy for backward computation, where only some specific participants, the "choice leaders", can trigger a rollback. We present a session type system

for this calculus and show that it enforces the expected properties of session fidelity, forward progress and backward progress. This work has been published in the journal [11].

### 6.7.2. *Multiparty Sessions with Internal Delegation*

We have investigated a new form of *delegation* for multiparty session calculi. Usually, the delegation mechanism allows a session participant to appoint a participant in another session to act on her behalf. This means that delegation is inherently an inter-session mechanism, which requires session interleaving. Hence delegation falls outside the descriptive power of global types, which specify single multiparty sessions. As a consequence, properties such as deadlock-freedom or lock-freedom are difficult to ensure in the presence of delegation. In our work, we adopt a different view of delegation, by allowing participants to delegate tasks to each other within the same multiparty session. This way, delegation occurs within a single session (whence the name “internal delegation”) and may be captured by its global type. To increase flexibility in the use of delegation, we use again connecting communications, in order to accommodate optional participants in the branches of choices. By this means, we are also able to express conditional delegation. We present a session type system based on global types with internal delegation, and show that it ensures the usual safety properties of multiparty sessions, together with a progress property.

This work has been published in a special issue of TCS dedicated to Maurice Nivat [12].

### 6.7.3. *Event Structure Semantics for Multiparty Sessions*

In the work [14] we investigate the relationship between multiparty session calculi and other concurrency models, by focussing on Event Structures as proposed in the late 80’s. We consider a standard multiparty session calculus where sessions are described as networks of sequential processes, and each process implements a participant in the session. We propose an interpretation of such networks as *Flow Event Structures* (FESs) (a subclass of Winskel’s Stable Event Structures), which allows concurrency between session communications to be explicitly represented. We then introduce global types for these networks, and define an interpretation of global types as *Prime Event Structures* (PESs). Since the syntax of global types does not allow all the concurrency among communications to be expressed, the events of the associated PES need to be defined as equivalence classes of communication sequences up to *permutation equivalence*. We show that when a network is typable by a global type, the FES semantics of the former is equivalent, in a precise technical sense, to the PES semantics of the latter.

This work has been published in a volume dedicated to Rocco De Nicola on the occasion of his 65th birthday [14]. An extended version is available as Research Report [21].

## 6.8. Web Reactive Programming

### 6.8.1. *HipHop.js*

This year, we have completed the design of the *HipHop* programming language. We have finalized the syntax of core instructions, stabilized the interfacing with JavaScript, added variables that supplement signals in local computation, and we have completed the synchronous/asynchronous connections. A paper describing this final version of the paper is currently under submission.

We have also improved significantly the *HipHop* implementation for speed and for debugging.

- Leveraging on the *Hop* speed improvement and by adding a new *HipHop* compilation stage we have been able to accelerate by a factor of about 10× the intrinsic execution time of the reactive machine. The optimization removes nets of the virtual electronic circuits that are generated by the *HipHop* compiler by propagating constant and by collapsing identical nodes. This contributions is included in the main development tree (<https://github.com/manuel-serrano/hiphop>).
- A central difficulty of the synchronous reactive programming is debugging and error messages. The *HipHop* compilation roughly consists in implementing efficiently and compactly a deterministic automata that represents the user source code. If a causality error is detected during that compilation, unless a precise isolation of the user source code fragments that are involved in that error, the error

message reported to the user is so imprecise that fixing the problem is difficult. We have implemented an algorithm based on *strongly connected components* that enables the needed isolation. This experimental feature is currently publicly available via a dedicating development branch under the *HipHop* github repository.

### 6.8.2. Interactive music composition

The production of a piece of music by school children using the Skini platform as part of SACEM's call for projects "Fabrique à musique" (Music Factory) was initiated in 2019. It ended in 2019 with the realization of a show at the Nice Conservatory in May 2019. The music piece thus created implemented all of Skini's functionalities, from the distributed sequencer that allowed the pupils to design the basic material, to the control of the live orchestration, not by the audience in this case, but by the 24 students who participated in the project. Following the success of this first experiment, the project is being extended for 2020/2021 by Inria, with another class, as part of the "les cordées de la réussite" program.

Beyond the improvement of the system, and in particular of the distributed sequencer, thanks to the significant performance improvements of HipHop.js, it has been possible to enrich the controls on musical orchestrations by driving transformation elements of Skini's basic elements (the patterns) such as transpositions, use of patterns of different durations, music mode conversions, or tempo control. The coupling of these new processes has enriched the range of possibilities for interaction and has opened up new horizons in the field of pattern-based generative music.

In terms of musical creation, we have been able to implement orchestrations using the platform's new technical possibilities in order to reduce musical processes perceived as too automatic. We can note as convincing results: the possibility to break the too big symmetries on the durations of the patterns, and the variations of tempi subjected to various controls. We were able to demonstrate that with the same HipHop.js music orchestration program, we could efficiently generate very different musical pieces.

Skini music composition has been described in a conference paper presented in the NIME 2019 conference [16].

### 6.8.3. Multiparty Reactive Sessions

Ensuring that communication-centric systems interact according to an intended protocol is a challenging problem, particularly for systems with some reactive or timed components. To rise to this challenge, we have studied the integration of Session-based Concurrency and Synchronous Reactive Programming (SRP).

*Synchronous Reactive Programming* (SRP) is a well-established programming paradigm whose essential features are logical instants, broadcast events and event-based preemption. This makes it an ideal vehicle for the specification and analysis of timed reactive systems. *Session-based Concurrency* is the model of concurrent computation induced by session types.

In the Research Report [20], we propose a multiparty session calculus enriched with features from SRP. In this calculus, protocol participants may broadcast messages, suspend themselves while waiting for a message, and react to events. Our main contribution is a session type system for this calculus, which enforces session correctness for non-interleaved sessions and additionally ensures *input timeliness*, a time-related property that entails livelock-freedom (while deadlock-freedom holds by construction in our calculus). Our type system departs significantly from existing ones, specifically as it captures the notion of "logical instant" typical of SRP.

## Kairos Project-Team

### 7. New Results

#### 7.1. Spatio-temporal constraints for mobile systems, with automotive driving assistance illustrations

**Participants:** Frédéric Mallet, Joëlle Abou Faysal, Robert de Simone, Xiaohong Chen.

The objective here is to extend constraint specifications to encompass spatial aspects in addition to logical multiform time. Spatio-temporal logics and requirement formalisms are thus an inspiration here. But mobility requests additionally that these spatio-temporal relations evolve in time. We are investigating in several directions:

- a target methodological approach is to consider these spatio-temporal relations to express safe driving rules as requirements or guarantees, meant to (in)validate trajectory proposals computed by a lower-level algorithmic system (itself operating on more direct neighborhood information). A realistic size case study is handled in collaboration with Renault Software Labs, as part of the CIFRE PhD contract of Joëlle Abou-Faysal, to define the precise needs in expressiveness and formal validation.
- Preliminary definitions of a spatio-temporal requirement specification languages, borrowing ideas from spatio-temporal logics and formal mobile process modeling (none of which being sufficient to our aim), is being progressed in collaboration with fellow researchers from ECNU Shanghai [20].

#### 7.2. System Engineering for Performance and Availability in satellite embedded COTS

**Participants:** Robert de Simone, Julien Deantoni, Amin Oueslati, Paul Bouche.

In the context of the IRT ATIPPIC project, which provided engineer position funding for Paul Bouche and Amin Oueslati, we investigated the application of a realistic formal design methodology applied on a real case study under construction by the ATIPPIC partners, in this case a prototype satellite based on general-purpose electronic Components-on-the-Shelf (COTS), not radiation-hardened. We focused on the one hand on the Model-Based Design of local interconnects, to provide analysis techniques regarding bandwidth and possible congestion of inter-process communications; on the other hand, we considered formal analysis of availability in case of fault (solar radiations), to study impact of alternative mitigation techniques for fault tolerance. Results were delivered in the form of Capella viewpoints and analysis tools to the IRT Saint-Exupéry, as free software. They were also published in [18], [23].

#### 7.3. Efficient solvers and provers for CCSL

**Participants:** Frédéric Mallet, Xiaohong Chen.

One of the goal of the team is to promote the use of logical time in various application domains. This requires to have efficient solvers for CCSL. We have made considerable progresses on this part along two lines. One by relying on SMT solvers (like Z3), the other by building a dynamic logic amenable to building semi-automatic proofs for logical time properties of reactive systems. Then for some classes of problems we can efficient solving tools.

- The first step is to have an efficient Z3 library for solving CCSL specifications. We have improved a lot the performances over last year by getting rid of some of the existential quantifiers in our properties [35].

- Second, we use this solver to help requirement engineers elicit the requirements. We use execution traces to help generate valid satisfied CCSL specifications [28].
- Third, we have built a dynamic logics based on CCSL, where the formulae are derived from CCSL relational operators and programs include some of CCSL expressions and some imperative reactive constructs akin to Esterel programs. Then we have an interactive proof system, that helps prove that some reactive program satisfies a set of formulas at all time. As we use only a subset of CCSL then, we can restrict to a decidable subset of the logics and the SMT solver is always efficient. The SMT helps guide the semi-automatic proof [34] by identifying the next proof rules that can be used (or not).

## 7.4. Formal temporal Smart Contracts

**Participants:** Frédéric Mallet, Marie-Agnès Peraldi Frati, Robert de Simone.

"Smart Contracts", as a way to define legal ledger evolution in Blockchain environments, can be seen as rule constraints to be satisfied by the set of their participants. Such contracts are often reflecting requirements or guarantees extracted from a legal or financial corpus of rules, while this can be carried to other technical fields of expertise. Our view is that Smart Contracts are often relying on logically timed events, thus welcoming the specification style of our formalisms (such as CCSL). The specialization of multiform logical time constraints to this domain is under study, in collaboration with local academic partners at UCA UMR LEAT and Gredeg, and industrial partners, such as Symag and Renault Software Labs. Local funding was obtained from UCA DS4H EUR Academy 1, which allowed preparation of the ANR project SIM that was accepted in 2019. One goal is to get acceptance from the lawyers while still preserving strong semantics for verification. This builds on our previous expertise [16].

## 7.5. CCSL extension to Stochastic logical time

**Participants:** Frédéric Mallet, Robert de Simone.

CCSL specifications allows distinct clocks with unfixed inter-relations. In settings such as cyber-physical modeling, probabilistic rates of relative occurrences may be provided as bounds. The objective is to provide construct to introduce such relations for the inclusion and precedence partial orders, but also to consider also constructs that associate them. Preliminary results have been obtained by Frédéric Mallet in collaboration with fellow researchers from ECNU Shanghai.

## 7.6. Semantic Resource Discovery in Internet

**Participant:** Luigi Liquori.

Results [30] are obtained in close collaboration with professors Matteo Sereno and Rossano Gaeta from the University of Turin. Internet in recent years has become a huge set of channels for content distribution highlighting limits and inefficiencies of the current protocol suite originally designed for host-to-host communication. We propose a Content Name System Service (CNS) that provides a new network aware Content Discovery Service. The CNS behavior and architecture uses the BGP inter-domain routing information. In particular, the service registers and discovers resource names in each Internet Autonomous System (AS): contents are discovered by searching through the augmented AS graph representation classifying ASes into customer, provider, and peering, as the BGP protocol does. An interesting extension of this Internet Service could be to scale up to Internet of Things and to Cyber Physical Systems inter-networked with networks different than Internet.

## 7.7. Raising Semantic Resource Discovery in IoT

**Participants:** Luigi Liquori, Marie-Agnès Peraldi Frati.



Within the standards for M2M and the Internet of Things, managed by ETSI, **oneM2M**, we are looking for suitable mechanisms and protocols to perform a Semantic Resource Discovery as described in the previous Subsection. More precisely, we are extending the (actually weak) Semantic Discovery mechanism of the IoT oneM2M standard. The goal is to enable an easy and efficient discovery of information and a proper inter-networking with external source/consumers of information (e.g. a data bases in a smart city or in a firm), or to directly search information in the oneM2M system for big data purposes. oneM2M ETSI standard has currently a rather weak native discovery capabilities that work properly only if the search is related to specific known sources of information (e.g. searching for the values of a known set of containers) or if the discovery is very well scoped and designed (e.g. the lights in a house). We submitted our vision in ETSI project submission “Semantic Discovery and Query in oneM2M” (currently under evaluation by ETSI) for extending oneM2M with a powerful Semantic Resource Discovery Service, taking into account additional constraints, such as topology, mobility (in space), intermittence (in time), scoping, routing ...

## 7.8. Empirical study of Amdahl’s law on multicore processors

**Participants:** Carsten Bruns, Sid Touati.

Since many years, we observe a shift from classical multiprocessor systems to multicores, which tightly integrate multiple CPU cores on a single die or package. This shift does not modify the fundamentals of parallel programming, but makes harder the understanding and the tuning of the performances of parallel applications. Multicores technology leads to sharing of microarchitectural resources between the individual cores, which Abel et al. classified in storage and bandwidth resources. In this research report [39], we empirically analyze the effects of such sharing on program performance, through repeatable experiments. We show that they can dominate scaling behavior, besides the effects described by Amdahl’s law and synchronization or communication considerations. In addition to the classification of Abel et al., we view the physical temperature and power budget also as a shared resource. It is a very important factor for performance nowadays, since DVFS over a wide range is needed to meet these constraints in multicores. Furthermore, we demonstrate that resource sharing not just leads a flat speedup curve with increasing thread count but can even cause slowdowns. Last, we propose a formal modeling of the performances to allow deeper analysis. Our work aims to gain a better understanding of performance limiting factors in high performance multicores, it shall serve as basis to avoid them and to find solutions to tune the parallel applications.

## 7.9. Communicating Networks of Data-Flow (sub)networks with limited memory

**Participant:** Robert de Simone.

Process Networks have been proposed a long time ago as models of concurrent, embedded streaming computations and communications, both amenable to formal analysis as models and executable as parallel program abstractions. As part of a larger effort at identifying precise connections between these models, programming models, and embedded parallel architectures altogether, we worked this year on the following problem: given a network of concurrent processes (Kahn-style) where each process is in turn a data-flow process network (SDF-style), can we decide in an efficient fashion (not NP-hard) whether a given assignment of communications to bounded local memories is schedulable (in a way that two simultaneous communications cannot require more than the available memory). A technical report is in preparation.

## 7.10. Behavioral Equivalence of Open Systems

**Participants:** Eric Madelaine, Cristian Grigoriu, Zechen Hou.

We consider Open (concurrent) Systems where the environment is represented as a number of processes which behavior is unspecified. Defining their behavioral semantics and equivalences from a Model-Based Design perspective naturally implies model transformations. To be proven correct, they require equivalence of “Open” terms, in which some individual component models may be omitted. Such models take into account various kind of data parameters, including, but not limited to, time. The middle term goal is to build a formal framework, but also an effective tool set, for the compositional analysis of such programs. In collaboration with ENS Lyon and Inria Lille, we studied an application of this approach to the verification of BIP architectures; this work extends previous dedicated approaches for compositional verification of BIP systems to data-dependent synchronizations [22]. Following last year results we have devised dedicated algorithms for checking equivalence of such systems [27], [41], currently under implementation in collaboration with ECNU Shanghai.

In order to facilitate the usage of our tools, we have also defined a language for defining open systems in terms of parameterized networks of synchronized automata (pNets, [4]), and implemented this language as an Eclipse-based editor in the VerCors tool (see Software section), together with interfaces to the semantic construction and equivalence checking algorithms.

## 7.11. Calculi with Union and Intersection types

**Participants:** Luigi Liquori, Claude Stolze.

Union and intersection types are interesting to improve actual programming languages static disciplines with alternative form of polymorphism. Since type inference is undecidable, our research vein focus on finding suitable “type decorations” in term syntax permitting to make type checking decidable, *i.e.*  $\lambda x.x : (\sigma \rightarrow \sigma) \cap (\tau \rightarrow \tau)$  becomes  $\langle \lambda x : \sigma.x, \lambda x : \tau.x \rangle : (\sigma \rightarrow \sigma) \cap (\tau \rightarrow \tau)$  in a fully-typed syntax. Those type systems uses intensively a subtyping relation stating *e.g.* that  $\sigma \cap \tau \leq \sigma$  or  $\sigma \leq \sigma \cup \tau$ . Deciding whether  $\sigma \leq \tau$  can be extremely difficult in complexity (space and time): actually, there are few algorithms in the literature dealing with union and intersection types. Recently [45] we have proved and certified in Coq a subtype algorithm of a type theory with union and intersection types; we have also extracted a running functional code. Subtyping constraints could be easily interpreted as temporal constraints in a suitable temporal algebra, like those that could be specified in CCSL. Advances of typed-calculi featuring those type disciplines are presented in [42], [31] and [14].

## 7.12. Bull, an Interactive Type Checker with Union and Intersection Types

**Participants:** Luigi Liquori, Claude Stolze.

Starting from our theoretical researches on Intersection and Union Types and related Subtype Theories, we have designed and implemented a prototype of an Interactive Typechecker based on the 2018 work on the  $\Delta$ -framework [43], on the 2017 work on decidable subtyping logic for Intersection and Union types [45], and on our recent advances on the  $\Delta$ -calculus [42] and [14]. The prototype is called *Bull*; Bull has a command-line interface where the user can declare axioms, terms, and perform computations. These terms can be incomplete, therefore the type checking algorithm uses unification to try to construct the missing subterms. A Read-Eval-Print-Loop allows to define axioms and definitions, and performs some basic terminal-style features like error pretty-printing, subexpressions highlighting, and file loading. Moreover, it can typecheck a proof and normalize it. We use the syntax of *Pure Type Systems* of Berardi to improve the compactness and the modularity of the kernel. Abstract and concrete syntax are mostly aligned: the concrete syntax is similar to the concrete syntax of the ITP Coq. We have also designed and implemented a *higher-order unification algorithm* *à la* Huet for terms, while typechecking and partial type inference are done by our *bidirectional refinement algorithm*. The refinement can be split into two parts: the essence refinement and the typing refinement. The bidirectional refinement algorithm aims to have partial type inference, and to give as much information as possible to the unifier. For instance, if we want to find a  $?y$  such that  $\vdash_{\Sigma} \langle \lambda x : \sigma.x, \lambda x : \tau.?y \rangle : (\sigma \rightarrow \sigma) \cap (\tau \rightarrow \tau)$ , we can infer that  $x : \tau \vdash ?y : \tau$  and that  $\lambda ?y \lambda =_{\beta} x$ . We are experimenting with classical examples in Bull, like the ones formalized by Pfenning with his Refinement Types in LF, and we are looking for examples taking into account preorders, constraints and operators (like

e.g.  $<, \leq, >, \geq, \cup, \cap, \dots$ ) that could be interpreted as timed algebras expressions *à la* CCSL. This would be a little step toward the formal and certified definition of a simple timed type systems for the  $\lambda$ -calculus and a Timed Logical Framework.

The software can be actually retrieved on the GitHub repository [Bull](#) (registration to the BIL Inria data base is in progress).

### 7.13. Co-Modeling for Better Co-Simulations

**Participants:** Julien Deantoni, Giovanni Liboni.

A Collaborative simulation consists in coordinating the execution of heterogeneous models executed by different tools. In most of the approaches from the state of the art, the coordination is unaware of the behavioral semantics of the different models under execution; *i.e.*, each model and the tool to execute it is seen as a black box. We highlighted that it introduces performance and accuracy problems [44].

In order to improve the performance and correctness of co-simulations, we proposed a language to defined model behavioral interfaces, *i.e.*, to expose some information about the model behavioral semantics. We also proposed another language to make explicit the way to coordinate the different models by using dedicated connectors. The goal is to provide few information about the models to avoid intellectual property violations, but enough to allow an expert to make relevant choices concerning their coordination. The resulting models can then be exploited to generate a dedicated coordination, aware of the specificity of each model [29]. Future work mainly consists in experimenting a new co-simulation interface taking advantage of the model behavioral interface and proposed as a generalization of co-simulation interfaces from the state of the art.

This work is realized in the context of the GLOSE project (see Section 1 ) in collaboration with Safran and other Inria teams (namely HyCOMES and DiVerSE).

### 7.14. CCSL for Models Behavioral Composition

**Participants:** Julien Deantoni, Frédéric Mallet, Hui Zhao.

The growing use of models for separating concerns in complex systems has lead to a proliferation of model composition operators. These composition operators have traditionally been defined from scratch following various approaches differing in formality, level of detail, chosen paradigm, and styles. Due to the lack of proper foundations for defining model composition (concepts, abstractions, or frameworks), it is difficult to compare or reuse composition operators. In [17], we proposed research directions towards a unifying framework that reduces all structural composition operators to structural merging, and all composition operators acting on discrete behaviors to event scheduling. Our belief is that CCSL, embedding both synchronous and asynchronous relations, is a good candidate to specify the event scheduling corresponding to the coordination of the different behaviors. However, as already stated in previous sections, to achieve such a status, some extensions to CCSL must be proposed. One of them was the possibility to prioritize events in the presence of synchronous relations. This was formally defined in [26] and implemented in the TimeSquare tool. Other interesting extensions are under study in the context of heterogeneous models, see Section 7.13 .

As part of Zhao Hui's PhD work, we have proposed a language to bring together subsets of existing predefined languages in a bid to combine their expressiveness. Rather than trying to build the ultimate unified language, sum of all languages, we would rather select meaningful features in existing languages and build a new language based on those features. As an example of application, we have shown how to combine the functional models of Capella with the security models of SysML-sec in an ad-hoc security-aware language for functional analysis [36].

### 7.15. Expressing IoT security constraints

**Participants:** Stéphanie Challita, Robert de Simone.

In the framework of Inria Project Lab SPAI, we are considering extensions of the logical time constraint style of CCSL, in order to encompass locality information as well as the duality between (dynamic) agents and (static) resources. Once an appropriate framework has been defined to express occupancy of resources by agents through (logical) time, notions of access rights, enclaves, privileges and priorities may be encoded straightforwardly, and rules governing their proper secure use can be expressed as properties. Results will be presented at the completion of Stephanie Challita postdoctoral period.

## 7.16. Real-Time Systems Compilation

**Participants:** Dumitru Potop Butucaru, Hugo Pompougnac, Jad Khatib.

This work took place in the framework of the PIA ES3CAP project (see section 9.2.5 ) and in close collaboration with Inria PARKAS, Airbus, Safran Aircraft Engines, Kalray, and the IRT Saint-Exupéry. It funded the last year of Keryan Didier PhD thesis (before the Paris Kairos subteam was created).

The key difficulty of real-time scheduling is that timing analysis and resource allocation depend on each other. An exhaustive search for the optimal solution not being possible for complexity reasons, heuristic approaches are used to break this dependency cycle. Two such approaches are typical in real-time systems design. The first one uses unsafe timing characterizations for the tasks (*e.g.* measurements) to build the system, and then checks the respect of real-time requirements through a global timing analysis. The second approach uses a formal model of the hardware platform enabling timing characterizations that are safe for all possible resource allocations (worst-case bounds). So far, the practicality of the second approach had never been established. Automated real-time parallelization flows still relied on simplified hypotheses ignoring much of the timing behavior of concurrent tasks, communication and synchronization code. And even with such unsafe hypotheses, few studies and tools considered the (harmonic) multi-periodic task graphs of real-world control applications, and the problem of statically managing all their computational, memory, synchronization and communication resources.

Our work has provided the first demonstration of the feasibility of the second approach, showing good practical results for classes of real-world applications and multiprocessor execution platforms whose timing predictability allows keeping pessimism under control. This requires something that is missing in previous work: the tight orchestration of all implementation phases: WCET analysis, resource allocation, generation of glue code ensuring the sequencing of tasks on cores and the synchronization and memory coherency between the cores, compilation and linking of the resulting C code. This orchestration is conducted on a very detailed timing model that considers both the tasks and the generated glue code, and which includes resource access interferences due to multi-core execution. Orchestration is not a mere combination of existing tools and algorithms. Enabling predictable execution and keeping pessimism under control requires the formal and algorithmic integration of all design phases, which in turn required the definition of an application normalization phase that facilitates timing analysis, of an original code generation algorithm designed to provide mapping-independent worst-case execution time bounds, and of new real-time scheduling algorithms capable of orchestrating memory allocation and scheduling.

Extensive results on the application of this method to real-file avionics case studies (>5000 unique nodes) mapped on the Kalray MPPA256 Bostan many-core have been presented in [15], [21] and in the PhD thesis of Keryan Didier, defended in September.

The Kalray MPPA platform provides excellent support for safety-critical real-time implementation, by allowing the computation of static WCET bounds. This is no longer true on more classical multi-cores such as those with ARM and POWER micro-architecture. We are currently aiming at extending our method to allow mapping on such multi-cores. Full schedulability guarantees cannot be provided on such platforms. Instead, our aim is to allow the synthesis of implementations that are functionally correct, efficient, and where unpredictability is reduced to a minimum by eliminating controllable sources of timing variability. This line of work has been pursued in the context of the collaboration contracts with Airbus and IRT Saint-Exupéry. First results are promising.

Further extensions of our method are under way, most notably to cover timing predictable architectures different from the Kalray MPPA 256.

## 7.17. Formal Modeling of Concurrent Implementations

**Participant:** Dumitru Potop Butucaru.

Concurrent programming is notoriously difficult, especially in constrained embedded contexts. Threads, in particular, are wildly non-deterministic as a model of computation, and difficult to analyze in the general case. Fortunately, it is often the case that multi-threaded, semaphore-synchronized embedded software implements high-level functional specifications written in a deterministic data-flow language such as Scade or (safe subsets of) Simulink. We claim that in this case the implementation process should build not just the multi-threaded C code, but (first and foremost) a richer model exposing the data-flow organization of the computations performed by the implementation. From this model, the C code is extracted through selective pretty-printing, while knowledge of the data-flow organization facilitates analysis.

This year, we have proposed a language for describing such implementation models that expose the data-flow behavior hiding under the form of a multi-threaded program. The language allows the representation of efficient implementations featuring pipelined scheduling and optimized memory allocation and synchronization. We showed applicability on a large-scale industrial avionics case study and on a commercial many-core [24].

## 7.18. Scalability of Constraint Programming for Real-Time Scheduling

**Participants:** Dumitru Potop Butucaru, Robert de Simone.

Given two abstract modeling descriptions, one of a dataflow process network for the application, one of a block diagram structure for the computing platform and its interconnects, together with cost functions for the elementary computations and communications, one is bound to seek optimal mappings pairing the two. Amongst all the possible techniques, an obvious one consists in using general constraint solvers (real, integer, or boolean constraint programming, SMT solvers, CP solvers, etc.). Given the NP-hard nature of the problem, the issue here is to experimentally determine the empirical complexity of various scheduling problems, and thus help in determining when solvers can be used for the resolution of scheduling problems.

In previous years we addressed this issue for ILP and SMT solvers. This year, we considered a Constraint Programming solver with dedicated support for modeling and solving real-time scheduling problems (IBM ILOG CPLEX CP Optimizer). The work was conducted in the framework of Bimael Iosif's student internship, and the writing of a paper is under way.

## LEMON Project-Team

# 6. New Results

## 6.1. Inland flow processes

### 6.1.1. Shallow water models with porosity

We propose in [10] a discussion on the publication 'Dam break in rectangular channels with different upstream-downstream widths' (Valiani and Caleffi, 2019). The authors consider an augmented shallow water system for modelling the dam-break problem in a channel with discontinuous width and present its analytical solutions depending on the upstream-downstream water depth and channel's width ratios. In this discussion we contest the conservation of the hydraulic head through the width's discontinuity, which is stated by the authors, and we exemplify it by performing 2D Shallow water simulations reproducing some test cases presented in the paper.

### 6.1.2. Forcing

A book chapter entitled *Space-time simulations of extreme rainfall : why and how ?* involving among others two members of the team, Vincent Guinot and Gwladys Toulemonde has been written and accepted for publication [6]. The book whose title is *Mathematical Modeling of Random and Deterministic Phenomena* will be published by Wiley. This chapter aims to present practical interest of doing space-time simulations of extreme rainfall and to propose a state-of-art about that.

## 6.2. Marine and coastal systems

### 6.2.1. Numerical Modelling of Hydrokinetic Turbines

Recent studies have pointed out the potential of several coastal or river areas to provide significant energy resources in the near future. However, technological processes for extracting energy using Marine Current Energy Converters (MCEC) are not generically "field-ready" and still require significant research to be set up. The book chapter [8] comes within this framework: we develop the numerical model OceaPoS, useful to carry out a comprehensive description of turbulent flow patterns past MCEC and forward optimize the turbine arrays configurations and evaluate their environmental effects. The OceaPos model consists in describing the fluid as an ensemble of Lagrangian particles ruled by a Stochastic process. OceaPos follows the same methodology than SDM-WindPoS model for wind farm simulations and adapts the Lagrangian stochastic downscaling method (SDM) to the tidal and oceanic boundary layer. We also introduce a Lagrangian version of actuator discs to take account of one or several MCEC's devices and their effects on the flow dynamics. Several benchmarks are presented, and numerical predictions are compared to experimental results.

### 6.2.2. Multi-scale ocean modeling

In [3], we derive discrete transparent boundary conditions for a class of linearized Boussinesq equations. These conditions happen to be non-local in time and we test numerically their accuracy with a Crank-Nicolson time-discretization on a staggered grid. We use the derived transparent boundary conditions as interface conditions in a domain decomposition method, where they become local in time. We analyze numerically their efficiency thanks to comparisons made with other interface conditions.



In **Cemracs 2019** in Marseille, Joao CALDAS was enrolled in the project "Model analysis for tsunami generation by landslides", with Louis EMERALD (PhD student, Université de Rennes), Emmanuel AUDUSSE (maître de conférences, Université Paris 13), Martin PARISOT (chargé de recherche, Inria Bordeaux, CARDAMOM team), Philippe HEINRICH (researcher, CEA) and Alexandre PARIS (PhD student, CEA). The project, funded by CEA, aims to study and compare different fluid mechanics models (Navier-Stokes, Boussinesq, Shallow Water equations) in the simulation of waves generated by landslides. The observed behaviour of the models is correlated to the amount of energy transferred from the sediments to the fluid, both in the wave generation zone (next to the landslide) and in the wave propagation zone (far away from it). An inverse problem is proposed for recovering the landslide from a given evolution of the free surface elevation. A publication will appear in the proceedings of CEMRACS 2019.

## 6.3. Stochastic models for extreme events

### 6.3.1. Hierarchical space-time modeling of exceedances

This novel approach is presented in this subsection but it is important to note that it also could have been presented in the subsection *Forcing* because the proposed method could be used as rainfall forcing and because it answers to some mentioned challenges.

The statistical modeling of space-time extremes in environmental applications is a valuable approach to understand complex dependencies in observed data and to generate realistic scenarios for impact models. Motivated by hourly rainfall data in Southern France presenting asymptotic independence, we propose in a joint work (J.N. Bacro, C. Gaetan, T. Opitz and G. Toulemonde) published in the Journal of the ASA [2] a novel hierarchical model for high threshold exceedances leading to asymptotic independence in space and time. Our approach is based on representing a generalized Pareto distribution as a Gamma mixture of an exponential distribution, enabling us to keep marginal distributions which are coherent with univariate extreme value theory. The key idea is to use a kernel convolution of a space-time Gamma random process based on influence zones defined as cylinders with an ellipsoidal basis to generate anisotropic spatio-temporal dependence in exceedances. Statistical inference is based on a composite likelihood for the observed censored excesses. The practical usefulness of our model is illustrated on the previously mentioned hourly precipitation data set from a region in Southern France. This work has also been presented by Gwladys Toulemonde in 2019 in two invited talks (EVA, Zagreb 2019; CMStatistics, ERCIM, London 2019), in one contributed international conference (ISI, Kuala Lumpur, 2019) and one seminar organized by the "Ecole Polytechnique" (Paris, 2019).

### 6.3.2. Extension of the XGumbel copula to the spatial framework

An extension of the XGumbel copula to the spatial framework has been developed. This work has been presented in the international conference Extreme Value Analysis (EVA 2019, Zagreb) and is currently under review [9]. The XGumbel copula combines two Gumbel copulas with weight parameters, termed extra-parameters, taking values in the unit hyper-cube. In a multisite study, the copula dimension being the number of sites, the XGumbel copula quickly becomes over-parametrized. In addition, interpolation to ungauged locations is not easily achieved. We propose a spatial model for maxima that combines a spatial regression for GEV marginals built with a vector generalized linear model and the spatialized XGumbel copula defined thanks to a spatial mapping for the extra-parameters. The mapping is designed shaped as a disk according to bivariate properties of the XGumbel copula. An Approximate Bayesian Computation (ABC) scheme that seeks to reproduce upper tail dependence coefficients for distance classes is used to infer the parameters. The extension of the XGumbel copula to the spatial framework has been used to study annual maxima of daily precipitation totals at 177 gauged stations over a 57 year period in the French Mediterranean.

## MATHNEURO Project-Team

# 5. New Results

## 5.1. Neural Networks as dynamical systems

### 5.1.1. Metastable Resting State Brain Dynamics

**Participants:** Peter Beim Graben [Brandenburg University of Technology Cottbus, Germany], Antonio Jimenez-Marin [Computational Neuroimaging Lab, BioCruces-Bizkaia Health Research Institute, Spain], Ibai Diez [Harvard Medical School, Massachusetts General Hospital, Boston, MA, USA], Jesus M Cortes [Computational Neuroimaging Lab, BioCruces-Bizkaia Health Research Institute, Spain], Mathieu Desroches, Serafim Rodrigues [Ikerbasque & MCEN team, Basque Center for Applied Mathematics, Spain].

Metastability refers to the fact that the state of a dynamical system spends a large amount of time in a restricted region of its available phase space before a transition takes place, bringing the system into another state from where it might recur into the previous one. Beim Graben and Hutt (2013) [74] suggested to use the recurrence plot (RP) technique introduced by Eckmann et al. (1987) [57] for the segmentation of system's trajectories into metastable states using recurrence grammars. Here, we apply this recurrence structure analysis (RSA) for the first time to resting-state brain dynamics obtained from functional magnetic resonance imaging (fMRI). Brain regions are defined according to the brain hierarchical atlas (BHA) developed by Diez et al. (2015) [56], and as a consequence, regions present high-connectivity in both structure (obtained from diffusion tensor imaging) and function (from the blood-level dependent-oxygenation–BOLD–signal). Remarkably, regions observed by Diez et al. were completely time-invariant. Here, in order to compare this static picture with the metastable systems dynamics obtained from the RSA segmentation, we determine the number of metastable states as a measure of complexity for all subjects and for region numbers varying from 3 to 100. We find RSA convergence toward an optimal segmentation of 40 metastable states for normalized BOLD signals, averaged over BHA modules. Next, we build a bistable dynamics at population level by pooling 30 subjects after Hausdorff clustering. In link with this finding, we reflect on the different modeling frameworks that can allow for such scenarios: heteroclinic dynamics, dynamics with riddled basins of attraction, multiple timescale dynamics. Finally, we characterize the metastable states both functionally and structurally, using templates for resting state networks (RSNs) and the automated anatomical labeling (AAL) atlas, respectively.

This work has been published in *Frontiers in Computational Neuroscience* and is available as [20].

### 5.1.2. Controlling seizure propagation in large-scale brain networks

**Participants:** Simona Olmi, Spase Petkoski [Institut de Neurosciences des Systèmes, Marseille], Maxime Guye [CEMEREM, Hôpital de la Timone, Marseille], Fabrice Bartolomei [Hôpital de la Timone, Marseille], Viktor Jirsa [Institut de Neurosciences des Systèmes, Marseille].

Information transmission in the human brain is a fundamentally dynamic network process. In partial epilepsy, this process is perturbed and highly synchronous seizures originate in a local network, the so-called epileptogenic zone (EZ), before recruiting other close or distant brain regions. We studied patient-specific brain network models of 15 drug-resistant epilepsy patients with implanted stereotactic electroencephalography (SEEG) electrodes. Each personalized brain model was derived from structural data of magnetic resonance imaging (MRI) and diffusion tensor weighted imaging (DTI), comprising 88 nodes equipped with region specific neural mass models capable of demonstrating a range of epileptiform discharges. Each patients virtual brain was further personalized through the integration of the clinically hypothesized EZ. Subsequent simulations and connectivity modulations were performed and uncovered a finite repertoire of seizure propagation patterns. Across patients, we found that (i) patient-specific network connectivity is predictive for the subsequent seizure propagation pattern; (ii) seizure propagation is characterized by a systematic sequence of brain states; (iii) propagation can be controlled by an optimal intervention on the connectivity matrix; (iv) the degree of invasiveness can be significantly reduced via the here proposed seizure control as compared to traditional

resective surgery. To stop seizures, neurosurgeons typically resect the EZ completely. We showed that stability analysis of the network dynamics using graph theoretical metrics estimates reliably the spatiotemporal properties of seizure propagation. This suggests novel less invasive paradigms of surgical interventions to treat and manage partial epilepsy.

This work has been published in [PLoS Computational Biology](#) and is available as [29].

### 5.1.3. *Chimera states in pulse coupled neural networks: the influence of dilution and noise*

**Participants:** Simona Olmi, Alessandro Torcini [Institute of Complex Systems, Florence, Italy].

We analyse the possible dynamical states emerging for two symmetrically pulse coupled populations of leaky integrate-and-fire neurons. In particular, we observe broken symmetry states in this set-up: namely, breathing chimeras, where one population is fully synchronized and the other is in a state of partial synchronization (PS) as well as generalized chimera states, where both populations are in PS, but with different levels of synchronization. Symmetric macroscopic states are also present, ranging from quasi-periodic motions, to collective chaos, from splay states to population anti-phase partial synchronization. We then investigate the influence disorder, random link removal or noise, on the dynamics of collective solutions in this model. As a result, we observe that broken symmetry chimera-like states, with both populations partially synchronized, persist up to 80 % of broken links and up to noise amplitudes 8 % of threshold-reset distance. Furthermore, the introduction of disorder on symmetric chaotic state has a constructive effect, namely to induce the emergence of chimera-like states at intermediate dilution or noise level.

This work has been published as a chapter in the book [Nonlinear Dynamics in Computational Neuroscience](#) (Springer, 2019) and is available as [35].

### 5.1.4. *Enhancing power grid synchronization and stability through time delayed feedback control*

**Participants:** Halgurd Taher, Simona Olmi, Eckehard Schöll [Technical University Berlin, Germany].

We study the synchronization and stability of power grids within the Kuramoto phase oscillator model with inertia with a bimodal frequency distribution representing the generators and the loads. We identify critical nodes through solitary frequency deviations and Lyapunov vectors corresponding to unstable Lyapunov exponents. To cure dangerous deviations from synchronization we propose time-delayed feedback control, which is an efficient control concept in nonlinear dynamic systems. Different control strategies are tested and compared with respect to the minimum number of controlled nodes required to achieve synchronization and Lyapunov stability. As a proof of principle, this fast-acting control method is demonstrated using a model of the German power transmission grid.

This work has been published in [Physical Review E](#) and is available as [32].

### 5.1.5. *Stability and control of power grids with diluted network topology*

**Participants:** Liudmila Tumash [gipsa-lab, CNRS, Grenoble], Simona Olmi, Eckehard Schöll [Technical University Berlin, Germany].

In the present study we consider a random network of Kuramoto oscillators with inertia in order to mimic and investigate the dynamics emerging in high-voltage power grids. The corresponding natural frequencies are assumed to be bimodally Gaussian distributed, thus modeling the distribution of both power generators and consumers: for the stable operation of power systems these two quantities must be in balance. Since synchronization has to be ensured for a perfectly working power grid, we investigate the stability of the desired synchronized state. We solve this problem numerically for a population of  $N$  rotators regardless of the level of quenched disorder present in the topology. We obtain stable and unstable solutions for different initial phase conditions, and we propose how to control unstable solutions, for sufficiently large coupling strength, such that they are stabilized for any initial phase. Finally, we examine a random Erdős-Renyi network under the impact of white Gaussian noise, which is an essential ingredient for power grids in view of increasing renewable energy sources.

This work has been published in [Chaos: An Interdisciplinary Journal of Nonlinear Science](#) and is available as [33].

### 5.1.6. Modeling dopaminergic modulation of clustered gamma rhythms

**Participants:** Denis Zakharov [Center for Cognition and Decision Making, HSE, Moscow, Russia], Martin Krupa [UCA, LJAD, Inria MathNeuro], Boris Gutkin [Laboratoire de Neurosciences Cognitives, ENS, Paris].

Gamma rhythm (20-100Hz) plays a key role in numerous cognitive tasks: working memory, sensory processing and in routing of information across neural circuits. In comparison with lower frequency oscillations in the brain, gamma-rhythm associated firing of the individual neurons is sparse and the activity is locally distributed in the cortex. Such “weak” gamma rhythm results from synchronous firing of pyramidal neurons in an interplay with the local inhibitory interneurons in a “pyramidal-interneuron gamma” or PING. Experimental evidence shows that individual pyramidal neurons during such oscillations tend to fire at rates below gamma, with the population showing clear gamma oscillations and synchrony. One possible way to describe such features is that this gamma oscillation is generated within local synchronous neuronal clusters. The number of such synchronous clusters defines the overall coherence of the rhythm and its spatial structure. The number of clusters in turn depends on the properties of the synaptic coupling and the intrinsic properties of the constituent neurons. We previously showed that a slow spike frequency adaptation current in the pyramidal neurons can effectively control cluster numbers. These slow adaptation currents are modulated by endogenous brain neuro-modulators such as dopamine, whose level is in turn related to cognitive task requirements. Hence we postulate that dopaminergic modulation can effectively control the clustering of weak gamma and its coherence. In this paper we study how dopaminergic modulation of the network and cell properties impacts the cluster formation process in a PING network model.

This work has been accepted for publication in [Communications in Nonlinear Science and Numerical Simulation](#) and is available as [34].

## 5.2. Mean field theory and stochastic processes

### 5.2.1. Mean-field limit of interacting 2D nonlinear stochastic spiking neurons

**Participants:** Benjamin Aymard, Fabien Campillo, Romain Veltz.

In this work, we propose a nonlinear stochastic model of a network of stochastic spiking neurons. We heuristically derive the mean-field limit of this system. We then design a Monte Carlo method for the simulation of the microscopic system, and a finite volume method (based on an upwind implicit scheme) for the mean-field model. The finite volume method respects numerical versions of the two main properties of the mean-field model, conservation and positivity, leading to existence and uniqueness of a numerical solution. As the size of the network tends to infinity, we numerically observe propagation of chaos and convergence from an individual description to a mean-field description. Numerical evidences for the existence of a Hopf bifurcation (synonym of synchronised activity) for a sufficiently high value of connectivity, are provided.

This work has been submitted for publication and is available as [38].

### 5.2.2. Stochastic modeling for biotechnologies Anaerobic model AM2b

**Participants:** Fabien Campillo, Mohsen Chebbi [ENIT, University of Tunis, Tunisia], Salwa Toumi [INSAT, University of Carthage, Tunisia].

The model AM2b is conventionally represented by a system of differential equations. However, this model is valid only in a large population context and our objective is to establish several stochastic models at different scales. At a microscopic scale, we propose a pure jump stochastic model that can be simulated exactly. But in most situations this exact simulation is not feasible, and we propose approximate simulation methods of Poisson type and of diffusive type. The diffusive type simulation method can be seen as a discretization of a stochastic differential equation. Finally, we formally present a result of law of large numbers and of functional central limit theorem which demonstrates the convergence of these stochastic models towards the initial deterministic models.

This work has been published in [ARIMA](#) and is available as [22].

### 5.2.3. *Cross frequency coupling in next generation inhibitory neural mass models*

**Participants:** Andrea Ceni [University of Exeter, UK], Simona Olmi, Alessandro Torcini [Institute of Complex Systems, Florence, Italy], David Angulo-Garcia [Polytechnic University of Cartagena, Colombia].

Coupling among neural rhythms is one of the most important mechanisms at the basis of cognitive processes in the brain. In this study we consider a neural mass model, rigorously obtained from the microscopic dynamics of an inhibitory spiking network with exponential synapses, able to autonomously generate collective oscillations (COs). These oscillations emerge via a super-critical Hopf bifurcation, and their frequencies are controlled by the synaptic time scale, the synaptic coupling and the excitability of the neural population. Furthermore, we show that two inhibitory populations in a master-slave configuration with different synaptic time scales can display various collective dynamical regimes: namely, damped oscillations towards a stable focus, periodic and quasi-periodic oscillations, and chaos. Finally, when bidirectionally coupled the two inhibitory populations can exhibit different types of theta-gamma cross-frequency couplings (CFCs): namely, phase-phase and phase-amplitude CFC. The coupling between theta and gamma COs is enhanced in presence of a external theta forcing, reminiscent of the type of modulation induced in Hippocampal and Cortex circuits via optogenetic drive.

This work has been submitted for publication and is available as [40].

### 5.2.4. *Conductance-Based Refractory Density Approach for a Population of Bursting Neurons*

**Participants:** Anton Chizhov [IOFFE Institute, St Petersburg, Russia], Fabien Campillo, Mathieu Desroches, Antoni Guillamon [Polytechnic University of Catalonia, Barcelona, Spain], Serafim Rodrigues [Ikerbasque & MCEN team, Basque Center for Applied Mathematics, Spain].

The conductance-based refractory density (CBRD) approach is a parsimonious mathematical-computational framework for modelling interacting populations of regular spiking neurons, which, however, has not been yet extended for a population of bursting neurons. The canonical CBRD method allows to describe the firing activity of a statistical ensemble of uncoupled Hodgkin-Huxley-like neurons (differentiated by noise) and has demonstrated its validity against experimental data. The present manuscript generalises the CBRD for a population of bursting neurons; however, in this pilot computational study, we consider the simplest setting in which each individual neuron is governed by a piecewise linear bursting dynamics. The resulting population model makes use of slow-fast analysis, which leads to a novel methodology that combines CBRD with the theory of multiple timescale dynamics. The main prospect is that it opens novel avenues for mathematical explorations, as well as, the derivation of more sophisticated population activity from Hodgkin-Huxley-like bursting neurons, which will allow to capture the activity of synchronised bursting activity in hyper-excitable brain states (e.g. onset of epilepsy).

This work has been published in [Bulletin of Mathematical Biology](#) and is available as [23].

### 5.2.5. *Long time behavior of a mean-field model of interacting neurons*

**Participants:** Quentin Cormier [Inria Tosca], Étienne Tanré [Inria Tosca], Romain Veltz.

We study the long time behavior of the solution to some McKean-Vlasov stochastic differential equation (SDE) driven by a Poisson process. In neuroscience, this SDE models the asymptotic dynamics of the membrane potential of a spiking neuron in a large network. We prove that for a small enough interaction parameter, any solution converges to the unique (in this case) invariant measure. To this aim, we first obtain global bounds on the jump rate and derive a Volterra type integral equation satisfied by this rate. We then replace temporary the interaction part of the equation by a deterministic external quantity (we call it the external current). For constant current, we obtain the convergence to the invariant measure. Using a perturbation method, we extend this result to more general external currents. Finally, we prove the result for the non-linear McKean-Vlasov equation.

This work has been published in [Stochastic Processes and their Applications](#) and is available as [24].



### 5.2.6. *Effective low-dimensional dynamics of a mean-field coupled network of slow-fast spiking lasers*

**Participants:** Axel Dolcemascolo [INPHYNI, Nice], Alexandre Miazek [INPHYNI, Nice], Romain Veltz, Francesco Marino [National Institute of Optics, Italy], Stéphane Barland [INPHYNI, Nice].

Low dimensional dynamics of large networks is the focus of many theoretical works, but controlled laboratory experiments are comparatively very few. Here, we discuss experimental observations on a mean-field coupled network of hundreds of semiconductor lasers, which collectively display effectively low-dimensional mixed mode oscillations and chaotic spiking typical of slow-fast systems. We demonstrate that such a reduced dimensionality originates from the slow-fast nature of the system and of the existence of a critical manifold of the network where most of the dynamics takes place. Experimental measurement of the bifurcation parameter for different network sizes corroborate the theory.

This work has been submitted for publication and is available as [42].

### 5.2.7. *The mean-field limit of a network of Hopfield neurons with correlated synaptic weights*

**Participants:** Olivier Faugeras, James Maclaurin [NJIT, USA], Étienne Tanré [Inria Tosca].

We study the asymptotic behaviour for asymmetric neuronal dynamics in a network of Hopfield neurons. The randomness in the network is modelled by random couplings which are centered Gaussian correlated random variables. We prove that the annealed law of the empirical measure satisfies a large deviation principle without any condition on time. We prove that the good rate function of this large deviation principle achieves its minimum value at a unique Gaussian measure which is not Markovian. This implies almost sure convergence of the empirical measure under the quenched law. We prove that the limit equations are expressed as an infinite countable set of linear non Markovian SDEs.

This work has been submitted for publication and is available as [43].

### 5.2.8. *Asymptotic behaviour of a network of neurons with random linear interactions*

**Participants:** Olivier Faugeras, Émilie Soret, Étienne Tanré [Inria Tosca].

We study the asymptotic behaviour for asymmetric neuronal dynamics in a network of linear Hopfield neurons. The randomness in the network is modelled by random couplings which are centered i.i.d. random variables with finite moments of all orders. We prove that if the initial condition of the network is a set of i.i.d random variables with finite moments of all orders and independent of the synaptic weights, each component of the limit system is described as the sum of the corresponding coordinate of the initial condition with a centered Gaussian process whose covariance function can be described in terms of a modified Bessel function. This process is not Markovian. The convergence is in law almost surely w.r.t. the random weights. Our method is essentially based on the CLT and the method of moments.

This work has been submitted for publication and is available as [44].

### 5.2.9. *On a toy network of neurons interacting through their dendrites*

**Participants:** Nicolas Fournier [LPSM, Sorbonne Université], Étienne Tanré [Inria Tosca], Romain Veltz.

Consider a large number  $n$  of neurons, each being connected to approximately  $N$  other ones, chosen at random. When a neuron spikes, which occurs randomly at some rate depending on its electric potential, its potential is set to a minimum value  $v_{min}$ , and this initiates, after a small delay, two fronts on the (linear) dendrites of all the neurons to which it is connected. Fronts move at constant speed. When two fronts (on the dendrite of the same neuron) collide, they annihilate. When a front hits the soma of a neuron, its potential is increased by a small value  $w_n$ . Between jumps, the potentials of the neurons are assumed to drift in  $[v_{min}, \infty)$ , according to some well-posed ODE. We prove the existence and uniqueness of a heuristically derived mean-field limit of the system when  $n, N \rightarrow \infty$  with  $w_n \simeq N^{-1/2}$ . We make use of some recent versions of the results of Deuschel and Zeitouni [55] concerning the size of the longest increasing subsequence of an i.i.d. collection of points in the plan. We also study, in a very particular case, a slightly different model where the neurons spike when their potential reach some maximum value  $v_{max}$ , and find an explicit formula for the (heuristic) mean-field limit.



This work has been accepted for publication in *Annales de l'Institut Henri Poincaré (B) Probabilités et Statistiques* and is available as [27].

### 5.2.10. Bumps and oscillons in networks of spiking neurons

**Participants:** Helmut Schmidt [Max Planck Institute for Human Cognitive and Brain Science, Germany], Daniele Avitabile [VU Amsterdam, Inria MathNeuro].

We study localized patterns in an exact mean-field description of a spatially-extended network of quadratic integrate-and-fire (QIF) neurons. We investigate conditions for the existence and stability of localized solutions, so-called bumps, and give an analytic estimate for the parameter range where these solutions exist in parameter space, when one or more microscopic network parameters are varied. We develop Galerkin methods for the model equations, which enable numerical bifurcation analysis of stationary and time-periodic spatially-extended solutions. We study the emergence of patterns composed of multiple bumps, which are arranged in a snake-and-ladder bifurcation structure if a homogeneous or heterogeneous synaptic kernel is suitably chosen. Furthermore, we examine time-periodic, spatially-localized solutions (oscillons) in the presence of external forcing, and in autonomous, recurrently coupled excitatory and inhibitory networks. In both cases we observe period doubling cascades leading to chaotic oscillations.

This work has been submitted for publication and is available as [46].

### 5.2.11. Slow-fast dynamics in the mean-field limit of neural networks

**Participants:** Daniele Avitabile [VU Amsterdam, Inria MathNeuro], Emre Baspinar, Mathieu Desroches, Olivier Faugeras.

In the context of the Human Brain Project (HBP, see section 5.1.1.1. below), we have recruited Emre Baspinar in December 2018 for a two-year postdoc. Within MathNeuro, Emre is working on analysing slow-fast dynamical behaviours in the mean-field limit of neural networks.

In a first project, he has been analysing the slow-fast structure in the mean-field limit of a network of FitzHugh-Nagumo neuron models; the mean-field was previously established in [3] but its slow-fast aspect had not been analysed. In particular, he has proved a persistence result of Fenichel type for slow manifolds in this mean-field limit, thus extending previous work by Berglund *et al.* [47], [48]. A manuscript is in preparation.

In a second project, he has been looking at a network of Wilson-Cowan systems whose mean-field limit is an ODE, and he has studied elliptic bursting dynamics in both the network and the limit: its slow-fast dissection, its singular limits and the role of canards. In passing, he has obtained a new characterisation of elliptic bursting via the construction of periodic limit sets using both the slow and the fast singular limits and unravelled a new singular-limit scenario giving rise to elliptic bursting via a new type of torus canard orbits. A manuscript is in preparation.

## 5.3. Neural fields theory

### 5.3.1. Next-generation neural field model: The evolution of synchrony within patterns and waves

**Participants:** Áine Byrne [Center for Neural Science, New York University, USA], Daniele Avitabile [VU Amsterdam, Inria MathNeuro], Stephen Coombes [University of Nottingham, UK].

Neural field models are commonly used to describe wave propagation and bump attractors at a tissue level in the brain. Although motivated by biology, these models are phenomenological in nature. They are built on the assumption that the neural tissue operates in a near synchronous regime, and hence, cannot account for changes in the underlying synchrony of patterns. It is customary to use spiking neural network models when examining within population synchronization. Unfortunately, these high-dimensional models are notoriously hard to obtain insight from. In this paper, we consider a network of  $\theta$ -neurons, which has recently been shown to admit an exact mean-field description in the absence of a spatial component. We show that the inclusion of space and a realistic synapse model leads to a reduced model that has many of the features of a standard neural field model coupled to a further dynamical equation that describes the evolution of network synchrony. Both Turing instability analysis and numerical continuation software are used to explore the existence and stability of spatiotemporal patterns in the system. In particular, we show that this new model can support states above and beyond those seen in a standard neural field model. These states are typified by structures within bumps and waves showing the dynamic evolution of population synchrony.

This work has been published in [Physical Review E](#) and is available as [21].

### 5.3.2. *The hyperbolic model for edge and texture detection in the primary visual cortex*

**Participant:** Pascal Chossat [CNRS, Inria MathNeuro].

The modelling of neural fields in the visual cortex involves geometrical structures which describe in mathematical formalism the functional architecture of this cortical area. The case of contour detection and orientation tuning has been extensively studied and has become a paradigm for the mathematical analysis of image processing by the brain. Ten years ago an attempt was made to extend these models by replacing orientation (an angle) with a second-order tensor built from the gradient of the image intensity and named the structure tensor. This assumption does not follow from biological observations (experimental evidence is still lacking) but from the idea that the effectiveness of texture processing with the structure tensor in computer vision may well be exploited by the brain itself. The drawback is that in this case the geometry is not Euclidean but hyperbolic instead, which complicates substantially the analysis. The purpose of this review is to present the methodology that was developed in a series of papers to investigate this quite unusual problem, specifically from the point of view of tuning and pattern formation. These methods, which rely on bifurcation theory with symmetry in the hyperbolic context, might be of interest for the modelling of other features such as color vision, or other brain functions.

This work has been accepted for publication in [Journal of Mathematical Neuroscience](#) and is available as [41].

### 5.3.3. *A neural field model for color perception unifying assimilation and contrast*

**Participants:** Anna Song [ENS Paris, France], Olivier Faugeras, Romain Veltz.

We address the question of color-space interactions in the brain, by proposing a neural field model of color perception with spatial context for the visual area V1 of the cortex. Our framework reconciles two opposing perceptual phenomena, known as simultaneous contrast and chromatic assimilation. They have been previously shown to act synergistically, so that at some point in an image, the color seems perceptually more similar to that of adjacent neighbors, while being more dissimilar from that of remote ones. Thus, their combined effects are enhanced in the presence of a spatial pattern, and can be measured as larger shifts in color matching experiments. Our model supposes a hypercolumnar structure coding for colors in V1, and relies on the notion of color opponency introduced by Hering. The connectivity kernel of the neural field exploits the balance between attraction and repulsion in color and physical spaces, so as to reproduce the sign reversal in the influence of neighboring points. The color sensation at a point, defined from a steady state of the neural activities, is then extracted as a nonlinear percept conveyed by an assembly of neurons. It connects the cortical and perceptual levels, because we describe the search for a color match in asymmetric matching experiments as a mathematical projection on color sensations. We validate our color neural field alongside this color matching framework, by performing a multi-parameter regression to data produced by psychophysicists and ourselves. All the results show that we are able to explain the nonlinear behavior of shifts observed along one or two dimensions in color space, which cannot be done using a simple linear model.

This work has been published in [PLoS Computational Biology](#) and is available as [31].

## 5.4. Slow-fast dynamics in Neuroscience

### 5.4.1. Local theory for spatio-temporal canards and delayed bifurcations

**Participants:** Daniele Avitabile [VU Amsterdam, Inria MathNeuro], Mathieu Desroches, Romain Veltz, Martin Wechselberger [University of Sydney, Australia].

We present a rigorous framework for the local analysis of canards and slow passages through bifurcations in a wide class of infinite-dimensional dynamical systems with time-scale separation. The framework is applicable to models where an infinite-dimensional dynamical system for the fast variables is coupled to a finite-dimensional dynamical system for slow variables. We prove the existence of centre-manifolds for generic models of this type, and study the reduced, finite-dimensional dynamics near bifurcations of (possibly) patterned steady states in the layer problem. Theoretical results are complemented with detailed examples and numerical simulations covering systems of local- and nonlocal-reaction diffusion equations, neural field models, and delay-differential equations. We provide analytical foundations for numerical observations recently reported in literature, such as spatio-temporal canards and slow-passages through Hopf bifurcations in spatially-extended systems subject to slow parameter variations. We also provide a theoretical analysis of slow passage through a Turing bifurcation in local and nonlocal models.

This work has been submitted for publication and is available as [37].

### 5.4.2. Pseudo-plateau bursting and mixed-mode oscillations in a model of developing inner hair cells

**Participants:** Harun Baldemir, Daniele Avitabile [VU Amsterdam, Inria MathNeuro], Krasimira Tsaneva-Atanasova [University of Exeter, UK].

Inner hair cells (IHCs) are excitable sensory cells in the inner ear that encode acoustic information. Before the onset of hearing IHCs fire calcium-based action potentials that trigger transmitter release onto developing spiral ganglion neurones. There is accumulating experimental evidence that these spontaneous firing patterns are associated with maturation of the IHC synapses and hence involved in the development of hearing. The dynamics organising the IHCs' electrical activity are therefore of interest.

Building on our previous modelling work we propose a three-dimensional, reduced IHC model and carry out non-dimensionalisation. We show that there is a significant range of parameter values for which the dynamics of the reduced (three-dimensional) model map well onto the dynamics observed in the original biophysical (four-dimensional) IHC model. By estimating the typical time scales of the variables in the reduced IHC model we demonstrate that this model could be characterised by two fast and one slow or one fast and two slow variables depending on biophysically relevant parameters that control the dynamics. Specifically, we investigate how changes in the conductance of the voltage-gated calcium channels as well as the parameter corresponding to the fraction of free cytosolic calcium concentration in the model affect the oscillatory model behaviour leading to transition from pseudo-plateau bursting to mixed-mode oscillations. Hence, using fast-slow analysis we are able to further our understanding of this model and reveal a path in the parameter space connecting pseudo-plateau bursting and mixed-mode oscillations by varying a single parameter in the model.

This work has been accepted for publication in [Communications in Nonlinear Science and Numerical Simulation](#) and is available as [18].

### 5.4.3. Parabolic bursting, spike-adding, dips and slices in a minimal model

**Participants:** Mathieu Desroches, Jean-Pierre Françoise [LJLL, Sorbonne Université, Paris], Martin Krupa [LJAD, UCA, Inria MathNeuro].

A minimal system for parabolic bursting, whose associated slow flow is integrable, is presented and studied both from the viewpoint of bifurcation theory of slow-fast systems, of the qualitative analysis of its phase portrait and of numerical simulations. We focus the analysis on the spike-adding phenomenon. After a reduction to a periodically forced one-dimensional system, we uncover the link with the dips and slices first discussed by J.E. Littlewood in his famous articles on the periodically forced van der Pol system.

This work has been published in [Mathematical Modelling of Natural Phenomena](#) and is available as [26].

#### 5.4.4. *Anticipation via canards in excitable systems*

**Participants:** Elif Köksal Ersöz [INSERM, Rennes, Inria MathNeuro], Mathieu Desroches, Claudio Mirasso [University of the Balearic Islands, Spain], Serafim Rodrigues [Ikerbasque & Basque Center for Applied Mathematics, Spain].

Neurons can anticipate incoming signals by exploiting a physiological mechanism that is not well understood. This article offers a novel explanation on how a receiver neuron can predict the sender's dynamics in a unidirectionally-coupled configuration, in which both sender and receiver follow the evolution of a multi-scale excitable system. We present a novel theoretical viewpoint based on a mathematical object, called *canard*, to explain anticipation in excitable systems. We provide a numerical approach, which allows to determine the transient effects of canards. To demonstrate the general validity of canard-mediated anticipation in the context of excitable systems, we illustrate our framework in two examples, a multi-scale radio-wave circuit (the van der Pol model) that inspired a caricature neuronal model (the FitzHugh-Nagumo model) and a biophysical neuronal model (a 2-dimensional reduction of the Hodgkin-Huxley model), where canards act as messengers to the senders' prediction. We also propose an experimental paradigm that would enable experimental neuroscientists to validate our predictions. We conclude with an outlook to possible fascinating research avenues to further unfold the mechanisms underpinning anticipation. We envisage that our approach can be employed by a wider class of excitable systems with appropriate theoretical extensions.

This work has been published in [Chaos: An Interdisciplinary Journal of Nonlinear Science](#) and is available as [28].

#### 5.4.5. *Canard-induced complex oscillations in an excitatory network*

**Participants:** Elif Köksal Ersöz, Mathieu Desroches, Antoni Guillamon [Polytechnic University of Catalunya, Spain], John Rinzel [Center for Neural Science and Courant Institute of Mathematical Sciences, New York University, USA], Joel Tabak [University of Exeter, UK].

In this work we have revisited a rate model that accounts for the spontaneous activity in the developing spinal cord of the chicken embryo [69]. The dynamics is that of a classical square-wave burster, with alternation of silent and active phases. Tabak et al. [69] have proposed two different three-dimensional (3D) models with variables representing average population activity, fast activity-dependent synaptic depression and slow activity-dependent depression of two forms. In [66], [67], [68] various 3D combinations of these four variables have been studied further to reproduce rough experimental observations of spontaneous rhythmic activity. In this work, we have first shown the spike-adding mechanism via canards in one of these 3D models from [69] where the fourth variable was treated as a control parameter. Then we discussed how a canard-mediated slow passage in the 4D model explains the sub-threshold oscillatory behavior which cannot be reproduced by any of the 3D models, giving rise to mixed-mode bursting oscillations (MMBOs); see [10]. Finally, we related the canard-mediated slow passage to the intervals of burst and silent phase which have been linked to the blockade of glutamatergic or GABAergic/glycinergic synapses over a wide range of developmental stages [68].

This work has been submitted for publication and is available as [12].

### 5.5. Mathematical modeling of neuronal excitability

#### 5.5.1. *Modeling cortical spreading depression induced by the hyperactivity of interneurons*

**Participants:** Mathieu Desroches, Olivier Faugeras, Martin Krupa [LJAD, UCA, Inria MathNeuro], Massimo Mantegazza [Institut de Pharmacologie Moléculaire et Cellulaire (IPMC), Sophia Antipolis].

Cortical spreading depression (CSD) is a wave of transient intense neuronal firing leading to a long lasting depolarizing block of neuronal activity. It is a proposed pathological mechanism of migraine with aura. Some forms of migraine are associated with a genetic mutation of the  $\text{Na}_{v1.1}$  channel, resulting in its gain of function and implying hyperexcitability of interneurons. This leads to the counterintuitive hypothesis that intense firing of interneurons can cause CSD ignition. To test this hypothesis *in silico*, we developed a computational model of an E-I pair (a pyramidal cell and an interneuron), in which the coupling between the cells is not just synaptic, but takes into account also the effects of the accumulation of extracellular potassium caused by the activity of the neurons and of the synapses. In the context of this model, we show that the intense firing of the interneuron can lead to CSD. We have investigated the effect of various biophysical parameters on the transition to CSD, including the levels of glutamate or GABA, frequency of the interneuron firing and the efficacy of the  $\text{KCC}_2$  co-transporter. The key element for CSD ignition in our model was the frequency of interneuron firing and the related accumulation of extracellular potassium, which induced a depolarizing block of the pyramidal cell. This constitutes a new mechanism of CSD ignition.

This work has been published in [Journal of Computational Neuroscience](#) and is available as [25].

The extension of this work is the topic of the PhD of Louisiane Lemaire, who started in October 2018. A first part of Louisiane's PhD has been to improve and extend the model published in [25] in a number of ways: replace the GABAergic neuron model used in [25], namely the Wang-Buszáki model, by a more recent fast-spiking cortical interneuron model due to Golomb and collaborators; implement the effect of the HM1a toxin used by M. Mantegazza to mimic the genetic mutation of sodium channels responsible for the hyperactivity of the GABAergic neurons; take into account ionic concentration dynamics (relaxing the hypothesis of constant reversal potentials) for the GABAergic as well whereas in [25] this was done only for the Pyramidal neuron. This required a great deal of modelling and calibration and the simulation results are closer to the actual experiments by Mantegazza than in our previous study. A manuscript is in preparation.

## 5.6. Modelling the visual system

### 5.6.1. Uniqueness of viscosity mean curvature flow solution in two sub-Riemannian structures

**Participants:** Emre Baspinar, Giovanna Citti [University of Bologna, Italy].

We provide a uniqueness result for a class of viscosity solutions to sub-Riemannian mean curvature flows. In a sub-Riemannian setting, uniqueness cannot be deduced by the comparison principle, which is known only for graphs and for radially symmetry surfaces. Here we use a definition of continuous viscosity solutions of sub-Riemannian mean curvature flows motivated from a regularized Riemannian approximation of the flow. With this definition, we prove that any continuous viscosity solution of the equation is a limit of a sequence of solutions of Riemannian flow and obtain as a consequence uniqueness and the comparison principle. The results are provided in the settings of both 3-dimensional rototranslation group  $SE(2)$  and Carnot groups of step 2, which are particularly important due to their relation to the surface completion problem of a model of the visual cortex.

This work has been published in [SIAM Journal on Mathematical Analysis](#) and is available as [19].

### 5.6.2. A sub-Riemannian model of the visual cortex with frequency and phase

**Participants:** Emre Baspinar, Alessandro Sarti [CAMS, EHESS, Paris, France], Giovanna Citti [University of Bologna, Italy].

In this paper we present a novel model of the primary visual cortex (V1) based on orientation, frequency and phase selective behavior of the V1 simple cells. We start from the first level mechanisms of visual perception: receptive profiles. The model interprets V1 as a fiber bundle over the 2-dimensional retinal plane by introducing orientation, frequency and phase as intrinsic variables. Each receptive profile on the fiber is mathematically interpreted as a rotated, frequency modulated and phase shifted Gabor function. We start from the Gabor function and show that it induces in a natural way the model geometry and the associated horizontal connectivity modeling the neural connectivity patterns in V1. We provide an image enhancement algorithm employing the model framework. The algorithm is capable of exploiting not only orientation but

also frequency and phase information existing intrinsically in a 2-dimensional input image. We provide the experimental results corresponding to the enhancement algorithm.

This work has been submitted for publication and is available as [\[39\]](#).



## MCTAO Project-Team

## 7. New Results

### 7.1. Analysis of singularities in minimum time control problems

**Participants:** Jean-Baptiste Caillaud, Jacques Féjóz [Université Paris-Dauphine & Observatoire de Paris], Michaël Orioux [SISSA], Robert Roussarie [Université de Bourgogne-Franche Comté].

An important class of problems is affine control problems with control on the disk (or the Euclidean ball, in higher dimensions). Such problems show up for instance in space mechanics and have been quite extensively studied from the mathematical (geometric) and numerical point of view. Still, even for the simplest cost, namely time minimization, the analysis of singularities occurring was more or less open. Building on previous results of the team and on recent studies of Agrachev and his collaborators, we give a detailed account of the behaviour of minimum time extremals crossing the so-called singular locus (typically a switching surface). The result is twofold. First, we show that there the set of initial conditions of the Hamiltonian flow can be stratified, and that the flow is smooth on each stratum, one of them being the codimension stratum leading to the singular locus. This generalizes in higher codimension the known case of switching conditions of codimension one encountered, for instance, in  $L^1$ -minimization (consumption minimization, in aerospace applications). We give a clear geometric interpretation of this first result in terms of normally hyperbolic invariant manifold. Secondly, we provide a model for the singularity on the flow when strata are crossed, proving that it is of logarithmic type. This paves the way for *ad hoc* numerical methods to treat this kind of extremal flow. The crucial tool for the analysis is a combination of blow-up and normal form techniques for dynamical systems.

### 7.2. The Sard Conjecture in sub-Riemannian Geometry

**Participants:** Ludovic Rifford, André Belotto Da Silva [Univ. Aix-Marseille], Adam Parusinski [Univ. Côte d'Azur].

In a work in progress, we address the Sard conjecture for sub-Riemannian structures on analytic manifolds and related problems. We present a description of singular horizontal curves of a totally nonholonomic analytic distribution in term of the projections of the orbits of some integrable and isotropic subanalytic distribution in the cotangent bundle. In the generic smooth case, we obtain an extension of an important result by Chitour, Jean and Trélat by showing that singular curves are the projection of a Hamiltonian singular vector field. As a by-product of our first result, we obtain a proof of the so-called minimal rank Sard conjecture in some analytic cases. It establishes that from a given point the set of points accessible through singular horizontal curves of minimal rank, which corresponds to the rank of the distribution, has Lebesgue measure zero under additional technical assumptions.

### 7.3. Local controllability of magnetic micro-swimmers and more general classes of control systems

**Participants:** Laetitia Giraldi, Pierre Lissy [Univ. Paris Dauphine], Clément Moreau, Jean-Baptiste Pomet.

As a part of Clément Moreau's PhD, we gave fine results on local controllability of magnetized micro swimmers actuated by an external magnetic field. We had shown that the "two-link" magnetic swimmer had some local controllability around its straight configuration but that it was not Small Time Locally Controllable" (STLC) in the classical sense that asks that points close to the initial condition can be reached using "small" controls.

We derived in [30] some necessary conditions for STLC of affine control systems with two scalar controls, around an equilibrium where not only the drift vector field vanishes but one of the two control vector fields vanishes too; we state various necessary conditions (involving the value at the equilibrium of some iterated Lie brackets of the system vector fields), where the "smallness" of the controls is intended in the  $L^\infty$  (classical) or  $W^{1,\infty}$  (less classical, used in recent work by K. Beauchard and F. Marbach).

We also arrived to local controllability results in higher dimension than the “two-link” micro-robots, see [9]. This relies on the following remark: classical STLC does not hold, but STLC is concerned with small controls, hence with variations around the zero control... but, due to one of the control fields vanishing, the system also rests at the equilibrium for (infinitely many) nonzero constant values of the control. It is proved that there is one nonzero value of the control such that STLC holds when considered *around this constant control* and not around the zero control. In other terms, classical STLC holds after a constant feedback transformation.

#### 7.4. Time-optimal deorbiting maneuvers of solar sails

**Participants:** Jean-Baptiste Caillau, Lamberto Dell’Elce, Jean-Baptiste Pomet.

Increasing interest in optimal low-thrust orbital transfers was triggered in the last decade by technological progress in electric propulsion and by the ambition of efficiently leveraging on orbital perturbations to enhance the maneuverability of small satellites. This work was aimed at investigating time optimal propellantless deorbiting maneuvers in low-Earth orbit using solar sails. The solution of this problem was achieved by doubly averaging the optimal control Hamiltonian with respect to both satellite and Sun longitudes. Initial conditions for the osculating trajectory were inferred via a near-identity transformation that approximates the quasi-periodic oscillations of both state and adjoint variables [61]. The outcomes of the study were presented at the 4th KePASSA meeting in Logrono [18].

#### 7.5. Long-term evolution of quasi-satellite orbits

**Participants:** Lamberto Dell’Elce, Nicola Baresi [Univ. of Surrey, UK], Josué Cardoso Dos Santos [Sao Paulo State Univ., Brazil], Yasuhiro Kawakatsu [JAXA, Japan].

The Martian Moons eXploration mission is currently under development at the Japan space agency (JAXA) and will be the first spacecraft mission to retrieve pristine samples from the surface of Phobos. In preparation for the sampling operations, MMX will collect observations of Phobos from stable retrograde relative trajectories, which are referred to as quasi-satellite orbits (QSOs). This study, started in 2018 in collaboration with JAXA, investigates the navigability of mid- and high-altitude QSOs in terms of relative orbit element. Our developments are based on the Yamanaka-Ankersen solution of the Tschauner-Hempel equations and capture the effects of the secondary’s gravity and orbital eccentricity on the shape and orientation of near-equatorial retrograde relative orbits. The analytic solution that we obtained by averaging the equations of motion with respect to the longitude of the satellite is suitable to gain insight into the long-term evolution of QSOs. These results were recently published in [38].

#### 7.6. Non-singular analytical solution of perturbed satellite motion using Milankovitch elements

**Participants:** Lamberto Dell’Elce, Pini Gurfil [Technion, Israel], Gianpaolo Izzo [Technion, Israel], Aaron J. Rosengren [Univ. of Arizona, US].

In the brief span of time after the launch of Sputnik, a whole succession of analyses was devoted to the problem poised by the drag-free motion of an artificial satellite about an oblate planet, employing almost every known perturbation method. Although in a sense, the problem is a classic one that also occurred among the natural satellites, it was necessary in the applications of artificial satellite motion to obtain a more general, detailed, and accurate solution. In this study, we developed a new formulation of the mean-to-osculating conversion for first-order oblateness perturbations based on the Milankovitch elements [74] that corrects the critical-inclination deficiency. We use the direct method of Kozai [67], and present an explicit analytical short-period correction in vector form that is valid for all orbits with nonzero angular momentum. Preliminary results were presented at the International Symposium of Space Flight Mechanics (ISSFM) [19].

#### 7.7. Sub-Riemannian Geometry and Micro-Swimmers and Extensions to Control in Hydrodynamics

**Participants:** Bernard Bonnard, Piernicola Bettiol [Univ. Bretagne Ouest], Alice Nolot [Univ. de Bourgogne Franche Comté], Jérémy Rouot.

We pursue our study concerning the 1-copepod swimmer using techniques from SR-geometry and numerical simulations, see [40] for previously obtained results. Following Takagi model, a 2d-swimmer is currently analyzed whose aim is to perform a 2d-motion where the copepod swimmer can change its orientation. Preliminary study concerning this problem was analysed during the internship of A. Lenc in relation with the motion planning of a car. Under the impulse of O. Cots and B. Wempe an extension of the project is the developments of the geometric optimal control techniques in hydrodynamics. In particular we studied a Zermelo navigation problem in a current with a vortex [25] (submitted to ESAIM-COCV). An interesting and new phenomenon detected in optimal control is the existence for the geodesic flow of a Reeb foliation.

## 7.8. Swimming at low Reynolds number an optimal control problem

**Participants:** François Alouges [École Polytechnique], Luca Berti, Antonio Desimone [SISSA Trieste], Yacine El Alaoui-Faris, Laetitia Giraldi, Yizhar Or [Technion, Israel], Christophe Prud'Homme [Univ. de Strasbourg], Jean-Baptiste Pomet, Stéphane Régnier [Sorbonne Université], Oren Wiezel [Technion, Israel].

This part is devoted to study the displacement of micro-swimmers. We attack this problem using numerical tools and optimal control theory. Micro-scale swimmers move in the realm of negligible inertia, dominated by viscous drag forces, the fluid is governed by the Stokes equation. We study two types of models. First, deriving from the PDE system, in [5] we use Feel++, a finite elements library in order to simulate the motion of a one-hinged swimmer, which obeys to the scallop theorem. Then, we address the flagellar microswimmers. In [31] we formulate the leading order dynamics of a  $2D$  slender multi-link microswimmer assuming small-amplitude undulations about its straight configuration. The energy optimal stroke to achieve a given prescribed displacement in a given time period is obtained as the largest eigenvalue solution of a constrained optimal control problem. We prove that the optimal stroke is an ellipse lying within a two-dimensional plane in the  $(N - 1)$  dimensional space of shape variables, where  $N$  can be arbitrarily large. If the number of shape variables is small, we can consider the same problem when the prescribed displacement in one time period is large, and not attainable with small variations of the joint angles. The fully non-linear optimal control problem is solved numerically for the cases  $N = 3$  and  $N = 5$  showing that, as the prescribed displacement becomes small, the optimal solutions obtained using the small-amplitude assumption are recovered. We also show that, when the prescribed displacements become large, the picture is different. Finally, in [28] we present an automated procedure for the design of optimal actuation for flagellar magnetic microswimmers based on numerical optimization. Using this method, a new magnetic actuation method is provided which allows these devices to swim significantly faster compared to the usual sinusoidal actuation. This leads to a novel swimming strategy which shows that a faster propulsion is obtained when the swimmer is allowed to go out-of-plane. This approach is experimentally validated on a scaled-up flexible swimmer.

## 7.9. Periodic body deformations are optimal for locomotion

**Participants:** Laetitia Giraldi, Frédéric Jean.

A periodic cycle of body's deformation is a common strategy for locomotion (see for instance birds, fishes, humans). The aim of this work (see [29]) is to establish that the auto-propulsion of deformable object is optimally achieved using periodic strategies of body's deformations. This property is proved for a simple model using optimal control theory framework.

## 7.10. Optimal Control of Chemical Networks by Temperature Control

**Participants:** Bernard Bonnard, Jérémy Rouot.

The objective of the project is to develop previous results obtained at the end of the 90's by B. Bonnard and his collaborators to control the production of batch reactors by temperature control in relation with the Shell Company. These results were derived to analyze the simple (but relevant for applications) irreversible reaction scheme  $A \rightarrow B \rightarrow C$ . More complicated weakly reversible scheme like the McKeithan network are currently under investigation taking into account the bridge phenomenon detected in [7], where complicated optimal policies with two singular arcs can occur. Preliminary results are presented in [3] where also the geometric techniques are described. See also the article in the 58th IEEE-CDC Nice conference [11].

### 7.11. Muscular Isometric Force Contraction by Electric Stimulation

**Participants:** Bernard Bonnard, Jérémy Rouot, Toufik Bakir [Univ. de Bourgogne Franche Comté].

This project started two years ago under the impulse of T. Bakir (ImVia-UBFC) who defended his HDR on the subject (November, 2018). The problem is the one of optimizing the train pulses of the FES signal to produce the muscular contraction. It is based on the Hill model refined by Ding et al to take into account the variations of the fatigue variable. Preliminary closed loop results were obtained using an MPC-method where the state variable is estimated with a non linear observer [2]. The problem can be stated in the optimal sampled-control data framework; with the collaboration of L. Bourdin (Maths Dept Limoges), Pontryagin-type necessary conditions were derived and partially numerically implemented [1]. The project is supported by a PEPS 1 AMIES and a PGM0 Project. A CIFRE Thesis is planned to start in January, 2020 (Phd Student: Quentin Arnaud) in the Company **SEGULA**, supervised by T. Bakir and co-Supervised by B. Bonnard. See section 8.1 .

### 7.12. Selection of microalgae

**Participants:** Walid Djema, Laetitia Giraldi, Olivier Bernard [BIOCORE project-team].

We investigate a minimal-time control problem in a chemostat continuous photo-bioreactor model that describes the dynamics of two distinct microalgae populations. Our objective is to optimize the time of separation between two species of microalgae by controlling the dilution rate. We focus on Droop's model. Using Pontryagin's principle, we develop a dilution-based control strategy that steers the model trajectories to a suitable target in minimal time. Our study reveals that the optimal solution has a turpike property [14] [27]. A numerical optimal-synthesis, based on direct optimal control tools, is performed in [15] and it shows that the optimal solution is of type bang-singular.

### 7.13. Extensions of the Zermelo-Markov-Dubins problem in optimal control

**Participants:** Ahmed Dieng, Jean-Baptiste Caillaud, Jean-Baptiste Pomet, Sofya Maslovskaya.

Motivated by a collaboration with **CGG** in 2018, we continued investigating minimum time problems for simplified kinematic models of a marine vessel towing some equipments, with various curvature constraints. These are extensions (by adding the towed equipment) of the so-called Zermelo-Markov-Dubins problem. In [12], we describe the problem with the simplest possible model of the trailer, and show that the Hamiltonian system resulting from Pontryagin Principle for minimum time is integrable in that case, both for the "regular" flow and for the flow giving singular extremals; without giving an explicit analytic solution, this drastically simplifies the computation of optimal solutions; a description of the marine application solution is also given.

Ahmed Dieng's internship was the opportunity to test more complex models numerically and to have a qualitative approach of the results from [12].

Note that the collaboration with CGG (we had a short bilateral contract with this company in 2018) did not continue mainly because they stopped this activity and more generally marine acquisition. This recent **press release** details the transactions.

### 7.14. Stability of nonlinear high frequency amplifiers and stability of linear time-varying time-delay systems

**Participants:** Laurent Baratchart [FACTAS project-team], Sébastien Fueyo, Jean-Baptiste Pomet, Gilles Lebeau.

These amplifiers contain on the one hand nonlinear active components and on the other hand lines, that induce some sort of delays and make the system infinite-dimensional: they are, for each choice of a periodic input, a nonlinear infinite dimensional dynamical system. The Computer Aided Design tools mentioned in Section 4.4 provide a periodic solution under this periodic forcing and may also give the frequency response of the linearized system along this trajectory with some artificial "small" excitation. The goal is to deduce stability from these data.

It is an opportunity to build theoretical basis and justification to a stability analysis through harmonic identification; the latter is one of the specialties of FACTAS, we collaborate on the infinite-dimensional non-linear stability analysis for periodic solutions and how it works with the results of harmonic identification. This is the topic of Sébastien Fueyo's PhD.

On academic examples of simple circuits, we have given full justification (with some possible obstructions) to the prediction of stability through transfer function identification. The theoretical interest is that the spectrum of the operator that gives stability is not as elementary as predicted in the literature, but stability can be predicted nonetheless. Publication in progress on this point, a preliminary version was presented in [17].

It was also the opportunity to re-visit stability of time-delay time-varying linear system. A new sufficient condition can be found in [22], and a more general result is the purpose of a publication to come. These results are important to the domain of linear time-delay systems because the time-varying case has seldom been touched.

## MORPHEME Project-Team

### 6. New Results

#### 6.1. Exact biconvex reformulation of the $\ell_2 - \ell_0$ minimization problem

**Participants:** Gilles Aubert, Arne Henrik Bechensteen, Laure Blanc-Féraud.

We focus on the problem of minimizing the least-squares loss function under the constraint that the reconstructed signal is at maximum  $k$ -sparse. This is called the  $\ell_2 - \ell_0$  constrained problem. The  $\ell_0$  pseudo-norm counts the number of non-zero elements in a vector. The minimization problem is of interest in signal processing, with a wide range of applications as compressed sensing, source separation, and super-resolution imaging, for example.

Based on the results of [31], we reformulate the  $\ell_0$  pseudo-norm exactly as a convex minimization problem by introducing an auxiliary variable. We then propose an exact biconvex reformulation of the  $\ell_2 - \ell_0$  constrained and penalized problems. We give correspondence results between minimizer of the initial function and the reformulated ones. The reformulation is biconvex. This property is used to derive two minimization algorithm, CoBic (Constrained Biconvex) and PeBic (Penalized Biconvex).

We apply the algorithms to the problem of Single-Molecule Localization Microscopy and compare the results with the well-known IHT algorithm [22]. Both visually and numerically the biconvex reformulations perform better. Furthermore, the algorithm has been compared to the IRL1-CEL0 [23] and Deep-STORM [25]. The IRL1-CEL0 minimizes an exact relaxation [29] of the  $\ell_2 - \ell_0$  penalized form and Deep-STORM is an algorithm that uses deep-learning and convolutional network to localize the molecules. This work has been presented at the ISBI 2019 conference [6], as well as a more mathematical article was presented as a poster at GRETSI 2019 [12]. A full journal article has been submitted to the Biomedical Optics Express for a feature issue: Superresolution Microscopy on the 25th Anniversary of STED Microscopy and the 20th Anniversary of SIM.

#### 6.2. Biological Image Super-resolution Enhanced with Tensor

**Participants:** Jose Henrique de Morais Goulart, Laure Blanc-Féraud, Eric Debreuve, Sébastien Schaub.

*This work is part of the BISET project, funded by the académie I RISE (Réseaux, Information et Société numérique) of Idex UCA JEDI.*

Fluorescence microscopy imaging has numerous applications in biological sciences, but has limited resolution due to light diffraction. Recently proposed super-resolution techniques acquire an image time series at a high frame rate and exploit independent random fluorophore blinking for reconstruction. This approach holds great potential for observing live-cell sub-cellular phenomena, which is a challenging scenario with strict constraints over the deployed excitation levels and the acquisition time.

The BISET project aimed to develop tensor-based super-resolution fluorescence microscopy algorithms based on this approach. Assuming a known separable PSF  $h(x, y) = g(x)g(y)$ , a third-order tensor model with two spatial diversities and one temporal diversity was proposed. The model unknowns are high-dimensional fluorophore spatial profiles along  $x$  and  $y$  directions and temporal fluorophore profiles modeling blinking. Our formulation employs a least-squares loss term and penalty functions promoting spatial profile sparsity (necessary for fluorophore locality) and temporal profile group sparsity (which controls the number of fluorophores).



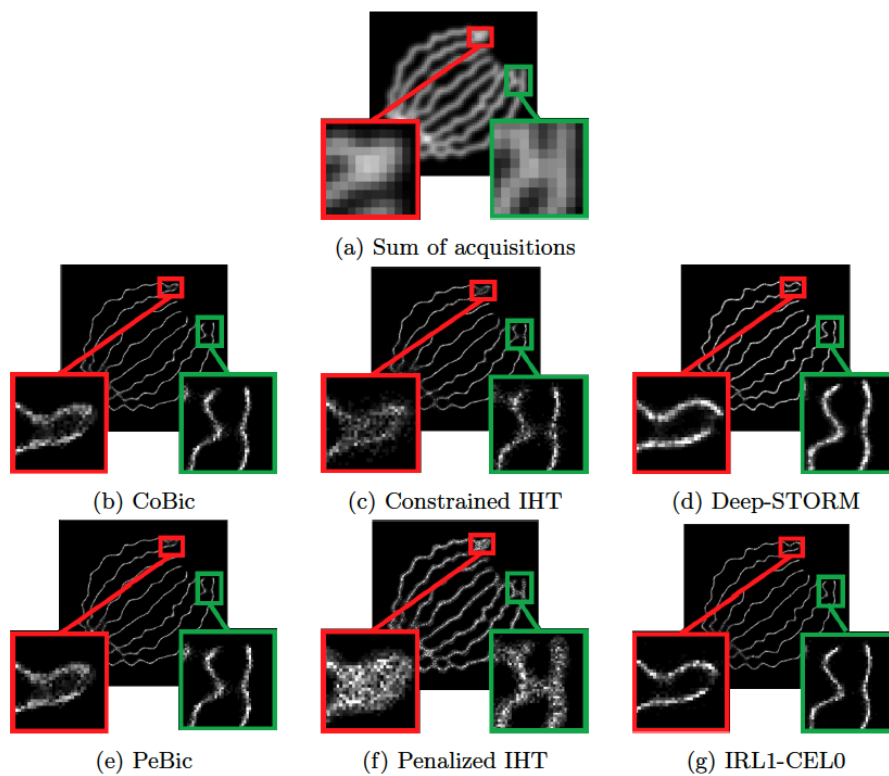


Figure 1. Reconstructed images from the simulated ISBI dataset [28], 99 non-zero pixels on average. Top: Sum of the acquisitions. Middle: From left to right: CoBic, Constrained IHT and Deep-STORM. Bottom: From left to right: PeBic, Penalized IHT and IRL1-CELO.

The formulation is nonconvex but block-convex in the unknown profiles and thus can be solved by alternating minimization. It has a significantly smaller number of unknowns in comparison with a matrix-based convex one (with frames as columns), in consonance with the current trend of employing nonconvex formulations rather than overparameterized convex ones which are often too costly. However, its resolution is numerically challenging for high-density acquisitions. Indeed, even though the proposed algorithm is able to reveal the overall target structure in our simulations, it produces a “dotted” reconstruction. For comparison, we developed a matrix-based formulation with nonconvex group-sparsity regularization, which is more costly to solve but achieves better results. These findings were published in the IEEE CAMSAP 2019 conference [11], and were also presented on October 2019 in a GdR ISIS (Information, Signal, Image et Vision)/MIA (Mathématiques de l’Imagerie et de ses Applications)/ONDES meeting<sup>0</sup> held in Paris and entitled “Co-conception: hybrid sensors and algorithms for innovative systems”. An illustration of the results produced by the developed tensor and matrix methods is given in Figure 2, along with outcomes of other state-of-art methods. In conclusion, though our tensor approach is innovative and was shown to be promising, further research is needed to overcome the model estimation difficulties.

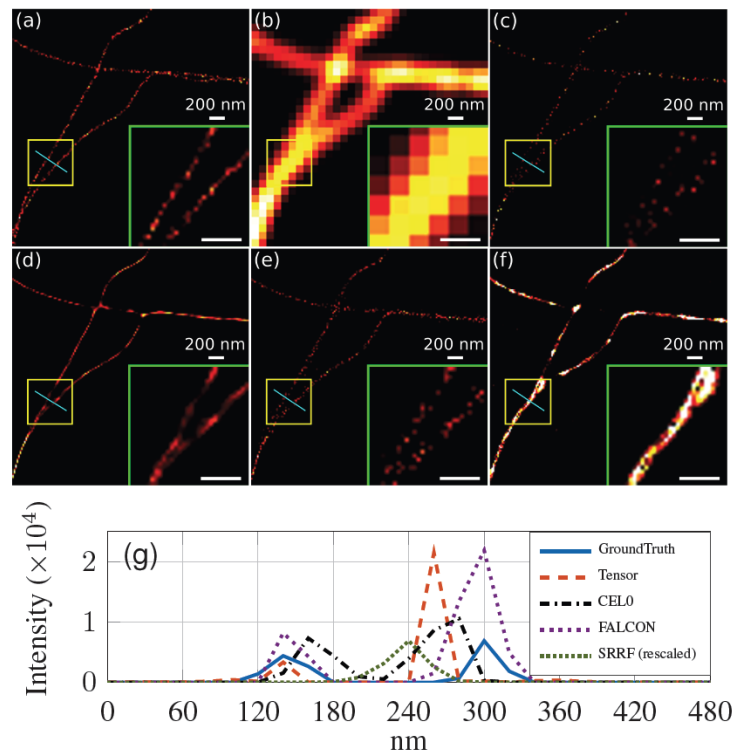


Figure 2. Results for reconstruction of simulated microtubules: (a) integrated ground truth; (b) integrated observed stack ( $5\times$  zoom); (c) proposed tensor approach; (d) proposed matrix approach; (e) FALCON; (f) SRRF; (g) intensity profiles along the shown blue line. The frame in the bottom right corner shows a  $2.66\times$  zoom of the smaller yellow frame.

### 6.3. Classification and Modeling of the Fibronectin Networks in Extracellular Matrices

<sup>0</sup>Meeting webpage: <http://www.gdr-isis.fr/index.php?page=reunion&idreunion=401>.

**Participants:** Anca-Ioana Grapa, Laure Blanc-Féraud, Xavier Descombes.

*This work is done in collaboration with Ellen Van Obberghen-Schilling and Georgios Efthymiou (iBV).*

We are interested in the numerical analysis and modeling of the Fibronectin (FN) networks, a major extracellular matrix (ECM) molecule, expressed in pathological states (fibrosis, cancer, etc). Our goal is to develop numerical quantitative biomarkers that describe the geometrical organization of the different four variants of the FN fiber networks, from 2D confocal microscopy images. Since the functions of these variants are not well defined in the context of their role within the tumour microenvironment, we hope that a computational model might be able to provide a meaningful description that incorporates the structural differences among the variants.

In a previous work, we have derived a pipeline to classify a given tissue among the four FN variants (cell-derived matrices), based on a decomposition into discrete fast curvelet transform coefficients. We ensured the invariance to rotation of the coefficients and then fed them to a DAG-SVM multiclassifier, in order to prove their discriminative ability in the context of classification of the four FN variants. The results were published in [24] and show that the curvelet coefficients are capable of discerning among the four FN variants with similar performances to those of a human annotator.

The second step of our work consisted in setting up the modeling of the FN networks starting from a graph-based representation, built on top of Gabor features (fiber scale, orientation, etc). The graph parameters corresponding to the geometrical and topological features of the improved skeletonizations (i.e. median pore circularity, ratio of fiber thinness, fiber thickness kurtosis, fiber connectivity) of the four FN variants, are then classified by a DAG-SVM. It is thus shown through the analysis of the feature distribution over the four variants, features PCA analysis and SVM-based classification, that graph features can discriminate among the FN variants almost as well as our first work. This proves that the graph representation embeds the most relevant information provided by the image.

The next step focused on the development of a metric between graphs that takes into account their topology and geometry. This distance is bound to provide a quantitative but also a qualitative comparison of the four FN variants as well as a differentiation between normal and tumour-like FN fibers. In order to evaluate the distance among graphs, we have referred to graph-matching techniques, which are considered standard problems that deal with graph comparison. The main idea is to obtain an evaluation of the similarity between two graphs, by finding the optimal correspondence between their nodes, such as to align their structure, i.e their adjacency matrices. We expect to obtain invariance with respect to translation, rotation and scale.

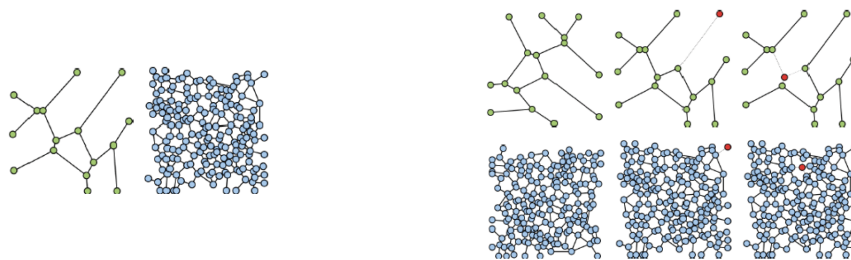


*Figure 3. Generated toy-graphs with different dimensions: 16, 181 nodes (left side). Right side illustrates the database of toy-graphs derived from the initial ones, but having small modifications in terms of node order (first column) and different number of nodes (second and third column). The purpose is to match the nodes of every pair of graph (initial-modified) using the graph-matching and optimal assignment framework and compare the performances of the two methods.*

More specifically, we are interested in one of the various techniques to perform many-to-many graph matching [32], where the merging of multiple nodes to match another one is allowed, especially in the case of graphs with different dimensions (i.e. different number of total vertices). Alternatively, we considered a different line of work, based on optimal transport for the comparison of structured objects (e.g. graphs) with associated probability distributions. We focus on the work of Peyré et al. [26] that have considered a metric called Gromov-Wasserstein, capable of comparing objects that lie in spaces with different dimensions, by minimizing the cost of mass transport from one discrete distribution to the other. In the context of graph matching techniques, this can be regarded as a probabilistic assignment problem.

In [13], we have compared the two aforementioned approaches from a graph-matching perspective, on randomly generated graphs (Figure 3), in the context of a preliminary study for the future modeling of FN graph-based representations. We have tested different graph scenarios, with various information captured by the adjacency matrix (binary adjacency matrix, shortest path between nodes). Moreover, we have slightly modified the second method by optimal transport, to make it feasible for direct one-to-one matching, by adding dummy masses. We have concluded that the graph matching by many-to-many assignment, captures a meaningful distance between two given graphs with good performances, while the Gromov-Wasserstein discrepancy is computed faster but with lower performances.

One advantage of using graph-matching techniques for comparing fiber networks, comes from the possibility of defining a median graph that will be representative of a FN class. Currently, we are developing methodologies for deriving the representative graph for FN variants, using the metric provided by the many-to-many graph assignment problem. The challenges range from deciding a good technique to perform a meaningful matching among the graphs, to determining the adjacency of the median graph and the corresponding physical localization of the nodes.

A second advantage is given by the possibility of computing various deformation maps between FN fiber networks: the matching serves as a registration between the graphs, and once after having obtained an assignment between the corresponding graph edges, we can compute the differences in terms of fiber length, orientation, etc (see Figure 4 for an example of a deformation map in terms of fiber length - which can be regarded as a local stretching of the fibers that should be applied to first graph in order to obtain the second one)).

The deformation maps can subsequently be analyzed in a test hypothesis framework that decides whether the variation of a certain parameter (e.g. length) is due to the the variance within the same class or not.

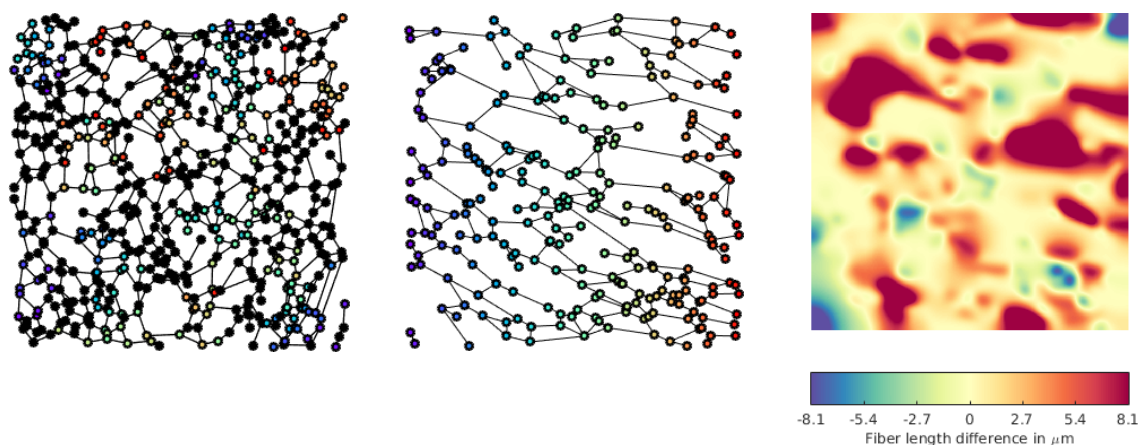


Figure 4. From left to right: graph network FN A+; graph network FN A+ ("tumour-like"); Deformation map between FN A+ and FN A+ (tumour-like)

Once we have derived a meaningful median graph based on graph-matching distances, we might be able to perform classification of the graph networks. Additionally, the fiber properties statistics inferred from the graph local properties, as well as Gabor filters parameters, can be of use to interpret the local differences within a specific class and among FN variants.

Anca Grapa's work is supported by the French Government (National Research Agency, ANR) through the "Investments for the Future" LABEX SIGNALIFE: program reference ANR-11-LABX-0028-01.

#### 6.4. Classification of the Fibronectin Networks in Extracellular Matrices using CNN and DAG-SVM of confocal and coverslip scanner images

**Participants:** Ghosh Avrajit, Anca-Ioana Grapa, Laure Blanc-Féraud, Xavier Descombes.

*This work is done in collaboration with Ellen Van Obberghen-Schilling and Georgios Efthymiou (iBV).*

We are interested in the numerical analysis and modeling of the Fibronectin (FN) networks, a major extracellular matrix (ECM) molecule, expressed in pathological states (fibrosis, cancer, etc).

Firstly, during one experiment, confocal images  $3128 \times 3128$  pixels with a lateral resolution of  $0.27 \mu\text{m}/\text{pixel}$  were acquired with a Zeiss LSM710 confocal system 10X/0.45 with the pinhole diameter set to its maximal value. Subsequently, images of FN variants in a different experiment were acquired using a coverslip scanner (Vectra Polaris Automated Quantitative Pathology Imaging System) based on fluorescence whole-slide scanning on a similar resolution to that of the confocal system.

For each of the experiments, 70 images (for every FN variant) corresponding to a representative region of  $512 \times 512$  pixels were selected for feature extraction and classification. The set of 280 gray-scale images was classified with a DAG-SVM classifier using curvelet features using the parametrization from [24]. Additionally, it was classified with the GoogLeNet [30] pretrained Convolutional Neural Net (CNN) architecture using the MATLAB Deep Learning Toolbox and a 22-layer deep network trained on more than 1 million images for classification into 1000 object categories. A set of 196 images was used for the training of the algorithm, and the remaining 84 for testing it. The training image set was presented to the algorithm 25 times (epochs), in order to improve classification accuracy.

The results (Figures 5, 7, 6, and 8) show that the information in the FN images is relevant enough in a CNN-based classification to distinguish FN variants better than curvelet-based features. Additionally, the coverslip scanner acquired samples are classified with a higher accuracy, underlining the potential benefit of using the scanner for future experiments.

Actual / Predicted	FN B-A+	FN B-A-	FN B+A-	FN B+A+
FN B-A+	85.7	0	28.5	14.3
FN B-A-	0	80.9	14.3	4.8
FN B+A-	0	9.5	90.5	0
FN B+A+	9.5	14.3	0	76.2

Figure 5. Confusion matrix in percentage form of the CNN classification of FN variant confocal images. General mean accuracy of classification is 83.3%.

#### 6.5. Tumor cell tracking for automatic detection of cell death time, and classification of its type

**Participants:** Deborah Cottais, Eric Debreuve.

Actual/ Predicted	FN B-A+	FN B-A-	FB B+A-	FN B+A+
FN B-A+	64.3	2.9	25.7	7.1
FN B-A-	0	90	0	10
FN B+A-	25.7	4.3	45.7	24.3
FN B+A+	0	15.7	8.6	75.7

Figure 6. Confusion matrix in percentage form of the DAG-SVM classification of FN variants, using curvelets features. General mean accuracy of classification is 68.9%.

Actual/ Predicted	FN B-A+	FN B-A-	FB B+A-	FN B+A+
FN B-A+	95.2	0	0	4.7
FN B-A-	0	100	0	0
FN B+A-	0	4.7	62	33
FN B+A+	0	0	0	100

Figure 7. Confusion matrix in percentage form of the CNN classification of FN variant coverslip scanner images. General mean accuracy of classification is 89.3%.

Actual/ Predicted	FN B-A+	FN B-A-	FB B+A-	FN B+A+
FN B-A+	72.8	0	0	27.1
FN B-A-	0	85.7	8.5	5.7
FN B+A-	0	10	65.7	24.2
FN B+A+	15.7	0	11.43	72.8

Figure 8. Confusion matrix in percentage form of the DAG-SVM classification of FN variant coverslip scanner images (curvelet features). General mean accuracy of classification is 74.2%.



*This work was made in collaboration with Jérémie Roux (IRCAN, Nice, France).*

The available data were multi-channel videos acquired in fluorescence microscopy. We first performed cell segmentation on the channel in which the geometrical information was predominant. Then we performed tracking of the segmented cells. More precisely, we refer to tracking as the construction of cell trajectories along the video (see Fig. 9). By *transferring* this cell tracking onto the channel in which the radiometric information of the cells is the richest (mean intensity, variance, texture), we were able to extract characteristics for each cell, and study their temporal evolution to deduce the moment of cell death. Next, we are planning to develop a method of classification of the cell deaths into predefined types.

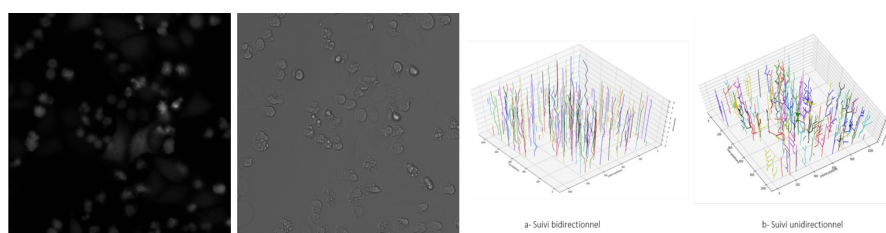


Figure 9. From left to right: two channels of a video frame and tracking trajectories of the segmented cells.

## 6.6. Cytoplasm segmentation from cells confocal microscopy images

**Participants:** Somia Rahmoun, Eric Debreuve, Xavier Descombes, Fabienne de Graeve.

As part of the ANR project RNAGRIMP, two series of images have been acquired using fluorescence microscopy: one where the cell cytoplasm has been stained with GFP (Green Fluorescent Protein), the second where the nuclei have been stained with DAPI (4',6-diamidino-2-phenylindole). The first steps are detecting the nuclei on the DAPI images and learning a classification procedure into living cell or dead cell based on morphological and radiometric nuclei properties (average intensity, area, granularity, circularity, ...).

The next step is to segment (i.e., extract automatically the region of) the cell cytoplasm on the GFP images. Indeed, the target RNP-IMP granules appear in that compartment of the cell and are visible through their GFP response. This segmentation problem is particularly difficult due to the heterogeneity of the cells intensity. This heterogeneity even appears within a given cell. Besides, cells sometimes form clusters in which there is no clear separation between adjacent cells.

In this context, we have considered a two-step algorithm to segment the cytoplasm. The first step consists of the image segmentation in small areas called superpixels that represent adjacent pixels with similar intensity. An automatic algorithm based on the watershed transform has been chosen after evaluating and comparing different strategies (based on iterative clustering, minimum spanning tree, persistent edge selection ...).

The second step of the proposed approach performs superpixels merging to obtain the final segmentation. Starting from the previously detected nuclei to define cell seeds, the neighboring superpixels are merged iteratively if a radiometric similarity is detected. Ambiguities between neighboring cells are solved by combining radiometric and shape criteria. This cell growth process is considered layer by layer and performed in parallel.

## 6.7. Adaptive thresholding using persistent diagrams

**Participants:** Paul Emmanuel Ponsenard, Xavier Descombes.

In this project we have proposed a new algorithm for adaptive thresholding based on persistence diagrams. A common difficulty in binarizing biological images lies in the heterogeneity of the signal. This heterogeneity can be due to the sensor itself but also to variability in the cell response to a given marker. Therefore the binarization can not be adequately performed by using the same threshold on the whole image. In this context, adaptive approaches that estimate a local or regional proper threshold are needed. Last year, we have proposed a solution that embedded both a contrast term and a shape criterion to select the most relevant connected components among the different level sets of the image. In this work we focus on the connected component trajectories along the grey values defining the levels sets. More precisely, the persistent diagram studies the evolution of the different connected components of a binarized image for successive thresholds. The life time of a connected component is thus defined as the timelapse between its birth (gray level for which the component appears) and its death (gray level for which the component is merged with a neighboring one). As a final result for the binarization, we propose to keep the connected components with the longest lifetimes. A result on mitochondrial network binarization is shown on figure 10 .

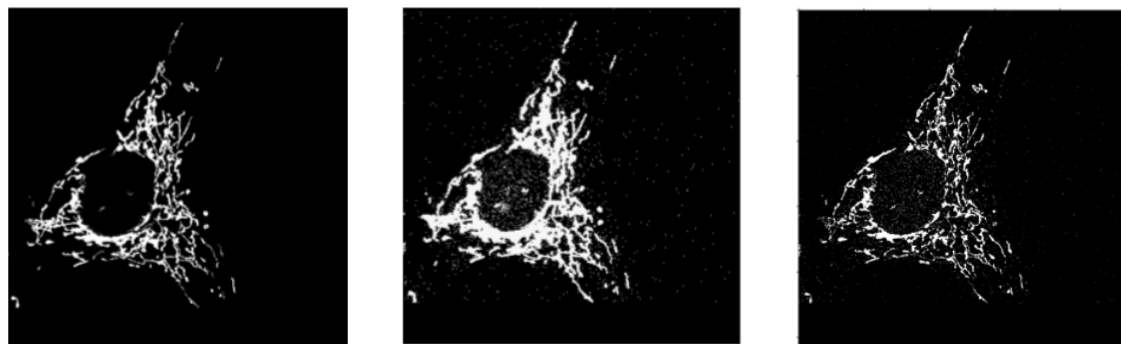


Figure 10. Image of Mitochondria from Bost team at C3M (left), Binarization obtained with a global threshold (middle) and with the persistence diagram approach. (right).

## 6.8. Graph matching and median graph through simulating annealing

**Participants:** Zhankeng Zhang, Xavier Descombes.

Graph matching when the number of nodes and edges differs is known as an NP-hard problem. Therefore, sub-optimal optimization algorithms have been proposed to solve this problem. In this work, we evaluate the possibility to reach, at least theoretically, the global optimum by using simulated annealing. We have developed an improved version of the simulating annealing scheme based on a Metropolis sampler. To solve the problem of dimension matching (different number of nodes) we have classically added dummy nodes in the smaller graph. Besides, we have shown that adding dummy nodes in both graphs provides more flexibility in the matching, thus improving the matching result. Finally, within this framework we were able to define and compute "median" graph as shown on figure 11 . The algorithm consists in aligning all the graphs in a first step. The median graph is then obtained by considering two types of move in the simulated annealing: adding/removing an edge and switching two nodes. To validate this work we have considered a classification scheme between graphs. The obtained results overcome those obtained with state of the art graph matching algorithms while the computational time remains reasonable.

## 6.9. Botrytis cinerea phenotype recognition and classification: toward the establishment of links between phenotypes and antifungal molecules

**Participants:** Sarah Laroui, Eric Debreuve, Xavier Descombes.

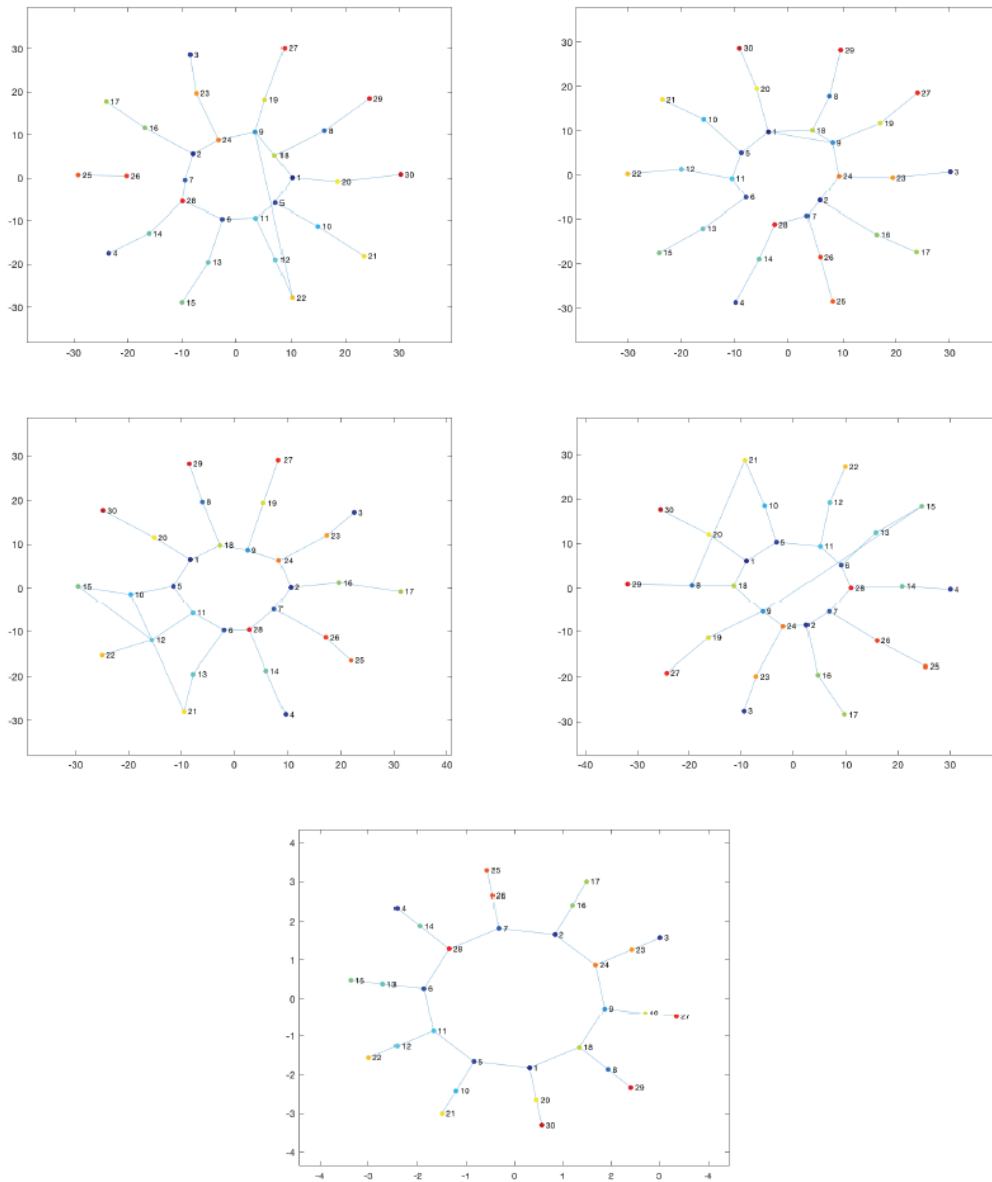


Figure 11. Four samples of noisy SUN graph and computed median graph

*This work is made in collaboration with Aurelia Vernay and Florent Villiers (Bayer).*

*Botrytis cinerea* is a reference model of filamentous phytopathogen fungi. Some chemical treatments can lead to characteristic morphological changes, or phenotypic signatures. These phenotypes could be associated with the treatment Mode of Action (Figure 12). In order to recognise and characterise different phenotypes and associate them with the different modes of action of the molecules (Figure 13), 24-hour images are taken by transmitted light microscopy. Because of the different dose-response effects, each given molecule is tested at ten concentrations.

We compared the results of classification of these images using two methods: random forests and convolutional neural networks (Deep Learning).

To learn the Random Forest classifier, we developed a robust image analysis and classification framework relying on morphometric and topological characteristics. A number of 16 features are extracted from three representations of the objects (binary mask, skeleton and graph). Some are calculated globally over all the objects of an image (ex: the skeleton length variance) while others are calculated on each object of an image (ex: the number of nodes of the graph). The second method uses a convolutional neural network. It has been implemented using Tensorflow, an open source library for Machine Learning, created by Google to develop applications in Deep Learning.

This method achieves better results than Random Forests, and it proved to be very robust to inter-experiment variations with an average classification accuracy of 88%. In addition, it does not require data pre-processing for feature extraction. However the explanatory aspect that exists with random forests is lost.

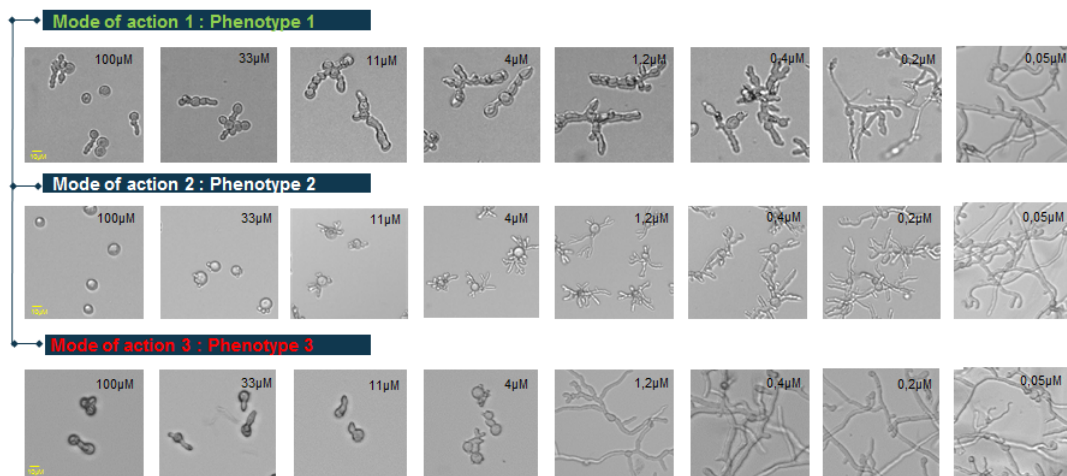


Figure 12. Characteristic phenotypic signatures for different chemical treatments at different concentrations (transmitted light microscopy, ImageXpress microscope, 10x lens).

## 6.10. Estimating the volume of a copepod from a single image with Deep Learning

**Participants:** Cédric Dubois, Eric Debreuve.

*This work was made in collaboration with Jean-Olivier Irisson (Laboratoire d’Océanographie de Villefranche).*

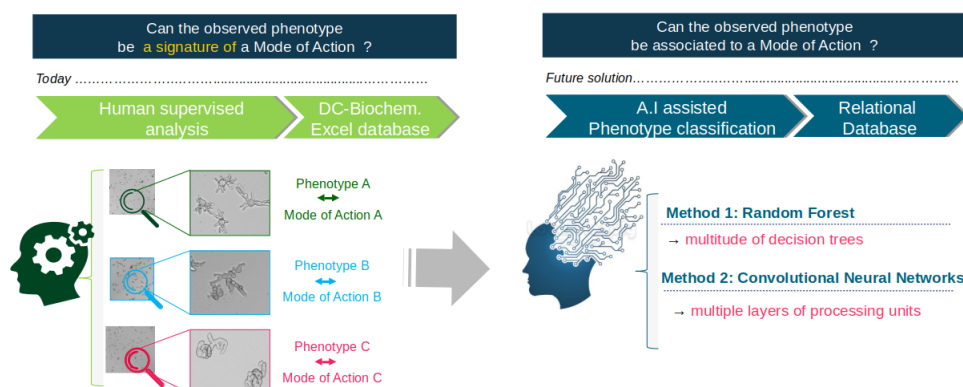


Figure 13. Example of phenotypic signatures obtained with molecules with three different mode of action. Strategy of automatic recognition and characterisation of different phenotypes and associate them with the different modes of action of the molecules.

Ecologists and biogeochemists are interested in estimating the volume of copepods (to then convert it into a biomass), a subclass of zooplankton, in order to estimate how much carbon it can store and how much it will store in the future. Those studies are made thanks to the online database EcoTaxa, which gives access to a large number of plankton images. The standard method used in ecology produces partially incorrect results due to geometric approximations and projection issues (from 3D to the 2D image plane). We first proposed a study of the error made by this method on the volume estimation of copepods. Then we proposed a new method based on the deep learning framework. Its performances have been analyzed on simulated data (Fig. 14) and preliminary tests have been made on a subset of the data of the *UVP5hd GreenEdge 2016* acquisition campaign available on EcoTaxa. Our work pointed out the limitations of both methods, indicating that a broader study is needed to improve the computation of copepod volumes.

This work formed the basis for Cédric Dubois's PhD which began on October 1st 2019 with a Ministère de la Recherche funding.

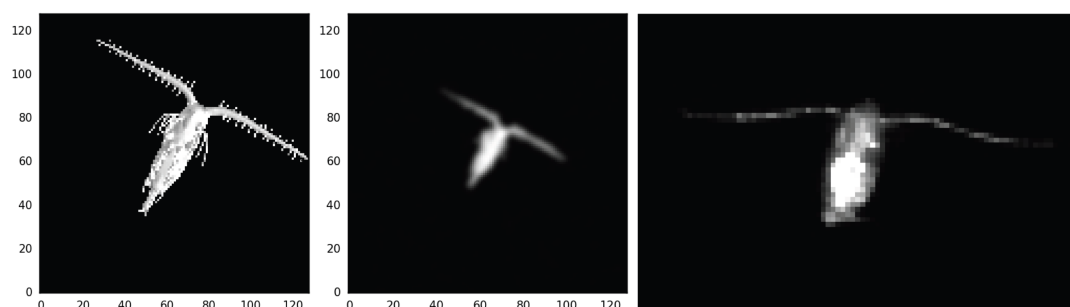


Figure 14. Left: synthetic 3D model of a typical copepod. Middle: a simulated 2D observation of the model. Right: a real observation.

## 6.11. Cell lineage calculation

**Participants:** Manuel Petit [Mosaic, Lyon], Christophe Godin [Mosaic, Lyon], Grégoire Malandain.

*This work is made within the IPL Naviscope.*

In recent years, techniques to image the development of biological organisms have made spectacular progresses. Researchers are now able to observe the trajectories corresponding to the development of 3D- plant tissues or animal embryo with cellular resolution. However, such observations yield a large amount of data, which, in turn, require fast and robust analysis tools to extract information while minimizing user interaction. The goal of M. Petit, which PhD thesis has begun november the 1st, is first to propose new lineage extraction schemes, and then analysis tools over a population of lineages.

## 6.12. Morphogenesis of the sea urchin embryo

**Participants:** Angie Moullet, Grégoire Malandain.

*This work is made in collaboration with Barthélemy Delorme and Matteo Rauzi (iBV, Nice).*

The goal of the project is to understand how biophysical forces are generated and how they work to produce exquisitely precise and controlled tissue shape changes in embryo development. Tissue morphogenesis is a process by which the embryo is reshaped into the final form of a developed animal. Tissues are constituted by cells that are interconnected one another: local changes of cell mechanical properties and shape drive consequent tissue shape change. Nevertheless, the knowledge per se of the mechanisms and mechanics at the cell level which drive cell shape changes is insufficient to explain how tissues change their shape. Emerging properties arise at higher scales resulting from the interaction of cells within tissues and of tissues coordinating and interacting with one another.

To study the embryo evolution at a cellular scale, temporal series will be acquired by a multi-view light-sheet microscope. We will use the Mediterranean sea urchin embryo species *Paracentrotus lividus* as a model system and focus on the process of tissue folding, that will process that is vital since folding defects can impair neurulation in vertebrates and gastrulation in all animals which are organized into the three germ layers. From the technological perspective, new tools are needed to be able to visualize cells and to provide quantifiable data at high temporal and spatial resolution over large regions and across the entire embryo.

The goal of A. Moullet's internship (that begins dec. the 1st) is to measure and study the archenteron length evolution over a population of sea urchin embryos.

## 6.13. 3D Coronary vessel tracking in x-ray projections

**Participants:** Emmanuelle Poulain, Grégoire Malandain.

*This work is made in collaboration with Régis Vaillant (GE-Healthcare, Buc, France) and Nicholas Ayache (Inria Epione team).*

Percutaneous Coronary Intervention (PCI) is a minimally procedure which is used to treat coronary artery narrowing. The physician intervenes on the patient under the guidance of an x-ray imaging system. This system is not able to display a visual assessment of the coronary wall, contrary to the pre-operative Computed Tomography Angiography (CTA). To help physician to exploit this information during the course of the procedure, registering these two modalities would be useful. To this aim, we first proposed in a previous work a method of 3D coronary tracking of the main vessel in x-ray projections [27]. This approach is only applicable when the operator has avoided vessel superimposition over the vessel of interest. To further extend the concept, we explore the benefit of doing the deformable registration over the whole coronary tree. This benefit is illustrated in Fig. 15 and through tracking videos presented in <https://3dvtracking.github.io/>.

The proposed approach involves several algorithmic steps: a rigid registration of the tree to an iso-cardiac phase projection followed by a deformation of the tree represented as a tree-spline.



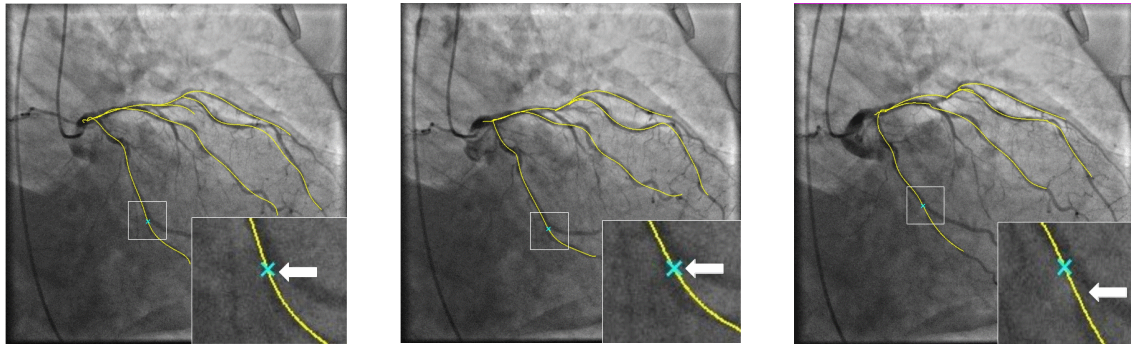


*Figure 15. Tracking results for one patient over one cardiac cycle. The yellow curve represents the projected 3D vessel, the blue cross represents the point tracked as the bifurcation, and the white arrow points to the bifurcation. Those images come from a 15 frames sequence. This figure shows the frames 1, 6, 15, from left to right.*

Indeed, a tree-spline i.e. a tree with a spline attached to each edge and shared control points between these points describes a 3D coronary tree and is able to represent its deformation along the time. We combine this description with a registration algorithm operating between the tree-spline and the angiographic projection of the coronary tree. It starts by the estimation of a rigid transformation for the iso cardiac phase time followed by a non-rigid deformation of the tree driven by the pairings formed between the projection of the edges of the tree-spline and the observed x-ray projection of the coronary arteries. The pairings are built taking into account the tree topology consistency. Anatomical constraints of length preservation is enforced when deforming the arteries.

This work has been published in FIMH [9].

## NACHOS Project-Team

## 6. New Results

### 6.1. Electromagnetic wave propagation

#### 6.1.1. *POD-based reduced-order DGTD method*

**Participants:** Stéphane Lanteri, Kun Li [UESTC, Chengdu, China], Liang Li [UESTC, Chengdu, China].

This study is concerned with reduced-order modeling for time-domain electromagnetics and nanophotonics. More precisely, we consider the applicability of the proper orthogonal decomposition (POD) technique for the system of 3D time-domain Maxwell equations, possibly coupled to a Drude dispersion model, which is employed to describe the interaction of light with nanometer scale metallic structures. We introduce a discontinuous Galerkin (DG) approach for the discretization of the problem in space based on an unstructured tetrahedral mesh. A reduced subspace with a significantly smaller dimension is constructed by a set of POD basis vectors extracted offline from snapshots that are obtained by the global DGTD scheme with a second order leap-frog method for time integration at a number of time levels. POD-based ROM is established by projecting (Galerkin projection) the global semi-discrete DG scheme onto the low-dimensional space. The stability of the POD-based ROM equipped with the second order leap-frog time scheme has been analysed through an energy method. Numerical experiments have allowed to verify the accuracy, and demonstrate the capabilities of the POD-based ROM. These very promising preliminary results are currently consolidated by assessing the efficiency of the proposed POD-based ROM when applied to the simulation of 3D nanophotonic problems.

#### 6.1.2. *Study of 3D periodic structures at oblique incidences*

**Participants:** Claire Scheid, Nikolai Schmitt, Jonathan Viquerat.

In this work, we focus on the development of the use of periodic boundary conditions with sources at oblique incidence in a DGTD framework. Whereas in the context of the Finite Difference Time Domain (FDTD) methods, an abundant literature can be found, for DGTD, the amount of contributions reporting on such methods is remarkably low. In this work, we supplement the existing references using the field transform technique with an analysis of the continuous system using the method of characteristics and provide an energy estimate. Furthermore, we also study the numerical stability of the resulting DGTD scheme. After numerical validations, two realistic test problems have been considered in the context of nanophotonics with our DIOGENeS DGTD solver. This work has been accepted for publication in 2019.

#### 6.1.3. *Stability and asymptotic properties of the linearized Hydrodynamic Drude model*

**Participants:** Serge Nicaise [Université de Valenciennes], Claire Scheid.

We go a step further toward a better understanding of the fundamental properties of the linearized hydrodynamical model studied in the PhD of Nikolai Schmitt [16]. This model is especially relevant for small nanoplasmonic structures (below 10nm). Using a hydrodynamical description of the electron cloud, both retardation effects and non local spatial response are taken into account. This results in a coupled PDE system for which we study the linear response. In [45] (submitted, under revision), we concentrate on establishing well posedness results combined to a theoretical and numerical stability analysis. We especially prove polynomial stability and provide optimal energy decay rate. Finally, we investigate the question of numerical stability of several explicit time integration strategies combined to a Discontinuous Galerkin spatial discretization.

#### 6.1.4. *Toward thermoplasmonics*

**Participants:** Yves d'Angelo, Stéphane Lanteri, Claire Scheid.

Although losses in metal is viewed as a serious drawback in many plasmonics experiments, thermoplasmonics is the field of physics that tries to take advantage of the latter. Indeed, the strong field enhancement obtained in nanometallic structures lead to a localized raise of the temperature in its vicinity leading to interesting photothermal effects. Therefore, metallic nanoparticles may be used as heat sources that can be easily integrated in various environments. This is especially appealing in the field of nanomedicine and can for example be used for diagnosis purposes or nanosurgery to cite but just a few. This year, we initiated a preliminary work towards this new field in collaboration with Y. D'Angelo (Université Côte d'Azur) and G. Baffou (Fresnel Institute, Marseille) who is an expert in this field. Due to the various scales and phenomena that come into play, the numerical modeling present great challenges. The laser illumination first excite a plasmon oscillation (reaction of the electrons of the metal) that relaxes in a thermal equilibrium and in turn excite the metal lattice (phonons). The latter is then responsible for heating the environment. A relevant modeling approach thus consists in describing the electron-phonon coupling through the evolution of their respective temperature. Maxwell's equations is then coupled to a set of coupled nonlinear hyperbolic equations describing the evolution of the temperatures of electrons, phonons and environment. The nonlinearities and the different time scales at which each thermalization occurs make the numerical approximation of these equations quite challenging.

#### 6.1.5. *Corner effects in nanoplasmonics*

**Participants:** Camille Carvalho [Applied Mathematics Department, University of California Merced, USA], Claire Scheid.

In this work, we study nanoplasmonic structures with corners (typically a diedral/triangular structure); a situation that raises a lot of issues. We focus on a lossless Drude dispersion model and propose to investigate the range of validity of the amplitude limit principle. The latter predicts the asymptotic harmonic regime of a structure that is monochromatically illuminated, which makes a frequency domain approach relevant. However, in frequency domain, several well posedness problems arise due to the presence of corners (addressed in the PhD thesis of Camille Carvalho). This should impact the validity of the limit amplitude principle and has not yet been addressed in the literature in this precise setting. Here, we combine frequency-domain and time-domain viewpoints to give a numerical answer to this question in two dimensions. We show that the limit amplitude principle does not hold for whole interval of frequencies, that are explicitated using the well-posedness analysis. This work is now being finalized.

#### 6.1.6. *MHM methods for the time-domain Maxwell equations*

**Participants:** Alexis Gobé, Stéphane Lanteri, Diego Paredes Concha [Instituto de Matemáticas, Universidad Católica de Valparaíso, Chile], Claire Scheid, Frédéric Valentin [LNCC, Petropolis, Brazil].

Although the DGTD method has already been successfully applied to complex electromagnetic wave propagation problems, its accuracy may seriously deteriorate on coarse meshes when the solution presents multiscale or high contrast features. In other physical contexts, such an issue has led to the concept of multiscale basis functions as a way to overcome such a drawback and allow numerical methods to be accurate on coarse meshes. The present work, which is conducted in the context of the HOMAR Associate Team, is concerned with the study of a particular family of multiscale methods, named Multiscale Hybrid-Mixed (MHM) methods. Initially proposed for fluid flow problems, MHM methods are a consequence of a hybridization procedure which characterize the unknowns as a direct sum of a coarse (global) solution and the solutions to (local) problems with Neumann boundary conditions driven by the purposely introduced hybrid (dual) variable. As a result, the MHM method becomes a strategy that naturally incorporates multiple scales while providing solutions with high order accuracy for the primal and dual variables. The completely independent local problems are embedded in the upscaling procedure, and computational approximations may be naturally obtained in a parallel computing environment. In this study, a family of MHM methods is proposed for the solution of the time-domain Maxwell equations where the local problems are discretized either with a continuous FE method or a DG method (that can be viewed as a multiscale DGTD method). Preliminary results have been obtained in the two-dimensional case.

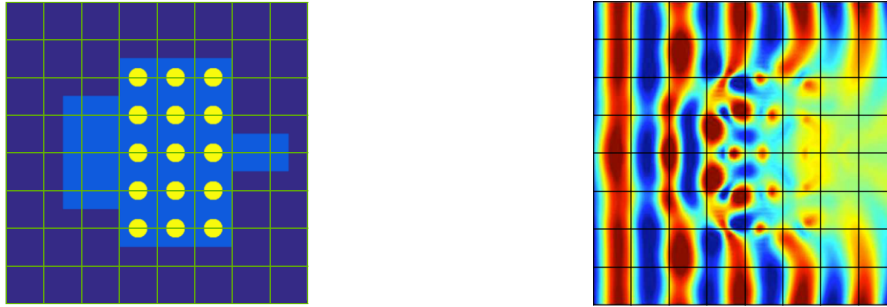


Figure 4. Light propagation in a photonic crystal structure using a MHM-DGTD method for solving the 2D Maxwell's equations. Left: quadrangular mesh. Right: contour lines of the amplitude of the electric field.

### 6.1.7. HDG methods for the time-domain Maxwell equations

**Participants:** Théophile Chaumont-Frelet, Stéphane Descombes, Stéphane Lanteri, Georges Nehmetallah.

Hybridizable discontinuous Galerkin (HDG) methods have been investigated in the team since 2012. This family of method employs face-based degrees of freedom that can be viewed as a fine grain domain decomposition technique. We originally focused on frequency-domain applications, for which HDG methods enable the use of static condensation, leading to drastic reduction in computational time and memory consumption. More recently, we have investigated the use of HDG discretization to solve time-dependent problems. Specifically, in the context of the PhD thesis of Georges Nehmetallah, we focused on two particular aspects. On the one hand, HDG methods exhibit a superconvergence property that allows, by means of local postprocessing, to obtain new improved approximations of the unknowns. Our first contribution is to apply this methodology to time-dependent Maxwell's equations, where the post-processed approximation converges with order  $k + 1$  instead of  $k$  in the  $H(\text{curl})$ -norm, when using polynomial of degree  $k \geq 1$ . The proposed method has been implemented for dealing with general 3D problems. Fig. 5 highlights the improved accuracy of the post-processed approximation on a cavity benchmark.

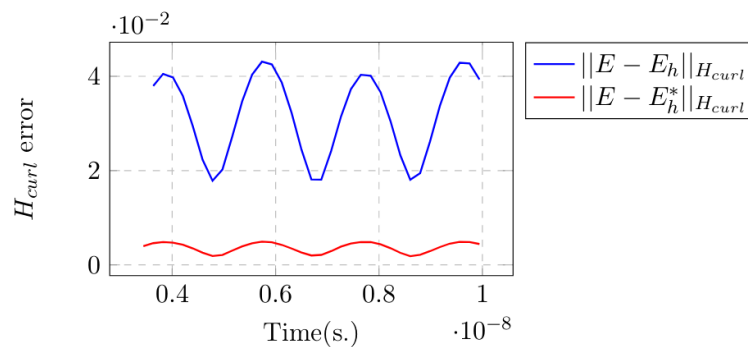


Figure 5. Time evolution of the  $H(\text{curl})$ -error before and after postprocessing for  $P_2$  interpolation and a fixed mesh constituted by 3072 elements

Another interesting aspect of the HDG method is that it can be conveniently employed to blend different time-integration schemes in different regions of the mesh. This is especially useful to efficiently handle locally refined space grids, that are required to take into account geometrical details. These ideas have already been explored for standard discontinuous Galerkin discretization in the context of the PhD thesis of Ludovic Moya [13], [14]. Here, we focused on HDG methods and we introduced a family of coupled implicit-explicit (IMEX) time integration methods for solving time-dependent Maxwell's equations. We established stability conditions that are independent of the size of the small elements in the mesh, and are only constrained by the coarse part. Numerical experiments on two-dimensional benchmarks illustrate the theory and the usefulness of the approach.

### 6.1.8. *A posteriori* error estimators

**Participants:** Théophile Chaumont-Frelet, Alexandre Ern [SERENA project-team], Patrick Vega, Martin Vohralík [SERENA project-team].

The development of *a posteriori* error estimators and is a new topic of interest for the team. Concerning *a posteriori* estimators, a collaboration with the SERENA project-team has been initiated. We mainly focus on a technique called equilibrated fluxes, which has the advantage to produce  $p$ -robust error estimators together with guaranteed error estimates. This means in particular that these estimators are particularly suited for high-order discretization schemes. Our first results deal with the Helmholtz equation, and have been recently submitted [39] and presented at the Enumath international conference [29]. Fig. 6 depicts the ability of the estimators to accurately describe the error distribution in a realistic application. Future works in this line will include the treatment of Maxwell's equations. The recently hired postdoctoral fellow Patrick Vega will actively participate in these developments.

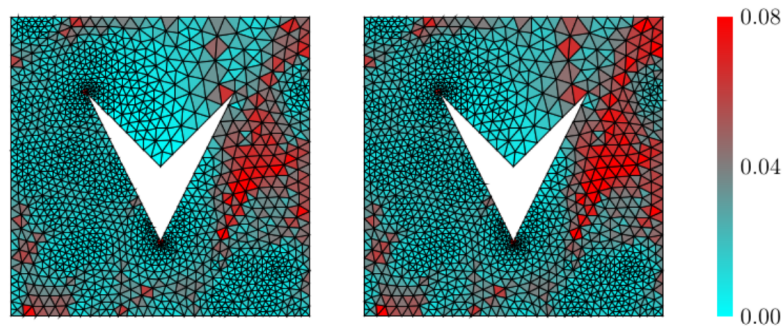


Figure 6. Estimators  $\eta_K$  (left) and elementwise errors  $\|u - u_h\|_K$  (right) for a scattering problem discretized with  $\mathcal{P}_3$  elements

### 6.1.9. $hp$ -adaptivity

**Participants:** Théophile Chaumont-Frelet, David Pardo [Basque Center for Applied Mathematics, Bilbao, Spain].

Together with the development of *a posteriori* estimators, a novel activity in the team is the design of efficient  $hp$ -adaptive strategy. In this regard, we propose a multi-level hierarchical data structure imposing Dirichlet nodes to manage the so-called hanging nodes. Our  $hp$ -adaptive strategy is based on performing quasi-optimal unrefinements. Taking advantage of the hierarchical structure of the basis functions both in terms of the element size  $h$  and the polynomial order of approximation  $p$ , we mark those with the lowest contributions to the energy of the solution and remove them. This straightforward unrefinement strategy does not require from a fine grid or complex data structures, making the algorithm flexible to many practical situations and

existing implementations. Our first contribution has been recently submitted [42], and deals with the Poisson equation. Fig. 7 shows how the algorithm is able to correctly refine the computational grid to capture a shock wave.

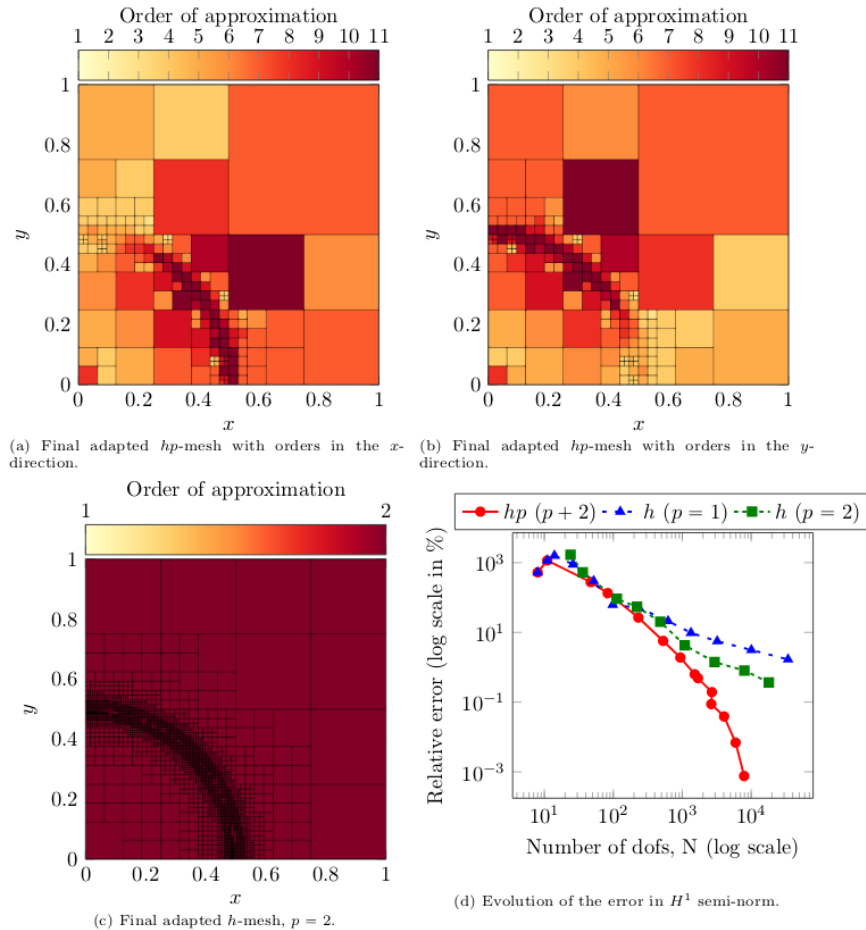


Figure 7. Different  $hp$ -adaptive strategies for capturing a shock wave

### 6.1.10. Multiscale methods for frequency-domain wave propagation

**Participants:** Théophile Chaumont-Frelet, Zakaria Kassali, Stéphane Lanteri, Frédéric Valentin.

The design and analysis of multiscale methods for wave propagation is an important research line for team. The team actually mainly specializes in one family of multiscale methods, called multiscale hybrid-mixed (MHM). These developments started thanks to the close collaboration with Frédéric Valentin, who has recently been awarded an Inria international chair. Previous investigations in the context of this collaboration focused on time-dependent Maxwell's equations [10]. Recent efforts have been guided towards the realization of a MHM method for time-harmonic Maxwell's equations. We first focused on the Helmholtz equation, that modelizes the particular case of polarized waves. Our first results include the implementation of the method for two-dimensional problems as well as rigorous, frequency-explicit, stability and convergence analysis. These findings have recently been accepted for publication [40]. In the context of the internship of Zakaria Kassali,



the method has been further adapted for the propagation of polarized waves in solar cells. Specifically, it is required in this case to take into account “quasi-periodic” boundary conditions that deserve a special treatment. We are currently undertaking further developments guided toward full three-dimensional Maxwell’s equations with the PhD of Zakaria Kassali, which started in November 2019.

## 6.2. High performance numerical computing

### 6.2.1. High order HDG schemes and domain decomposition solvers for frequency-domain electromagnetics

**Participants:** Emmanuel Agullo [HIEPACS project-team, Inria Bordeaux - Sud-Ouest], Théophile Chaumont-Frelet, Luc Giraud [HIEPACS project-team, Inria Bordeaux - Sud-Ouest], Stéphane Lanteri.

This work is undertaken in the context of PRACE 6IP project and aims at the development of scalable frequency-domain electromagnetic wave propagation solvers, in the framework of the DIOGENeS software suite. This solver is based on a high order HDG scheme formulated on an unstructured tetrahedral grid for the discretization of the system of three-dimensional Maxwell equations in dispersive media, leading to the formulation of large sparse indefinite linear system for the hybrid variable unknowns. This system is solved with domain decomposition strategies that can be either a purely algebraic algorithm working at the matrix operator level (i.e. a black-box solver), or a tailored algorithm designed at the continuous PDE level (i.e. a PDE-based solver). In the former case, we collaborate with the HIEPACS project-team at Inria Bordeaux - Sud-Ouest in view of adapting and exploiting the MaPHYs (Massively Parallel Hybrid Solver - <https://gitlab.inria.fr/solverstack/maphys>) algebraic hybrid iterative-direct domain decomposition solver. More precisely, this collaboration is concerned with two topics: one one hand,= the improvement of the iterative convergence of MaPHYs for the HDG hybrid variable linear system.

## 6.3. Applications

### 6.3.1. Inverse design of metasurfaces using statistical learning methods

**Participants:** Régis Duvigneau [ACUMES project-team, Inria Sophia Antipolis-Méditerranée], Mahmoud Elsayy, Patrice Genevet [CRHEA laboratory, Sophia Antipolis], Stéphane Lanteri.

Metasurfaces are flat optical nanocomponents, that are the basis of several more complicated optical devices. The optimization of their performance is thus a crucial concern, as they impact a wide range of applications. Yet, current design techniques are mostly based on *engineering knowledge*, and may potentially be improved by a rigorous analysis based on accurate simulation of Maxwell’s equations. The goal of this study is to optimize phase gradient metasurfaces by taking advantage of our fullwave high order Discontinuous Galerkin time-Domain solver implemented in DIOGENeS, coupled with two advanced optimization techniques based on statistical learning and evolutionary strategies. Our key findings are novel designs for Gan semiconductor phase gradient metasurfaces operating at visible wavelengths. Our numerical results reveal that rectangular and cylindrical nanopillar arrays can achieve more than respectively 88% and 85% of diffraction efficiency for TM polarization and both TM and TE polarization respectively, using only 150 fullwave simulations. To the best of our knowledge, this is the highest blazed diffraction efficiency reported so far at visible wavelength using such metasurface architectures. Fig. 8 depicts the superiority of the proposed statistical learning approaches over standard gradient-based optimization strategies. This work has been recently published [22].

### 6.3.2. Optimization of light-trapping in nanocone gratings

**Participants:** Stéphane Collin [Sunlit team, C2N-CNRS, Marcoussi], Alexis Gobé, Julie Goffard [Sunlit team, C2N-CNRS, Marcoussi], Stéphane Lanteri.

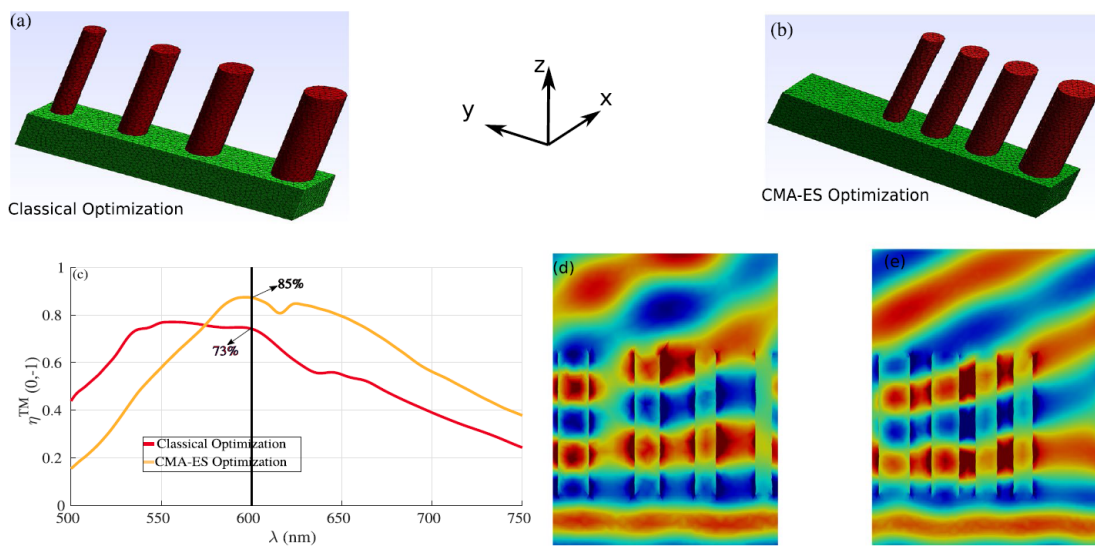


Figure 8. Comparison between the classical approach to phase gradient metasurface design and our optimized geometries for the cylindrical nanopillars with  $h = 800$  nm. (a,b) The geometry obtained using the classical approach in which each nanopillar is optimized manually by changing the diameter and finally placed together in order to obtain the desired phase shift needed to maximize the light deflection for the first order mode at  $\lambda = 600$  nm with period 1500 nm in  $y$ -direction. (c) Results obtained using the CMA-ES for the cylindrical nanopillars (see Table 3) for the corresponding parameters. (c) Comparison between the deflection efficiency for the first order mode obtained using the classical (red curve) and the CMA-ES (orange curve). (d,e) Represent field maps of  $Re(E_y)$  obtained using the classical optimization design and the CMA-ES results, respectively

There is significant recent interest in designing ultrathin crystalline silicon solar cells with active layer thickness of a few micrometers. Efficient light absorption in such thin films requires both broadband antireflection coatings and effective light trapping techniques, which often have different design considerations. In collaboration with physicists from the Sunlit team at C2N-CNRS, we conduct a numerical study of solar cells based on nanocone gratings. Indeed, it has been previously shown that by employing a double-sided grating design, one can separately optimize the geometries for antireflection and light trapping purposes to achieve broadband light absorption enhancement [60]. In the present study, we adopt the nanocone grating considered in [60]. This structure contains a crystalline silicon thin film with nanocone gratings also made of silicon. The circular nanocones form two-dimensional square lattices on both the front and the back surfaces. The film is placed on a perfect electric conductor (PEC) mirror. The ultimate objective of this study is to devise a numerical optimization strategy to infer optimal values of the geometrical characteristics of the nanocone grating on each side of the crystalline silicon thin film. Absorption characteristics are here evaluated using the high order DGTd solver from the DIOGENeS software suite. We use two efficient global optimization techniques based on statistical learning to adapt the geometrical characteristics of the nanocones in order to maximize the light absorption properties of this type of solar cells.

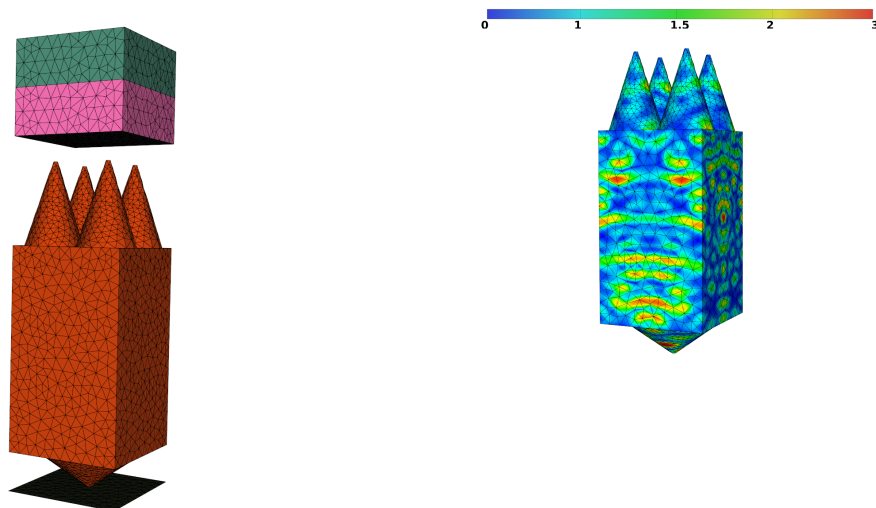


Figure 9. Simulation of light trapping in a solar cell based on nanocone gratings. Geometrical model (left) and contour lines of the module of the DFT of  $\mathbf{E}$  for a wavelength  $\lambda = 857$  nm (right).

### 6.3.3. Influence of spatial dispersion on surface plasmons and grating couplers

**Participants:** Stéphane Lanteri, Antoine Moreau [Institut Pascal, Université Blaise Pascal], Armel Pitelet [Institut Pascal, Université Blaise Pascal], Claire Scheid, Nikolai Schmitt, Jonathan Viquerat.

Recent experiments have shown that spatial dispersion may have a conspicuous impact on the response of plasmonic structures. This suggests that in some cases the Drude model should be replaced by more advanced descriptions that take spatial dispersion into account, like the hydrodynamic model. Here we show that nonlocality in the metallic response affects surface plasmons propagating at the interface between a metal and a dielectric with high permittivity. As a direct consequence, any nanoparticle with a radius larger than 20 nm can be expected to be sensitive to spatial dispersion whatever its size. The same behavior is expected for a simple metallic grating allowing the excitation of surface plasmons, just as in Woods famous experiment. Finally, we carefully set up a procedure to measure the signature of spatial dispersion precisely, leading the way

for future experiments. Importantly, our work suggests that for any plasmonic structure in a high permittivity dielectric, nonlocality should be taken into account.

#### **6.3.4. Optimization and uncertainty quantification of gradient index metasurfaces**

**Participants:** Gauthier Brière [CRHEA laboratory, Sophia Antipolis], Herbert de Gersem [TEMF institute, TU Darmstadt, Germany], Patrice Genevet [CRHEA laboratory, Sophia Antipolis], Niklas Georg [TEMF institute, TU Darmstadt, Germany], Stéphane Lanteri, Dimitrios Loukrezis [TEMF institute, TU Darmstadt, Germany], Ulrich Römer [TEMF institute, TU Darmstadt, Germany], Nikolai Schmitt.

The design of intrinsically flat two-dimensional optical components, i.e., metasurfaces, generally requires an extensive parameter search to target the appropriate scattering properties of their constituting building blocks. Such design methodologies neglect important near-field interaction effects, playing an essential role in limiting the device performance. Optimization of transmission, phase-addressing and broadband performances of metasurfaces require new numerical tools. Additionally, uncertainties and systematic fabrication errors should be analysed. These estimations, of critical importance in the case of large production of metaoptics components, are useful to further project their deployment in industrial applications. Here, we report on a computational methodology to optimize metasurface designs. We complement this computational methodology by quantifying the impact of fabrication uncertainties on the experimentally characterized components. This analysis provides general perspectives on the overall metaoptics performances, giving an idea of the expected average behavior of a large number of devices.

## NEO Project-Team

# 7. New Results

## 7.1. Stochastic Modeling

**Participants:** Sara Alouf, Eitan Altman, Konstantin Avrachenkov, Alain Jean-Marie, Giovanni Neglia.

### 7.1.1. Network growth models

Network growth models that embody principles such as preferential attachment and local attachment rules have received much attention over the last decade. Among various approaches, random walks have been leveraged to capture such principles. In the framework of joint team with Brazil (Thanes), G. Neglia, together with G. Iacobelli and D. Figueiredo (both from UFRJ, Brazil), has studied a simple model where network growth and a random walker are coupled [23]. In particular, they consider the No Restart Random Walk model where a walker builds its graph (tree) while moving around. The walker takes  $s$  steps (a parameter) on the current graph. A new node with degree one is added to the graph and connected to the node currently occupied by the walker. The walker then resumes, taking another  $s$  steps, and the process repeats. They have analyzed this process from the perspective of the walker and the network, showing a fundamental dichotomy between transience and recurrence for the walker as well as power law and exponential degree distribution for the network.

### 7.1.2. Controlled Markov chains

E. Altman in collaboration with D. Josselin and S. Boularouk (CERI/LIA, Univ Avignon) study in [26] a multiobjective dynamic program where all the criteria are in the form of total expected sum of costs till absorption in some set of states. They assume that instantaneous costs are strictly positive and make no assumption on the ergodic structure of the Markov Decision Process. Their main result is to extend the linear program solution approach that was previously derived for transient Constrained Markov Decision Processes to the general ergodic structure. Several (additive) cost metrics are defined and (possibly randomized) routing policies are sought which minimize one of the costs subject to constraints over the other objectives.

### 7.1.3. Escape probability estimation in large graphs

Consider large graphs as the object of study and specifically the problem of escape probability estimation. Generally, this characteristic cannot be calculated analytically nor even numerically due to the complexity and large size of the investigation object. In [32], K. Avrachenkov and A. Borodina (Karelian Institute of Applied Mathematical Research, Russia) have presented an effective method for estimating the probability that the random walk on graph first enters a node  $b$  before returning into the starting node  $a$ . Regenerative properties of the random walk allow the use of an accelerated method for the simulation of cycles based on the splitting technique. The results of numerical experiments confirm the advantages of the proposed method.

### 7.1.4. Random surfers and prefetching

Prefetching is a basic technique used to reduce the latency of diverse computer services. Deciding what to prefetch amounts to make a compromise between latency and the waste of resources (network bandwidth, storage, energy) if contents is mistakenly prefetched. Modeling the problem in case of web/video/gaming navigation, is done by identifying a graph of “documents” connected by links representing the possible chaining. A surfer, either random or strategic, browses this graph. The prefetching controller must make it sure that the documents browsed are always available locally. In the case where the surfer is random and/or the graph is not completely known in advance, the question is largely unexplored. Q. Petitjean, under the supervision of S. Alouf and A. Jean-Marie, has determined through extensive simulations that when the graph is a tree, neither the greedy strategy, nor the one optimal when the tree is completely known, are optimal when the tree is discovered progressively.

### 7.1.5. The marmoteCore platform

The development of marmoteCore (see Section 6.1) has been pursued. Its numerical features for computing stationary distributions, average hitting times and absorption probabilities have been used in a joint work with F. Cazals, D. Mazauric and G. Santa Cruz (ABS team) and J. Roux (Univ Cote d'Azur) [52]. The software has been presented to young researchers in networking at the ResCom 2019 summer school.

## 7.2. Random Graph and Matrix Models

**Participants:** Konstantin Avrachenkov, Andrei Bobu.

### 7.2.1. Random geometric graphs

Random geometric graphs are good examples of random graphs with a tendency to demonstrate community structure. Vertices of such a graph are represented by points in Euclid space  $R^d$ , and edge appearance depends on the distance between the points. Random geometric graphs were extensively explored and many of their basic properties are revealed. However, in the case of growing dimension  $d \rightarrow \infty$  practically nothing is known; this regime corresponds to the case of data with many features, a case commonly appearing in practice. In [30], K. Avrachenkov and A. Bobu focus on the cliques of these graphs in the situation when average vertex degree grows significantly slower than the number of vertices  $n$  with  $n \rightarrow \infty$  and  $d \rightarrow \infty$ . They show that under these conditions random geometric graphs do not contain cliques of size 4 a.s. As for the size 3, they present new bounds on the expected number of triangles in the case  $\log^2(n) \ll d \ll \log^3(n)$  that improve previously known results.

Network geometries are typically characterized by having a finite spectral dimension (SD), that characterizes the return time distribution of a random walk on a graph. The main purpose of this work is to determine the SD of random geometric graphs (RGGs) in the thermodynamic regime, in which the average vertex degree is constant. The spectral dimension depends on the eigenvalue density (ED) of the RGG normalized Laplacian in the neighborhood of the minimum eigenvalues. In fact, the behavior of the ED in such a neighborhood characterizes the random walk. Therefore, in [33] K. Avrachenkov together with L. Cottatellucci (FAU, Germany and Eurecom) and M. Hamidouche (Eurecom) first provide an analytical approximation for the eigenvalues of the regularized normalized Laplacian matrix of RGGs in the thermodynamic regime. Then, we show that the smallest non zero eigenvalue converges to zero in the large graph limit. Based on the analytical expression of the eigenvalues, they show that the eigenvalue distribution in a neighborhood of the minimum value follows a power-law tail. Using this result, they find that the SD of RGGs is approximated by the space dimension  $d$  in the thermodynamic regime.

In [42] K. Avrachenkov together with L. Cottatellucci (FAU, Germany and Eurecom) and M. Hamidouche (Eurecom) have analyzed the limiting eigenvalue distribution (LED) of random geometric graphs. In particular, they study the LED of the adjacency matrix of RGGs in the connectivity regime, in which the average vertex degree scales as  $\log(n)$  or faster. In the connectivity regime and under some conditions on the radius  $r$ , they show that the LED of the adjacency matrix of RGGs converges to the LED of the adjacency matrix of a deterministic geometric graph (DGG) with nodes in a grid as the size of the graph  $n$  goes to infinity. Then, for  $n$  finite, they use the structure of the DGG to approximate the eigenvalues of the adjacency matrix of the RGG and provide an upper bound for the approximation error.

## 7.3. Data Analysis and Learning

**Participants:** Konstantin Avrachenkov, Maximilien Drevet, Giovanni Neglia, Chuan Xu.

### 7.3.1. Almost exact recovery in label spreading

In semi-supervised graph clustering setting, an expert provides cluster membership of few nodes. This little amount of information allows one to achieve high accuracy clustering using efficient computational procedures. Our main goal is to provide a theoretical justification why the graph-based semi-supervised learning works very well. Specifically, for the Stochastic Block Model in the moderately sparse regime, in



[34] K. Avrachenkov and M. Dreveton have proved that popular semi-supervised clustering methods like Label Spreading achieve asymptotically almost exact recovery as long as the fraction of labeled nodes does not go to zero and the average degree goes to infinity.

### 7.3.2. *Similarities, kernels and proximity measures on graphs*

In [13], K. Avrachenkov together with P. Chebotarev (RAS Trapeznikov Institute of Control Sciences, Russia) and D. Rubanov (Google) have analytically studied proximity and distance properties of various kernels and similarity measures on graphs. This helps to understand the mathematical nature of such measures and can potentially be useful for recommending the adoption of specific similarity measures in data analysis.

### 7.3.3. *The effect of communication topology on learning speed*

Many learning problems are formulated as minimization of some loss function on a training set of examples. Distributed gradient methods on a cluster are often used for this purpose. In [47], G. Neglia, together with G. Calbi (Univ Côte d'Azur), D. Towsley, and G. Vardoyan (UMass at Amherst, USA), has studied how the variability of task execution times at cluster nodes affects the system throughput. In particular, a simple but accurate model allows them to quantify how the time to solve the minimization problem depends on the network of information exchanges among the nodes. Interestingly, they show that, even when communication overhead may be neglected, the clique is not necessarily the most effective topology, as commonly assumed in previous works.

In [48] G. Neglia and C. Xu, together with D. Towsley (UMass at Amherst, USA) and G. Calbi (Univ Côte d'Azur) have investigated why the effect of the communication topology on the number of epochs needed for machine learning training to converge appears experimentally much smaller than what predicted by theory.

## 7.4. Game Theory

**Participants:** Eitan Altman, Konstantin Avrachenkov, Mandar Datar, Swapnil Dhamal, Alain Jean-Marie.

### 7.4.1. *Resource allocation: Kelly mechanism and Tullock game*

The price-anticipating Kelly mechanism (PAKM) is one of the most extensively used strategies to allocate divisible resources for strategic users in communication networks and computing systems. It is known in other communities as the Tullock game. The users are deemed as selfish and also benign, each of which maximizes his individual utility of the allocated resources minus his payment to the network operator. E. Altman, A. Reiffers-Masson (IISc Bangalore, India), D. Sadoc-Menasche (UFJR, Brazil), M. Datar, S. Dhamal, C. Touati (Inria Grenoble-Rhone-Alpes) and R. El-Azouzi (CERI/LIA, Univ Avignon) have first applied this type of games to competition in crypto-currency protocols between miners in blockchain [11]. Blockchain is a distributed synchronized secure database containing validated blocks of transactions. A block is validated by special nodes called miners and the validation of each new block is done via the solution of a computationally difficult problem, which is called the proof-of-work puzzle. The miners compete against each other and the first to solve the problem announces it, the block is then verified by the majority of miners in this network, trying to reach consensus. After the propagated block reaches the consensus, it is successfully added to the distributed database. The miner who found the solution receives a reward either in the form of crypto-currencies or in the form of a transaction reward. The authors show that the discrete version of the game is equivalent to a congestion game and thus has an equilibrium in pure strategies.

E. Altman, M. Datar, C. Touati (Inria Grenoble-Rhone-Alpes) and G. Burnside (Nokia Bell Labs) then introduce further constraints on the total amount of resources used and study pricing issues in this constrained game. They show that a normalized equilibrium (in the sense of Rosen) exists which implies that pricing can be done in a scalable way, i.e; prices can be chosen to be independent of the player. A possible way to prove this structure is to show that the utilities are strict diagonal concave (which is an extension to game setting of concavity) which they did in [27].

In [25], Y. Xu, Z. Xiao, T. Ni, X. Wang (all from Fudan Univ, China), J. H. Wang (Tsinghua Univ, China) and E. Altman formulate a non-cooperative Tullock game consisting of a finite amount of benign users and one misbehaving user. The maliciousness of this misbehaving user is captured by his willingness to pay to trade for unit degradation in the utilities of benign users. The network operator allocates resources to all the users via the price-anticipating Kelly mechanism. They present six important performance metrics with regard to the total utility and the total net utility of benign users, and the revenue of network operator under three different scenarios: with and without the misbehaving user, and the maximum. We quantify the robustness of PAKM against the misbehaving actions by deriving the upper and lower bounds of these metrics.

#### **7.4.2. A stochastic game with non-classical information structure**

In [44], V. Kavitha, M. Maheshwari (both from IIT Bombay, India) and E. Altman introduce a stochastic game with partial, asymmetric and non-classical information. They obtain relevant equilibrium policies using a new approach which allows managing the belief updates in a structured manner. Agents have access only to partial information updates, and their approach is to consider optimal open loop control until the information update. The agents continuously control the rates of their Poisson search clocks to acquire the locks, the agent to get all the locks before others would get reward one. However, the agents have no information about the acquisition status of others and will incur a cost proportional to their rate process. The authors solved the problem for the case with two agents and two locks and conjectured the results for a general number of agents. They showed that a pair of (partial) state-dependent time-threshold policies form a Nash equilibrium.

#### **7.4.3. Zero-Sum stochastic games over the field of real algebraic numbers**

In [14], K. Avrachenkov together with V. Ejov (Flinders Univ, Australia), J. Filar and A. Moghaddam (both from Univ of Queensland, Australia) have considered a finite state, finite action, zero-sum stochastic games with data defining the game lying in the ordered field of real algebraic numbers. In both the discounted and the limiting average versions of these games, they prove that the value vector also lies in the same field of real algebraic numbers. Their method supplies finite construction of univariate polynomials whose roots contain these value vectors. In the case where the data of the game are rational, the method also provides a way of checking whether the entries of the value vectors are also rational.

#### **7.4.4. Evolutionary Markov games**

I. Brunetti (CIRED), Y. Hayel (CERI/LIA, Univ Avignon) and E. Altman extend in [59] evolutionary game theory by introducing the concept of individual state. They analyze a particular simple case, in which they associate a state to each player, and suppose that this state determines the set of available actions. They consider deterministic stationary policies and suppose that the choice of a policy determines the fitness of the player and it impacts the evolution of the state. They define the interdependent dynamics of states and policies and introduce the State Policy coupled Dynamics in order to study the evolution of the population profile. They prove the relation between the rest points of the system and the equilibria of the game. Then they assume that the processes of states and policies move with different velocities: this assumption allows them to solve the system and then find the equilibria of the game with two different methods: the singular perturbation method and a matrix approach.

#### **7.4.5. Stochastic replicator dynamics**

In [12], K. Avrachenkov and V.S. Borkar (IIT Bombay, India) have considered a novel model of stochastic replicator dynamics for potential games that converts to a Langevin equation on a sphere after a change of variables. This is distinct from the models of stochastic replicator dynamics studied earlier. In particular, it is ill-posed due to non-uniqueness of solutions, but is amenable to the Kolmogorov selection principle that picks a unique solution. The model allows us to make specific statements regarding metastable states such as small noise asymptotics for mean exit times from their domain of attraction, and quasi-stationary measures. We illustrate the general results by specializing them to replicator dynamics on graphs and demonstrate that the numerical experiments support theoretical predictions.

#### **7.4.6. Stochastic coalitional better-response dynamics for finite games with application to network formation games**

In [57], K. Avrachenkov and V.V. Sing (IIT Delhi, India) have considered coalition formation among players in  $n$ -player finite strategic game over infinite horizon. At each time a randomly formed coalition makes a joint deviation from a current action profile such that at new action profile all the players from the coalition are strictly benefited. Such deviations define a coalitional better-response (CBR) dynamics that is in general stochastic. The CBR dynamics either converges to a  $\mathcal{K}$ -stable equilibrium or becomes stuck in a closed cycle. The authors also assume that at each time a selected coalition makes mistake in deviation with small probability that add mutations (perturbations) into CBR dynamics. They prove that all  $\mathcal{K}$ -stable equilibria and all action profiles from closed cycles, that have minimum stochastic potential, are stochastically stable. A similar statement holds for strict  $\mathcal{K}$ -stable equilibrium. They apply the CBR dynamics to study the dynamic formation of the networks in the presence of mutations. Under the CBR dynamics all strongly stable networks and closed cycles of networks are stochastically stable.

#### **7.4.7. Strong Stackelberg equilibria in stochastic games**

In a joint work with V. Bucarey López (Univ Libre de Bruxelles, Belgium and Inria team INOCS), E. Della Vecchia (Univ Nacional de Rosario, Argentina), and F. Ordóñez (Univ de Chile, Chile), A. Jean-Marie has considered Stackelberg equilibria for discounted stochastic games. The motivation originates in applications of Game Theory to security issues, but the question is of general theoretical and practical relevance. The solution concept of interest is that of Stationary Strong Stackelberg Equilibrium (SSSE) policies: both players apply state feedback policies; the leader announces her strategy and the follower plays a best response to it. Tie breaks are resolved in favor of the leader. The authors provide classes of games where the SSSE exists, and we prove via counterexamples that SSSE does not exist in the general case. They define suitable dynamic programming operators whose fixed points are referred to as Fixed Point Equilibrium (FPE). They show that the FPE and SSSE coincide for a class of games with Myopic Follower Strategy. Numerical examples shed light on the relationship between SSSE and FPE and the behavior of Value Iteration, Policy Iteration and Mathematical programming formulations for this problem. A security application illustrates the solution concepts and the efficiency of the algorithms introduced. The results are presented in [67], [50], [51].

#### **7.4.8. Routing on a ring network**

R. Burra, C. Singh and J. Kuri (IISc Bangalore, India), study in [60] with E. Altman routing on a ring network in which traffic originates from nodes on the ring and is destined to the center. The users can take direct paths from originating nodes to the center and also multihop paths via other nodes. The authors show that routing games with only one and two hop paths and linear costs are potential games. They give explicit expressions of Nash equilibrium flows for networks with any generic cost function and symmetric loads. They also consider a ring network with random number of users at nodes, all of them having same demand, and linear routing costs. They give explicit characterization of Nash equilibria for two cases: (i) General i.i.d. loads and one and two hop paths, (ii) Bernoulli distributed loads. They also analyze optimal routing in each of these cases.

#### **7.4.9. Routing games applied to the network neutrality debate**

The Network Neutrality issue has been at the center of debate worldwide lately. Some countries have established laws so that principles of network neutrality are respected. Among the questions that have been discussed in these debates there is whether to allow agreements between service and content providers, i.e. to allow some preferential treatment by an operator to traffic from some providers (identity-based discrimination). In [63], A. Reiffers-Masson (IISc Bangalore), Y. Hayel, T. Jimenez (CERI/LIA, Univ Avignon) and E. Altman, study this question using models from routing games.

#### **7.4.10. Peering vs transit: A game theoretical model for autonomous systems connectivity**

G. Accongiagioco (IMT, Italy), E. Altman, E. Gregori (Institute of Informatics and Telematics, Univ Pisa) and Luciano Lenzini (Dipartimento di Informatica, Univ Pisa) propose a model for network optimization in a non-cooperative game setting with specific reference to the Internet connectivity. The model describes the

decisions taken by an Autonomous System when joining the Internet. They first define a realistic model for the interconnection costs incurred; then they use this cost model to perform a game theoretic analysis of the decisions related to link creation and traffic routing, keeping into account the peering/transit dichotomy. The proposed model does not fall into the standard category of routing games, hence they devise new tools to solve it by exploiting specific properties of the game. They prove analytically the existence of multiple equilibria.

#### **7.4.11. Altruistic behavior and evolutionary games**

Within some species like bees or ants, the one who interacts is not the one who reproduces. This implies that the Darwinian fitness is related to the entire swarm and not to a single individual and thus, standard Evolutionary Game models do not apply to these species. Furthermore, in many species, one finds altruistic behaviors, which favors the group to which the playing individual belongs, but which may hurt the single individual. In [58], [62], I. Brunetti (CIRED), R. El-Azouzi, M. Haddad, H. Gaiech, Y. Hayel (LIA/CERI, Univ Avignon) and E. Altman define evolutionary games between group of players and study the equilibrium behavior as well as convergence to equilibrium.

### **7.5. Applications in Telecommunications**

**Participants:** Eitan Altman, Konstantin Avrachenkov, Giovanni Neglia.

#### **7.5.1. Elastic cloud caching services**

In [37], G. Neglia, together with D. Carra (Univ of Verona, Italy) and P. Michiardi (Eurecom), has considered in-memory key-value stores used as caches, and their elastic provisioning in the cloud. The cost associated to such caches not only includes the storage cost, but also the cost due to misses: in fact, the cache miss ratio has a direct impact on the performance perceived by end users, and this directly affects the overall revenues for content providers. The goal of their work is to adapt dynamically the number of caches based on the traffic pattern, to minimize the overall costs. They present a dynamic algorithm for TTL caches whose goal is to obtain close-to-minimal costs and propose a practical implementation with limited computational complexity: their scheme requires constant overhead per request independently from the cache size. Using real-world traces collected from the Akamai content delivery network, they show that their solution achieves significant cost savings specially in highly dynamic settings that are likely to require elastic cloud services.

#### **7.5.2. Neural networks for caching**

In [19] G. Neglia, together with V. Fedchenko (Univ Côte d'Azur) and B. Ribeiro (Purdue Univ, USA), has proposed a caching policy that uses a feedforward neural network (FNN) to predict content popularity. This scheme outperforms popular eviction policies like LRU or ARC, but also a new policy relying on the more complex recurrent neural networks. At the same time, replacing the FNN predictor with a naive linear estimator does not degrade caching performance significantly, questioning then the role of neural networks for these applications.

#### **7.5.3. Similarity caching**

In similarity caching systems, a user request for an object  $o$  that is not in the cache can be (partially) satisfied by a similar stored object  $o'$ , at the cost of a loss of user utility. Similarity caching systems can be effectively employed in several application areas, like multimedia retrieval, recommender systems, genome study, and machine learning training/serving. However, despite their relevance, the behavior of such systems is far from being well understood. In [41], G. Neglia, together with M. Garetto (Univ of Turin, Italy) and E. Leonardi (Politechnic of Turin, Italy), provides a first comprehensive analysis of similarity caching in the offline, adversarial, and stochastic settings. They show that similarity caching raises significant new challenges, for which they propose the first dynamic policies with some optimality guarantees. They evaluate the performance of the proposed schemes under both synthetic and real request traces.

#### **7.5.4. Performance evaluation and optimization of 5G wireless networks**

In small cell networks, high mobility of users results in frequent handoff and thus severely restricts the data rate for mobile users. To alleviate this problem, one idea is to use heterogeneous, two-tier network structure where static users are served by both macro and micro base stations, whereas the mobile (i.e., moving) users are served only by macro base stations having larger cells; the idea is to prevent frequent data outage for mobile users due to handoff. In [16], A. Chattopadhyay and B. Błaszczyszyn (Inria DYOGENE team) in collaboration with E. Altman use the classical two-tier Poisson network model with different transmit powers, assume independent Poisson process of static users and doubly stochastic Poisson process of mobile users moving at a constant speed along infinite straight lines generated by a Poisson line process. Using stochastic geometry, they calculate the average downlink data rate of the typical static and mobile (i.e., moving) users, the latter accounted for handoff outage periods. They consider also the average throughput of these two types of users.

In [15], the same authors consider location-dependent opportunistic bandwidth sharing between static and mobile downlink users in a cellular network. Each cell has some fixed number of static users. Mobile users enter the cell, move inside the cell for some time and then leave the cell. In order to provide higher data rate to mobile users, the authors propose to provide higher bandwidth to the mobile users at favourable times and locations, and provide higher bandwidth to the static users in other times. They formulate the problem as a long run average reward Markov decision process (MDP) where the per-step reward is a linear combination of instantaneous data volumes received by static and mobile users, and find the optimal policy. The transition structure of this MDP is not known in general. To alleviate this issue, they propose a learning algorithm based on single timescale stochastic approximation. Also, noting that the unconstrained MDP can be used to solve a constrained problem, they provide a learning algorithm based on multi-timescale stochastic approximation. The results are extended to address the issue of fair bandwidth sharing between the two classes of users. Numerical results demonstrate performance improvement by their scheme, and also the trade-off between performance gain and fairness.

#### **7.5.5. The age of information**

Two decades after the seminal paper on software aging and rejuvenation appeared in 1995, a new concept and metric referred to as the age of information (AoI) has been gaining attention from practitioners and the research community. In the vision paper [46], D.S. Menasche (UFRJ, Brazil), K. Trivedi (Duke Univ, USA) and E. Altman show the similarities and differences between software aging and information aging. In particular, modeling frameworks that have been applied to software aging, such as the semi Markov approach can be immediately applied in the realm of age of information. Conversely, they indicate that questions pertaining to sampling costs associated with the age of information can be useful to assess the optimal rejuvenation trigger interval for software systems.

The demand for Internet services that require frequent updates through small messages has tremendously grown in the past few years. Although the use of such applications by domestic users is usually free, their access from mobile devices is subject to fees and consumes energy from limited batteries. If a user activates his mobile device and is in the range of a publisher, an update is received at the expense of monetary and energy costs. Thus, users face a tradeoff between such costs and their messages aging. It is then natural to ask how to cope with such a tradeoff, by devising aging control policies. An aging control policy consists of deciding, based on the utility of the owned content, whether to activate the mobile device, and if so, which technology to use (WiFi or cellular). In [28] E. Altman, R. El-Azouzi (CERI/LIA, Univ Avignon), D.S. Menasche (UFRJ, Brazil) and Y. Xu (Fudan Univ, China) show the existence of an optimal strategy in the class of threshold strategies, wherein users activate their mobile devices if the age of their podcasts surpasses a given threshold and remain inactive otherwise. The accuracy of their model is validated against traces from the UMass DieselNet bus network. The first version of this paper, among the first to introduce the age of information, appeared already in arXiv on 2010.

#### **7.5.6. Wireless transmission vehicle routing**

The Wireless Transmission Vehicle Routing Problem (WT-VRP) consists of searching for a route for a vehicle responsible for collecting information from stations. The new feature w.r.t. classical vehicle routing is the



possibility of picking up information via wireless transmission, without visiting physically the stations of the network. The WT-VRP has applications in underwater surveillance and environmental monitoring. In [53], L. Flores Luyo and E. Ocaña Anaya (IMCA, Brazil), A. Agra (Univ Aveiro, Brazil), R. Figueiredo (CERI/LIA, Univ Avignon) and E. Altman, study three criteria for measuring the efficiency of a solution and propose a mixed integer linear programming formulation to solve the problem. Computational experiments were done to access the numerical complexity of the problem and to compare solutions under the three criteria proposed.

### 7.5.7. Video streaming in 5G cellular networks

Dynamic Adaptive Streaming over HTTP (DASH) has become the standard choice for live events and on-demand video services. In fact, by performing bitrate adaptation at the client side, DASH operates to deliver the highest possible Quality of Experience (QoE) under given network conditions. In cellular networks, in particular, video streaming services are affected by mobility and cell load variation. In this context, DASH video clients continually adapt the streaming quality to cope with channel variability. However, since they operate in a greedy manner, adaptive video clients can overload cellular network resources, degrading the QoE of other users and suffer persistent bitrate oscillations. In [40] R. El-Azouzi (CERI/LIA, Univ Avignon), A. Sunny (IIT Palakkad, India), L. Zhao (Huazhong Agricultural Univ, China), E. Altman, D. Tsilimantos (Huawei Technologies, France), F. De Pellegrini (CERI/LIA Univ Avignon), and S. Valentin (Darmstadt Univ, Germany) tackle this problem using a new scheduler at base stations, named Shadow-Enforcer, which ensures minimal number of quality switches as well as efficient and fair utilization of network resources.

While most modern-day video clients continually adapt quality of the video stream, they neither coordinate with the network elements nor among each other. Consequently, a streaming client may quickly overload the cellular network, leading to poor Quality of Experience (QoE) for the users in the network. Motivated by this problem, A. Sunny (IIT Palakkad, India), R. El-Azouzi, A. Arfaoui (both from CERI/LIA, Univ Avignon), E. Altman, S. Poojary (BITS, India), D. Tsilimantos (Huawei Technologies, France) and S. Valentin (Darmstadt Univ, Germany) introduce in [24] D-VIEWS — a scheduling paradigm that assures video bitrate stability of adaptive video streams while ensuring better system utilization. The performance of D-views is then evaluated through simulations.

In [39], R. El-Azouzi, K.V. Acharya (ENS Lyon), M. Haddad (CERI/LIA, Univ Avignon), S. Poojary (BITS, India), A. Sunny (IIT Palakkad, India), D. Tsilimantos (Huawei Technologies, France), S. Valentin (Darmstadt Univ, Germany) and E. Altman, develop an analytical framework to compute the Quality-of-Experience (QoE) metrics of video streaming in wireless networks. Their framework takes into account the system dynamics that arises due to the arrival and departure of flows. They also consider the possibility of users abandoning the system on account of poor QoE. Considering the coexistence of multiple services such as video streaming and elastic flows, they use a Markov chain based analysis to compute the user QoE metrics: probability of starvation, prefetching delay, average video quality and bitrate switching. The simulation results validate the accuracy of their model and describe the impact of the scheduler at the base station on the QoE metrics.

### 7.5.8. A learning algorithm for the Whittle index policy for scheduling web crawlers

In [31] K. Avrachenkov and V.S. Borkar (IIT Bombay, India) have revisited the Whittle index policy for scheduling web crawlers for ephemeral content and developed a reinforcement learning scheme for it based on LSPE(0). The scheme leverages the known structural properties of the Whittle index policy.

### 7.5.9. Distributed cooperative caching for VoD with geographic constraints

Consider the caching of video streams in a cellular network in which each base station is equipped with a cache. Video streams are partitioned into multiple substreams and the goal is to place substreams in caches such that the residual backhaul load is minimized. In [36] K. Avrachenkov together with J. Goseling (UTwente, The Netherlands) and B. Serbetci (Eurecom) have studied two coding mechanisms for the substreams: Layered coding (LC) mechanism and multiple description coding (MDC). They develop a distributed asynchronous algorithm for deciding which files to store in which cache to minimize the residual bandwidth, i.e., the cost for downloading the missing substreams of the user's requested video with a certain video quality from the gateway (i.e., the main server). They show that their algorithm converges rapidly. Finally, they show that MDC



partitioning is better than the LC mechanism when the most popular content is stored in caches; however, their algorithm enables to use the LC mechanism as well without any performance loss.

Further, in [35], K. Avrachenkov together with J. Goseling (UTwente, The Netherlands) and B. Serbetci (Eurecom), have considered the same setting as above but maximized the expected utility. The utility depends on the quality at which a user is requesting a file and the chunks that are available. They impose alpha-fairness across files and qualities. Similarly to [36] they have developed a distributed asynchronous algorithm for deciding which chunks to store in which cache.

## 7.6. Applications in Social Networks

**Participants:** Eitan Altman, Swapnil Dhamal, Giovanni Neglia.

### 7.6.1. Utility from accessing an online social network

The retention of users on online social networks has important implications, encompassing economic, psychological and infrastructure aspects. In the framework of our joint team with Brazil (Thanes), G. Neglia, together with E. Hargreaves and D. Menasche (both from UFRJ, Brazil) investigated the following question: what is the optimal rate at which users should access a social network? To answer this question, they have proposed an analytical model to determine the value of an access (VoA) to the social network. In the simple setting they considered, VoA is defined as the chance of a user accessing the network and obtaining new content. Clearly, VoA depends on the rate at which sources generate content and on the filtering imposed by the social network. Then, they have posed an optimization problem wherein the utility of users grows with respect to VoA but is penalized by costs incurred to access the network. Using the proposed framework, they provide insights on the optimal access rate. Their results are parameterized using Facebook data, indicating the predictive power of the approach. This research activity led to two publications in 2019 [49], [43].

Last year, the same researchers, together with E. Altman, A. Reiffers-Masson (IISc, India), and the journalist C. Agosti (Univ of Amsterdam, Netherlands), have worked on Facebook News Feed personalization algorithm. The publication [21] complete that line of work described in NEO's 2018 technical report.

### 7.6.2. Optimal investment strategies for competing camps in a social network

S. Dhamal, W. Ben-Ameur (Telecom SudParis), T. Chahed (Telecom SudParis), and E. Altman have studied the problem of optimally investing in nodes of a social network in [17], wherein two camps attempt to maximize adoption of their respective opinions by the population. Several settings are analyzed, namely, when the influence of a camp on a node is a concave function of its investment on that node, when one of the camps has uncertain information regarding the values of the network parameters, when a camp aims at maximizing competitor's investment required to drive the overall opinion of the population in its favor, and when there exist common coupled constraints concerning the combined investment of the two camps on each node. Extensive simulations are conducted on real-world social networks for all the considered settings.

S. Dhamal, W. Ben-Ameur (Telecom SudParis), T. Chahed (Telecom SudParis), and E. Altman have studied a two-phase investment game for competitive opinion dynamics in social networks, in [18]. The existence of Nash equilibrium and its polynomial time computability is shown under reasonable assumptions. A simulation study is conducted on real-world social networks to quantify the effects of the initial biases and the weigh attributed by nodes to their initial biases, as well as that of a camp deviating from its equilibrium strategy. The study concludes that, if nodes attribute high weight to their initial biases, it is advantageous to have a high investment in the first phase, so as to effectively influence the biases to be harnessed in the second phase.

### 7.6.3. Extending the linear threshold model

S. Dhamal has proposed a generalization of the linear threshold model to account for multiple product features, in [38]. An integrated framework is presented for product marketing using multiple channels: mass media advertisement, recommendations using social advertisement, and viral marketing using social networks. An approach for allocating budget among these channels is proposed.

#### **7.6.4. Public retention in Youtube**

There exist many aspects involved in a video turning viral on YouTube. These include properties of the video such as the attractiveness of its title and thumbnail, the recommendation policy of YouTube, marketing and advertising policies and the influence that the video's creator or owner has in social networks. E. Altman and T. Jimenez (CERI/LIA, Univ Avignon), study in [29] audience retention measurements provided by YouTube to video creators, which may provide valuable information for improving the videos and for better understanding the viewers' potential interests in them. They then study the question of when is a video too long and can gain from being shortened. They examine consistency between several existing audience retention measures. They end in a proposal for a new audience retention measure and identify its advantages.

#### **7.6.5. The medium selection game**

F. Lebeau (ENS Lyon), C. Touati (Inria Grenoble-Rhone-Alpes), E. Altman and N. Abuzainab (Virginia Tech, USA) consider in [45] competition of content creators in routing their content through various media. The routing decisions may correspond to the selection of a social network (e.g. twitter versus facebook or linkedin) or of a group within a given social network. The utility for a player to send its content to some medium is given as the difference between the dissemination utility at this medium and some transmission cost. The authors model this game as a congestion game and compute the pure potential of the game. In contrast to the continuous case, they show that there may be various equilibria. They show that the potential is M-concave which allows them to characterize the equilibria and to propose an algorithm for computing it. They then introduce a learning mechanism which allows them to give an efficient algorithm to determine an equilibrium. They finally determine the asymptotic form of the equilibrium and discuss the implications on the social medium selection problem.

### **7.7. Applications to Environmental Issues**

**Participant:** Alain Jean-Marie.

#### **7.7.1. Sustainable management of water consumption**

Continuing a series of game-theoretic studies on sustainable management of water resources, A. Jean-Marie, jointly with T. Jimenez (CERI/LIA, Univ Avignon) and M. Tidball (INRA), consider in [54] the basic groundwater exploitation problem, in the case where agents (farmers) have incomplete information about other agents' profit functions and about pumping cost functions. Farmers behave more or less myopically. The authors analyze two models where they assume that each agent relies on simple beliefs about the other agents' behavior. In a first model, a variation of their own extraction has a first order linear effect on the extractions of others. In a second model, agents consider that extraction of the others players is a proportion of the available water. Farmers' beliefs are updated through observations of the resource level over time. The paper also considers two models with a myopic feature and no learning. In the first one, agents do not know the profit function of the other agents and cost is announced before extraction. In the second one agents know the profit function of the other player and cost is announced after extraction. In this last case agents play a Nash equilibrium. The four behaviors are compared from the economic and environmental points of view.

#### **7.7.2. Pollution permit trading**

In a joint work with K. Fredj (Univ of Northern British Columbia, Canada), G. Martín-Herrán (Univ Valladolid, Spain) and Mabel Tidball (INRA), A. Jean-Marie investigated in [20] the strategic behaviour of two countries or firms that minimize costs facing emission standards. Emission standards can be reached through emission reduction, banking or borrowing, and emission trading in a given and fixed planning horizon. The authors extend classical models with: the introduction of transaction costs in tradeable emission markets on the one hand, and using a dynamic game setting, on the other hand. They analyze the case with and without transaction costs and the case with and without discount rate. They characterize socially optimal solutions and Nash equilibria in each case and, depending on the initial allocation, characterize the buyer and seller in the emission trading market. The main findings prove that the agents' equilibrium is not efficient when transaction costs are positive.

## PRIVATICS Project-Team

### 6. New Results

#### 6.1. Differential Inference Testing

**Participant:** Claude Castelluccia.

In order to protect individuals' privacy, data have to be "well-sanitized" before sharing them, i.e. one has to remove any personal information before sharing data. However, it is not always clear when data shall be deemed well-sanitized. In [10], we argue that the evaluation of sanitized data should be based on whether the data allows the inference of sensitive information that is specific to an individual, instead of being centered around the concept of re-identification. We propose a framework to evaluate the effectiveness of different sanitization techniques on a given dataset by measuring how much an individual's record from the sanitized dataset influences the inference of his/her own sensitive attribute. Our intent is not to accurately predict any sensitive attribute but rather to measure the impact of a single record on the inference of sensitive information. We demonstrate our approach by sanitizing two real datasets in different privacy models and evaluate/compare each sanitized dataset in our framework.

#### 6.2. Analyse des impacts de la reconnaissance faciale - Quelques éléments de méthode (in French)

**Participants:** Claude Castelluccia, Daniel Le Métayer.

Significant technical progress has been made in recent years in the field of image processing, in particular in facial recognition. The deployments and experiments of this type of systems are more and more numerous. However, opinions differ on their use, especially in public space. Noting the lack of consensus on a technology that can have a significant impact on society, many organizations have alerted public opinion and asked for a public debate on the subject. We believe that such a debate is indeed necessary. However, for it to be truly productive, it is necessary to be able to confront the arguments in a rigorous manner while avoiding, as far as possible, the preconceptions, and by distinguishing established facts from assumptions or opinions. The purpose of this document [14] is precisely to help put the terms of the debate on solid foundations. It is therefore not a question here of taking a position on facial recognition in general nor of providing an exhaustive review of its applications but of proposing elements of method, illustrated by a few examples. We first present a quick overview of the applications of facial recognition before detailing the reasons that make it a particularly sensitive subject, emphasizing in particular the risks linked to a possible generalization of its use. We then present an incremental, comparative and rigorous approach to analyze the impacts of a facial recognition system.

#### 6.3. Towards a generic framework for black-box explanation methods

**Participants:** Daniel Le Métayer, Clément Hénin.

Explainability has generated increased interest during the last decade because the most accurate ML techniques often lead to opaque Algorithmic Decision Systems (ADS) and opacity is a major source of mistrust. Indeed, even if explanations are not a panacea, they can play a key role, not only to enhance trust in the system, but also to allow its users to better understand its outputs and therefore to make a better use of it. In addition, they are necessary to make it possible to challenge the decisions resulting from an ADS. Explanations can take different forms, they can target different types of users and different types of methods can be used to produce them. Our work on this topic [15] focuses on a category of methods, called "black-box", that do not make any assumption about the availability of the code of the ADS or its implementation techniques. Our first contribution is to bring to light a common structure for Black-box Explanation Methods and to define a generic framework allowing us to compare and classify different approaches. This framework consists of three components, called respectively

Sampling, Generation and Interaction. Beyond its interest as a systematic presentation of the state of the art, we believe that this framework can also provide new insights for the design of new explanation systems. For example, it may suggest new combinations of Sampling and Generation components or criteria to choose the most appropriate combination to produce a given type of explanation.

#### **6.4. A generic information and consent framework for the IoT**

**Participants:** Daniel Le Métayer, Mathieu Cunche, Victor Morel.

The development of the Internet of Things (IoT) raises specific privacy issues especially with respect to information and consent. People are generally unaware of the devices collecting data about them and do not know the organizations operating them. Solutions such as stickers or wall signs are not effective information means in most situations. As far as consent is concerned, individuals do not have simple means to express and communicate it to the entities collecting data. Furthermore, the devices used to collect data in IoT environments have scarce resources; some of them do not have any user interface, are battery-operated or operate passively. The Working Party 29 (now “European Data Protection Board”) advocates the design of new consent mechanisms, such as “privacy proxies”, on the devices themselves. Starting from their recommendations, we have defined general requirements that have to be met to ensure that information and consent are managed in a manner that is satisfactory both for data subjects and for data controllers. We have shown in [8] how these requirements can be implemented in different situations, in particular through declaration registers and beacons. Depending on the context and the types of devices involved, not all technical options are always possible. In order to provide guidance to IoT system designers, we have outlined the main choice factors in the design space and illustrated the framework with several challenging case studies. We have also implemented a Proof of Concept prototype implementation of these techniques.

#### **6.5. Analysis of privacy policies to enhance informed consent**

**Participant:** Daniel Le Métayer.

A privacy policy language must meet a number of requirements to be able to express the valid consent of the data subject for the processing of their personal data. For example, under the GDPR, valid consent must be freely given, specific, informed and unambiguous. Therefore, the language must be endowed with a formal semantics in order to avoid any ambiguity about the meaning of a privacy policy. However, the mere existence of a semantics does not imply that DSs properly understand the meaning of a policy and its potential consequences. One way to enhance the understanding of the data subjects is to provide them information about the potential risks related to a privacy policy. This is in line with Recital 39 of the GDPR which stipulates that data subjects should be “made aware of the risks, rules, safeguards and rights in relation to the processing of personal data and how to exercise their rights in relation to such processing”. To address this need, we have defined a language in [11], called PILOT, meeting these requirements and shown its benefits to define precise privacy policies and to highlight the associated privacy risks. In order to automatically answer questions related to privacy risks, we use the verification tool SPIN and the modeling language PROMELA. Risk properties are encoded in Linear Temporal Logic properties that can be automatically checked by SPIN.

#### **6.6. Understanding algorithmic decision-making: Opportunities and challenges, Study for the European Parliament (STOA)**

**Participants:** Claude Castelluccia, Daniel Le Métayer.

Algorithms are far from being a recent invention but they are increasingly involved in systems used to support decision making. Algorithmic Decision Systems (ADS) often rely on the analysis of large amounts of personal data to infer correlations or, more generally, to derive information deemed useful to make decisions. Humans may have a role of varying degree in the decision making and may even be completely out of the loop in entirely automated systems. In many situations, the impact of the decision on people can be significant: access to credit, employment, medical treatment, judicial sentences, etc. Entrusting ADS to make or to influence such decisions raises a variety of issues that differ in nature such as ethical, political, legal, technical, etc. and great care must be taken to analyse and address these issues. If they are neglected, the expected benefits of these systems may be offset by the variety of risks for individuals (discrimination, unfair practices, loss of autonomy, etc.), the economy (unfair practices, limited access to markets, etc.) and society as a whole (manipulation, threat to democracy, etc.).

We have written a report for the European Parliament reviewing the opportunities and risks related to the use of ADS. We present existing options to reduce these risks and explain their limitations. We sketch some recommendations to benefit from the tremendous possibilities of ADS while limiting the risks related to their use. Beyond providing an up-to-date and systematic review of the situation, the report gives a precise definition of a number of key terms and an analysis of their differences. This helps clarify the debate. The main focus of the report is the technical aspects of ADS. However, other legal, ethical and social dimensions are considered to broaden the discussion.

## 6.7. Saving Private Addresses: An Analysis of Privacy Issues in the Bluetooth-Low-Energy Advertising Mechanism

**Participants:** Mathieu Cunche, Guillaume Celiosa.

The Bluetooth Low Energy (BLE) protocol is being included in a growing number of connected objects such as fitness trackers and headphones. As part of the service discovery mechanism of BLE, devices announce themselves by broadcasting radio signals called advertisement packets that can be collected with off-the-shelf hardware and software. To avoid the risk of tracking based on those messages, BLE features an address randomization mechanism that substitutes the device address with random temporary pseudonyms, called Private addresses. We analyze the privacy issues associated with the advertising mechanism of BLE, leveraging a large dataset of advertisement packets collected in the wild. First, we identified in [7] that some implementations fail at following the BLE specifications on the maximum lifetime and the uniform distribution of random identifiers. Furthermore, we found that the payload of the advertisement packet can hamper the randomization mechanism by exposing counters and static identifiers. In particular, we discovered that advertising data of Apple and Microsoft proximity protocols can be used to defeat the address randomization scheme. Finally, we discuss how some elements of advertising data can be leveraged to identify the type of device, exposing the owner to inventory attacks

## 6.8. Fingerprinting Bluetooth-Low-Energy Devices Based on the Generic Attribute Profile

**Participants:** Mathieu Cunche, Guillaume Celiosa.

Bluetooth Low Energy (BLE) is a short range wireless technology included in many consumer devices such as smartphones, earphones and wristbands. As part of the Attribute (ATT) protocol, discoverable BLE devices expose a data structure called Generic Attribute (GATT) profile that describes supported features using concepts of services and characteristics. This profile can be accessed by any device in range and can expose users to privacy issues. We study how the GATT profile can be used to create a fingerprint that can be exploited to circumvent anti-tracking features of the BLE standard (i.e. MAC address randomization). Leveraging a dataset of more than 13000 profiles, we analyze the potential of this fingerprint and show that it can be used to uniquely identify a number of devices. We also shed light in [6] on several issues where GATT profiles can be mined to infer sensitive information that can impact privacy of users. Finally, we suggest solutions to mitigate those issues.

## 6.9. Privacy implications of switching ON a light bulb in the IoT world

**Participants:** Vincent Roca, Mathieu Thiery.

The number of connected devices is increasing every day, creating smart homes and shaping the era of the Internet of Things (IoT), and most of the time, end-users are unaware of their impacts on privacy. We analyze in [23] the ecosystem around a Philips Hue smart white bulb in order to assess the privacy risks associated to the use of different devices (smart speaker or button) and smartphone applications to control it. We show that using different techniques to switch ON or OFF this bulb has significant consequences regarding the actors involved (who mechanically gather information on the user's home) and the volume of data sent to the Internet (we measured differences up to a factor 100, depending on the control technique we used). Even when the user is at home, these data flows often leave the user's country, creating a situation that is neither privacy friendly (and the user is most of the time ignorant of the situation), nor sovereign (the user depends on foreign actors), nor sustainable (the extra energetic consumption is far from negligible). We therefore advocate a complete change of approach, that favors local communications whenever sufficient.

## 6.10. Security Analysis of Subject Access Request Procedures How to authenticate data subjects safely when they request for their data

**Participants:** Cédric Lauradoux, Coline Boniface.

With the GDPR in force in the EU since May 2018, companies and administrations need to be vigilant about the personal data they process. The new regulation defines rights for data subjects and obligations for data controllers but it is unclear how subjects and controllers interact concretely. In [4], we try to answer two critical questions: is it safe for a data subject to exercise the right of access of her own data? When does a data controller have enough information to authenticate a data subject? To answer these questions, we have analyzed recommendations of Data Protection Authorities and authentication practices implemented in popular websites and third-party tracking services. We observed that some data controllers use unsafe or doubtful procedures to authenticate data subjects. The most common flaw is the use of authentication based on a copy of the subject's national identity card transmitted over an insecure channel. We define how a data controller should react to a subject's request to determine the appropriate procedures to identify the subject and her data. We provide compliance guidelines on data access response procedures.

## 6.11. Plausible Deniability for Practical Privacy-Preserving Live Streaming

**Participant:** Antoine Boutet.

Video consumption is one of the most popular Internet activities worldwide. The emergence of sharing videos directly recorded with smartphones raises important privacy concerns. In this work we propose P3LS, the first practical privacy-preserving peer-to-peer live streaming system. To protect the privacy of its users, P3LS relies on  $k$ -anonymity when users subscribe to streams, and on plausible deniability for the dissemination of video streams. Specifically, plausible deniability during the dissemination phase ensures that an adversary is never able to distinguish a user's stream of interest from the fake streams from a statistical analysis (i.e., using an analysis of variance). We exhaustively evaluate P3LS and show that adversaries are not able to identify the real stream of a user with very high confidence. Moreover, P3LS consumes 30% less bandwidth than the standard  $k$ -anonymity approach where nodes fully contribute to the dissemination of  $k$  streams.

## 6.12. Protecting motion sensor data against sensitive inferences through an adversarial network approach

**Participants:** Antoine Boutet, Théo Jourdan.



With the widespread development of the quantified self movement, more and more motion sensor data are captured and transmitted through the intermediary of smartphones. However, granting to applications a direct access to sensor data expose users to many privacy risks, including in particular the possibility of inferring their activities and transportation mode to more sensitive inferences such as their demographic attributes or even mobility deficiency. In this work, we propose a privacy-preserving scheme to protect sensor data for activity recognition while at the same time preventing unwanted sensitive inferences on specific information. To achieve this objective, we leverage on the powerful framework of generative adversarial networks (GANs) to sanitize the sensor data. More precisely in our framework three neural networks are jointly trained, a generator that aim at sanitizing the data given at input as well two discriminators that try to infer respectively the sensitive attributes and the current activity of the user. By letting these neural networks compete against each other, the mechanism improves the protection while providing a good accuracy in terms of activity recognition and limiting sensitive inferences on specified attributes. Preliminary results demonstrate that the approach is promising in terms of achieving a good utility-privacy trade-off.

### **6.13. Inria white book on Cybersecurity: Current challenges and Inria's research directions**

**Participant:** Vincent Roca.

This book provides an overview of research areas in cybersecurity, illustrated by contributions from Inria teams. The first step in cybersecurity is to identify threats and define a corresponding attacker model. Threats, including malware, physical damage or social engineering, can target the hardware, the network, the operating system, the applications, or the users themselves.

Then, detection and protection mechanisms must be designed to defend against these threats. One of the core mechanisms is cryptography, in order to ensure the confidentiality and integrity of data. These primitives must be the object of continuous cryptanalysis to ensure the highest level of security. However, secure cryptographic primitives alone are not sufficient for secure communications and services: cryptographic protocols, implementing richer interactions on top of the primitives, are needed. These protocols are distributed systems. Ensuring that they achieve their goals in the presence of an adversary requires the use of formal verification techniques, which have been extremely successful in this field.

Additional security services, such as authentication and access control, are needed to enforce a security policy. These security services, usually provided by the operating system or the network devices, can themselves be attacked and sometimes bypassed. Therefore, activities on the information system are monitored in order to detect any violation of the security policy. Finally, as attacks can spread extremely fast, the system must react automatically or at least reconfigure itself to avoid propagating attacks.

Privacy has also become an intrinsic part of cybersecurity. Privacy has its own properties, techniques, and methodology. Moreover, the study of privacy often requires to take legal, economical, and sociological aspects into account.

All these security mechanisms need to be carefully integrated in security-critical applications. These applications include traditional safety-critical applications that are becoming increasingly connected and therefore more vulnerable to security attacks, as well as new infrastructures running in the cloud or connected to a multitude of Things (IoT).

### **6.14. Inspect what your location history reveals about you - Raising user awareness on privacy threats associated with disclosing his location data**

**Participant:** Antoine Boutet.

Location is one of the most extensively collected personal data on mobile by applications and third-party services. However, how the location of users is actually processed in practice by the actors of targeted advertising ecosystem remains unclear. Nonetheless, these providers have a strong incentive to create very detailed profile of users to better monetize the collected data. End users are usually not aware about the strength and wide range of inference that can be performed from their mobility traces. In this work, users interact with a web-based application to inspect their location history and to discover the inferential power of this kind of data. Moreover to better understand the possible countermeasures, users can apply a sanitization to protect their data and visualize the impact on both the mobility traces and the associated inferred information. The objective of this work is to raise the user awareness on the profiling capabilities and the privacy threats associated with disclosing his location data as well as how sanitization mechanisms can be efficient to mitigate these privacy risks. In addition, by collecting users feedbacks on the personal information revealed and the usage of a geosanitization mechanism, we hope that this work will also be useful to constitute a new and valuable dataset on users perceptions on these questions.

## **6.15. Pseudonymisation techniques and best practices**

**Participant:** Cédric Lauradoux.

This ENISA report explores further the basic notions of pseudonymisation, as well as technical solutions that can support implementation in practice. Starting from a number of pseudonymisation scenarios, the report defines first the main actors that can be involved in the process of pseudonymisation along with their possible roles. It then analyses the different adversarial models and attacking techniques against pseudonymisation, such as brute force attack, dictionary search and guesswork. Moreover, it presents the main pseudonymisation techniques and policies available today.

## STAMP Project-Team

### 6. New Results

#### 6.1. Hol-Light and Elpi

**Participants:** Enrico Tassi, Marco Maggesi [University of Florence, Italy].

We implemented an elaborator for HOL-Light in Elpi. In particular the new elaborator supports coercions and overloaded notations for algebraic structures.

#### 6.2. Generating equality tests for inductive types

**Participant:** Enrico Tassi.

We show how to derive in a modular fashion equality tests for a wide variety of inductive type definitions. This makes an instrumental use of parametricity. This work has been published in an international conference [10]. This is also an interesting case study for the Elpi language [2].

#### 6.3. Re-designing the state machine of Coq

**Participants:** Enrico Tassi, Maxime Dénès.

We redesigned the state machine of Coq to improve its support for LSP-based user interfaces<sup>0</sup>. In particular, we decoupled the representation of the document as seen by the User-Interface and the structured document as used by the STM to decide what to compute and how (in which order).

#### 6.4. Formal proofs on session types

**Participants:** Enrico Tassi, Cinzia Di Giusto [University of Nice], Marco Giunti [New University of Lisbon], Kirstin Peters [University of Darmstadt], Antonio Ravara [New University of Lisbon].

We formalized in Coq and Isabelle a linear, monadic Pi calculus, its labelled transition system, and type system. We proved the properties of subject reduction and absence of linearity violation. These are based on De Bruijn levels and Nominals with the objective of comparing the approaches and provide automation for recurrent goals. This is done in Project PROSE (Provers for Sessions).

#### 6.5. Formal proofs of an axiomatization of graphs with tree-width two

**Participants:** Christian Doczkal, Damien Pous [CNRS, ENS de Lyon].

We finished the formalization of a completeness proof for an axiomatization of graphs of treewidth at most two in Coq+MathComp. This work was submitted for publication in a conference [11]. We are also revising the article presenting our proof of the Minor-Exclusion property for Treewidth-Two graphs [15] for publication in a journal. Most of the formal proofs are available from the following web-site <https://perso.ens-lyon.fr/damien.pous/covece/graphs/>.

#### 6.6. Formal study of double-word arithmetic algorithms

**Participants:** Laurence Rideau, Jean-Michel Muller [CNRS, ENS de Lyon].

We finished the formalization of double-word arithmetic algorithms, described in the article *Tight and rigorous error bounds for basic building blocks of double-word arithmetic* [16].

---

<sup>0</sup>LSP stands for Language Server Protocol

Thanks to the formalization, errors were found in the proofs, but the stated results (correction of algorithms and error limits) were proven correct. On the other hand, for the purposes of this formalization, we had to develop a more general version of the proof of the Fast2Sum algorithm, which should soon be integrated into the Floccq library.

An article describing this work of formalisation is being written.

## 6.7. Approximations using Chebyshev polynomials

**Participants:** Laurent Théry, Florian Steinberg [Inria Saclay, Toccata project-team].

Florian Steinberg and Laurent Théry have been working on polynomial approximations using Chebyshev polynomials. This work has been presented at the ANR FastRelax final meeting (Lyon, June 2019) and is available as a library at <https://github.com/FlorianSteinberg/Cheby>.

## 6.8. Formalizing computational analysis

**Participants:** Laurent Théry, Florian Steinberg [Inria Saclay, Toccata project-team], Holger Thies [Kyushu University, Fukuoka].

Florian Steinberg, Holger Thies, and Laurent Théry have been working on formalizing computational analysis. This work is described in a paper to be submitted for publication [13]. A shorter version was published in a conference [9].

## 6.9. Formal study of probabilistic programs

**Participants:** Cécile Baritel-Ruet, Benjamin Grégoire, José Bacelar Almeida [INESC TEC], Manuel Barbosa [INESC TEC], Gilles Barthe [IMDEA], Sonia Belaïd [CryptoExpert], Matthew Campagna [AWS], Gaëtan Cassiers [UCL], Sunjay Cauligi [UC San Diego], Ernie Cohen [AWS], François Dupressoir [University of Surrey], Pierre-Alain Fouque [Université Rennes 1], Charlie Jacomme [LSV], Steve Kremer [Inria Nancy Grand-Est, PESTO project Team], Adrien Koutsos [LSV], Vincent Laporte [Inria], Tiago Oliveira [INESC TEC], Vitor Pereira [INESC TEC], Bernardo Portela [INESC TEC], Alley Stoughton [Boston University], François-Xavier Standaert [UCL], Deian Stefan [UC San Diego], Pierre-Yves Strub [Ecole Polytechnique], Serdar Tasiran [AWS].

We provide two different tools:

- EasyCrypt (see <http://www.easycrypt.info/>) is a toolset for reasoning about relational properties of probabilistic computations with adversarial code. Its main application is the construction and verification of game-based cryptographic proofs.
- Jasmin (see <https://github.com/jasmin-lang/jasmin>) is certified compiler to generate high-speed and high-assurance cryptographic code.

## 6.10. Security of a key management service

**Participants:** Benjamin Grégoire, José Bacelar Almeida [INESC TEC], Manuel Barbosa [INESC TEC], Gilles Barthe [IMDEA], Matthew Campagna [AWS], Vitor Pereira [INESC TEC], Bernardo Portela [INESC TEC], Pierre-Yves Strub [Ecole Polytechnique], Serdar Tasiran [AWS].

We have developed a machine-checked proof of security for the domain management protocol of Amazon Web Services' KMS (Key Management Service) a critical security service used throughout AWS and by AWS customers. Domain management is at the core of AWS KMS; it governs the toplevel keys that anchor the security of encryption services at AWS. We show that the protocol securely implements an ideal distributed encryption mechanism under standard cryptographic assumptions. The proof is machine-checked in the EasyCrypt proof assistant and is the largest EasyCrypt development to date. This work corresponds to a contract with AWS and has been published in a major computer security conference [3].

### 6.11. High-assurance and high-speed SHA-3

**Participants:** Cécile Baritel-Ruet, Benjamin Grégoire, José Bacelar Almeida [INESC TEC], Manuel Barbosa [INESC TEC], Gilles Barthe [IMDEA], François Dupressoir [University of Surrey], Vincent Laporte [Inria], Tiago Oliveira [INESC TEC], Alley Stoughton [Boston University], Pierre-Yves Strub [Ecole Polytechnique].

We have developed a high-assurance and high-speed implementation of the SHA-3 hash function. Our implementation is written in the Jasmin programming language, and is formally verified for functional correctness, provable security and timing attack resistance in the EasyCrypt proof assistant. Our implementation is the first to achieve simultaneously the four desirable properties (efficiency, correctness, provable security, and side-channel protection) for a non-trivial cryptographic primitive. Concretely, our mechanized proofs show that:

1. The SHA-3 hash function is indiffereniable from a random oracle, and thus is resistant against collision, first and second preimage attacks;
2. The SHA-3 hash function is correctly implemented by a vectorized x86 implementation.

Furthermore, the implementation is provably protected against timing attacks in an idealized model of timing leaks. The proofs include new EasyCrypt libraries of independent interest for programmable random oracles and modular indiffereniability proofs. This work has been published at an international conference [4].

### 6.12. A domain-specific language for timing sensitive computation

**Participants:** Benjamin Grégoire, Sunjay Cauligi [UC San Diego], Gilles Barthe [IMDEA], Deian Stefan [UC San Diego].

Real-world cryptographic code is often written in a subset of C intended to execute in constant-time, thereby avoiding timing side channel vulnerabilities. This C subset eschews structured programming as we know it: if-statements, looping constructs, and procedural abstractions can leak timing information when handling sensitive data. The resulting obfuscation has led to subtle bugs, even in widely-used high profile libraries like OpenSSL. To address the challenge of writing constant-time cryptographic code, we have participate to the development of FaCT, a crypto DSL that provides high-level but safe language constructs. The FaCT compiler uses a secrecy type system to automatically transform potentially timing-sensitive high-level code into low-level, constant-time LLVM bitcode. While the language and the type system has been developed by our collaborator, we have formalized the constant-time transformation. We have performed an empirical evaluation that uses FaCT to implement core crypto routines from several open-source projects including OpenSSL, libsodium, and curve25519-donna. Our evaluation shows that FaCT's design makes it possible to write readable, high-level cryptographic code, with efficient, constant-time behavior. This work has been published at an international conference [7].

### 6.13. Proving equivalence between probabilistic programs

**Participants:** Benjamin Grégoire, Gilles Barthe [IMDEA], Steve Kremer [Inria Nancy Grand-Est, PESTO project Team], Pierre-Yves Strub [Ecole Polytechnique].

We have developed principled methods for proving equivalence between probabilistic programs that operate over finite fields and related algebraic structures. We have focused on three essential properties: program equivalence, information flow, and uniformity. We give characterizations of these properties based on deducibility and other notions from symbolic cryptography. We use (sometimes improve) tools from symbolic cryptography to obtain decision procedures or sound proof methods for program equivalence, information flow, and uniformity. A partial implementation of our approach is integrated in EasyCrypt and in MaskVerif. This work has been published at an international conference [6].

### 6.14. MaskVerif: automated verification of higher-order masking in presence of physical defaults

**Participants:** Benjamin Grégoire, Gilles Barthe [IMDEA], Sonia Belaïd [CryptoExpert], Gaëtan Cassiers [UCL], Pierre-Alain Fouque [Université Rennes 1], François-Xavier Standaert [UCL].

Power and electromagnetic based side-channel attacks are serious threats against the security of cryptographic embedded devices. In order to mitigate these attacks, implementations use countermeasures, among which masking is currently the most investigated and deployed choice. Unfortunately, commonly studied forms of masking rely on underlying assumptions that are difficult to satisfy in practice. This is due to physical defaults, such as glitches or transitions, which can recombine the masked data in a way that concretely reduces an implementation's security. We have developed and implemented an automated approach for verifying security of masked implementations in presence of physical defaults (glitches or transitions). Our approach helps to recover the main strengths of masking: rigorous foundations, composability guarantees, automated verification under more realistic assumptions. This work contributes to demonstrate the benefits of language-based approaches (specifically probabilistic information flow) for masking. This work was published at an international conference [5].

### 6.15. Frame type theory

**Participants:** Cyril Cohen, Assia Mahboubi [Inria Rennes Bretagne Atlantique, Gallinette project-team], Xavier Montillet [University of Nantes].

Writing modular programs in proof assistants is notoriously difficult. A significant literature and implementation effort is devoted to the topic, with approaches ranging from adding new constructions to the underlying logic, to adding features to the proof assistant. However, all current options (including records, sections and modules) are unsatisfactory in one way or another. In this work in progress we aim at reconciling several options using frames. The central idea is to consider records where some fields do not have a value yet. We will call these generalized records frames, and will say that a field is a definition (resp. abstraction) if it has (resp. does not have) a value. Frames can also be thought of as a reification of the contexts of CiC, as presented in the Coq manual.

### 6.16. Automated refinements on algorithms in Lean

**Participants:** Cyril Cohen, Tobias Grosser [ETH Zurich], Utz Haus [CRAY EMEA Research Lab], Chris Hughes [Imperial college].

We have experimented with Applying manual and automated program refinements techniques to a simple algorithm, in Lean, with Tobias Grosser, Utz Haus and Chris Hughes, in Zürich. Experiments on this topic are available at the following address <https://github.com/ChrisHughes24/LP>.

This work also includes investigations on parametricity in Lean as visible at the following address <https://github.com/CohenCyril/mathlib/tree/param>.

### 6.17. Parametricity in Template Coq

**Participants:** Cyril Cohen, Damien Rouhling, Assia Mahboubi [Inria Rennes Bretagne Atlantique, Gallinette project team], Nicolas Tabareau [Inria Rennes Bretagne Atlantique, Gallinette project team].

We study the implementation of parametricity in Template Coq and improve on the work proposed the article *Equivalence for free!* [17]. This work is available at <https://github.com/CoqHott/parametricity-a-la-carte>.

### 6.18. A hierarchy builder

**Participants:** Kazuhiko Sakaguchi, Cyril Cohen.

We are studying how to generate mathematical structures from their axioms using the high-level language provided by the Coq-Elpi experiment. Ongoing experiments are visible at the following address <https://github.com/math-comp/hierarchy-builder>.



## 6.19. Adding measure theory to mathematical components analysis

**Participants:** Cyril Cohen, Damien Rouhling, Laurence Rideau, Reynald Affeldt [AIST, Japan], Georges Gonthier [Inria Saclay Ile de France, Specfun project team], Marie Kerjean [Inria Rennes Bretagne Atlantique, Gallinette project team], Assia Mahboubi [Inria Rennes Bretagne Atlantique, Gallinette project team], Pierre-Yves Strub [Ecole Polytechnique].

We started extending mathematical components analysis [14] with measure theory and Lebesgue-Stieljes integral. We are taking inspiration from work done on Coquelicot and in the MILC project (DIM-RFSI).

## 6.20. A formal description of exact real arithmetic

**Participants:** Yves Bertot, Nicolas Magaud [University of Strasbourg].

We revisited an old package available in the contributions to the Coq system, where algorithms to perform real number computations were described. This package was using primitives described using axioms. We showed that these axioms were faulty and proposed solutions to salvage the package and make it more safely usable in the future.

## 6.21. Formal study of a triangulation algorithm

**Participant:** Yves Bertot.

We wish to describe a triangulation algorithm in a way that respects both a high level of abstraction and a precise account of pointer manipulations. Using refinements approaches as in CoqEAL, we hope that this can lead to efficient implementation that are derived from the formal description.

## 6.22. Formal study of Voronoi diagrams and Fortune's algorithm

**Participants:** Ahmed Khulaif A Alharbi, Yves Bertot.

Voronoi diagrams are an example of data that can be used to solve problems in robot motion planning. In this experiment, we provided a formal description of Fortune's algorithm to compute such diagrams, together with a framework to animate this algorithm. Formal proofs of correctness will be the next step.

## 6.23. Formal study of a cell-decomposition algorithm

**Participants:** Julien Lamiroy, Yves Bertot.

To solve robot motion planning problems, a simple approach is to decompose the available space into obstacle-free cells and to move from one cell to another only by boundaries that are also obstacle free. We developed a formal description of an algorithm producing this kind of decomposition, with the aim of providing formal proofs of correctness in the long run.

## 6.24. A guide to use Coq for security evaluations

**Participants:** Maxime Dénès, Yves Bertot, Vincent Laporte, Arnaud Fontaine [ANSSI], Thomas Letan [ANSSI].

Common Criteria are an international standard for computer security certification. Evaluations are rated with Evaluation Assurance Levels, from 1 to 7. EAL6 and EAL7 require developers to conduct a formal analysis of their product with respect to certain security properties.

In France, the Certification Body (the entity emitting Common Criteria certificates) is part of the ANSSI (*l'Agence Nationale de la Sécurité des Systèmes d'Information*, also referred to as the French Cybersecurity Agency), and is one of the few emitters of EAL6 and EAL7 certificates.

Coq has already been used to support Common Criteria formal analysis. The ANSSI and Inria have been collaborating on an authoritative document to introduce guidelines and rules for formal analyses supported by Coq, in order to make these developments easier to read and evaluate.

## 6.25. Formalization of the Poincaré disk model in Isabelle

**Participants:** Pierre Boutry, Danijela Simić [University of Belgrade], Filip Marić [University of Belgrade].

The Poincaré disk model is a model that can be shown to satisfy all axioms of Tarski's system of geometry at the exception of the parallel postulate. We developed a formal proof of this fact in the Isabelle system and submitted an article for publication. Reviewers suggested that we add a proof that the postulate of the existence of limiting parallels does hold. This completes neatly the work on this topic, as it allows us to exhibit that the Poincaré disk model is not only a counter-model for the parallel postulate but also a model of hyperbolic geometry. An improved version of the article will be submitted soon.

## 6.26. Integration of the GeoCoq library to Logipedia

**Participants:** Pierre Boutry, Gaspard Ferey [Inria Saclay Ile de France, Deducteam project team].

We have proofs of independence of the parallel postulate for several models of hyperbolic geometry (among which the Poincaré disk model). An objective is to provide formal proofs that these models are actually isomorphic. An issue for this objective is the question of re-usability, because the formal proofs that we have so far exist in the realms of different theorem provers. The Logipedia effort is an attempt to make proofs from different proofs systems work together, by using a tool called Dedukti as a go-between. A particular point is to be able to translate proofs already done in Coq, namely the GeoCoq library, into proofs verifiable by Dedukti. This requires handling tactics based on internal computation (reflective tactics), that we used intensively in our Coq proof. However, handling reflective tactics is currently not well supported by Dedukti. This is our current point of attention.

## 6.27. Performance improvements for a reflective tactic in the GeoCoq library

**Participants:** Pierre Boutry, Benjamin Grégoire, Enrico Tassi.

The GeoCoq library relies on a reflective tactic. It is an interesting topic to understand how to make such a tactic more efficient. A first pass on the algorithm makes that we manage to gain 15% of performance for the whole library and several orders of magnitude on specific subgoals. Another area of the tactic can also be improved by relying on Coq-Elpi.

## 6.28. Mutual interpretability of cartesian planes with Tarski's system of geometry

**Participants:** Pierre Boutry, Cyril Cohen.

A previous result by Pierre Boutry is that cartesian planes over pythagorean ordered fields are mutually interpretable with Tarski's system of geometry without the continuity axiom. This result can be extended by linking cartesian planes over real closed fields and the full Tarski system of geometry, understanding the continuity axiom as an implementation of Dedekind cuts. On the one hand, this requires a new proof that is not already found in the literature, on the other hand, this will result in a verified quantifier elimination procedure for Tarski's system of geometry, thus extending previous work by Cyril Cohen.

## 6.29. Simplification of a constructive version of Tarski's system of geometry

**Participant:** Pierre Boutry.

Our long term project is to show the independence of all thirteen axioms in a variant of Tarski's system of geometry. In the current situation, ten axioms have been checked to be independent using counter-models. Specific questions arise around the continuity axiom and decidability of equality between points. This is related to investigations concerning mutual interpretability with cartesian planes and an alternative system proposed by Michael Beeson.

### **6.30. Formal proofs of Tarjan's strongly connected components algorithm**

**Participants:** Cyril Cohen, Laurent Théry, Ran Chen [Institute of Software, Chinese Academy of Science, Beijing], Jean-Jacques Lévy [Inria Paris,  $\pi.r^2$  project-team], Stephan Merz [Inria Nancy Grand Est, Veridis project-team].

Comparing provers on a formalization of the same problem is always a valuable exercise. In this work, we present the formal proof of correctness of a non-trivial algorithm from graph theory that was carried out in three proof assistants: Why3, Coq, and Isabelle. This was published in an international conference [8].

## Stars Project-Team

## 6. New Results

### 6.1. Introduction

This year Stars has proposed new results related to its three main research axes: (i) perception for activity recognition, (ii) action recognition and (iii) semantic activity recognition.

#### 6.1.1. Perception for Activity Recognition

**Participants:** François Brémond, Juan Diego Gonzales Zuniga, Abhijit Das, Antitza Dantcheva, Ujjwal Ujjwal, Srijan Das, David Anghelone, Monique Thonnat.

The new results for perception for activity recognition are:

- Handling the Speed-Accuracy Trade-off in Deep Learning based Pedestrian Detection (see 6.2 )
- Deep Learning applied on Embedded Systems for People Tracking (see 6.3 )
- Partition and Reunion: A Two-Branch Neural Network for Vehicle Re- identification (see 6.4 )
- Improving Face Sketch Recognition via Adversarial Sketch-Photo Transformation (see 6.5 )
- Impact and Detection of Facial Beautification in Face Recognition: An Overview (see 6.6 )
- Computer Vision and Deep Learning applied to Facial analysis in the invisible spectra (see 6.7 )

#### 6.1.2. Action Recognition

**Participants:** François Brémond, Juan Diego Gonzales Zuniga, Abhijit Das, Antitza Dantcheva, Ujjwal Ujjwal, Srijan Das, Monique Thonnat.

The new results for action recognition are:

- ImaGINator: Conditional Spatio-Temporal GAN for Video Generation (see 6.8 )
- Characterizing the State of Apathy with Facial Expression and Motion Analysis (see 6.9 )
- Dual-threshold Based Local Patch Construction Method for Manifold Approximation And Its Application to Facial Expression Analysis (see 6.10 )
- A Weakly Supervised Learning Technique for Classifying Facial Expressions (see 6.11 )
- Robust Remote Heart Rate Estimation from Face Utilizing Spatial- temporal Attention (see 6.12 )
- Quantified Analysis for Epileptic Seizure Videos (see 6.13 )
- Toyota Smarthome: Real-World Activities of Daily Living (see 6.15 )
- Looking deeper into Time for Activities of Daily Living Recognition (see 6.15.1 )
- Self-Attention Temporal Convolutional Network for Long-Term Daily Living Activity Detection (see 6.16 )

#### 6.1.3. Semantic Activity Recognition

**Participants:** François Brémond, Elisabetta de Maria, Antitza Dantcheva, Srijan Das, Abhijit Das, Daniel Gaffé, Thibaud L'Yvonnet, Sabine Moisan, Jean-Paul Rigault, Annie Ressouche, Ines Sarray, Yaohui Wang, S L Happy, Alexandra König, Philippe Robert, Monique Thonnat.

For this research axis, the contributions are:

- DeepSpa Project (see 6.17 )
- Store Connect and Solitaria (see 6.18 )
- Synchronous Approach to Activity Recognition (see 6.19 )
- Probabilistic Activity Modeling (see 6.20 )

## 6.2. Handling the Speed-Accuracy Trade-off in Deep Learning based Pedestrian Detection

**Participants:** François Brémond, Ujjwal Ujjwal.

Pedestrian detection is a specific instance of the more general problem of object detection. Pedestrian detection plays a fundamental role in many modern applications involving but not limited to *autonomous vehicles* and *surveillance systems*. These applications as many others are safety-critical. This implies that the cost of not correctly detecting a pedestrian is very high. At the same time applications such as the ones mentioned before, are expected to be real-time. This implies that a pedestrian be detected with minimum time delay. The subject of our recent work has been to design a pedestrian detector which is capable of detecting pedestrians with a high accuracy and high speed – two traits which are known to be difficult to achieve simultaneously.

Most of the pedestrian detectors in computer vision are derived from general-category object detectors. We reflect upon its implication in terms of speed and accuracy below.

### 6.2.1. Speed-Accuracy Trade-off

Speed and accuracy of object detectors are mutually trade-off factors. Emphasis on higher accuracy usually entails intensive computations which sacrifice the detection speed. On the other hand, emphasis on higher detection speed usually leads to simpler computations which sacrifice the detection accuracy.

We have recently been able to balance this trade-off by identifying that the means of computations on anchors are a major source of the speed-accuracy trade-off. Anchors are hypothetical bounding boxes and are reminiscent of sliding windows used in earlier works on object detection. There are two distinct means of processing anchors – *feature pooling* and *feature probing*. We have recently demonstrated that feature pooling is a costlier strategy than feature probing in terms of computational cost. However, in contrast, feature pooling is a more precise means to process anchors.

We leverage this difference in our approach by utilizing feature pooling throughout in our system. However, in order to gain in terms of run-time performance, we reduce the number of anchors to be processed. This reduction does allow us to process a small number of relevant anchors with high precision.

The block diagram of our proposed approach is shown in figure 4 .

We fuse the feature maps of multiple layers in order to improve the feature diversity. An increased feature diversity assists in learning from a range of hierarchical features generated by a convolutional neural network, often abbreviated as CNN. A depth-wise separable convolutional layer then further processes the fused feature map in order to reduce the number of feature dimensions. One of the prime novelties in our work is the use of pseudo-semantic segmentation. Pseudo-semantic segmentation allows one to obtain a rough estimate of the localization of pedestrians in the form of a heatmap. This step is important, as it provides us with a basis to select a small set of anchors instead of processing all the tiling anchors on the feature map. An anchor classification layer uses anchor-specific kernel sizes to classify a given anchor as positive or negative. A positive or negative anchor is characterized by the overlap between the anchor and the ground truth bounding box during training. This overlap is measured in terms of the well known intersection-over-union (IoU) metric in computer vision. The positive anchors are then pooled from, followed by classification and regression to obtain the final detection.

### 6.2.2. Results

Figure 5 summarizes the performance of the proposed approach vis-à-vis other approaches. The proposed approach provides significant improvements over other approaches in terms of both speed and accuracy. From figure 5 it is clear that we benefit from initial training on the citypersons data set. Moreover, we obtain the state-of-art performance on the citypersons data set, improving the existing best performing techniques by nearly 4 LAMR points.

## 6.3. Deep Learning applied on Embedded Systems for People Tracking

**Participants:** Juan Diego Gonzales Zuniga, Ujjwal Ujjwal, François Brémond, Serge Tissot [Kontron].

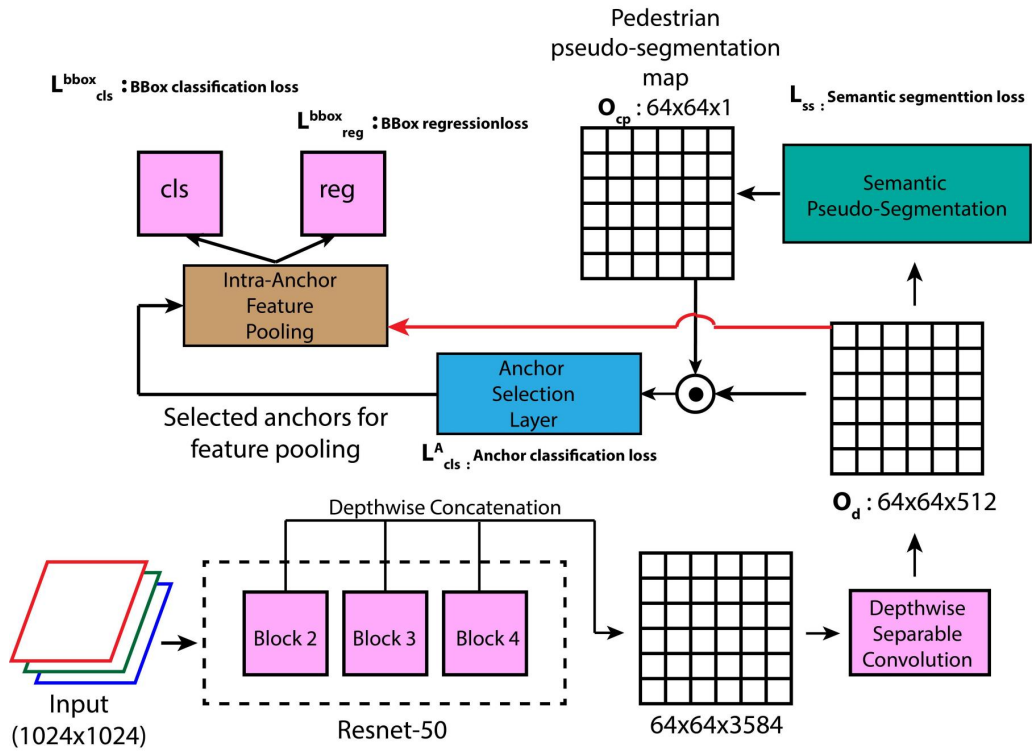


Figure 4. The block diagram of our proposed approach

Method	Stages	LAMR		Speed
		caltech-reasonable (test) (w/o CP pre-training) (CP pre-trained)	citypersons (val) (trained only on CP)	
Faster-RCNN	2	12.10	15.4	7
SSD	1	17.78 (16.36)	19.69	48
YOLOv2	1	21.62 (20.83)	NA	60
RPN-BF	2	9.6 (NA)	NA	7
MS-CNN	2	10.0 (NA)	NA	8
SDS-RCNN	2	7.6 (NA)	NA	5
ALF-Net	1	4.5 (NA)	12.0	20
Rep-Loss	2	5.0 (4.0)	13.2	-
<b>Ours</b>	1.5	<b>4.76 (3.99)</b>	<b>8.12</b>	<b>32</b>

Figure 5. Performance comparison of the proposed method with other methods for caltech-reasonable test set and citypersons validation set. The speed figures are in frames per second.



Our work objective is two-fold: a) Perform tracking of multiple people in videos, which is an instance of Multiple Object Tracking (MOT) problem, and b) optimize this tracking on embedded and open source hardware platforms such as OpenVINO and ROCm.

People tracking is a challenging and relevant problem since it needs multiple additional modules to perform the data association between nodes. In addition, state-of-the-art solutions require intensive memory allocation and power consumption which are not available on embedded hardware. Most architectures either require great amounts of memory or large computing time to achieve a state-of-the-art performance, these results are mostly achieved with dedicated hardware at data centers.

### 6.3.1. Online Joint Detection and Tracking

In people tracking, we are questioning the main paradigm that is tracking-by-detection which heavily relies on the performance of the underlying detection method. This requires access to a highly accurate and robust people detector. On the other hand, few frameworks attempt detect and track people jointly. Our intent is to perform people tracking *online* and *jointly with detection*.

We are trying to determinate a manner in which a single model can both perform detection and tracking simultaneously. Along these lines, we experimented with a variation of I3D on the Posetrack data set that takes an input of 8 frames in order to create heatmaps along multiple frames as seen in Figure 6 . Giving that the data of Posetrack or MOT cannot train a network as I3D, we are doing the pretraining with the synthetic JTA-Dataset.

This work is inspired by the less common methods of tracking-by-tracks and tracking-by-tracklets. Both [40] and [41] generate multi-frame bounding box tuple proposals and extract detection scores and features with a CNN and LSTM, respectively. Recent researches improve object detection by applying optical flow to propagate scores between frames.

Another method we implemented is by using the detections of previous frames as proposal for the data association, it only uses the IOU between two objects as a distance metric. This approach is simple and efficient assuming the objects do not move drastically. An improved method increases the performance by using a siamese network to conserve identity across frames and predictions for death and birth of tracks.

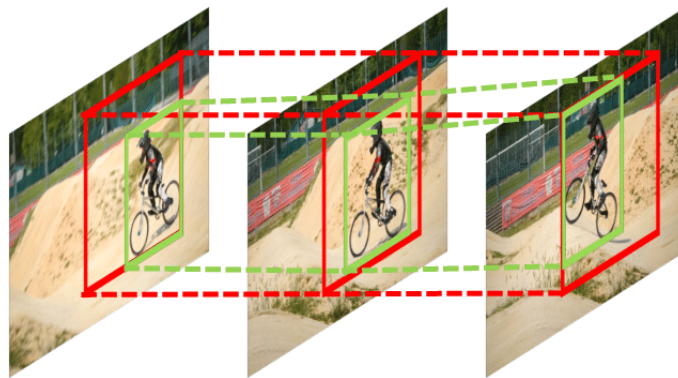


Figure 6. People tracking by tubelets

### 6.3.2. OpenVINO and ROCm

Regarding embedded hardware, we focus on enlarging both implementation and experimentation of two specific frameworks; OpenVINO and ROCm.

OpenVINO allows us to transfer deep learning models into Myriad and KeemBay chips, taking advantage of their capacity to compute multiple operations without the need of much power consumption. We have thoroughly tested their power consumption under different scenarios as well as implemented many qualitative algorithms with these two platforms, Figure 7 shows the Watt consumption and frame rate of the most popular backbone networks, making it viable to use on embedded applications with a reasonable 25FPS.

For ROCm, we have used the approach of [38] to optimize the compiler execution for a variety of CNN features and filters using a substitute GPU with similar computation capability as Nvidia but still remaining a low branch consumption around 15 Watts.

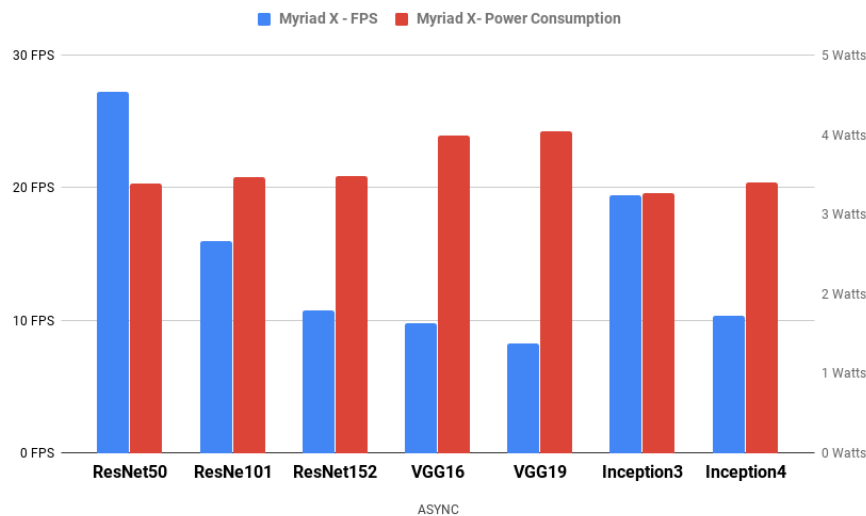


Figure 7. Power Consumption vs Frame rate

## 6.4. Partition and Reunion: A Two-Branch Neural Network for Vehicle Re-identification

**Participants:** Hao Chen, Benoit Lagadec, François Brémond.

The smart city vision raises the prospect that cities will become more intelligent in various fields, such as more sustainable environment and a better quality of life for residents. As a key component of smart cities, intelligent transportation system highlights the importance of vehicle re-identification (Re-ID). However, as compared to the rapid progress on person Re-ID, vehicle Re-ID advances at a relatively slow pace. Some previous state-of-the-art approaches strongly rely on extra annotation, like attributes (vehicle color and type) and key-points (wheels and lamps). Recent work on person Re-ID shows that extracting more local features can achieve a better performance without considering extra annotation. In this work, we propose an end-to-end trainable two-branch Partition and Reunion Network (PRN) for the challenging vehicle Re-ID task. Utilizing only identity labels, our proposed method outperforms existing state-of-the-art methods on four vehicle Re-ID benchmark datasets, including VeRi-776, VehicleID, VRIC and CityFlow-ReID by a large margin. The general architecture of our proposed method is represented in the Figure 8 .

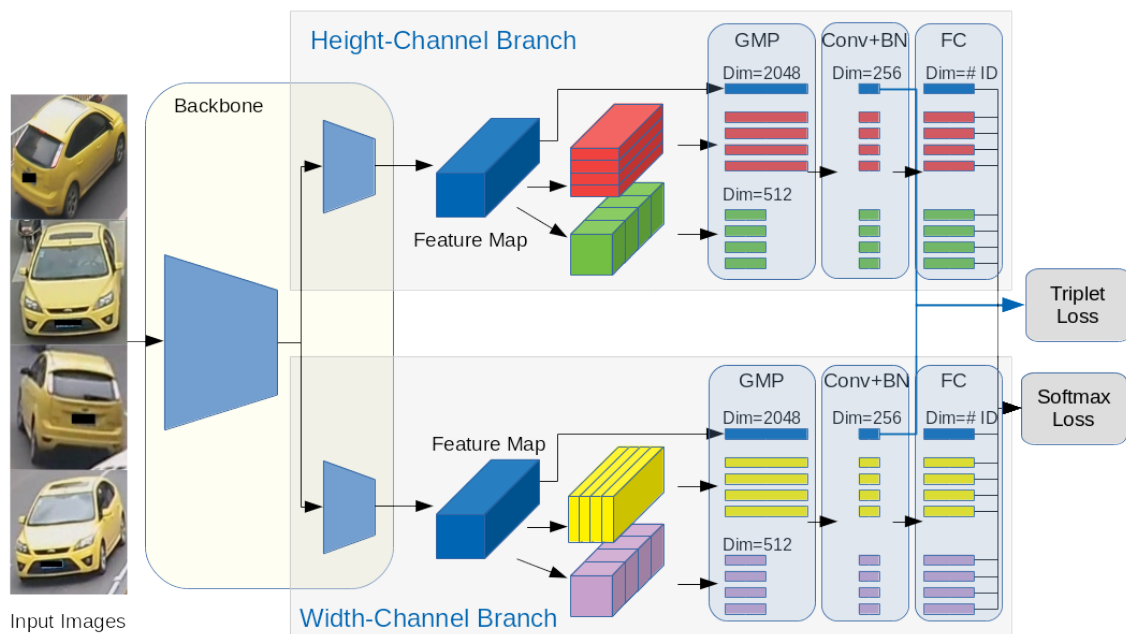


Figure 8. General architecture of our proposed model. In this work, a ResNet-50 is used as our backbone network. Layers after conv4\_1 in Resnet-50 are duplicated to split our network into 2 independent branches. GMP refers to Global Max Pooling. Conv refers to 1\*1 convolutional layer, which aims to unify dimensions of global and local feature vectors. FC refers to fully connected layer. BN refers to Batch Normalization layer. In the test phase, all the feature vectors (Dim=256) after Batch Normalization layer are concatenated together as an appearance signature (Dim=256\*18).

### 6.4.1. Learning Discriminative and Generalizable Representations by Spatial-Channel Partition for Person Re-Identification

In Person Re-Identification (Re-ID) task, combining local and global features is a common strategy to overcome missing key parts and misalignment on models based only on global features. Using this combination, neural networks yield impressive performance in Re-ID task. Previous part-based models mainly focus on spatial partition strategies. Recently, operations on channel information, such as Group Normalization and Channel Attention, have brought significant progress to various visual tasks. However, channel partition has not drawn much attention in Person Re-ID. We conduct a study to exploit the potential of channel partition in Re-ID task [32]. Based on this study, we propose an end-to-end Spatial and Channel partition Representation network (SCR) in order to better exploit both spatial and channel information. Experiments conducted on three mainstream image-based evaluation protocols including Market-1501, DukeMTMC-ReID and CUHK03 and one video-based evaluation protocol MARS validate the performance of our model, which outperforms previous state-of-the-art in both single and cross domain Re-ID tasks. The general architecture of our proposed method is represented in the Figure 9 .

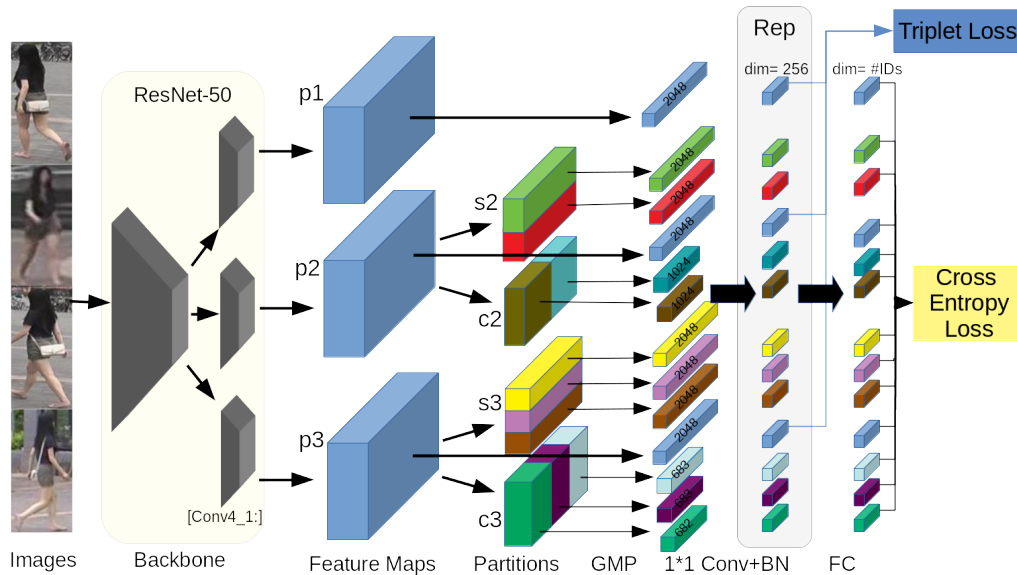


Figure 9. Spatial and Channel Partition Representation network. For the backbone network, we duplicate layers after conv4\_1 into 3 identical but independent branches that generate 3 feature maps "p1", "p2" and "p3". Then, multiple spatial-channel partitions are conducted on the feature maps. "s2" and "c2" refer to 2 spatial parts and 2 channel groups. "s3" and "c3" refer to 3 spatial parts and 3 channel groups. After global max pooling (GMP), dimensions of global ( $dim = 2048$ ) and local ( $dim = 2048, 1024*2$  and  $683*2+682$ ) features are unified by  $1*1$  convolution ( $1*1$  Conv) and batch normalization (BN) to 256. Then, fully connected layers (FC) give identity predictions of input images. All the dimension unified feature vectors ( $dim = 256$ ) are aggregated together as appearance representation (Rep) for testing.

## 6.5. Improving Face Sketch Recognition via Adversarial Sketch-Photo Transformation

**Participants:** Antitza Dantcheva, Shikang Yu [Chinese Academy of Sciences], Hu Han [Chinese Academy of Sciences], Shiguang Shan [Chinese Academy of Sciences], Xilin Chen [Chinese Academy of Sciences].

### participants

Face sketch-photo transformation has broad applications in forensics, law enforcement, and digital entertainment, particular for face recognition systems that are designed for photo-to-photo matching. While there are a number of methods for face photo-to-sketch transformation, studies on sketch-to-photo transformation remain limited. In this work, we proposed a novel conditional CycleGAN for face sketch-to-photo transformation. Specifically, we leveraged the advantages of CycleGAN and conditional GANs and designed a feature-level loss to assure the high quality of the generated face photos from sketches. The generated face photos were used, as a replacement of face sketches, and particularly for face identification against a gallery set of mugshot photos. Experimental results on the public-domain database CUFSF showed that the proposed approach was able to generate realistic photos from sketches, and the generated photos were instrumental in improving the sketch identification accuracy against a large gallery set. This work has been presented at the IEEE International Conference on Automatic Face and Gesture Recognition (FG 2019) [30].

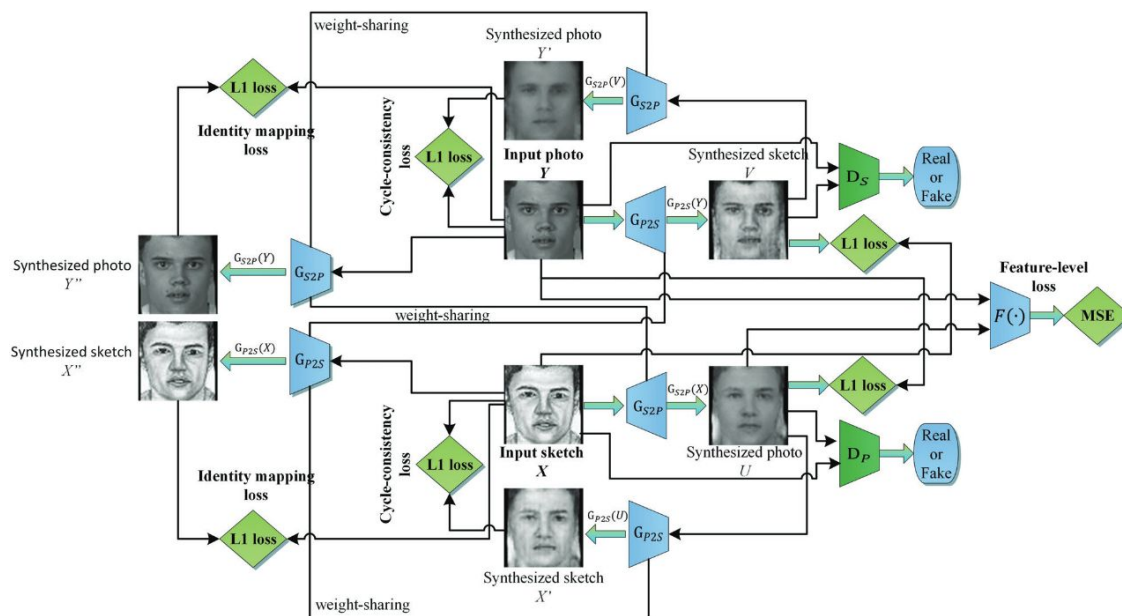


Figure 10. Overview of the proposed GAN for sketch-to-photo transformation using feature-level loss.

## 6.6. Impact and Detection of Facial Beautification in Face Recognition: An Overview

**Participants:** Antitza Dantcheva, Christian Rathgeb [Hochschule Darmstadt], Christoph Busch [Hochschule Darmstadt].

Facial beautification induced by plastic surgery, cosmetics or retouching has the ability to substantially alter the appearance of face images. Such types of beautification can negatively affect the accuracy of face recognition systems. In this work, a conceptual categorisation of beautification was presented, relevant scenarios with respect to face recognition were discussed, and related publications were revisited. Additionally, technical considerations and trade-offs of the surveyed methods were summarized along with open issues and challenges in the field. This survey is targeted to provide a comprehensive point of reference for biometric researchers

and practitioners working in the field of face recognition, who aim at tackling challenges caused by facial beautification. This work was published in IEEE Access [18].

## 6.7. Computer Vision and Deep Learning applied to Facial analysis in the invisible spectra

**Participants:** David Anghelone, Antitza Dantcheva.

The goal of our work is to analyze faces, as well as recognize events in the invisible spectra. In the last few years, face analysis has been a highly active area and has attracted a lot of interest from the scientific community. Limitations encountered in the visible spectrum such as illumination-restriction have the ability to be overcome in the infrared spectrum. We explored the state-of-the-Art of facial analysis in the invisible spectrum including low energy infrared waves, as well as ultraviolet waves. In this context we have captured images in each spectra and intend to process the data. We aim at designing a model, which extracts biometric features. The key challenges are the processing of contours, shape, etc. This subject is within the framework of the national project *SafeCity*: Security of Smart Cities.

## 6.8. ImaGINator: Conditional Spatio-Temporal GAN for Video Generation

**Participants:** Yaohui Wang, Antitza Dantcheva, Piotr Bilinski [University of Warsaw], François Brémond.

**keywords:** GANs, Video Generation

Generating human videos based on single images entails the challenging simultaneous generation of realistic and visual appealing appearance and motion. In this context, we propose a novel conditional GAN architecture, namely ImaGINator [35] (see Figure 11), which given a single image, a condition (label of a facial expression or action) and noise, decomposes appearance and motion in both latent and high level feature spaces, generating realistic videos. This is achieved by (i) a novel spatio-temporal fusion scheme, which generates dynamic motion, while retaining appearance throughout the full video sequence by transmitting appearance (originating from the single image) through all layers of the network. In addition, we propose (ii) a novel transposed (1+2)D convolution, factorizing the transposed 3D convolutional filters into separate transposed temporal and spatial components, which yields significant gains in video quality and speed. We extensively evaluate our approach on the facial expression datasets MUG and UvA-NEMO, as well as on the action datasets NATOPS and Weizmann. We show that our approach achieves significantly better quantitative and qualitative results than the state-of-the-art (see Table 1).

Table 1. Evaluation of VGAN, MoCoGAN and proposed ImaGINator with respect to image quality (SSIM/PSNR) and video quality (FID).

	MUG		NATOPS	
	SSIM/PSNR	FID	SSIM/PSNR	FID
VGAN	0.28/14.54	74.72	0.72/20.09	167.71
MoCoGAN	0.58/18.16	45.46	0.74/21.82	49.46
ImaGINator	<b>0.75/22.63</b>	<b>29.02</b>	<b>0.88/27.39</b>	<b>26.86</b>
	Weizmann		UvA-NEMO	
	SSIM/PSNR	FID	SSIM/PSNR	FID
VGAN	0.29/15.78	127.31	0.21/13.43	30.01
MoCoGAN	0.42/17.58	116.08	0.45/16.58	29.81
ImaGINator	<b>0.73/19.67</b>	<b>99.80</b>	<b>0.66/20.04</b>	<b>16.16</b>

## 6.9. Characterizing the State of Apathy with Facial Expression and Motion Analysis

**Participants:** S L Happy, Antitza Dantcheva, Abhijit Das, François Brémond, Radia Zeghari [Cobtek], Philippe Robert [Cobtek].



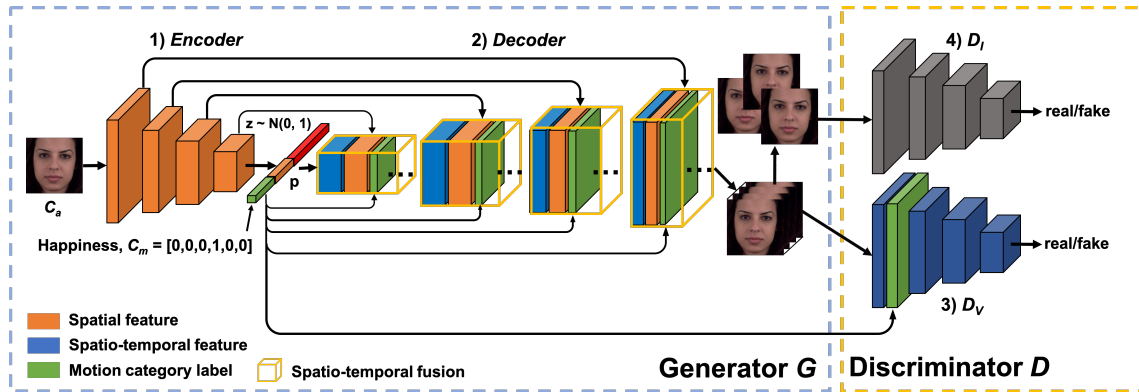


Figure 11. **Overview of the proposed ImmaGINator.** In the Generator  $G$ , the Encoder firstly encodes an input image  $c_a$  into a single vector  $p$ . Then, the Decoder produces a video based on a motion  $c_m$  and a random vector  $z$ . By using spatio-temporal fusion, low level spatial feature maps from the Encoder are directly concatenated into the Decoder. While  $D_I$  discriminates whether the generated images contain an authentic appearance,  $D_V$  additionally determines whether the generated videos contain an authentic motion.

Reduced emotional response, lack of motivation, and limited social interaction comprise the major symptoms of apathy. Current methods for apathy diagnosis require the patient's presence in a clinic, and time consuming clinical interviews and questionnaires involving medical personnel, which are costly and logistically inconvenient for patients and clinical staff, hindering among other large scale diagnostics. In this work we introduced a novel machine learning framework to classify apathetic and non-apathetic patients based on analysis of facial dynamics, entailing both emotion and facial movement. Our approach catered to the challenging setting of current apathy assessment interviews, which include short video clips with wide face pose variations, very low-intensity expressions, and insignificant inter-class variations. We tested our algorithm on a dataset consisting of 90 video sequences acquired from 45 subjects and obtained an accuracy of 84% in apathy classification. Based on extensive experiments, we showed that the fusion of emotion and facial local motion produced the best feature set for apathy classification. In addition, we trained regression models to predict the clinical scores related to the mental state examination (MMSE) and the neuropsychiatric apathy inventory (NPI) using the motion and emotion features. Our results suggested that the performance can be further improved by appending the predicted clinical scores to the video-based feature representation. This work has been presented at the IEEE International Conference on Automatic Face and Gesture Recognition (FG 2019) [25].

## 6.10. Dual-threshold Based Local Patch Construction Method for Manifold Approximation And Its Application to Facial Expression Analysis

**Participants:** S L Happy, Antitza Dantcheva, Aurobinda Routray [IIT Kharagpur].

In this paper, we propose a manifold based facial expression recognition framework which utilizes the intrinsic structure of the data distribution to accurately classify the expression categories. Specifically, we model the expressive faces as the points on linear subspaces embedded in a Grassmannian manifold, also called as expression manifold. We propose the dual-threshold based local patch (DTLP) extraction method for constructing the local subspaces, which in turn approximates the expression manifold. Further, we use the affinity of the face points from the subspaces for classifying them into different expression classes. Our method is evaluated on four publicly available databases with two well known feature extraction techniques. It is evident from the results that the proposed method efficiently models the expression manifold and improves

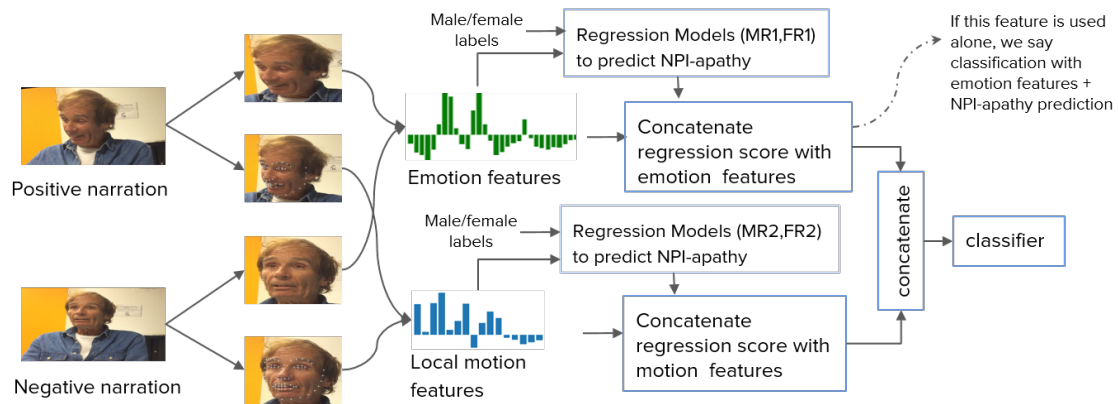


Figure 12. Overall framework for apathy detection from facial videos.

the recognition accuracy in spite of the simplicity of the facial representatives. This work has been presented at the European Signal Processing Conference (EUSIPCO'19) [26].

## 6.11. A Weakly Supervised Learning Technique for Classifying Facial Expressions

**Participants:** S L Happy, Antitza Dantcheva, François Brémond.

The universal hypothesis suggests that the six basic emotions: anger, disgust, fear, happiness, sadness, and surprise, are being expressed by similar facial expressions by all humans. While existing datasets support the universal hypothesis and comprise of images and videos with discrete disjoint labels of profound emotions, real-life data contains jointly occurring emotions and expressions of different intensities. Models, which are trained using categorical one-hot vectors often over-fit and fail to recognize low or moderate expression intensities. Motivated by the above, as well as by the lack of sufficient annotated data, we propose a weakly supervised learning technique for expression classification, which leveraged the information of unannotated data. Crucial in our approach was that we first trained a convolutional neural network (CNN) with label smoothing in a supervised manner and proceeded to tune the CNN-weights with both labelled and unlabelled data simultaneously. Experiments on four datasets demonstrated large performance gains in cross-database performance, as well as showed that the proposed method achieved to learn different expression intensities, even when trained with categorical samples. This work was published in Pattern Recognition Letters [15].

## 6.12. Robust Remote Heart Rate Estimation from Face Utilizing Spatial-temporal Attention

**Participants:** Antitza Dantcheva, Abhijit Das, Xuesong Niu [Chinese Academy of Sciences], Xingyuan Zhao [Chinese Academy of Sciences], Hu Han [Chinese Academy of Sciences], Shiguang Shan [Chinese Academy of Sciences], Xilin Chen [Chinese Academy of Sciences].

We proposed an end-to-end approach for robust remote heart rate (HR) measurement gleaned from facial videos. Specifically the approach was based on remote photoplethysmography (rPPG), which constitutes a pulse triggered perceivable chromatic variation, sensed in RGB-face videos. Incidentally rPPGs can be affected in less-constrained settings. To unpin the shortcoming, the proposed algorithm utilized a spatio-temporal attention mechanism, which placed emphasis on the salient features included in rPPG-signals. In addition,

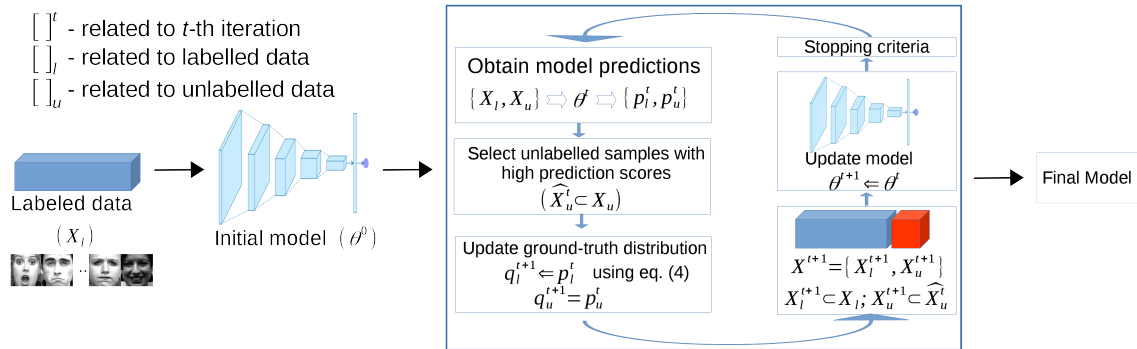


Figure 13. Workflow of the proposed method for weakly supervised learning of facial expressions.

we proposed an effective rPPG augmentation approach, generating multiple rPPG signals with varying HRs from a single face video. Experimental results on the public datasets VIPL-HR and MMSE-HR showed that the proposed method outperformed state-of-the-art algorithms in remote HR estimation. This work has been presented at the IEEE International Conference on Automatic Face and Gesture Recognition (FG 2019) [28].

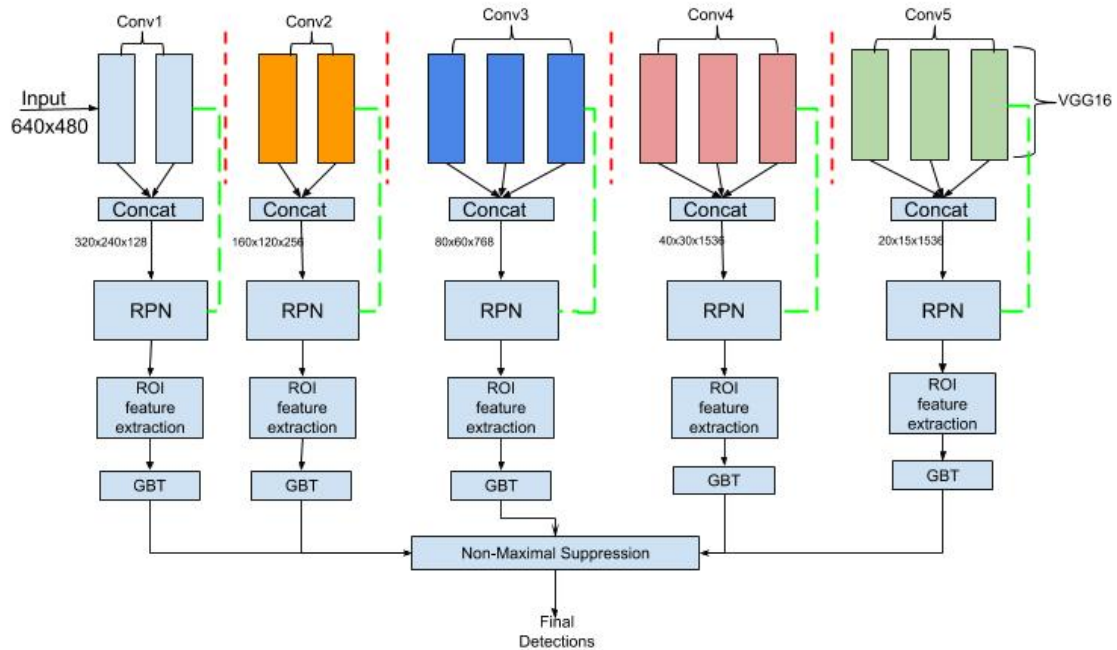


Figure 14. Overview of the proposed end-to-end trainable approach for rPPG based remote HR measurement via representation learning with spatial-temporal attention.

### 6.13. Quantified Analysis for Epileptic Seizure Videos

**Participants:** Jen-Cheng Hou, Monique Thonnat.

Epilepsy is a type of neurological disorder, affecting around 50 million people worldwide. Epilepsy's main symptoms are seizures, which are caused by abnormal neuronal activities in the brain. To determine appropriate treatments, neurologists assess manifestation of patients' behavior when seizures occur. Nevertheless, there are few objective criteria regarding the procedure, and diagnosis could be biased due to subjective evaluation. Hence it is important to quantify patients' ictal behaviors for better assessment of the disorder. In collaboration with Dr. Fabrice Bartolomei and Dr. Aileen McGonigal from Timone Hospital, Marseille, we have access to video recordings from epilepsy monitoring unit for analysis, with consent from ethics committee (IRB) and the patients involved.

### **6.13.1. Seizure Video Classification and Background Video Collection**

In an epilepsy monitoring unit, EEG and video recording are usually collected. For patients who need brain surgery to remove lobes that produce seizures, stereo-EEG (SEEG) recordings are particularly measured. SEEG is an intrusive measurement and provides information of the seizure type. We have 86 seizure videos from 20 patients along with the corresponding SEEG conclusion (i.e. pre-frontal epilepsy, occipital epilepsy, etc.). In this study, the goal is to classify seizure videos to their seizure types. Classification was conducted by fine-tuning a pre-trained video classification model, I3D, with 10-fold cross-validation. Due to the relatively small volume of data we have and the challenging nature of our videos, the performance was not satisfactory enough. Inspired by recent semi-supervised works in leveraging large unlabeled dataset for better adaptation to certain tasks, we are collecting large volume of background videos in the epilepsy monitoring unit, in which patients' behavior are normal, such as eating, sleeping, and talking. The volume of the background video can be up to 1000 hours, which could be taken as unlabeled dataset for semi-supervised learning in our case.

### **6.13.2. Quantifying Rhythmic Rocking Movement with Head Tracking**

In this study, six seizures from three patients with pre-frontal epilepsy were analyzed. The duration of rocking was 15-40 seconds, with marked regularity throughout each seizure. Our objective is to document time-evolving frequencies of antero-posterior rocking body movements occurring during seizures. We adopted MobileNet [39] as our backbone model for detecting head of the patient, and hence obtain the trajectories of head movement (see Figure 15). After smoothing the trajectories and find the valid peaks corresponding to the antero-posterior movement, we compute the time-evolving movement frequency for each seizure video. Whereas the rocking frequency varied substantially between patients and seizures (0.3-1Hz), coefficient of variation of frequency was low ( $\leq 12\%$ ). The study report is under review for a medical journal.

## **6.14. Skeleton Image Representation for 3D Action Recognition**

**Participants:** Carlos Caetano, François Brémond.

Due to the availability of large-scale skeleton datasets, 3D human action recognition has recently called the attention of computer vision community. Many works have focused on encoding skeleton data as skeleton image representations based on spatial structure of the skeleton joints, in which the temporal dynamics of the sequence is encoded as variations in columns and the spatial structure of each frame is represented as rows of a matrix. To further improve such representations, we introduce a novel skeleton image representation to be used as input of Convolutional Neural Networks (CNNs), named SkeleMotion. The proposed approach encodes the temporal dynamics by explicitly computing the magnitude and orientation values of the skeleton joints. Different temporal scales are employed to compute motion values to aggregate more temporal dynamics to the representation making it able to capture long-range joint interactions involved in actions as well as filtering noisy motion values. Experimental results demonstrate the effectiveness of the proposed representation on 3D action recognition outperforming the state-of-the-art on NTU RGB+D 120 dataset. This work has been published in AVSS 2019 [31].

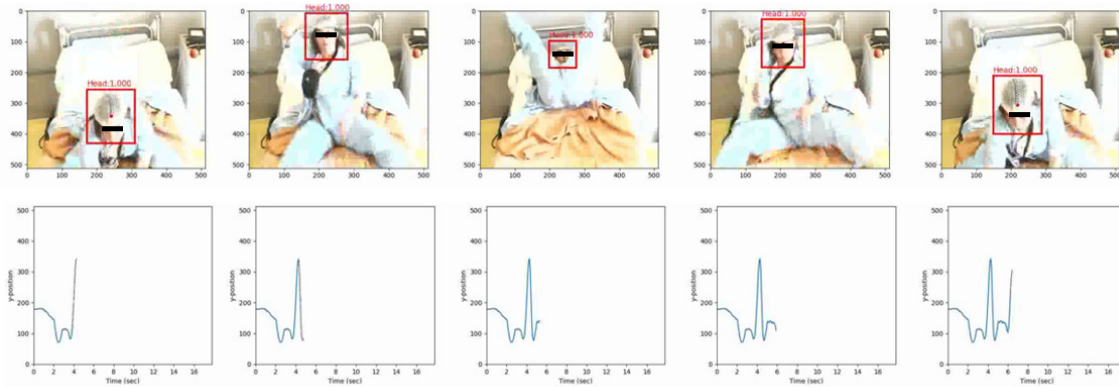


Figure 15. The first row demonstrates the image samples of the antero-posterior movement. The second row shows the position of the head through time in the vertical direction.

In another work, we have explore how to better represent motion information in a video. The temporal component of videos provides an important clue for activity recognition, as a number of activities can be reliably recognized based on the motion information. In view of that, this work proposes a novel temporal stream for two-stream convolutional networks based on images computed from the optical flow magnitude and orientation, named Magnitude-Orientation Stream (MOS), to learn the motion in a better and richer manner. Our method applies simple non-linear transformations on the vertical and horizontal components of the optical flow to generate input images for the temporal stream. Moreover, we also employ depth information to use as a weighting scheme on the magnitude information to compensate the distance of the subjects performing the activity to the camera. Experimental results, carried on two well-known datasets (UCF101 and NTU), demonstrate that using our proposed temporal stream as input to existing neural network architectures can improve their performance for activity recognition. Results demonstrate that our temporal stream provides complementary information able to improve the classical two-stream methods, indicating the suitability of our approach to be used as a temporal video representation. two-stream convolutional networks, spatiotemporal information, optical flow, depth information. This work has been published in the Journal of Visual Communication and Image Representation [14].

## 6.15. Toyota Smarthome: Real-World Activities of Daily Living

**Participants:** Srijan Das, Rui Dai, François Brémond.

The performance of deep neural networks is strongly influenced by the quantity and quality of annotated data. Most of the large activity recognition datasets consist of data sourced from the Web, which does not reflect challenges that exist in activities of daily living. In this work, we introduce a large real-world video dataset for activities of daily living: Toyota Smarthome. The dataset consists of 16K RGB+D clips of 31 activity classes, performed by seniors in a smarthome. Unlike previous datasets, videos were fully unscripted. As a result, the dataset poses several challenges: high intra-class variation, high class imbalance, simple and composite activities, and activities with similar motion and variable duration. Activities were annotated with both coarse and fine-grained labels. These characteristics differentiate Toyota Smarthome from other datasets for activity recognition as illustrated in 16 .

As recent activity recognition approaches fail to address the challenges posed by Toyota Smarthome, we present a novel activity recognition method with attention mechanism. We propose a pose driven spatio-temporal attention mechanism through 3D ConvNets. We show that our novel method outperforms state-of-the-art methods on benchmark datasets, as well as on the Toyota Smarthome dataset. We release the dataset



for research use at <https://project.inria.fr/toyotasmarthome>. This work is done in collaboration with Toyota Motors Europe and is published in ICCV 2019 [21].



Figure 16. Sample frames from Toyota Smarthome dataset: 1-7 label at the right top corner respectively correspond to camera view 1, 2, 3, 4, 5, 6 and 7 as marked in the plan of the apartment on the right. Image from camera view (1) Drink from can, (2) Drink from bottle, (3) Drink form glass and (4) Drink from cup are all fine grained activities with a coarse label drink. Image from camera view (5) Watch TV and (6) Insert tea bag show activities with large source-to-camera distance and occlusion. Images with camera view (7) Enter illustrate the RGB image and the provided 3D skeleton.

### 6.15.1. Looking deeper into Time for Activities of Daily Living Recognition

**Participants:** Srijan Das, Monique Thonnat, François Brémond.

In this work, we introduce a new approach for Activities of Daily Living (ADL) recognition. In order to discriminate between activities with similar appearance and motion, we focus on their temporal structure. Actions with subtle and similar motion are hard to disambiguate since long-range temporal information is hard to encode. So, we propose an end-to-end Temporal Model to incorporate long-range temporal information without losing subtle details. The temporal structure is represented globally by different temporal granularities and locally by temporal segments as illustrated in fig. 17. We also propose a two-level pose driven attention mechanism to take into account the relative importance of the segments and granularities. We validate our approach on 2 public datasets: a 3D human activity dataset (NTU-RGB+D) and a human action recognition dataset with object interaction dataset (Northwestern-UCLA Multiview Action 3D). Our Temporal Model can also be incorporated with any existing 3D CNN (including attention based) as a backbone which reveals its robustness. This work has been accepted in WACV 2020 [20].

## 6.16. Self-Attention Temporal Convolutional Network for Long-Term Daily Living Activity Detection

**Participants:** Rui Dai, François Brémond.



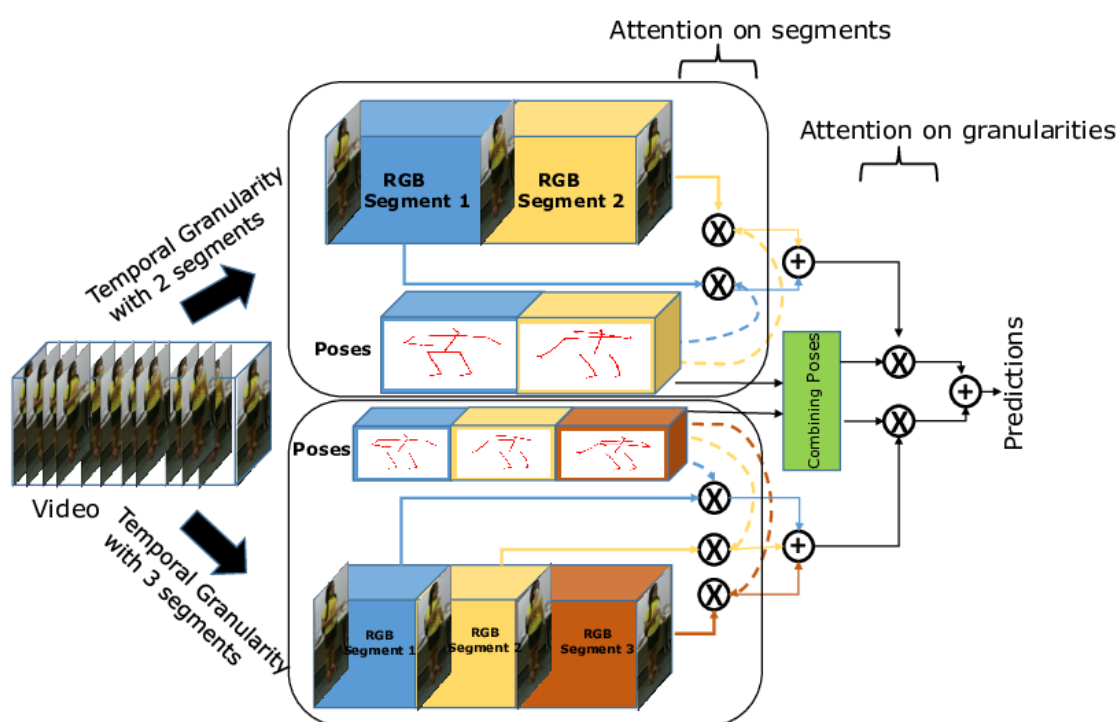


Figure 17. Framework of the proposed approach in a nutshell for two temporal granularities. The articulated poses soft-weight the temporal segments and the temporal granularities using a two-level attention mechanism.

This year, we proposed a Self-Attention - Temporal Convolutional Network (SA-TCN), which is able to capture both complex activity patterns and their dependencies within long-term untrimmed videos [34]. This attention block can also embed with other TCN-based models. We evaluate our proposed model on Daily Home Life Activity Dataset (DAHLIA) and Breakfast datasets. Our proposed method achieves state-of-the-art performance on both datasets.

### 6.16.1. Work Flow

Given an untrimmed video, we represent each non-overlapping snippet by a visual encoding over 64 frames. This visual encoding is the input to the encoder-TCN, which is the combination of the following operations: 1D temporal convolution, batch normalization, ReLU, and max pooling. Next, we send the output of the encoder-TCN into the self-attention block to capture long-range dependencies. After that, the decoder-TCN applies the 1D convolution and up sampling to recover a feature map of the same dimension as visual encoding. Finally, the output will be sent to a fully connected layer with softmax activation to get the prediction. Fig 18 and 19 provide the structure of our model.

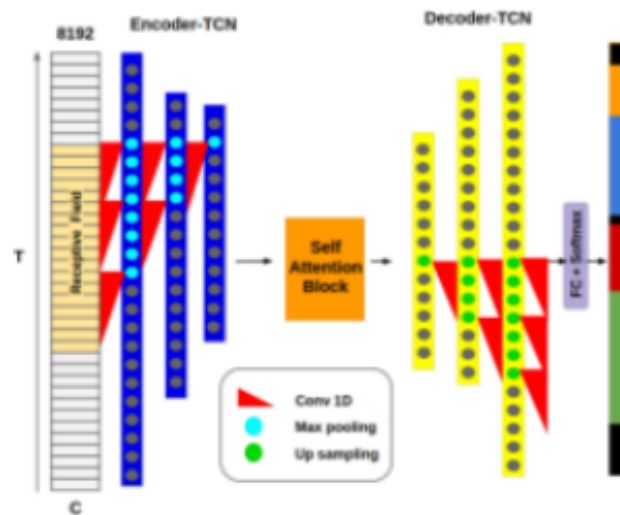


Figure 18. **Overview.** The model contains mainly three parts: (1) visual encoding, (2) encoder-decoder structure, (3) attention block

### 6.16.2. Result

We evaluated the proposed method on two daily-living activity datasets (DAHLIA, Breakfast) and achieved state-of-the-art performances. We compared with these following State-of-the arts: DOHT, Negin *et al.*, GRU, ED-TCN, TCFPN.

## 6.17. DeepSpa Project

**Participants:** Alexandra König, Rachid Guerchouche, Minh Tran-Duc, Antitza Dantcheva, S L Happy, Abhijit Das.

The DeepSpa (Deep Speech Analysis, January 2019 - June 2020) project aims to deliver telecommunication-based neurocognitive assessment tools for early screening, early diagnostic and follow-up of cognitive disorders, mainly in elderly. The target is also clinical trials addressing Alzheimer's and other neurodegenerative diseases. By combining AI in speech recognition and video analysis for facial expression recognition, the proposed tools allow remote cognitive and psychological testing, thereby saving time and money.

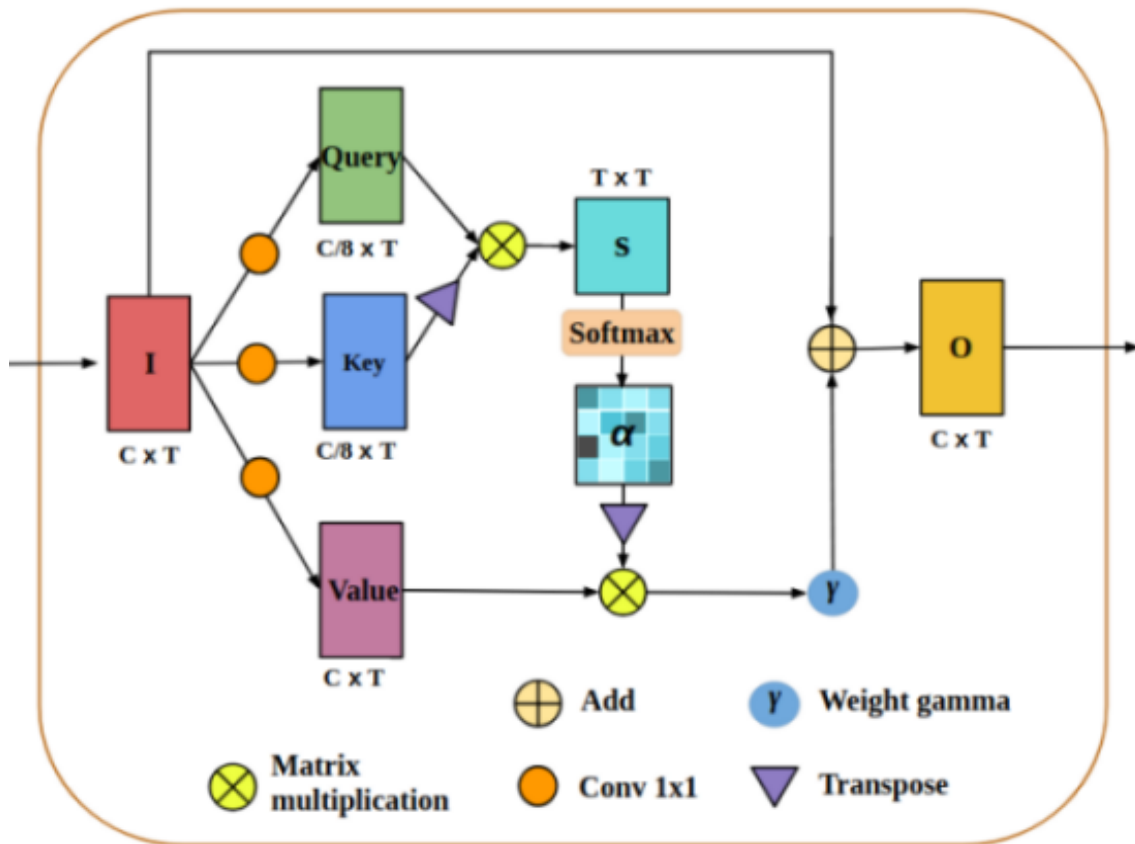


Figure 19. Attention block. This figure presents the structure of attention block

Table 2. Activity detection results on DAHLIA dataset with the average of view 1, 2 and 3. \* marked methods have not been tested on DAHLIA in their original paper.

Model	FA1	F-score	IoU	mAP
DOHT	0.803	0.777	0.650	-
GRU*	0.759	0.484	0.428	0.654
ED-TCN*	0.851	0.695	0.625	0.826
Negin <i>et al.</i>	0.847	0.797	0.723	-
TCFPN*	0.910	<b>0.799</b>	0.738	<b>0.879</b>
<b>SA-TCN</b>	<b>0.921</b>	0.788	<b>0.740</b>	0.862

Table 3. Activity detection results on Breakfast dataset.

Model	FA1	F-Score	IoU	mAP
GRU	0.368	0.295	0.198	0.380
ED-TCN	0.461	0.462	0.348	0.478
TCFPN	<b>0.519</b>	0.453	0.362	0.466
<b>SA-TCN</b>	0.497	<b>0.494</b>	<b>0.385</b>	<b>0.480</b>

Table 4. Average precision of ED-TCN on DAHLIA.

<b>Activities</b>	<b>Background</b>	<b>House work</b>	<b>Working</b>	<b>Cooking</b>
<b>AP</b>	0.36	0.65	0.95	0.96
<b>Activities</b>	<b>Laying table</b>	<b>Eating</b>	<b>Clearing table</b>	<b>Wash dishes</b>
<b>AP</b>	0.90	0.97	0.80	0.97

Table 5. Combination of attention block with other TCN-based model: TCFPN. (Evaluated on DAHLIA dataset)

<b>Model</b>	<b>FA1</b>	<b>F-score</b>	<b>IoU</b>	<b>mAP</b>
TCFPN	0.910	<b>0.799</b>	0.738	0.879
<b>SA-TCFPN</b>	<b>0.917</b>	<b>0.799</b>	<b>0.748</b>	<b>0.894</b>

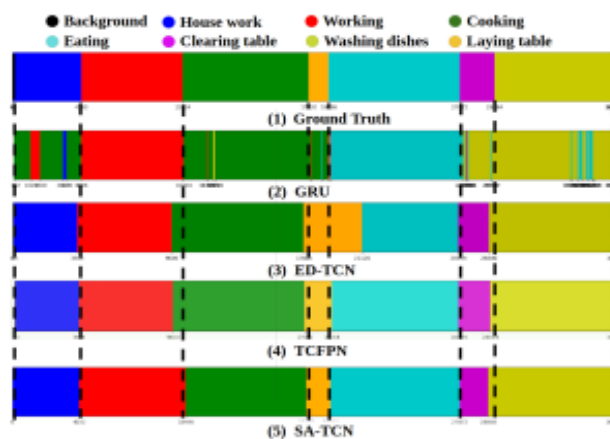


Figure 20. **Detection visualization.** The detection visualization of video 'S01A2K1' in DAHLIA: (1) ground truth, (2) GRU, (3) ED-TCN, (4) TCFPN and (5) SA-TCN.

The partners of the project are:

- Inria: technical partner and project coordinator
- University of Maastricht: clinical partner
- Jansen & Jansen: pharma partner and business champion
- Association Innovation Alzheimer: subgranted clinical partner
- Ki-element: subgranted technical partner.

### 6.17.1. Project structure

The DeepSpA project is structured in two use-cases:

- Use-case 1: remote assessment through phone for early screening of cognitive disorders (University of Maastricht, Jansen & Jansen and Ki-element): using AI based speech recognition; assessments through phone are made possible. A clinical trial is currently running in Maastricht (by end 2019, 70 subjects will be included, and 50 others will be included in 2020), the goal is to study the feasibility of such phone assessment in comparison to face-to-face assessment.
- Use-case 2: remote assessment through video-conference system (telemedicine tool) (Inria, Jansen & Jansen and Association Innovation Alzheimer): Inria developed a telemedicine tool which allows complete remote assessment. AI based speech and facial expression recognition empower the cognitive assessment by providing extra features useful for clinicians.

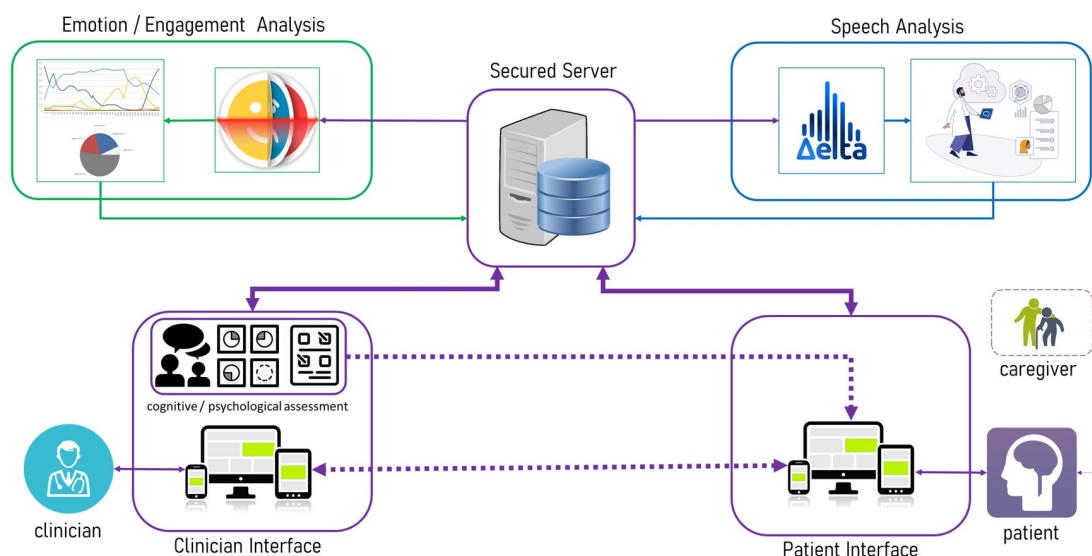


Figure 21. Global view of the telemedicine tool developed by Inria (STARS).

### 6.17.2. Telemedicine / Clinical Study with Digne-les-Bains

In order to evaluate the feasibility of remote assessment through the telemedicine tool, a collaboration with the city of Digne-les-Bains started in March 2019. The Hospital of Digne-les-Bains, la Maison de la Santé and the ADMR (association dealing with isolated people) are involved in a running clinical study, which aims at evaluating the feasibility of the remote assessment in two different setups:

- Clinical setup: a fixed place where the participant will undergo the telemedicine session: clinic, hospital, pharmacy, health centres ....
- Mobile Units: a mobile unit goes to the subjects home, the telemedicine session is done inside the mobile unit (e.g., van).

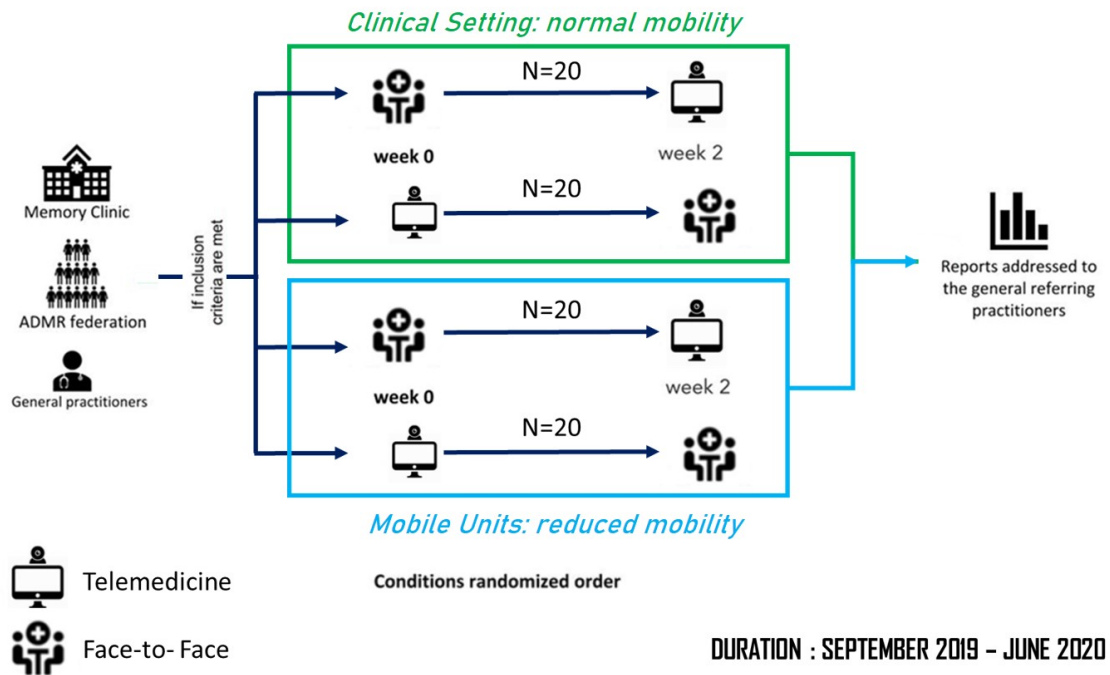


Figure 22. Global view of the clinical study with Digne-les-Bains.

We already started including subjects in the clinical setup case. By end 2019, we expect to include about 15 subjects, 25 extra subjects will be included during 2020. Mobile units setup will be tested during 2020.

First results and observations already showed that the telemedicine tool allows full assessments. Clinicians and patients showed strong interest and appreciation of such tool.

### 6.17.3. Facial expressions recognition and engagement evaluation in the telemedicine tool

The STARS team is doing research on facial expressions analysis, which could be integrated as part of the vision module of the telemedicine tool [25].

Notable software related to this research is the provided API on the cloud, which allows sending video files and retrieving emotions, gaze direction, facial movements and head direction (implemented by S L Happy).

## 6.18. Store Connect and Solitaria

**Participants:** Sébastien Gilabert, Minh Khue Phan Tran, François Brémond.

Store-Connect was a consortium aiming at detecting and positioning people in a supermarket. Several technologies were explored such as computing and merging trajectories obtained from the mobile phone of customers and from video cameras. In a second step, the goal was to detect all the 'stop' events of the customers while shopping in the store.



### 6.18.1. SupICP

We have developed with the SED team, SupICP, a platform for integrating all plugins developed by STARS team. Our main contribution is the Ontology Language Plugin. With this plugin, we can use contextual and knowledge information inside scenarios designed for video event recognition. Currently, we are improving this plugin for combining the Ontology Language with Deep Learning technology towards “Action recognition based on Deep Learning and Ontology Language”.

We have also installed this software at the Institute Claude Pompidou, in order to conduct clinical trials, and to work with medical scientists.

### 6.18.2. Solitaria

The aim of this project is to combine data extracted from domestic sensors and from video cameras, and to implement this plugin into SupICP to monitor older people at home.

## 6.19. Synchronous Approach to Activity Recognition

**Participants:** Daniel Gaffé, Sabine Moisan, Annie Ressouche, Jean-Paul Rigault, Ines Sarray.

Activity Recognition aims at recognizing and understanding sequences of actions and movements of mobile objects (human beings, animals or artifacts), that follow the predefined model of an activity. We propose to describe activities as a series of actions, triggered and driven by environmental events.

This year we mainly refined the ADeL description language, the semantics of some of its instructions and their compilation into equation systems. We also improved the recognition engine and the synchronizer to better handle the synchronous/asynchronous transformation.

Work remains to be done to complete a full framework to generate generic recognition systems and automatic tools to interface with static and dynamic analysis tools, such as model checkers or performance monitors.

### 6.19.1. Activity Description Language

The ADeL language was designed to describe various activities, it provides two different (and equivalent) formats: graphical and textual. This year we started to describe use case examples in the medical domain: serious games and exercises for patients having cognitive problems, such as Alzheimer or autistic persons. This kind of games are used to test patients and to evaluate their behavior and interactions. These use cases lead us to improve the language and part of its semantics. An example of the graphical format describing a simple exercise activity is given in figure 23 .

Work remains to be done to improve the usability of the language by our end-users.

### 6.19.2. Synchronizer

Using the synchronous paradigm makes time manipulation easy thanks to determinism and synchronous parallelism; moreover, tools exist to support formal verification. However, the sensor environment is asynchronous and it is thus necessary to transform asynchronous events given by sensors into synchronous logical instants. It is a difficult problem that does not have an exact and complete solution. We introduced a component called "synchronizer" between the environment sensors and the recognition engine. The synchronizer is responsible for filtering the sensor data, grouping them into logical instants, and sending these instants to the recognition engine.

We specified a generic algorithm, based on *awaited* events, i.e. the events which may trigger transitions to a next state. These events are provided by each automaton in each state. This algorithm is parametrized by heuristics to adapt to different situations. There are two main points of variation in the synchronizer where heuristics can be applied: when processing data coming from the sensors (to collect and combine raw data) and when building logical instants (to decide on the end of instants and to manage preemptions).

This year we finished to implement a first version of the synchronizer (for one single activity to recognize), we defined different heuristics, and we tested the synchronizer algorithm on some uses cases with these heuristics [11].

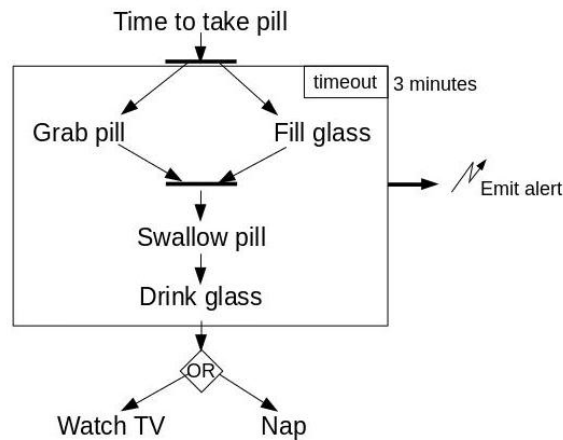


Figure 23. Example of a simple activity (patient should take a pill at a given time) including a parallel and a timeout instructions.

## 6.20. Probabilistic Activity Modeling

**Participants:** Elisabetta de Maria, Sabine Moisan, Jean-Paul Rigault, Thibaud L'Yvonnet.

Serious games constitute a domain in which real-time activity recognition is particularly relevant: the expected behavior is well identified and it is possible to rely on different sensors (biometric and external) while playing the game. We focus on games to help in diagnosis and treatment of patients.

We developed a formal approach to model such activities, taking into account possible variations in human behavior. All the scenarios of an activity are not equivalent: some are typical (thus frequent) while others seldom happen. We propose to quantify the likelihood of these variations by associating probabilities with the key actions of the activity description. We rely on a formal model based on probabilistic discrete-time Markov chains (DTMCs). We used the PRISM framework and its model checking facilities to express and check interesting temporal logic properties (PCTL).

As a use case, we considered a serious game to analyze the behavior of Alzheimer patients. We encoded this game as a DTMC in PRISM and we defined several meaningful PCTL properties that are then automatically tested thanks to the PRISM model checker. Two kinds of properties may be defined: those to verify the model and those oriented toward the medical domain. The latter may give indications to a practitioner regarding a patient's behavior. These properties include the use of PRISM "rewards" to quantify the performance of patients.

We expect that such a modeling approach could provide doctors with new indications for interpreting patients' performance and we identified three medically interesting outcomes for this approach. First, to evaluate a new patient before the first diagnosis of doctors, we can compare her game performance to a reference model representing a "healthy" behavior. Second, to monitor known patients, a customized model can be created according to their first results, and, over time, their health improvement or deterioration could be monitored. Finally, to pre-select a cohort of patients, we can use a reference model to determine, in a fast way, whether a new group of patients belongs to this specific category.

This year we first addressed the model definition and its suitability to check behavioral properties of interest [24]. Indeed, this is mandatory before envisioning any clinical study.

The next step will be to validate our approach as well as to test its scalability on three other serious games selected with the help of clinicians. We wrote a medical protocol to be submitted to CERNI proposing clinical experimentations with patients. This protocol will be a collaboration with the ICP institute, member of the CoBTEX laboratory. The new games will be modeled in PRISM and different configurations (for example for Mild, Moderate or Severe Alzheimer) will be set up with the participation of clinicians. Then, several groups of patients will play these games and their results will be recorded to calibrate our initial models.

## TITANE Project-Team

# 7. New Results

## 7.1. Analysis

### 7.1.1. Pyramid scene parsing network in 3D: improving semantic segmentation of point clouds with multi-scale contextual information

**Participants:** Hao Fang, Florent Lafarge.

Analyzing and extracting geometric features from 3D data is a fundamental step in 3D scene understanding. Recent works demonstrated that deep learning architectures can operate directly on raw point clouds, i.e. without the use of intermediate grid-like structures. These architectures are however not designed to encode contextual information in-between objects efficiently. Inspired by a global feature aggregation algorithm designed for images, we propose a 3D pyramid module to enrich pointwise features with multi-scale contextual information. Our module can be easily coupled with 3D semantic segmentation methods operating on 3D point clouds. We evaluated our method on three large scale datasets with four baseline models. Experimental results show that the use of enriched features brings significant improvements to the semantic segmentation of indoor and outdoor scenes (See Figure 1 ). This work was published in the ISPRS journal of Remote Sensing and Photogrammetry [6].

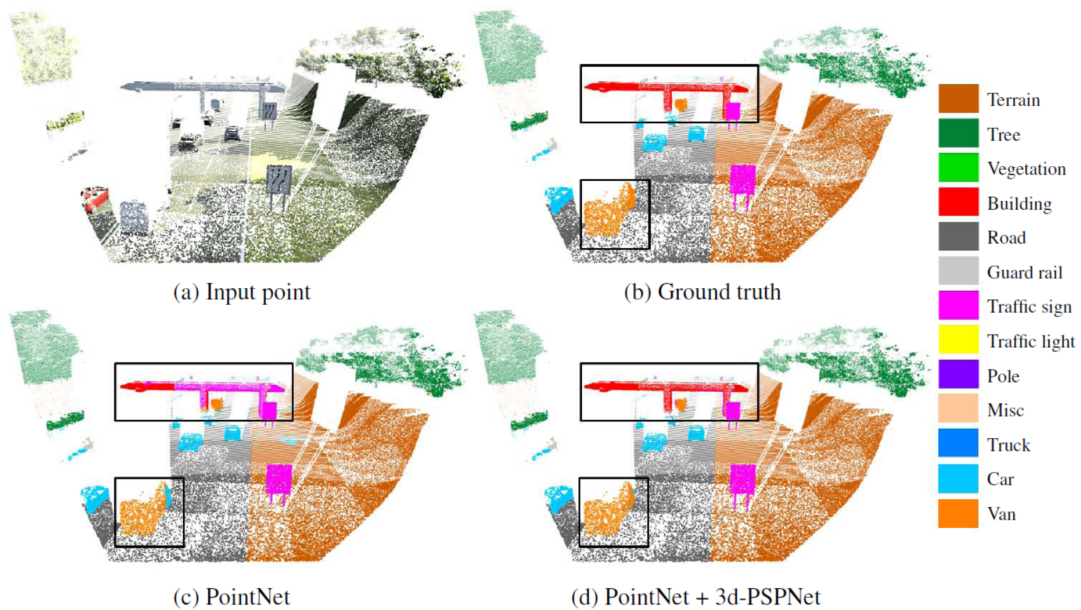


Figure 1. Semantic segmentation of a point cloud with and without our 3d-PSPNet module. Given an input point cloud (a), PointNet fails to predict correct labels for points describing large-scale objects (see rectangles in (c)). PointNet equipped with our 3d-PSPNet module gives better prediction results by enriching global contextual information (d).

### 7.1.2. *Low-power neural networks for semantic segmentation of satellite images*

**Participants:** Gaetan Bahl, Florent Lafarge.

*In collaboration with Lionel Daniel and Matthieu Moretti (IRT Saint-Exupéry).*

Semantic segmentation methods have made impressive progress with deep learning. However, while achieving higher and higher accuracy, state-of-the-art neural networks overlook the complexity of architectures, which typically feature dozens of millions of trainable parameters. As a result, these networks require high computational resources and are mostly not suited to perform on edge devices with tight resource constraints, such as phones, drones, or satellites. In this work, we propose two highly-compact neural network architectures for semantic segmentation of images, which are up to 100 000 times less complex than state-of-the-art architectures while approaching their accuracy. To decrease the complexity of existing networks, our main ideas consist in exploiting lightweight encoders and decoders with depth-wise separable convolutions and decreasing memory usage with the removal of skip connections between encoder and decoder. Our architectures are designed to be implemented on a basic FPGA such as the one featured on the Intel Altera Cyclone V family. We demonstrate the potential of our solutions in the case of binary segmentation of remote sensing images, in particular for extracting clouds and trees from RGB satellite images. This work was published in the Low-Power Computer Vision ICCV workshop [13].

### 7.1.3. *A learning approach to evaluate the quality of 3D city models*

**Participants:** Oussama Ennafii, Florent Lafarge.

*In collaboration with Arnaud Le Bris and Clément Mallet (IGN).*

The automatic generation of 3D building models from geospatial data is now a standard procedure. An abundant literature covers the last two decades and several softwares are now available. However, urban areas are very complex environments. Inevitably, practitioners still have to visually assess, at city-scale, the correctness of these models and detect frequent reconstruction errors. Such a process relies on experts, and is highly time-consuming with approximately two hours per square kilometer for one expert. This work proposes an approach for automatically evaluating the quality of 3D building models. Potential errors are compiled in a novel hierarchical and versatile taxonomy. This allows, for the first time, to disentangle fidelity and modeling errors, whatever the level of detail of the modeled buildings. The quality of models is predicted using the geometric properties of buildings and, when available, Very High Resolution images and Digital Surface Models. A baseline of handcrafted, yet generic, features is fed into a Random Forest classifier. Both multi-class and multi-label cases are considered: due to the interdependence between classes of errors, it is possible to retrieve all errors at the same time while simply predicting correct and erroneous buildings. The proposed framework was tested on three distinct urban areas in France with more than 3,000 buildings. 80% – 99% F-score values are attained for the most frequent errors. For scalability purposes, the impact of the urban area composition on the error prediction was also studied, in terms of transferability, generalization and representativeness of the classifiers. It shows the necessity of multimodal remote sensing data and mixing training samples from various cities to ensure stability of the detection ratios, even with very limited training set sizes. This work was presented at the IGARSS conference [16] and published in the PE&RS journal [5].

### 7.1.4. *Robust joint image reconstruction from color and monochrome cameras*

**Participant:** Muxingzi Li.

*In collaboration with Peihan Tu (Uni. of Maryland) and Wolfgang Heidrich (KAUST).*

Recent years have seen an explosion of the number of camera modules integrated into individual consumer mobile devices, including configurations that contain multiple different types of image sensors. One popular configuration is to combine an RGB camera for color imaging with a monochrome camera that has improved performance in low-light settings, as well as some sensitivity in the infrared. In this work we introduce a method to combine simultaneously captured images from such a two-camera stereo system to generate a high-quality, noise reduced color image. To do so, pixel-to-pixel alignment has to be constructed between the two captured monochrome and color images, which however, is prone to artifacts due to parallax. The joint image

reconstruction is made robust by introducing a novel artifact-robust optimization formulation. We provide extensive experimental results based on the two-camera configuration of a commercially available cell phone. This work was presented at the BMVC conference [18].

### 7.1.5. *Noisy supervision for correcting misaligned cadaster maps without perfect Ground Truth data*

**Participants:** Nicolas Girard, Yuliya Tarabalka.

*In collaboration with Guillaume Charpiat (Tau Inria project-team).*

In machine learning the best performance on a certain task is achieved by fully supervised methods when perfect ground truth labels are available. However, labels are often noisy, especially in remote sensing where manually curated public datasets are rare. We study the multi-modal cadaster map alignment problem for which available annotations are misaligned polygons, resulting in noisy supervision. We subsequently set up a multiple-rounds training scheme which corrects the ground truth annotations at each round to better train the model at the next round. We show that it is possible to reduce the noise of the dataset by iteratively training a better alignment model to correct the annotation alignment. This work was presented at the IGARSS conference [10].

### 7.1.6. *Incremental Learning for Semantic Segmentation of Large-Scale Remote Sensing Data*

**Participants:** Onur Tasar, Pierre Alliez, Yuliya Tarabalka.

In spite of remarkable success of the convolutional neural networks on semantic segmentation, they suffer from catastrophic shortcomings: a significant performance drop for the already learned classes when new classes are added on the data having no annotations for the old classes. We propose an incremental learning methodology, enabling to learn segmenting new classes without hindering dense labeling abilities for the previous classes, although the entire previous data are not accessible. The key points of the proposed approach are adapting the network to learn new as well as old classes on the new training data, and allowing it to remember the previously learned information for the old classes. For adaptation, we keep a frozen copy of the previously trained network, which is used as a memory for the updated network in absence of annotations for the former classes. The updated network minimizes a loss function, which balances the discrepancy between outputs for the previous classes from the memory and updated networks, and the mis-classification rate between outputs for the new classes from the updated network and the new ground-truth. We either regularly feed samples from the stored, small fraction of the previous data or use the memory network, depending on whether the new data are collected from completely different geographic areas or from the same city (see Figure 2 ). Our experimental results prove that it is possible to add new classes to the network, while maintaining its performance for the previous classes, despite the whole previous training data are not available. This work was published in the IEEE journal of Selected Topics in Applied Earth Observations and Remote Sensing [9].

### 7.1.7. *Multi-Task Deep Learning for Satellite Image Pansharpening and Segmentation*

**Participants:** Onur Tasar, Yuliya Tarabalka.

*In collaboration with Andrew Khalel (Cairo University), Guillaume Charpiat (Inria, TAU team)*

In this work, we propose a novel multi-task framework, to learn satellite image pansharpening and segmentation jointly (Figure 3 ). Our framework is based on the encoder-decoder architecture, where both tasks share the same encoder but each one has its own decoder. We compare our framework against single-task models with different architectures. Results show that our framework outperforms all other approaches in both tasks. This work was presented at the IGARSS conference [11].

### 7.1.8. *A Generic Framework for Combining Multiple Segmentations in Geographic Object-Based Image Analysis*

**Participant:** Onur Tasar.

*In collaboration with Sébastien Lefèvre (Université Bretagne Sud, IRISA) and David Sheeren (DYNAFOR, University of Toulouse, INRA)*



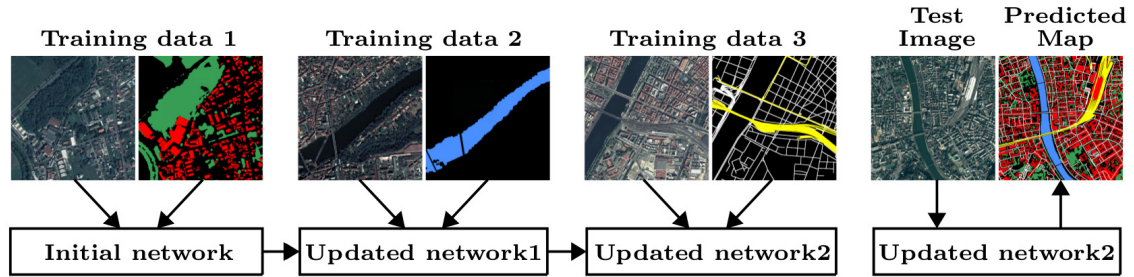


Figure 2. An example of an incremental learning scenario. Firstly, satellite images as well as their label maps for building and high vegetation classes are fed to the network. Then, from the second training data, the network learns the water class without forgetting building and high vegetation classes. Finally, road and railway classes are taught to the network. Whenever new training data are obtained, we store only a small part of the previous ones for the network to remember. When a new test image is provided, the network is able to detect all the classes.

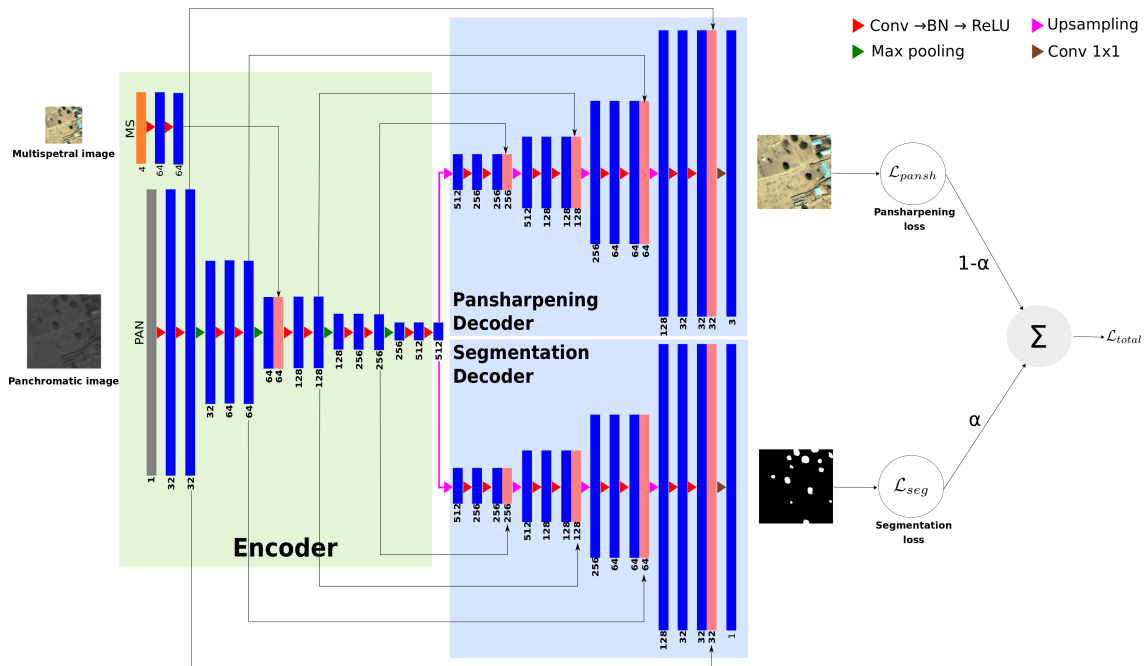


Figure 3. The overall pansharpening and segmentation framework.

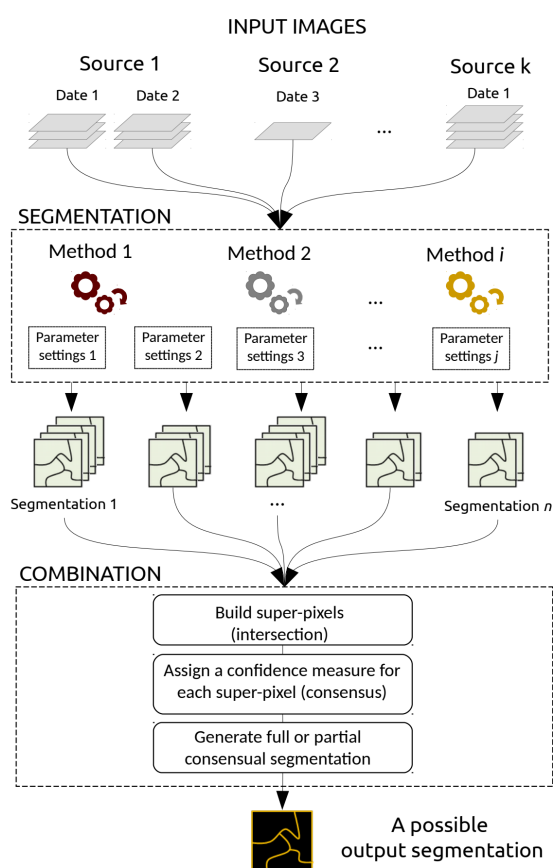


Figure 4. Our generic framework to combine multiple segmentations in the GEOBIA paradigm. Segmentations can come from different data sources (e.g., optical and radar sensors) and be acquired at different dates. They may also be produced using different methods (e.g., region-based or edge-based) relying on different parameter values.

The Geographic Object-Based Image Analysis (GEOBIA) paradigm relies strongly on the segmentation concept, i.e., partitioning of an image into regions or objects that are then further analyzed. Segmentation is a critical step, for which a wide range of methods, parameters and input data are available. To reduce the sensitivity of the GEOBIA process to the segmentation step, here we consider that a set of segmentation maps can be derived from remote sensing data. Inspired by the ensemble paradigm that combines multiple weak classifiers to build a strong one, we propose a novel framework for combining multiple segmentation maps (Figure 4). The combination leads to a fine-grained partition of segments (super-pixels) that is built by intersecting individual input partitions, and each segment is assigned a segmentation confidence score that relates directly to the local consensus between the different segmentation maps. Furthermore, each input segmentation can be assigned some local or global quality score based on expert assessment or automatic analysis. These scores are then taken into account when computing the confidence map that results from the combination of the segmentation processes. This means the process is less affected by incorrect segmentation inputs either at the local scale of a region, or at the global scale of a map. In contrast to related works, the proposed framework is fully generic and does not rely on specific input data to drive the combination process. We assess its relevance through experiments conducted on ISPRS 2D Semantic Labeling. Results show that the confidence map provides valuable information that can be produced when combining segmentations, and fusion at the object level is competitive w.r.t. fusion at the pixel or decision level. This work was published in the ISPRS journal of Geo-Information [8].

## 7.2. Reconstruction

### 7.2.1. City Reconstruction from Airborne Lidar: A Computational Geometry Approach

**Participants:** Jean-Philippe Bauchet, Florent Lafarge.

We introduce a pipeline that reconstructs buildings of urban environments as concise polygonal meshes from airborne LiDAR scans. It consists of three main steps: classification, building contouring, and building reconstruction, the two last steps being achieved using computational geometry tools. Our algorithm demonstrates its robustness, flexibility and scalability by producing accurate and compact 3D models over large and varied urban areas in a few minutes only (See Figure 5). This work was published in the ISPRS international conference 3D GeoInfo [14].

### 7.2.2. Extracting geometric structures in images with Delaunay point processes

**Participant:** Florent Lafarge.

*In collaboration with Jean-Dominique Favreau (Ekinnox), Adrien Bousseau (GraphDeco Inria team) and Alex Auvolat (Wide Inria team).*

We introduce Delaunay Point Processes, a framework for the extraction of geometric structures from images. Our approach simultaneously locates and groups geometric primitives (line segments, triangles) to form extended structures (line networks, polygons) for a variety of image analysis tasks. Similarly to traditional point processes, our approach uses Markov Chain Monte Carlo to minimize an energy that balances fidelity to the input image data with geometric priors on the output structures. However, while existing point processes struggle to model structures composed of interconnected components, we propose to embed the point process into a Delaunay triangulation, which provides high-quality connectivity by construction. We further leverage key properties of the Delaunay triangulation to devise a fast Markov Chain Monte Carlo sampler. We demonstrate the flexibility of our approach on a variety of applications, including line network extraction, object contouring, and mesh-based image compression (See Figure 6). This work was published in the IEEE journal TPAMI [7].

## 7.3. Approximation

### 7.3.1. Cost-driven framework for progressive compression of textured meshes

**Participants:** Cédric Portaneri, Pierre Alliez.

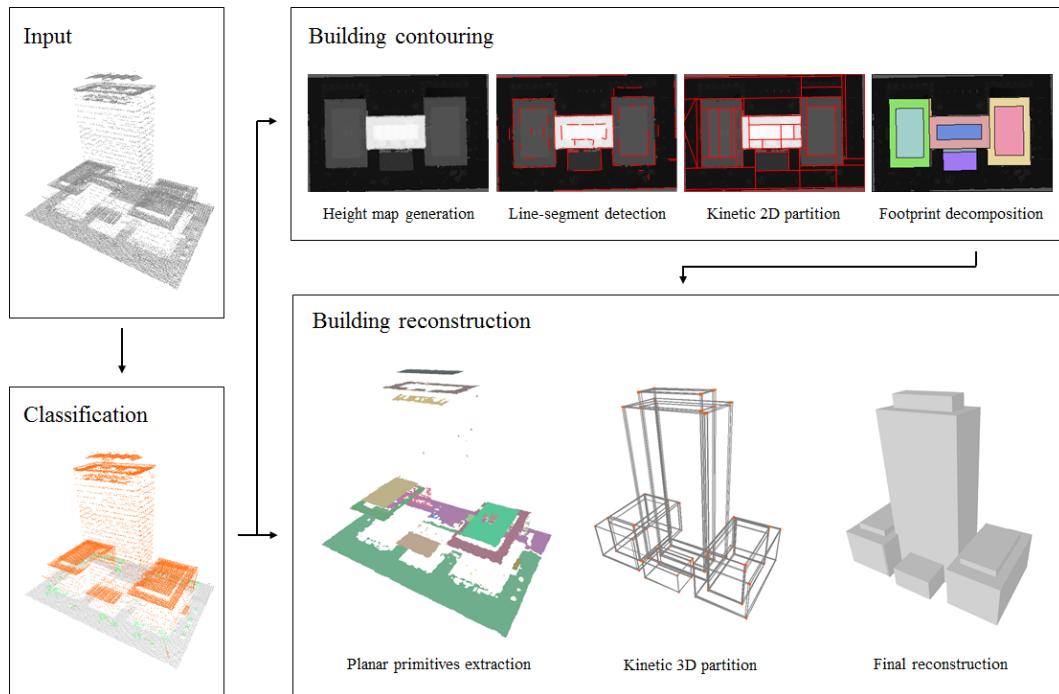


Figure 5. City Reconstruction from Airborne Lidar. Our method consists of three main steps. We first label points of the LiDAR scan as ground, vegetation or roof. Then, we apply a contouring algorithm to the height map, revealing the facades initially absent in the point set. Finally, we extract and propagate planar primitives from the point cloud, dividing the space into polyhedra that are labeled to obtain a 3D reconstruction of buildings.



Figure 6. Example applications of Delaunay Point Processes to extract planar graphs representing blood vessels in retina images (left), and complex polygons representing object silhouettes (right). The point distribution creates a dynamic Delaunay triangulation while edge and facet labels specify the geometric structure (see red edges on close-ups).

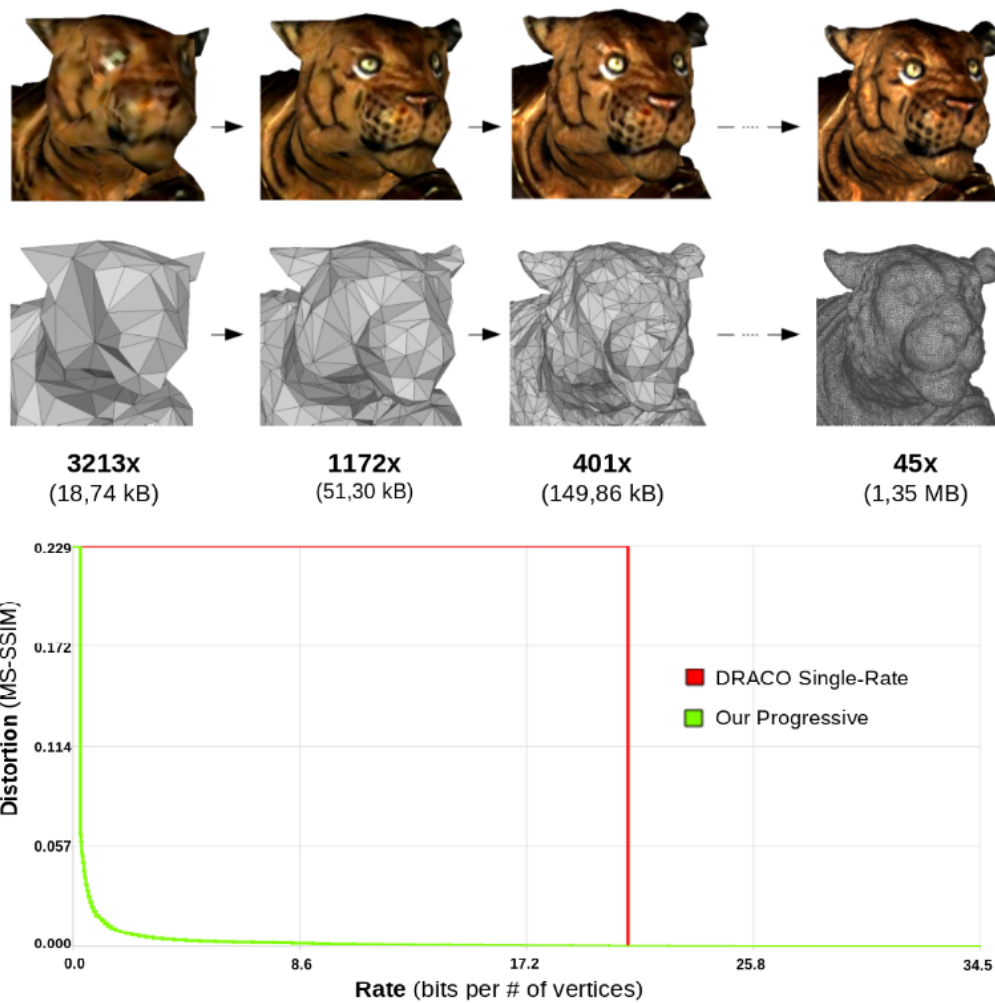


Figure 7. Progressive decomposition of a textured surface triangle mesh. Top: key levels of detail with their size and compression rate compared to the raw obj file (texture data not included). Bottom: Distortion against the bit consumption, in bits per vertex, where the number of vertices refers to the input mesh. Green is our progressive approach, red is the state-of-the-art single-rate DRACO encoder.

*In collaboration with Michael Hemmer (Google X), Lukas Birklein and Elmar Schoemer (Uni. of Mainz).*

Recent advances in digitization of geometry and radiometry generate in routine massive amounts of surface meshes with texture or color attributes. This large amount of data can be compressed using a progressive approach which provides at decoding low complexity levels of details (LODs) that are continuously refined until retrieving the original model. The goal of such a progressive mesh compression algorithm is to improve the overall quality of the transmission for the user, by optimizing the rate-distortion trade-off. In this paper, we introduce a novel meaningful measure for the cost of a progressive transmission of a textured mesh by observing that the rate-distortion curve is in fact a staircase, which enables an effective comparison and optimization of progressive transmissions in the first place. We contribute a novel generic framework which utilizes the cost function to encode triangle surface meshes via multiplexing several geometry reduction steps (mesh decimation via half-edge or full-edge collapse operators, xyz quantization reduction and uv quantization reduction). This framework can also deal with textures by multiplexing an additional texture reduction step. We also design a texture atlas that enables us to preserve texture seams during decimation while not impairing the quality of resulting LODs. For encoding the inverse mesh decimation steps we further contribute a significant improvement over the state-of-the-art in terms of rate-distortion performance and yields a compression-rate of 22:1, on average. Finally, we propose a unique single-rate alternative solution using a selection scheme of a subset among LODs, optimized for our cost function, and provided with our atlas that enables interleaved progressive texture refinements (see Figure 7). This work was presented at the ACM Multimedia Systems conference [19] and obtained the best paper award.

### 7.3.2. *Selective padding for Polycube-based hexahedral meshing*

**Participant:** Pierre Alliez.

*In collaboration with Gianmarco Cherchi and Riccardo Scateni from University of Cagliari (Sardinia), Max Lyon from University of Aachen and David Bommes from University of Bern.*

Hexahedral meshes generated from polycube mapping often exhibit a low number of singularities but also poor quality elements located near the surface. It is thus necessary to improve the overall mesh quality, in terms of the minimum Scaled Jacobian (MSJ) or average Scaled Jacobian (ASJ). Improving the quality may be obtained via global padding (or pillowing), which pushes the singularities inside by adding an extra layer of hexahedra on the entire domain boundary. Such a global padding operation suffers from a large increase of complexity, with unnecessary hexahedra added. In addition, the quality of elements near the boundary may decrease. We propose a novel optimization method which inserts sheets of hexahedra so as to perform selective padding, where it is most needed for improving the mesh quality. A sheet can pad part of the domain boundary, traverse the domain and form singularities. Our global formulation, based on solving a binary problem, enables us to control the balance between quality improvement, increase of complexity and number of singularities. We show in a series of experiments that our approach increases the MSJ value and preserves (or even improves) the ASJ, while adding fewer hexahedra than global padding. (See Figure 8). This work was published in an international journal and was presented at the EUROGRAPHICS conference [4].



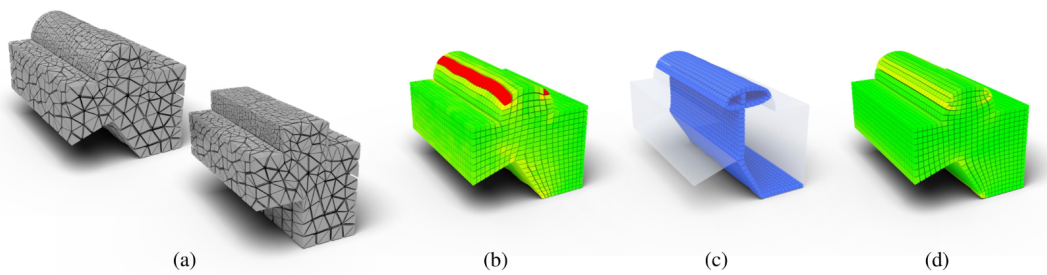


*Figure 8. Polycube-based hexahedral meshing. Our pipeline takes as input a model and its polycube mapping (a); we compute the relative hex-mesh and locate the surface areas in need of padding analyzing the mapping quality (b); we set and solve a binary problem to find a set of facets to extrude in order to create a selective padding layer (c); we compute and analyze the mapping with the new hex-mesh structure (d).*

## TOSCA Team

## 6. New Results

### 6.1. Probabilistic numerical methods, stochastic modeling and applications

**Participants:** Sofia Allende Contador, Alexis Anagnostakis, Mireille Bossy, Lorenzo Campana, Nicolas Champagnat, Quentin Cormier, Madalina Deaconu, Aurore Dupre, Coralie Fritsch, Vincent Hass, Pascal Helson, Christophe Henry, Ulysse Herbach, Igor Honore, Antoine Lejay, Rodolphe Loubaton, Radu Maftai, Kerlyns Martinez Rodriguez, Victor Martin Lac, Hector Olivero-Quinteros, Édouard Strickler, Denis Talay, Etienne Tanré, Denis Villemonais.

#### 6.1.1. Published works and preprints

- H. AlRachid (Orléans University), M. Bossy, C. Ricci (University of Florence) and L. Szpruch (University of Edinburgh and The Alan Turing Institute, London) introduced several new particle representations for *ergodic* McKean-Vlasov SDEs. They construct new algorithms by leveraging recent progress in weak convergence analysis of interacting particle system. In [12] they present detailed analysis of errors and associated costs of various estimators, highlighting key differences between long-time simulations of linear (classical SDEs) versus non-linear (McKean-Vlasov SDEs) process.
- M. Di Iorio (Marine Energy Research and Innovation Center, Santiago, Chile), M. Bossy, C. Mokrani (Marine Energy Research and Innovation Center, Santiago, Chile), and A. Rousseau (LEMON team) obtained advances in stochastic Lagrangian approaches for the simulation of hydrokinetic turbines immersed in complex topography [42].
- M. Bossy, J.-F. Jabir (University of Edinburgh) and K. Martinez (University of Valparaiso) consider the problem of the approximation of the solution of a one-dimensional SDE with non-globally Lipschitz drift and diffusion coefficients behaving as  $x^\alpha$ , with  $\alpha > 1$  [44]. They propose an (semi-explicit) exponential-Euler scheme and study its convergence through its weak approximation error. To this aim, they analyze the  $C^{1,4}$  regularity of the solution of the associated backward Kolmogorov PDE using its Feynman-Kac representation and the flow derivative of the involved processes. From this, under some suitable hypotheses on the parameters of the model ensuring the control of its positive moments, they recover a rate of weak convergence of order one for the proposed exponential Euler scheme. Numerical experiments are analyzed in order to complement their theoretical result.
- L. Campana et al. developed some Lagrangian stochastic model for anisotropic particles in turbulent flow [35]. Suspension of anisotropic particles can be found in various industrial applications. Microscopic ellipsoidal bodies suspended in a turbulent fluid flow rotate in response to the velocity gradient of the flow. Understanding their orientation is important since it can affect the optical or rheological properties of the suspension (e.g. polymeric fluids). The equations of motion for the orientation of microscopic ellipsoidal particles was obtained by Jeffery. But so far this description has been always investigated in the framework of direct numerical simulations (DNS) and experimental measurements. In this work, the orientation dynamics of rod-like tracer particles, i.e. long ellipsoidal particles (in the limit of infinite aspect-ratio) is studied. The size of the rod is assumed smaller than the Kolmogorov length scale but sufficiently large that its Brownian motion need not be considered. As a result, the local flow around a particle can be considered as inertia-free and Stokes flow solutions can be used to relate particle rotational dynamics to the local velocity gradient. The orientation of rod can be described as the normalised solution of the linear ordinary differential equation for the separation vector between two fluid tracers, under the action of the velocity gradient tensor. In this framework, the rod orientation is described by a Lagrangian stochastic model where cumulative velocity gradient fluctuations are represented by a white-noise tensor such that the incompressibility condition is preserved. A numerical scheme based on the decomposition into skew/symmetric part of the process dynamics is proposed.

- Together with M. Andrade-Restrepo (Univ. Paris Diderot) and R. Ferrière (Univ. Arizona and École Normale Supérieure), N. Champagnat studied deterministic and stochastic spatial eco-evolutionary dynamics along environmental gradients. This work focuses on numerical and analytical analysis of the clustering phenomenon in the population, and on the patterns of invasion fronts [13].
- Together with M. Benaïm (Univ. Neuchâtel), N. Champagnat and D. Villemonais studied stochastic algorithms to approximate quasi-stationary distributions of diffusion processes absorbed at the boundary of a bounded domain. They study a reinforced version of the diffusion, which is resampled according to its occupation measure when it reaches the boundary. They show that its occupation measure converges to the unique quasi-stationary distribution of the diffusion process [43].
- N. Champagnat, C. Fritsch and S. Billiard (Univ. Lille) studied models of food web adaptive evolution. They identified the biomass conversion efficiency as a key mechanism underlying food webs evolution and discussed the relevance of such models to study the evolution of food webs [51].
- N. Champagnat and J. Claisse (Univ. Paris-Dauphine) studied the ergodic and infinite horizon controls of discrete population dynamics with almost sure extinction in finite time. This can either correspond to control problems in favor of survival or of extinction, depending on the cost function. They have proved that these two problems are related to the quasi-stationary distribution of the processes controlled by Markov controls [18].
- N. Champagnat and B. Henry (Univ. Lille 1) studied a probabilistic approach for the Hamilton-Jacobi limit of non-local reaction-diffusion models of adaptive dynamics when mutations are small. They used a Feynman-Kac interpretation of the partial differential equation and large deviation estimates to obtain a variational characterization of the limit. They also studied in detail the case of finite phenotype space with exponentially rare mutations, where they were able to obtain uniqueness of the limit [19].
- N. Champagnat and D. Villemonais solved a general conjecture on the Fleming-Viot particle systems approximating quasi-stationary distributions (QSD): in cases where several quasi-stationary distributions exist, it is expected that the stationary distributions of the Fleming-Viot processes approach a particular QSD, called minimal QSD. They proved that this holds true for general absorbed Markov processes with soft obstacles [20].
- N. Champagnat and D. Villemonais studied the geometric convergence of normalized unbounded semigroups. They proved in [47] that general criteria for this convergence can be easily deduced from their recent results on the theory of quasi-stationary distributions.
- N. Champagnat, S. Méléard (École Polytechnique) and V.C. Tran (Univ. Paris Est Marne-la-Vallée) studied evolutionary models of bacteria with horizontal transfer. They considered in [46] a scaling of parameters taking into account the influence of negligible but non-extinct populations, allowing them to study specific phenomena observed in these models (re-emergence of traits, cyclic evolutionary dynamics and evolutionary suicide).
- M. Bahlali (CEREA, France), C. Henry and B. Carissimo (CEREA, France) clarify issues related to the expression of Lagrangian stochastic models used for atmospheric dispersion applications. They showed that accurate simulations are possible only if two aspects are properly addressed: the respect of the well-mixed criterion (related to the incorporation of the mean pressure-gradient term in the mean drift-term) and the consistency between Eulerian and Lagrangian turbulence models (regarding turbulence models, boundary and divergence-free conditions).
- A. Lejay and A. Brault have continued their work on rough flows, which provides an unified framework to deal with the theory of rough paths from the point of view of flows. In particular, they have studied consistency, stability and generic properties of rough differential equations [45].
- A. Lejay and P. Pigato have provided an estimator of a discontinuous drift coefficients [30], which follows their previous work on the oscillating Brownian motion and its application to financial models.

- A. Lejay and H. Mardones (U. la Serenan, Chile), have completed their work on the Monte Carlo simulation of the Navier-Stokes equations based on a new representation by Forward-Backward Stochastic Differential Equations [53].
- O. Faugeras, E. Soret and E. Tanré have obtained a Mean-Field description of thermodynamics limits of large population of neurons with random interactions. They have obtained the asymptotic behaviour for an asymmetric neuronal dynamics in a network of linear Hopfield neurons. They have a complete description of this limit with Gaussian processes. Furthermore, the limit object is not a Markov process [50].
- E. Tanré, P. Grazieschi (Univ. Warwick), M. Leocata (Univ. Pisa), C. Mascart (Univ. Côte d'Azur), J. Chevallier (Univ. of Grenoble) and F. Delarue (Univ. Côte d'Azur) have extended the previous work [9] to sparse networks of interacting neurons. They have obtained a precise description of the limit behavior of the mean field limit according to the probability of (random) interactions between two individual LIF neurons [24].
- P. Helson has studied the learning of an external signal by a neural network and the time to forget it when this network is submitted to noise. He has constructed an estimator of the initial signal thanks to the synaptic currents, which are Markov chains. The mathematical study of the Markov chains allow to obtain a lower bound on the number of external stimuli that the network can receive before the initial signal is forgotten [52].
- Q. Cormier and E. Tanré studied with Romain Veltz (team MATHNEURO) the long time behavior of a McKean-Vlasov SDE modeling a large assembly of neurons. A convergence to the unique (in this case) invariant measure is obtained assuming that the interactions between the neurons are weak enough. The key quantity in this model is the "firing rate": it gives the average number of jumps per unit of times of the solution of the SDE. They derive a non-linear Volterra equation satisfied by this rate. They used methods from integral equation to control finely the long time behavior of this firing rate [21].
- E. Tanré has worked with Nicolas Fournier (Sorbonne Université) and Romain Veltz (MATHNEURO Inria team) on a network of spiking networks with propagation of spikes along the dendrites. Consider a large number  $n$  of neurons randomly connected. When a neuron spikes at some rate depending on its electric potential, its membrane potential is set to a minimum value  $v_{min}$ , and this makes start, after a small delay, two fronts on the dendrites of all the neurons to which it is connected. Fronts move at constant speed. When two fronts (on the dendrite of the same neuron) collide, they annihilate. When a front hits the soma of a neuron, its potential is increased by a small value  $w_n$ . Between jumps, the potentials of the neurons are assumed to drift in  $[v_{min}, \infty)$ , according to some well-posed ODE. They prove the existence and uniqueness of a heuristically derived mean-field limit of the system when  $n \rightarrow \infty$  [23].
- O. Faugeras, James Maclaurin (Univ. of Utah) and E. Tanré have worked on the asymptotic behavior of a model of neurons in interaction with correlated gaussian synaptic weights. They have obtained the limit equation as a singular non-linear SDE and a Large Deviation Principle for the law of the finite network [49].
- E. Tanré has worked with Alexandre Richard (Centrale-Supelec) and Soledad Torres (Universidad de Valparaíso, Chile) on a one-dimensional fractional SDE with reflection. They have proved the existence of the reflected SDE with a penalization scheme (suited to numerical approximation). Penalization also gives an algorithm to approach this solution [55].
- The Neutron Transport Equation (NTE) describes the flux of neutrons over time through an inhomogeneous fissile medium. A probabilistic solution of the NTE is considered in order to demonstrate a Perron-Frobenius type growth of the solution via its projection onto an associated leading eigenfunction. The associated eigenvalue, denoted  $k_{eff}$ , has the physical interpretation as being the ratio of neutrons produced (during fission events) to the number lost (due to absorption in the reactor or leakage at the boundary) per typical fission event. Together with A. M. G. Cox, E. L. Horton and A. E. Kyprianou (Univ. Bath), D. Villemonais developed the stochastic analysis of the NTE by giving a rigorous probabilistic interpretation of  $k_{eff}$  [48].

- In [34], D. Villemonais obtained a lower bound for the coarse Ricci curvature of continuous-time pure-jump Markov processes, with an emphasis on interacting particle systems. Applications to several models are provided, with a detailed study of the herd behavior of a simple model of interacting agents.
- In collaboration with C. Coron (Univ. Paris Sud) and S. Méléard (École Polytechnique), D. Villemonais studied in [22] the way alleles extinctions and fixations occur for a multiple allelic proportions model based on diffusion processes. It is proved in particular that alleles extinctions occur successively and that a 0-1 law holds for fixation and extinction: depending on the population dynamics near extinction, either fixation occurs before extinction, or the converse, almost surely.
- Mean telomere length in human leukocyte DNA samples reflects the different lengths of telomeres at the ends of the 23 chromosomes and in an admixture of cells. Together with S. Toupance (CHRU Nancy), D. Germain (Univ. Lorraine), A. Gégout-Petit (Univ. Lorraine and BIGS Inria team), E. Albuissou (CHRU Nancy) and A. Benetos (CHRU Nancy), D. Villemonais analysed telomere length distributions dynamics in adults individuals. It is proved in [33] that the shape of this distribution is stable over the lifetime of individuals.
- J. Bion-Nadal (Ecole Polytechnique) and D. Talay have pursued their work on their Wasserstein-type distance on the set of the probability distributions of strong solutions to stochastic differential equations. This new distance is defined by restricting the set of possible coupling measures and can be expressed in terms of the solution to a stochastic control problem, which allows one to deduce a priori estimates or to obtain numerical evaluations [15].

A notable application concerns the following modeling issue: given an exact diffusion model, how to select a simplified diffusion model within a class of admissible models under the constraint that the probability distribution of the exact model is preserved as much as possible? The objective being to select a model minimizing the above distance to a target model, approximations of the optimal model have been established. The construction and analysis of an efficient stochastic algorithm are being in progress.

- D. Talay and M. Tomašević have continued to work on their new type of stochastic interpretation of the parabolic-parabolic Keller-Segel systems. It involves an original type of McKean-Vlasov interaction kernel. At the particle level, each particle interacts with all the past of each other particle. D. Talay and M. Tomašević are studying the well-posedness and the propagation of chaos of the particle system related to the two-dimensional parabolic-parabolic Keller-Segel system.
- V. Martin Lac, R. Maftai D. Talay and M. Tomašević have continued to work on theoretical and algorithmic questions related to the simulation of the Keller-Segel particle systems. The library DIAMSS has been developed.
- H. Olivero (Inria, now University of Valparaiso, Chile) and D. Talay have continued to work on their hypothesis test which helps to detect when the probability distribution of complex stochastic simulations has a heavy tail and thus possibly an infinite variance. This issue is notably important when simulating particle systems with complex and singular McKean-Vlasov interaction kernels which make it extremely difficult to get a priori estimates on the probability laws of the mean-field limit, the related particle system, and their numerical approximations. In such situations the standard limit theorems do not lead to effective tests. In the simple case of independent and identically distributed sequences the procedure developed this year and its convergence analysis are based on deep tools coming from the statistics of semimartingales.
- I. Honoré and D. Talay have worked on statistical issues related to numerical approximations of invariant probability measures of ergodic diffusions. These approximations are based on the simulation of one single trajectory up to long time horizons. I. Honoré and D. Talay handle the critical situations where the asymptotic variance of the normalized error is infinite.
- V. Martin Lac, H. Olivero-Quinteros and D. Talay have worked on theoretical and algorithmic questions related to the simulation of large particle systems under singular interactions and to critical numerical issues related to the simulation of independent random variables with heavy tails. A preliminary version of a library has been developed.

- C. Graham (École Polytechnique) and D. Talay have ended the second volume of their series on Mathematical Foundation of Stochastic Simulation to be published by Springer.

### 6.1.2. Other works in progress

- K. Martinez, M. Bossy, C. Henry, R. Maftai and S. Sherkarforush work on a refined algorithm for macroscopic simulations of particle agglomeration using population balance equations (PBE). More precisely, their study is focused on identifying regions with non-homogeneous spatial distribution of particles. This is indeed a major drawback of PBE formulations which require a well-mixed condition to be satisfied. The developed algorithm identifies higher/lower density regions to treat them separately.
- S. Allende (CEMEF, France), J. Bec (CEMEF, France), M. Bossy, L. Campana, M. Ferrand (EDF, France), C. Henry and J.P. Minier (EDF, France) work together on a macroscopic model for the dynamics of small, flexible, inextensible fibers in a turbulent flow. Following the model developed at Inria, they perform numerical simulations of the orientation of such fibers in wall-bounded turbulent flows and compare it to microscopic simulations obtained with Direct Numerical Simulation (DNS). This work is performed under the POPART project.
- N. Champagnat, C. Fritsch and U. Herbach are working with A. Harlé (Institut de Cancérologie de Lorraine), J.-L. Merlin (ICL), E. Pencreac'h (CHRU Strasbourg), A. Gégout-Petit, P. Vallois, A. Muller-Gueudin (Inria BIGS team) and A. Kurtzmann (Univ. Lorraine) within an ITMO Cancer project on modeling and parametric estimation of dynamical models of circulating tumor DNA (ctDNA) of tumor cells, divided into several clonal populations. The goal of the project is to predict the emergence of a clonal population resistant to a targeted therapy in a patient's tumor, so that the therapy can be modulated more efficiently.
- N. Champagnat and R. Loubaton are working with P. Vallois (Univ. Lorraine and Inria BIGS team) and L. Vallat (CHRU Strasbourg) on the inference of dynamical gene networks from RNAseq and proteome data.
- N. Champagnat, E. Strickler and D. Villemonais are working on the characterization of convergence in Wasserstein distance of conditional distributions of absorbed Markov processes to a quasi-stationary distribution.
- N. Champagnat and V. Hass are studying evolutionary models of adaptive dynamics under an assumption of large population and small mutations. They expect to recover variants of the canonical equation of adaptive dynamics, which describes the long time evolution of the dominant phenotype in the population, under less stringent biological assumptions than in previous works.
- Q. Cormier, E. Tanré and Romain Veltz (team MATHNEURO) are working on the local stability of a stationary solution of some McKean-Vlasov equation. They also obtain spontaneous oscillation of the solution for critical values of the external currents or the interactions.
- M. Deaconu, A. Lejay and E. Mordecki (U. de la República, Uruguay) are studying an optimal stopping problem for the Snapping Out Brownian motion.
- M. Deaconu and A. Lejay are currently working on the simulation and the estimation of the fragmentation equation through its probabilistic representation.
- S. Allende (CEMEF, France), C. Henry and J. Bec (CEMEF, France) work on the dynamics of small, flexible, inextensible fibers in a turbulent flow. They show that the fragmentation of fibers smaller than the smallest fluid scale in a turbulent flow occurs through tensile fracture (i.e. when the fiber is stretched along its main axis) or through flexural failure (i.e. when the fiber curvature is too high as it buckles under compressive load). Statistics of such events are provided together with measures of the rate of fragmentation and daughter size distributions, which are basic ingredients for macroscopic fragmentation models.



- C. Henry and M.L. Pedrotti (LOV, France) are working together on the topic of sedimentation of plastic that are populated by biological organisms (this is called biofouling). Biofouling modifies the density of plastic debris in the ocean and can lead to their sedimentation towards deeper regions. This work is done under the PLAISE project, which comprises measurements (by the LOV) and simulations (by C. Henry).
- C. Fritsch is working with A. Gégout-Petit (Univ. Lorraine and EPI BIGS), B. Marçais (INRA, Nancy) and M. Grosdidier (INRA, Avignon) on a statistical analysis of a Chalara Fraxinea model.
- C. Fritsch is working with Tanjona Ramiadantsoa (Univ. Wisconsin-Madison) on a model of extinction of orphaned plants.
- A. Lejay and M. Clausel (U. Lorraine) are studying the clustering method based on the use of the signature and the iterated integrals of time series. It is based on asymmetric spectral clustering [41].
- In collaboration with L. Lenotre (postdoc at IECL between Oct. 2018 and Sep. 2019), A. Gégout-Petit (Univ. Lorraine and Inria BIGS team) and O. Coudray (Master degree student), D. Villemonais conducted preliminary researches on branching models for the telomeres' length dynamics across generations.

## WIMMICS Project-Team

## 7. New Results

### 7.1. Users Modeling and Designing Interaction

#### 7.1.1. *Design of a User-Centered Evaluation Method for Exploratory Search Systems: Consolidation of the CheXplore plugin*

**Participants:** Alain Giboin, Jean-Marie Dormoy, Emilie Palagi, Fabien Gandon.

Designed and implemented in the context of the PhD of Emilie Palagi [64], CheXplore is a Chrome plugin that supports the user-centered evaluation of exploratory search systems. This year, CheXplore has been consolidated, i.e., in particular, refactoring of the source code – from jQuery to JavaScript; addition of some new functionalities mentioned in Emilie Palagi’s PhD thesis.

#### 7.1.2. *User Evaluation of the WASABI demonstrators*

**Participants:** Alain Giboin, Michel Buffa, Elmahdi Korfed.

In the context of the ANR project WASABI, and in collaboration with Guillaume Pellerin (IRCAM), we specified a generic methodological framework for evaluating the WASABI musical demonstrators through their use. The demonstrators are targeted to six kinds of users: composers, musicologists, journalists, content providers, music school students and teachers, and sound-engineers.

#### 7.1.3. *Territoriality-theory-based Rules and Method for Designing Multi-device Games*

**Participant:** Alain Giboin.

A research action performed in the context of a collaboration with Anne-Marie Dery-Pinna, Philippe Renevier (I3S, Sparks team) and Sophie Lepreux (UVHC, LAMIH Lab). Observing that “territorial behavior” occurs during human interaction at a table – i.e. that humans engaged in a collaborative task partition the table workspace into different zones (so-called personal territory, group territory and storage territory), in order to get collaborative benefits –, Scott and Carpendale [65] proposed to rely on a tabletop territoriality (or workspace partitioning) theory to support the design of collaborative digital tabletop applications. Concerned by competitive game applications involving multiple devices (e.g., tabletop, tablet, smartphone), we adapted Scott and Carpendale’s theory, and, based on this adapted theory, we developed a set of rules and a method for designing the user interfaces of these multi-device applications [57]. This year, we refined this set of rules and this method after having tested them [58].

#### 7.1.4. *Linked Data Visualization*

**Participants:** Yun Tian, Olivier Corby.

We started a collaboration with M. Winckler from I3S, UNS, on Linked Data visualization with Yun Tian, a Polytech’Nice Master internship. During this internship, we have connected the HAL open data server<sup>0</sup> with the MGEExplorer graphic library. The result is a graphic browser for copublications. This work resulted in a server prototype<sup>0</sup>.

#### 7.1.5. *Linked Data Path Finder*

**Participants:** Marie Destandeu, Olivier Corby, Alain Giboin.

We started a collaboration with the ILDA Inria team from Saclay where we developed an algorithm to explore the content of remote Semantic Web triple stores.

<sup>0</sup><http://sparql.archives-ouvertes.fr/sparql>

<sup>0</sup><http://sparks-vm9.i3s.unice.fr:8080/index.html>

## 7.2. Communities and Social Interactions Analysis

### 7.2.1. Fake News Detection

**Participants:** Elena Cabrio, Serena Villata, Jérôme Delobelle.

This work is part of the DGA project RAPID CONFIRMA (COntre argumentation contre les Fausses InfoRMAtion) aiming to automatically detect fake news and limit their diffusion. In this purpose, a framework is developed to detect fake news, to reduce their propagation and to propose the best response strategies. Thus, in addition to identifying the communities propagating these fake news, our goal is to propose a method to convince a person that the information is actually false is a key element in fighting the spread of such a kind of dangerous information. To achieve this goal, we orientate our research towards the generation of counter-argumentation. Counter-argumentation is a process aiming to put forward counter-arguments in order to provide evidences against a certain argument previously proposed. In the case of fake news, in order to convince a person that the (fake) information is true, the author of the fake news will use different methods of persuasion via arguments. Thus, identifying these arguments and attacking them by using carefully constructed arguments from safe sources is a way to fight this phenomenon and its spread along the social network. More precisely, we have identified four steps to address the counter-argumentation process: (1) Identifying the arguments used in the fake news (Argument mining); (2) Determining, for each of the arguments, whether it is for or against the topic of the fake news (Stance detection); (3) Identifying the key arguments that our system must attack (Classification task); and (4) Providing a set of arguments from safe sources to attack the targeted fake arguments (Counter-Argumentation).

We are also interested in studying, from a formal point of view, how to cast the notion of interpretability (i.e. the degree to which an observer can understand the cause(s) of a result) in abstract argumentation so that the reasons leading to the acceptability of one or a set of arguments in a framework (returned by a particular semantics) may be explicitly assessed [13]. More precisely, this research question breaks down into the following sub-questions: (i) how to formally define and characterise the notion of *impact* of an argument with respect to the acceptability of the other arguments in the framework? and (ii) how does this impact play a role in the interpretation process of the acceptability of arguments in the framework?

### 7.2.2. Hate Speech Detection

**Participants:** Elena Cabrio, Alain Giboin, Sara Tonelli, Michele Corazza, Pinar Arslan, Stefano Menini.

On the topic of cyberbullying event detection and hate speech detection, we proposed a message-level cyberbullying annotation on an Instagram dataset. Moreover, we used the correlations on the Instagram dataset annotated with emotion, sentiment and bullying labels. Finally, we built a message-level emotion classifier automatically predicting emotion labels for each comment in the Vine bullying dataset. We built a session-based bullying classifier with the use of n-grams, emotion, sentiment and concept-level features. For both emotion and bullying classifiers, we used Linear Support Vector Classification. Our results showed that “anger” and “negative” labels have a positive correlation with the presence of bullying. Concept-level features, emotion and sentiment features in different levels contribute to the bullying classifier, especially to the bullying class. Our best performing bullying classifier with n-grams and concept-level features (e.g., polarity, averaged polarity intensity, moodtags and semantics features) reached to an F1-score of 0.65 for bullying class and a macro average F1-score of 0.7520. The results of this research have been published at SAC 2019 [7].

Together with some colleagues at FBK Trento, we performed a comparative evaluation on datasets for hate speech detection in Italian, extracted from four different social media platforms, i.e. Facebook, Twitter, Instagram and WhatsApp. We showed that combining such platform-dependent datasets to take advantage of training data developed for other platforms is beneficial, although their impact varies depending on the social network under consideration. The results of this research have been published at SAC 2019 [11].

## 7.3. Vocabularies, Semantic Web and Linked Data Based Knowledge Representation and Artificial Intelligence Formalisms on the Web

### 7.3.1. Semantic Web for Biodiversity

**Participants:** Franck Michel, Catherine Faron Zucker, Antonia Ettore.

The development of an activity related to biodiversity data sharing and integration is going on through the sustained collaboration with the "Muséum National d'Histoire Naturelle" of Paris (MNHN).

First, at the very end of 2018, we published a journal paper about the SPARQL Micro-Services architecture and how this can be useful in the biodiversity domain [62]. Then, through the internship of a Ubinet master student, we explored how SPARQL Micro-Services can help biologists in editing taxonomic information by confronting multiple, heterogeneous biodiversity-related data sources. We presented some results of this work at the Biodiversity\_Next conference 2019 [28].

Within the same internship we continued the work meant to publish biodiversity data as linked data (TAXREF-LD<sup>0</sup>). The goal is to extend the dataset from simple taxonomic data to new types of data: species interactions, multi-lingual names, conservation and legal statuses. This work should lead to a publication in 2020.

During the last two years, we have lead the biodiversity task within the Bioschemas.org W3C community group that seeks the definition and adoption of common biology-related markup terms. We proposed the creation of the Taxon term<sup>0</sup> whose adoption in Schema.org is under discussion. The work now starts bearing fruits as 180.000+ webpages of the MNHN are now annotated with the Taxon term, paving the way to more biodiversity resources being published as structured data that search engines can process to provide more accurate search results.

### 7.3.2. *Semantic Web for eEducation*

**Participants:** Catherine Faron Zucker, Géraud Fokou Pelap.

In the framework of the EduMICS project we developed and populated an ontology to represent the students' activity on the Educlever learning platform.

### 7.3.3. *Semantic Web for B2B applications*

**Participants:** Molka Dhouib, Catherine Faron Zucker, Andrea Tettamanzi.

In the framework of the collaborative project with Silex France company aiming to model the social network of service providers and companies, as a preliminary step, we developed an ontology alignment approach combining word embedding and the radius measure to detect matching concepts and determining equivalence or hierarchical relations between them. We report and discuss the results of the evaluation of our approach on the OAEI complex alignment benchmark and on the SILEX use case: aligning reference vocabularies to annotate B2B services (ESCO to Cigref, ESCO to ROME, NAF to kompass and NAF to Silex activity domains) [35].

### 7.3.4. *Integration of Heterogeneous Data Sources*

**Participants:** Franck Michel, Catherine Faron Zucker, Fabien Gandon.

With the incentive of fostering the integration of Linked Data and non RDF data sources, we continued the work initiated around the SPARQL Micro-Service architecture that harnesses the Semantic Web standards to enable automatic combination of Linked Data and data residing in Web APIs. We published a paper at the LDOW workshop of the Web Conference that explores how we can leverage Schema.org to enable web-scale discovery and querying of Web APIs using SPARQL micro-services [27].

### 7.3.5. *Uncertainty in the Semantic Web*

**Participants:** Ahmed El Amine Djebri, Fabien Gandon, Andrea Tettamanzi.

In the framework of Ahmed El Amine Djebri's thesis, we proposed an approach to publishing uncertainty on the Semantic Web [15] and to link and negotiate uncertainty theories [14].

### 7.3.6. *Uncertainty in Human Geography*

**Participant:** Andrea Tettamanzi.

---

<sup>0</sup><http://agroportal.lirmm.fr/ontologies/TAXREF-LD>

<sup>0</sup><http://bioschemas.org/devSpecs/Taxon/>

In the framework of the Incertimmo collaborative project between Université Côte d'Azur and Kinaxia, we applied machine learning and urban morphology theory to the investigation of the influence of the urban environment on the value of residential real estate [6].

### 7.3.7. *Ontology Design Rule*

**Participants:** Olivier Corby, Catherine Faron Zucker, Philippe Martin.

We worked on the topic of Ontology Design Rules with Philippe Martin, from université de la Réunion, during his visit to the Wimmics team. This work resulted in a publication at Semantics [25].

### 7.3.8. *Suggestion of Data Sources for SPARQL Queries over Linked Open Data*

**Participants:** Hai Huang, Fabien Gandon.

For querying processing over Linked Open Data, suggestion of relevant data sources with respect to a SPARQL query is crucial since it highly affects the performance of querying. In this work, we focus on the problem of suggesting  $k$  relevant data sources with respect to a SPARQL query. We propose a summarization method which models the RDF graph of linked data sources and query graphs as sets of feature paths (star, sink and chain paths) and an effective algorithm to extract these feature paths for data sources and query graphs. To obtain candidate data sources we propose a time and space efficient search algorithm based on locality sensitive hashing. We perform a large-scale experiment on real world linked datasets which shows that our algorithm outperforms existing baselines.

## 7.4. Analyzing and Reasoning on Heterogeneous Semantic Graphs

### 7.4.1. *SPARQL Function*

**Participant:** Olivier Corby.

We wrote a SHACL interpreter with the LDScript language. Within the SPARQL Function LDScript [56] language we introduced new datatypes for JSON and XML DOM. We have written a technical documentation for the whole language: <http://ns.inria.fr/sparql-extension>.

### 7.4.2. *Ontology alignment approach based on Embedded Space*

**Participants:** Molka Dhoub, Catherine Faron Zucker, Andrea Tettamanzi.

In the framework of a collaborative project with Silex France company aiming to model the social network of service providers and companies, as a preliminary step, we developed last year a dedicated vocabulary of competences and fields of activities to semantically annotate B2B service offers. This year, we proposed a new ontology alignment approach based on a set of rules exploiting the embedded space and measuring clusters of labels to discover the relationship between concepts. We tested our system on the OAEI conference complex alignment benchmark track and then applied it to aligning ontologies in a real-world case study of Silex company. The experimental results show that the combination of word embedding and the radius measure make it possible to determine, with good accuracy, not only equivalence relations, but also hierarchical relations between concepts. This work has been presented at the 15th International Conference, SEMANTiCS 2019 [35].

### 7.4.3. *Argument Mining and Argumentation Theory*

**Participants:** Elena Cabrio, Shohreh Haddadan, Tobias Mayer, Milagro Teruel, Laura Alonso Alemany, Johanna Frau.

We have proposed an Argument Mining approach to political debates [23]. We have addressed this task in an empirical manner by annotating 39 political debates from the last 50 years of US presidential campaigns, creating a new corpus of 29k argument components, labeled as premises and claims. We then proposed two tasks: (1) identifying the argumentative components in such debates, and (2) classifying them as premises and claims. We showed that feature-rich SVM learners and Neural Network architectures outperform standard baselines in Argument Mining over such complex data. We released the new corpus USElecDeb60To16 and the accompanying software under free licenses to the research community. As a result of these findings, we have also realized the DISPUTool system [22]. The results of this research have been published at ACL 2019 and IJCAI 2019.

We have contributed to the definition of the ACTA tool, aiming at applying argument mining to clinical text, given the importance of argument-based decision making in medicine [26]. ACTA is a tool for automating the argumentative analysis of clinical trials. The tool is designed to support doctors and clinicians in identifying the document(s) of interest about a certain disease, and in analyzing the main argumentative content and PICO elements. The results of this research have been published at IJCAI 2019.

Finally, together with Laura Alonso Alemany (Univ. Cordoba), Johanna Frau (Univ. Cordoba) and Milagro Teruel (Univ. Cordoba), we evaluated different attention mechanisms applied over a state-of-the-art architecture for sequence labeling [18]. Argument mining is a rising area of Natural Language Processing (NLP) concerned with the automatic recognition and interpretation of argument components and their relations. Neural models are by now mature technologies to be exploited for automating the argument mining tasks, despite the issue of data sparseness. This could ease much of the manual effort involved in these tasks, taking into account heterogeneous types of texts and topics. They assessed the impact of different flavors of attention in the task of argument component detection over two datasets: essays and legal domain. They showed that attention not models the problem better but also supports interpretability. The results of this research have been published at FLAIRS 2019.

#### **7.4.4. Mining and Reasoning on Legal Documents**

**Participants:** Serena Villata, Cristian Cardellino, Milagro Teruel, Laura Alonso Alemany, Guido Governatori, Leendert Van Der Torre, Beishui Liao, Nir Oren.

Together with Cristian Cardellino (Univ. Cordoba), Santiago Marro (Univ. Cordoba), Milagro Teruel (Univ. Cordoba) and Laura Alonso Alemany (Univ. Cordoba), we have adapted the semi-supervised deep learning architecture known as Convolutional Ladder Networks, from the domain of computer vision, and explored how well it works for a semi-supervised Named Entity Recognition and Classification task with legal data. The idea of exploring a semi-supervised technique is to assess the impact of large amounts of unsupervised data (cheap to obtain) in specific tasks that have little annotated data, in order to develop robust models that are less prone to overfitting. In order to achieve this, first we checked the impact on a task that is easier to measure. We presented some preliminary results, however, the experiments carried out showed some interesting insights that foster further research in the topic. The results of this research have been published at FLAIRS 2019 [9].

Together with some colleagues from Data61 Queensland (Australia) and Antonino Rotolo (University of Bologna), Serena Villata proposed a framework for modelling legislative deliberation in the form of dialogues. Roughly, in legislative dialogues coalitions can dynamically change and propose rule-based theories associated with different utility functions, depending on the legislative theory the coalitions are trying to determine. The results of this research have been published at ICAIL 2019 [21].

Finally, together with Nir Oren (Univ. Aberdeen), Leendert van der Torre (Univ. Luxembourg) and Beishui Liao (Univ. Zhejiang), we defined, using hierarchical abstract normative systems (HANS), three kinds of prioritized normative reasoning approaches called Greedy, Reduction and Optimization. Then, after formulating an argumentation theory for a HANS, we showed that for a totally ordered HANS, Greedy and Reduction can be represented in argumentation by applying the weakest link and the last link principles, respectively, and Optimization can be represented by introducing additional defeats capturing the idea that for each argument that contains a norm not belonging to the maximal obeyable set then this argument should be rejected. The results of this research have been published on the Journal of Logic and Computation [3].

#### **7.4.5. Natural Language Processing of Song Lyrics**

**Participants:** Michael Fell, Elena Cabrio, Fabien Gandon, Alain Giboin.

We progressed our work in the WASABI ANR project in two directions. First, we tackled the problem of summarizing song lyrics. Given the peculiar structure of songs, applying generic text summarization methods to lyrics can lead to the generation of highly redundant and incoherent text. We thus proposed to enhance state-of-the-art text summarization approaches with a method inspired by audio thumbnailing. We showed how these summaries that take into account the audio nature of the lyrics outperform the generic methods according to both an automatic evaluation and human judgments. The work resulted in an RANLP publication



[17]. Second, we investigated the task of detecting swear words and other potential harmful content in lyrics. The Parental Advisory Label (PAL) is a warning label that is placed on audio recordings in recognition of profanity or inappropriate references, with the intention of alerting parents of material potentially unsuitable for children.

Since 2015, digital providers such as iTunes, Spotify, Amazon Music and Deezer also follow PAL guidelines and tag such tracks as explicit.

Nowadays, such labelling is carried out mainly manually on voluntary basis, with the drawbacks of being time consuming and therefore costly, error prone and partly a subjective task. Therefore, we compared automated methods ranging from dictionary-based lookup to state-of-the-art deep neural networks to automatically detect explicit contents in English lyrics. We showed that more complex models perform only slightly better on this task, and relying on a qualitative analysis of the data, we discussed the inherent hardness and subjectivity of the task. The work was published at the RANLP conference [16]. We are currently modelling emotion in song lyrics, with the focus on the hierarchical and sequential structure of these texts, in which lines make up segments which make up the full lyric. And later parts may be perceived differently in light of the emotion previous parts have caused.

#### 7.4.6. RDF Mining

**Participants:** Thu Huong Nguyen, Andrea Tettamanzi.

In collaboration with our former PhD student Tran Duc Minh, Claudia d'Amato of the University of Bari, and Nguyen Thanh Binh of the Danang University, we made a comparison of rule evaluation metrics for EDMAR, our evolutionary approach to discover multi-relational rules from ontological knowledge bases exploiting the services of an OWL reasoner [36].

In the framework of Nguyen Thu Huong's thesis, we have proposed a grammar-based evolutionary method to mine RDF datasets for OWL class disjointness axioms [31], [30].

#### 7.4.7. Machine Learning for Operations Research

**Participant:** Andrea Tettamanzi.

Together with Alberto Ceselli and Saverio Basso of the University of Milan we used machine learning techniques to understand good decompositions of linear programming problems [1].

#### 7.4.8. Image recognition with Semantic Data

**Participants:** Anna Bobasheva, Fabien Gandon, François Raygagne, Frédéric Precioso.

The objective of the MonaLIA 2.0 project is to exploit the crossover between the Deep Learning methods of image analysis and knowledge-based representation and reasoning and its application to the semantic indexing of annotated works and images in JocondeLab dataset. The goal is to identify automated or semi-automated tasks to improve the annotation and information retrieval. This project was an 11-month contract with Ministry of Culture plus 6-month internship.

- Training dataset preparation
  - Developed SPARQL query to extract the subsets of images to train the multi-label Deep Learning classifiers for a given set of categories
  - Developed Python scripts to filter and balance training images and Joconde specific data loader
  - Identified categories that are not linked by Garnier Thesaurus but visually related and extended the Joconde metadata with the new RDF triples (e.g. category "Rider" is linked to categories "Horse" and "Human being")
  - Researched effects of various image transformations on the object detection performance (resizing, cropping, padding, scaling)

For the underrepresented categories (bicycle, airplane, cat, etc. ) downloaded the images from the external sources such as Kaggles’ “Painter by Number”, the Behance Artistic Media Set, and Cleveland Museum of Art. This has been done with the internship of François Raygagne.

- Building Deep Learning model
  - Adapted the pre-trained VGG16 and Inception v3 PyTorch implementations for multi-label classification of the artwork images
  - Tuned models hyperparameters
  - Experimented with scaling the multi-labeled for 10, 20, 40 classes
  - Experimented with binary classifiers for a single category
- Classification results consumption
  - Studied the possible dependencies between knowledge graph metrics and classification performance (average precision of object detection)
  - Extended the Joconde metadata with prediction scores produced by the classifiers
  - Included the scores into category search queries to filter and order the results to produce more relevant results

Results were presented at atelier Culture - Inria, on december 2nd, Institut national d’histoire de l’art in Paris.

#### 7.4.9. Hospitalization Prediction

**Participants:** Raphaël Gazzotti, Catherine Faron Zucker, Fabien Gandon.

HealthPredict is a project conducted in collaboration with the Département d’Enseignement de Recherche en Médecine Générale (DERMG) at Université Côte d’Azur and the SynchroNext company. It aims at providing a digital health solution for the early management of patients through consultation with their general practitioner and health care circuit. Concretely, it is a predictive Artificial Intelligence interface that allows us to cross the data of symptoms, diagnosis and medical treatments of the population in real time to predict the hospitalization of a patient. We propose and evaluate different ways to enrich the features extracted from electronic medical records with ontological resources before turning them into vectors used by Machine Learning algorithms to predict hospitalization. We reported and discussed the results of our first experiments on the database PRIMEGE PACA at EGC 2019 [38] and ESWC 2019 [19]. We propose a semi-supervised approach based on DBpedia to extract medical subjects from EMRs and evaluate the impact of augmenting the features used to represent EMRs with these subjects in the task of predicting hospitalization. Our results will be presented at SAC 2020 [61]. We designed an interface to assist in the decision-making process of general practitioners that allows them to identify in patients the first signs that lead to hospitalization and medical problems to be treated as a priority. It has been presented at [55].

#### 7.4.10. Learning Analytics and Adaptive learning

**Participants:** Oscar Rodríguez Rocha, Catherine Faron Zucker.

We developed semantic queries to analyse the student activity data available in the Educlever knowledge graph and the SIDES knowledge graph, showing the added value of Semantic Web modelling enabling ontology-based reasoning. The results of our analysis of the SIDES knowledge graph have been presented at the 2019 French workshop on AI and Health [39].

The faculties of medicine, all grouped together under the auspices of the *Conférence des doyens*, are collectively proposing to upgrade the SIDES solution to an innovative solution called Intelligent Health Education System 3.0 (SIDES 3.0). As part of this community-based approach, the coordination of the project will be carried out by the *Université Numérique Thématique (UNT) en Santé et Sport*, the *GIP UNESS.fr*. This structure offers an ideal national positioning for support and coordination of training centers (UFR) and also offers long-term financial sustainability.

In particular, Inria through the Wimmics research team focuses on the recommendation of existing questions to the students according to their profile. For this, research activities are performed to classify the questions present in the platform by difficulty levels according to the Bloom's revised taxonomy, considering the information contained in text of the question. Also, research activities have focused to predict the probability of the outcomes of the students to questions considering previous answers stored in the SIDES graph.

With the ultimate goal of recommending resources adapted to the student's profile and context, we developed an approach to predict the success of students when answering training or test questions by learning a student model from the SIDES knowledge graph. To learn a user model from the SIDES knowledge graph, we combine state-of-the-art features with node embeddings. Our first results will be presented at SAC 2020.

The level of complexity and specificity of the learning objective associated with a question may be a key criterion to integrate in the recommendation process. For this purpose, we developed an approach to classify the questions of the SIDES platform according to the reference Bloom's taxonomy, by extracting the level of complexity and specificity of their learning objectives from their textual descriptions with semantic rules.

## ZENITH Project-Team

# 7. New Results

## 7.1. Scientific Workflows

### 7.1.1. *User Steering in Dynamic Workflows*

**Participants:** Renan Souza, Patrick Valduriez.

In long-lasting scientific workflow executions in HPC machines, computational scientists (users) often need to fine-tune several workflow parameters. These tunings are done through user steering actions that may significantly improve performance or improve the overall results. However, in executions that last for weeks, users can lose track of what has been adapted if the tunings are not properly registered. In [18], we address the problem of tracking online parameter fine-tuning in dynamic workflows steered by users. We propose a lightweight solution to capture and manage provenance of the steering actions online with negligible overhead. The resulting provenance database relates tuning data with data for domain, dataflow provenance, execution, and performance, and is available for analysis at runtime. We show how users may get a detailed view of execution, providing insights to determine when and how to tune. We discuss the applicability of our solution in different domains and validate it with a real workflow in Oil and Gas extraction. In this experiment, the user could determine which tuned parameters influence simulation accuracy and performance. The observed overhead for keeping track of user steering actions at runtime is negligible.

### 7.1.2. *ProvLake: Efficient Runtime Capture of Multiworkflow Data*

**Participants:** Renan Souza, Patrick Valduriez.

Computational Science and Engineering (CSE) projects are typically developed by multidisciplinary teams. Despite being part of the same project, each team manages its own workflows, using specific execution environments and data processing tools. Analyzing the data processed by all workflows globally is critical in a CSE project. However, this is hard because the data generated by these workflows are not integrated. In addition, since these workflows may take a long time to execute, data analysis needs to be done at runtime to reduce cost and time of the CSE project. A typical solution in scientific data analysis is to capture and relate workflow runtime data in a provenance database, thus allowing for runtime data analysis. However, such data capture competes with the running workflows, adding significant overhead to their execution. To solve this problem, we introduce a system called ProvLake [39]. While capturing the data, ProvLake logically integrates and ingests them into a provenance database ready for runtime analysis. We validate ProvLake in a real use case in Oil and Gas extraction with four workflows that process 5 TB datasets for a deep learning classifier. Compared with Komadu, the closest competing solution, our approach has much smaller overhead.

### 7.1.3. *Adaptive Caching of Scientific Workflows in the Cloud*

**Participants:** Gaetan Heidsieck, Christophe Pradal, Esther Pacitti, Patrick Valduriez.

We consider the efficient execution of data-intensive scientific workflows in the cloud. Since it is common for workflow users to reuse other workflows or data generated by other workflows, a promising approach for efficient workflow execution is to cache intermediate data and exploit it to avoid task re-execution. In [27], we propose an adaptive caching solution for data-intensive workflows in the cloud. Our solution is based on a new scientific workflow management architecture that automatically manages the storage and reuse of intermediate data and adapts to the variations in task execution times and output data size. We evaluated our solution by implementing it in the OpenAlea system and performing extensive experiments on real data with a data-intensive application in plant phenotyping. The results show that adaptive caching can yield major performance gains.

## 7.2. Query Processing

### 7.2.1. *Top-k Query Processing Over Encrypted Data in the Cloud*

**Participants:** Sakina Mahboubi, Reza Akbarinia, Patrick Valduriez.

Cloud computing provides users and companies with powerful capabilities to store and process their data in third-party data centers. However, the privacy of the outsourced data is not guaranteed by the cloud providers. One solution for protecting the user data against security attacks is to encrypt the data before being sent to the cloud servers. Then, the main problem is to evaluate user queries over the encrypted data.

In [12], we propose a system, called SD-TOPK (Secure Distributed TOPK), that encrypts and stores user data in a cloud across a set of nodes, and is able to evaluate top-k queries over the encrypted data. SD-TOPK comes with a novel top-k query processing algorithm that finds a set of encrypted data that is proven to contain the top-k data items. This is done without having to decrypt the data in the nodes where they are stored. In addition, we propose a powerful filtering algorithm that removes the false positives as much as possible without data decryption. We implemented and evaluated the performance of our system over synthetic and real databases. The results show excellent performance for SD-TOPK compared to TA-based approaches.

### 7.2.2. *Parallel Query Rewriting in Key-Value Stores under Single-Key Constraints*

**Participant:** Reza Akbarinia.

Semantic constraints bring important knowledge about the structure and the domain of data. They allow users to better exploit their data thanks to the possibility of formulating high-level queries, which use a vocabulary richer than that of the single sources. However, the constraint-based rewriting of a query may lead to a huge set of new queries, which has a consequent impact on the query answering time.

In [37], we propose a novel technique for parallelizing both the generation and the evaluation of the rewriting set of a query serving as the basis for distributed query evaluation under constraints. Our solution relies on a schema for encoding the possible rewritings of a query on an integer interval. This allows us to generate equi-size partitions of rewritings, and thus to balance the load of the parallel working units that are in charge of generating and evaluating the queries. The experimental evaluation of our technique shows a significant reduction of query rewriting and execution time by means of parallelization.

## 7.3. Data Analytics

### 7.3.1. *SAVIME: Simulation Data Analysis and Visualization*

**Participant:** Patrick Valduriez.

Limitations in current DBMSs prevent their wide adoption in scientific applications. In order to make scientific applications benefit from DBMS support, enabling declarative data analysis and visualization over scientific data, we present an in-memory array DBMS system called SAVIME. In [34], we describe the system SAVIME, along with its data model. Our preliminary evaluation show how SAVIME, by using a simple storage definition language (SDL) can outperform the state-of-the-art array database system, SciDB, during the process of data ingestion. We also show that it is possible to use SAVIME as a storage alternative for a numerical solver without affecting its scalability.

### 7.3.2. *Massively Distributed Indexing of Time Series*

**Participants:** Djamel Edine Yagoubi, Reza Akbarinia, Boyan Kolev, Oleksandra Levchenko, Florent Maseglia, Patrick Valduriez, Dennis Shasha.

Indexing is crucial for many data mining tasks that rely on efficient and effective similarity query processing. Consequently, indexing large volumes of time series, along with high performance similarity query processing, have become topics of high interest. For many applications across diverse domains though, the amount of data to be processed might be intractable for a single machine, making existing centralized indexing solutions inefficient.

In [20], we propose a parallel solution to construct the state of the art iSAX-based index over billions of time series by making the most of the parallel environment by carefully distributing the work load. Our solution takes advantage of frameworks such as MapReduce or Spark. We provide dedicated strategies and algorithms for a deep combination of parallelism and indexing techniques. We also propose a parallel query processing algorithm that, given a query, exploits the available processing nodes to answer the query in parallel using the constructed parallel index. We implemented our index construction and query processing algorithms, and evaluated their performance over large volumes of data (up to 4 billion time series of length 256, for a total volume of 6 TB). Our experiments demonstrate high performance of our algorithm with an indexing time of less than 2 hours for more than 1 billion time series, while the state of the art centralized algorithm needs more than 5 days. They also illustrate that our approach is able to process 10M queries in less than 140 seconds, while the state of the art centralized algorithm need almost 2300 seconds.

We have implemented our solutions in the Imitates software. The demonstration of Imitates [32] is available at <http://imitates.gforge.inria.fr/>. The demo visitors are able to choose query time series, see how each algorithm approximates nearest neighbors and compare times in a parallel environment.

### 7.3.3. *Online Correlation Discovery in Sliding Windows of Time Series*

**Participants:** Djamel Edine Yagoubi, Reza Akbarinia, Boyan Kolev, Oleksandra Levchenko, Florent Masegla, Patrick Valduriez, Dennis Shasha.

In some important applications (such as finance, retail, etc.), we need to find correlated time series in a time window, and then continuously slide this window. Doing this efficiently in parallel could help gather important insights from the data in real time. In [30], we address the problem of continuously finding highly correlated pairs of time series over the most recent time window. Our solution, called ParCorr, uses the sketch principle for representing the time series. We implemented ParCorr on top of UPM-CEP, a Complex Event Processing streaming engine developed by our partner Universitat Politecnica de Madrid. Our solution improves the parallel processing of UPM-CEP, allowing higher throughput using less resources. An interesting aspect of our solution is the discovery of time series that are correlated to a certain subset of time series. The discovered correlations can be used to select features for training a regression model for prediction.

### 7.3.4. *Time Series Clustering via Dirichlet Mixture Models*

**Participants:** Khadidja Meguelati, Florent Masegla.

Dirichlet Process Mixture (DPM) is a model used for clustering with the advantage of discovering the number of clusters automatically and offering nice properties like, *e.g.*, the potential convergence to the actual clusters in the data. These advantages come at the price of prohibitive response times, which impairs its adoption and makes centralized DPM approaches inefficient. In [35], we propose DC-DPM (Distributed Computing DPM), a parallel clustering solution that gracefully scales to millions of data points while remaining DPM compliant, which is the challenge of distributing this process. In [36], we propose HD4C (High Dimensional Data Distributed Dirichlet Clustering), a parallel clustering solution that addresses the curse of dimensionality by distributed computing and performs clustering of high dimensional data such as time series (as a function of time), hyperspectral data (as a function of wavelength) etc. For both methods, our experiments on synthetic and real world data show high performance.

## 7.4. Machine Learning for Biodiversity Informatics

### 7.4.1. *Phenological Stage Annotation with Deep Convolutional Neural Networks*

**Participants:** Titouan Lorieul, Herve Goeau, Alexis Joly.



Herbarium based phenological research offers the potential to provide novel insights into plant diversity and ecosystem processes under future climate change. The goal of this study [11], conducted in collaboration with US and French ecologists, is to automate the scoring of reproductive phenological stages within a huge amount of digitized herbaria and provide significant resources for the ecological and organismal scientific communities. Specifically, we address three questions: 1) Can fertility, i.e., the presence of reproductive structures, be automatically detected from digitized specimens using deep learning? 2) Are the detection models generalizable to different herbarium data sets? and 3) Is it possible to automatically record stages (i.e., phenophases) within longer phenological events on herbarium specimens? This is the first time that such an analysis has been conducted at this scale, on such a large number of herbarium specimens and species. The results obtained for 7782 species of plants representing angiosperms, gymnosperms, and ferns suggest that it is possible to consider large-scale phenological annotation across broad phylogenetic groups.

#### 7.4.2. Deep Species Distribution Modelling

**Participants:** Benjamin Deneu, Christophe Botella, Alexis Joly.

Species distribution models (SDM) are widely used for ecological research and conservation purposes. Given a set of species occurrences and environmental data (such as climatic rasters, soil occupation, altitude, etc.), the aim is to infer the spatial distribution of the species over a given territory. In a previous work, we showed that using deep convolutional networks significantly improved predictive performance compared to conventional punctual approaches. We have deepened this methodology with two main contributions. The first one is to extend the model to explicitly take into account species co-occurrences [22]. This is achieved through a new multimodal architecture that allows the joint learning of biotic and abiotic patterns in a common representation space. The second contribution is to experiment deep SDMs at the scale of several tens of thousands of species and tens of millions of occurrences. These contributions were made possible thanks to the use of supercomputer Jean Zay (more than 1000 GPUs) of the GENCI national infrastructure.

#### 7.4.3. Evaluation of Species Identification and Prediction Algorithms

**Participants:** Alexis Joly, Herve Goeau, Christophe Botella, Benjamin Deneu, Fabian Robert Stoter.

We run a new edition of the LifeCLEF evaluation campaign [29] with the involvement of 16 research teams worldwide. The main outcomes of the 2019-th edition are:

- **GeoLifeCLEF.** The main result of the second edition of this challenge [24] is that deep convolutional models outperform the most efficient machine learning models used in ecology (such as random forests or boosted trees). In particular, they are able to transfer knowledge from animals distribution to plant distribution, which had never been shown before.
- **PlantCLEF.** The 2019-th edition of the plant identification challenge [26] was designed to evaluate automated identification on the flora of data deficient regions, tropical ones in particular. It is based on a dataset of 10K species mainly focused on the Guiana shield and the Northern Amazon rainforest, an area known to have one of the greatest diversity of plants and animals in the world. The results reveal that the identification performance in this context is considerably lower than the one obtained on temperate plants of Europe and North America. The performance of convolutional neural networks fall due to the very low number of training images for most species and the higher degree of noise that is occurring in such data.
- **Bird sounds identification.** The 2019-th edition of the BirdCLEF challenge [41] focuses on the difficult task of recognizing all birds vocalizing in omni-directional soundscape recordings. Therefore, the dataset of the previous year has been extended with more than 350 hours of manually annotated soundscapes that were recorded using 30 field recorders in Ithaca (NY, USA). The main outcome is that the recognition performance can be significantly improved thanks to sophisticated data augmentation methods adapted to the problem.

In addition to organizing these challenges, we published a synthesis of the LifeCLEF evaluation campaign since its inception in 2011. This synthesis [44] is part of a larger book published on the occasion of the 20th anniversary of the CLEF international research forum. It highlights the rapid progress that automatic identification has made over the past decade, and allows us to take a step back on the future challenges of this discipline.

#### 7.4.4. *Optimal Checkpointing for Heterogeneous Chains: How to Train Deep Neural Networks with Limited Memory*

**Participants:** Alena Shilova, Alexis Joly.

In many deep learning tasks for biodiversity, limited GPU memory is a performance limiting factor. The use of larger image sizes, in particular, is often not possible because the back-propagation algorithm requires storing all network activation maps in memory during for the backward stage. A larger image size could improve the performance of many tasks such as the analysis of digitized herbarium beds, range modeling or early detection of crop weeds in precision agriculture.

In this work [47], done in collaboration with the REAL-OPT team, we introduce a new activation checkpointing method which allows to significantly decrease memory usage when training Deep Neural Networks with the back-propagation algorithm. Similarly to checkpointing techniques coming from the literature on Automatic Differentiation, it consists in dynamically selecting the forward activations that are saved during the training phase, and then automatically recomputing missing activations from those previously recorded. We propose an original computation model that combines two types of activation savings: either only storing the layer inputs, or recording the complete history of operations that produced the outputs (this uses more memory, but requires fewer recomputations in the backward phase), and we provide an algorithm to compute the optimal computation sequence for this model, when restricted to memory persistent sequences. We provide a PyTorch implementation that processes the entire chain, dealing with any sequential DNN whose internal layers may be arbitrarily complex and automatically executing it according to the optimal checkpointing strategy computed given a memory limit. Through extensive experiments, we show that our implementation consistently outperforms existing checkpointing approaches for a large class of networks, image sizes and batch sizes.

### 7.5. Machine Learning for Audio Heritage Data

Audio data is typically exploited through large repositories. For instance, music right holders face the challenge of exploiting back catalogues of significant sizes while ethnologists and ethnomusicologists need to browse daily through archives of heritage audio recordings that have been gathered across decades. The originality of our research on this aspect is to bring together our expertise in large volumes and probabilistic music signal processing to build tools and frameworks that are useful whenever audio data is to be processed in large batches. In particular, we leverage on the most recent advances in probabilistic and deep learning applied to signal processing from both academia (e.g. Telecom Paris, PANAMA & Multispeech Inria project-teams, Kyoto University) and industry (e.g. Mitsubishi, Sony), with a focus towards large scale community services.

#### 7.5.1. *Setting the State of the Art in Music Demixing*

**Participants:** Fabian-Robert Söter, Antoine Liutkus.

We have been very active in the topic of music demixing, with a prominent role in defining the state of the art in this domain. This has been achieved through several means.

- In the previous years, we have been organizing the Signal Separation Evaluation Challenge (SiSEC), an international event in the signal processing community that is held since 2007. Its objective is to bring together researchers to evaluate their algorithms on music separation/demixing on the same data and with the same metrics. From 2016 to 2019, A. Liutkus was the lead chair of SiSEC.
- We have developed the *open-unmix* [19] software, which is a reference implementation for music source separation. For the first time, it makes it possible for any researcher to use and improve a state-of-the art implementation (MIT-licensed) in the domain. In terms of performance, open-unmix matches the best results we observed over the years as the organizers of SiSEC. The open-unmix software won the second place at the Global Pytorch Summer Hackaton 2019 organized by FaceBook.

The *pro* private version of this software is currently under active development for transfer to industry.

- In [6], we present the field to the non-specialist researcher, in a wide-audience scientific magazine. We are also core contributors of the audio section for the position paper on the use of AI for the creation industry [48].

### 7.5.2. *Generative Modelling for Audio*

**Participants:** Antoine Liutkus, Fabian-Robert Söter, Mathieu Fontaine.

Discriminative training for audio signal processing is inherently limited in the sense that it boils down to assuming that the target signals are present in the input, and can be recovered through some kind of filtering, even if this involves sophisticated deep models. We move forward to a new paradigm for signal processing, in which the observed signals and time series are not assumed to comprise the totality of the target, but rather some arbitrarily degraded version of it. The objective then can be understood as *generating new content given this input*. For instance, bandwidth extension may be thought of as audio super-resolution.

Our research on generative modelling concerns both methodological/theoretical aspects and applied research. On the former, we introduce the Sliced Wasserstein Flow in our ICML paper [33], which enables the optimal transport of particles from two probability spaces in a principled way. On the latter, we study the combination of heavy-tailed probabilistic models with generative audio models for source separation in [31], [25].

Our strategy is to go beyond our current expertise on music demixing to address the new and very active topics of audio style transfer and enhancement, with large scale applications for the exploitation and repurposing of large audio corpora.

### 7.5.3. *Robust Probabilistic Models for Time-series*

**Participants:** Mathieu Fontaine, Antoine Liutkus, Fabian-Robert Söter.

Processing large amounts of data for denoising or analysis comes with the need to devise models that are robust to outliers and permit efficient inference. For this purpose, we advocate the use of non-Gaussian models for this purpose, which are less sensitive to data-uncertainty. Our contributions on this topic can be split in two parts. First, we develop new filtering methods that go beyond least-squares estimation. In collaboration with researchers from Telecom Paris, we introduce several methods that generalize least-squares Wiener filtering to the case of  $\alpha$ -stable processes [2]. This work is currently also under review as a journal paper. Second, as mentioned in the previous section, we have been working on generative models for audio, with the particular twist that the deep models we consider are trained probabilistically under  $\alpha$ -stable assumptions. This has the remarkable effect of significantly augmenting robustness [31], [25].